

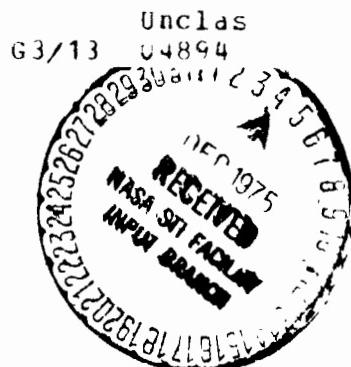
**NASA TECHNICAL
MEMORANDUM**

NASA TM X-71838

NASA TM X-71838

(NASA-TM-X-71838) TITAN/CENTAUR D-1 TC-2,
HELIOS A FLIGHT DATA REPORT (NASA) 343 p HC
\$10.00 CSCI 22C

N76-13140



**TITAN/CENTAUR D-1T
TC-2, HELIOS A
FLIGHT DATA REPORT**

Lewis Research Center
Cleveland, Ohio
September 1975

TC-2 FLIGHT DATA REPORT

HELIOS A

Contents

	<u>Page</u>
I SUMMARY	2
II INTRODUCTION	4
Helios A Mission Background	4
Helios A Mission Scientific Objectives	5
Centaur Extended Mission Experiments	5
III SPACE VEHICLE DESCRIPTION	8
Helios A Spacecraft	8
Launch Vehicle Configuration	12
Titan IIIE	15
Centaur D-1TR	17
Delta TE-M-364-4	19
Centaur Standard Shroud	20
IV MISSION PROFILE AND PERFORMANCE SUMMARY	24
Flight Trajectory and Performance Data	24
Titan Phase of Flight	33
Centaur Phase of Flight - Primary and Extended Mission	34
V VEHICLE DYNAMICS	37
VI SOFTWARE PERFORMANCE	59
Airborne	59
Computer Controlled Launch Set	60
VII TITAN IIIE SYSTEMS ANALYSIS	62
Mechanical Systems	62
Airframe Structures	62
Propulsion Systems	63
SRM Thrust Vector Control	77
Hydraulic Systems	79

	<u>Page</u>
Flight Controls and Sequencing System	81
Electrical/Electronic Systems	95
Airborne Electrical System	95
Flight Termination System	100
Instrumentation and Telemetry System	101
VIII CENTAUR STANDARD SHROUD	105
Preflight/Liftoff Functions and Venting	105
CSS and Vehicle Aerodynamics	127
CSS Structures	156
CSS In-flight Events and Jettison	160
IX CENTAUR D-1TR SYSTEMS ANALYSIS	185
Mechanical Systems	185
Structures	185
Propulsion/Propellant Feed System	199
Hydrogen Peroxide Supply and Reaction Control System	222
Hydraulic System	226
Pneumatics and Tank Vent Systems	228
Computer Controlled Vent and Pressurization System	239
Centaur D-1TR and CSS Thermal Environment and Propellant Behavior	248
Centaur and CSS Component and Environmental Temperatures	248
Centaur Propellant Management	263
Electrical/Electronic Systems	271
Electrical Power Systems	271
Digital Computer Unit	275
Inertial Measurement Group	276
Flight Control System	278
Propellant Loading/Propellant Utilization	287
Instrumentation and Telemetry Systems	290
Tracking and Range Safety Systems	298
X DELTA TE-M-364-4 SYSTEMS ANALYSIS	301
Mechanical System	301
Propulsion System	302
Electrical System	303
Telemetry and Tracking Systems	304

	<u>Page</u>
XI FACILITIES AND AGE	306
Complex 41 Facilities	306
Fluid Systems Operations	307
Pneumatic Ground Systems	310
Environmental Control Systems	316
Electrical Ground Systems	329
Delta Stage Support Systems	338
Helios A Spacecraft Support Systems	339

I SUMMARY

I SUMMARY

by K. A. Adams

Titan/Centaur TC-2 was launched from the Eastern Test Range, Complex 41, at 02:11 EST on Tuesday, December 10, 1974. This was the first operational flight of the newest NASA unmanned launch vehicle. The spacecraft was the Helios A, the first of the two solar probes designed and built by the Federal Republic of Germany.

The primary mission objective, to place the Helios spacecraft on a heliocentric orbit in the ecliptic plane with a perihelion distance of 0.31 AU, was successfully accomplished.

After successful injection of the Helios spacecraft, a series of experiments was performed with the Centaur stage to demonstrate its operational capabilities. These experiments included a one-hour zero "g" coast period and subsequent engine burn to demonstrate the capability to fly long coast planetary missions such as MJS'77 and a three-hour zero "g" coast and subsequent engine burn to demonstrate the capability to perform geosynchronous missions. All objectives of this Centaur extended mission experiment phase were successfully met.

II INTRODUCTION

II INTRODUCTION

by K. A. Adams

Helios A Mission Background

In June 1969 the Federal Republic of Germany and the United States of America agreed on the joint cooperative Helios solar probe project. This basic agreement provided for the design, development, test and launch of two flight spacecraft to within 0.3 AU of the sun. Germany was assigned the responsibility for providing the two spacecraft, seven scientific experiments on each spacecraft, and controlling the spacecraft throughout the mission. The United States was assigned the task of providing three scientific experiments on each spacecraft, two Titan IIIE/Centaur/Delta (TE-M-364-4) launch vehicles and tracking and data reception from the NASA Deep Space Network (DSN). Major contractual effort on the program began in 1970. In March of 1971 the German Government (BMBW) proposed an additional experiment, Celestial Mechanics, for the Helios mission. Late in the program, a Faraday Rotation experiment was also approved.

This joint project is expected to provide new understanding of fundamental solar processes and Sun/Earth relationships by obtaining information and measurements on the solar wind, magnetic and electric fields, cosmic rays, cosmic dust and solar disc. It will also test the theory of general relativity. The NASA Lewis Research Center (LeRC) has prime responsibility for the launch vehicle. The NASA Goddard Space Flight Center (GSFC) through its Helios Project is responsible for the activities of the United States agencies which are involved in Helios and for provision of the United States sponsored experiments. The Gesellschaft fur Weltraumforschung (GfW) of the Federal Republic of Germany is responsible for the technical direction of the prime spacecraft contractor, Messerschmidt-Boelkow-Blohm GmbH (MBB-Ottobrunn), for the German experiments, and for all other German organizations which contribute to the Helios project.

The Titan IIIE and Centaur D-1TR, fitted with a spin-stabilized solid propellant TE-M-364-4 (Delta) stage, is designed to launch the Helios A unmanned spacecraft into a heliocentric orbit, in the ecliptic plane, with a perihelion of approximately 0.31 AU and an aphelion of approximately 1.0 AU. This was the first of two planned Helios spacecraft. The launch of Helios A was from the AFETR Launch Complex 41, Cape Canaveral, Florida, utilizing a parking orbit ascent mode. The launch of Helios B is planned for late 1975.

Flight time of the Helios A primary mission is approximately 120 days, extending through the first solar occultation. The total mission life time, however, is expected to exceed 18 months with primary interest in the region of the orbit between perihelion and solar occultation.

After the spacecraft was placed into its desired heliocentric trajectory, the Centaur vehicle continued into an experimental flight phase. During this post Helios experiment phase developmental data was obtained relative to the Centaur's capability for extended periods of zero-g coast and multiple engine starts.

Helios A Mission Scientific Objectives

The principal objective of the Helios A mission is the exploration of interplanetary space in the proximity of the Sun by:

- Measuring the magnetic field, the density, temperature, velocity and direction of the solar wind.
- Studying discontinuities and shock phenomena in the interplanetary medium magnetically, electrically, and by observing the behavior of the solar wind particles.
- Studying radio waves and the electron plasma oscillations in their natural state.
- Measuring the propagation and spatial gradient of solar and galactic cosmic rays.
- Studying the spatial gradient and dynamics of the interplanetary dust and chemical composition of dust grains.
- X-ray monitoring the solar disc by means of a Geiger-Muller counter.
- Testing the theory of General Relativity with respect to both orbital and signal propagation effects.

Helios A successfully accomplished its mission objectives on March 15, 1975, when it satisfied the agreed scientific measurement criteria during its perihelion passage (0.309 AU). All instruments were working and good scientific data was received from each of the 10 active experiments. Data has also been received from the two passive experiments (Celestial Mechanics and Faraday Rotation), but their period of maximum interest is just before first solar occultation (mid-April). All spacecraft systems operated nominally with temperatures generally falling within a few degrees centigrade of predictions (except for the German Magnetometer Experiment 2). Preliminary indications are that Helios B would be assigned a minimum perihelion of about 0.29 AU.

Centaur Extended Mission Experiments

Following injection of the Helios into its required trajectory, the Centaur vehicle was designed to perform developmental experiments. These Centaur experiments include:

- One-hour zero-g coast capability.
- Main engine ignition test following one-hour zero-g coast.
- Three-hour zero-g coast with thermal maneuvers.

- Boost pump operation experiment with ignitors on.
- Zero-g boost pump dead head operation.

Extensive special instrumentation was installed on Centaur to provide engineering data which will be used to assess its capability to meet the requirements of future NASA, international and commercial programs.

During the Centaur extended mission, all experiment objectives were successfully met. A detailed analysis of this mission phase will be published by LeRC in a separate engineering report.

III SPACE VEHICLE DESCRIPTION

III SPACE VEHICLE DESCRIPTION

Helios A Spacecraft

by K. A. Adams

The Helios A spacecraft (Figure 1) has a short 16-sided cylindrical central body with two conical solar arrays attached at its upper and lower end. Above the central body, within and protruding above the upper solar array, is the communications antenna assembly. This antenna assembly consists of a high gain antenna with a despun deflector that orients to face the earth, a medium gain antenna, and an omni antenna.

There are two deployable radial booms attached to the central body on which are mounted the three magnetometer sensors. These two rigid booms are diametrically opposite and when deployed the boom axes are approximately radial. The magnetometer booms are double hinged. Magnetometer Experiment 3 is located at the tip of one boom and Magnetometer Experiment 4 is located at the tip of the other boom. Magnetometer Experiment 2 is located part way along the Magnetometer Experiment 4 boom.

The spacecraft also deploys two radial flexible booms from reel type storage to provide a 32 meter tip to tip antenna for the Radiowave Experiment 5. The axis of this experiment antenna is normal to the axis of the two rigid booms when they are in the deployed position. In launch configuration, the two rigid booms are folded in against the central body and the experiment antenna booms are stored on their reels. The rigid booms and flexible antenna booms are deployed upon command after initial acquisition of the spacecraft RF signals by the DSN.

The central body has a circular equipment platform at each end with several radial equipment platforms in between. A conical adapter attached to the lower circular equipment platform mates with the Delta stage payload attach fitting to form the spacecraft to launch vehicle mechanical interface.

With the exception of the three magnetometer experiments sensors which are boom mounted, the experiment sensors, their electronic units and the spacecraft equipment are located on the radial equipment platforms within the central body or within the conical adapter.

The central body is thermally controlled by louver systems which, along with second surface mirrors covering the central body, maintain the temperature inside the central body reasonably constant during the mission.

A battery system provides spacecraft power up to the time of sun acquisition and then power is provided by the solar cells.

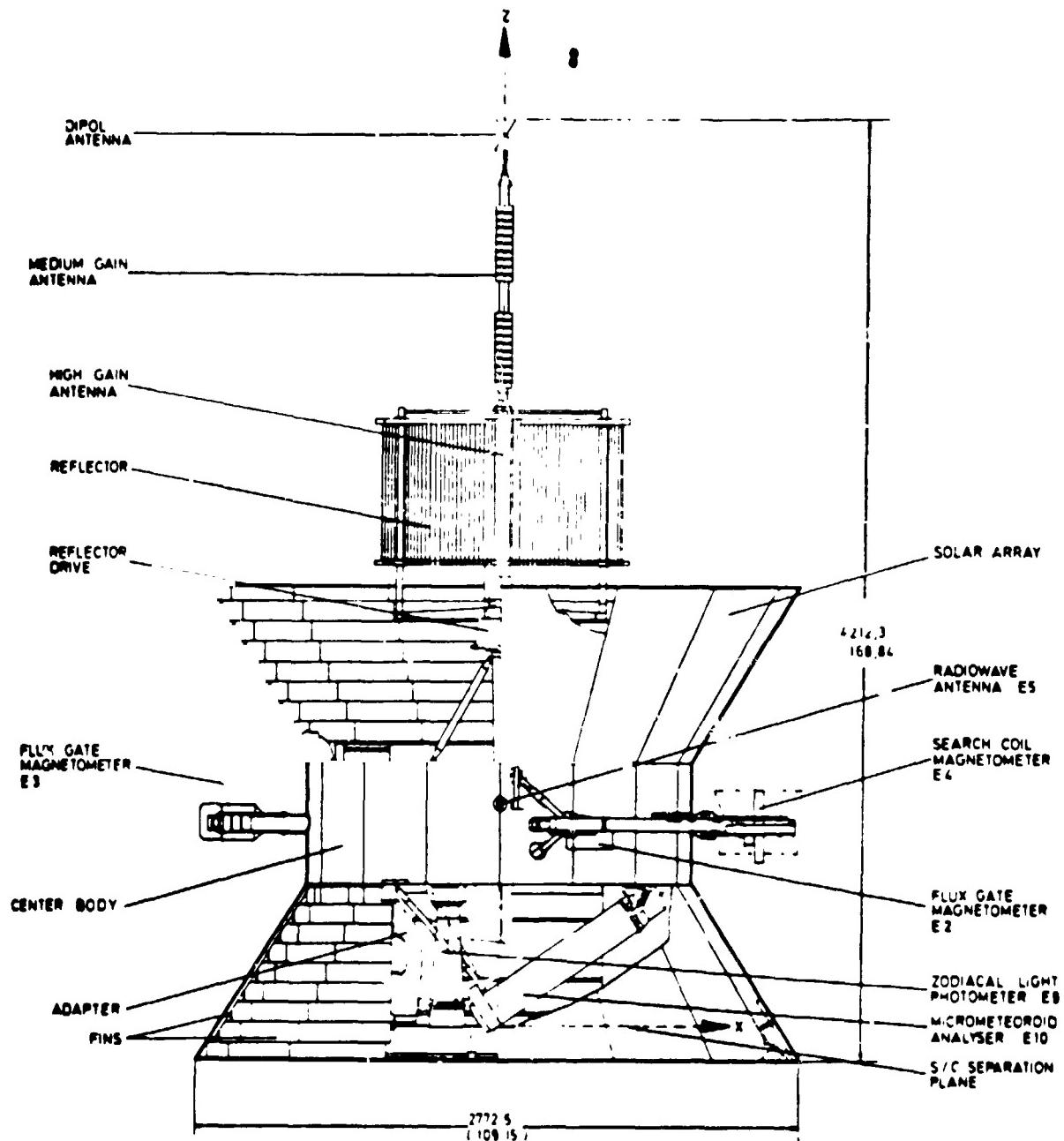


Figure 1 Spacecraft Launch Configuration

The spacecraft attitude control is performed by sun sensors and a cold nitrogen gas jet system. Coarse and fine sensors in the sun sensor assembly will be used to complete the initial acquisition sequence by orientation of the spacecraft spin axes to a position perpendicular to the spacecraft - sun line. Antenna signal strength measurements are used to bring the spin axes of the spacecraft perpendicular to the ecliptic plane. The final spin rate, 60 ± 1 RPM, will be achieved by the gas jet system, implemented by the ground command based on telemetered spin rate information.

A listing of the Helios A scientific experiments and the principal investigators is presented in Table 1.

TABLE I HELIOS SCIENTIFIC EXPERIMENTS

NUMBER	EXPERIMENT	INVESTIGATOR	AFFILIATION	SCIENTIFIC OBJECTIVES
1	Plasma Experiment	Rosenbauer and Pekoffer	Max Planck Institute, Garching	Solar wind velocity measurement
		Wolfe	Ames Research Center	
2	Flux-Gate Magnetometer	Neubauer and Maier	Technical University of Braunschweig	Interplanetary magnetic field measurement
3	Flux-Gate	Ness and Burlaga	Goddard Space Flight Center	Interplanetary magnetic field measurement
		Mariani and Cantarano	University of Rome	
4	Search-Coil Magnetometer	Neubauer and Dehmel	Technical University of Braunschweig	Interplanetary magnetic field measurement from 4.7 Hz to 2.2 kHz
5	Plasma and Radio Wave Experiment	Gurnett Kellogg	University of Iowa University of Minnesota	Radio wave measurement from 50 kHz to 2 MHz Plasma measurement from 10 Hz to 100 kHz
		Stone Bauer	Goddard Space Flight Center	
6	Cosmic Ray Experiment	Hasler and Kunow	University of Kiel	Energy measurements on solar and galactic particles
7	Cosmic Ray Experiment	McDonald, Trainor Teegarden Roelof McCracken	Goddard Space Flight Center CSIRO, Melbourne	Flow and energy measurements on solar and galactic particles Measurement of solar X-ray emission
8	Electron	Keppler and Wilken	Max Planck Institute, Lindau/Harz	Counting of solar electrons
		Williams	GSFC	
9	Zodiacal Light Photometer	Leinert and Pitz	Landessternwarte Heidelberg	Wavelength observation and polarization measurement of Zodiacal light
10	Micrometeroid Analyzer	Fechtig and Weihrauch	Max Planck Institute, Heidelberg	Mass and energy measurement of interplanetary dust particles
11	Celestial Mechanics Experiment	Kundt	University of Hamburg JPL	Verify relativity theories
12	Faraday Rotation Experiment	Levy	JPL	Measurement of S-Band polarization due to radio wave passage through solar corona
		Volland	University of Bonn	

Launch Vehicle Configuration

by K. A. Adams

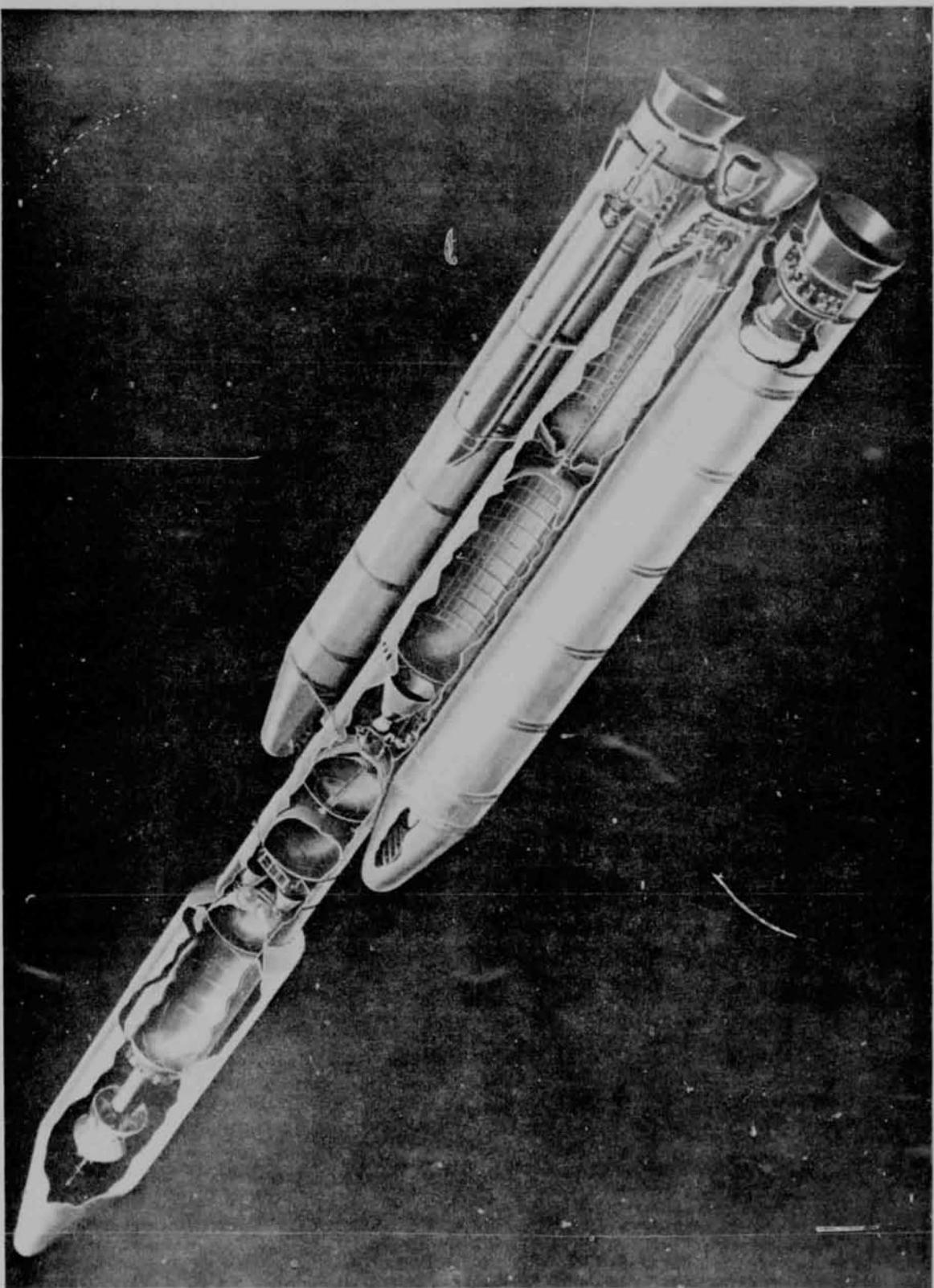
The launch vehicle for Helios A was the five stage Titan IIIE/Centaur D-ITR/Delta TE-M-364-4 configuration. This was the first operational flight of this combination of stages.

The overall vehicle configuration is shown in Figure 2. The Titan vehicle consists of a two-stage liquid propulsion core vehicle manufactured by the Martin Marietta Corporation and two solid rocket motors (zero stage) manufactured by United Technology Center. The Titan vehicle integrator is Martin Marietta. The third stage is the Centaur D-ITR manufactured by General Dynamics Convair Division. For the Helios A mission the Delta TE-M-364-4 solid rocket stage, manufactured by McDonnell Douglas and managed by Goddard Space Flight Center, was integrated into the configuration to provide additional velocity for this high energy mission.

The payload fairing for this configuration is the newly developed Centaur Standard Shroud (CSS) manufactured by Lockheed Missiles and Space Company, Inc. Figure 3 shows the Centaur/CSS/Helios A spacecraft general arrangement for this mission.

The following sections of the report give a summary description of the vehicle stage configurations. Detailed subsystem descriptions can be found in the Flight Data Report for Titan/Centaur IC-1 Proof Flight (NASA TM X-71692). Only configuration differences from TC-1 will be addressed in this report.

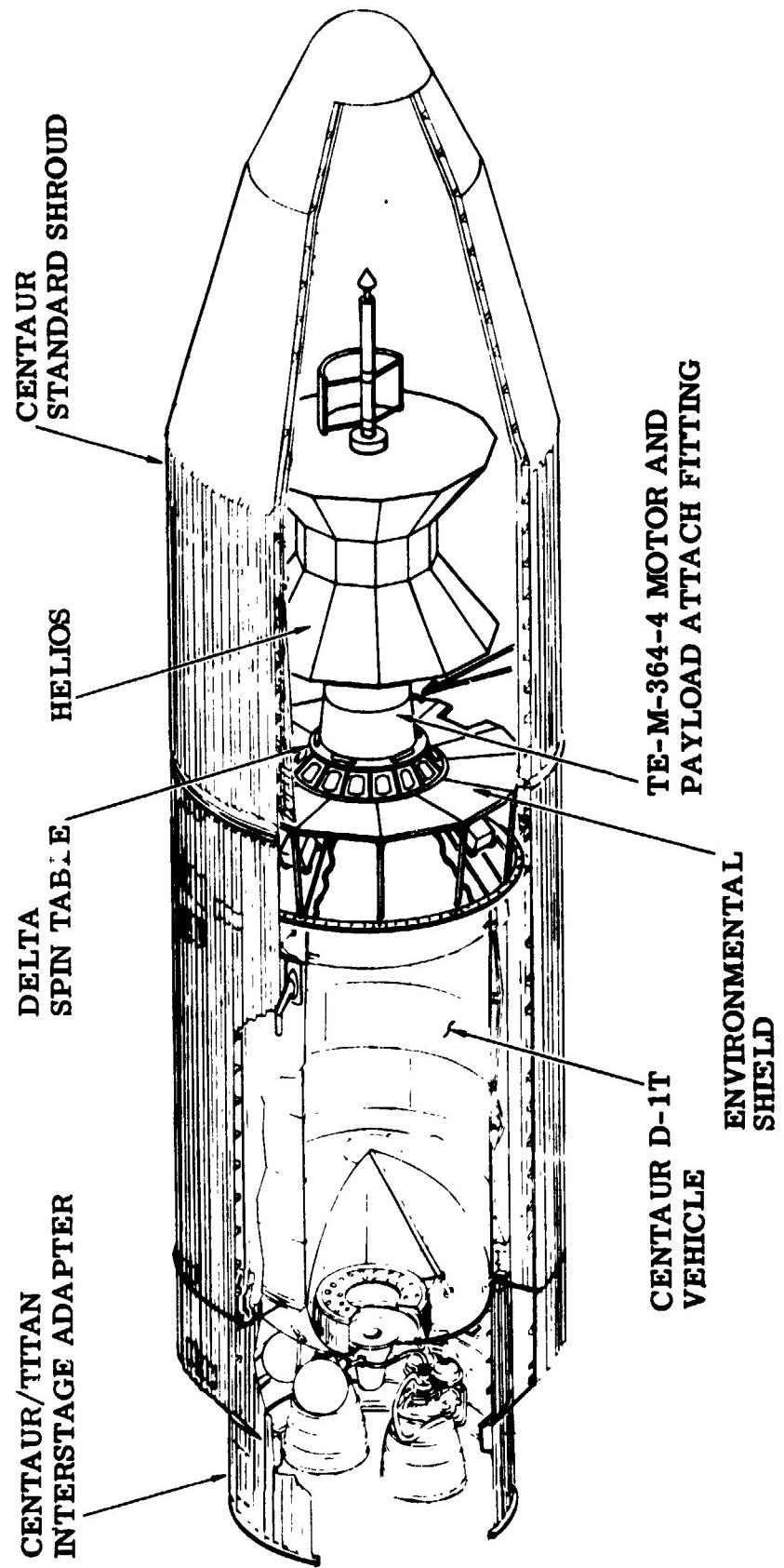
FIGURE 2 OVERALL TC-2 VEHICLE CONFIGURATION



ORIGINAL PAGE IS
OF POOR QUALITY

Figure 3

CENTAUR HELIOS GENERAL ARRANGEMENT



Titan IIIE

by J. L. Collins

The Titan/Centaur booster, designated Titan IIIE, was developed from the family of Titan III vehicles in use by the Air Force since 1964. The Titan IIIE is a modified version of the Titan IIID. Modifications were made to the Titan to accept steering commands and discretes from the Centaur inertial guidance system instead of a radio guidance system. In addition, a redundant programmer system was added. The Titan IIIE consists of two solid rocket motors designated Stage 0 and the Titan III core vehicle Stages I and II.

The two Solid Rocket Motors (SRM's) provide a thrust of 2.4 million pounds at liftoff. These motors, built by United Technology Center, use propellants which are basically aluminum and ammonium perchlorate in a synthetic rubber binder. Flight control during the Stage 0 phase of flight is provided by a Thrust Vector Control (TVC) system in response to commands from the Titan flight control computer. Nitrogen tetroxide injected into the SRM nozzle through TVC valves deflects the thrust vector to provide control. Pressurized tanks attached to each solid rocket motor supply the thrust vector control fluid. Electrical systems on each SRM provide power for the TVC system.

Titan core Stages I and II are built by the Martin Marietta Corporation. The Stages I and II propellant tanks are constructed of welded aluminum panels and domes while interconnecting skirts use conventional aluminum sheet and stringer construction. The Stage II forward skirt provides the attach point for the Centaur stage and also houses a truss structure supporting most of the Titan IIIE electronics. A thermal barrier was added to isolate the Titan IIIE electronics compartment from the Centaur engine compartment.

Stages I and II are both powered by liquid rocket engines made by the Aerojet Liquid Rocket Company. Propellants for both stages are nitrogen tetroxide and a 50/50 combination of hydrazine and unsymmetrical dimethylhydrazine. The Stage I engine consists of dual thrust chambers and turbopumps producing 520,000 pounds thrust at altitude. Independent gimbaling of the two thrust chambers, using a conventional hydraulic system, provides control in pitch, yaw, and roll during Stage I flight.

The Stage II engine is a single thrust chamber and turbopump producing 100,000 pounds thrust at altitude. The thrust chamber gimbals for flight control in pitch and yaw and the turbopump exhaust duct rotates to provide roll control during Stage II flight.

The Stage I oxidizer autogenous pressurization system consisted of one superheater to lower in-flight tank pressure levels from those experienced during TC-1 which had two superheaters. This pressurization system provides tank ullage pressure during Stage I burn time.

The Titan flight control computer provides pitch, yaw and roll commands to the solid rocket motor's thrust vector control system and the Stages I and II hydraulic actuators. The flight control computer receives attitude signals from the three-axis reference system which contains three displacement gyros.

Vehicle attitude rates in pitch and yaw are provided by the rate gyro system located in Stage I. In addition, the flight control computer generates preprogrammed pitch and yaw signals, provides signal conditioning, filtering and gain changes, and controls the dump of excess thrust vector control fluid. A roll axis control change was added to provide a variable flight azimuth capability for planetary launches. The Centaur computer provides steering programs for Stage 0 wind load relief and guidance steering for Titan Stages I and II.

A flight programmer provides timing for flight control programs, gain changes and other discrete events. A staging timer provides acceleration-dependent discretes for Stage I ignition and timed discretes for other events keyed to staging events. The flight programmer and staging timer, operating in conjunction with a relay package and enable-disable circuits, comprise the electrical sequencing system. On Titan IIIE a second programmer, relay packages and other circuits were added to provide redundancy. Also, capability for transmitting backup commands was added to the Titan systems for staging of the Centaur Standard Shroud and the Centaur.

The standard Titan uses three batteries: one for flight control and sequencing, one for telemetry and instrumentation, and one for ordnance. On Titan IIIE additional separate redundant Range Safety Command system batteries were added to satisfy Range requirements.

The Titan telemetry system is an S-band frequency, pulse code modulation/frequency modulation (PCM/FM) system consisting of one control converter and remote multiplexer units. The PCM format is reprogrammable.

For this Titan vehicle, the following measurements were added beyond the standard Titan IIIE instrumentation: six accelerometers on the Stage I engines, a Stage I oxidizer pump inlet pressure, two narrow band chamber pressure measurements on the two Stage I engines and an orifice and venturi pressure measurement in the Stage I autogenous system.

Many of the modifications to the Titan for Titan/Centaur were made to incorporate redundancy and reliability improvements. In addition to those modifications previously mentioned, a fourth retrorocket was added to Stage II in order to ensure proper Titan/Centaur separation if one motor does not fire. All redundancy modifications to Titan IIIE utilized Titan flight proven components.

Centaur D-1TR

by R. C. Kalo

The Centaur tank is a pressure-stabilized structure made from stainless steel (0.014 inches thick in cylindrical section). A double-walled, vacuum-insulated intermediate bulkhead separates the liquid oxygen tank from the liquid hydrogen tank.

The entire cylindrical section of the Centaur LH₂ tank is covered by a radiation shield. This shield consists of three separate layers of an aluminized Mylar-dacron net sandwich. The forward tank bulkhead and tank access door are insulated with a multilayer aluminized Mylar. The aft bulkhead is covered with a membrane which is in contact with the tank bulkhead and a rigid radiation shield supported on brackets. The membrane is a layer of dacron-reinforced aluminized Mylar. The radiation shield is made of laminated nylon fabric with aluminized Mylar on its inner surface and white polyvinyl flouride on its outer surface.

The forward equipment module, an aluminum conical structure, attaches to the tank by a short cylindrical stub adapter. Attached to the forward ring of the equipment module is an adapter which forms the mounting structure for the Delta (Fourth) Stage.

Two modes of tank pressurization are used. Before propellant tanking, a helium system maintains pressure. With propellants in the tank, pressure is maintained by propellant boiloff. During flight, the airborne helium system provides supplementary pressure when required. This system also provides pressure for the H₂O₂ and engine controls system.

Primary thrust is provided by two Pratt & Whitney RL10A3-3 engines, which develop 15,000 pounds total thrust each. The engines are fed by hydrogen peroxide fueled boost pumps. Engine gimbaling is provided by a separate hydraulic system on each engine.

During coast flight, attitude control is provided by four H₂O₂ engine cluster manifold assemblies mounted on the tank aft bulkhead on the peripheral center of each quadrant. Each assembly consists of two 6-lb lateral thrust engines manifolded together.

A retrothrust system consisting of two diametrically opposite nozzles mounted on the tank aft bulkhead and canted 45° from the vehicle longitudinal centerline provides the thrust for separating the Centaur from the Delta stage. Actuation of two parallel mounted pyrotechnic valves vent residual helium from the storage bottle through the two retrothrust nozzles.

A propellant utilization system controls the engine mixture ratio to ensure that both propellant tanks will be emptied simultaneously. Quantity measurement probes are mounted within the fuel and oxidizer tanks.

The Centaur D-IT astrionics system's Teledyne Digital Computer Unit (DCU) is an advanced, high speed computer with a 16,384 word random access memory. From the DCU discretes are provided to the Sequence Control Unit (SCU). Engine commands go to the Servo-Inverter Unit (SIU) through six digital-to-analog (D/A) channels.

The Honeywell Inertial Reference Unit (IRU) contains a four-gimbal, all-altitude stable platform. Three gyros stabilize this platform, on which are mounted three pulse-balanced accelerometers. A prism and window allow for optical azimuth alignment. Resolvers on the platform gimbals transform vector components from inertial to vehicle coordinates. A crystal oscillator, which is the primary timing reference, is also contained in the IRU.

The System Electronic Unit (SEU) provides conditioned power and sequencing for the IRU. Communication from the IRU to the DCU is through three analog-to-digital channels (for attitude and rate signals) and three incremental velocity channels. The SEU and IRU combination forms the Inertial Measuring Group (IMG).

The Centaur D-ITR system also provides guidance for Titan, with the stabilization function performed by the Titan.

The central controller for the Centaur pulse code modulation PCM telemetry system is housed in the DCU. System capacity is 267,000 bits per second. The central controller services two Teledyne remote-multiplexer units on the Centaur D-ITR.

The C-Band tracking system provides ground tracking of the vehicle during flight. The airborne transponder returns an amplified radio-frequency signal when it detects a tracking radar's interrogation.

The Centaur uses a basic d-c power system, provided by batteries and distributed via harnessing. The servo-inverter provides a-c power, 26 and 115 volts, single phase, 400 Hz.

Delta TE-M-364-4

by R. C. Kalo

The Delta Stage (alternately referred to as Fourth Stage or TE-M-364-4 Stage) major assemblies consist of a spin table, TE-M-364-4 solid propellant rocket motor, batteries, telemetry system, C-Band radar transponder, destruct system, motor separation clamp, payload attach fitting, and a spacecraft separation clamp. The Delta Stage-to-Centaur interface is between the Centaur cylindrical adapter and the Delta spin table lower (non-rotating) conical adapter.

The spin table assembly includes a four-segment petal adapter mounted on a bearing attached to the non-rotating conical adapter. During spinup, the eight spin rockets which are mounted on the spin table are ignited, the two redundant motor separation clamp explosive bolt assemblies are initiated, and centrifugal force swings the adapter segments back on their hinges to free the Delta Stage, the payload attach fitting and the Helios spacecraft.

The TE-M-364-4 rocket motor provides an average thrust of 14,900 pounds over its action time of about 44 seconds.

The MDAC 3731 Payload Attach Fitting (PAF) is a cylindrical aluminum structure, 31 inches high and approximately 37 inches in diameter. Fourteen vertical aluminum stiffeners are mounted externally on the attach fitting structure. Four formed stiffeners, mounted internally, serve as spacecraft separation spring supports. The base of the attach fitting is attached to the forward support ring of the TE-M-364-4 motor. The Helios spacecraft is fastened to the attach fitting by means of a V band clamp. Four separation springs are utilized, each exerting a force of approximately 130 pounds on the spacecraft in the mated configuration. After separation of the Helios spacecraft from the Delta stage, a yo-weight system is deployed on Delta to tumble the stage to neutralize residual motor thrust and prevent inadvertent impact with the spacecraft.

Centaur Standard Shroud

by T. P. Cahill

The Centaur Standard Shroud is a jettisonable fairing designed to protect the Centaur vehicle and its payloads for a variety of space missions. The Centaur Standard Shroud, as shown in Figure 4, consists of three major segments: a payload section, a tank section, and a boattail section. The 14-foot diameter of the shroud was selected to accommodate Viking spacecraft requirements. The separation joints sever the shroud into clamshell halves.

The shroud basic structure is a ring stiffened aluminum and magnesium shell. The cylindrical sections are constructed of two light gage aluminum sheets. The outer sheet is longitudinally corrugated for stiffness. The sheets are joined by spot welding through an epoxy adhesive bond. Sheet splices, ring attachments, and field joints employ conventional rivet and bolted construction. The bi-conic nose is a semi-monocoque magnesium-thorium single skin shell. The nose dome is stainless steel. The boattail section accomplishes the transition from the 14-foot shroud diameter to the 10-foot Centaur interstage adapter. The boattail is constructed of a ring stiffened aluminum sheet conical shell having external riveted hat section stiffeners.

The Centaur Standard Shroud modular concept permits installation of the tank section around the Centaur independent of the payload section. The payload section is installed around the spacecraft in a special clean room, after which the encapsulated spacecraft is transported to the launch pad for installation on the Centaur.

The lower section of the shroud provides insulation for the Centaur liquid hydrogen tank during propellant tanking and prelaunch ground hold operations. This section has seals at each end which close off the volume between the Centaur tanks and the shroud. A helium purge is required to prevent formation of ice in this volume.

The shroud is separated from the Titan/Centaur during Titan Stage II flight. Jettison is accomplished when an electrical command from the Centaur initiates the Super-Zip separation system detonation. Redundant dual explosive cords are confined in a flattened steel tube which lies between two notched plates around the circumference of the shroud near the base and up the sides of the shroud to the nose dome. The pressure produced by the explosive cord detonation expands the flattened tubes, breaking the two notched plates and separating the shroud into two halves.

To ensure reliability, two completely redundant electrical and explosive systems are used. If the first system should fail to function, the second is automatically activated as a backup within one-half second.

The Titan pyrotechnic battery supplies the electrical power to initiate the Centaur Standard Shroud electric pyrotechnic detonators. Primary and backup jettison discrete signals are sent to the Titan squib firing circuitry by the Centaur Sequence Control Unit (SCU). A tertiary jettison signal, for additional redundancy, is derived from the Titan staging timer.

Four base-mounted, coil-spring thrusters force each of the two severed shroud sections to pivot about hinge points at the base of the shroud. After rotating approximately 60 degrees, each shroud half separates from its hinges and continues to fall back and away from the launch vehicle.

Two additional sets of springs are installed laterally across the Centaur Standard Shroud split lines; one set of two springs in the upper nose cone to assist in overcoming nose dome rubbing friction and one set of two springs at the top of the tank section to provide additional impulse during Centaur/Shroud jettison disconnect breakaway.

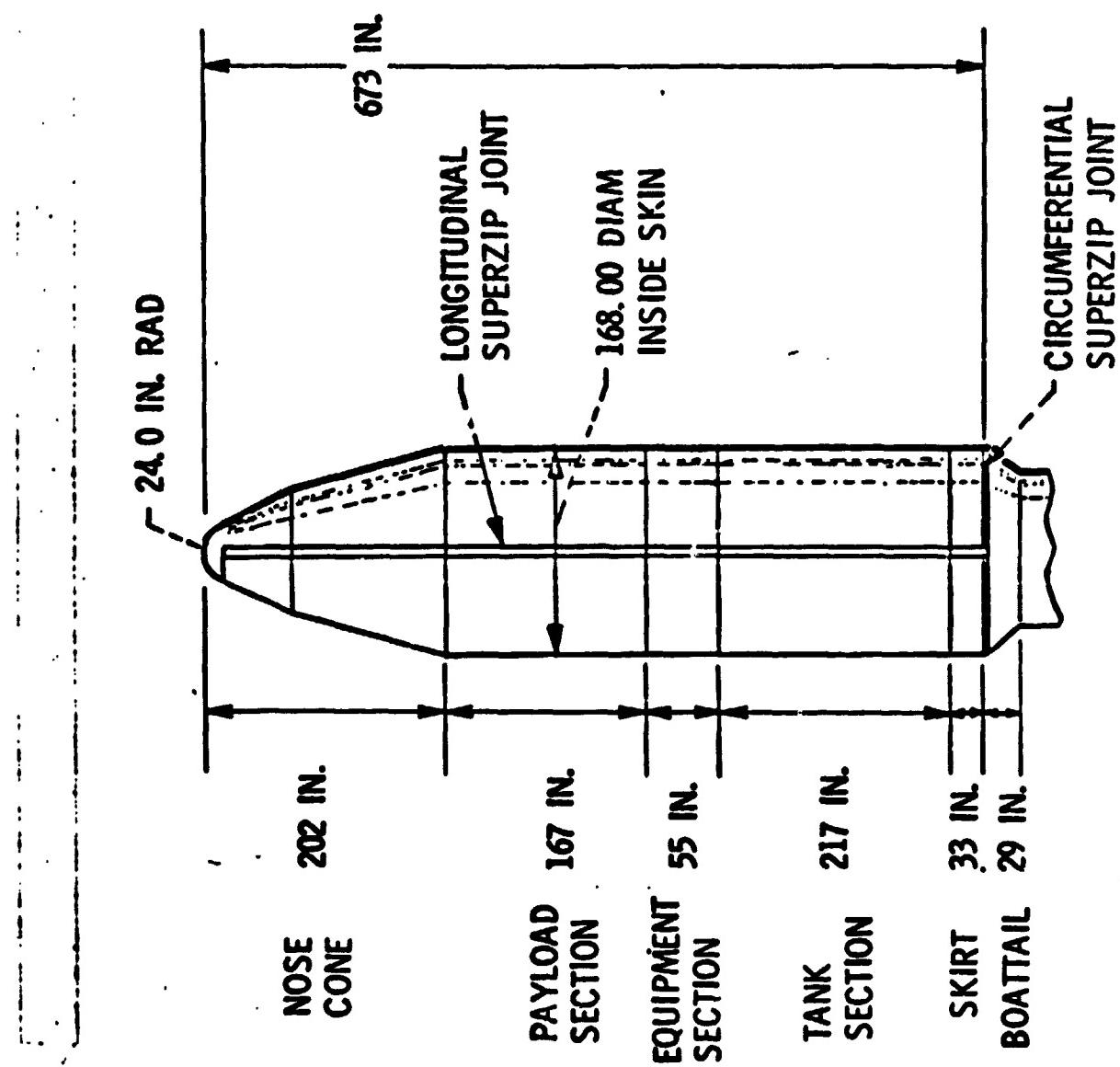


FIGURE 4 - CENTAUR STANDARD SHROUD CONFIGURATION

IV MISSION PROFILE AND PERFORMANCE SUMMARY

IV MISSION PROFILE AND PERFORMANCE SUMMARY

Flight Trajectory and Performance Data

by R. P. Kulvinen

Stage 0 ignition for the TC-2 launch vehicle occurred at 0711:01.057 GMT (0211:01.057 EST) on Tuesday, December 10, 1974, with liftoff occurring approximately 0.3 seconds later. The ADDJUST-designed Titan Stage 0 steering programs for aerodynamic load relief were based on a Windsonde balloon which was released 2.5 hours prior to the expected launch time.

The flight sequence of events is contained in Table 2. The Helios A portion of the mission extended from Stage 0 ignition through the TE-364-4 burn and spacecraft separation. The Centaur extended mission commenced after the separation of the TE-364-4/Helios A from the Centaur.

The Stage 0 phase of flight was nearly nominal. The ignition of the Stage I engines (87FS1) occurred at 111.6 seconds into the flight which was about 0.1 seconds earlier than predicted. 12.0 seconds after ignition, at 124.6 seconds into the flight, the solid rocket motors (SRM's) were jettisoned. The comparison of the actual trajectory with the preflight predicted trajectory showed the vehicle was extremely close to the predicted position and velocity at SRM jettison.

The duration of Stage I portion of flight was 3.7 seconds shorter than predicted. The Stage I/Stage II staging sequence commenced at 258.3 seconds with Stage I shutdown (87FS2) and was completed with separation occurring at 259.6 seconds. The Stage II ignition signal (91FS1) was sent simultaneously with the Stage II shutdown signal (87FS2). The vehicle was approximately 3000 feet higher in altitude and 80 feet/sec lower in velocity than predicted at the time of Stage I shutdown.

During the Titan Stage II portion of flight the Centaur Sequence Control Unit (SCU) commanded jettison of the Centaur Standard Shroud at 318.6 seconds into flight. This event is commanded by the Centaur SCU 60 seconds after the Centaur flight computer senses Titan Stage I shutdown.

The duration of the Titan Stage II portion of flight was 2.4 seconds longer than predicted, with Stage II shutdown occurring at 468.8 seconds into the flight. The Centaur DCU commanded Stage II separation 3.9 seconds after sensing the shutdown decelleration.

The vehicle was 528 ft low in altitude and 60 ft/sec low in velocity at Titan/Centaur separation. These dispersions were well within the expected tolerances.

Centaur main engine start (MES-1) for first burn occurred at 483.2 seconds into flight. The Centaur first burn terminated upon successful insertion into the parking orbit at 584.0 seconds into flight. Table 3 shows that a highly accurate parking orbit was achieved.

The Centaur coasted in parking orbit for 21.93 minutes in a propellant settled mode. The Centaur second burn of 273.4 seconds occurred at the end of the coast with main engine start (MES-2) at 1899.5 seconds into the flight with the guidance system commanding MECO-2 at 2172.9 seconds.

Seventy seconds after MECO-2, the TE-M-364-4 and spacecraft were spun up. Separation occurred two seconds later. The second burn orbital data is shown in Table 3 at TE-M-364-4 separation from the Centaur. The orbital data indicates a very accurate orbit was achieved by the Centaur second burn.

The TE-M-364-4 burn completed the Helios portion of flight placing the spacecraft into its final heliocentric orbit. The burn appeared to be about one second longer than expected. The orbital elements at spacecraft separation, which occurred at 2401.46 seconds, are presented in Table 3. A slightly higher velocity, approximately 30 ft/sec, was achieved by the TE-M-364-4. The free-fall trajectory simulation of the orbital elements to perihelion passage, which is presented in Table 4, shows that a very accurate Helios A heliocentric orbit was obtained.

The Centaur, after the TE-M-364-4 was separated, performed two additional firings of the main engines to demonstrate the capability to coast at least one hour in a zero-g mode and fire the engines as well as a longer zero-g coast which represented a typical geosynchronous mission sequence. Several propellant management experiments were performed in this Centaur extended mission.

The Centaur was aligned along the radius vector such that the resultant orbit after the third and fourth burns would be a highly elliptical geocentric orbit.

After the one-hour zero-g coast, the Centaur third burn occurred at 5773 seconds into the flight for a duration of 11 seconds. The Centaur then coasted for three hours in the zero-g mode performing thermal maneuvers. At 16584.1 seconds into the flight the Centaur fourth and final engine firing occurred. The duration of this burn was 47.9 seconds which was about 0.7 seconds shorter than expected. The orbital elements for the extended mission are tabulated in Table 5. The orbit accuracy is considered satisfactory since the third and fourth burns were not guided. The third burn was terminated on a fixed burn time and the fourth burn, on an acceleration level based upon a predetermined residual propellant weight. The inclination was 1.95 degrees greater than predicted, which indicated an out-of-plane thrust component. The inclination dispersion was investigated and was considered not to be unexpected for the autopilot software configuration that was flown. The investigation also revealed changes in some of the other orbital parameters during the coast phases. The orbital elements were computed from telemetered accelerometer data and it was concluded that these changes could be due to accelerometer bias errors. Because of insufficient tracking of the Centaur C-band during the extended mission, confirmation of these changes in orbital parameters was not possible.

TABLE 2
TC-2 HELIOS A SEQUENCE OF EVENTS

EVENT DESCRIPTION	NOMINAL (T+SECS)	ACTUAL (T+SEC)
GO INERTIAL	T-6	T-6
STAGE 0 (SRMs) IGNITION	T+0.0	T=0
LIFTOFF	0.2	0.3
FORWARD BEARING REACTOR SEPARATION	100.0	100.0
STAGE I IGNITION (87.FS1)	111.73	111.6
STAGE 0 (SRMs) JETTISON	123.8	123.6
STAGE I SHUTDOWN (87FS2/91FS1)	262.0	258.3
STEP I JETTISON/STAGE II IGNITION	262.8	259.2
CENTAUR STD SHROUD JETTISON	323.0	318.6
STAGE II SHUTDOWN (91FS1)	470.1	468.8
STAGE II JETTISON (T/C SEP)	476.1	472.7
CENTAUR MES 1	486.1	483.2
CENTAUR MECO 1	584.8	584.0
CENTAUR MES 2	1899.7	1899.5
CENTAUR MECO 2	2176.5	2172.9
TE-364-4 SPINUP	2246.5	2242.9
TE-364-4 SEPARATION	2248.5	2244.9
CENTAUR RETRO	2248.5	2244.9
TE-364-4 IGNITION	2290.5	2285.76
TE-364-4 BURNOUT	2334.3	2330.66

TABLE 2 (CONT'D.)
TC-2 HELIOS A SEQUENCE OF EVENTS

SPACECRAFT SEPARATION	2406.5	2401.46
TE-364-4 YO DEPLOY	2408.5	2405.36
CENTAUR MES 3	5776.4	5773.0
CENTAUR MECO 3	5787.4	5784.0
CENTAUR MES 4	16587.4	16584.1
CENTAUR MECO 4	16636.0	16632.0

SRM IGNITION TIME 07:11:01:057Z DECEMBER 10, 1974

TABLE 3.1

HELIOS A ORBITAL DATA

	PARKING ORBIT (MECO 1 + DECAY)		
	NOMINAL	ACTUAL	DIFF.
EPOCH (SECS)	585.3 (624)	585.8 (630.9) (1) (2)	+0.5 (+6.9)
PERIGEE ALT (N.MI.)	86.52 (87.22)	86.96 (88.834)	+0.48 (+1.61)
APOGEE ALT (N.MI.)	89.80 (89.80)	89.78 (90.138)	-0.02 (+.34)
SEMI MAJ. AXIS (N.MI.)	3532.1 (3532.4)	3532.3 (3533.42)	+0.2 (+1.0)
ECCECTRICITY (N.D.)	.000465 (.000366)	.000399 (.000185)	-0.000066 (-.000181)
INCLINATION (DEG)	29.843 (29.844)	29.868 (29.871)	+0.025 (+.03)
ARG. OF PERIGEE (DEG)	309.618 (303.87)	308.766 (229.880)	-0.852 (-73.99)
C ₃ (KM ² /SEC ²)	-60.935	-60.931	-0.004

DIFF = ACTUAL - NOMINAL (NOMINAL = PREFLIGHT ACTUAL LAUNCH TIME TRAJECTORY)

- (1) Derived Orbit from Guidance Data
 (2) Tracking Data from BDA, ANT & ASC

TABLE 3.2

HELIOS A ORBITAL DATA

CENTAUR 2ND BURN (TE-364-4 SEPARATION)			
	NOMINAL	ACTUAL (1)	DIFF.
EPOCH (SECS)	2248.5	2207.7	-40.8
PERIGEE ALT (N.MI.)	102.61	103.97	+1.36
APOGEE ALT (N.MI.)	HYP		
SEMI MAJ. AXIS (N.MI.)	-22913.07	-22857.16	+55.91
ECCENTRICITY (N.D.)	1.15478	1.15221	- .00257
INCLINATION (DEG)	29.808	29.820	+0.012
ARG. OF PERIGEE (DEG)	231.391	231.435	+0.054
C_3 (KM^2/SEC^2)	9.393	9.416	+0.023

DIFF = ACTUAL - NOMINAL (NOMINAL = PREFLIGHT ACTUAL LAUNCH TIME TRAJECTORY)

(1) Derived Orbit from Guidance Data

TABLE 3.3
HELIOS A ORBITAL DATA

SPACECRAFT ORBIT (SPACECRAFT SEPARATION)			
	NOMINAL	ACTUAL (1)	DIFF.
EPOCH (SECS)	2406.5	2330	-76.5
PERIGEE ALT (N.MI.)	148.9	156	+7.1
APOGEE ALT (N.MI.)	HYP	HYP	
SEMI MAJ. AXIS (N.MI.)	-2394.86	-2388	+6.86
ECCENTRICITY (N.D.)	2.50021	2.50670	+.00649
INCLINATION (DEG)	29.807	29.798	-0.009
ARG. OF PERIGEE (DEG)	237.725	237.883	.158
$C_3 (KM^2/SEC^2)$	89.871	90.139	.268

DIFF = ACTUAL - NOMINAL (NOMINAL = PREFLIGHT ACTUAL LAUNCH TIME TRAJECTORY)
(1) DSS 42 Tracking Solution

TABLE 4
SPACECRAFT HELIOCENTRIC TRAJECTORY

	NOMINAL	ACTUAL (1)	DIFF	3 SIGMA
PERHELION DISTANCE (A.U.)	0.30998	0.30958	-.0004	± .0015
INCLINATION (DEG)	0.0	0.0157	.0157	± .32

(1) Based on DSS-42 Track

TABLE 5
CENTAUR EXTENDED MISSION ORBITAL DATA

	CENTAUR 3RD BURN (MECO 3)			CENTAUR 4TH BURN (MECO 4)		
	NOMINAL	ACTUAL (1)	DIFF	NOMINAL	ACTUAL (1)	DIFF
EPOCH (SECS)	5787.9	5787.8	-0.1	16636.5	16637.8	+1.3
PERIGEE ALT (N.MI.)	200.35	208.35	+8.0	851.9	951.8	+100.1
APOGEE ALT (N.MI.)	HYP			81474.17	85674.97	+4200.8
SEMI. MAJ. AXIS (N.MI.)	-34759.69	-34649.76	+109.93	44606.94	46757.32	+2150.38
ECCENTRICITY (N.D.)	1.104842	1.105406	.000567	0.903697	0.90591	.0023
INCLINATION (DEG)	29.814	29.918	.104	29.815	31.765	+1.95
ARG. OF PERIGEE (DEG)	230.451	230.604	.153	215.651	216.248	.597
C ₃ (KM ² /SEC ²)	6.192	6.211	.019	-4.82	-4.60	.22

DIFF = ACTUAL - NOMINAL (NOMINAL = PREFLIGHT ACTUAL LAUNCH TIME TRAJECTORY)

(1) Guidance Derived Orbit Solution

Titan Phase of Flight

by J. L. Collins

The Stage 0 (Solid Rocket Motors) propulsion performance was very close to the preflight predicted parameters. This situation resulted in a nominal trajectory being flown during the Stage 0 burn.

The Stage I had a normal engine start transient, a normal exit closure jet-tison and normal oxidizer depletion shutdown characteristic. Propulsion parameters were very close to the preflight predicted values which yielded a nominal trajectory during Stage I burn. A ± 12 psi suction pressure oscillation at 16 Hz was noted at about 140 seconds into the Stage I burn.

The Stage II had a normal engine start transient and a fuel leading simultaneous depletion shutdown. Propulsion parameters indicated a nominal steady state flight except for a chamber pressure spike of 250 psi noted during shutdown.

Overall, the Titan E-2 performed its part of the overall mission in a satisfactory manner and at the end of Stage II burn the vehicle was nominal at 528 ft. low in altitude and 60.0/ft/sec low in velocity. These dispersions were within the expected flight tolerance.

From the Titan point of view there were several firsts which are listed below:

1. First flight of the -021 accelerometers
2. First flight of POGO instrumentation - Stage I
3. First flight with conformal coated Flight Control System Components

Centaur Phase of Flight - Primary and Extended Mission

by R. C. Kalo

Centaur (TC-2) successfully placed the Helios spacecraft into a highly accurate heliocentric orbit with the required attitude alignment. Following separation of the TE-M-364-4/Helios payload, the Centaur vehicle proceeded into a 4 1/2-hour experiment phase which successfully accomplished all objectives.

Performance of the Centaur was completely satisfactory. The Helios mission was performed using a two-burn, settled parking orbit ascent mode. The post Helios experiment phase consisted of a one-hour zero-G coast, a third burn (fixed duration of 11 seconds), a 3-hour zero-G coast with roll axis thermal maneuvers, and a fourth burn (cutoff based on vehicle weight) followed by a boost pump experiment and a H₂O₂ depletion test. All Helios mission objectives, Titan/Centaur operational capability objectives, and the Centaur experiment phase objectives were satisfied. These objectives are listed as follows:

Helios Mission Peculiar

1. The launch vehicle injected the Helios spacecraft into the required heliocentric orbit.
2. Centaur aligned the TE-M-364-4 stage for spacecraft injection burn.
3. Centaur generated the TE-M-364-4 stage spinup and separation commands.
4. Centaur executed a retrothrust maneuver following separation of the TE-M-364-4.
5. Vibration data on the TE-M-364-4 payload adapter was obtained.
6. Centaur Standard Shroud (CSS) payload cavity pressure and temperature data was obtained.
7. Total impulse of the TE-M-364-4 was verified.

Titan/Centaur Operational Capability

1. D-1TR Centaur operational 2-burn mission capability was demonstrated.
2. D-1TR Centaur vibration loads data were obtained.
3. Thermal performance of the D-1TR Centaur insulation system (2-burn mission) was demonstrated.
4. Performance of the computer controlled vent and pressurization system was demonstrated.

5. CSS ascent venting and control of cavity differential pressures was demonstrated.

Extended Mission Experiment Phase

1. Data was obtained to evaluate propellant behavior, heat transfer, and propellant tank temperature/pressure history during a one-hour zero-G coast of the type required for the 1977 Mariner Jupiter/Saturn mission.
2. The D-1TR Centaur hardware and software capability for performing multiple main engine starts was demonstrated.
3. Data was obtained to evaluate propellant behavior, heat transfer and propellant tank temperature/pressure history during a long zero-G coast which utilizes roll maneuvers for thermal control.
4. Data was obtained to evaluate boost pump operation in a "dead-head" and engine chilldown mode in a low-G environment.

V VEHICLE DYNAMICS

V VEHICLE DYNAMICS

by J. C. Estes and T. F. Gerus

Dynamic loads are imposed upon the vehicle from several sources. They are wind loads, acoustic fields, and loads due to system dynamic response from engines starting and stopping. Evaluation of the flight wind loads are as follows:

The ADDJUST system designed flight steering programs PIA2000*TC02 for the wind profile measured by a Windsonde balloon released at 0441Z, December 10, 1974. The pitch and yaw components of this wind are shown in Figure 5. During prelaunch verification of the flight steering programs, peak response to the 0441Z wind was calculated to be 78% of the weakest structural allowable (at 5434 feet) and 79% of the allowable TVC steering usage (at 60000 feet). It should be noted that these percentages include a combination of nominal wind responses with allowances for such unmeasured and/or non-nominal quantities as gusts, buffeting, trajectory dispersions, and two-hour wind changes.

A post-launch wind sounding was made with a Jimisphere balloon released at 0725Z, December 10, 1974. The pitch and yaw components of this wind are shown in Figure 6. The 0725Z sounding is the best available measurement of the flight winds, although it reached critical altitude about 45 minutes after launch. Peak calculated responses for this sounding were 85% of the weakest structural allowable (at 15371 feet) and 99.6% of the allowable TVC steering usage (at 56622 feet). These percentages include the same allowances for extreme conditions described above for the prelaunch verifications. As may be seen in the discussions of measured TVC steering usage (Section VII), Titan flight controls (Section VII), and shroud bending moments (Section VIII), all the measured flight wind responses were well below the allowable.

The acoustic levels measured above the Centaur equipment module are shown in Figures 7 and 8. The data is shown for both launch and transonic and is compared with TC-1. The acoustic level differences between TC-1 and TC-2 throughout the spectrum are well within expected deviations.

The measurements that are most sensitive to dynamic response from engines starting and stopping are those at the payload interface. The accelerometer locations relative to the preflight dynamic model coordinates are shown in Figure 9. Although CA 850 and CA 860 measured similar response to all transients, the discussion following will compare predictions to flight measurements on GA1A, GA2A and GA3A.

The highest lateral response measured in flight was at SRM ignition. The measured response and the upper limit predicted response are shown in Figures 10, 11, 12 and 13. The comparison between the moments resulting from the dynamic responses at three most critical stations are shown in Table 6. It must be noted that the moment computations have accuracy limitations since rotational degrees of freedom were not measured. As can be seen in the table, the moments resulting from the measured responses are well within the upper limit predicted values.

A tabulation of the accelerometer response due to gust and buffet is shown in Table 7. The maximum predicted response is also shown. A comparison of bending moments due to predicted and measured responses at the three most critical stations is shown in Table 8. As the table indicates, the moments which can be reconstructed most conservatively are well within the upper limit predicted values. As in the above launch transient, rotational degrees of freedom were not measured.

Longitudinal response due to POGO occurred during Stage I flight on TC-2. A simplified comparison of the response level and duration measured at the Stage I gimbal is shown in Figure 14 for the TC-1 and TC-2. The actual TC-2 response levels measured at the payload interface are shown on Figure 15. The response levels measured on TC-2 were not a problem because they were far below the maximum predicted values for the other critical conditions.

A comparison between measured acceleration and acceleration reconstructed using TC-2 chamber pressure at Stage I burnout are shown in Figures 16, 17 and 18. Evaluation of this data indicates that measured longitudinal response (Figure 16) agrees reasonably with that reconstructed using chamber pressure. Although lateral response (Figures 17 and 18) does not agree as well, both predicted and measured are very small. Therefore, the previously predicted dispersed values for loads at Stage I shutdown are also considered valid.

A comparison between predicted and measured acceleration response at MECO is shown in Figures 19, 20 and 21. Longitudinal response measured (Figure 19) is higher than predicted because the prediction was made early in the program when the most dispersed predicted propellant level at MECO was lower than the actual propellant level at TC-2 MECO. As in Stage I shutdown, lateral response predictions (Figures 20 and 21) did not accurately match measured values but both predicted and actual measured values are low.

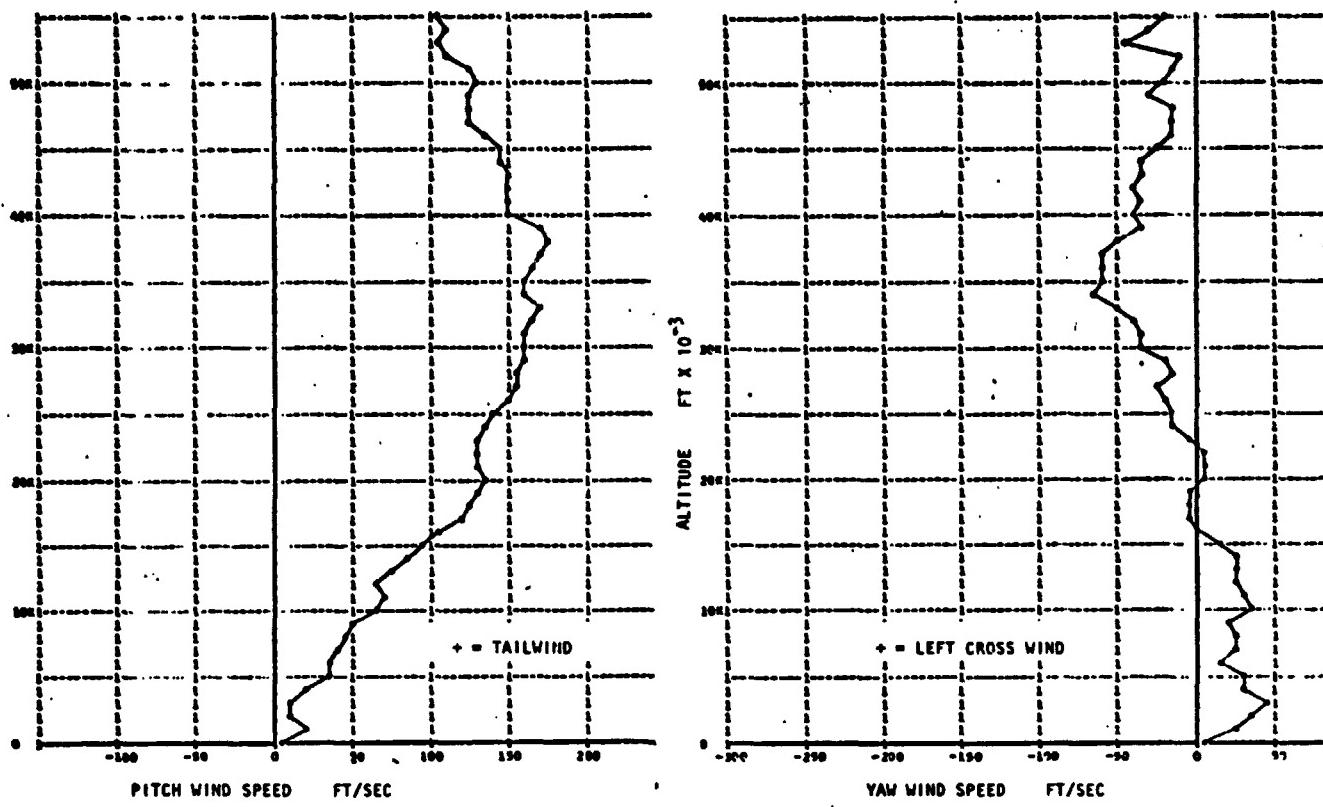


FIGURE 5

WINDSONDE COMPONENT WINDS, 0441Z, 12-10-74

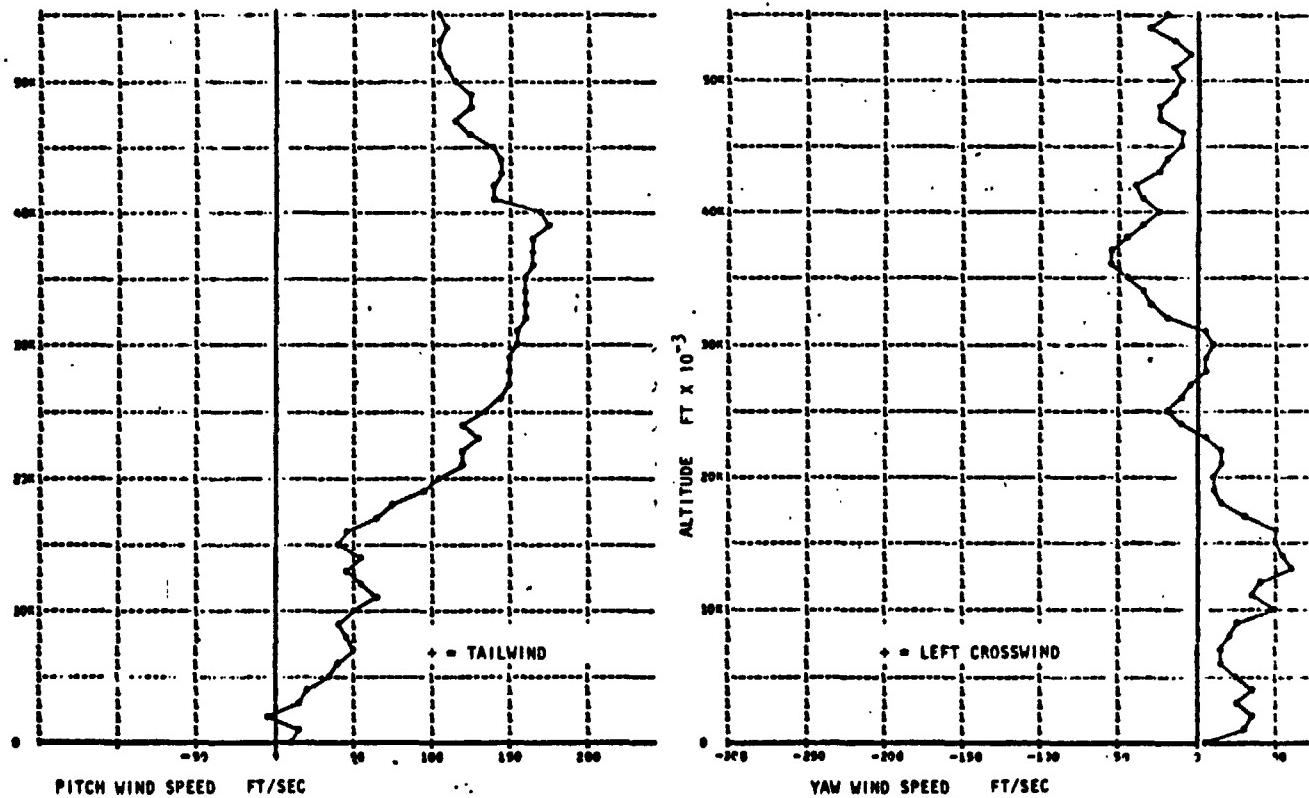


FIGURE 6

JIMSPHERE COMPONENT WINDS, 0725Z, 12-10-75

MEASUREMENT CASSCY - CENTAUR FORWARD EQUIPMENT MODULE

LEGEND: TC-1 -○-
TC-2 -●-

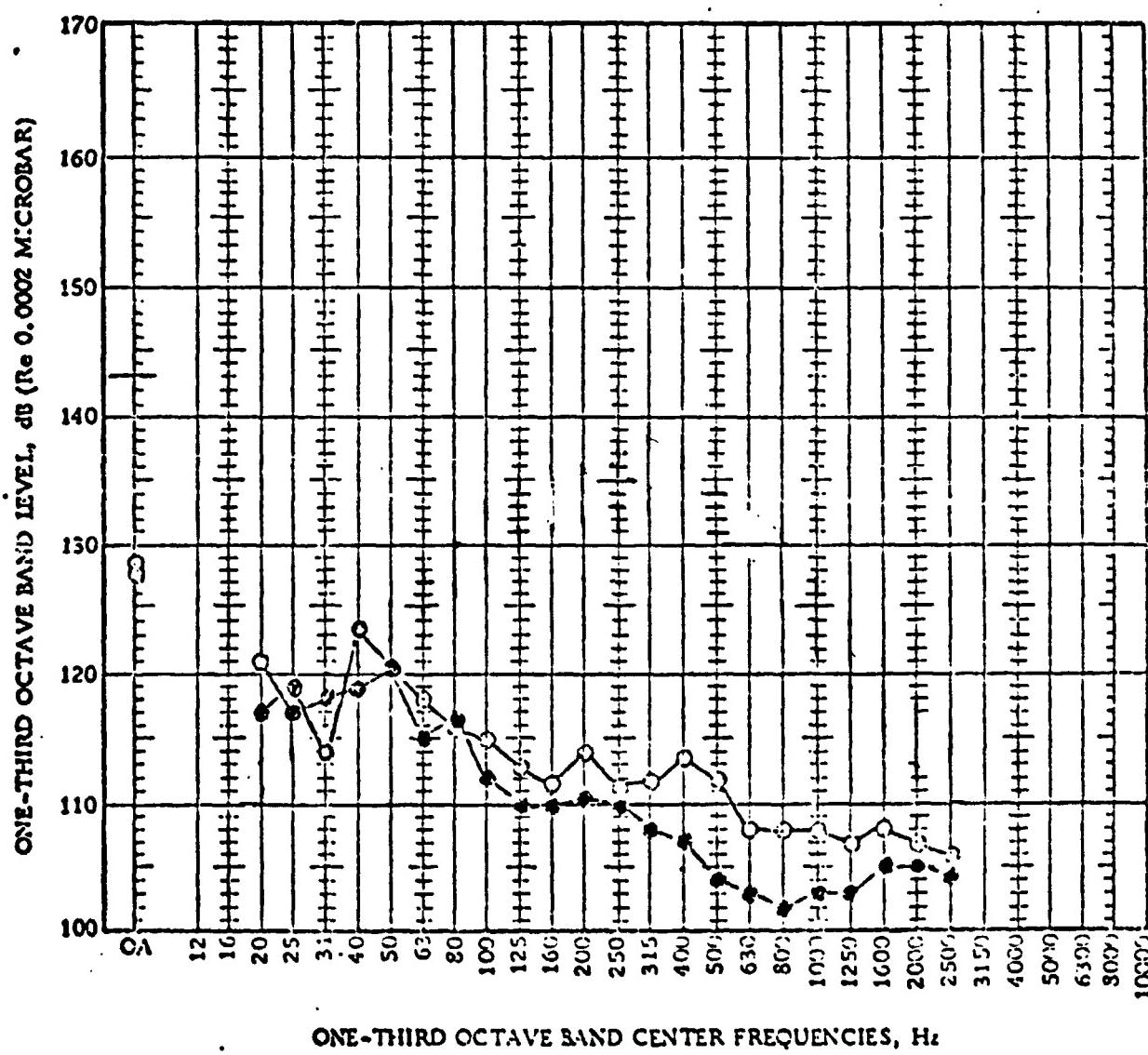


FIGURE 7 TC-1 AND TC-2 LAUNCH PEAK SOUND PRESSURE LEVELS

MEASUREMENT CASSGY - CENTAUR FORWARD EQUIPMENT MODULE

LEGEND: TC-1 —○—
TC-2 —●—

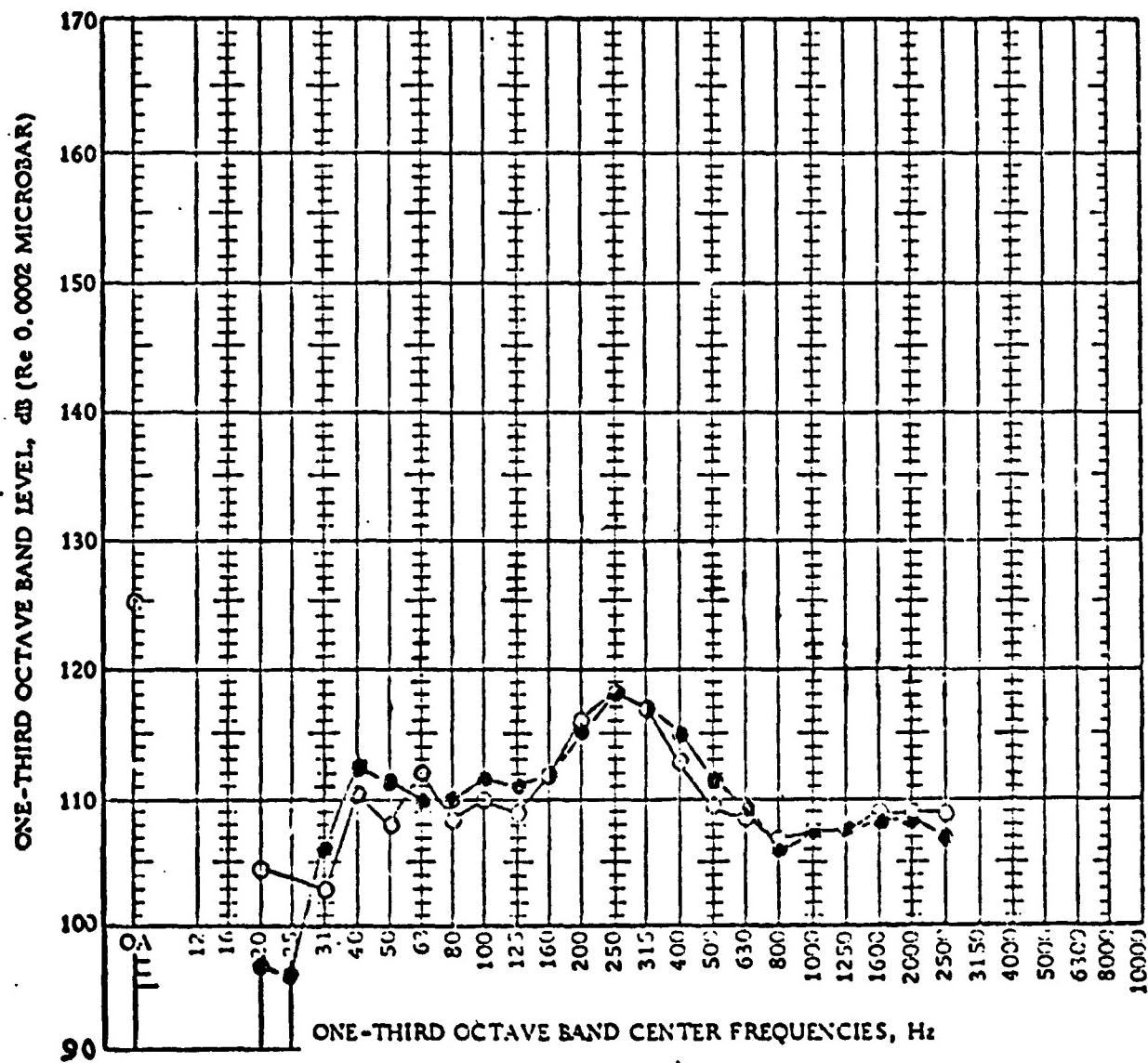


FIGURE 8 TC-1 AND TC-2 TRANSONIC PEAK SOUND PRESSURE LEVELS

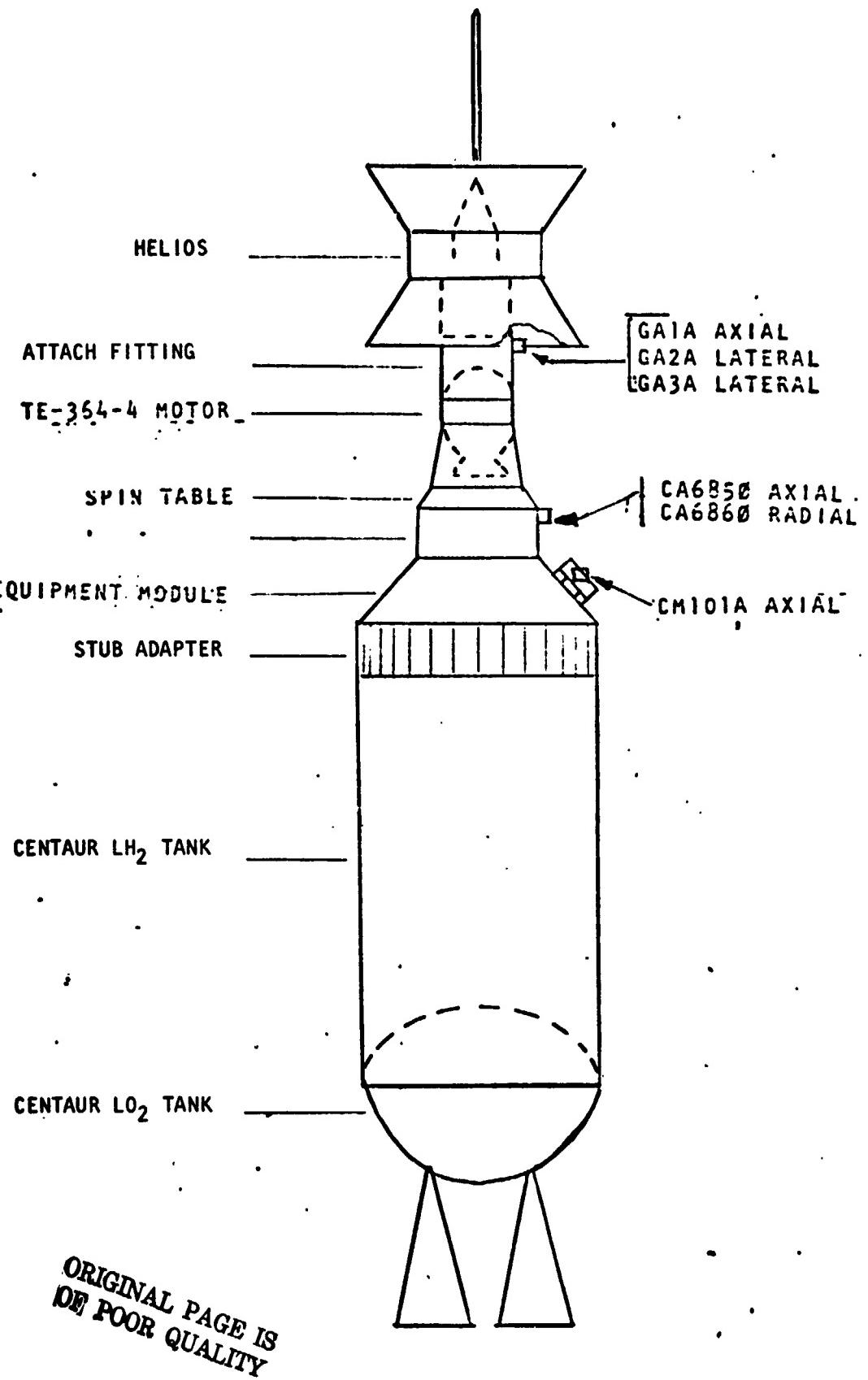


FIGURE 9 TC-2 INSTRUMENTATION LOCATION

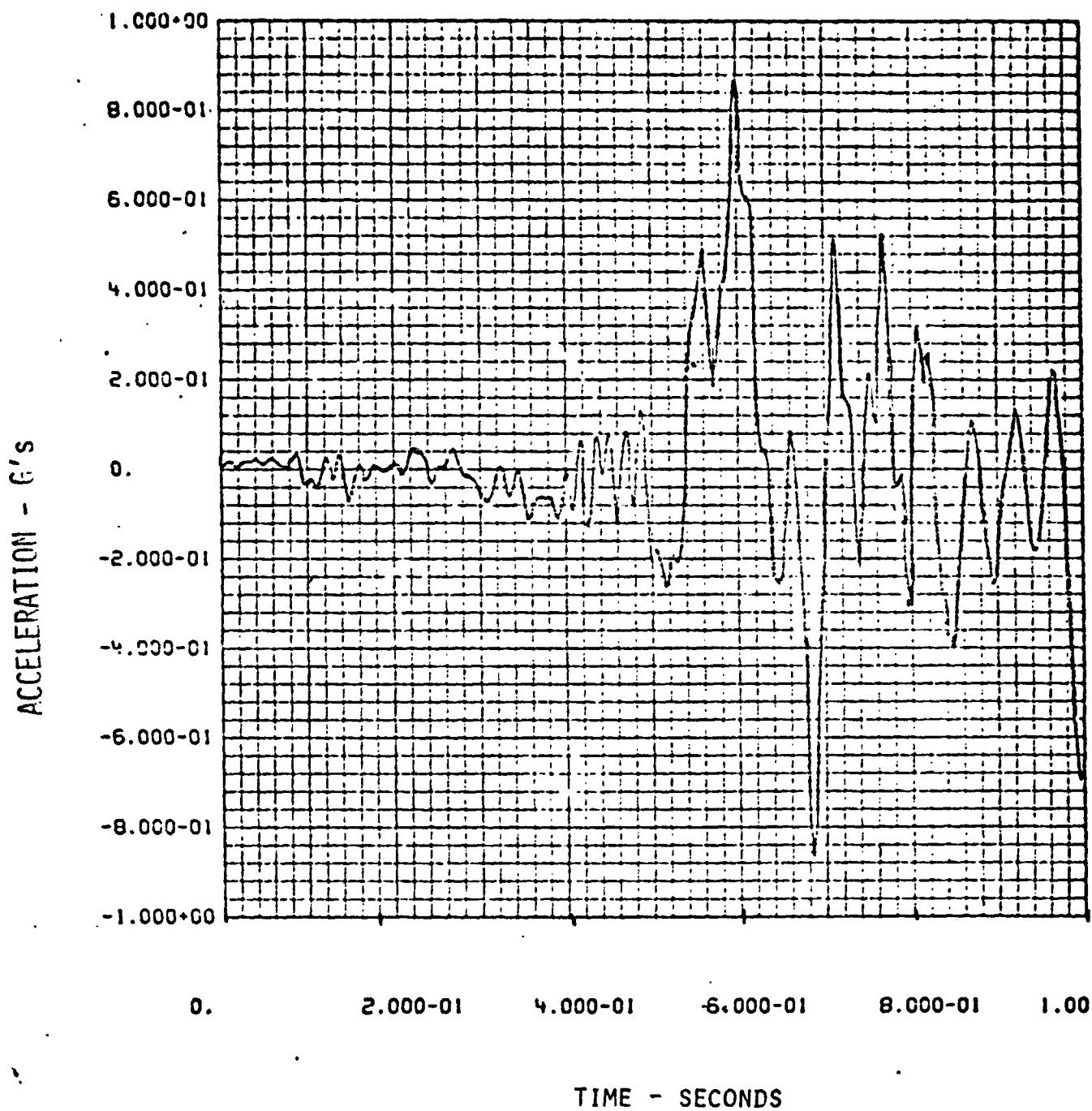


FIGURE 10 TC-2 MEASURED LATERAL ACCELERATION
(GA2A)

VS
TIME FROM LIFTOFF

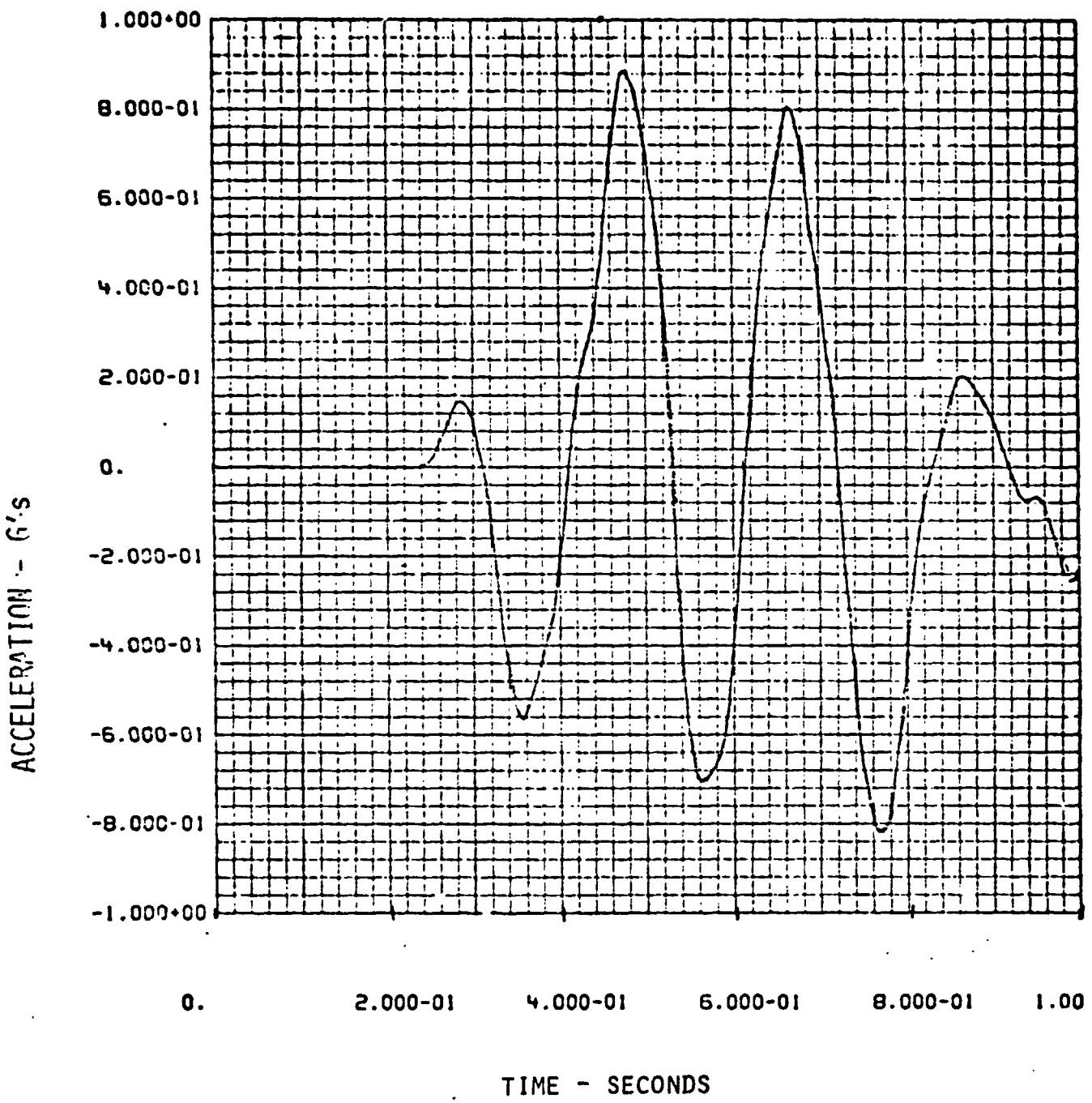


FIGURE 11 TC-2 PREDICTED LATERAL ACCELERATION (GA2A)
VS
TIME FROM LIFTOFF

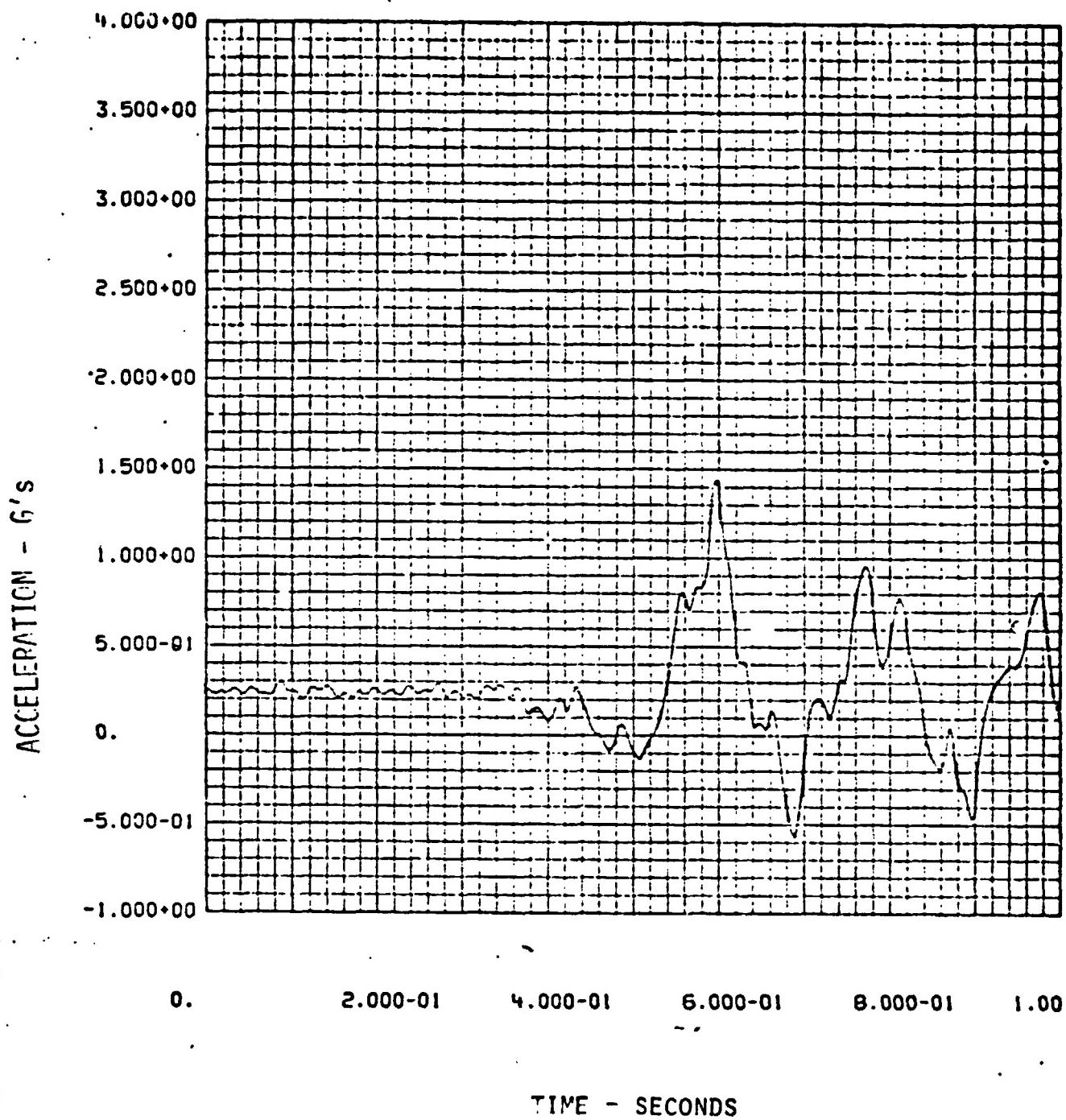


FIGURE 12 MEASURED LATERAL ACCELERATION (GA3A)
VS
TIME FROM LIFTOFF

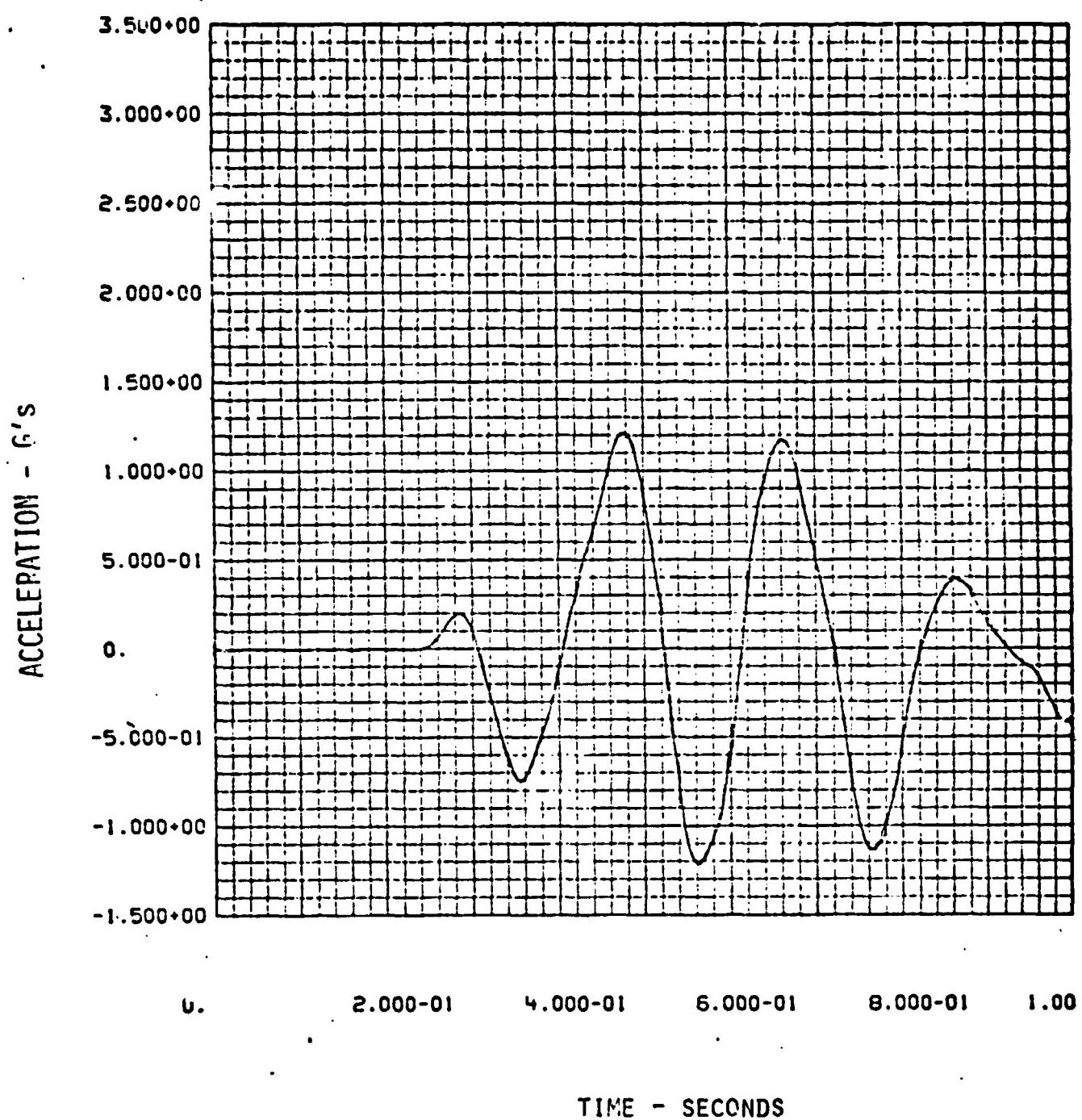


FIGURE 13 TC-2 PREDICTED LATERAL ACCELERATION (GA3A)
VS
TIME FROM LIFTOFF

TABLE 6

TC-2 SRM IGNITION PREDICTED UPPER LIMIT AND RECONSTRUCTED BENDING MOMENT
USING ACCELEROMETER DATA

<u>LOCATION</u>	<u>PREDICTED</u> (IN-LBS.)	<u>FLIGHT DATA</u> (IN-LBS.)
BASE OF ANTENNA	4,975	3,890
SPACECRAFT SEPARATION PLANE	147,400	87,000
TE-364 SPINTABLE	453,300	348,000

TABLE 7 TC-2 GUST AND BUFFET COMPARISON

- MAX LATERAL RESPONSE OCCURRED NEAR T+43 SEC, MN = 1.02, ON GA2A,
AND GA3A WAS ALSO NEAR MAXIMUM.
- GA3A MAY BE SLIGHTLY HIGHER AT T+40, MN = 0.93.
- USING 20HZ LOW PASS FILTER, PEAK AMPL. ARE:

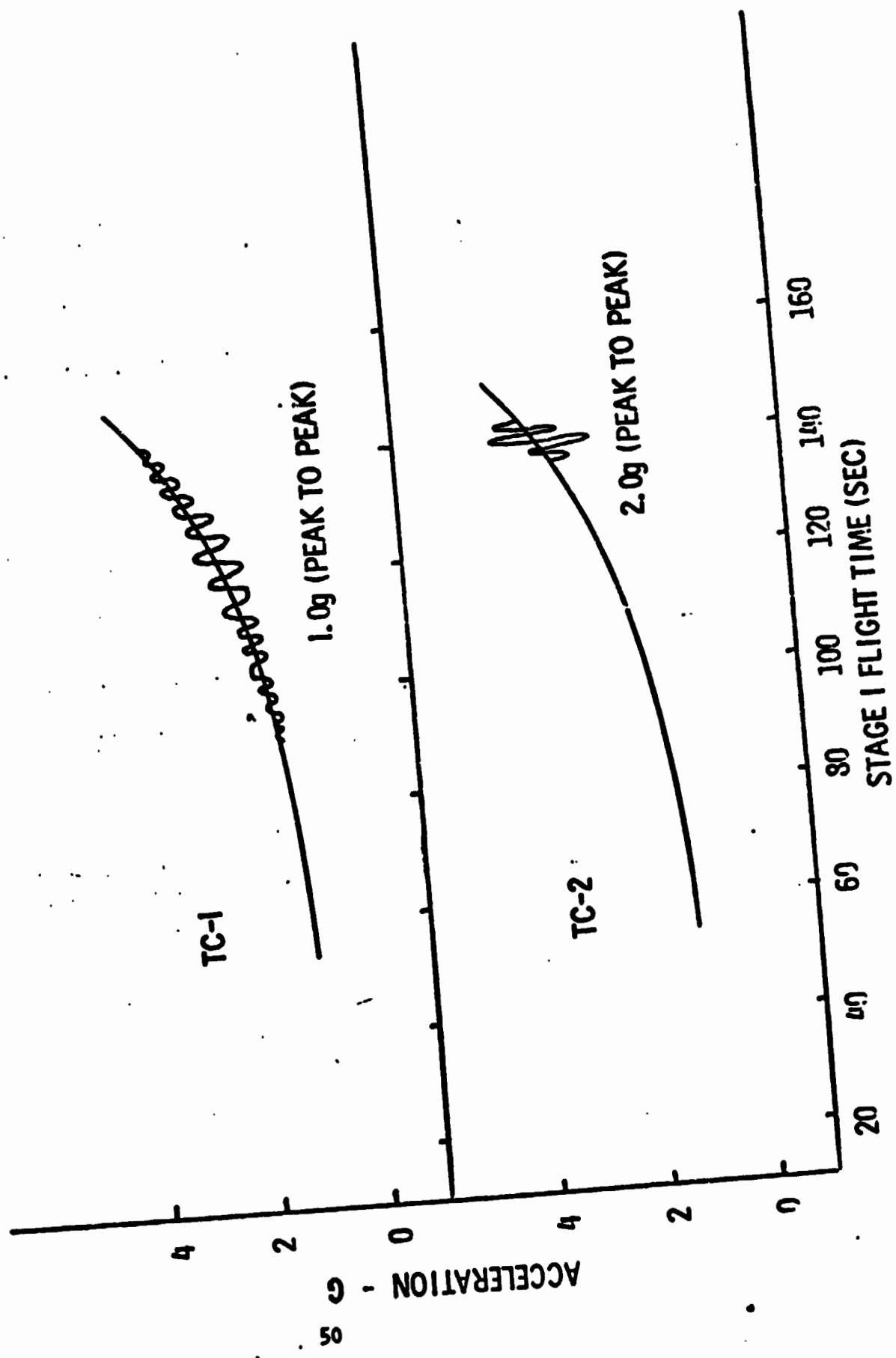
<u>FLIGHT RESULTS</u>			<u>BUFFET PREDICTION</u>			<u>GUST PREDICTION</u>		
ACCEL	FREQ. HZ	ACCEL G 0-PK NO.	MODE	FREQ.	G 0-PK	6 0-PK (ALREADY REDUCED BY 0.35 FACTOR)		
GA1A (AXIAL)	MAX	.38						
	19	0.30	54	18.4	.49			
5 3 X RMS =	MAX	0.35	RSS	ALL	= 0.56			
	15	0.18	50	15.8	0.1			
GA2A	MAX	0.60						
	4.8	0.4	25	.5	.75			
3 X RMS =	MAX	0.60						
	15	0.18	50	4.8	.52			
GA3A	MAX	0.58	RSS	ALL	= 1.11			
	4.7	0.3	25	4.6	.64			
3 X RMS =	MAX	0.33						
	15	0.1	50	4.8	.70			
3 X RMS =	MAX	0.40	RSS	ALL	= 1.19			
	15	0.1	51	15.8	0.23			

TABLE 8

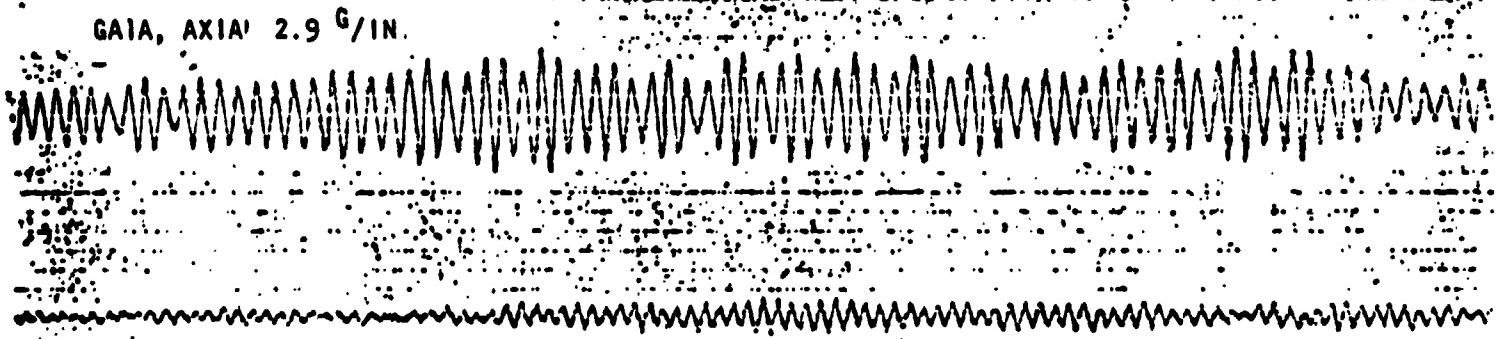
TC-2 GUST AND BUFFET PREDICTED AND RECONSTRUCTED BENDING MOMENT USING
ACCELEROMETER DATA

<u>LOCATION</u>	PREDICTED UPPER LIMIT (IN-LBS.)	MOST CONSERVATIVE MOMENT RECONSTRUCTION FROM FLIGHT DATA (IN-LBS.)
BASE OF ANTENNA	3,293	2,200
SPACECRAFT SEPARATION PLANE	135,900	95,000
TE-364 SPINTABLE	292,500	200,000

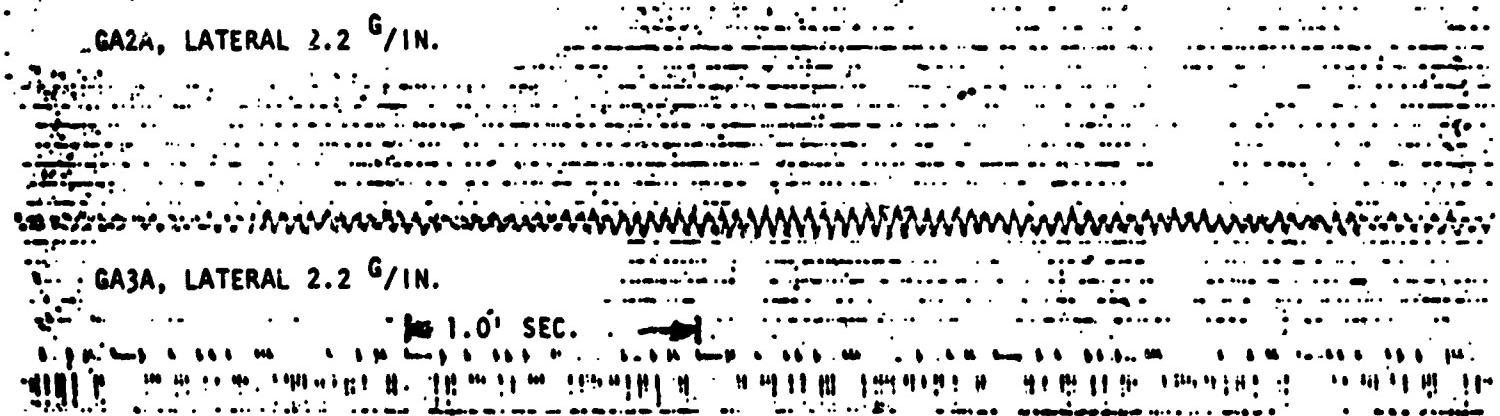
FIGURE 14
COMPARISON OF TC-2 AND TC-1 STAGE I POGO ACCELERATIONS AT THE GIMBAL STATION



GA1A, AXIAL 2.9 G/IN.



GA2A, LATERAL 2.2 G/IN.



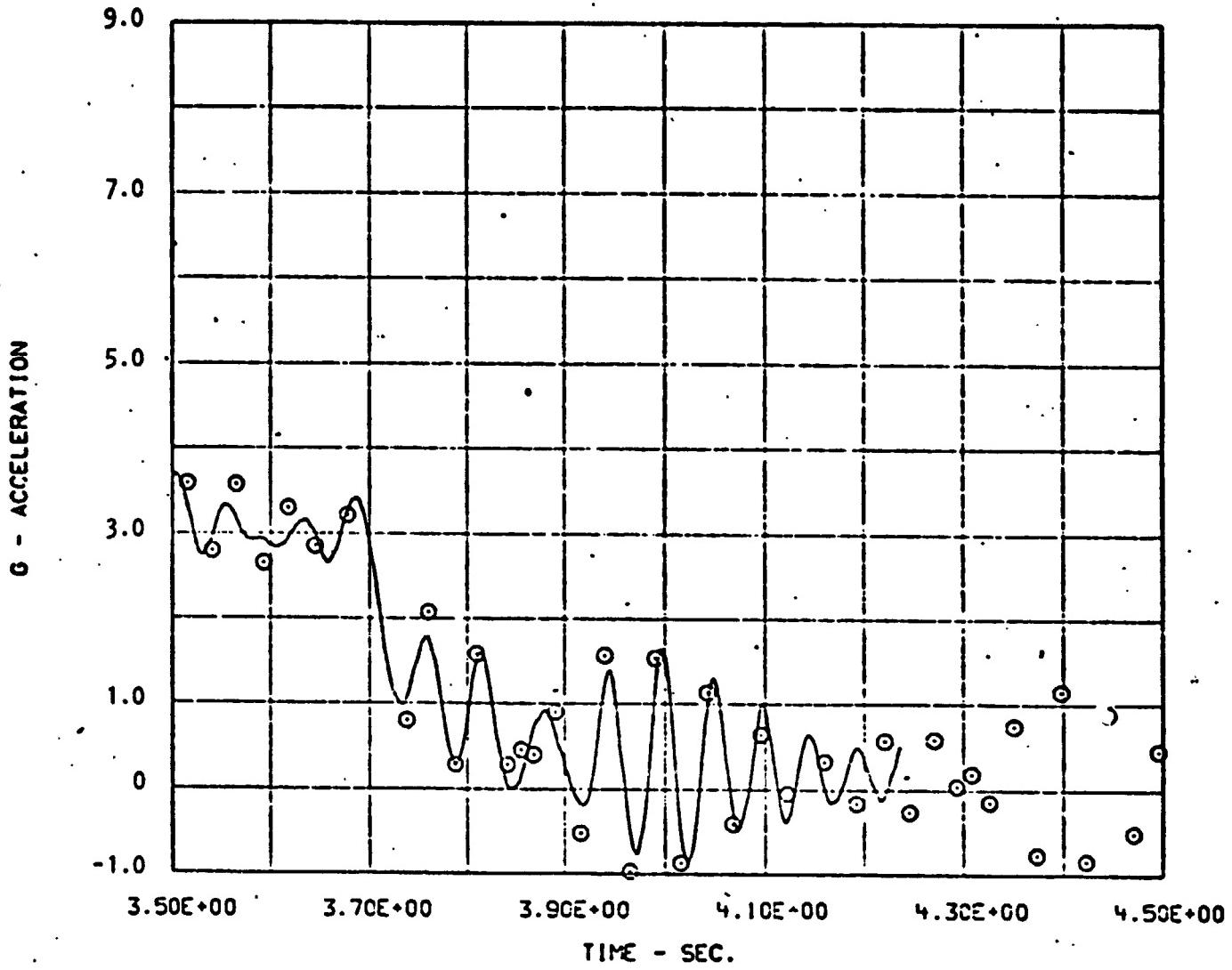
GA3A, LATERAL 2.2 G/IN.

1.0 SEC.

FIGURE 15

MAXIMUM STAGE I LONGITUDINAL OSCILLATIONS (POGO) AT T+140 SEC.

ORIGINAL PAGE IS
OF POOR QUALITY



LINE PLOT - TEST DATA 45 HZ FILTER
 POINT PLOT - ANALYTICAL DATA

FIGURE 16
 TC-2
 COMPARISON OF GAIA MEASURED RESPONSE AT STAGE I BURNOUT
 WITH ANALYTICALLY RECONSTRUCTED RESPONSE

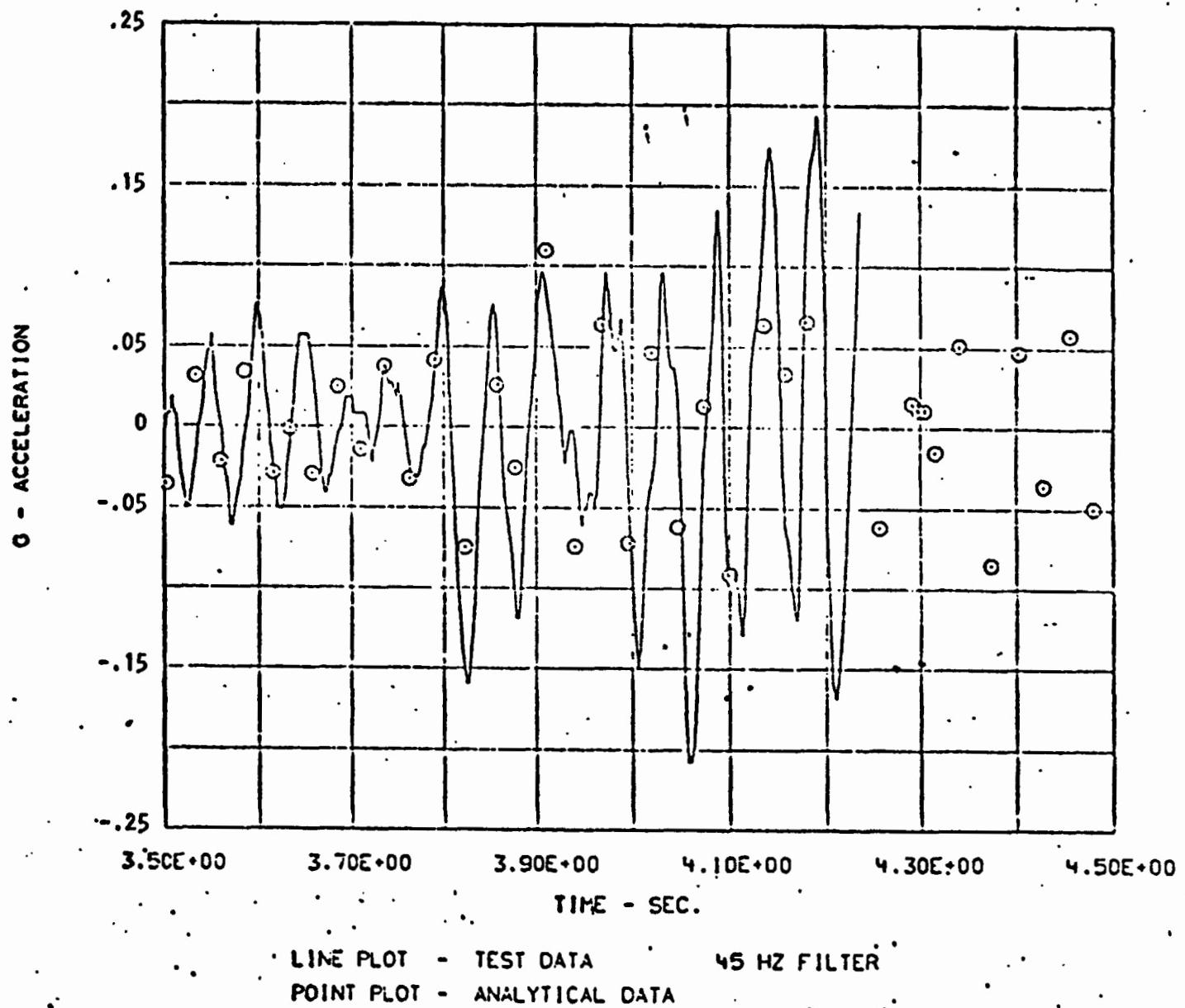


FIGURE 17

TC-2

COMPARISON OF GA2A MEASURED RESPONSE AT STAGE I BURNOUT
 WITH ANALYTICALLY RECONSTRUCTED RESPONSE

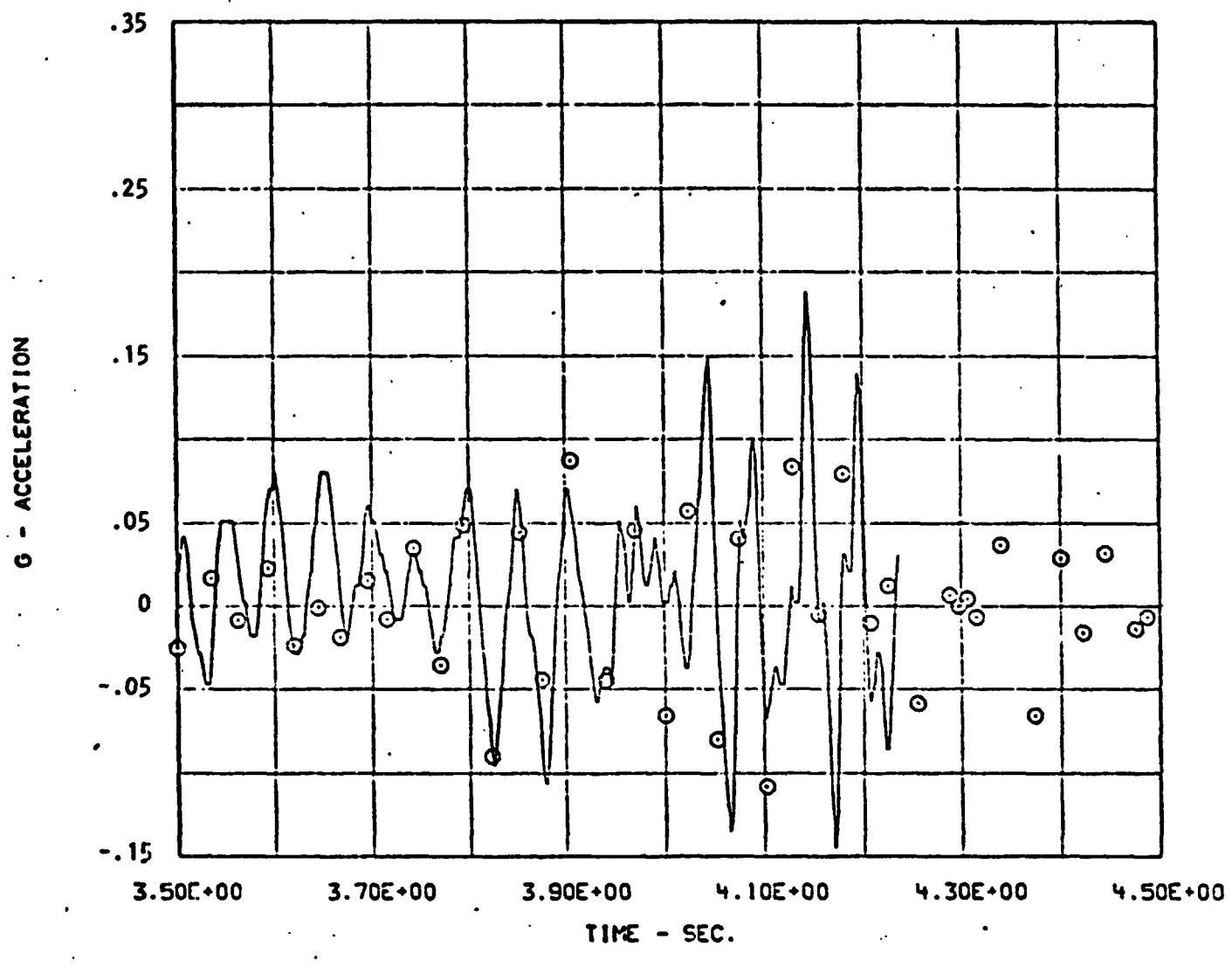


FIGURE 18

TC-2

COMPARISON OF GA3A MEASURED RESPONSE AT STAGE I BURNOUT
 WITH ANALYTICALLY RECONSTRUCTED RESPONSE

FIGURE 19 HELIOS/CENTAUR MECO LOADS ANALYSIS

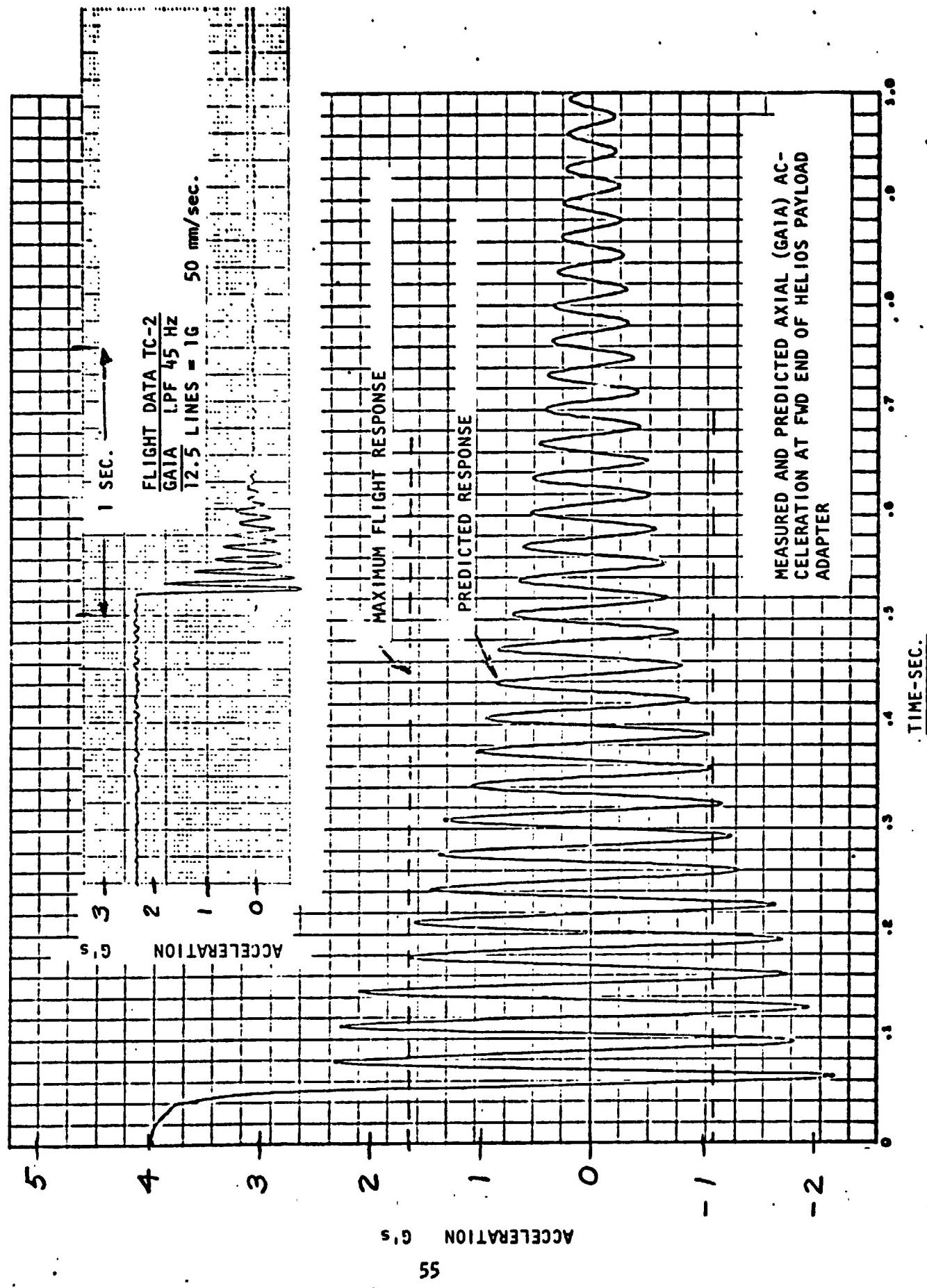
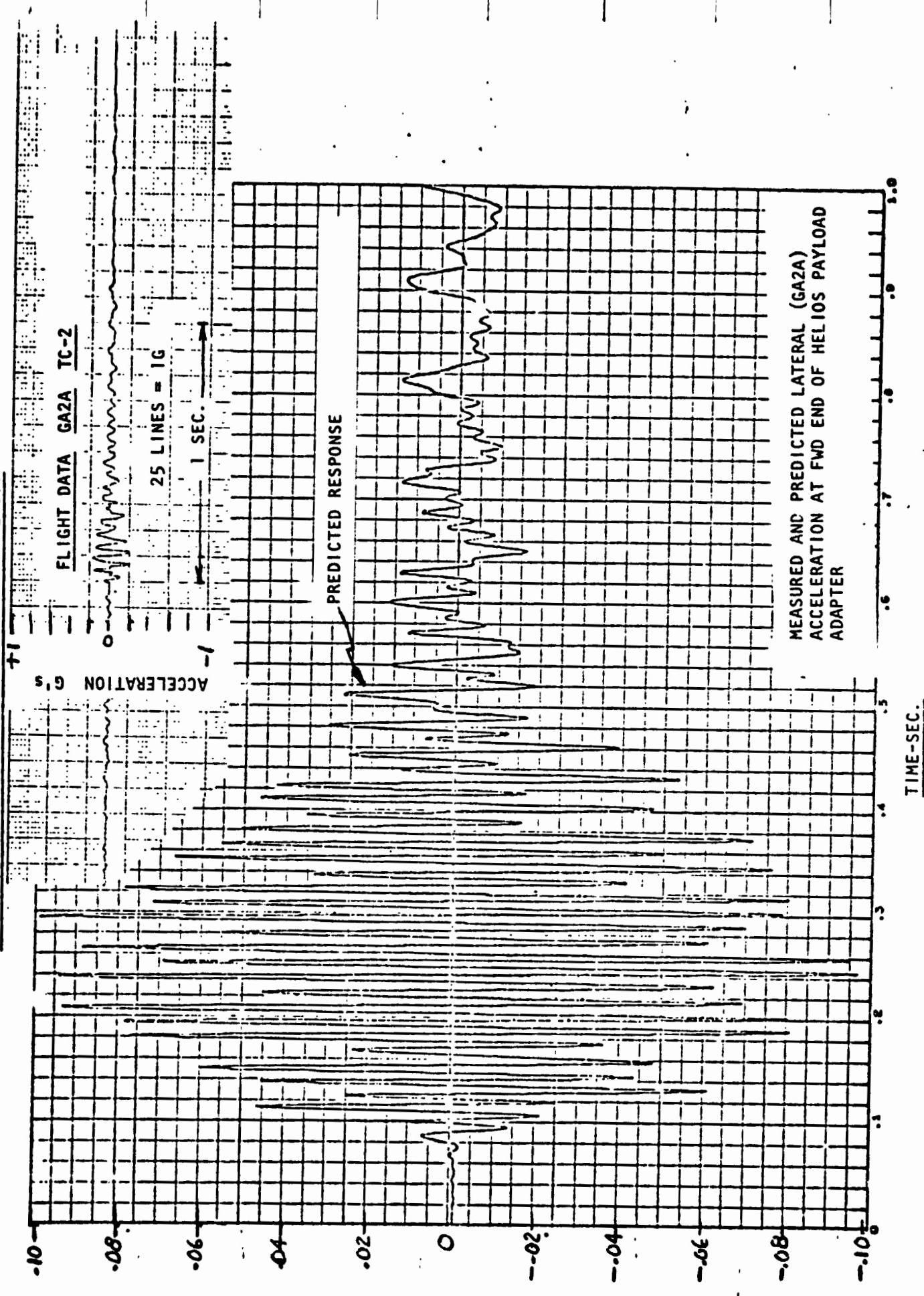


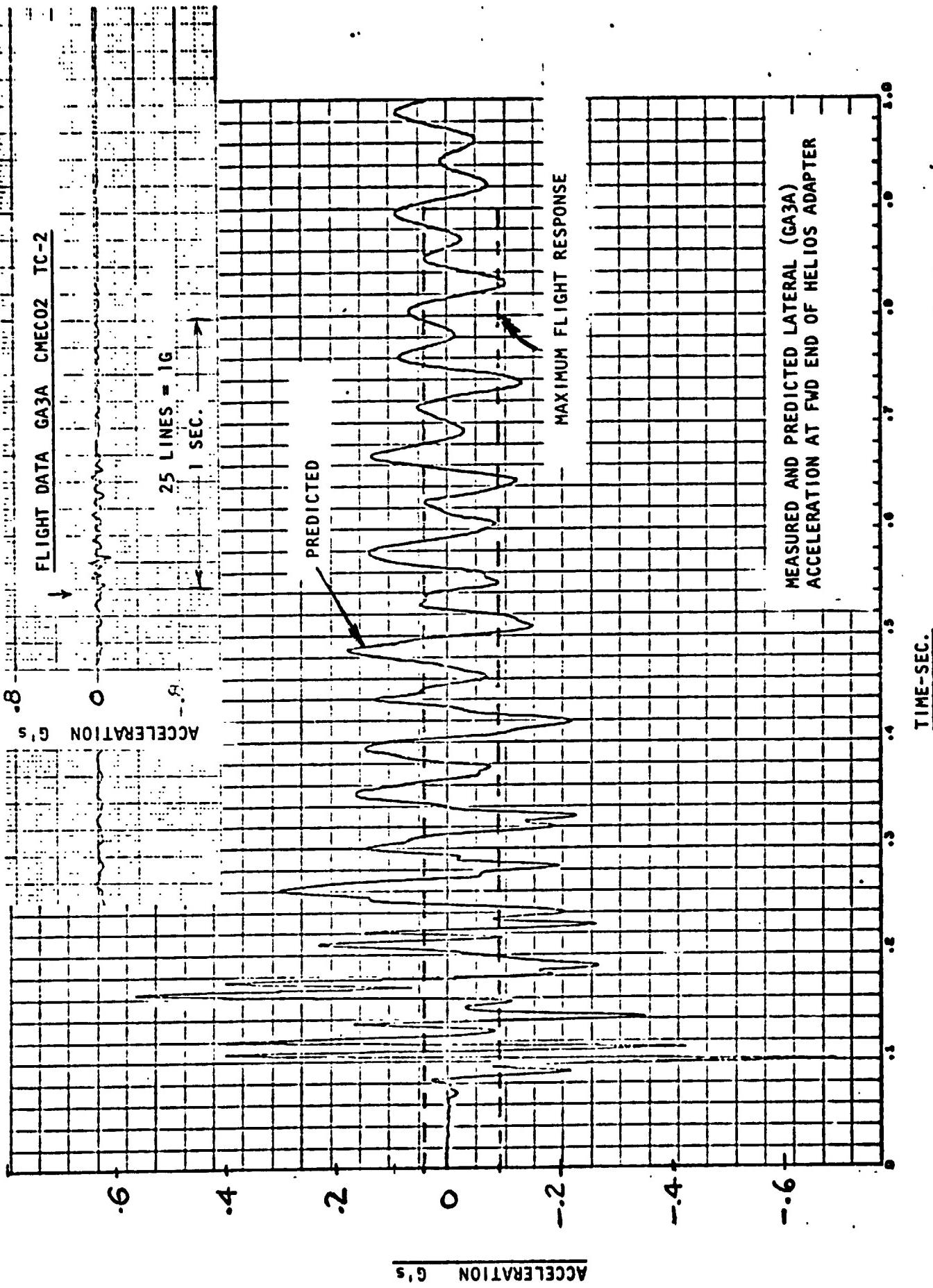
FIGURE 20 HELIOS/CENTAUR MECO LOADS ANALYSIS



ORIGINAL PAGE IS
OF POOR QUALITY

ACCELERATION g's

FIGURE 21 HELIOS/CENTAUR MECO LOADS ANALYSIS



VI SOFTWARE PERFORMANCE

VI SOFTWARE PERFORMANCE

Airborne

by J. L. Feagan

All available DCU flight telemetry data was thoroughly reviewed to verify that the flight software performed as designed. The data reviewed included analog plots of the DCU inputs (A/D's) and outputs (D/A's), and digital listings of the SCU switch commands and the software internal sequencing. The digital data was also used to verify the proper operation of each module of the flight program as well as the transfer of data between the various modules. The details of the software performance are elaborated upon in the descriptions of the various flight systems; e.g., PU, flight control, guidance, CCVAPS and trajectory.

Computer Controlled Launch Set (CCLS)

by A. L. Gordan

During the TC-2 launch countdown, the performance of the CCLS was normal. No hardware or software problems were encountered. All CCLS countdown procedure tasks were performed within the allowable time marks. This included the receiving and loading of the DCU with ADDJUST P/Y data coefficients via the ADDJUST transmission links from GDC, San Diego.

VII TITAN IIIE SYSTEMS ANALYSIS

VII TITAN IIIE SYSTEMS ANALYSIS

Mechanical Systems

Airframe Structures

by R. W. York

The Titan E2 vehicle airframe configuration remained unchanged from the E1 Proof Flight configuration. Response of the vehicle airframe to steady-state loads and transient events was nominal with peaks at expected levels. The magnitude of the longitudinal oscillation observed during the latter portion of Stage I flight did not adversely affect the Titan structure. Pressure measurements in Titan compartment 2A indicated that the compartment pressure and thermal barrier pressure differential time histories were in agreement with the design data (Figures 48 and 49.2, Section VIII).

Propellant tank ullage pressures measured during flight indicate limit levels required for structural stability were maintained during all phases of flight. The prelaunch lockup pressure for the Stage I oxidizer tank was intentionally 10 psi higher than that flown on E1 Proof Flight. The additional tank pressure was required to maintain adequate structural margin during flight in the absence of one ullage gas superheater. Flight ullage pressure data for the Stage I oxidizer tank indicates good correlation with predicted levels (Figure 25).

SRM separation and Stage I/Stage II separation occurred within predicted three-sigma event times. Flight data indicates Titan ordnance for these events performed as expected.

The Titan vehicle maintained structural integrity throughout all phases of booster ascent flight. Data from flight instrumentation agreed well with predicted flight values.

Propulsion Systems

by R. J. Salmi and R. J. Schroeder

SRMs

Table 9 summarizes the ballistic performance of the E-2 SRMs. All of the performance parameters were normal and well within the specified limits except for the maximum value of the forward end chamber pressure (P_c max.) which was 5 to 6 percent low. The low P_c max. was expected and has been a characteristic of the SRMs produced on certain contracts, and there is consideration to change the specification. On the P_c vs. time curves of Figures 22 and 23, P_c max. shows up as a spike at 0.5 seconds and its actual value has a negligible effect on the overall performance. The head end P_c transients are shown in Figure 24. They were smooth normal buildups as expected and well within the interface specifications. The specific impulse was well within limits but slightly lower (about 0.5 and 0.7 percent) than experienced on E-1. The main difference in the propellant mix between E-1 and E-2 is that E-2 is made with UTC PBAN and E-1 was made with ASR PBAN.

The Web Action Time (WAT) for E-2 was within the 106.9 seconds class, being slightly on the fast side whereas E-1 was of the slow burning 109.0 WAT class. The thrust differentials during ignition and tailoff were well within the specification limits. During ignition, the thrust differential was 26,200 lbs. (168,000 allowable) and 55,700 lbs. during tailoff (290,000 allowable).

Stage I and Stage II Propellant Feed System

The Titan propellant feed systems on Stage I and Stage II were the same configuration used on TC-1.

The Titan Stage I and Stage II propellant tanks were loaded with propellants based on an average expected in-flight propellant bulk temperature of 65°F. Stage I propellant tanks were loaded to provide a 2 sigma probability of having an oxidizer depletion shutdown. This was done to minimize the risk of encountering high stage II actuator loads during the Stage II engine start transient. A comparison of the actual loaded propellant weights for each tank with the expected loaded weights is shown in Table 10. Loaded propellant weights were within the allowable tolerance of \pm 0.4 percent for the oxidizer and \pm 0.3 percent for the fuel.

Stage I and Stage II propellant tanks were initially pressurized with nitrogen gas within the required prelaunch limits on F-1 day. Tank pressures were satisfactorily maintained. Table 11 compares the recorded telemetry tank pressures at liftoff with the required prelaunch limits.

TABLE 9

BALLISTIC PERFORMANCE COMPARISON
SRMs 35 AND 36

Parameter	Specification Rocket Motor		SRM 35		SRM 35		SRM 35	
	Nominal	Allowable Deviation, %	Measured	Corrected	Deviation, %	Measured	Corrected	Deviation, %
Test condition	Vacuum	-	Flight	Vacuum	-	Flight	Vacuum	-
Firing conditions, of	-	-	62.4	60	-	62.6	60	-
Web action time, sec	106.9	±2.16	104.8	105.1	-1.68	105.5	105.8	-1.03
Action time, sec	116.8	±3.43	115.2	115.6	-1.03	115.2	115.6	-1.03
Maximum forward end chamber pressure, psia	791	±3.76	755	749	-5.31	746	740	-6.45
Maximum initial sea level thrust, lb-sec x 10 ⁻⁶	1.1638	±6.23	1.1024	1.0945	-5.95	1.0881	1.0798	-7.22
Web action time total impulse, lb-sec x 10 ⁻⁶	108.43	±1.0	101.982	107.503	-0.85	102.396	107.918	-0.47
Action time total impulse, lb-sec x 10 ⁻⁶	112.52	±1.0	106.454	111.981	-0.48	106.492	112.019	-0.45
Web action time delivered specific impulse, sec	266.0	±0.7	251.2	264.7	-0.49	251.3	264.9	-0.41

NOTE: All thrust and impulse values are nozzle centerline

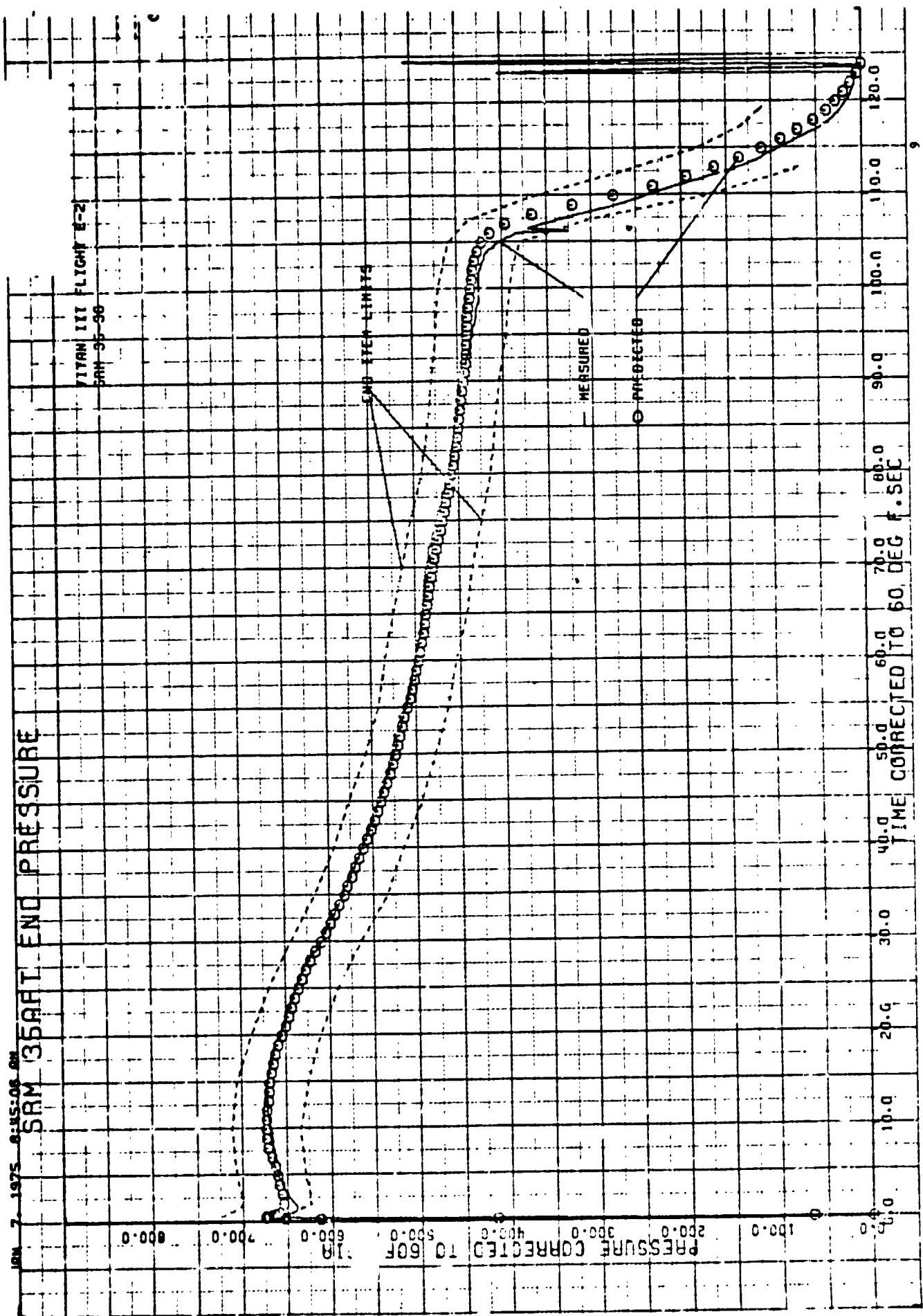


FIGURE 22 VARIATION OF AFT-END CHAMBER PRESSURE WITH TIME, SRM 35

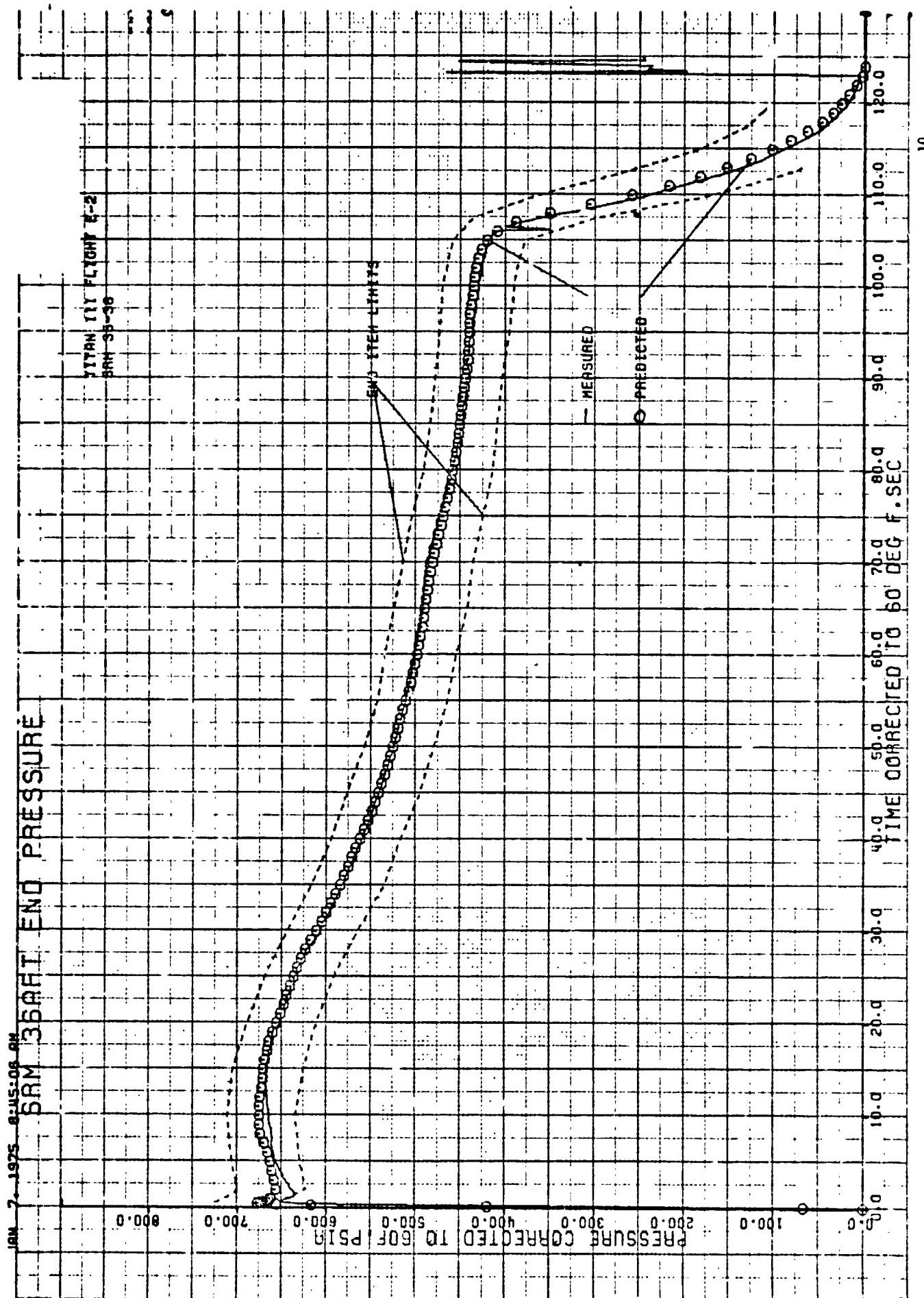


FIGURE 23 VARIATION OF AFT-END CHAMBER PRESSURE WITH TIME, SRM 36

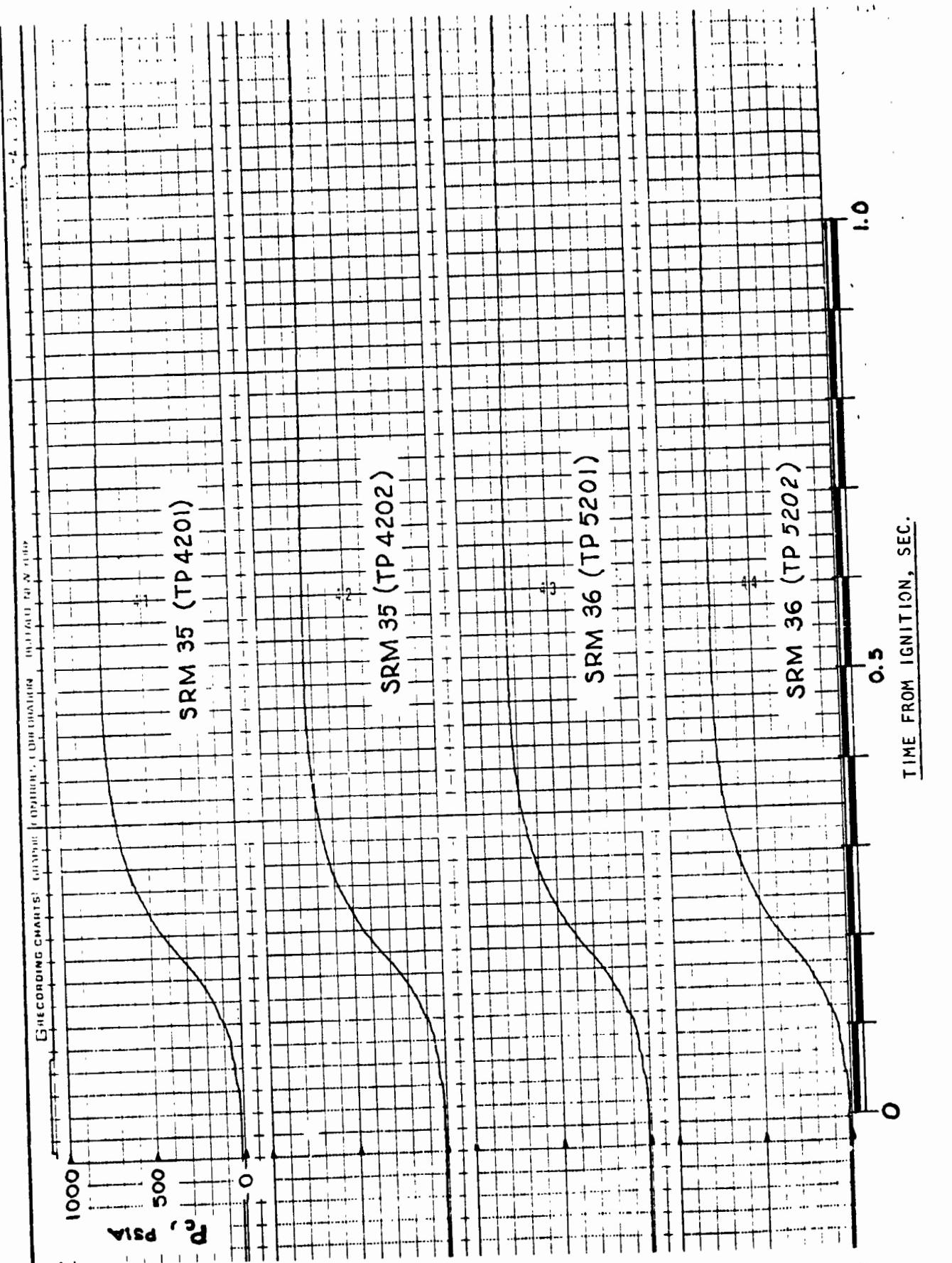


FIGURE 24 SRM CHAMBER PRESSURE IGNITION TRANSIENTS

TABLE 10 TITAN LOADED PROPELLANT WEIGHTS
STAGE I AND STAGE II - TC-2

	Expected (Lbs.)	Actual (Lbs.)
Stage I		
Oxidizer	165,701	165,850
Fuel	90,260	90,343
Stage II		
Oxidizer	43,173	43,242
Fuel	24,274	24,295

TABLE 11 TITAN PROPELLANT TANK PRELAUNCH
PRESSURIZATION, STAGE I AND STAGE II - TC-2

	Prelaunch Limits (psia)		Value at T-30 Sec. (psia)
	Lower	Upper	
Stage I			
Oxidizer Tank	43.6	55.0	51.6
Fuel Tank	24.0	32.0	28.8
Stage II			
Oxidizer Tank	45.0	57.0	52.0
Fuel Tank	50.0	56.0	52.8

The autogenous pressurization systems on Stage I and Stage II supplied adequate pressurization gases to the propellant tanks during engine operation. Table 12 compares the expected average tank pressures during engine operation with the actual flight values. Since the Stage I oxidizer autogenous pressurization system was modified for TC-2 (see Stage I Engine), a comparison of the expected and actual Stage I oxidizer tank pressure during Stage I engine operation was made (Figure 25). The oxidizer tank pressure during the Stage I engine operation was 0.8 to 2.0 psi higher than expected and within the 3 sigma limit of previous Titan III flights that used the single superheater configuration.

Stage I Engine

The Stage I engine configuration was the same as TC-1 with the following changes incorporated as a result of longitudinal oscillations encountered on TC-1 during Stage I operation. The oxidizer autogenous pressurization system was changed from a dual superheater configuration to a single superheater configuration. Accelerometers were mounted on the oxidizer pump housing, the gimbal block and the oxidizer discharge line of each engine subassembly. Two pressure measurements were added on the oxidizer autogenous pressurization lines. An oxidizer suction pressure measurement was added to the oxidizer feed line on engine subassembly two.

Flight performance of the Titan Stage I engine was satisfactory. Engine start signal (87FS1) occurred at T+111.6 seconds when the accelerometer in the Titan flight programmer sensed a reduction in acceleration to 1.5 g's during the tailoff period of the Stage 0 solid rocket motors.

Separation of the thrust chamber exit closures was satisfactory as indicated by the normal engine start transient. The time differential between subassembly one ignition and subassembly two ignition was 0.02 seconds. Eighty percent rated thrust level for each subassembly was reached with a 0.01 second time differential. There was no thrust overshoot produced in either subassembly. Stage I engine start transient data is shown in Table 13.

Engine performance during the steady-state period was satisfactory. Average engine thrust was 1.93 percent higher than expected, average specific impulse was 0.50 seconds lower than expected, and average engine mixture ratio was 1.17 percent higher than expected. The corresponding 3 sigma dispersion about the expected values were \pm 3.27 percent on thrust, \pm 2.3 seconds on specific impulse and \pm 2.17 percent on mixture ratio. Propellant outage was 2,308 pounds of fuel. This was 1,014 pounds greater than the expected mean outage but 868 pounds less than the expected maximum outage. Stage I engine steady-state performance data is shown in Table 14.

Performance of autogenous pressurization system during engine operation was satisfactory. (See Stage I and Stage II Propellant Feed System).

TABLE 12 TITAN PROPELLANT TANK AVERAGE PRESSURES
DURING ENGINE OPERATION - TC-2

	Expected Value (psia)	Actual Value (psia)
Stage I		
Oxidizer Tank	22.5	23.5
Fuel Tank	27.3	25.8
Stage II		
Oxidizer Tank	50.5	53.8
Fuel Tank	54.4	55.3

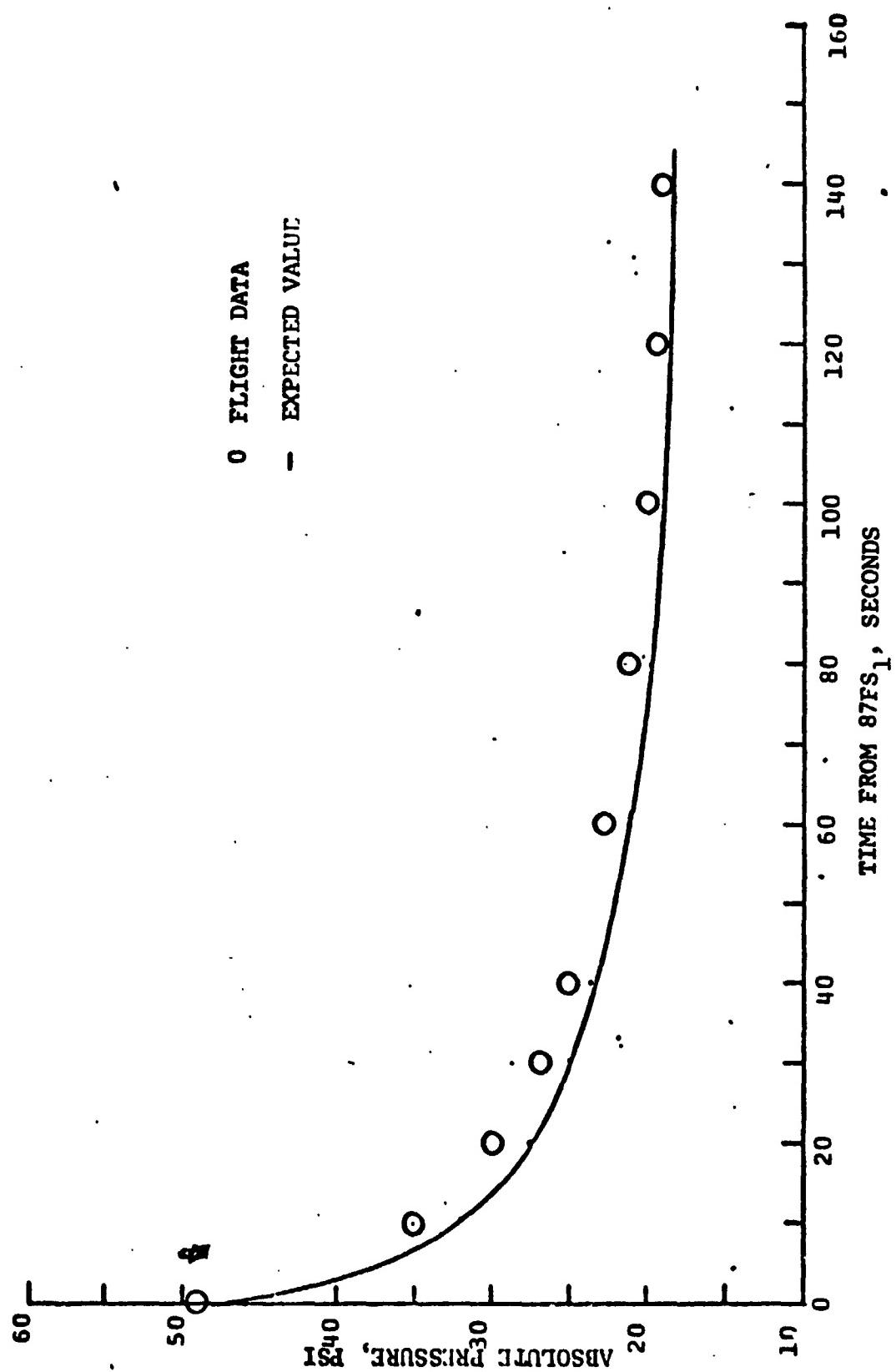


FIGURE 25 STAGE 1 OXIDIZER TANK GAS PRESSURE, TC-2

TABLE 13 TITAN STAGE I ENGINE START
TRANSIENT DATA - TC-2

Parameter	Units	Allowable	Flight Values	
			Subassembly 1	Actual Subassembly 2
FS ₁ to Ignition	Sec.	0.6 to 1.0	0.77	0.79
Ignition to 80% Rated Thrust Level	Sec.	0.125 minimum	0.20	0.21
Thrust Overshoot	Lbf.	323,000 maximum	No over- shoot	No over- shoot

TABLE 14 TITAN STAGE I ENGINE STEADY-STATE
PERFORMANCE - TC-2

Parameter	Units	Average Steady-State Flight Values	
		Expected (2)	Actual
Thrust, total	lbf.	510,383	520,212
Specific impulse	sec.	301.18	300.68
Mixture ratio, O/F	units	1.8686	1.8905
Overboard propellant flow rate, total (1)	lbm/sec.	1694.62	1731.49
Oxidizer flow rate, total	lbm/sec.	1105.53	1134.13
Fuel flow rate, total	lbm/sec.	591.64	599.91
Propellant outage	lbm	1294 mean 3176 max.	2308 (fuel)
Oxidizer temperature	°F	65	59.5
Fuel temperature	°F	65	60.2
FS ₁ to FS ₂	sec.	150.3	146.6

Notes: (1) Excludes autogenous pressurant flow

(2) Expected values are those used in the final preflight targeted trajectory

Stage I engine shutdown occurred at T+258.3 seconds when the thrust chamber pressure switches sensed a reduction in chamber pressure and issued the engine shutdown signal (87FS2). Engine shutdown was the result of oxidizer exhaustion as planned. The shutdown transient was normal for an oxidizer exhaustion mode. An 80 psi thrust chamber pressure spike occurred on engine subassembly one at 87FS2 + 0.55 seconds. This pressure spike is considered normal since similar spikes have been observed on three previous Titan III flights. Stage I engine operating time (FS1 to FS2) was 3.7 seconds shorter than expected as a result of the increased propellant flow rate.

Stage II Engine

The Stage II engine configuration was the same as TC-1.

Flight performance of the Titan Stage II engine was satisfactory. Engine start signal (91FS1) occurred at T+258.3 seconds (simultaneous with Stage I engine shutdown signal, 87FS2). The Stage II engine start transient was normal as shown in Table 15.

Engine steady-state performance was satisfactory. Average engine thrust was 0.56 percent lower than expected, average specific impulse was 0.57 seconds higher than expected and average engine mixture ratio was 0.68 percent lower than expected. The corresponding 3 sigma dispersions about the expected values were \pm 3.80 percent on thrust, \pm 3.5 seconds on specific impulse and \pm 2.66 percent on mixture ratio. Steady-state engine performance data is shown in Table 16.

The engine autogenous pressurization system performed satisfactory (see Stage I and Stage II Propellant Feed System).

Stage II engine shutdown (91FS2) occurred at T+468.8 seconds when the sensed vehicle acceleration dropped to 1.0 g's. Engine shutdown was the result of fuel exhaustion followed by oxidizer exhaustion during the shutdown transient. The shutdown transient was normal.

Stage II engine operating time (FS1 to FS2) was 2.3 seconds longer than expected.

TABLE 15 TITAN STAGE II ENGINE
START TRANSIENT DATA - TC-2

Parameter	Units	Flight Values	
		Allowable	Actual
FS ₁ to Ignition	Sec.	0.5 to 0.9	0.71
10% to 80% Rated Thrust	Sec.	0.150 minimum	0.20
Thrust at Over-shoot	Lbf.	128000 max.	98932

TABLE 16 TITAN STAGE II ENGINE STEADY-STATE
PERFORMANCE - TC-2

Parameter	Units	Average Steady-State Flight Values	
		Expected (3)	Actual
Thrust, total	lbf.	102166	101593
Specific impulse (1)	Sec.	314.89	315.46
Mixture ratio, O/F	Units	1.7864	1.7741
Overboard propel- lant flowrate, total (2)	lbm/sec.	321.66	319.42
Oxidizer flowrate, total	lbm/sec.	207.04	205.09
Fuel flowrate, total	lbm/sec.	115.90	115.61
Propellant outage	lbm	111 mean 538 max.	0
Oxidizer temperature	°F	65	61.2
Fuel temperature	°F	65	61.7
FS ₁ to FS ₂	Sec.	208.1	210.5

Notes: (1) Excludes roll nozzle thrust

(2) Excludes autogenous pressurant flow

(3) Expected values are those used in the final preflight
targeted trajectory

SRM Thrust Vector Control

by R. J. Salmi

The E-2 SRM TVC systems incorporated modified electro-mechanical valves from the type used on E-1. The E-2 valves were modified to incorporate a GN₂ purge system to prevent N₂O₄ seepage into the valve drive mechanism. A GN₂ vent port was added and the internal GN₂ flow path was slightly enlarged. The modification allowed the valves to meet the 75-day wet life criteria (including 30 days at pressure).

New criteria were also used for determining the TVC tank pressure at lock-up. In place of the constant-mass technique used on E-1, the new pressure technique is based on average seasonal temperature variations and daily temperature cycles so that the TVC tanks will not exceed the upper and lower pressure limits prior to liftoff. For E-2 the manifold pressures were 1041 psig and 1038 psig at liftoff which is nearly on the average target pressure of 1041 psig for liftoff (964 psig low and 1119 psig high).

The mechanical and electrical performance of the TVC system was normal; no anomalies were noted. The TVC dump was off 23.2 seconds on SRM 35 and 39.4 seconds on SRM 36 because of large injectant usage during the early part (20-40 seconds) of the flight. The maximum dumper off time for E-1 was about 8 seconds. The maximum steering command measured was 2.85 volts at t = 27 seconds. The hardware steering capability is for 10 volts. The TVC injectant usage is summarized in Table 17.

TABLE 17
INJECTANT FLUID USAGE

	<u>SRM 35</u>	<u>SRM 36</u>
NITROGEN TETROXIDE LOADED	8,415	8,419
TOTAL EXPENDED LB	6,637	6,722
TOTAL DUMPED LB	3,416	3,072
TOTAL TVC STEERING LB	3,221	3,650
MANIFOLD PRESSURE AT IGNITION	1,038	1,041
MANIFOLD PRESSURE AT SEPARATION	571	589

Hydraulic Systems

by T. W. Godwin

Performance of the hydraulic systems on Stage I and Stage II was normal. The electric motor driven pump in each stage supplied normal hydraulic pressure for the flight control system tests performed during countdown. Hydraulic pressures supplied by the turbine driven pump on each stage during engine operation were normal, except that the Stage I pressure indication was slightly low due to instrumentation error. Hydraulic reservoir levels were within limits throughout the countdown and flight. Stage I and Stage II hydraulic system performance data are presented in Table 18.

During flight, telemetry data indicated the Stage I hydraulic pressure to be 110 psi below the lower limit. Analysis of the data indicates that the pressure was normal, and that there was an error in the instrumentation or telemetry equipment.

At T+0.345 seconds, the DRS tape indicated a "NO-GO" condition on the Stage II accumulator-reservoir precharge pressure. The GO signal was maintained, however. Analysis indicated that the precharge pressure was indeed lower than average due to the low ambient temperature (58°F) on launch day. The pressure had been set at 1785 psia at 71°F, and had dropped to approximately 1740 psia on launch day. This condition, together with a high setting on the pressure switch and the vibration caused by the Stage 0 ignition apparently caused the temporary "NO-GO" indication. It is estimated that a further temperature drop of 20° to 25°F would be required to effect the loss of the "GO" signal.

The structural loads transmitted into the Stage I hydraulic actuators during the Stage I engine start transient were normal. A maximum load of 12,450 pounds compression was applied to subassembly 1 yaw/roll actuator 3-1. The allowable load for Stage I actuators is 50,000 pounds. The Stage II engine start transient produced a maximum load of 9,750 pounds compression on the Stage II yaw actuator 2-2. This is the highest loading yet observed for the 2-2 actuator, and the second highest load observed for Stage II. It is also the highest load ever observed for a Stage I oxidizer depleton shutdown. The Stage II actuators have a demonstrated load capacity of 18,000 pounds. Table 19 shows the maximum actuator loads encountered on TC-2 during the engine start transients. Also shown for comparison are the TC-1 loads and the maximum and minimum loads for all Titan vehicles.

TABLE 18
Titan Hydraulic Systems Flight Data - TC-2

Parameter	Units	Expected	Stage I	Stage II
Hydraulic Supply Pressure				
Max. at Pump Start	psi	4500 Max. (1)	3260	3790
Average Steady State	psi	2900-3000	2790(2)	2900
Reservoir Level				
Prior to Pump Start	%	47-62	49	55
At Max. Pump Start Press.	%	22-47	31	34.5
Average Steady State	%	22-47	30	36
Shutdown Minus 5 Sec.	%	22-47	32.5	39

(1) Proof pressure limit.
 (2) Out of tolerance - see text.

TABLE 19
Titan Hydraulic Actuator Maximum Loads
During Engine Start Transients

Vehicle	Stage I Actuators				Stage II Actuators	
	Subassembly One		Subassembly Two		Subassembly Three	
	Pitch 1-1	Yaw-Roll 2-1	Yaw-Roll 3-1	Pitch 4-1	Pitch 1-2	Yaw 2-2
TC-2	+3830 -9270	+ 3,320 - 5,530	+12,450 - 4,980	+9540 -4980	+5670 - 510	+9750(1) -7900
TC 1	+8250	+11,000	+11,000	-16,000	+9700	+5860
Titan Family (2)	+14,100 -12,490	+12,500 - 8,151	+14,100 - 6,920	+13,030 -16,000	+14,400 - 8,750	+9750(1) -11,184

+ Indicates compression load.
 - Indicates tension load.
 (1) Highest compression load yet observed.
 (2) Stage I data is from TIIID only.

Flight Controls and Sequencing System

by E. S. Jeris and T. W. Porada

The flight control system maintained vehicle stability throughout powered flight. All open loop pitch rates and preprogrammed events were issued as planned. No system or component anomalies occurred. Dump programming of TVC injectant fluid was satisfactory. The dump command was zero for 39.4 seconds due to the long duration of ADDJUST steering commands from Centaur. Dump command was at zero for only 8 seconds on E-1. After SRM jettison, the vehicle experienced an 11 deg/sec roll rate. This roll rate is the highest recorded on TIII vehicles. Peak rate on previous TIII vehicles was 8 deg/sec, and on E-1, the peak rate was 5 deg/sec. Prior to the SRM jettison event, the Stage I engines corrected for an apparent roll torque. The Stage I engines assumed a differential gimbal angle of approximately .53 degrees to counteract the roll torque. The cause of the roll torque is not well understood. Probable causes have been identified, but could not be proven conclusively. Among the possible causes are: (1) asymmetric shutdown behavior of the SRMs causing thrust dispersion, (2) SRM plume behavior during the shutdown causing impingement torques, (3) questionable aerodynamic coefficients, and (4) unknown angles of attack (wind data not available over 60,000 feet altitude) adding uncertainty in aerodynamic forces.

Command voltage to each SRM quadrant and the dynamic and static stability limits are shown in Figures 26 and 27. The stability limits represent the TIII-E-2 side force constraint in terms of TVC system quadrant voltage. This constraint is used in conjunction with launch day wind synthetic vehicle simulations as a go/no-go criterion with respect to vehicle stability and control authority. Simulation responses satisfying the constraint assures a 3 sigma probability of acceptable control authority and vehicle stability. Maximum command during Stage 0 flight was 2.85 volts which is 28.5 percent of the control system capability and 47.5 percent of the dynamic stability limit. The peak command occurred at T+27 seconds and was due to Centaur ADDJUST pitch up wind load relief steering.

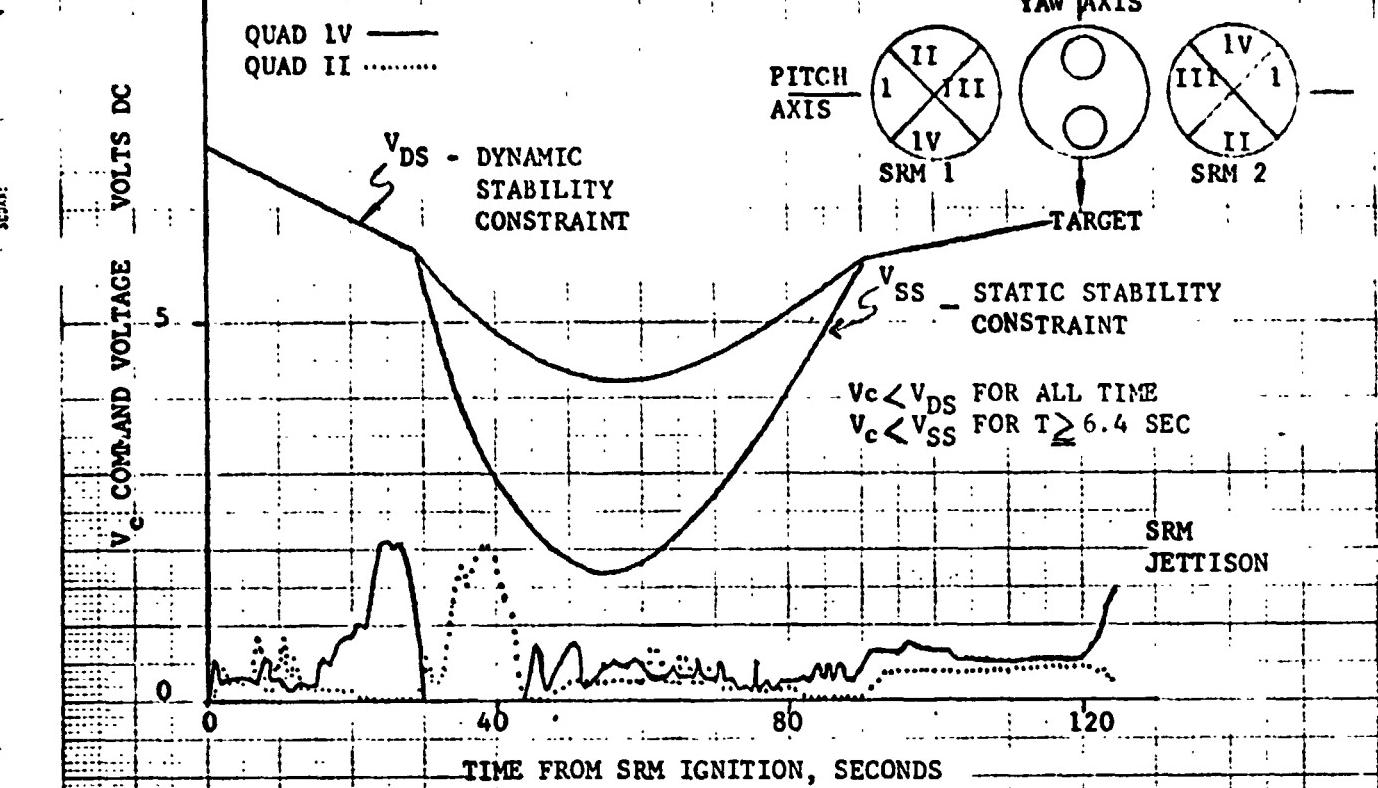
For Stage I and II, the control system limit is the maximum gimbal angle associated with the actuator stop. Actual gimbal angle used for Stages I and II versus flight time is plotted in Figures 28 through 33. During Stage I flight, the peak gimbal angle required for control was 1.06 degrees which is 25.7 percent of the maximum gimbal angle. The peak angle was required at SRM jettison. During Stage II, 7.6 degrees or 22.4 percent of peak gimbal angle was the maximum gimbal angle required at CSS jettison.

The control system response to vehicle dynamics was evaluated for each significant flight event. The amplitude, frequency and duration of vehicle transients, and the control system command capability required is shown in Table 20.

Both flight programmers and the staging timer issued all preprogrammed discretes at the proper times. The Centaur sent four discretes to the Titan at the proper times. The complete sequence of events with actual and nominal times from SRM ignition is shown in Table 21.

TITAN STAGE 0 FLIGHT CONTROL SYSTEM PERFORMANCE (E-2)

SRM 1 PITCH/ROLL COMMAND VOLTAGE VS. TIME



SRM 1 YAW COMMAND VOLTAGE VS. TIME

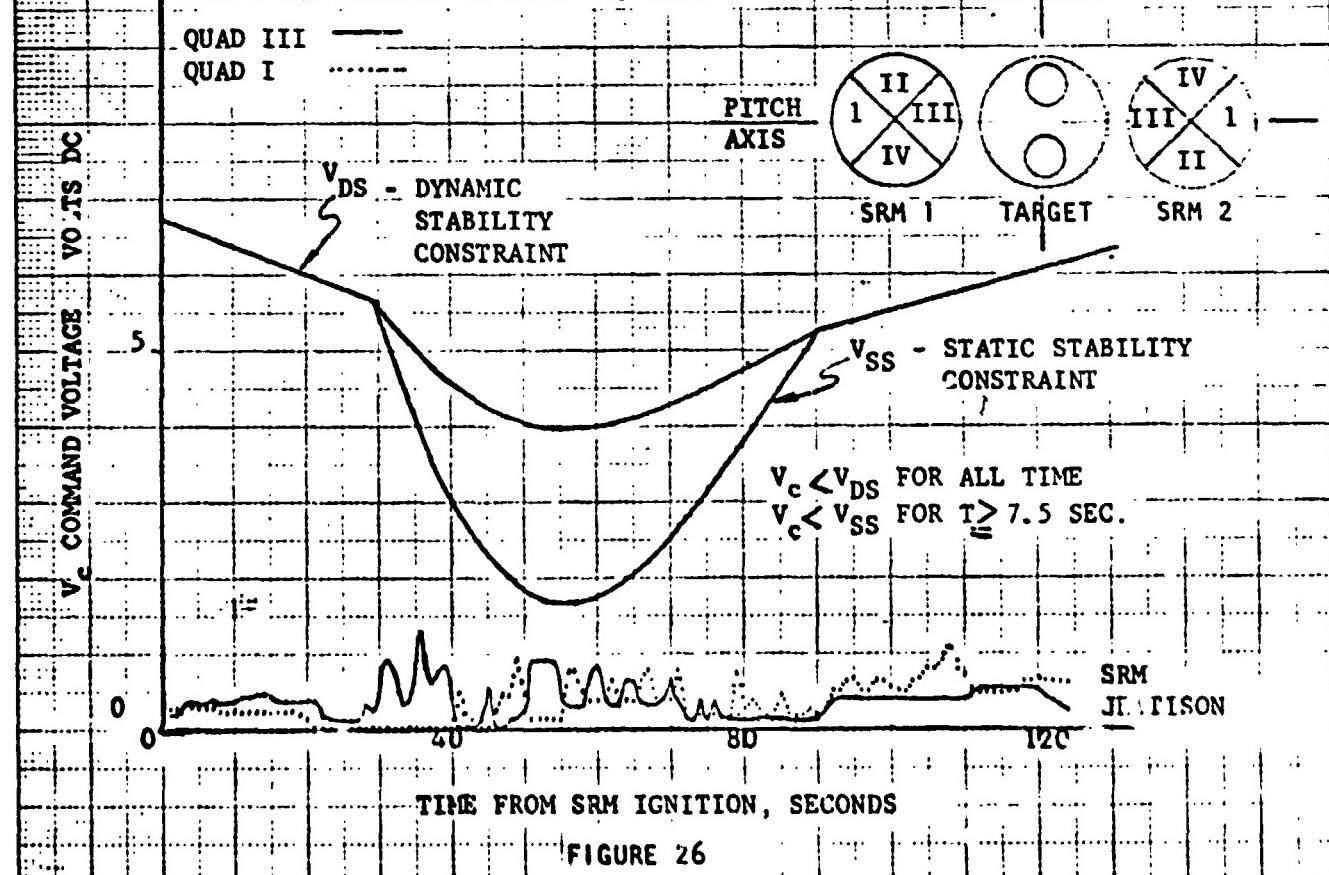
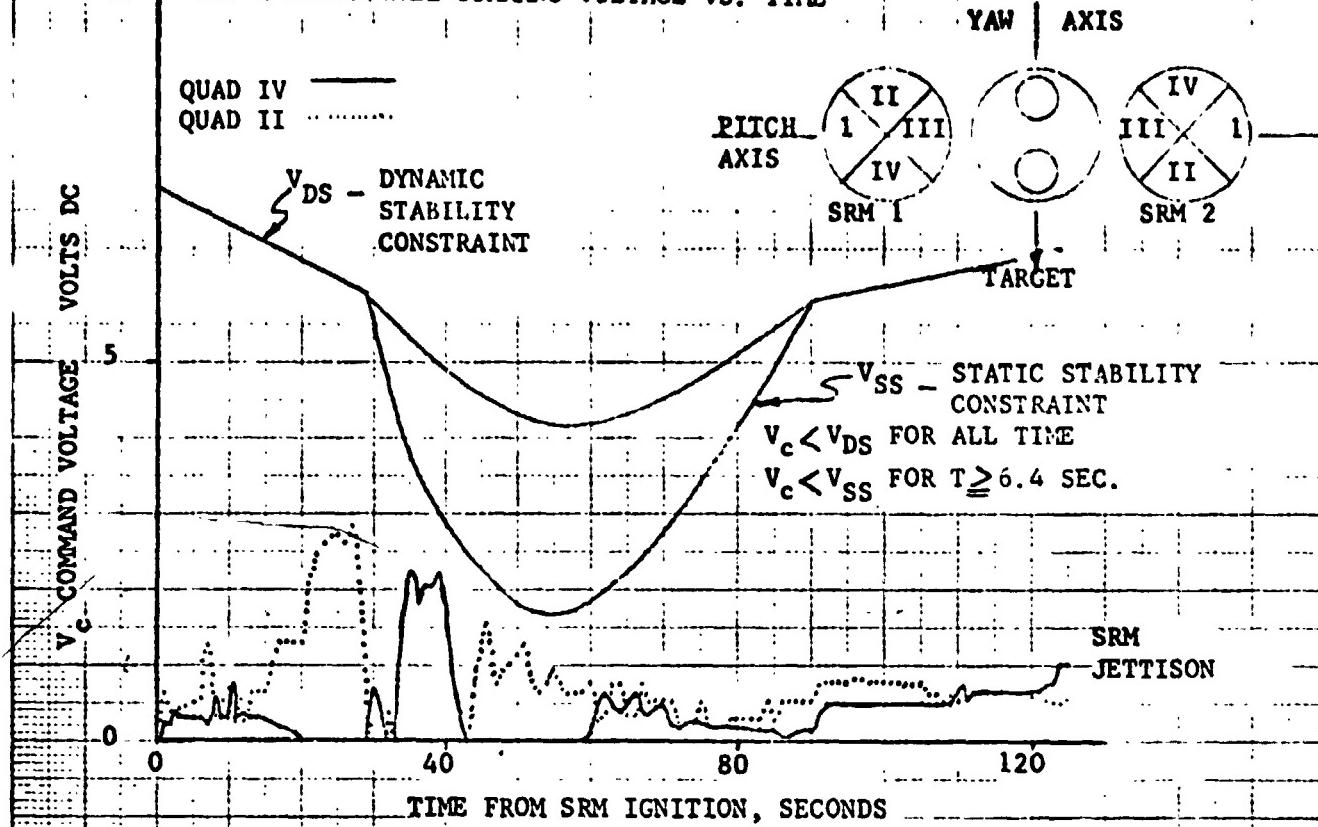


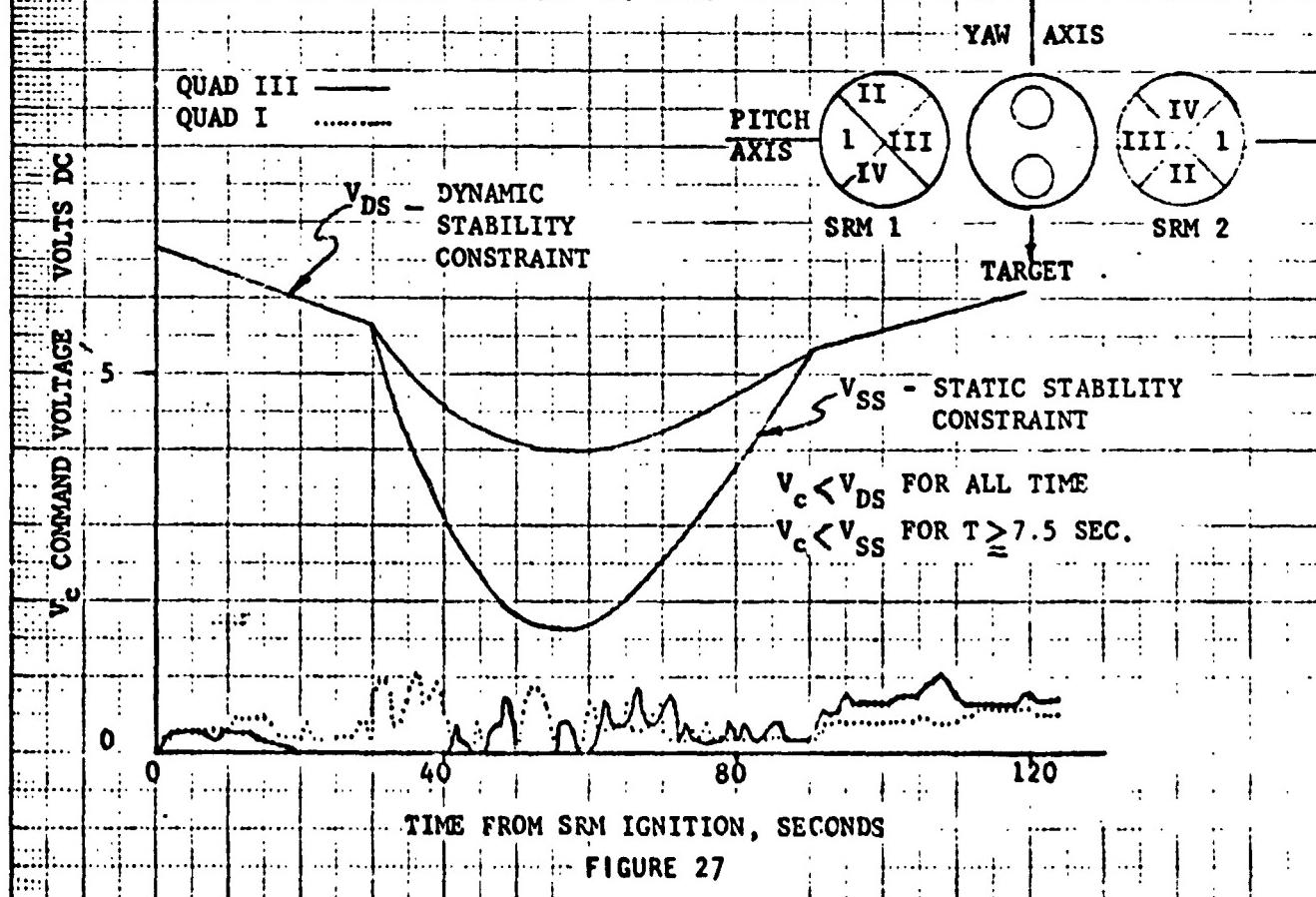
FIGURE 26

TITAN STAGE 0 FLIGHT CONTROL SYSTEM PERFORMANCE (E-2)

SRM 2 PITCH/ROLL COMMAND VOLTAGE VS. TIME



SRM 2 YAW COMMAND VOLTAGE VS. TIME



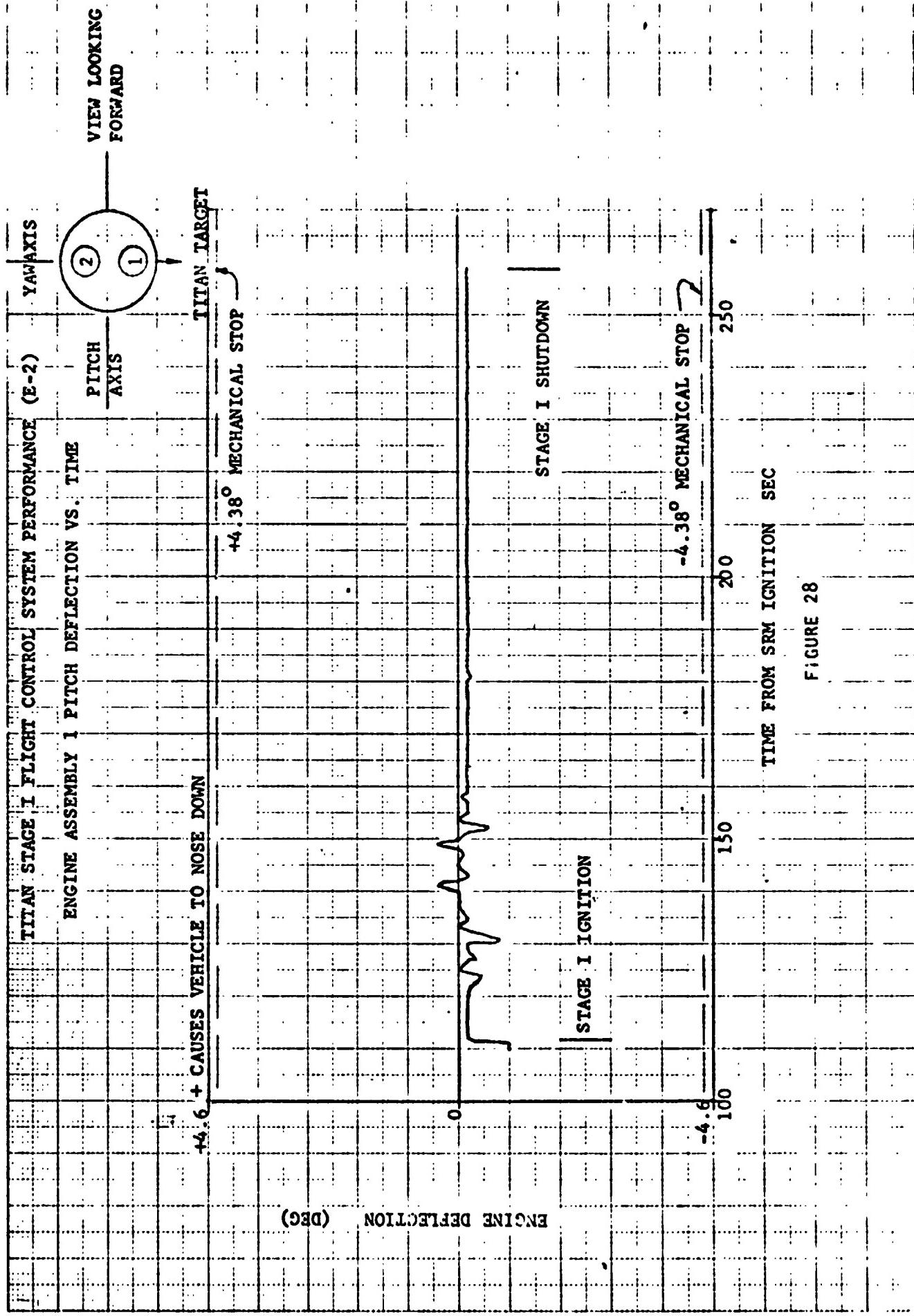
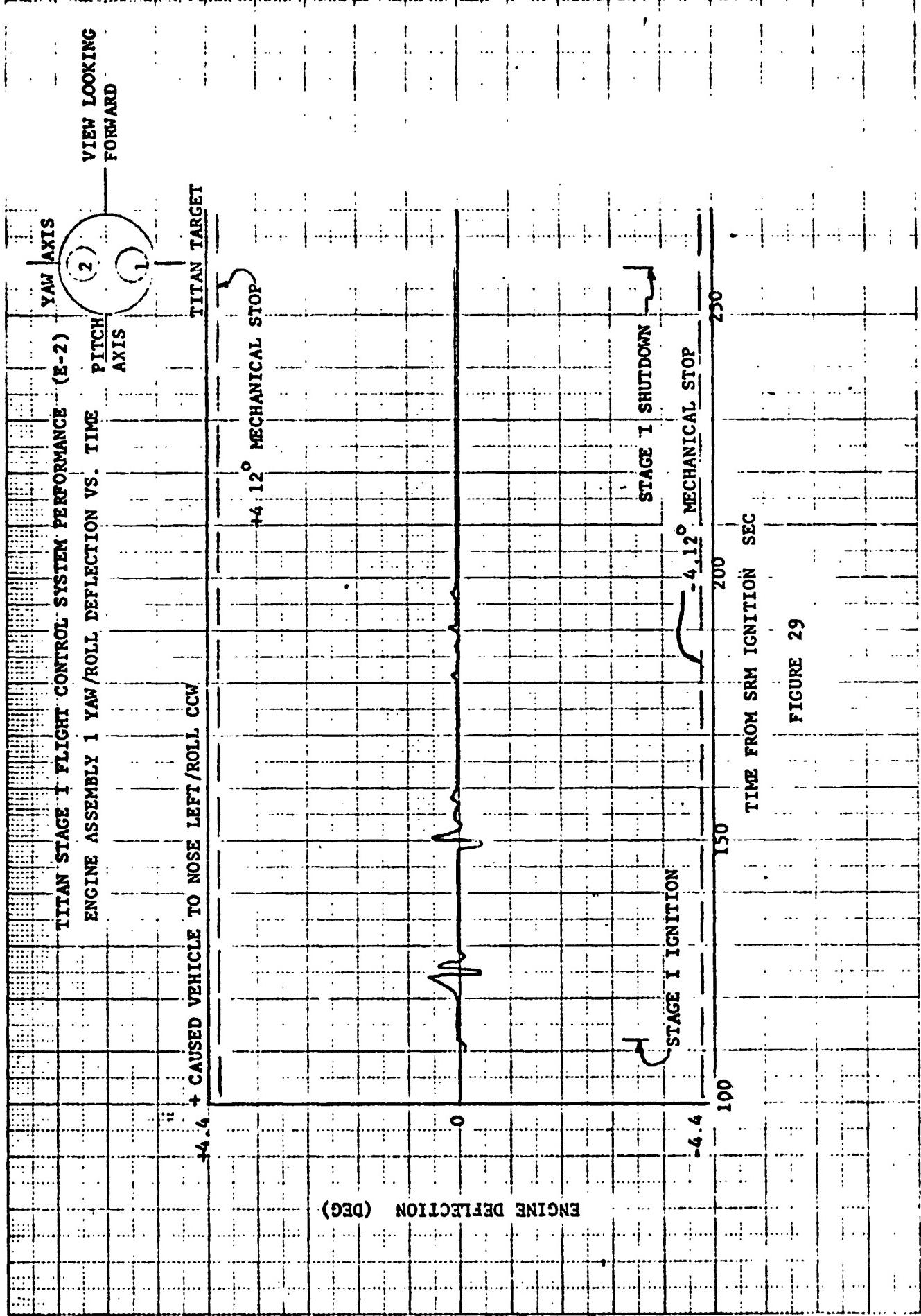


FIGURE 28



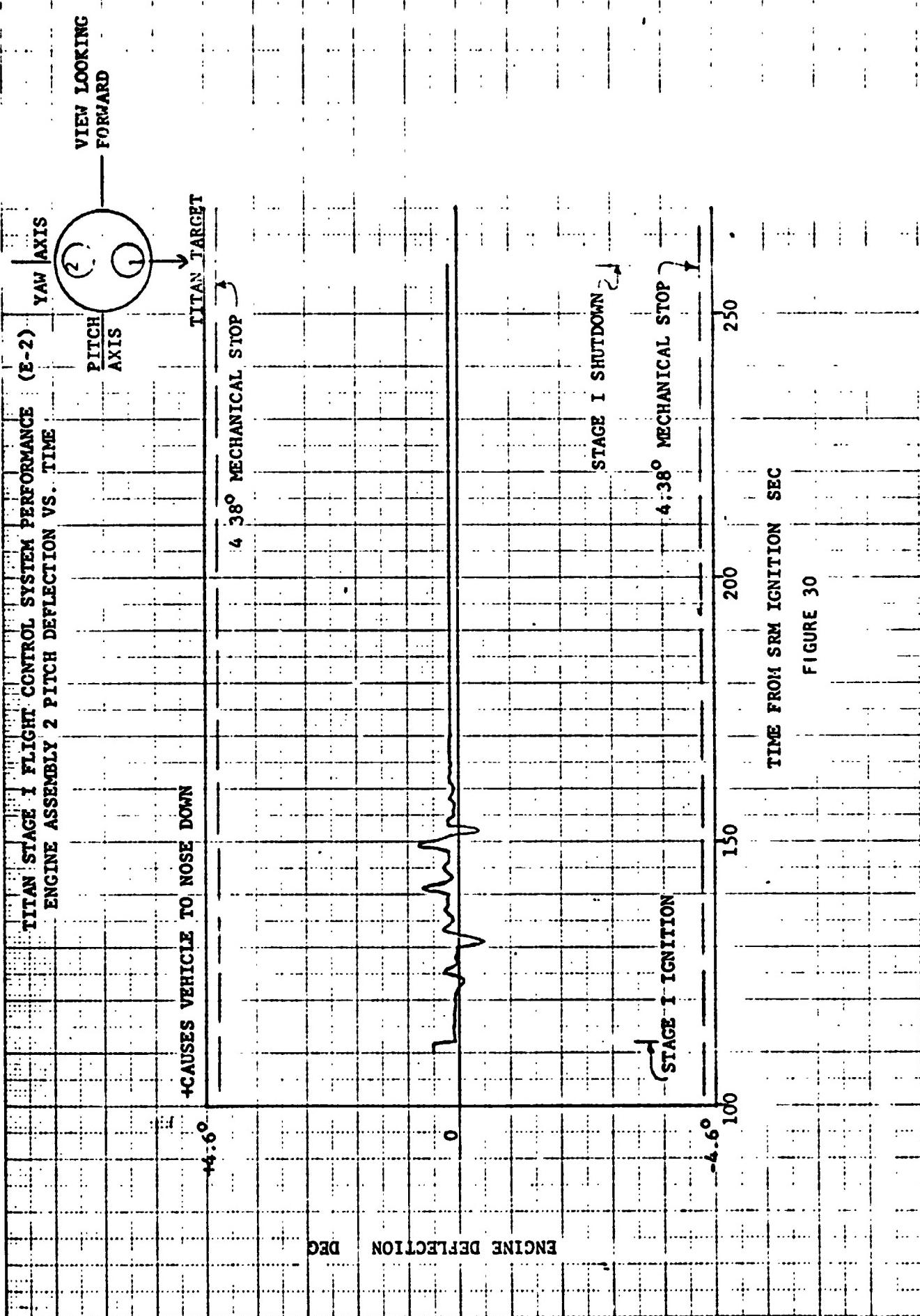


FIGURE 30

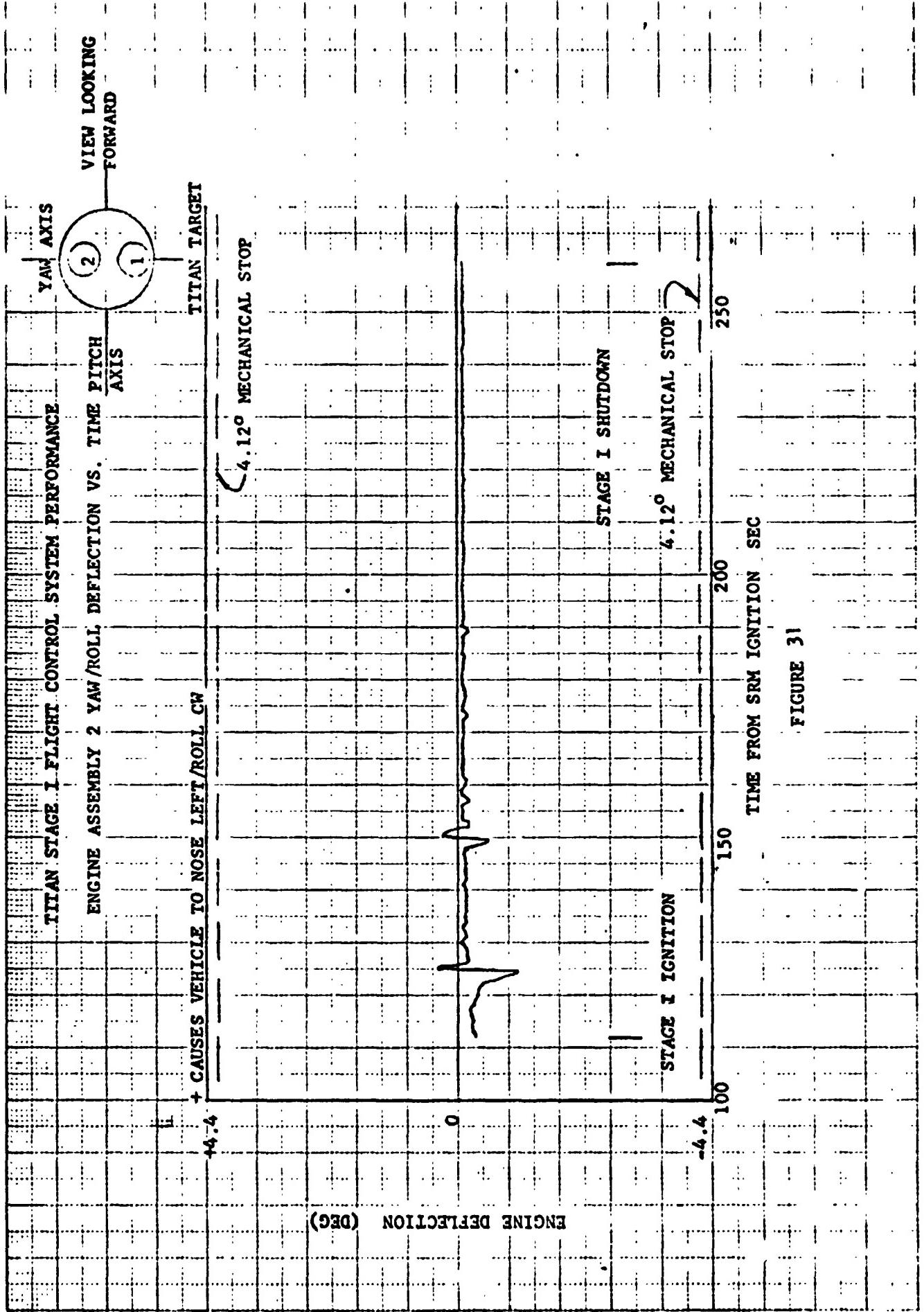


FIGURE 31

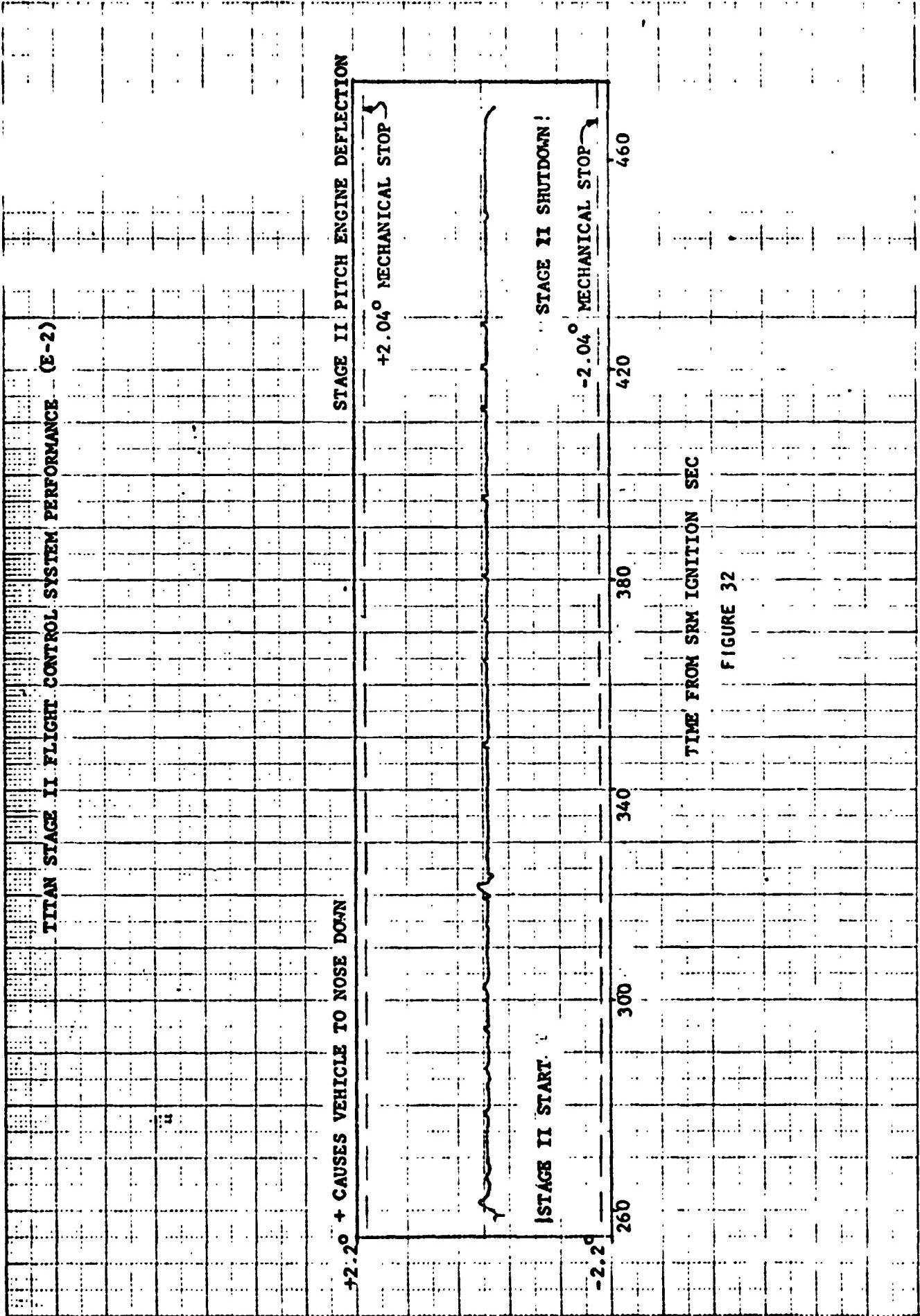
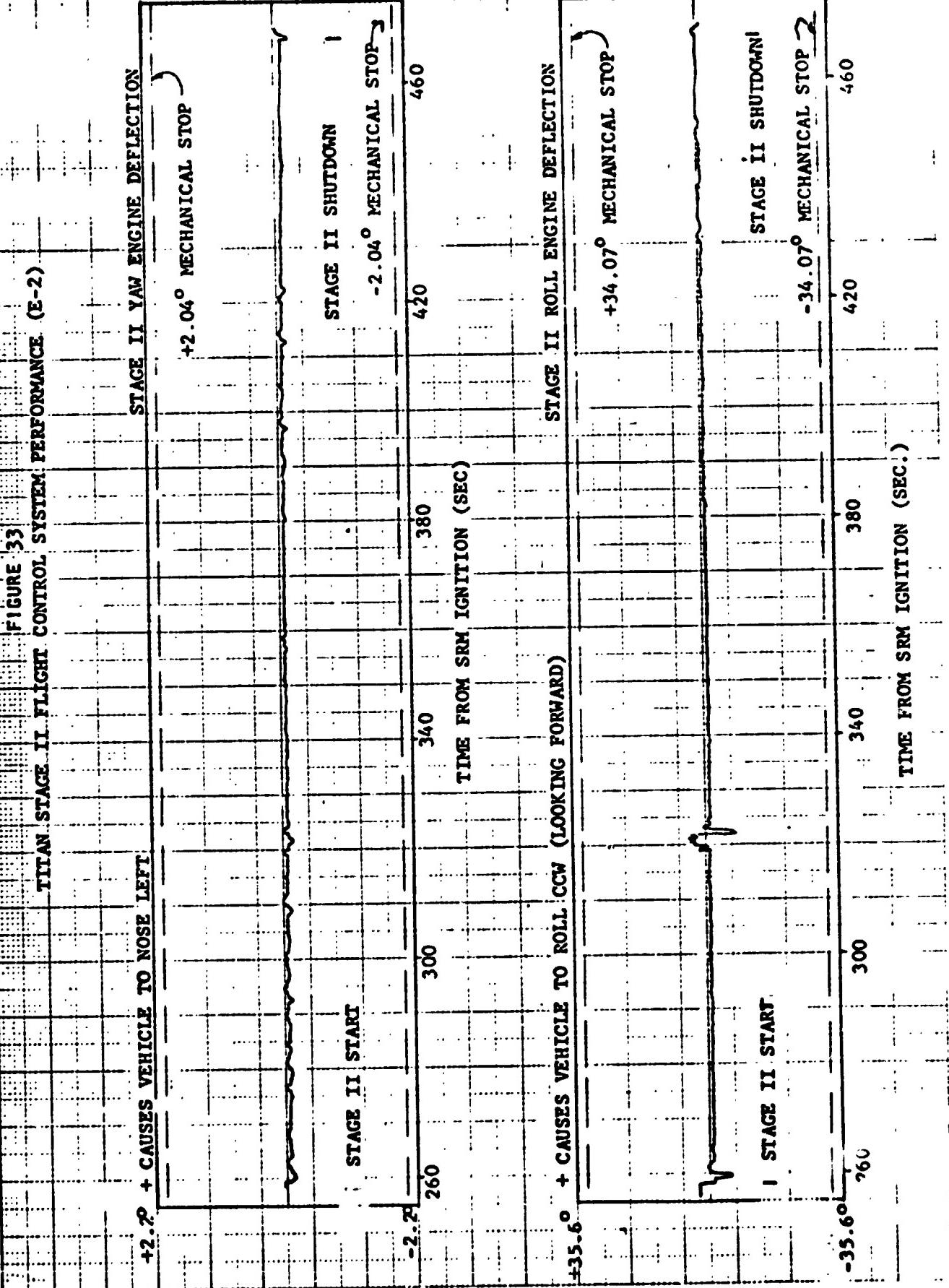


FIGURE 32



VEHICLE DYNAMIC RESPONSE

Event	Time Sec.	Axle	Zero to Peak Amplitude Deg./Sec.	Transient Frequency Hz	Transient Duration Sec.	Required Control % of Capability
Lift-off	0	P R Y	1.2 1.3 2.2	Mixed (20-30) 12 Mixed (20-30)	<1 <1 <1	{5 5 <1
Roll Maneuver	6.5	R	2	.3	5	13
Peak TARS Offset (Result of ADDJUST Steering and Winds)	27	P	-	-	-	28.5
Maximum Aerodynamic Pressure (45-60 Sec.)	4.3 40.2	P Y	6 6	Mixed (35-45) Mixed (30-40)	10	16 4
SRM Tail-off through Stage I Start	109	Y	.25	Drift	3	11
Stage I Ignition	123.6	P Y R	1.1 1.8 .72	Mixed (35-45) Mixed (35-40) 10	.25 1 1	<1 {10 {10
SRM Jettison (Initial Conditions)	122.6-123.6	R	.96	Drift	3.6	14.5
SRM Jettison Transient		P Y R	.54 5.8 11	Mixed (25-30) .3	5.5 3 6	2 {12.8 {12.8
Start of PR 7 (Only Pitch up Program)	131	P	1.44	N/A	N/A	12
Enable Guidance Steering (2.6° Pitch Down .8 YR)	~3	Y	2.5 .96	N/A N/A	N/A N/A	11.5 10.0

TABLE 20 (CONTINUED)

Event	Time Sec.	Axis	Zero to Peak Amplitude Deg./Sec.	Transient Frequency Hz	Transient Duration Sec.	Required Control % of Capability
Stage I Shutdown	259	P	.24	.2	5	4
Stage II Start		Y	.12	.33	3	2
		R	.48	.5	4	12
CSS Jettison	319	P	1.2	10	.5	8
	320-324	P	.24	.2	5	
	319	Y	.78	4	.4	2
	319	R	1.2	8	.5	4
	320-322	R	.72	10	2	15.6
	322.5	R	1.2	N/A	1.5	20.9

T-0 = 07:11:01.057 (SRM Ignition Command)

E-2 FLIGHT SEQUENCE OF EVENTS

Event	Predicted	(Times From T-0) Observed					Del
		F/P A	F/P B	S/T	DCU	Other	
Start Roll Program	6.50				6.575		+ 0.073
Stop Roll Program	--				6.613		-
Pitch Rate 1	10.000	10.004	10.009				+ 0.004
Pitch Rate 2	20.000	20.010	20.017				+ 0.010
Gain Change 1	29.000	29.014	29.026				+ 0.014
Pitch Rate 3	30.000	30.014	30.026				+ 0.014
Pitch Rate 4	62.000	62.031	62.057				+ 0.031
Gain Change 2	70.000	70.036	70.063				+ 0.036
Pitch Rate 5	75.000	75.038	75.068				+ 0.038
Enable S/T	75.000		75.069				+ 0.069
Gain Change 3	90.0.0	90.047	90.081				+ 0.047
Pitch Rate 6	95.000	95.048	95.087				+ 0.048
Enable F/P B	96.000	96.090	111.594	111.838			+ 0.090
Stage I Start CMD	112.038					111.605	- 0.444
Stage I Start	112.038						- 0.433
En Stg I ISDS Safe	118.038			117.606			- 0.432
0/1 Separation CMD	124.038			123.608	123.976		- 0.430
0/1 Separation	124.123					123.618	- 0.505
En Stg I ISDS Safe	124.044	123.795*					
Pitch Rate 7	130.000	130.067	131.416				+ 0.067
Pitch Rate 9	140.000	140.073	141.424				+ 0.073
Gain Change 5	192.000	192.102	193.674				+ 0.101
Gain Change 6	232.000	232.125	233.708				+ 0.123
Stg I S/D En	245.000	245.135	246.724				+ 0.135
Stg I S/D/Stg II Start	262.539					258.254	- 4.285
I/II Separation	263.235					259.631	- 4.204
Remove GC7, PRIC	310.000	310.169	311.582				+ 0.169
CSS Sep Prim	323.235					319.046	- 4.189
CSS Sep Sec	323.735					319.545	- 4.190
CSS Sep B/U	332.038						- 0.238
Gain Change 8	340.000	340.182	341.808				+ 0.182
Gain Change 9	400.000	400.215	401.862				+ 0.215

TABLE 21

TABLE 21 (CONTINUED)

E-2, LIGHT SEQUENCE OF EVENTS

T-0 = 07:11:01.057 (SRM Ignition Command)

Event	Predicted	(Times From T-0) Observed				Other	Delta
		F/P A	F/P B	S/T	DCU		
Stage II S/D En	448.000	448.244	449.008				+ 0.244
Stage II S/D	471.840			468.768			- 3.072
Stage II S/D	472.463	469.148					- 3.315
Stg II/Cen Sep	476.454			472.647			- 3.807
Stg II/Cen Sep B/U	479.863	476.559					- 3.304

* Event Masked by Noise; Time Approximated $\pm .65$ seconds

Electrical/Electronic Systems

Airborne Electrical System

by B. L. Beaton

Solid Rocket Motor Electrical System

The solid rocket motor (SRM) electrical system performance was satisfactory with no significant anomalies. All power requirements of the SRM electrical system were satisfied. One minor anomaly occurred at SRM ignition when a bridgewire apparently shorted to structure after initiation and simultaneous shorting occurred in the ignitor safe and arm device. TC-1 experienced the same condition.

The SRM electrical system was identical to that flown on TC-1.

The SRM electrical system supplied the requirements of the dependent systems at normal voltage levels. The SRM electrical system performance is summarized in Table 22.

The anomaly at SRM ignition was apparently caused by a short from an SRM igniter bridgewire positive to structure and simultaneous shorting from the transient return to readiness return within the igniter safe and arm device. As a result, the Titan core transfer current shunt indicated 10.4 amps for approximately 355 ms. The current dropped to zero simultaneous with the removal of the current path when the SRM umbilicals were ejected. The anomaly had no adverse effect on any airborne system.

Titan Core Electrical System

The core electrical system performance was satisfactory with no anomalies. All power requirements of the core electrical system were satisfied. All voltage and current measurements indicated expected values. Some bridgewire shorting (after initiation) was observed at every ordnance event.

The Titan electrical system was identical to that flown on TC-1.

The Titan core electrical system supplied the requirements of the dependent systems at normal voltage and current levels. The Titan core electrical system performance is summarized in Table 23.

The 800 Hz squarewave output of the static inverter was 38.15 volts during the entire flight.

The TPS bus voltage was 30.3 volts d-c at TPS bus enable and rose to 31.4 volts d-c at Titan/Centaur staging. This condition is normal due to increasing battery temperature since the battery internal heater and the TPS bus are enabled concurrently.

The TPS bus voltage and pyrotechnic firing currents during ordnance events are summarized in Table 24.

The transfer current indicated 10.4 amps at T-0 as previously discussed under SRM electrical system performance. The transfer current indicated that during short periods of high current demand on the APS bus, the IPS battery provided load sharing. This occurred at TPS enable, Stage I engine start and Stage I/II separation.

TABLE 22 SRM ELECTRICAL SYSTEM PERFORMANCE SUMMARY

	Power On Internal	Liftoff	SRM Jettison
TVC VOLTAGE	SRM-1 31.6	31.8	31.8
	SRM-2 32.0	32.0	32.0
AIPS VOLTAGE	SRM-1 29.9	29.7	29.7
	SRM-2 29.9	29.9	29.7
INSTRUMENTATION REGULATED BUS VOLTAGE	SRM-1 10.1	10.1	10.1
	SRM-2 10.0	10.0	10.1

TABLE 23 TITAN CORE VEHICLE ELECTRICAL SYSTEM PERFORMANCE SUMMARY

	Power on Internal	Liftoff	Enable TPS	Stage I Start	Stg 0/I Sep	Stg I/II Sep	CSS Jettison	Stage II S/D	T/C Staging
T-31.7	T-0	T+75	T+111.6	T+123.6	T+259	T+319	T+468.8	T+472.6	
APS VOLTAGE	28.2	28.5	28.2	27.6	27.9	27.2	28.2	27.9	27.9
APS CURRENT	8.4	8.0	8.9	10.3	10.7	13.1	7.5	8.5	9.5
IPS VOLTAGE	28.7	28.7	28.7	28.7	28.6	28.6	28.7	28.7	28.7
IPS CURRENT	9.7	9.5	9.7	9.7	9.7	9.8	8.9	8.9	8.9
TRANSFER CURRENT	0	10.4	0.5	0.4	0	0.6	0	0	0
TPS VOLTAGE	0	0	30.3	30.9	31.4	31.4	31.4	31.4	31.4

TABLE 24 TITAN CORE VEHICLE PYROTECHNIC SYSTEM PERFORMANCE

	STAGE I START	SRM JETTISON Separation	Stage I/I Staging Motors	Stage I/I Separation	CSS Jettison Motors	T/C and Retro-rocket	T/C Staging and Staging
TPS VOLTAGE	27.5	26.6	26.6	25.5	29.6	28.9	28.9
TPS CURRENT	33.5	205.9	239.5	263.4	31.9	64.6	28.9

Flight Termination System

by R. E. Orzechowski

The Titan flight termination system performance was nominal throughout the flight. Monitoring the receiver AGC voltages by telemetry indicated that sufficient signal was present throughout the powered flight to assure that any destruct or engine shutdown commands would have been properly executed. A list of station switching times is given in Table 25. Receiver safing command was issued at 07:21:02 GMT.

The Range Safety command battery voltages were 32.7 VDC at lift-off and remained steady throughout the flight. The commands from the flight programmer to safe the Stage I and the two SRM Inadvertent Separation Destruct Systems (ISDS) were issued at their expected times. The flight programmer also issued the command to safe the Destruct Initiator on Stage II prior to the Titan/Centaur separation.

Table 25 - Station Switching Times

Station	Carrier On	Carrier Off
Mainland (Sta. 1)	06:37:59 Z	07:13:51 Z
Grand Bahama Is. (Sta. 3)	07:13:51 Z	07:18:41 Z
Antigua (Sta. 91)	07:18:41 Z	07:23:14 Z

Instrumentation and Telemetry System

by R. E. Orzechowski

A total of 207 measurements were telemetered by the Titan Remote Multiplexed Instrumentation System (RMIS). A summary of the types of measurements versus the systems in which they were monitored is given in Table 26. Preliminary review of the flight data indicates that all measurements yielded satisfactory data.

Adequate telemetry coverage of the Titan vehicle was provided from lift-off to beyond Titan/Centaur separation. A summary of the predicted data coverage versus actual data coverage of the Titan telemetry link is given in Table 27.

There was a data dropout of 1.5 seconds duration at 07:13:04.8 GMT. This dropout was expected and is due to plume attenuation at the time of Stage 0 separation.

TABLE 26 TITAN BOOSTER MEASUREMENTS SUMMARY

SYSTEM	TYPE OF MEASUREMENT	ACCELERATION	VOLTAGE	CURRENT	PRESSURE	TEMPERATURE	DISPLACEMENT	RATES	DISCRETE	TOTAL
AIRFRAME		5			10				2	17
RANGE SAFETY			3						6	9
ELECTRICAL		15	10						25	
HYDRAULICS				8		2			10	
PROPELLION		6			34	8			4	52
FLIGHT CONTROL			32				33	11	11	86
TELEMETRY				6			1			7
TOTAL		11	56	10	52	9	35	11	15	207

TABLE 27

Summary of Predicted Data Coverage

Versus Actual Data Coverage

Titan 2287.5 MHZ Link

STATION	PREDICTED		ACTUAL	
	AOS	LOS	AOS	LOS
CIF (Mainland)	Turn On	450 sec	Turn On	490 sec
GBI (Grand Bahama)	76 sec	475 sec	64 sec	530 sec
GTK (Grand Turk)	250 sec	580 sec	184 sec	637 sec

VIII CENTAUR STANDARD SHROUD

VIII CENTAUR STANDARD SHROUD

Preflight/Liftoff Functions and Venting

by T. L. Seeholzer and W. K. Tabata

Pre-T-0 Disconnects and Door Closures

Included in this group of disconnects and door closures are the T-4 aft and the T-4 forward electrical and helium purge umbilicals shown in Figures 34, 35 and 36. Umbilical disconnect and door closings are accomplished by lanyards retracted by hydraulic cylinders. The forward T-4 door is closed by torsion springs and door weights and incorporates two secondary and two primary latches (Figure 37). The door springs and latches were modified in this flight to insure primary latching. The T-4 aft umbilical door (Figure 38) is closed by a door closing lanyard and incorporates two primary and one secondary latches.

Movies and television coverage verified disconnect of the forward umbilicals and door closing on the primary latches.

Microswitches mounted on the T-4 aft door verified the door closed on the primary latches following umbilical disconnect. Function of these microswitches was included in the launch ladder.

T-0/Liftoff Disconnects and Door Closures

T-0 disconnects and door closures were as follows: (Reference Figure 34).

Payload Air Conditioning - Disconnect of the payload air conditioning duct was accomplished by deflating the connecting seal and retracting the duct by a lanyard system. The door is closed by torsion springs. Both outer and inner doors are incorporated for redundancy (reference Figure 39).

Equipment Module Air Conditioning and Line of Sight - Disconnect of the equipment module air conditioning duct is similar to the payload air conditioning disconnect function. Door closure is accomplished by torsion springs and door weight. The door incorporates one primary and one secondary latch (reference Figure 40).

Forward Electrical Umbilical - Identical to the T-4 forward umbilical (reference Figures 36 and 37). This door and the equipment module air conditioning line of sight door springs and latches had been modified for this flight to insure primary latching.

LH₂ Vent Fin Disconnect - Disconnect of this duct is accomplished by a fly-away lanyard system (reference Figure 41).

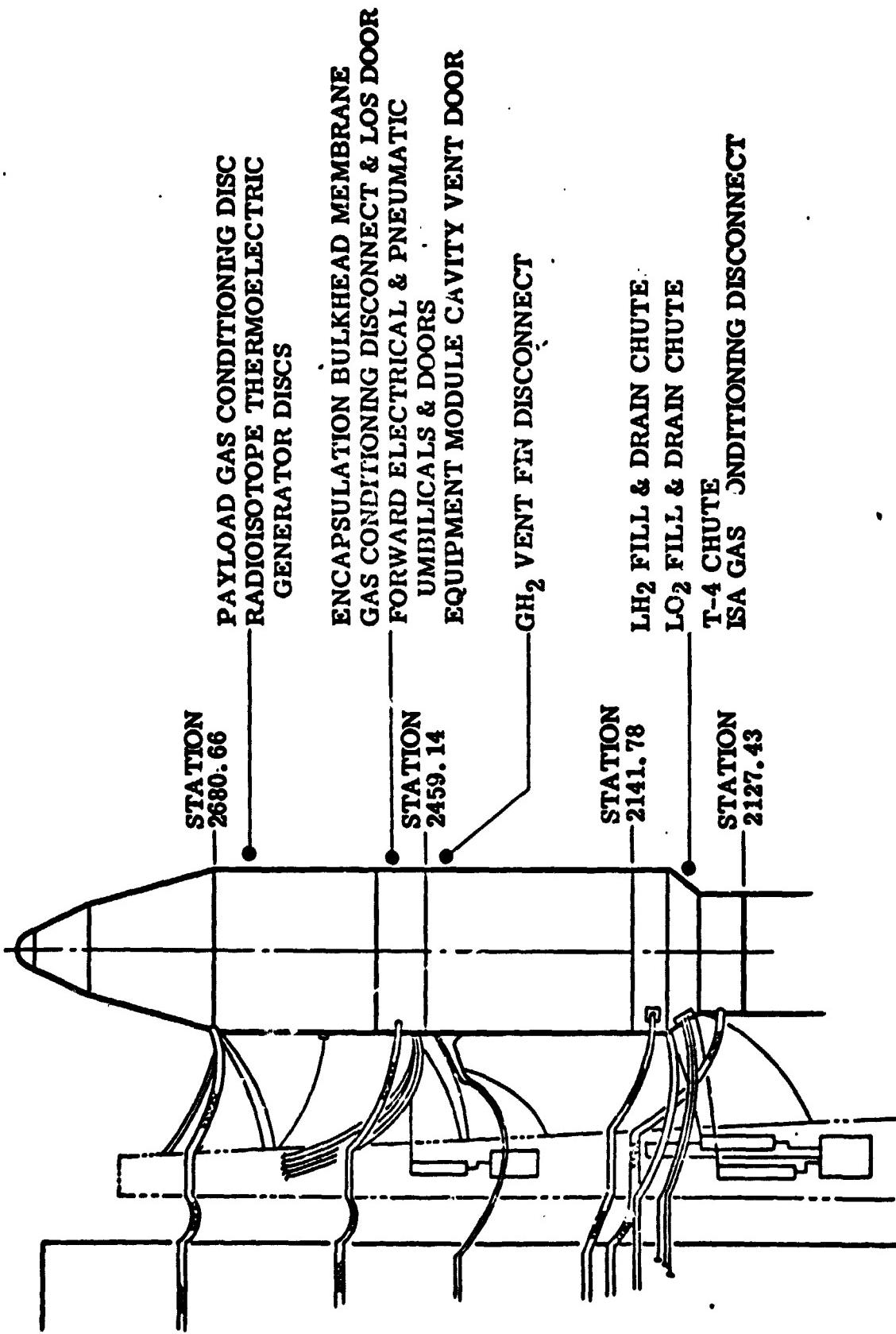


FIGURE 34 PREFLIGHT LIFTOFF FUNCTIONS

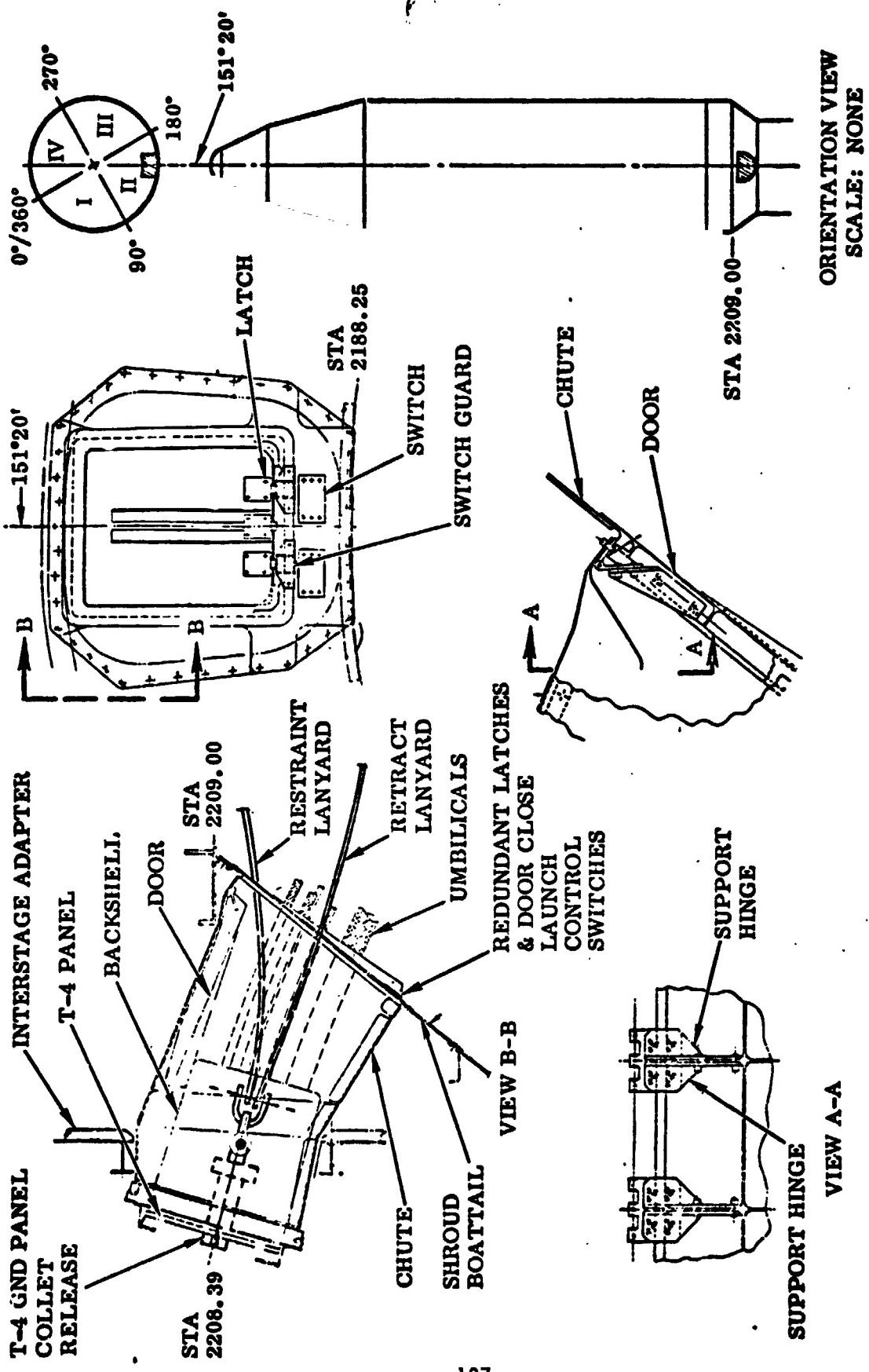


FIGURE 35 T-4 AFT PANEL, AND DOOR

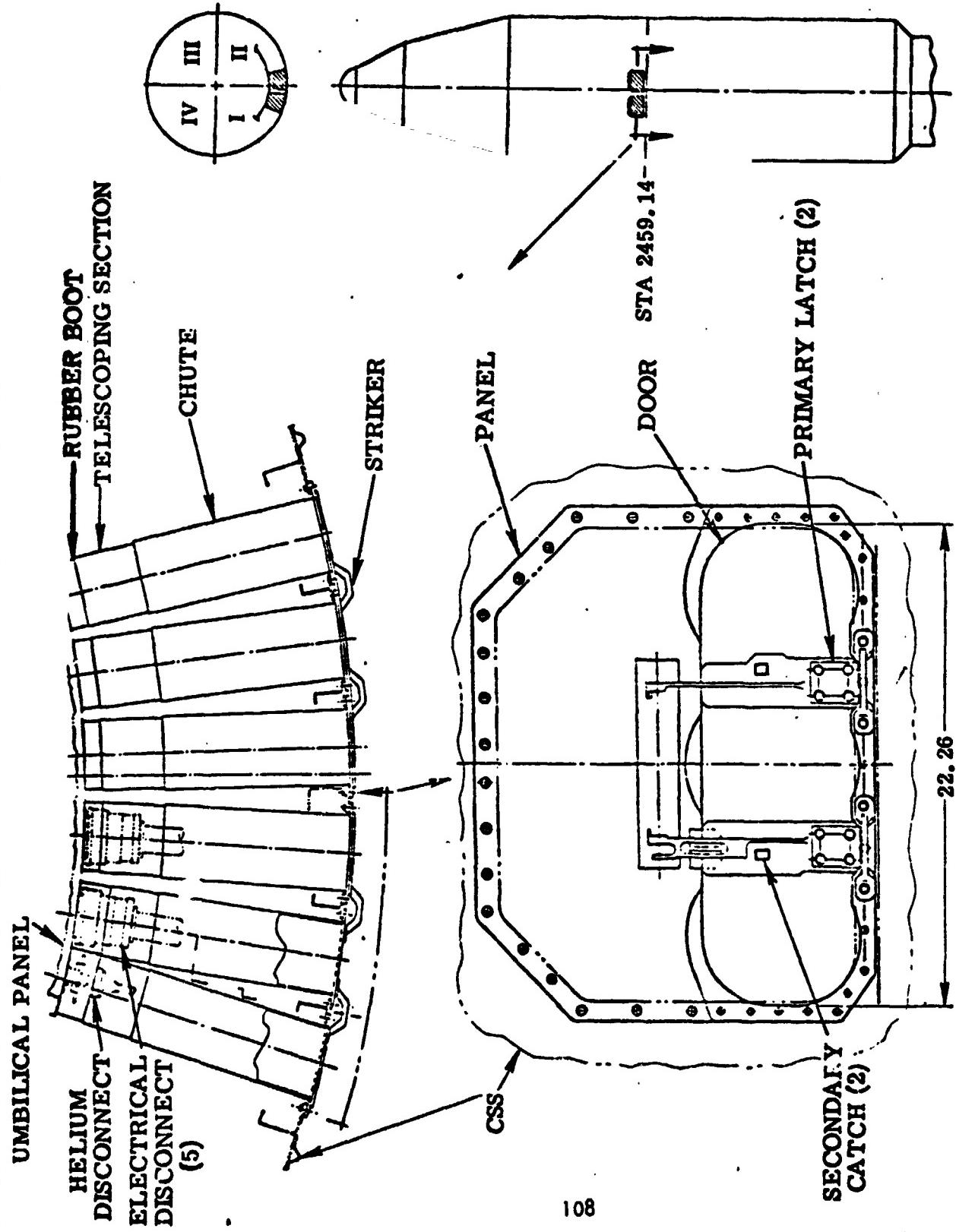


FIGURE 36 T-4 FORWARD UMBILICAL CHUTES AND DOOR

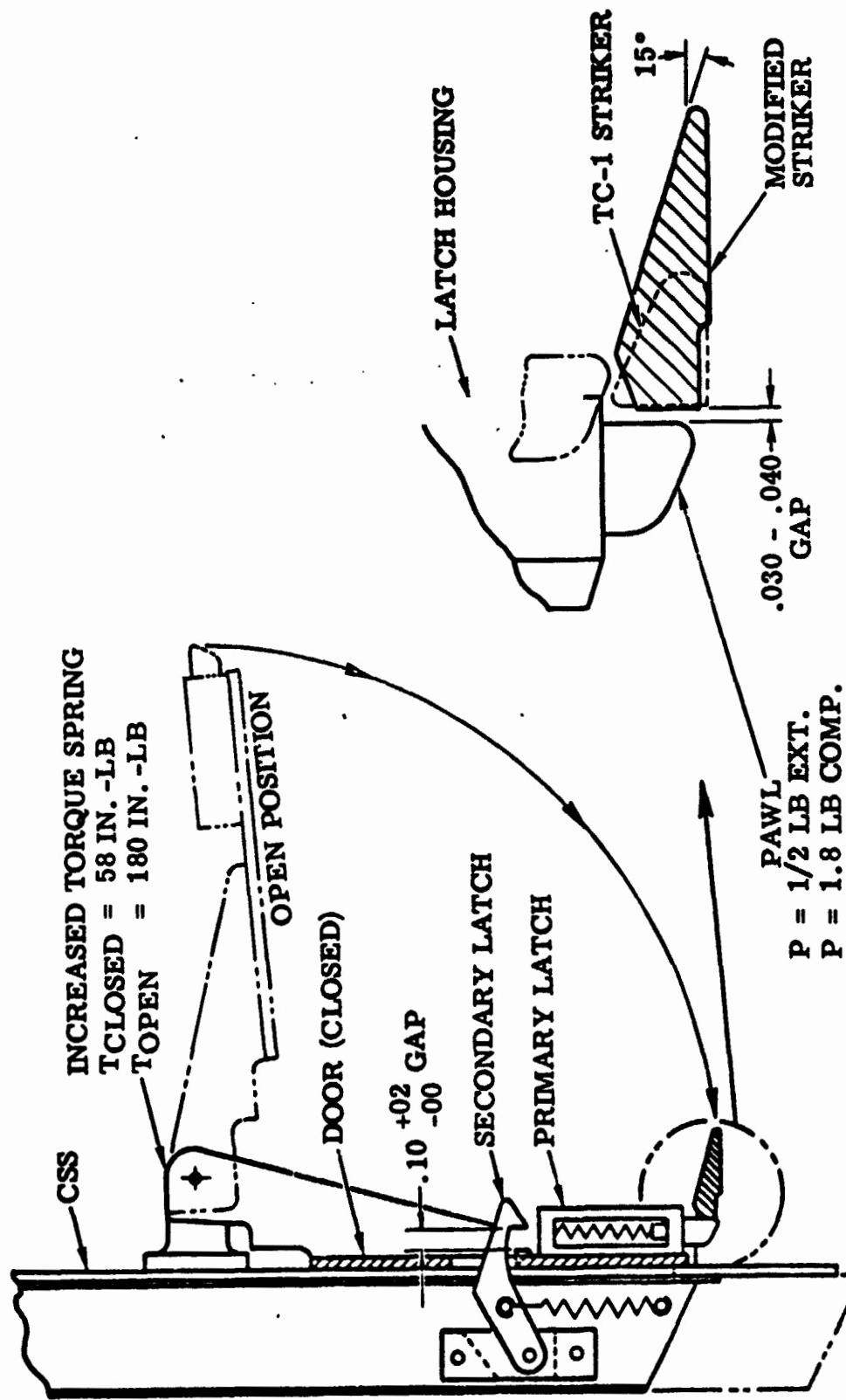
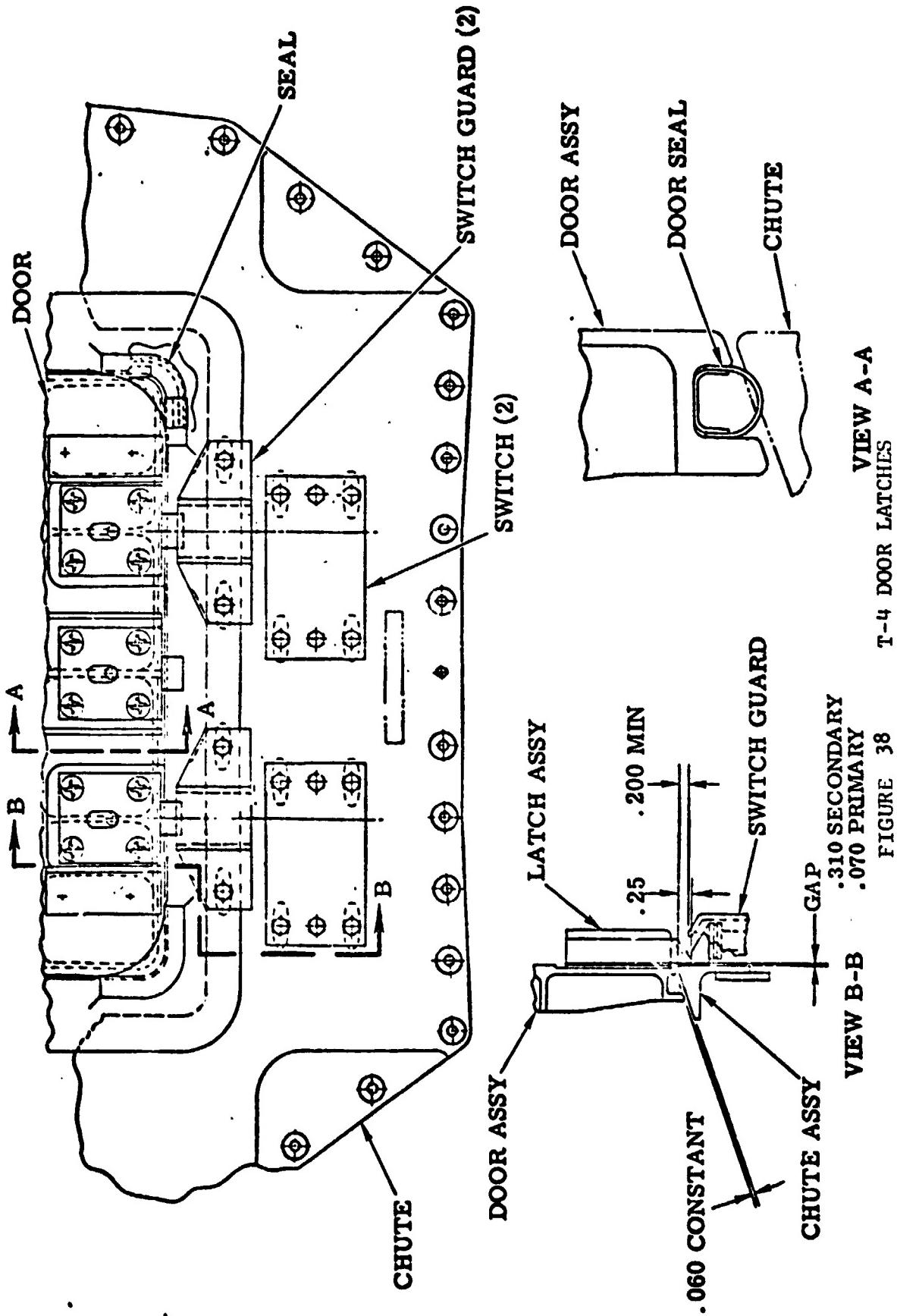


FIGURE 37 CSS T-4 FORWARD DOOR DETAILS
(TC-2 AND ON CONFIGURATION)



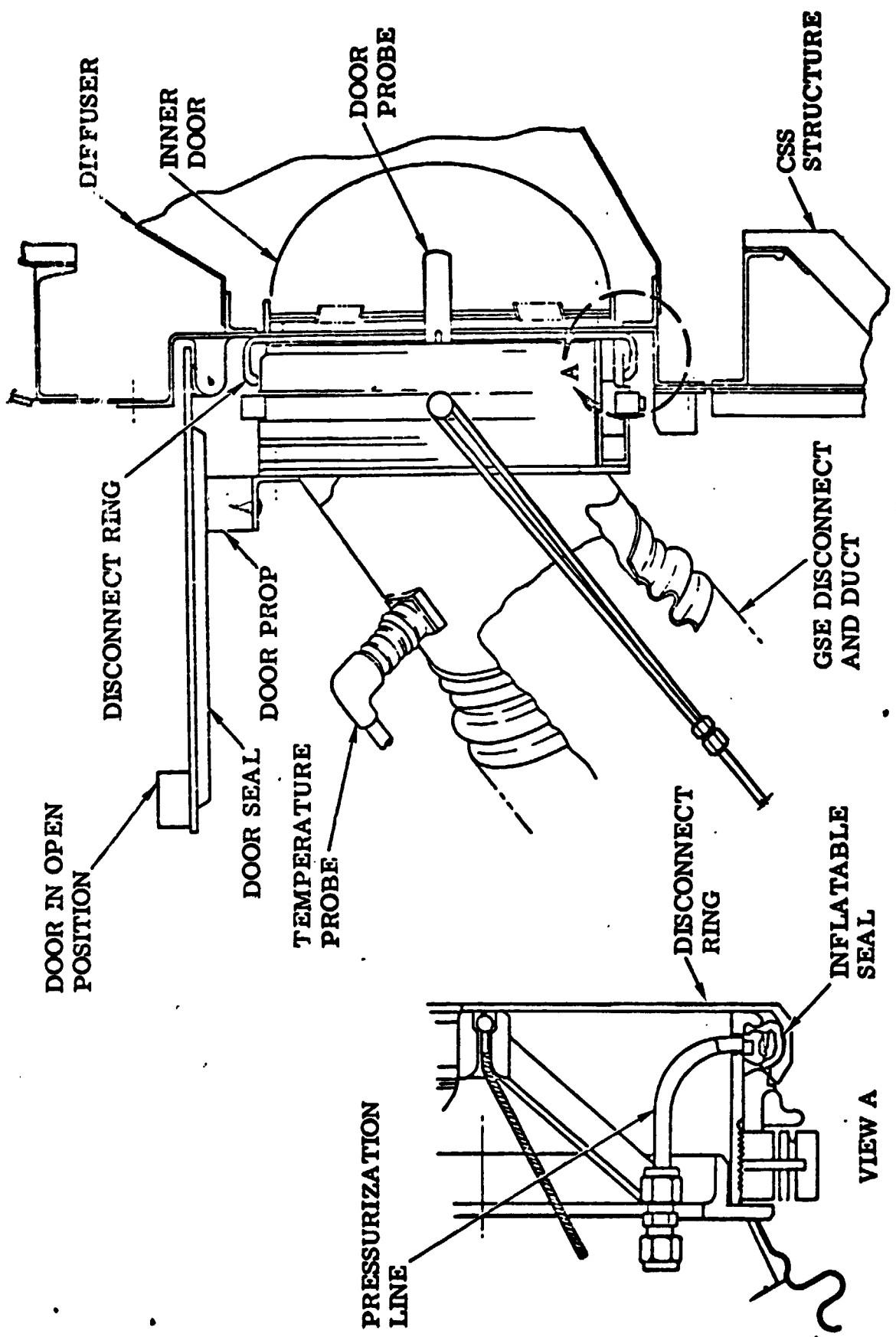


FIGURE 39 PAYLOAD AIR CONDITIONING DISCONNECT
II-A-3

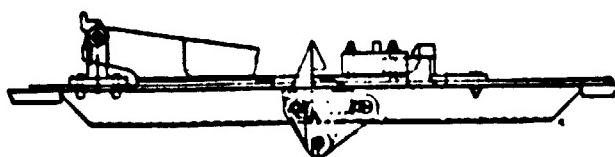
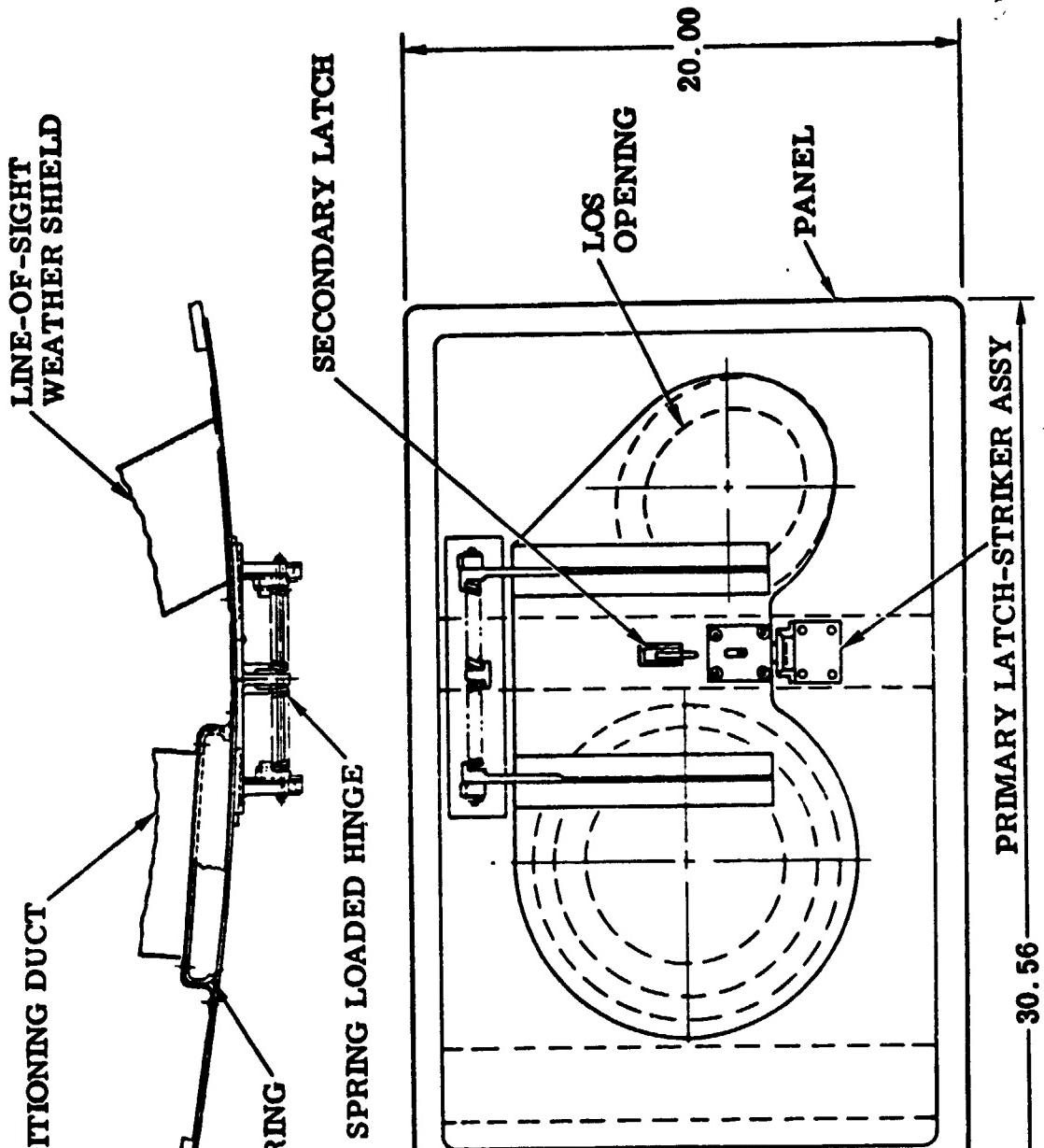


FIGURE 40

EQUIPMENT MODULE AIR CONDITIONING AND LINE OF SIGHT DOOR

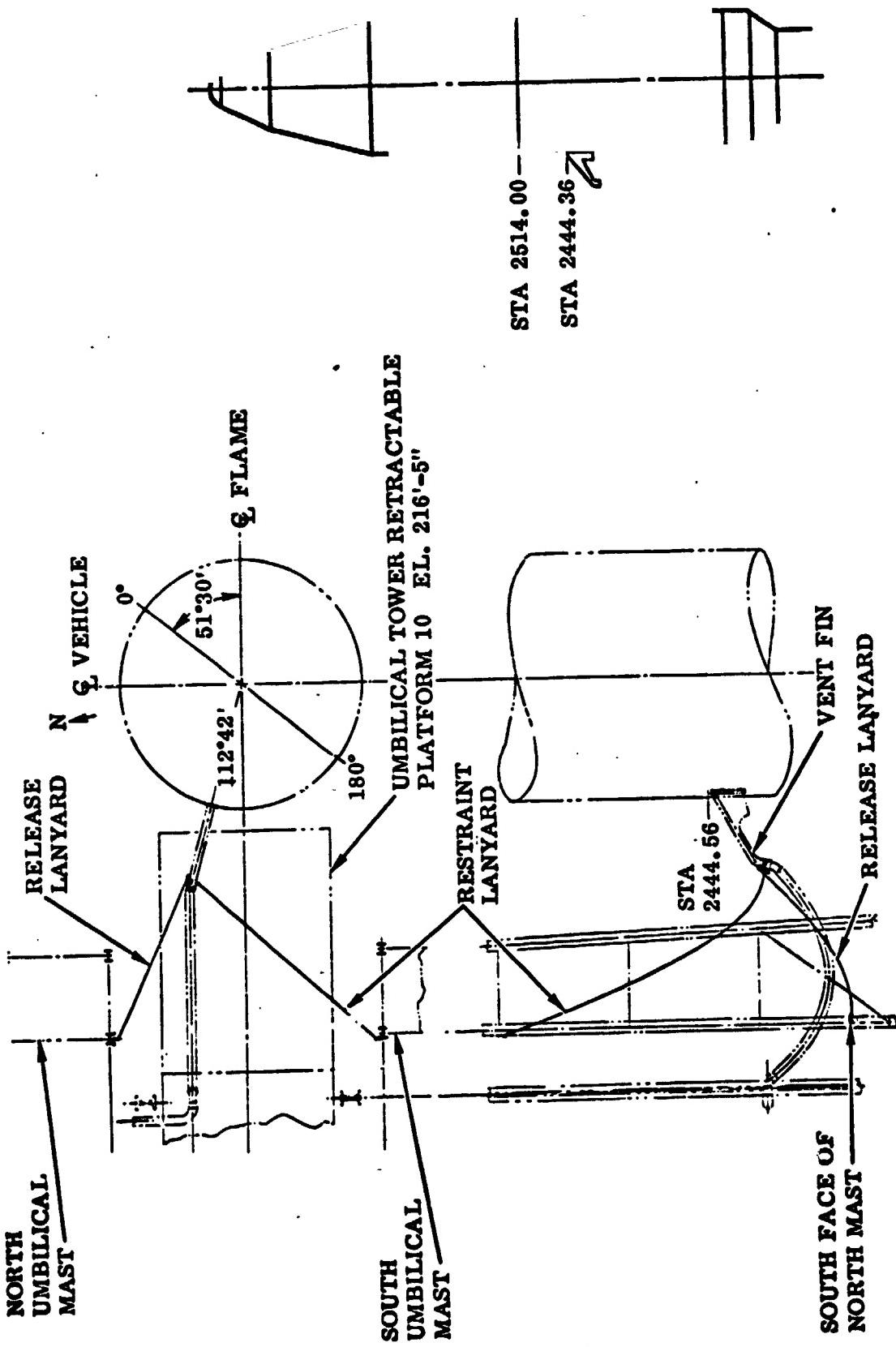


FIGURE 41 VENT FIN DISCONNECT

LH_2 and LO_2 Fill and Drain Valve Disconnects and Doors - Disconnect of the valve is accomplished by a lanyard system which disconnects the valve by fracturing frangible bolts. Doors are closed by lanyards and incorporate two primary and one secondary latches (reference Figures 42 and 43).

Interstage Adapter Air Conditioning - Disconnect and door closing are similar to the payload air conditioning (reference Figure 39).

All functions of the T-0 disconnects and doors were verified by movie and television camera data. For the T-4, T-0 and Equipment Module Air Conditioning Line of Sight doors, a reference line was painted on the primary latch housing and a dot was painted on the pawl retaining pin to assist in determining primary door latching (Figure 37). Movies covering these doors verified primary latching.

Centaur Standard Shroud Ascent Vent System

The Centaur Standard Shroud Ascent and Vent System controls the venting of seven separate compartments. The venting rates are controlled to minimize vehicle and spacecraft structural differential pressures during ascent through the atmosphere. The seven vented compartments, the contained gas media and volumes, the vent areas and the number of vents for the TC-2 vehicle are shown in Figure 44. The TC-2 and TC-1 Proof Flight CSS Ascent Vent Systems were identical except for how one compartment, Compartment 4A, was vented.

Compartment 1, the Helios A spacecraft, had an internal volume of 66 cubic feet of nitrogen which was vented into the CSS payload compartment. The Helios A spacecraft presented no venting problem.

Compartment 2, the payload compartment, and Compartment 3, the Centaur electronics compartment, were essentially one compartment. The Environmental Shield which separated the two compartments provided liberal communication between compartments. Compartment 2/3 had a combined volume of 3787 cubic feet of nitrogen gas.

Compartment 4A, the Centaur equipment module compartment, was bounded by the Centaur Equipment Module, the Centaur Stub Adapter and the top of the Centaur LH_2 tank. This 78 cubic feet compartment was purged with helium on the ground. The helium purge was required to prevent cryo-pumping of condensable gases into the LH_2 tank. During the launch countdown ladder just prior to liftoff, a spring-loaded door in the Equipment Module was opened by a pyrotechnic pin puller providing 9.5 square inches of vent area into Compartment 3 through a fiber-glas duct.

In flight, the nitrogen gas in Compartments 1 and 2/3 and the helium gas in Compartment 4A were vented through 125 square inches of vent area distributed in 11 rectangular vents distributed around the circumference of the CSS.

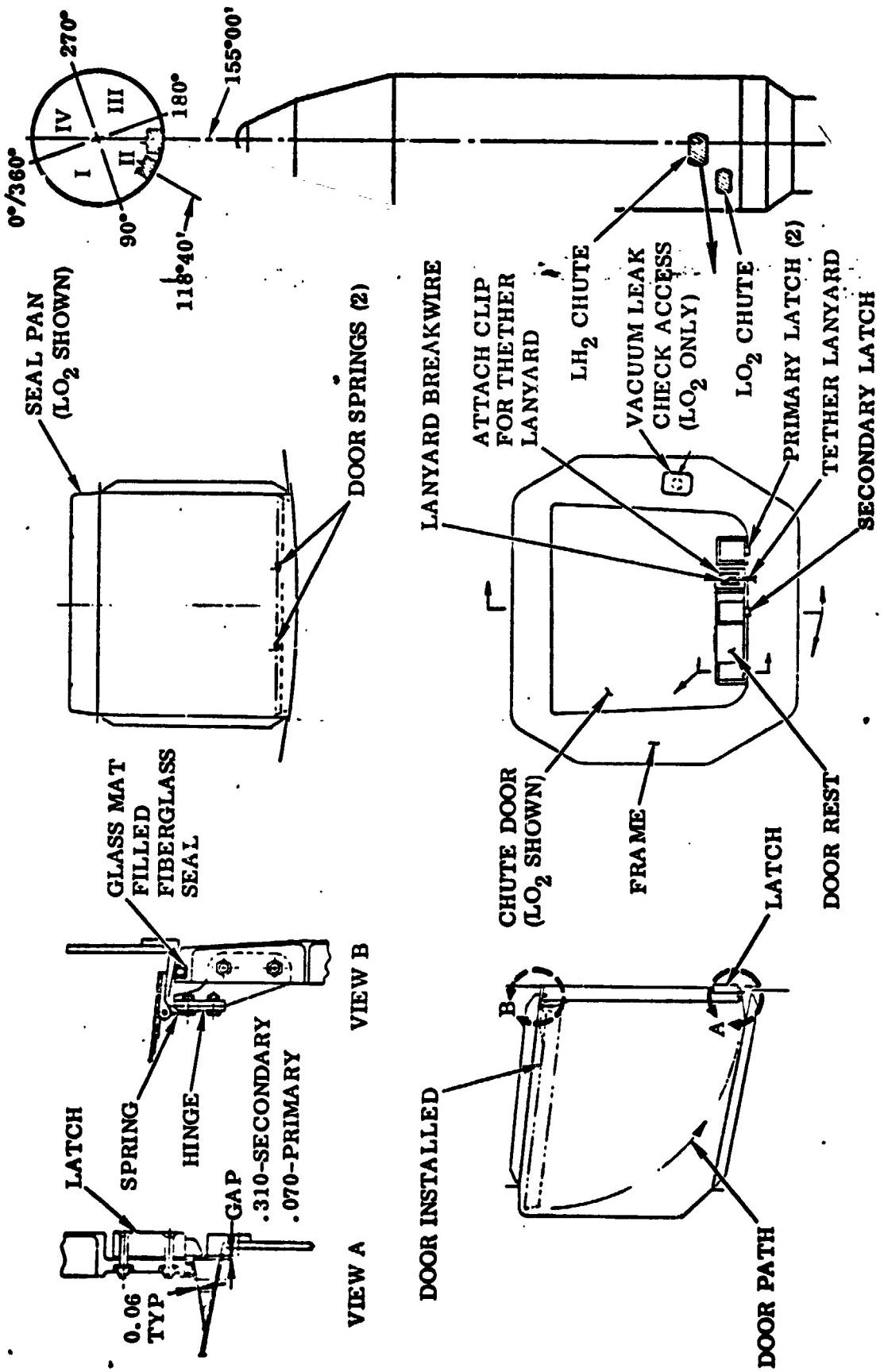


FIGURE 42 LH₂ AND LOX FILL AND DRAIN VALVE CHUTE AND DOOR

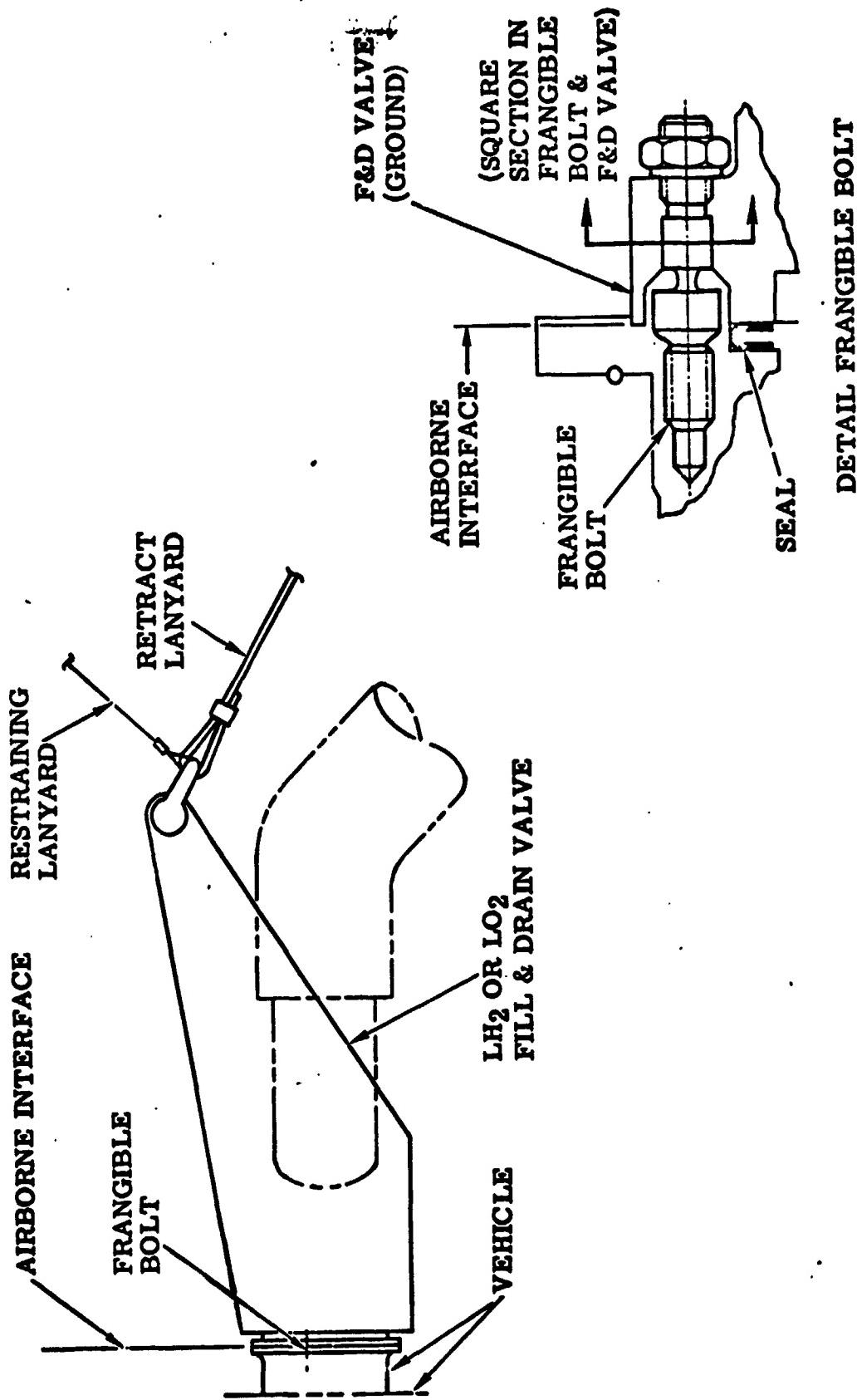


FIGURE 43 LH₂ AND LO₂ FILL AND DRAIN VALVE DISCONNECT DETAILS

TC-2 CENTAUR STANDARD SHROUD ASCENT VENT SYSTEM

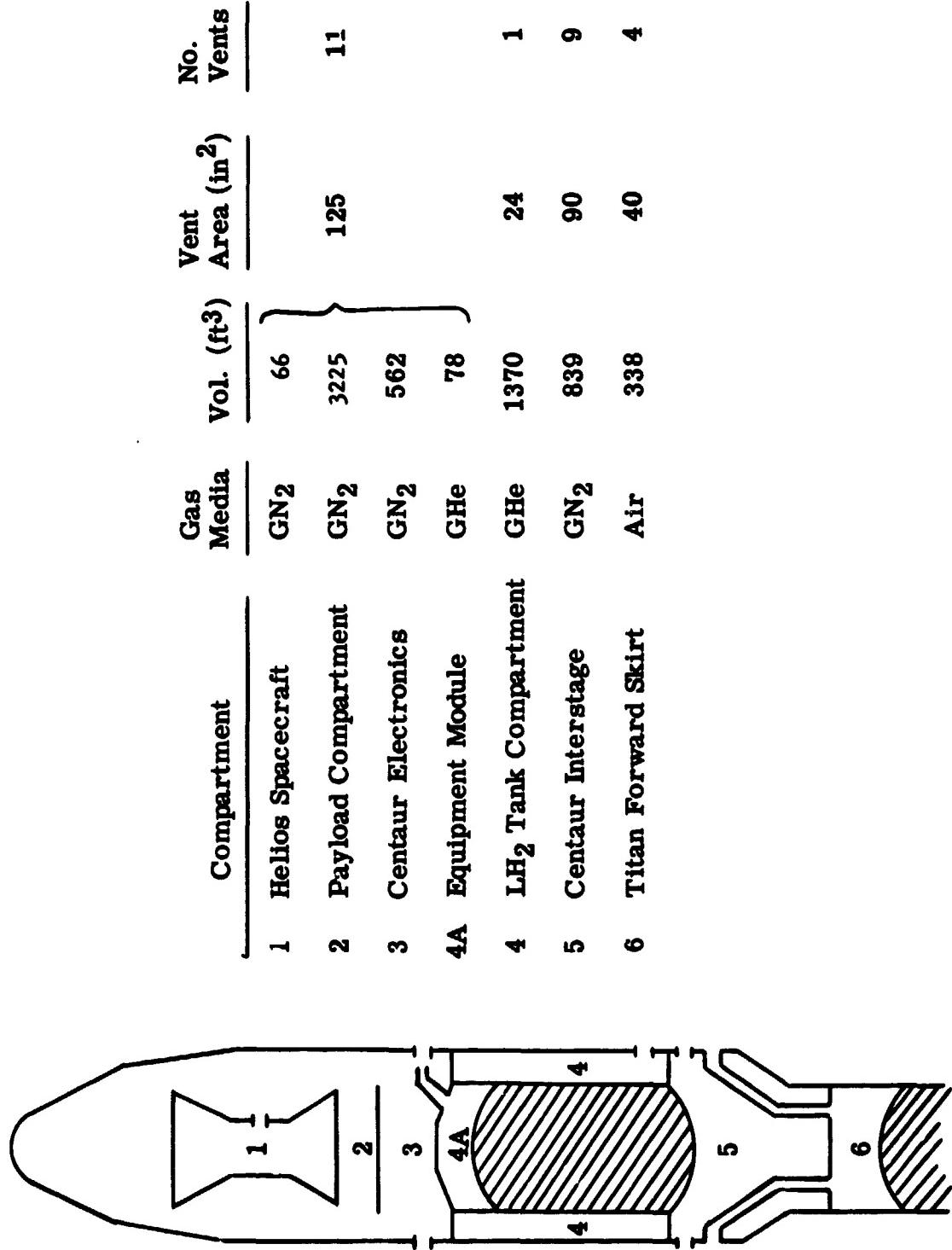


Figure 44 Centaur Standard Shroud Ascent Vent System Schematic

Compartment 4, the LH₂ Tank Compartment, was also purged on the ground with helium to prevent cryopumping. The compartment's 1370 cubic feet volume was bounded by the CSS Forward Seal and the CSS Aft Seal. Venting in flight was through five circular holes in the LH₂ Fill and Drain Valve Chute Door. The total vent area was 24 square inches.

Compartment 5 was the Centaur Interstage Compartment. The total volume was 839 cubic feet and was purged on the ground with 120°F dry nitrogen for thermal conditioning the Centaur Propulsion and H₂O₂ System components. Venting was accomplished through 90 square inches distributed in nine vents distributed around the circumference of the CSS just forward of the CSS conical boattail.

Compartment 6, the Titan Forward Skirt compartment, had a volume of 338 cubic feet. This compartment is vented through two ducts which lead to four vents (total 40 square inches) which are located at the same vehicle station as the Centaur Interstage compartment vents. The vents for the two compartments were co-station in order to minimize the differential pressure across the Thermal Barrier which separated the two compartments. The Thermal Barrier was required because Compartment 6 was conditioned on the ground with 70°F air.

As mentioned, the CSS Ascent Vent System was passive. All vents, except one, were rectangular in shape and contained fiberglass honeycomb inserts which were canted aft at 30 degrees. The only peculiar vent was the Compartment 4 vent which was five circular holes in the LH₂ Fill and Drain Valve Chute Door.

The TC-2 measured internal compartment pressures as a function of flight time for Compartments 2/3, 4, 5 and 6 are shown in Figures 45, 46, 47, 48, respectively. Shown with the TC-2 flight values are curves of preflight estimates and TC-1 Proof Flight data. For all four compartments, the agreement of TC-2 flight data with preflight estimates and TC-1 flight data were quite good. There is a time bias between flights and the preflight estimates due to actual trajectory flown. Compartment 4A pressure data are not presented. For TC-2, this compartment was vented to minimize differential pressure across the Centaur Equipment Module. Flight data indicate this was the case. Compartment 4A pressures were within 0.1 psi of Compartment 2/3 pressures during the flight.

A better indication of how well the Ascent Vent System functioned in flight is the comparison of compartment differential pressures rather than individual compartment internal pressures. The differential pressure across the CSS Forward Seal, the Centaur Stub Adapter, the Centaur Equipment Module, the CSS Aft Seal and the Thermal Barrier as a function of TC-2 flight time are shown in Figure 49.

The CSS Forward Seal differential pressures (Compartment 4-Compartment 2/3) agree well with TC-1 flight data and the preflight estimate. Again, a time bias exists because of the actual trajectory flown. The maximum values were -0.05 psid crush and +1.15 psid burst. Both values were well within the design limits of +2.8 psid burst and -1.6 psid crush.

CSS PAYLOAD/ELECTRONICS COMPARTMENT
COMPARTMENT 2/3

U.S. GOVERNMENT PRINTING OFFICE: 1964 10-1000
SPEECHES, DEBATES, AND DISCUSSIONS OF THE U.S. CONGRESS
AND OTHER PUBLIC DOCUMENTS

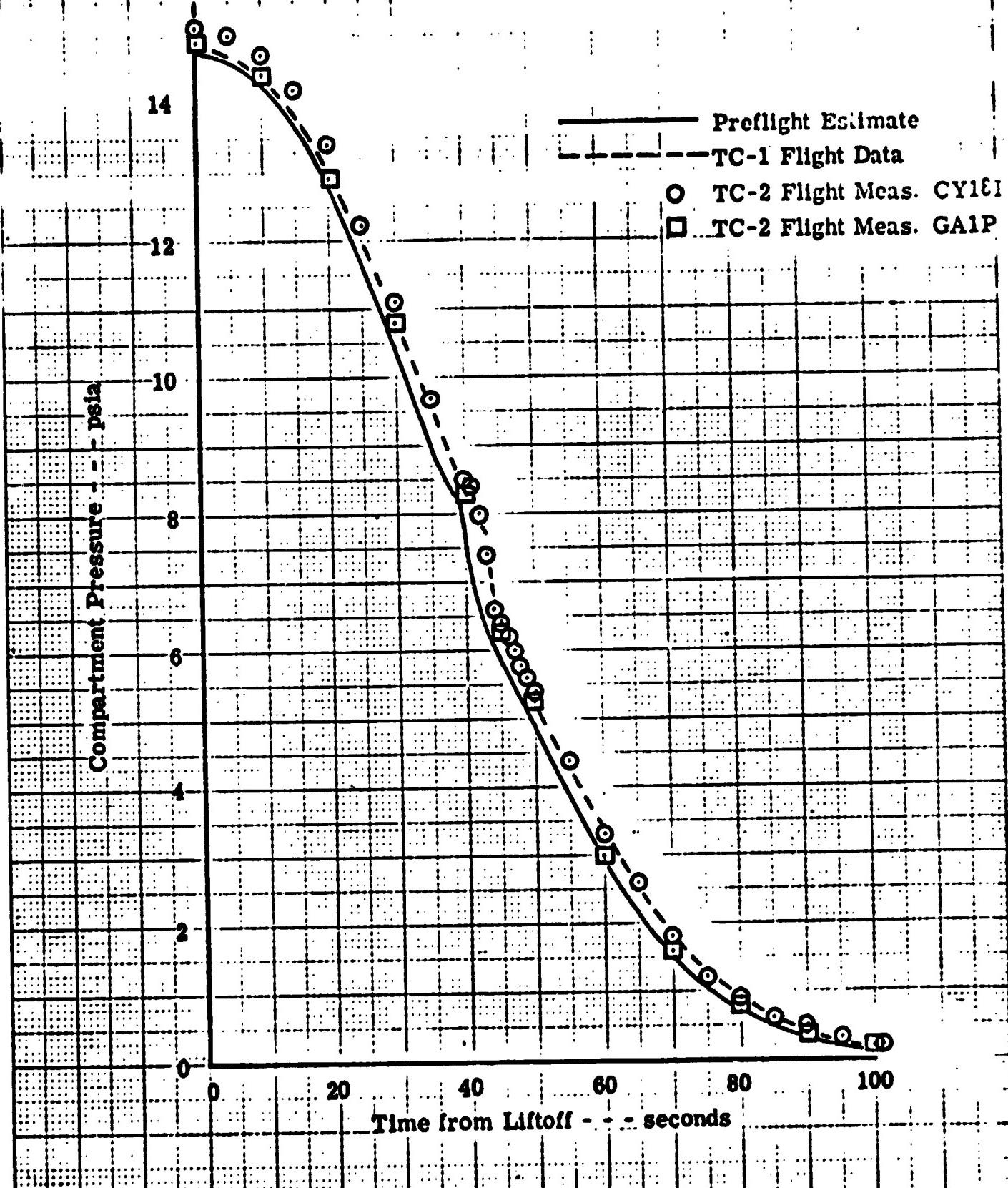
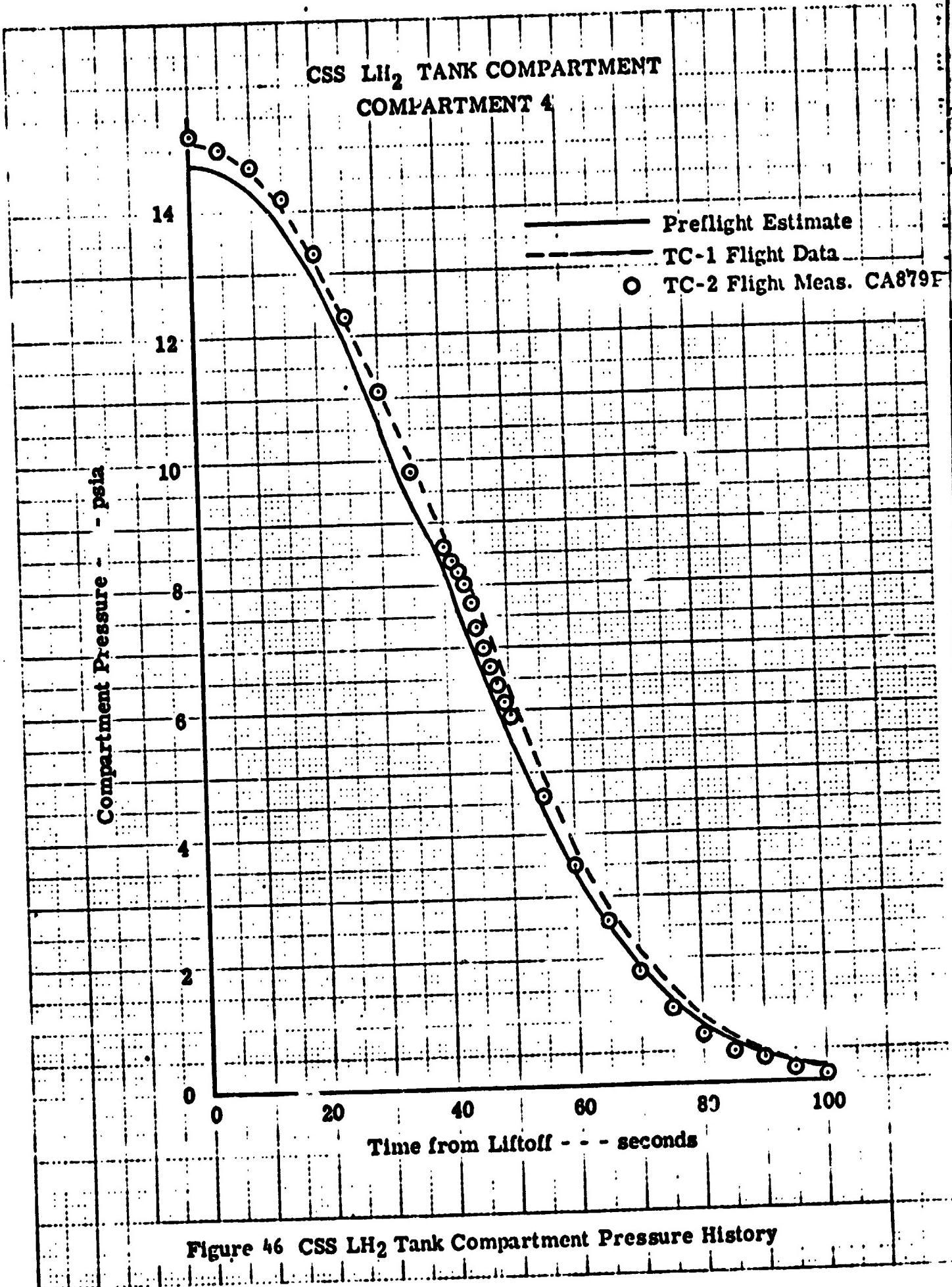


Figure 45 CSS Payload/Electronics Compartment Pressure History



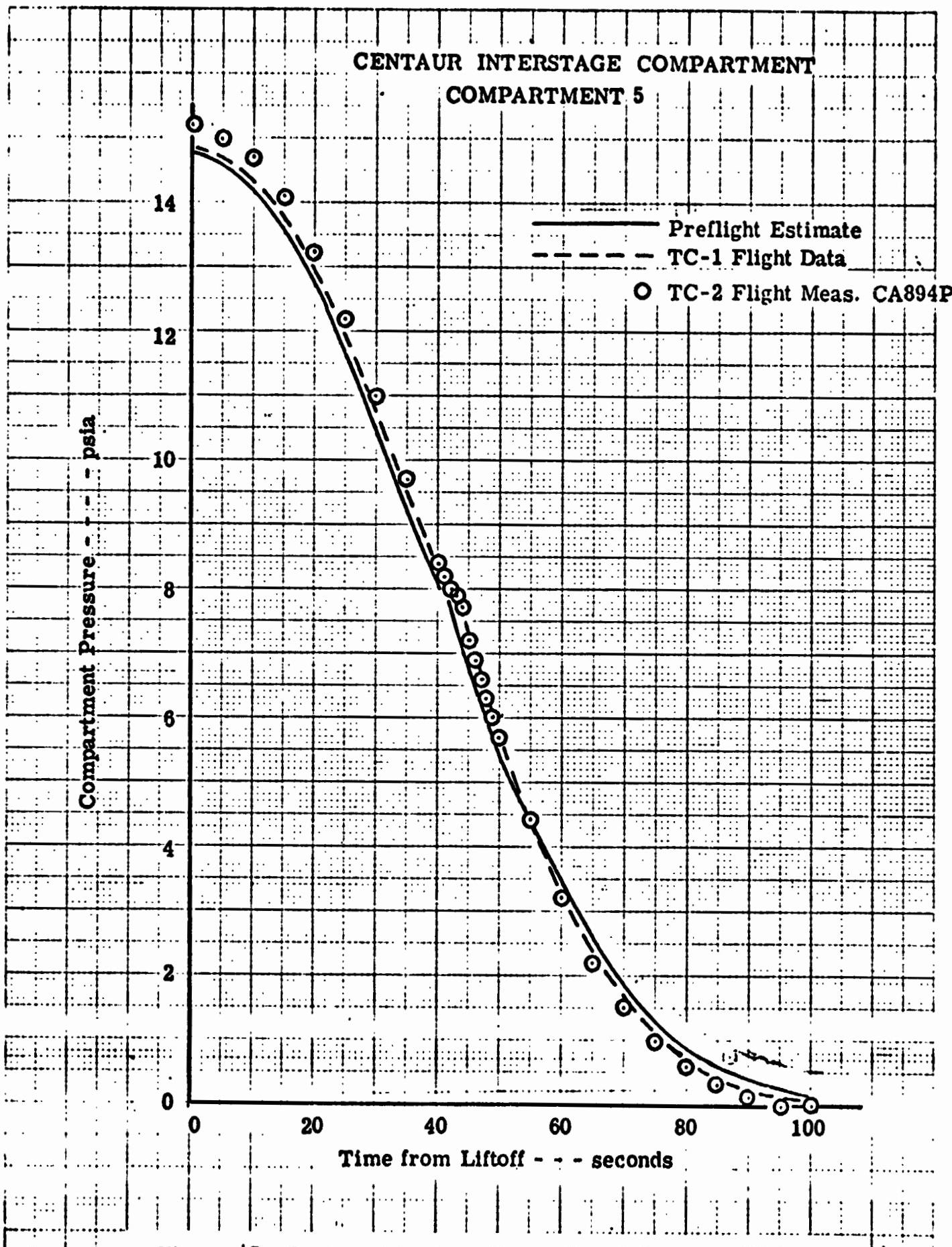


Figure 47 Centaur Interstage Compartment Pressure History

**TITAN FORWARD SKIRT COMPARTMENT
COMPARTMENT 6**

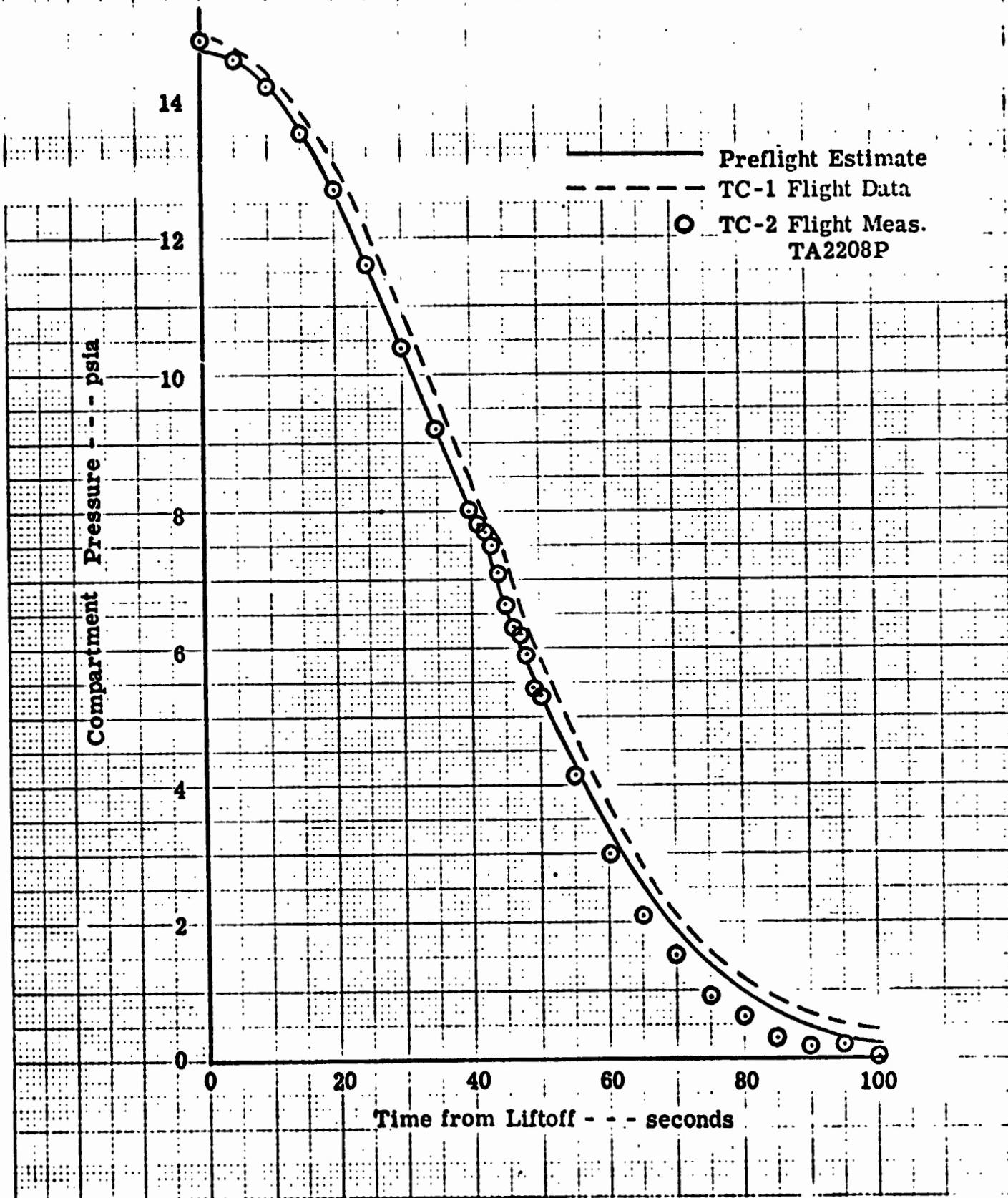


Figure 48 Titan Forward Skirt Compartment Pressure History

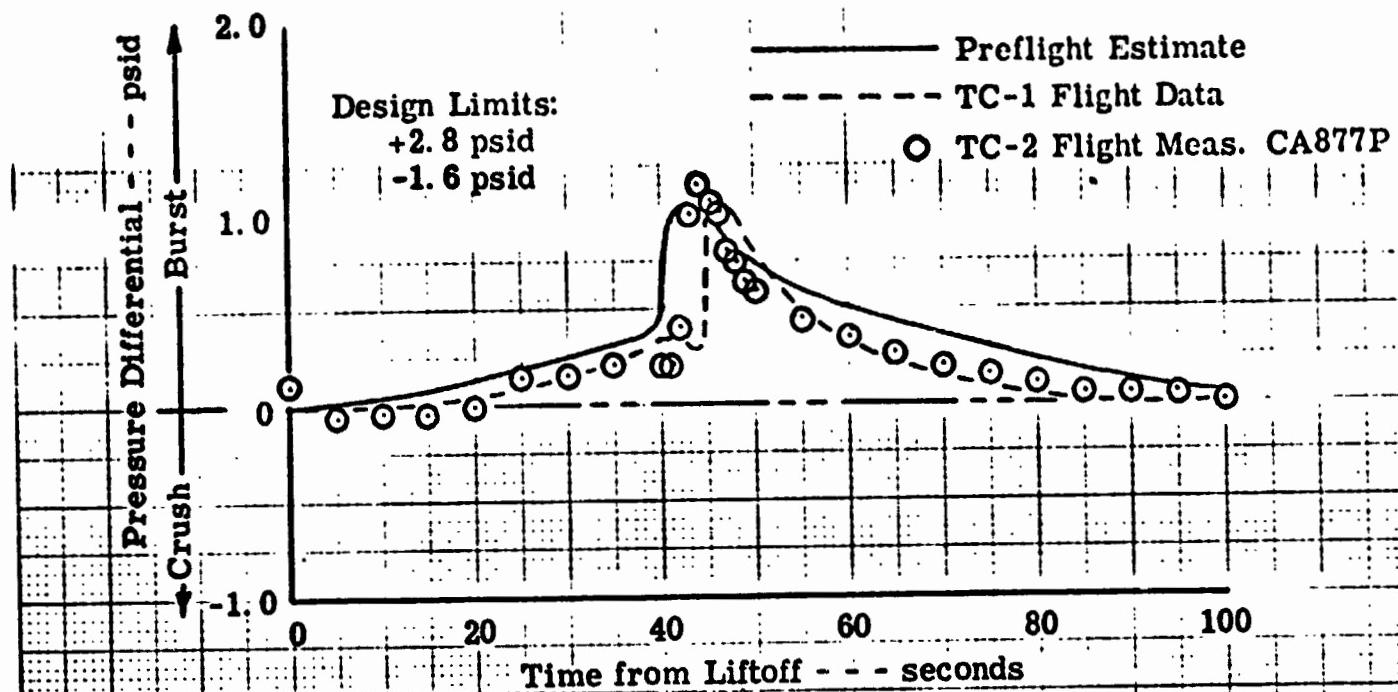
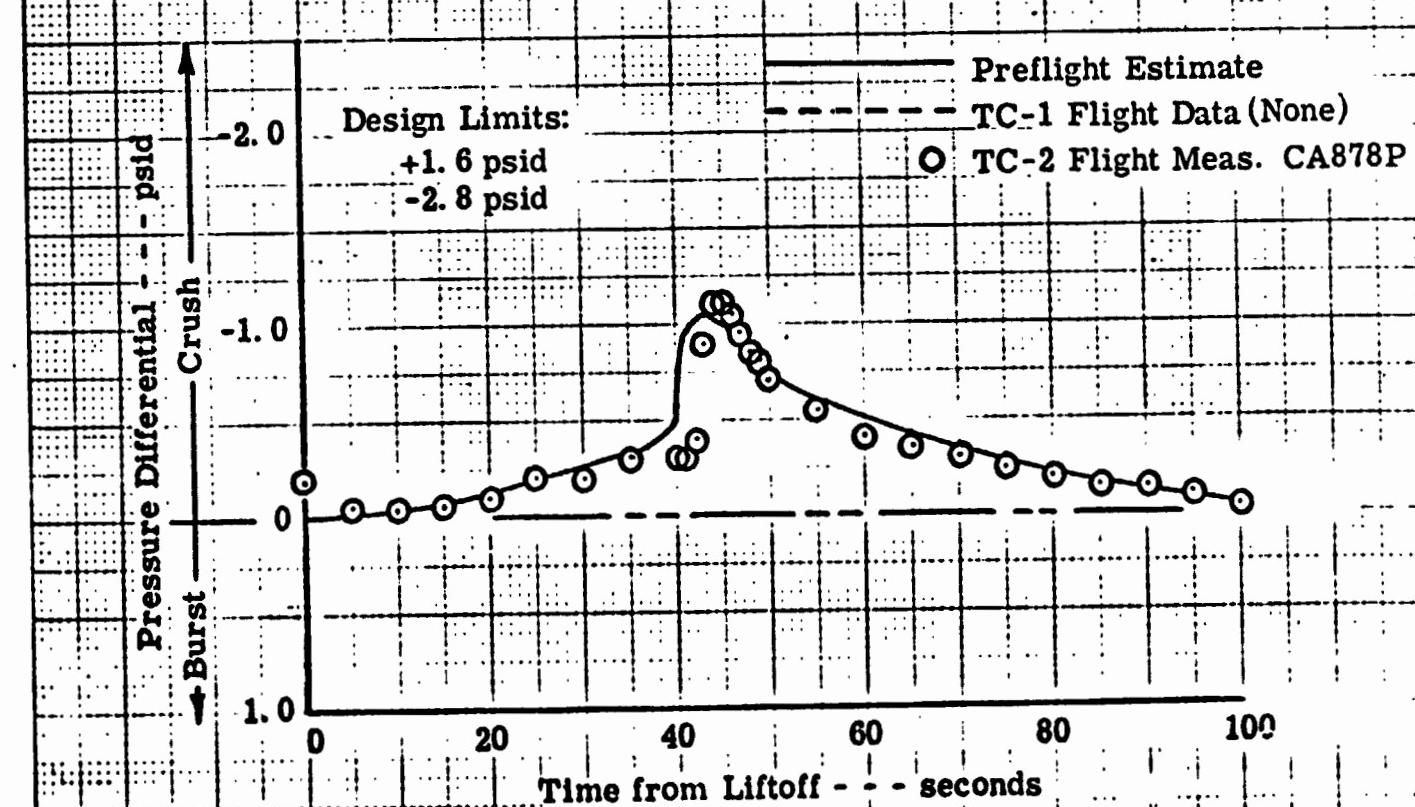
CSS FORWARD SEAL ΔP CENTAUR STUB ADAPTER ΔP 

Figure 49.1 Compartment Separator Differential Pressures

CENTAUR EQUIPMENT MODULE, ΔP

+1.0

Design Limits:
+0.20 psid
-0.06 psid

Preflight Estimate

TC-1 Flt. Data (None)

TC-2 Flight Meas.

CA882P

0

-1.0

0 20 40 60 80 100

Time from Liftoff - - - seconds

CSS AFT SEAL ΔP

+1.0

Design Limits:
+2.8 psid
-1.3 psid

Preflight Estimate

TC-1 Flight Data

TC-2 Flight Meas.

CA883P

-1.0

0 20 40 60 80 100

Time from Liftoff - - - seconds

THERMAL BARRIER ΔP

+1.0

Design Limits:
+1.3 psid
-1.0 psid

Preflight Estimate

TC-1 Flight Data

TC-2 Flight Meas.

TA2208P

0

0 20 40 60 80 100

Time from Liftoff - - - seconds

Figure 49.2

Compartment Separator Differential Pressures

The Centaur Stub Adapter differential pressures (Compartment 4A-Compartment 4) were identical to the Forward Seal data; i.e., no differential pressure across the Centaur Equipment Module, so burst pressures across the Forward Seal were crush pressures across the Stub Adapter. Flight data were well within the design limits of +1.6 psid burst and -2.8 psid crush and agreed well with the preflight estimate. TC-1 did not have a comparable Stub Adapter differential pressure because Compartment 4A was vented differently. On TC-1 with the payload mounted on a truss adapter directly to the Stub Adapter, Compartment 4A was vented directly into Compartment 4 in order to minimize crush pressure loading on the Stub Adapter. On TC-2 with the Helios A spacecraft mounted to the Centaur Equipment Module, Compartment 4A was vented into Compartment 3 in order to minimize crush pressure loading on the Equipment Module. This is a CSS Ascent Vent System mission peculiarity.

The differential pressure across the Equipment Module (Compartment 4A-Compartment 2/3) was essentially zero during flight. Again, there was no comparable measurement on TC-1 due to how Compartment 4A was vented.

The CSS Aft Seal differential pressures (Compartment 4-Compartment 5) were less than the preflight estimate and less than the TC-1 values. Maximum crush was -0.05 psid and the maximum burst was 0.35 psid. Both values were well within the design limits of +2.8 psid burst and -1.3 psid crush.

The maximum Thermal Barrier differential pressures (Compartment 5-Compartment 6) were -0.05 psid crush and +0.1 psid burst; well within the design limits of +1.3 psid burst and -1.0 psid crush.

Another indication of the performance of the CSS Ascent Vent System is the differential pressures across portions of the CSS, the Centaur Interstage Adapter, and the Titan Forward Skirt compartments. These data are presented in the report section entitled, CSS and Vehicle Aerodynamics.

The CSS Ascent Vent System also had a constraint to minimize the maximum rate of pressure decay in the spacecraft compartment during the transonic portion of flight. An expanded time plot of the spacecraft compartment (Compartment 2/3) internal pressures during the transonic is shown in Figure 50. As indicated in Figure 50, the maximum pressure decay rate was approximately -.75 psi/second. This value compares well with the preflight estimate of 0.89 psi/second and the TC-1 flight value of 0.75 psi/second. The time bias due to actual trajectory flown is again apparent in Figure 50.

The TC-2 Centaur Standard Shroud Ascent Vent System performed satisfactorily and as designed.

1. Compartment pressure time histories and compartment differential pressures agreed well with preflight estimates and with TC-1 flight data.
2. The spacecraft compartment maximum pressure decay rate during transonic agreed well with the preflight estimate and TC-1 flight data.

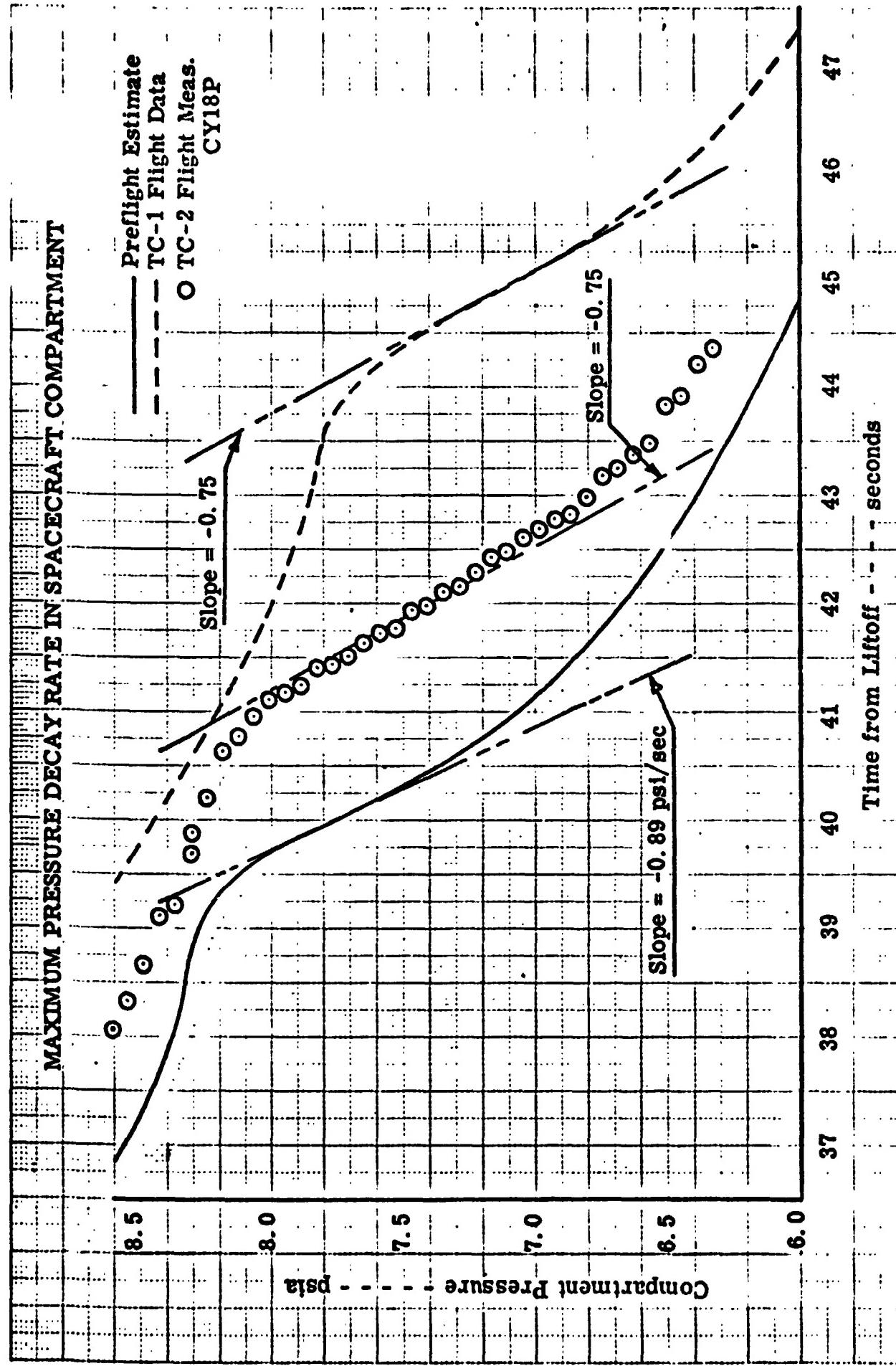


Figure 50 Maximum Pressure Decay Rate in Spacecraft Compartment During Transonic

CSS and Vehicle Aerodynamics

by J. C. Estes and M. L. Jones

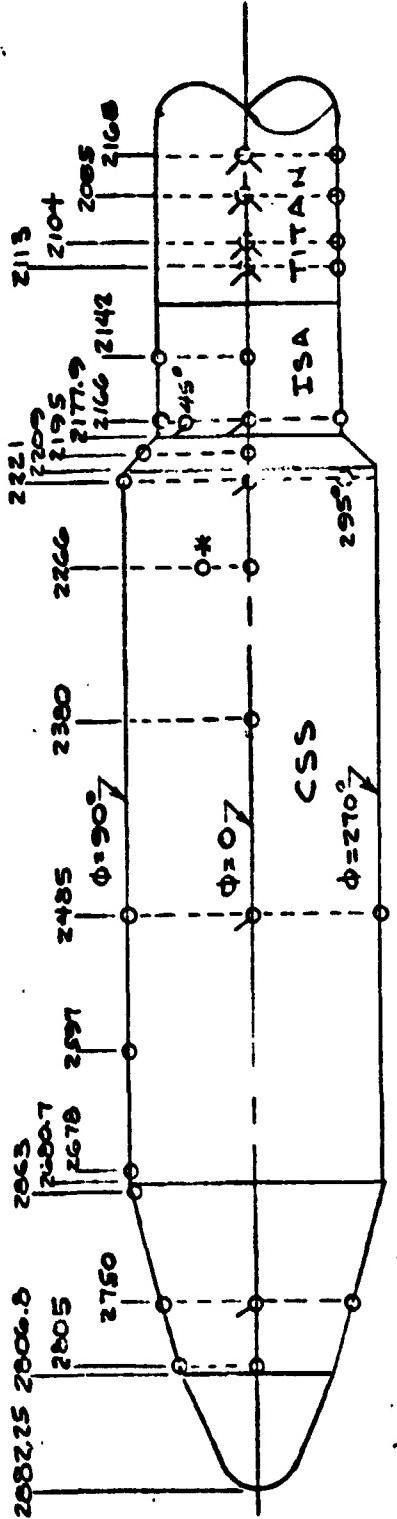
Aerodynamic Pressures - The location and the arrangement of the instrumentation used to measure the differential pressures across the walls of the CSS, the ISA and the Titan forward compartment are shown in Figure 51. The time history of these differential pressures is shown in Figure 52. Comparable data from the TC-1 flight are also shown on this figure. All differential pressures remained well below the design limits, which are included on the figure, throughout the atmospheric portion of the flight.

At Station 2678 measurement CA419P became noisy from approximately 32 to 36 seconds in the flight (Figure 52.4). The same phenomenon was observed on TC-1 and can probably be attributed to be a separated flow field at the cone/cylinder juncture (Station 2680.66) in the transonic speed range.

The proximity of the Titan forward compartment instrumentation to the solid rocket motors created a considerable amount of high frequency pressure oscillations. Consequently, the data shown for these measurements represent envelopes of the maximum burst and crush pressures.

It can be seen from the data at those stations where there was multiple instrumentation that there were only minor circumferential variations of pressure, indicating a very low vehicle angle of attack during the portion of the flight that had aerodynamic significance.

Aerodynamic Temperatures - Figure 53 shows the station and circumferential location of the 20 shroud and interstage adapter external temperature measurements. Time histories of the temperature measurements are shown in Figure 54. The TC-2 temperatures are generally lower than comparable measurements on the TC-1 flight. All flight measurements were well below the design temperatures used for the shroud heated jettison tests conducted at Plum Brook Station.



- * Located adjacent to LH₂ fill & drain valve door
- two locations - near & far sides
- one location - far side

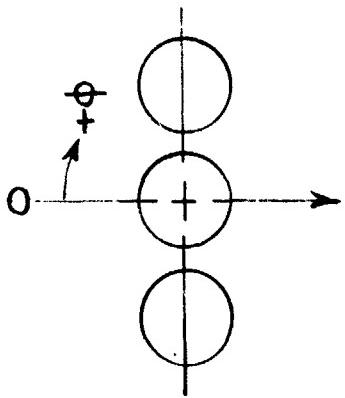


Figure 51 Location of CSS, ISA, & Titan Forward Compartment Differential Pressure Measurements

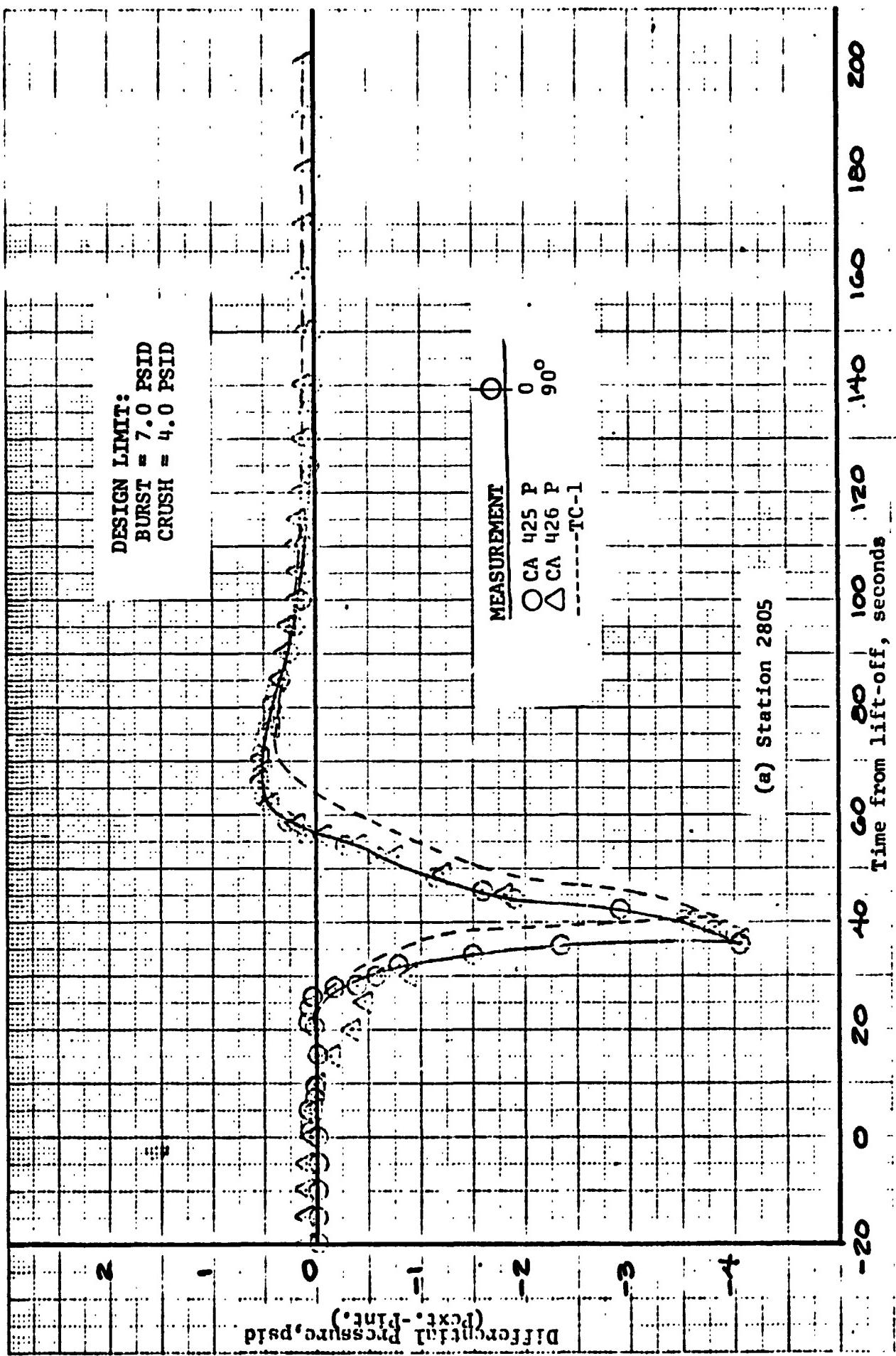


Figure 52.1 Vehicle Wall Differential Pressures,
52.1

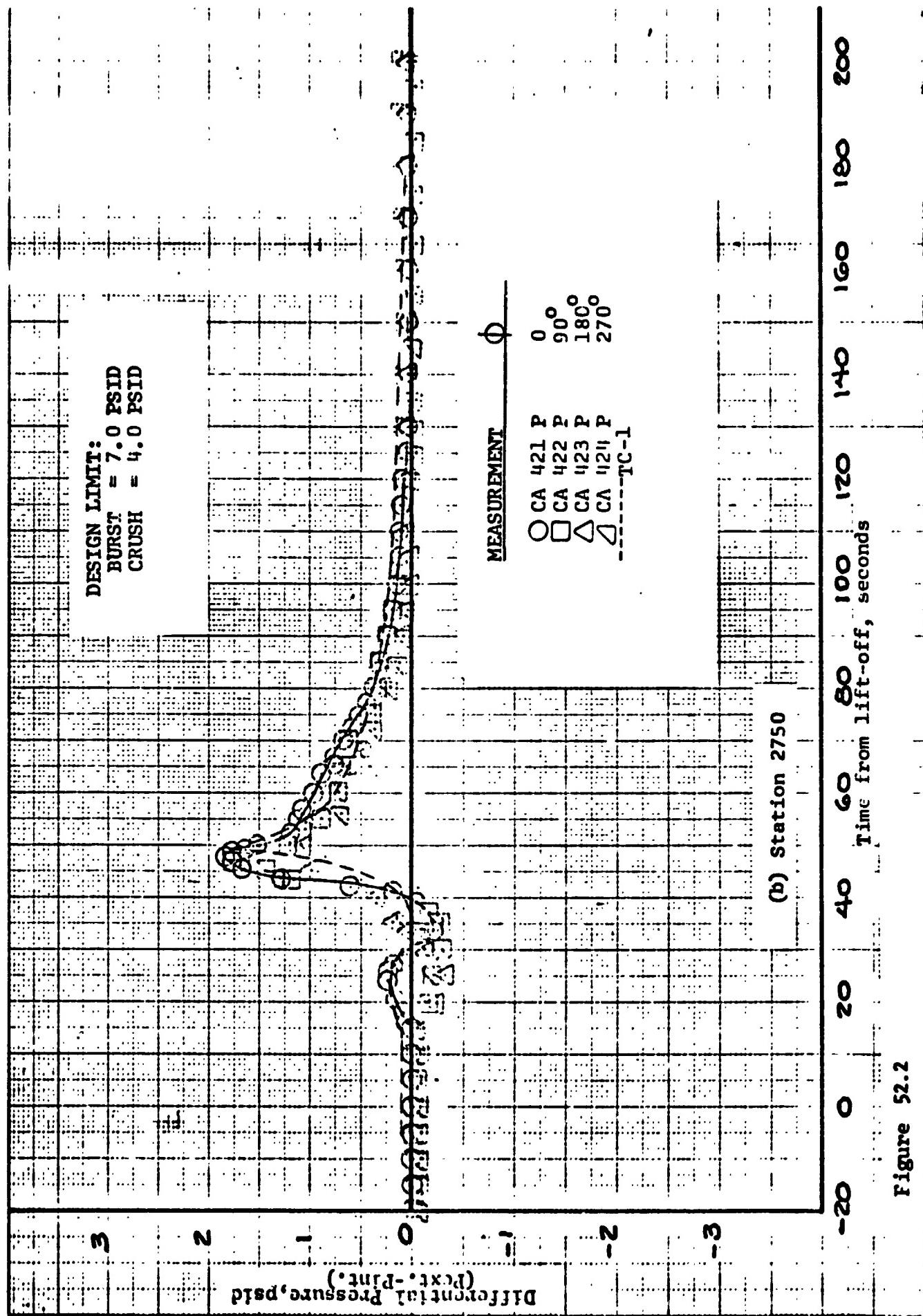


Figure 52.2

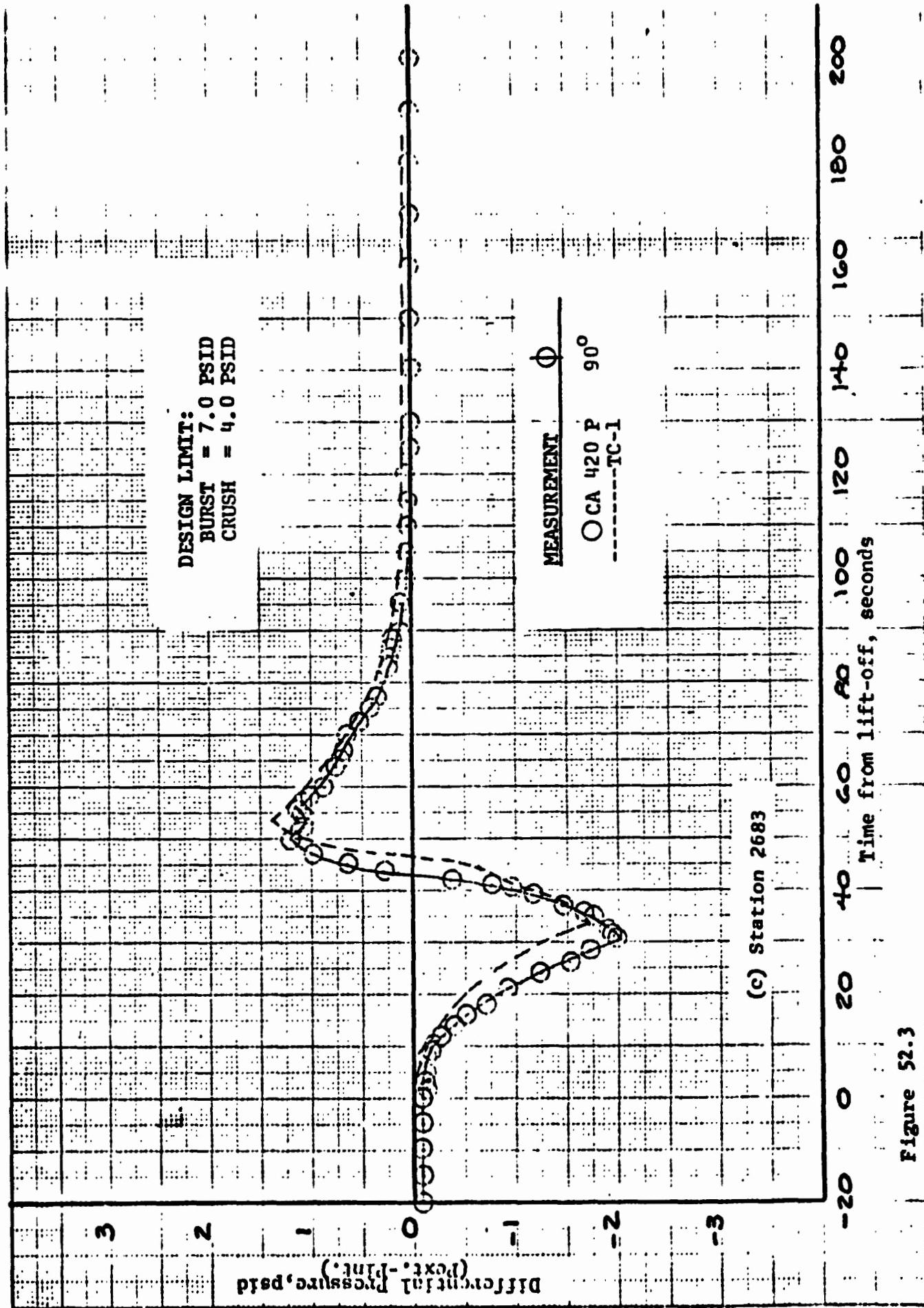


Figure 52.3

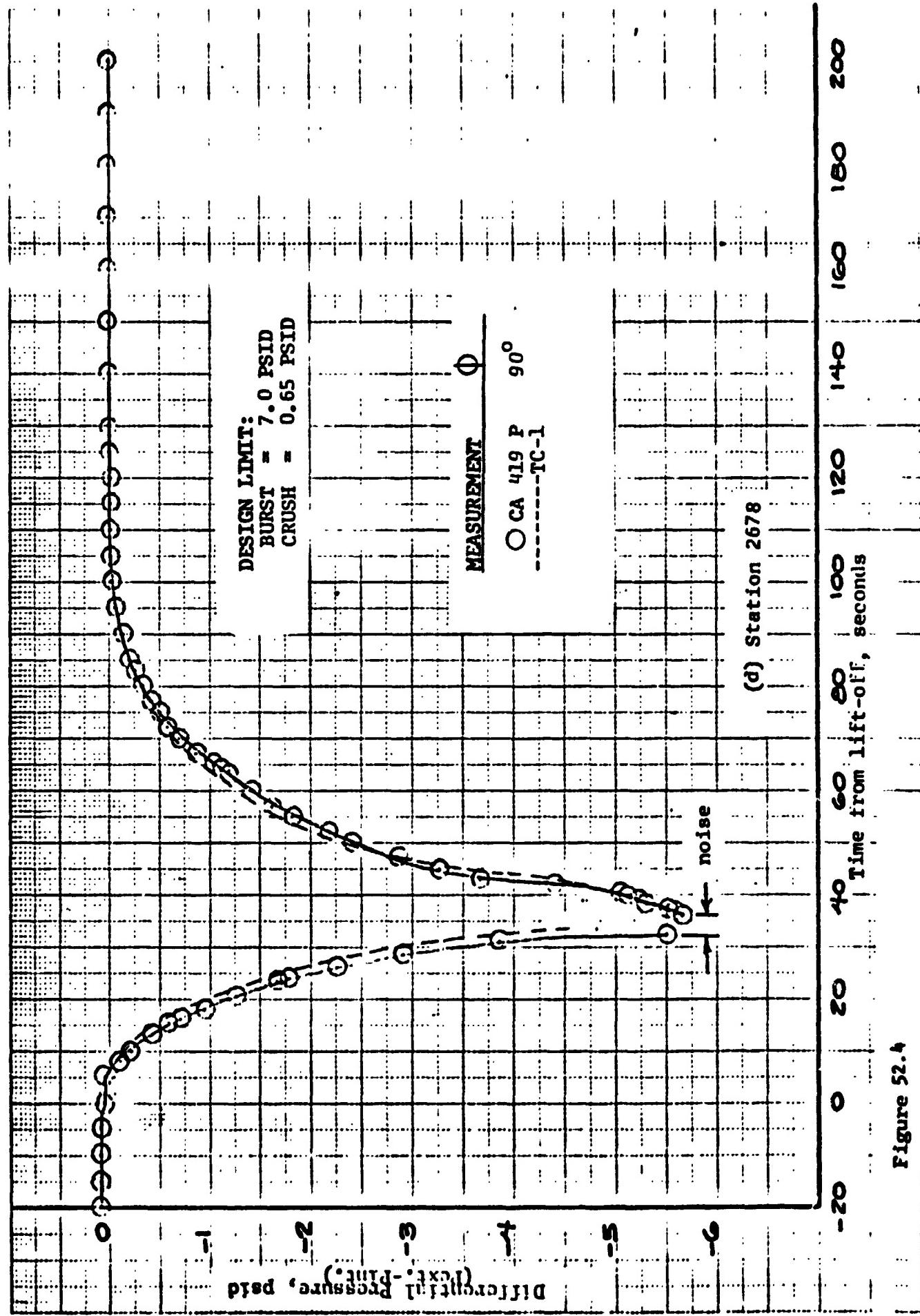


Figure 52.4

- K-E 10000 to the continuator 481513
10 x 1 cm

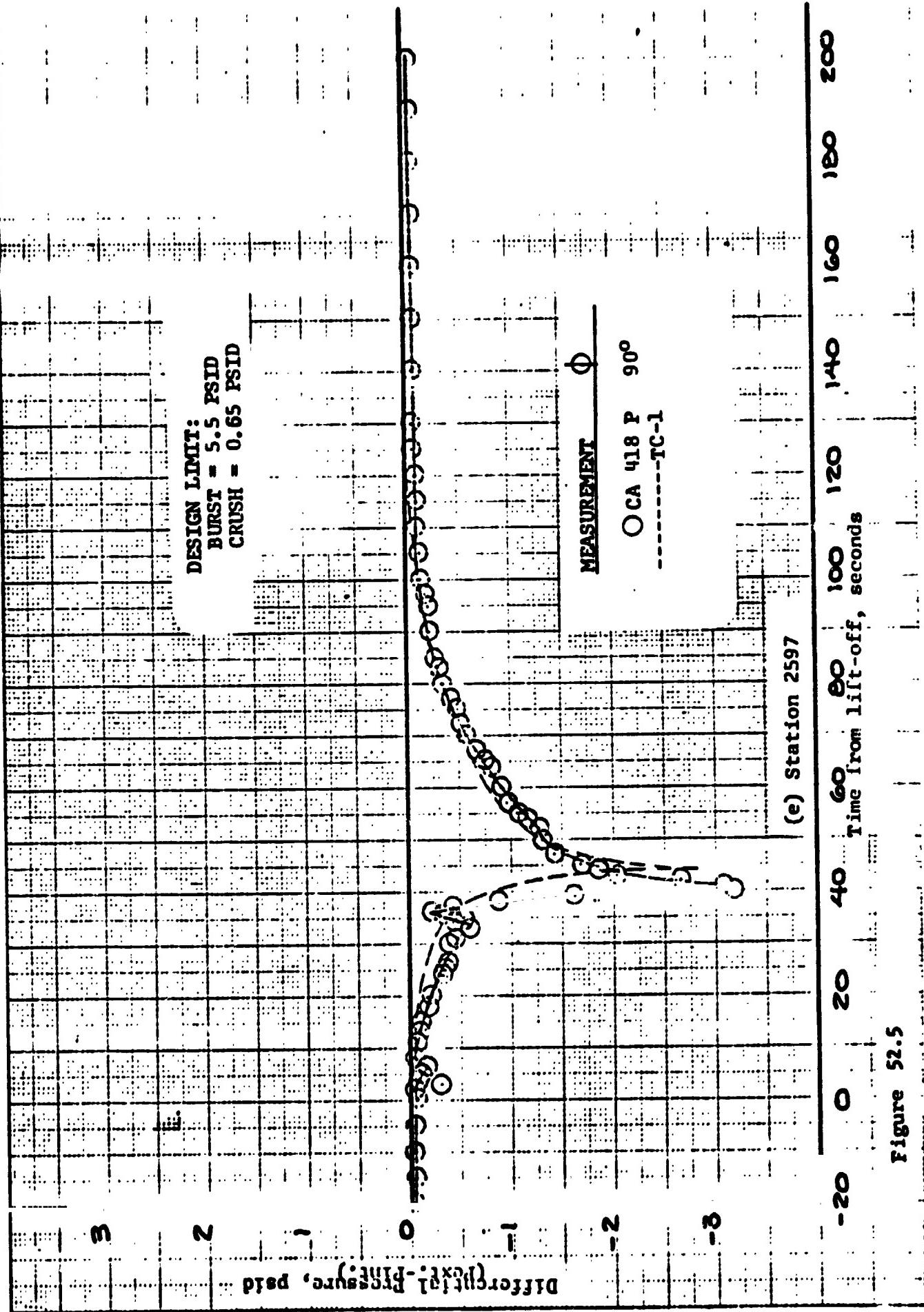


Figure 52.5

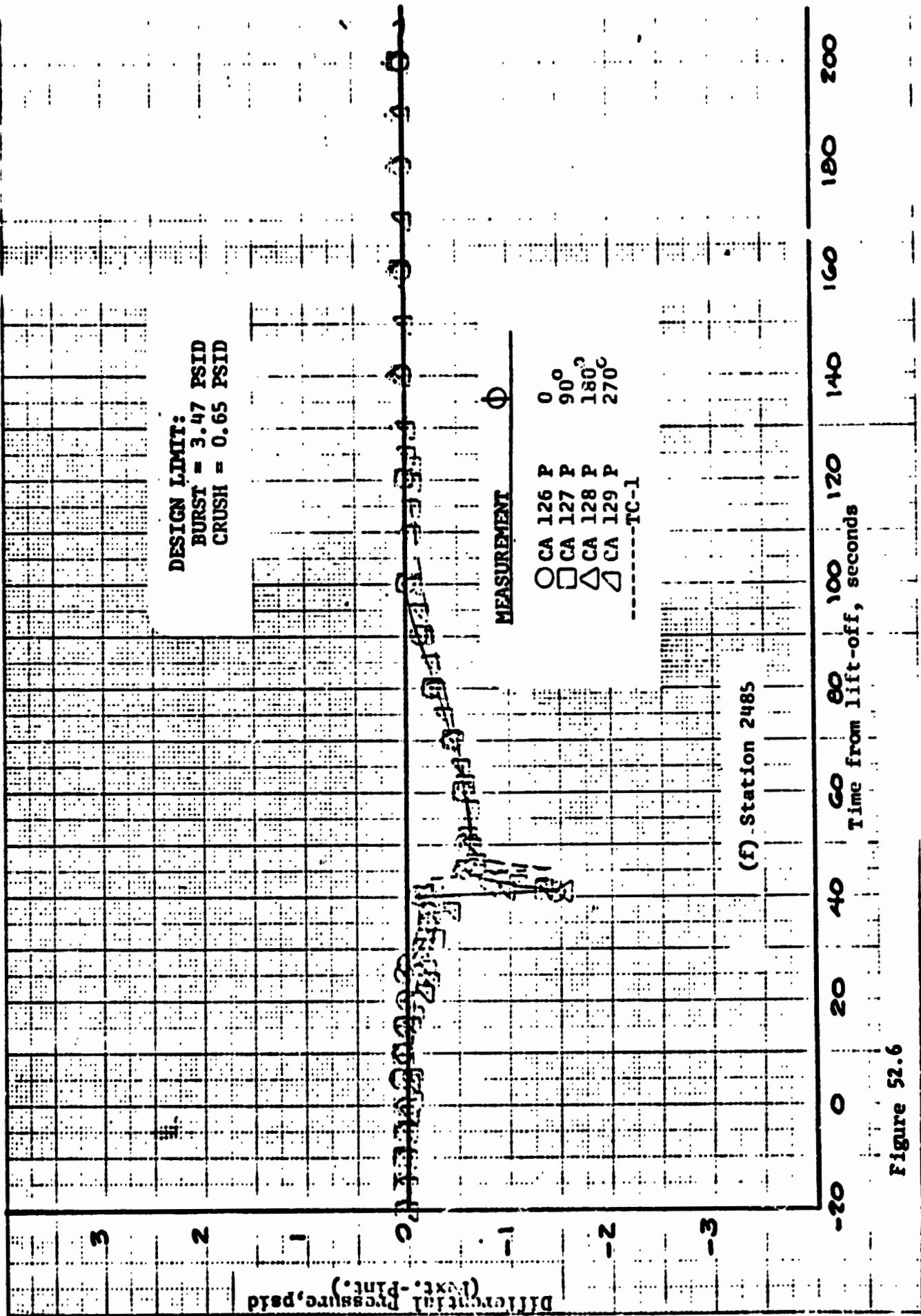


Figure 52.6

K-E 10' X 10' TO THE CENTERLINE 48 1913
KELPPEL & ECKER CO.

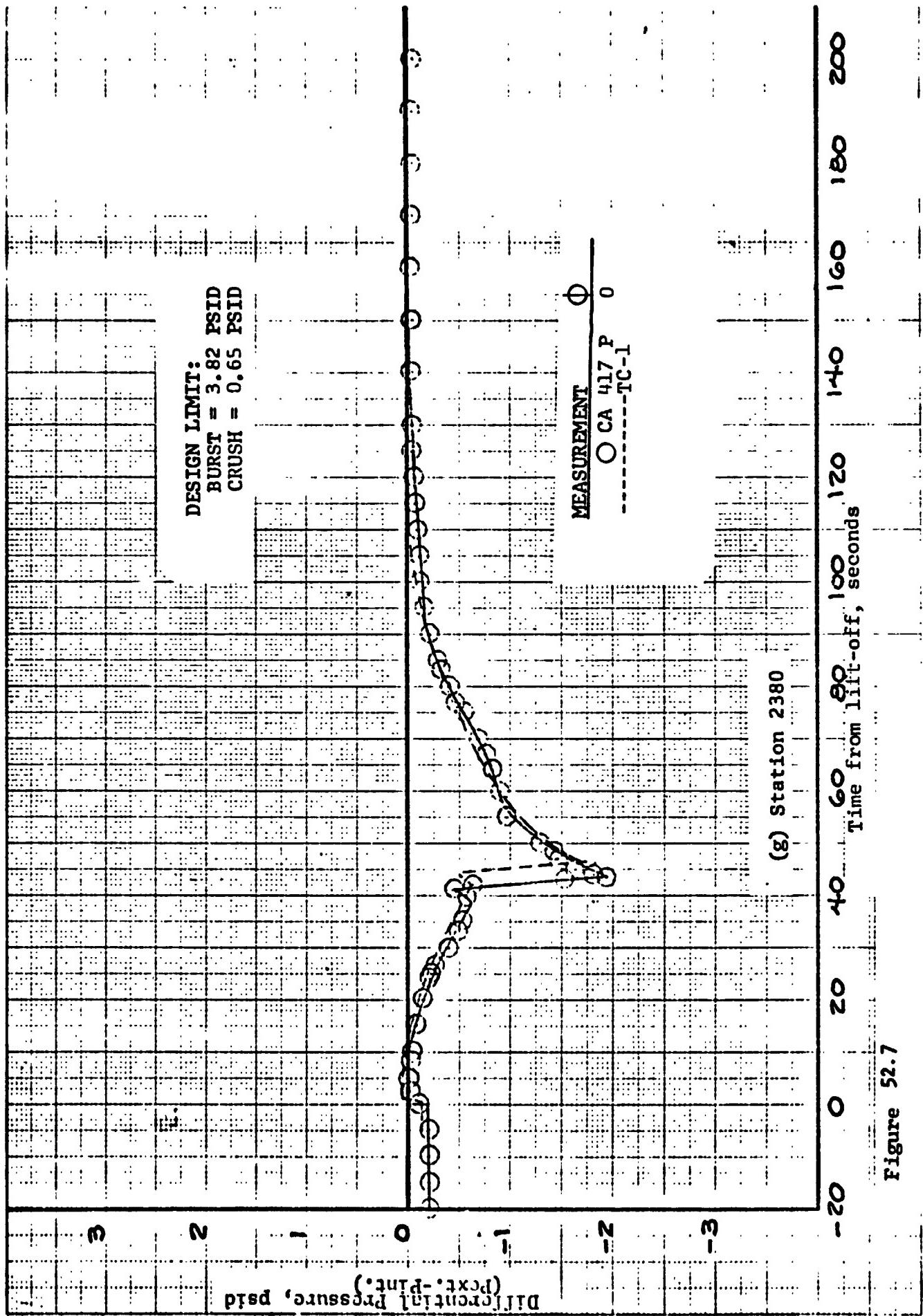


Figure 52.7

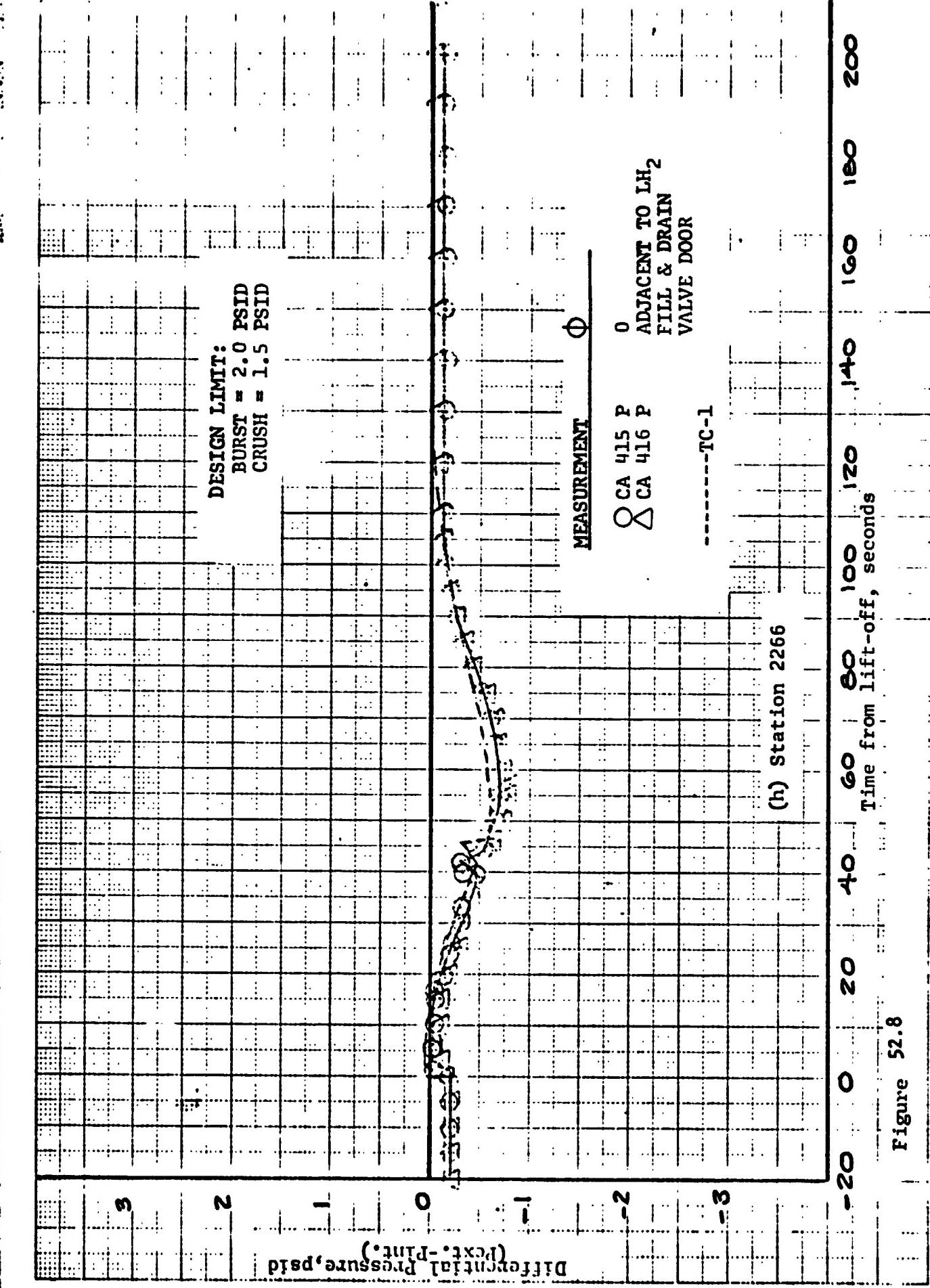


Figure 52.8

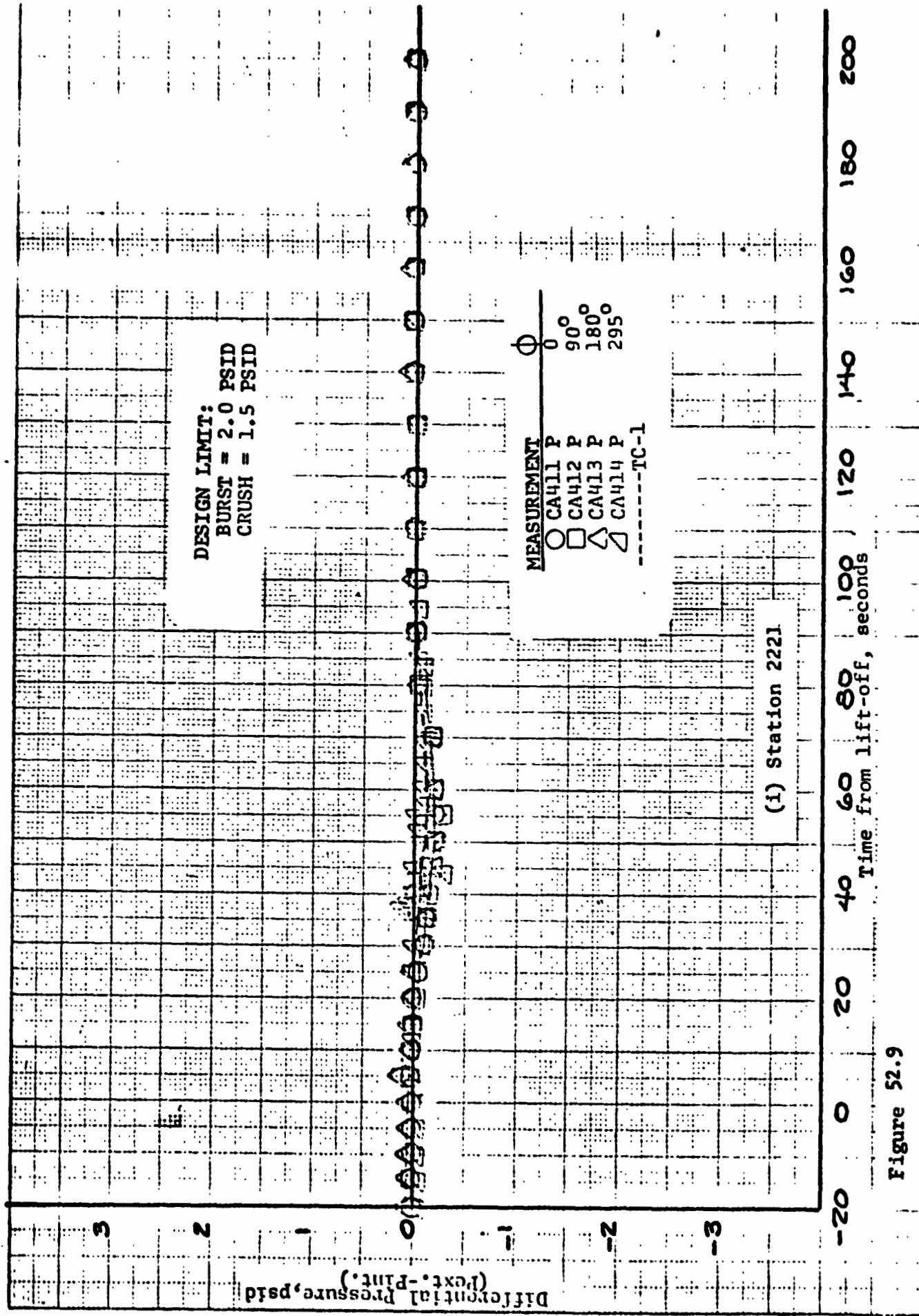


Figure 52.9

$\frac{1}{10}$ x 10 to THE CENTIMETER 40 1913
is 25 cm
KNUFFEL & ECKER CO.

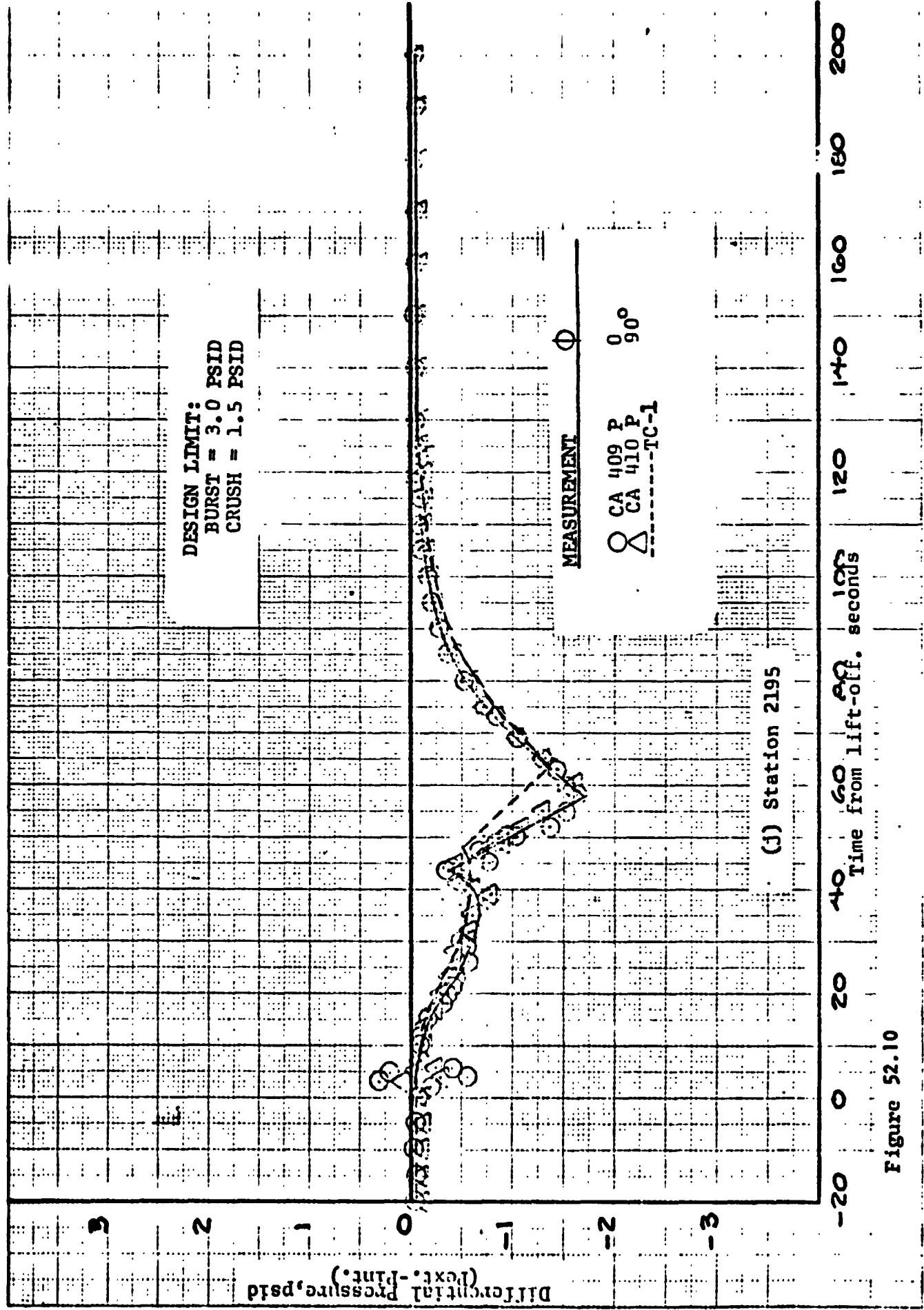


Figure 52.10

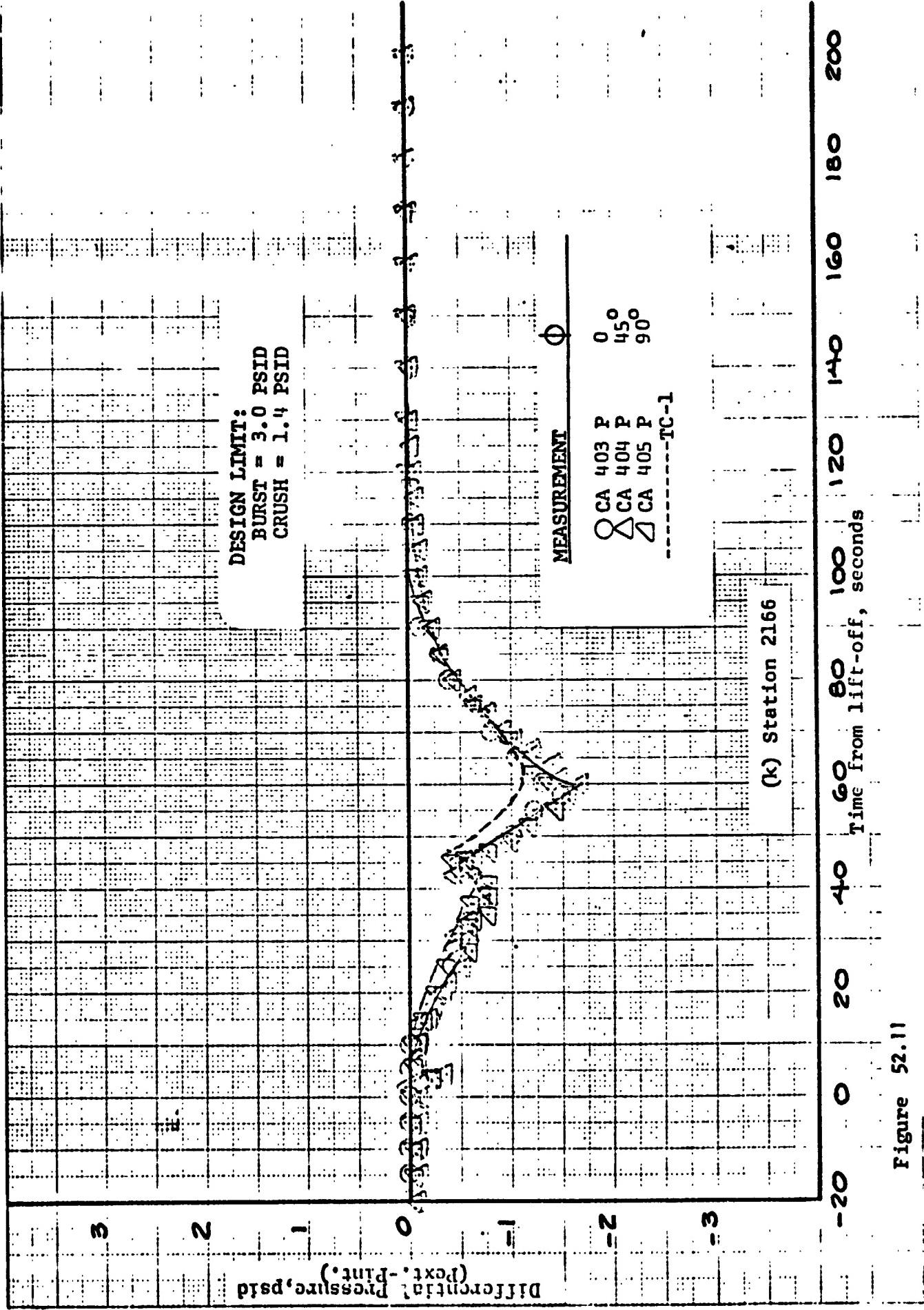


Figure 52.11

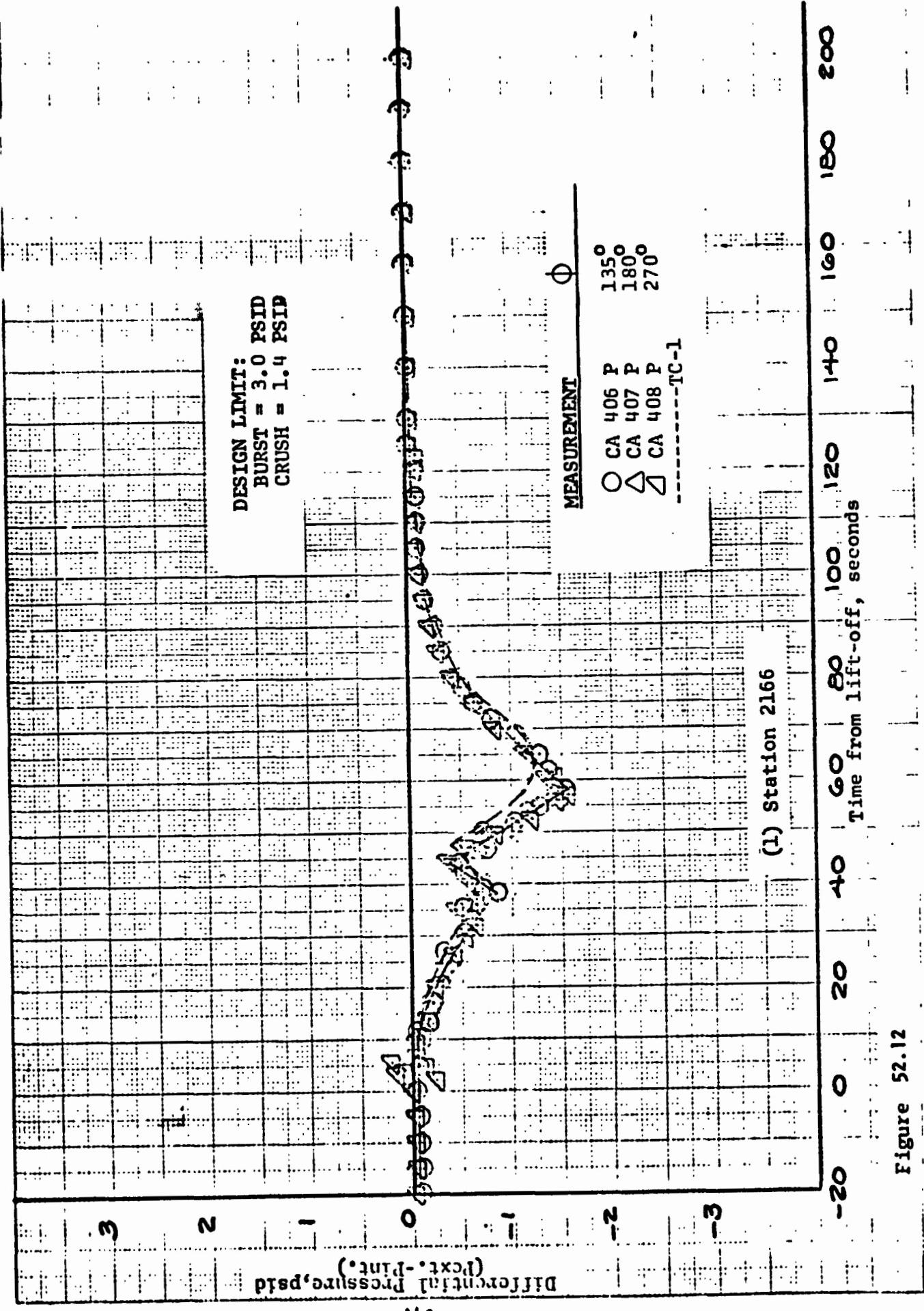


Figure 52.12

10⁻² TO THE CENTIMETER 48 1513
10⁻² CM
KELFELL & GREEN CO.

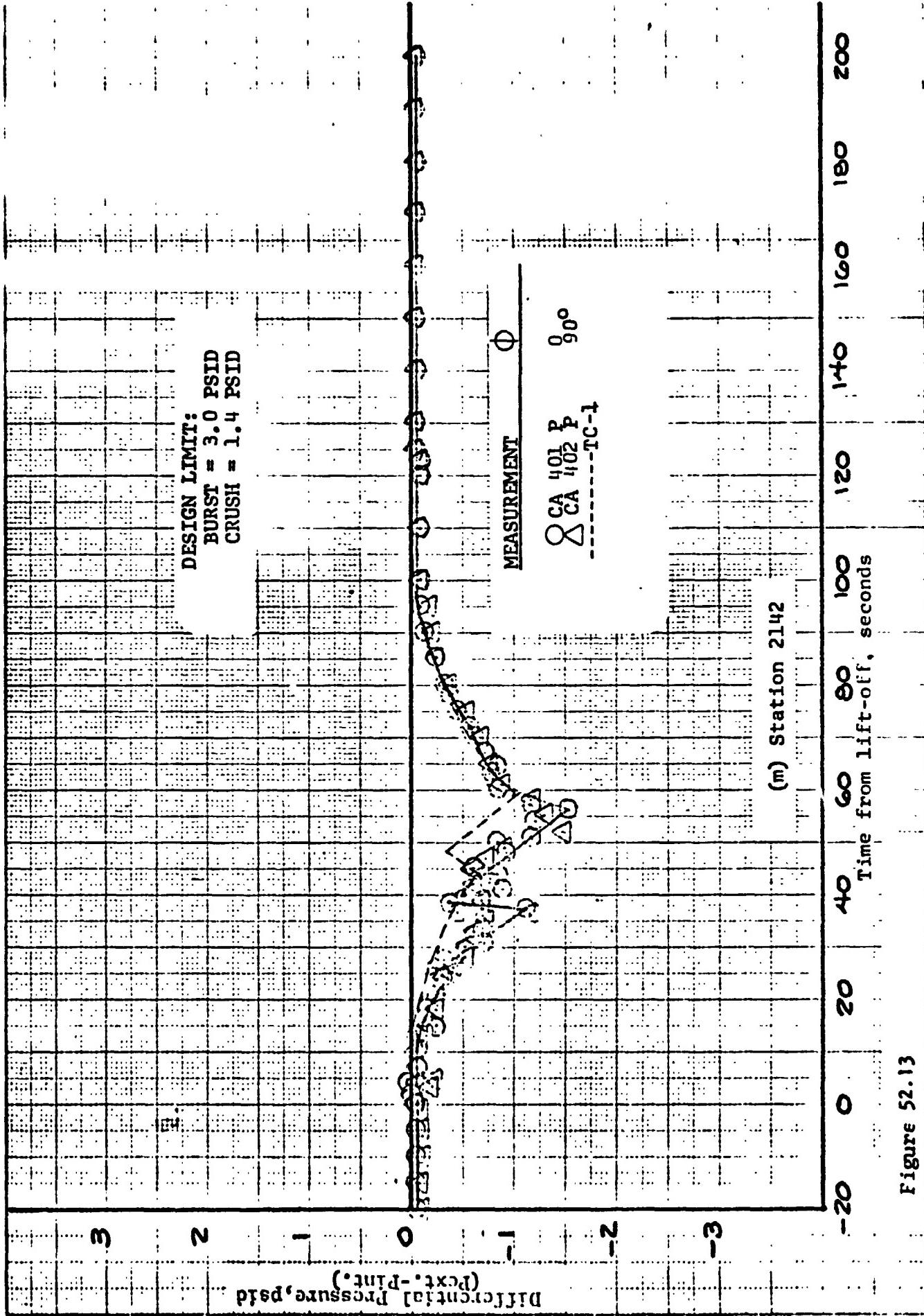


Figure 52.13

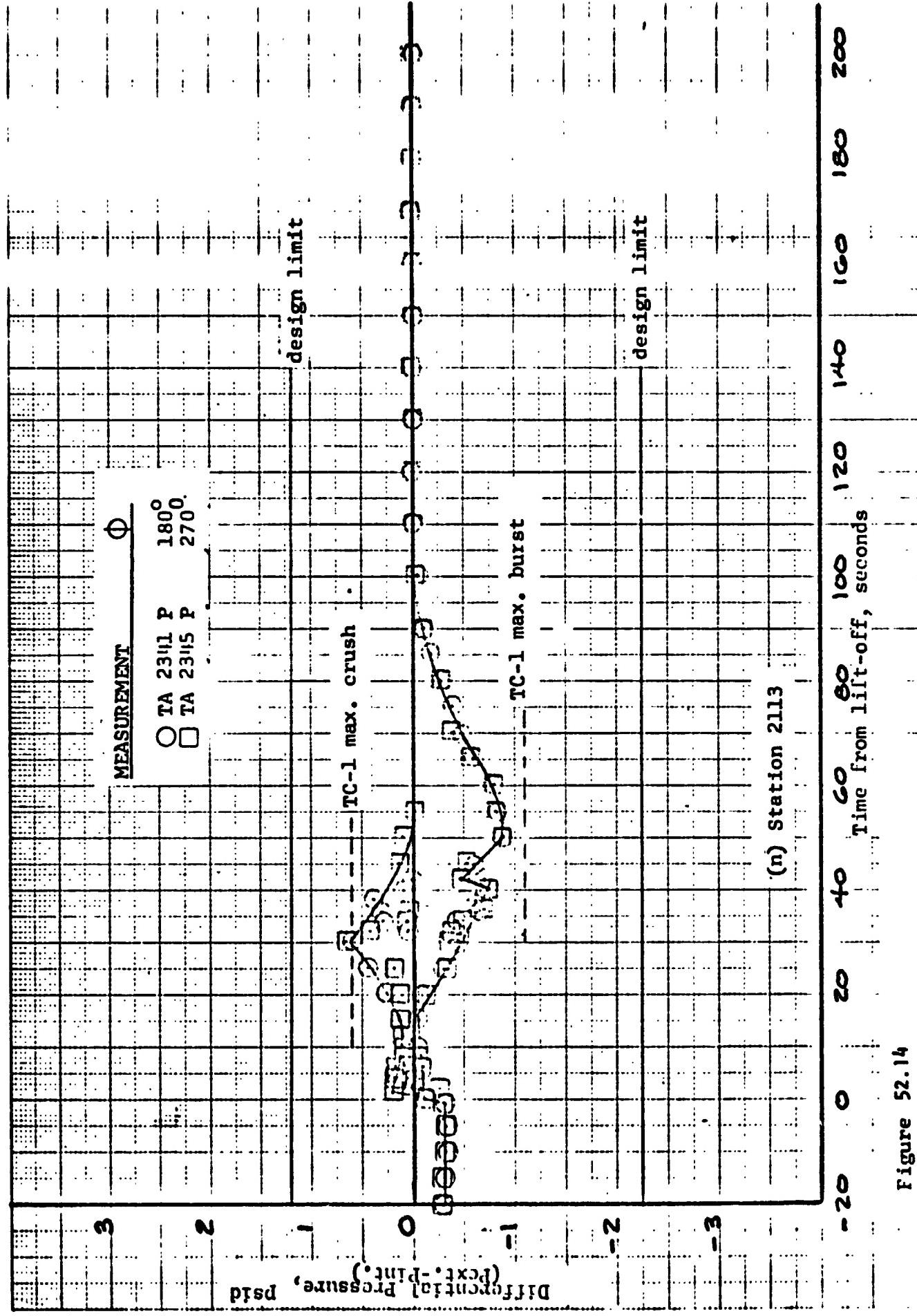


Figure 52.14

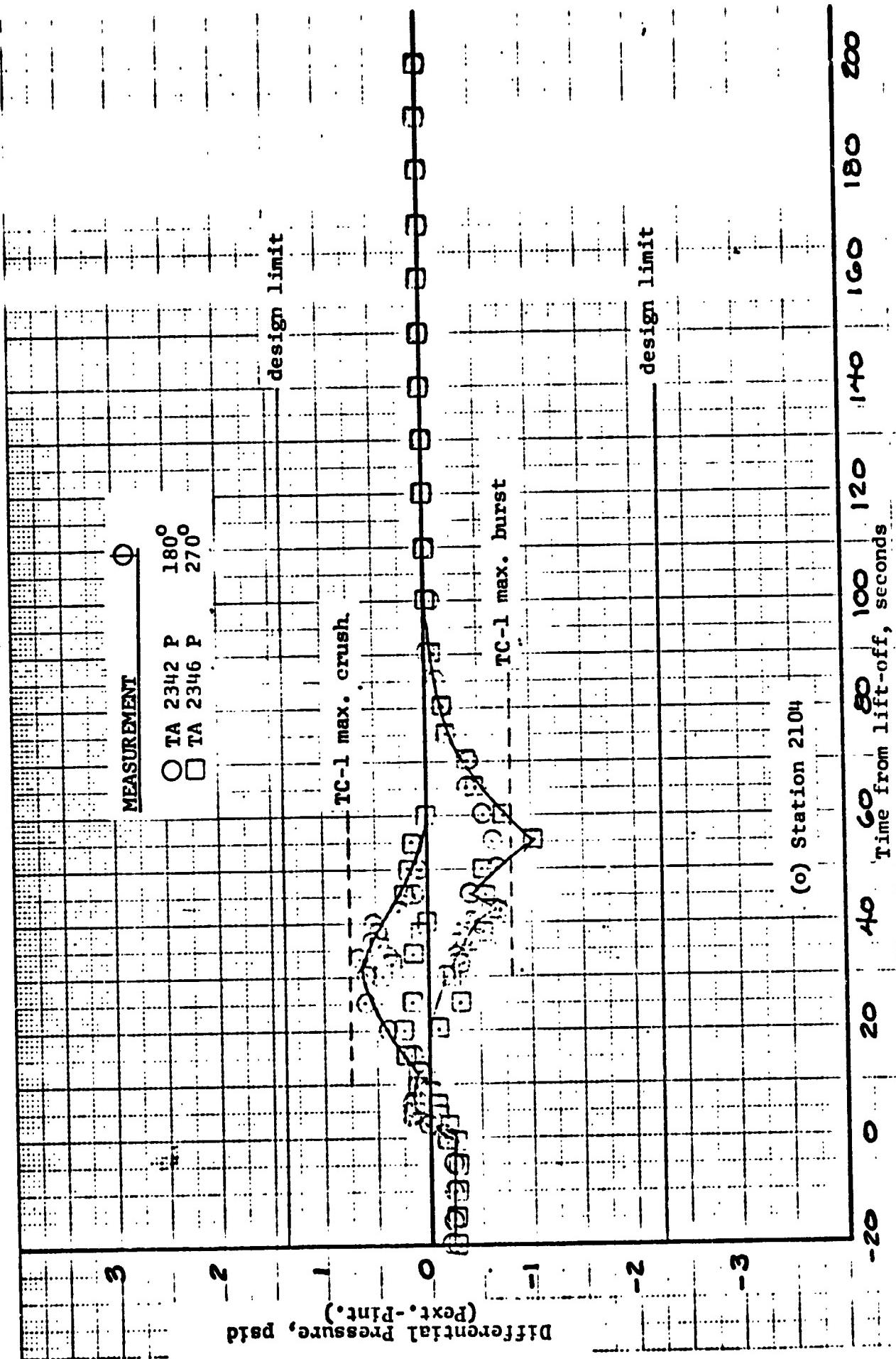


Figure 52.15

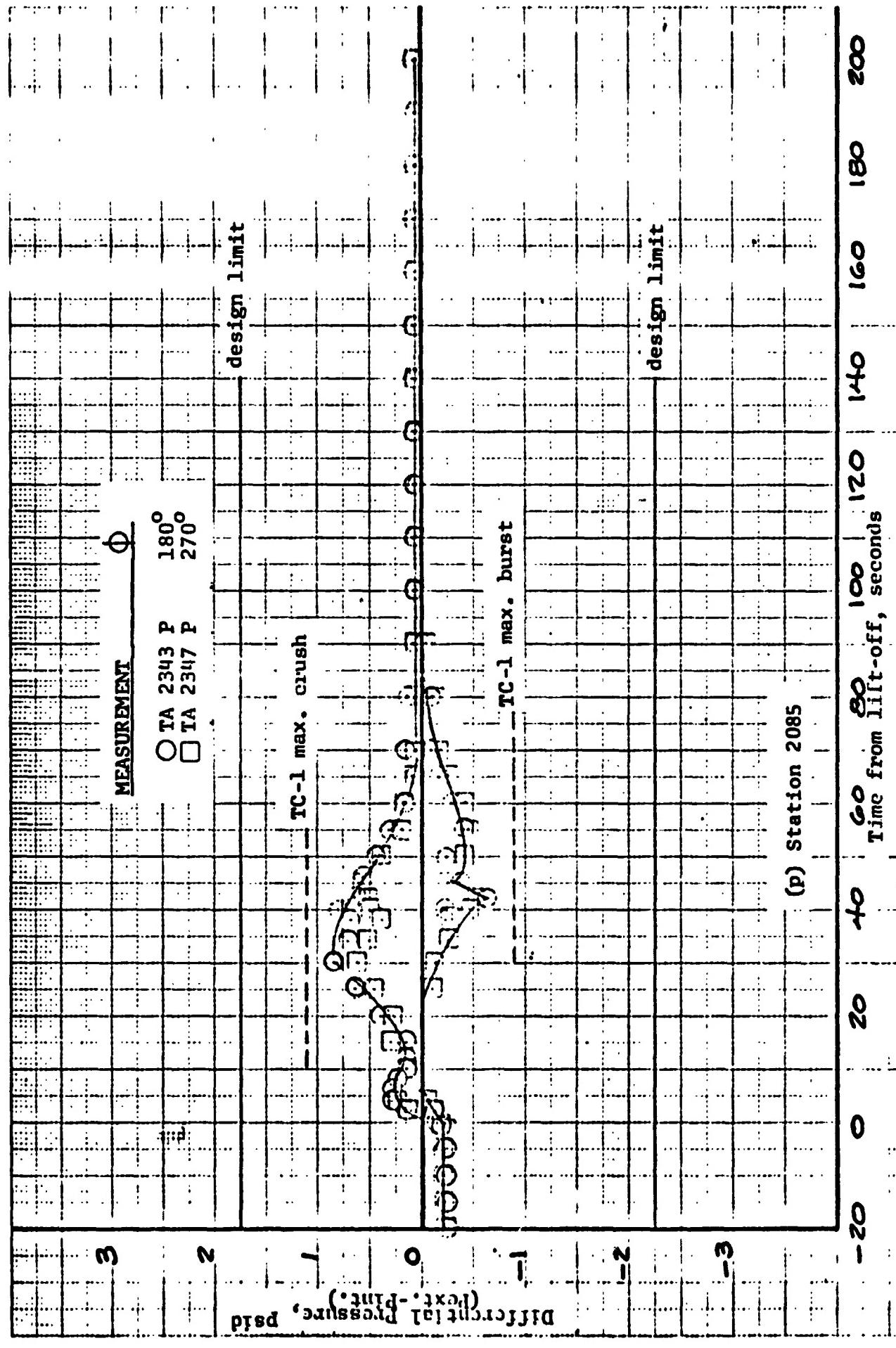


Figure 52.16

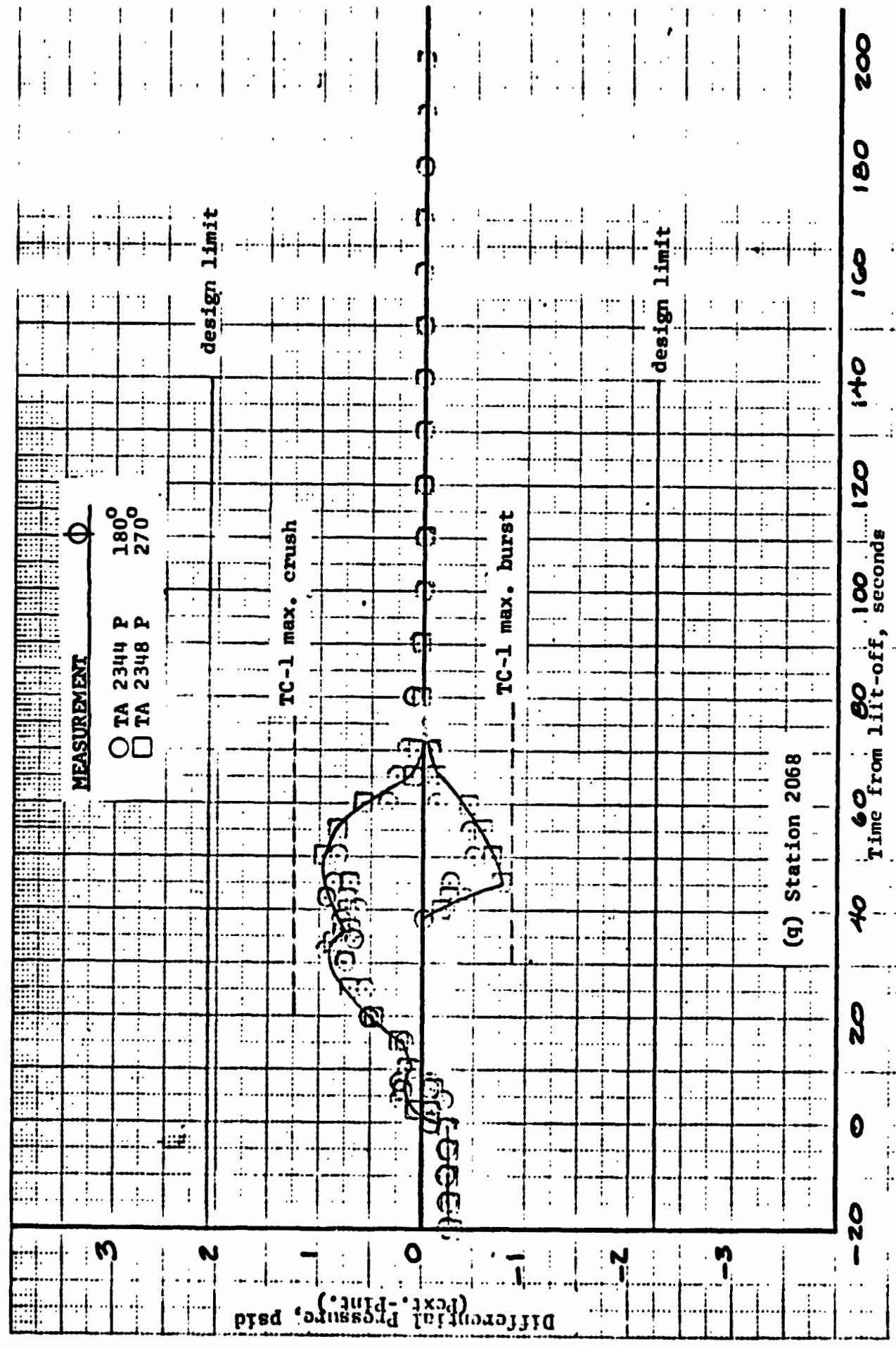


Figure 52.17

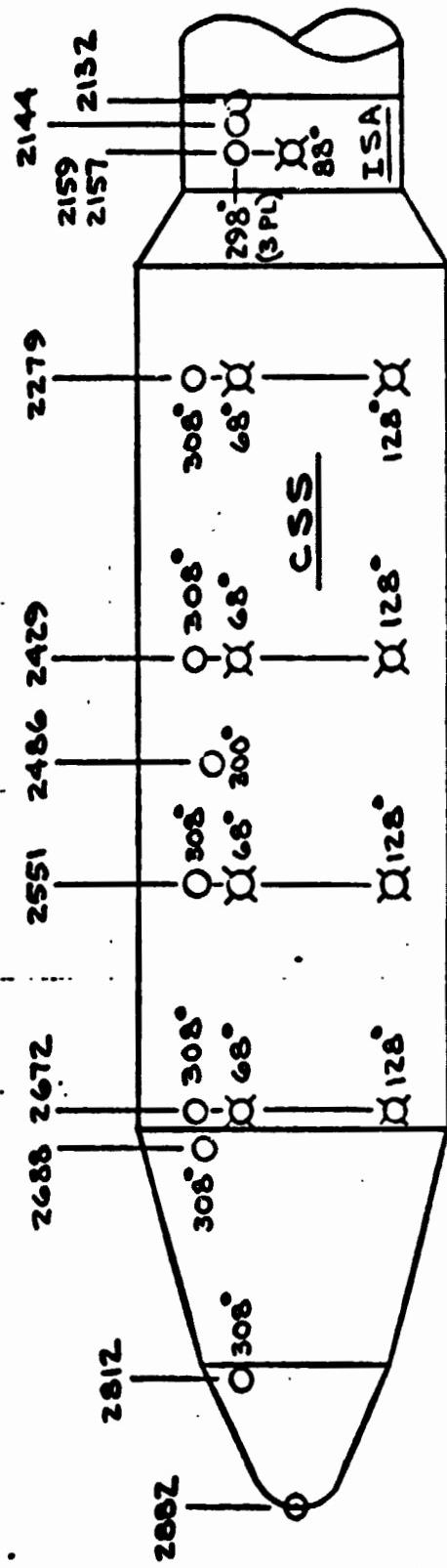
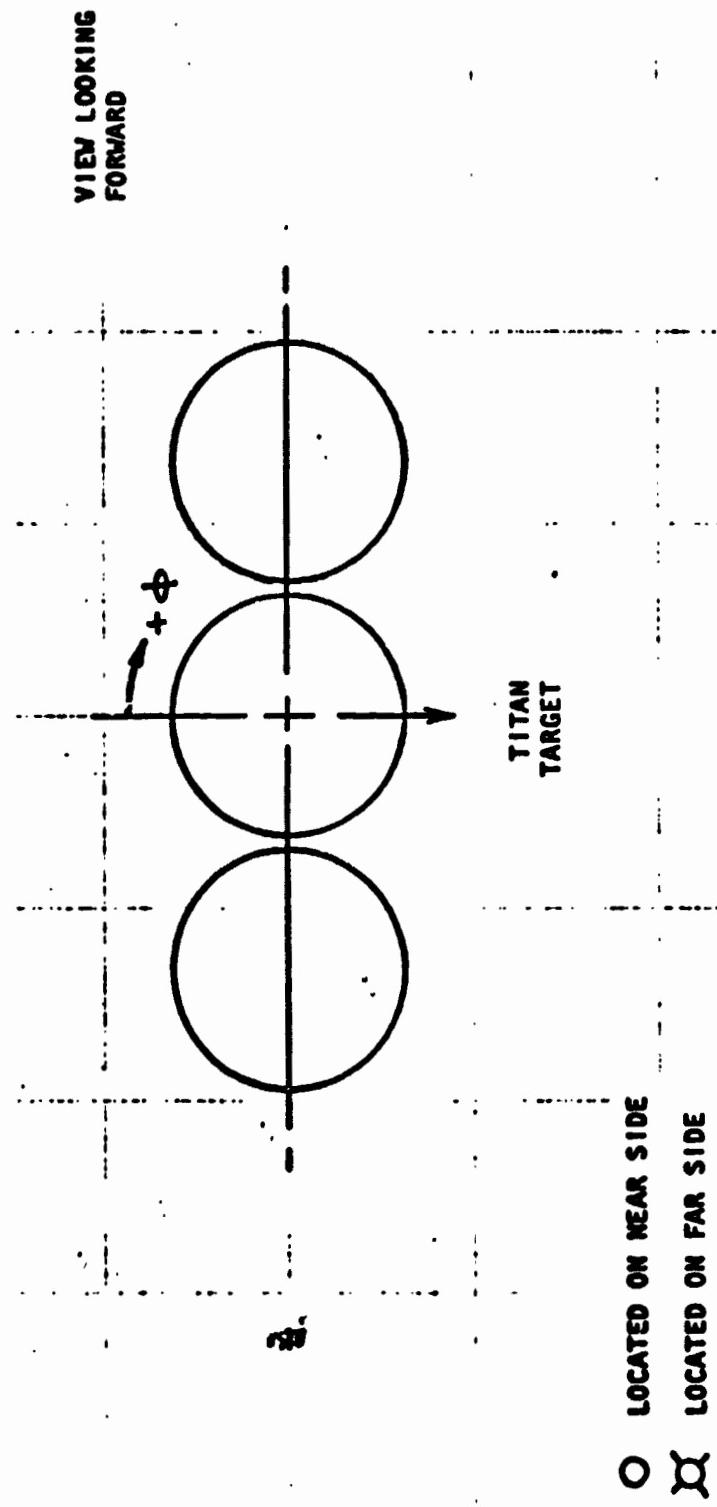
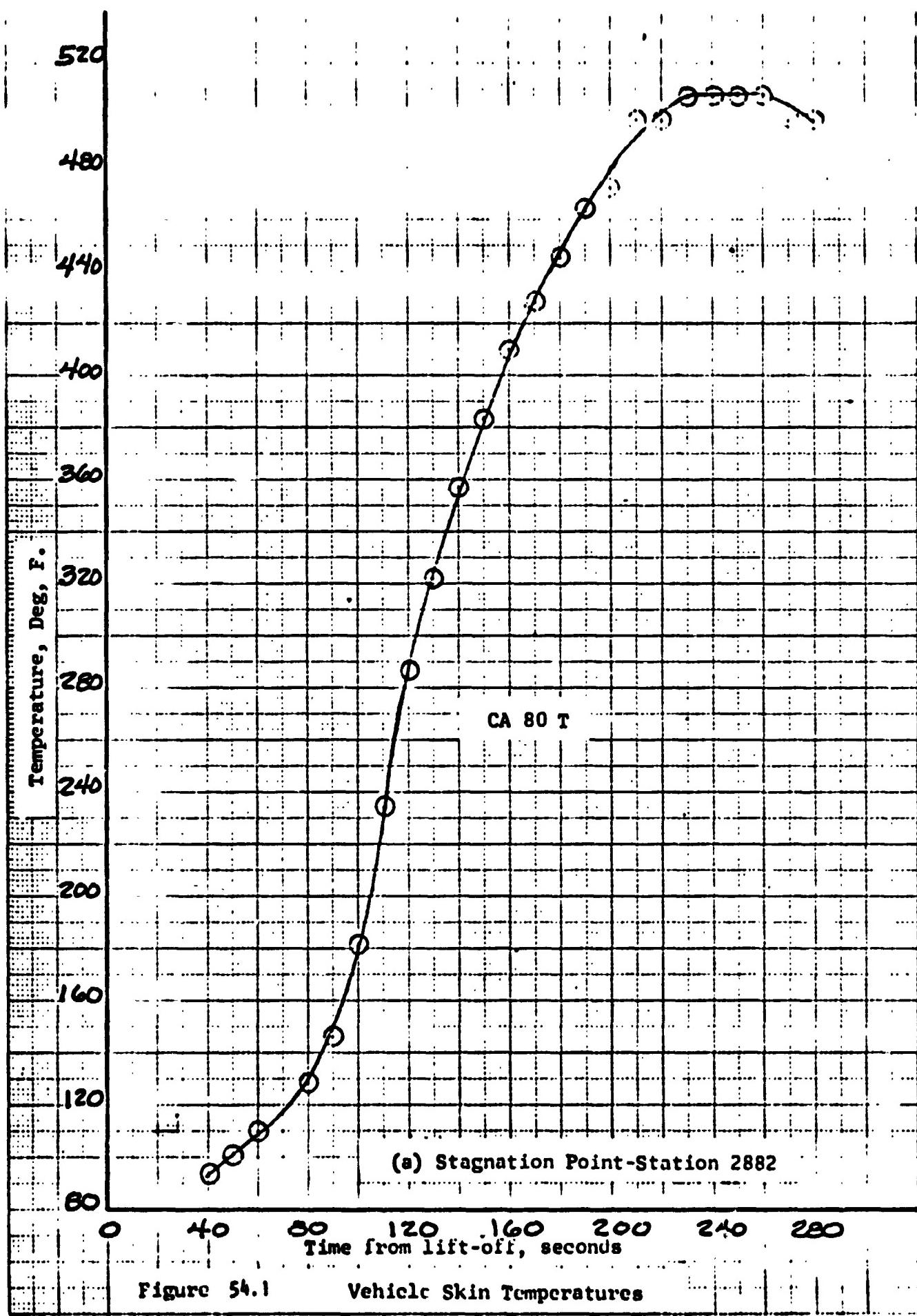
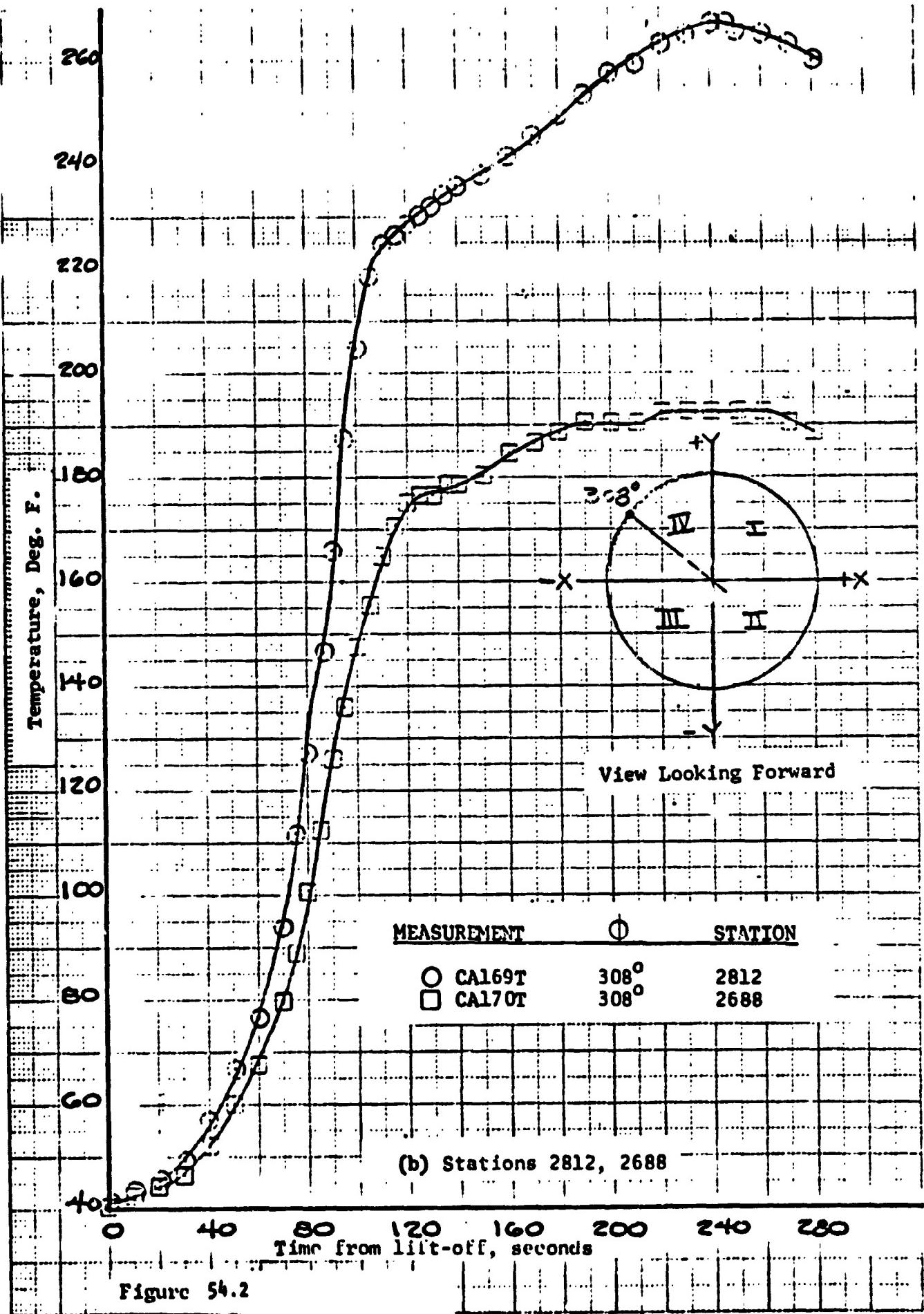


FIGURE E3 - LOCATION OF CSS AND ISA EXTERNAL TEMPERATURE MEASUREMENTS





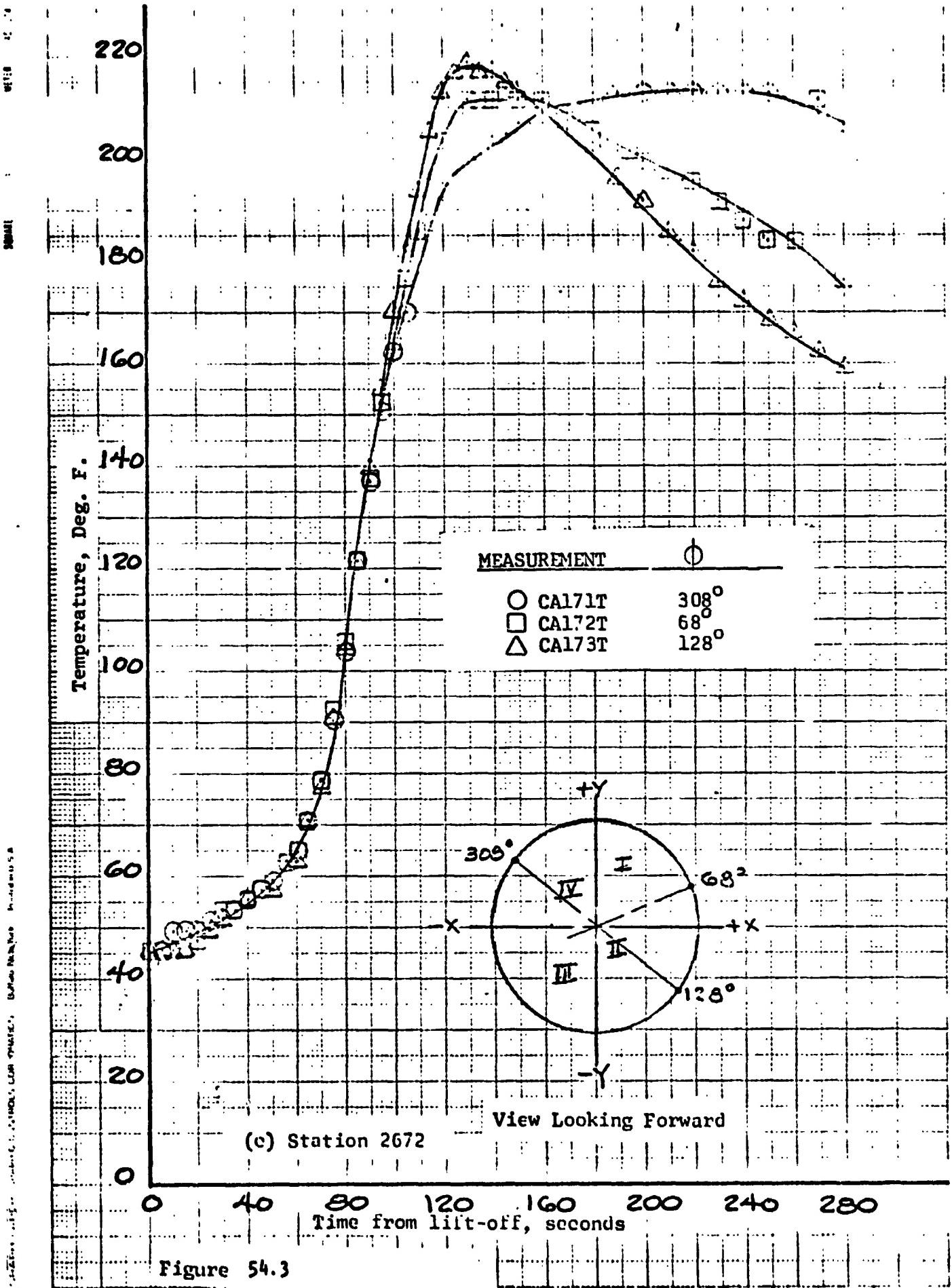


Figure 54.3

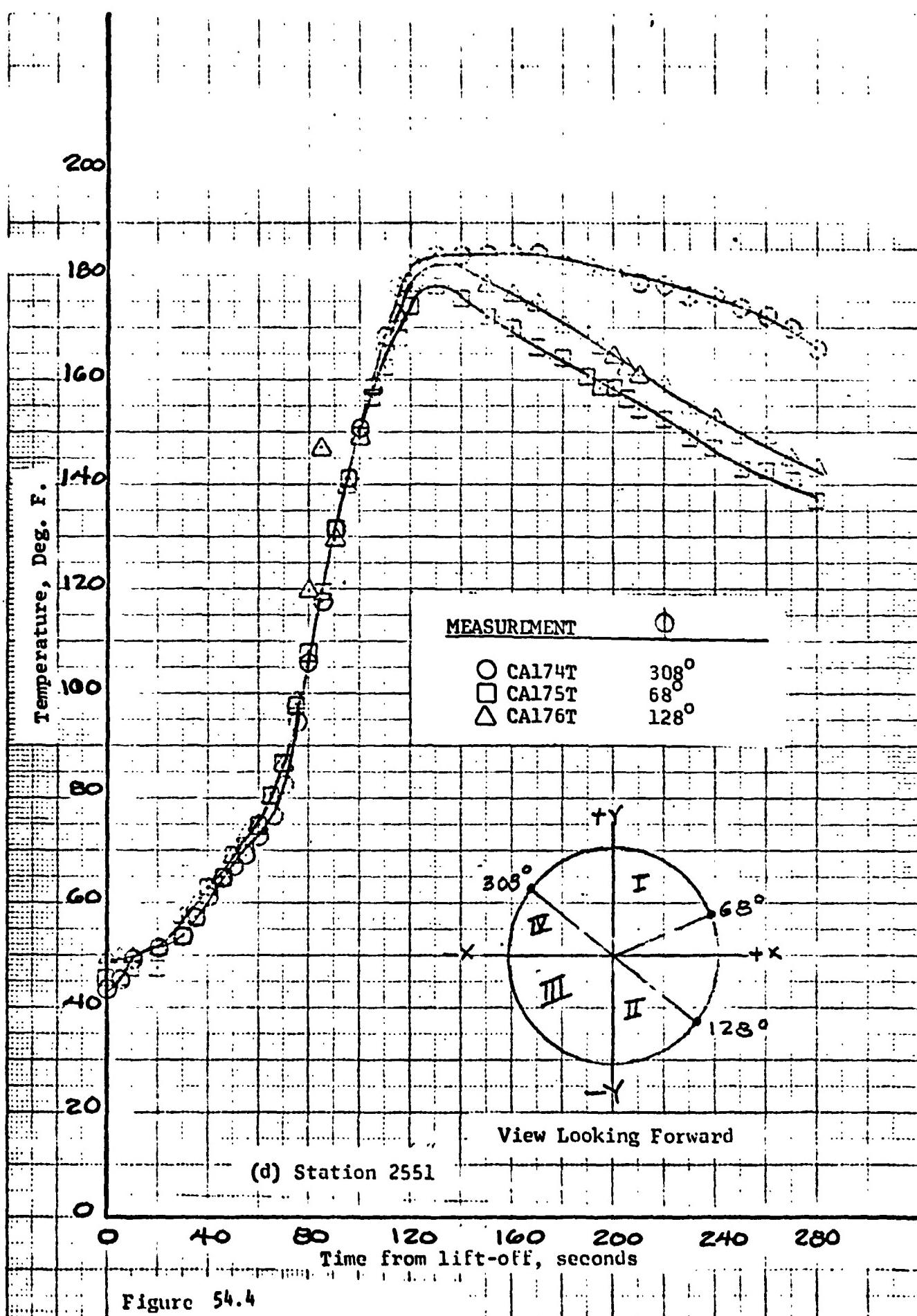
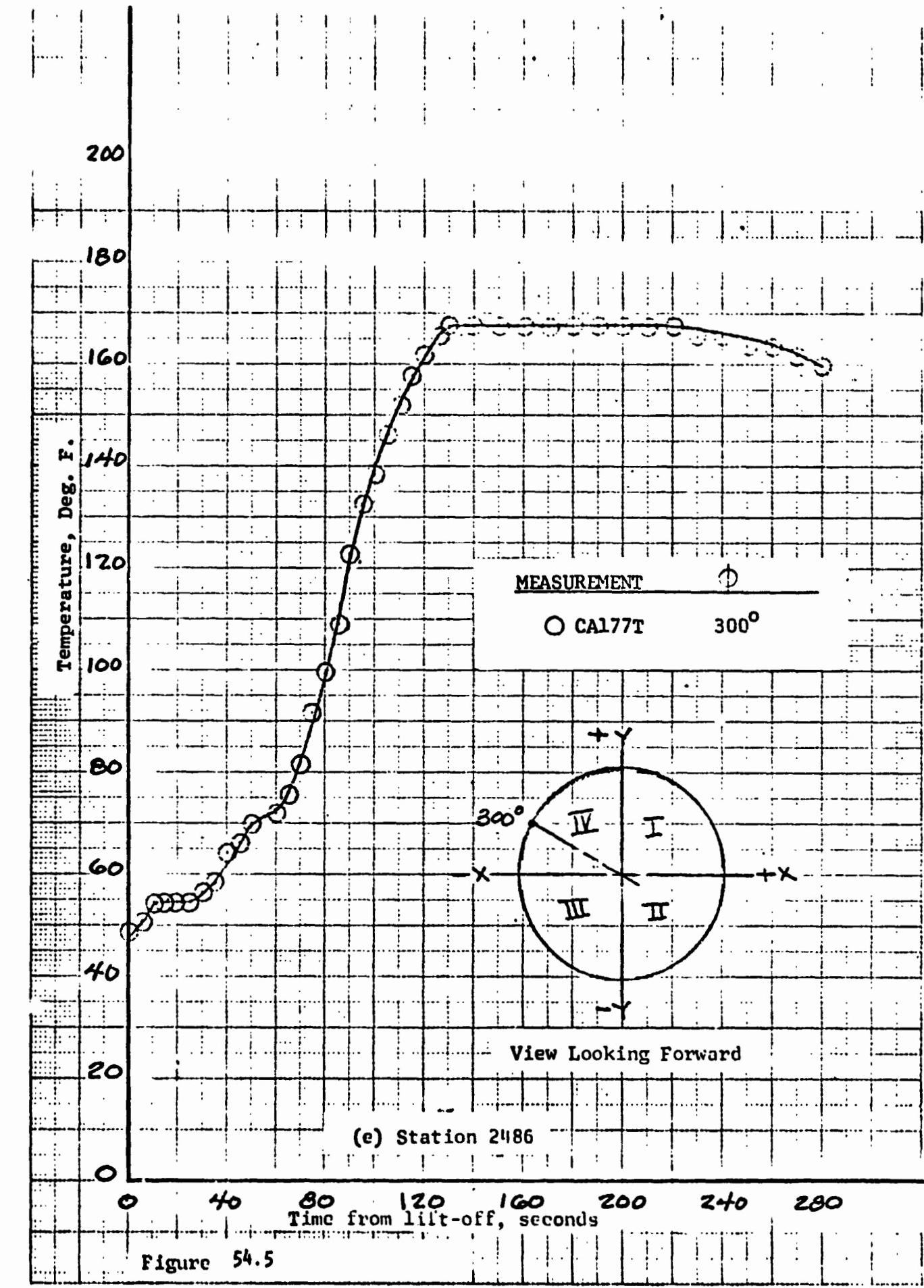
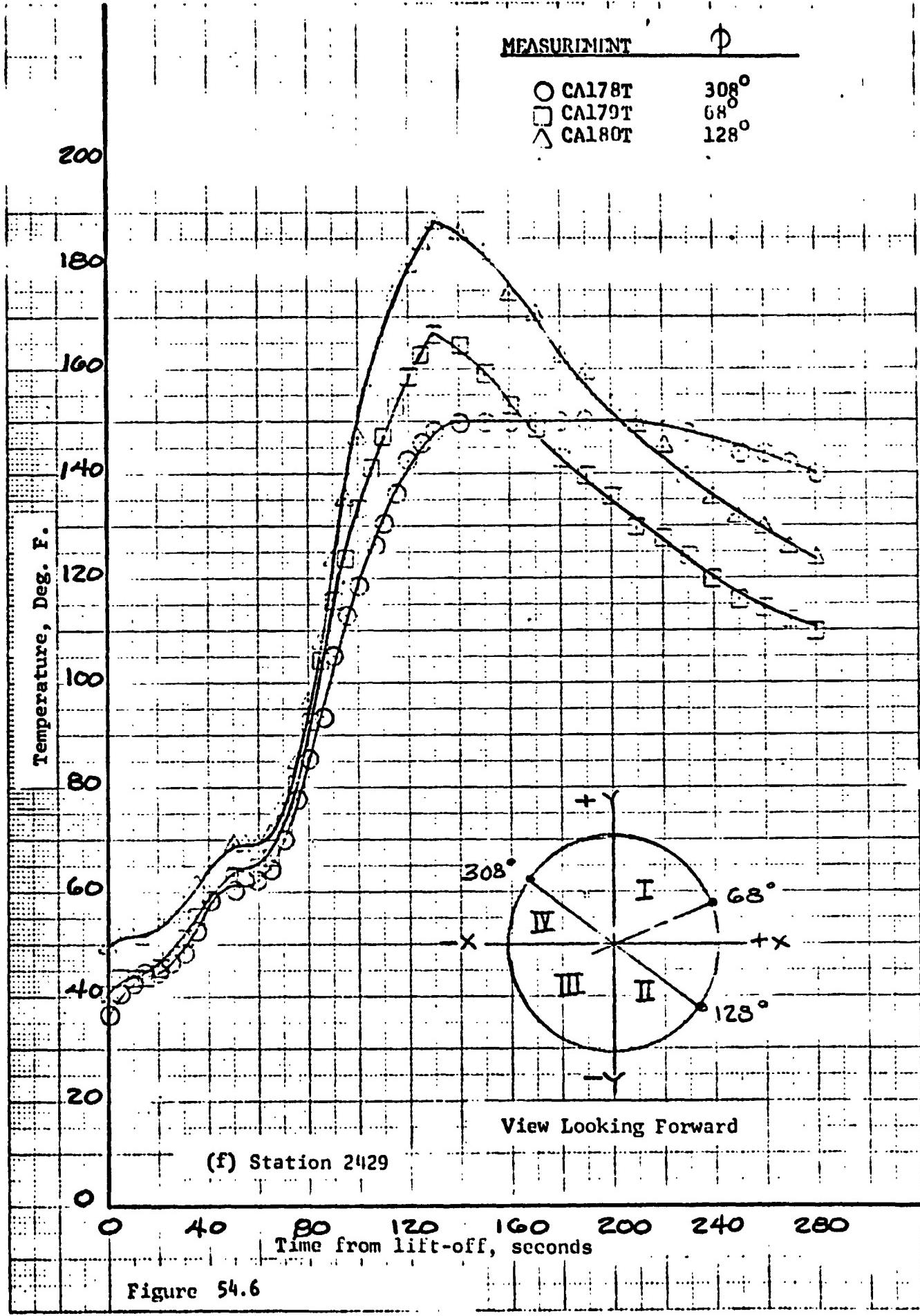
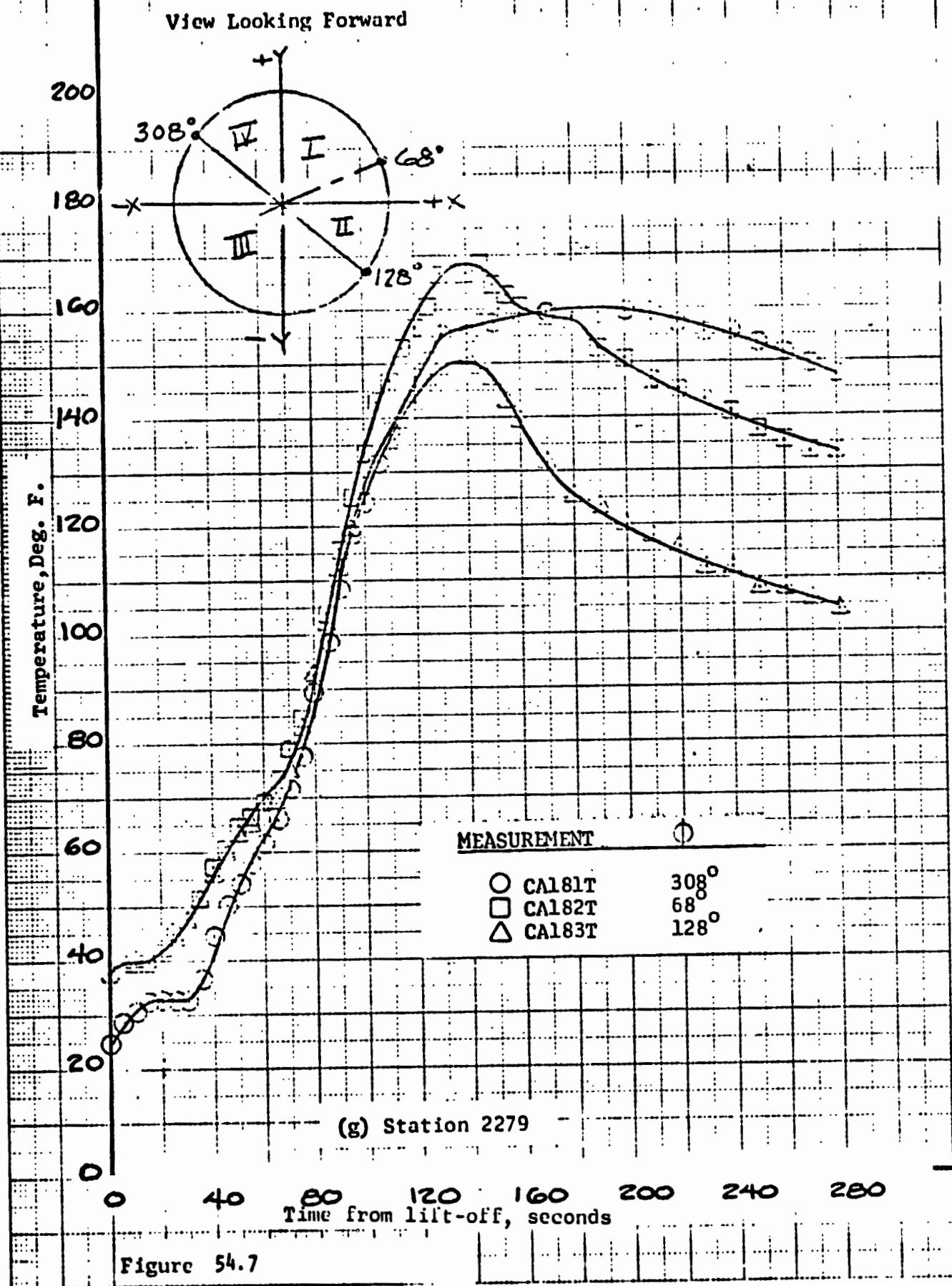


Figure 54.4







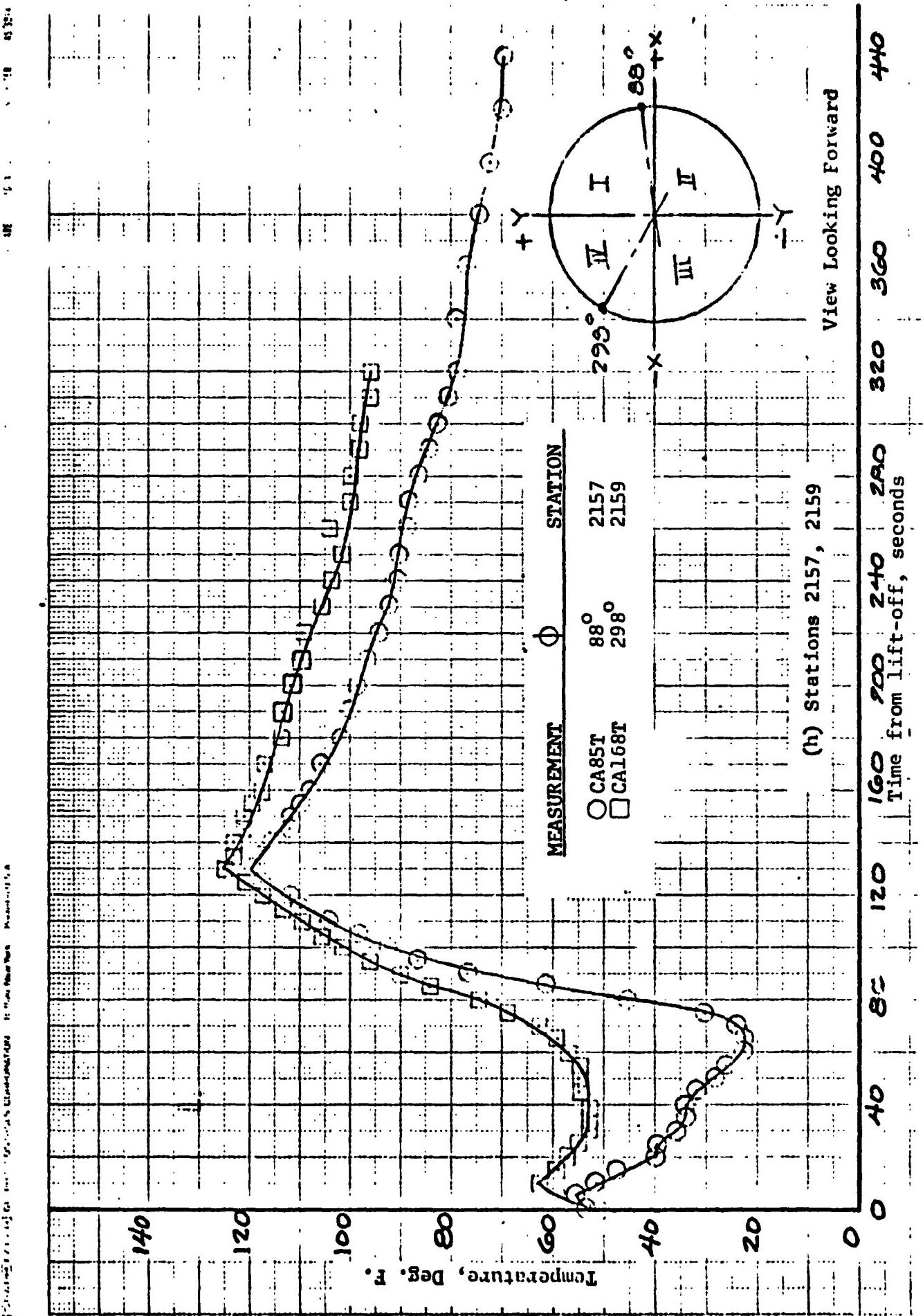


Figure 54.8

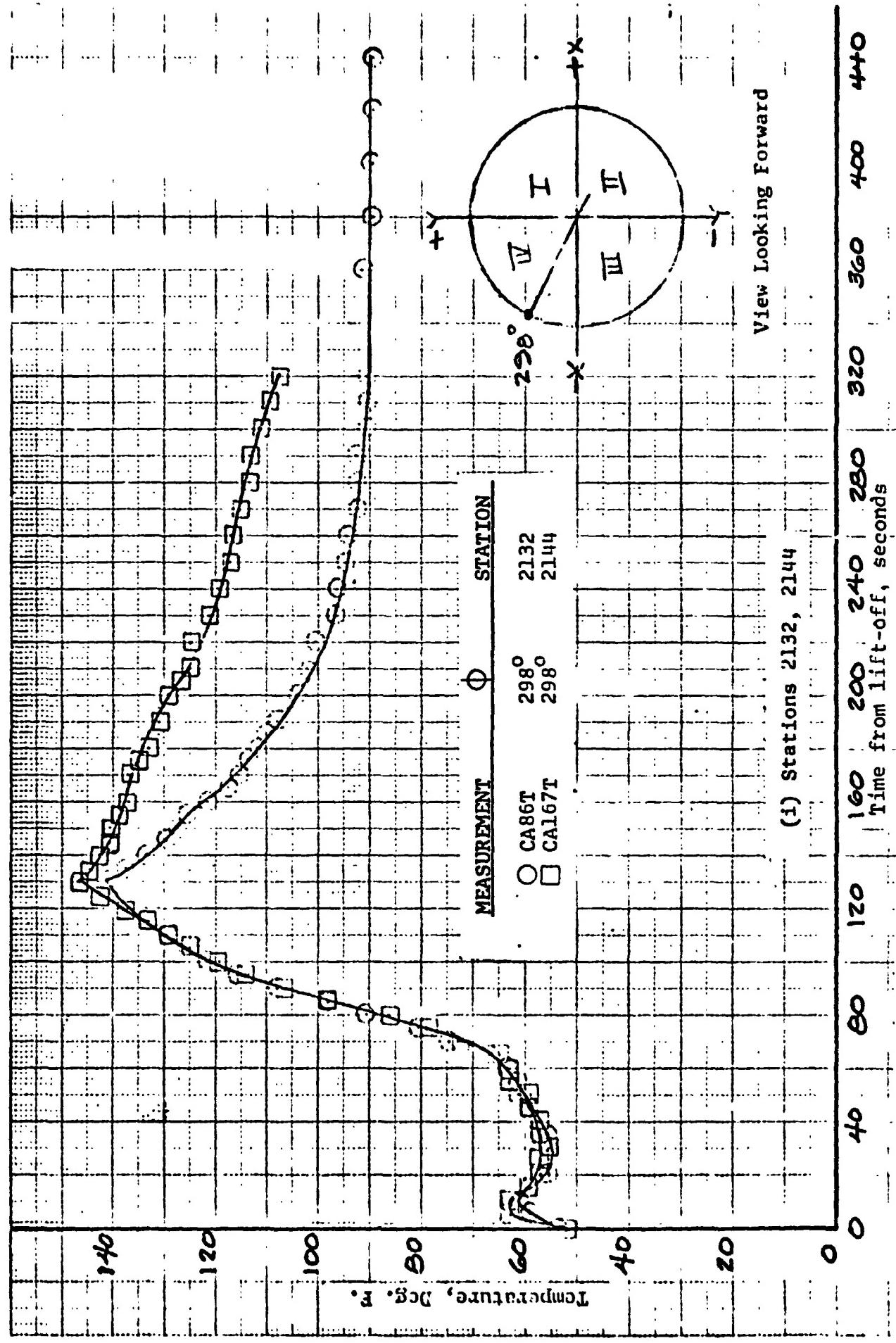


Figure 54.9

CSS Structures

by C. W. Eastwood

The flight loads, both axial and bending moments, on the shroud were calculated from structural strains that were sensed by strain measurements composed of strain gage arrays. Near the aft end of the shroud, four arrays were located at Station 2294 and spaced 90 degrees apart at azimuths 24° , 114° , 204° and 294° as shown in Figure 55. Each array consisted of four uniaxial gages mounted on the exterior skin corrugations and connected electrically as shown in Figure 56. The strain measurements were installed on the shroud prior to buildup on the vehicle and were zeroed after erection on the launch pad. Consequently, the tare weight of the shroud (50,000 lbs) forward of the strain gages was nulled-out. Although the value is small compared to the flight maximum load, the data presented has been corrected to include the shroud tare weight.

The maximum combined loads on the shroud at Station 2294 occurred at $T + 38.3$ seconds. The equivalent axial load at that time was 229,500 pounds on the compression side and 160,500 pounds tension load on the opposite side. Of this equivalent axial load, 34,500 pounds were direct axial load and 195,000 pounds were from a bending moment of 8.19×10^6 inch-pounds. The direct axial load was composed of 25,500 pounds of aerodynamic loading and 9,000 pounds of inertia loading from the vehicle acceleration of 1.8 g. The loads experienced by the CSS during TC-2 flight are listed in Table 28. Loads for TC-1 flight and loads applied to the test CSS also are included in the table for comparison. Maximum equivalent axial loads on the CSS for TC-2 flight, although higher than for TC-1 flight, were less than 47 percent of the test maximum values.

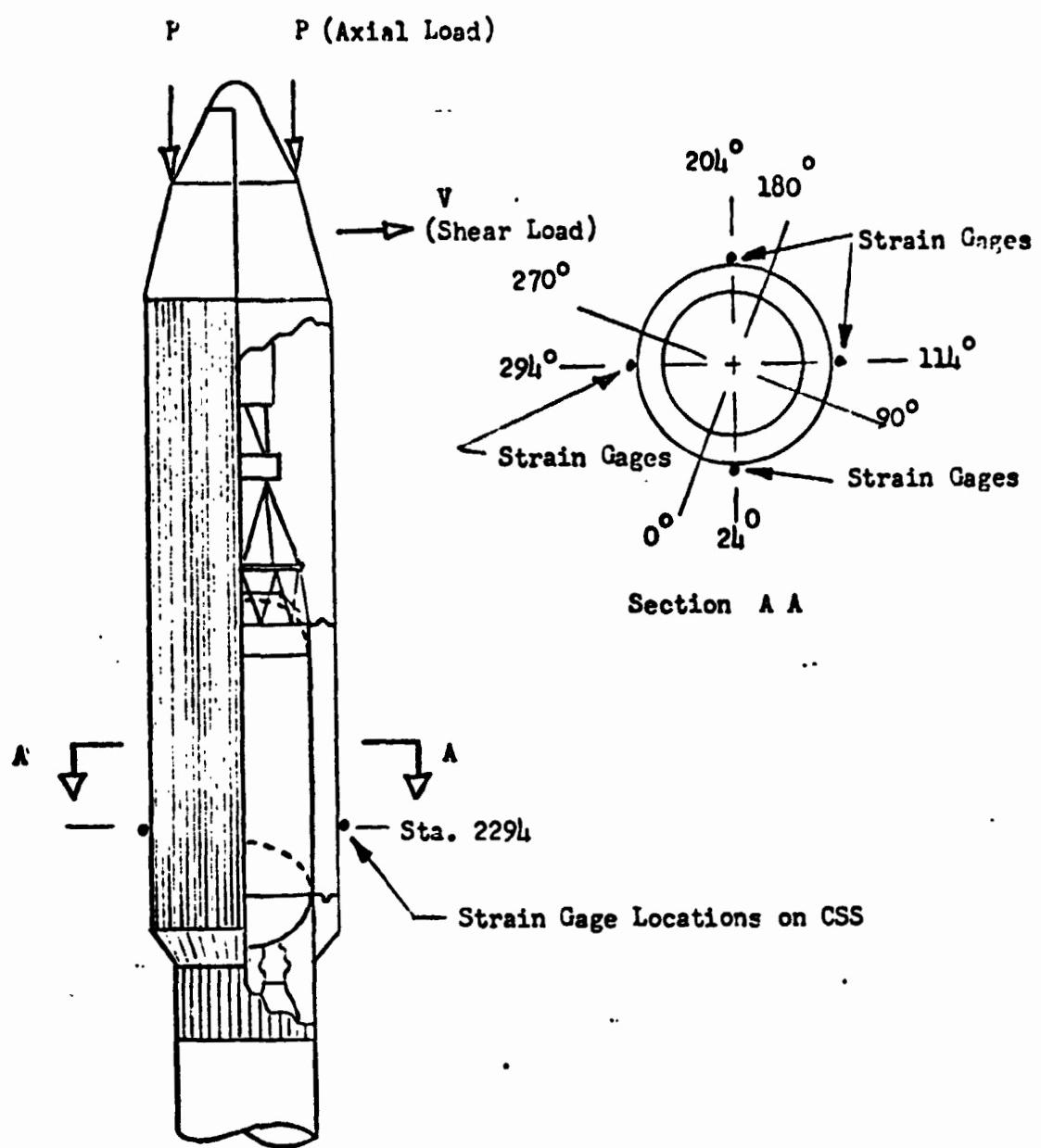


Figure 55 Structural Strain Measurement Locations on CSS.

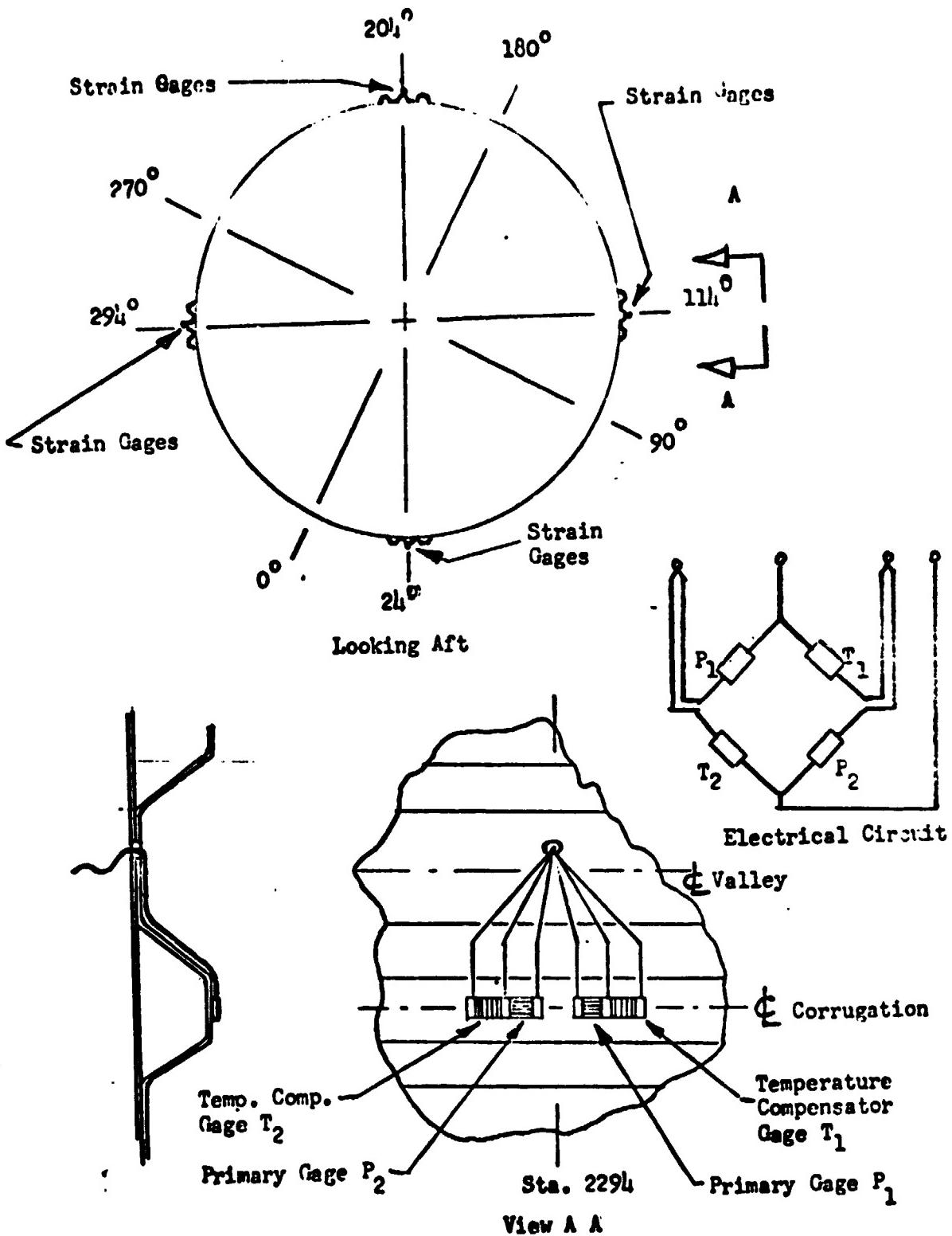


Figure 56 Centaur Standard Shroud Structural Strain Gages.

TABLE 28

CSS Structural Flight Loads and Limit Test Loads, Station 2294

(Includes weight of shroud forward of station 2294 in all axial values)

Flight Event	Nominal Time, Sec.	Total Axial Load, Lbs.	Bending Moment, in. lbs. x10 ⁶	Vehicle Accel., g	Total Equivalent Axial Load at Extreme Fiber, Lbs.	
	C=Comp. T=Tens.	Compression			TC-2	TC-1
Zero Reference	T-1.	5,000 C	1.77	1.00	17,200	5,000
-----	T+5.	36,300 C	0.97	1.60	58,500	97,900
Transonic	T+38.3	34,500 C	8.19	1.80	229,500	150,400
-----	T+41.	42,000 C	6.22	1.80	190,000	74,800
<hr/>						
Test Limit Loads						
With FBR		24,300 C	14.0	1.00	357,600	
Without FBR		94,600 C	17.0	1.00	499,100	

CSS In-flight Events and Jettison

by C. W. Eastwood and T. L. Seeholzer

Forward Bearing Reaction Separation

Separation of the six forward bearing reaction struts was accomplished by redundant explosive bolts. Following bolt separation, the strut halves were retracted against the CSS by a spring loaded retractor and against the stub adapter by a tension spring (reference Figures 57 and 58). Explosive separation bolts were located as shown in Figure 59. Bolt separation was caused by actuation of two electro-explosive devices (cartridge). Firing of either cartridge will separate the bolts. Pressure produced by the cartridge was converted into a force by means of two pistons and a silicone rubber force amplifier. (See Figure 60 for bolt details.) The resultant force fractured the bolts in the grooved area. This bolt had been successfully employed on the Atlas/Centaur vehicle for nose fairing separation. See Section VII for further description of the forward bearing reaction system.

Forward Bearing Reaction (FBR) system separation was nominally programmed to occur at $T + 100$ seconds. At this time, the vehicle has passed through the period of maximum loading. FBR separation actually occurred at $T + 100.0$ seconds. Separation of all six struts was verified by breakwires across the strut separation planes.

Forward Seal Release

The forward seal, illustrated by Figure 61, was located at Station 2454 between the CSS and Centaur stub adapter. The seal consisted of a silicone rubberized dacron fabric attached to the stub adapter by bolts and retained on the CSS forward bulkhead by a cable and retaining mechanism. A 5/16-inch diameter segmented teflon bead on the outboard edge of the seal held the seal under the cable.

A redundant explosive bolt was employed to release the seal. This is the same bolt as used for forward bearing reaction separation, see Figure 58. Two bolts, one at each split line, were attached to the seal retaining cable as shown in Figure 61. When the bolts separated, the cable tension was relaxed and the seal released. Seal release assist retractors were located around the periphery of the seal to assist in raising the seal bead over the retainer lip. Two seal retractors were located at the LH_2 vent nozzles to insure seal retraction over the nozzles (reference Figure 62).

Forward seal release occurred at $T + 211.2$ seconds. Breakwires mounted across each explosive bolt housing verified the bolts separated at this time releasing the seal retaining cable. Nominal jettison of the Centaur Standard Shroud verified the seal had completely released.

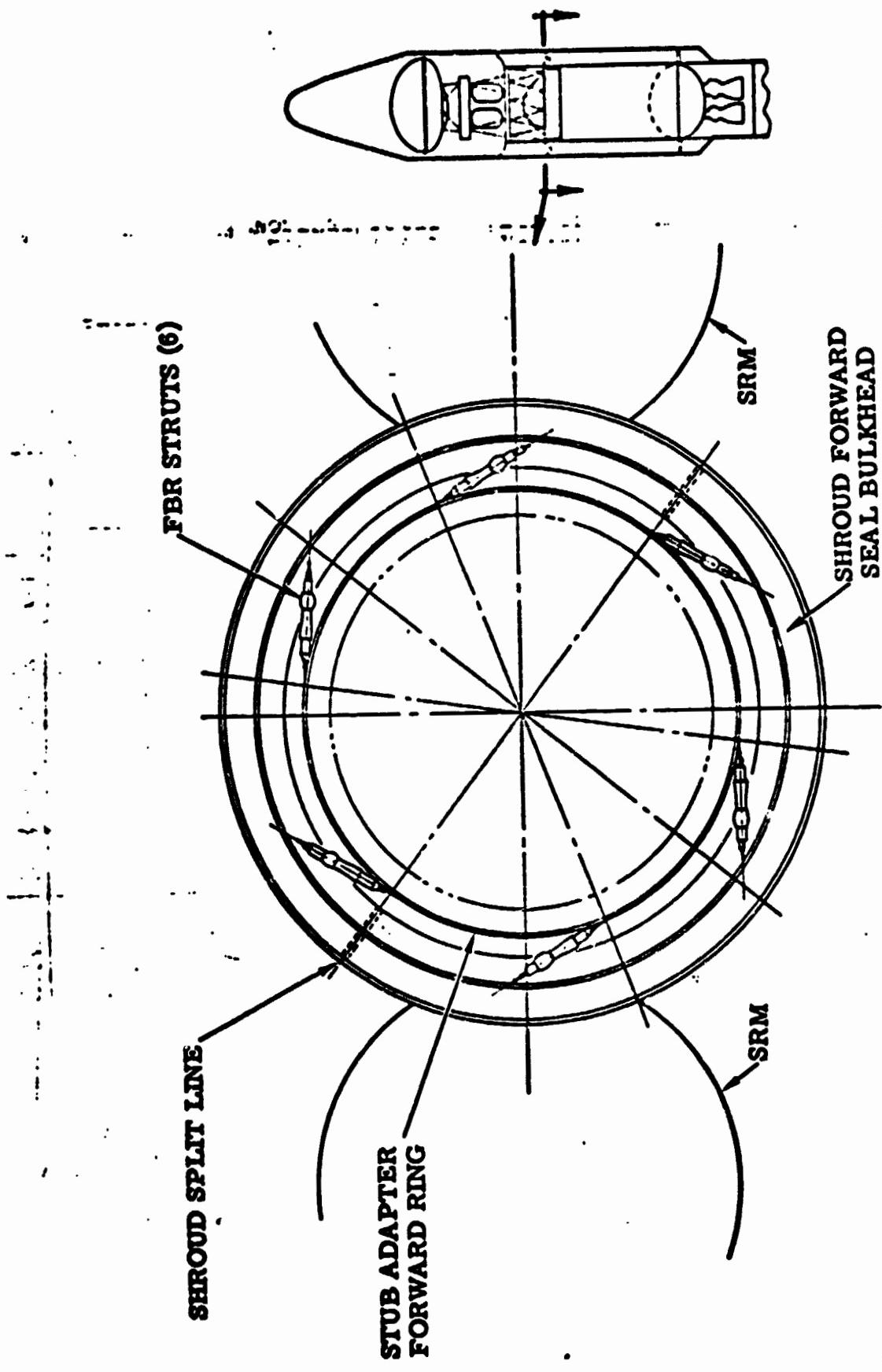


FIGURE 57 FORWARD BEARING REACTION SYSTEM

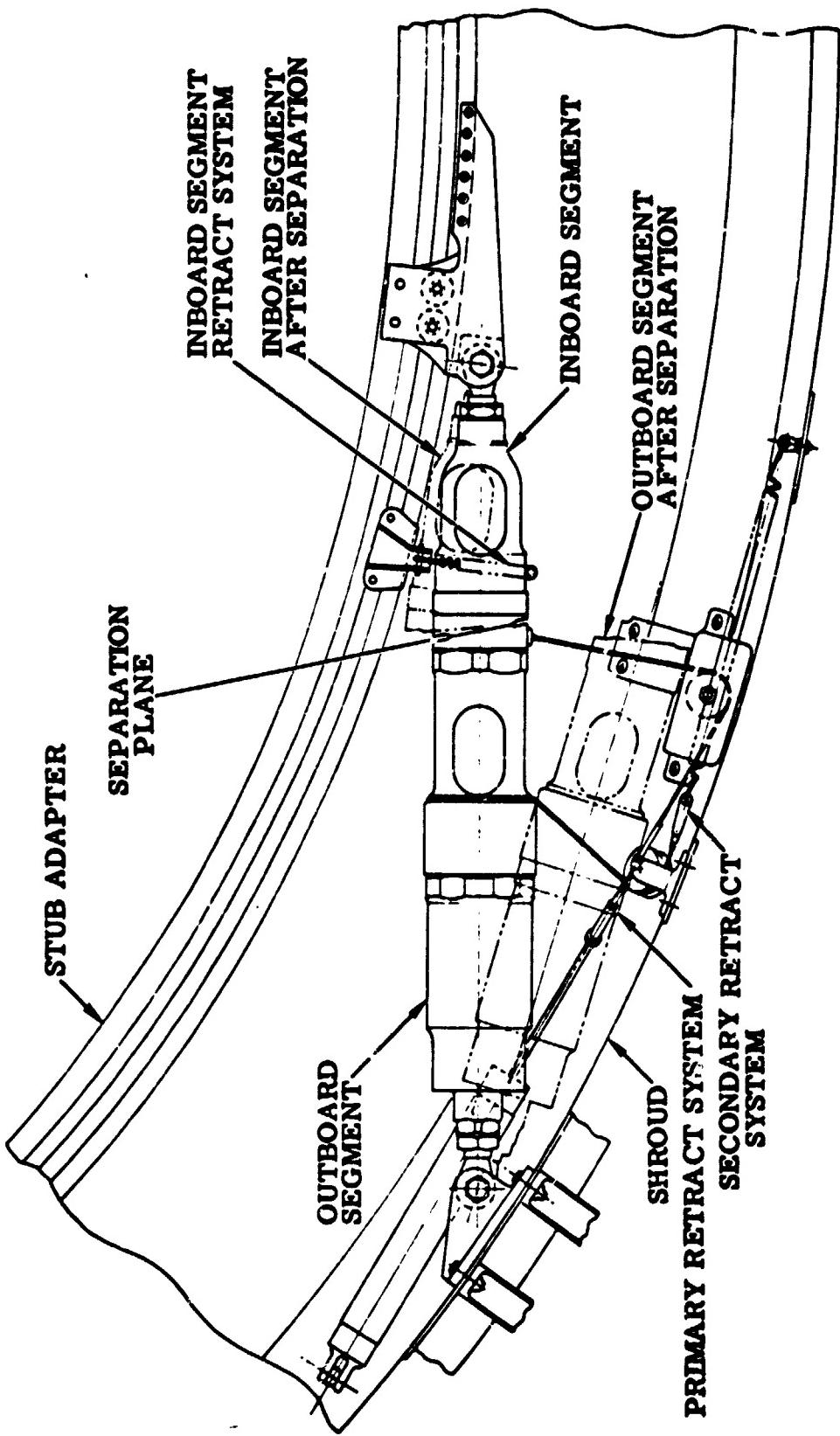


FIGURE 58 FORWARD BEARING REACTION STRUT INSTALLATION

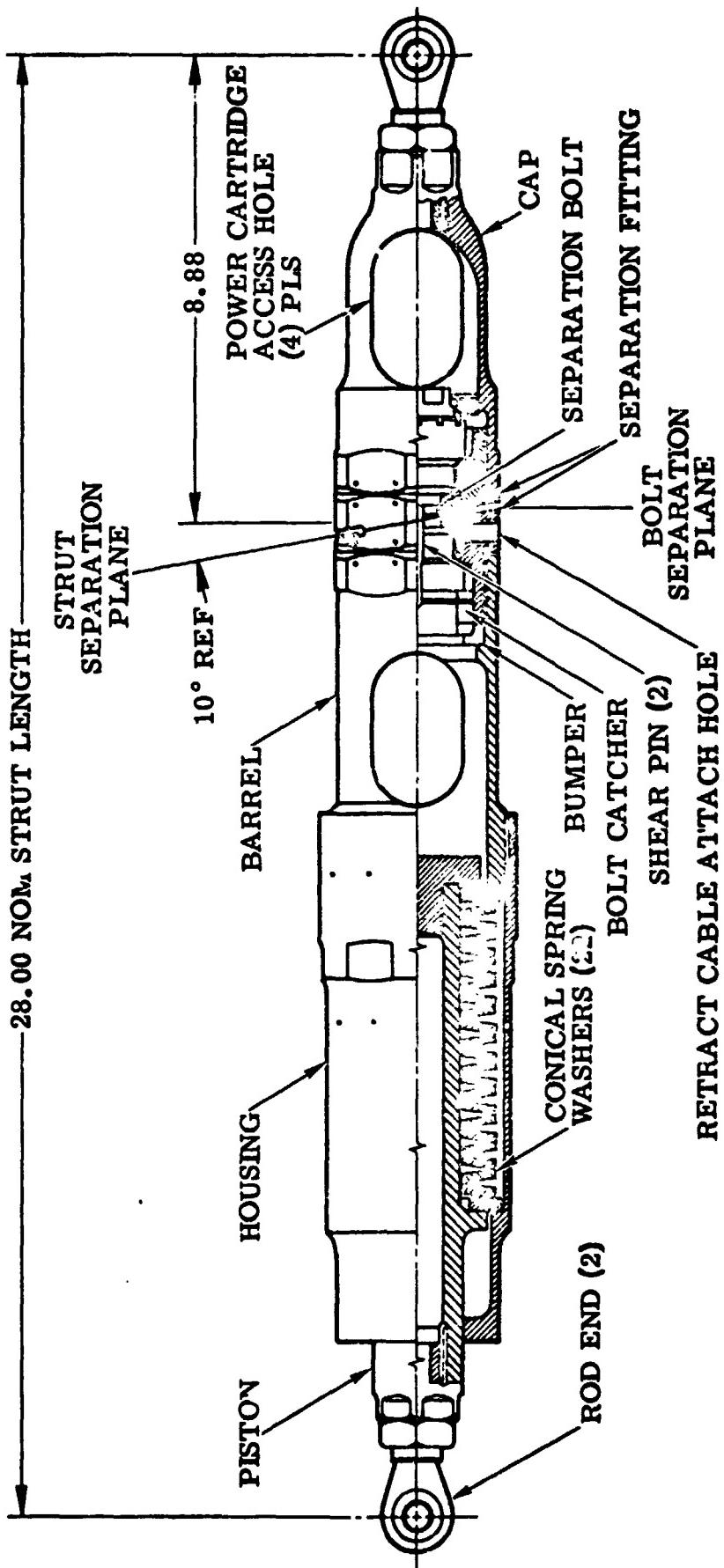


FIGURE 59 FORWARD BEARING REACTION STRUT

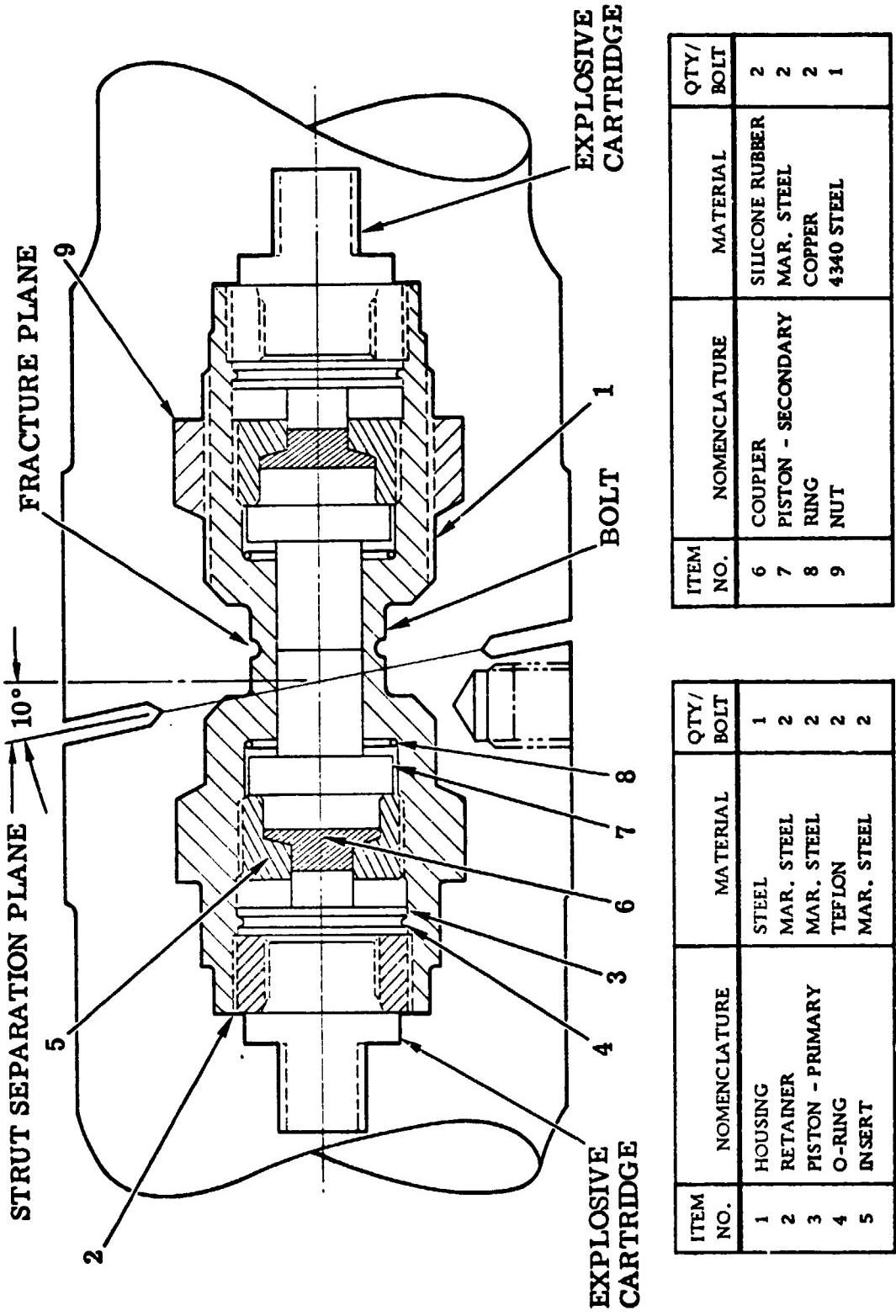


FIGURE 60 FORWARD BEARING REACTION SEPARATION BOLT LOCATION AND DETAILS

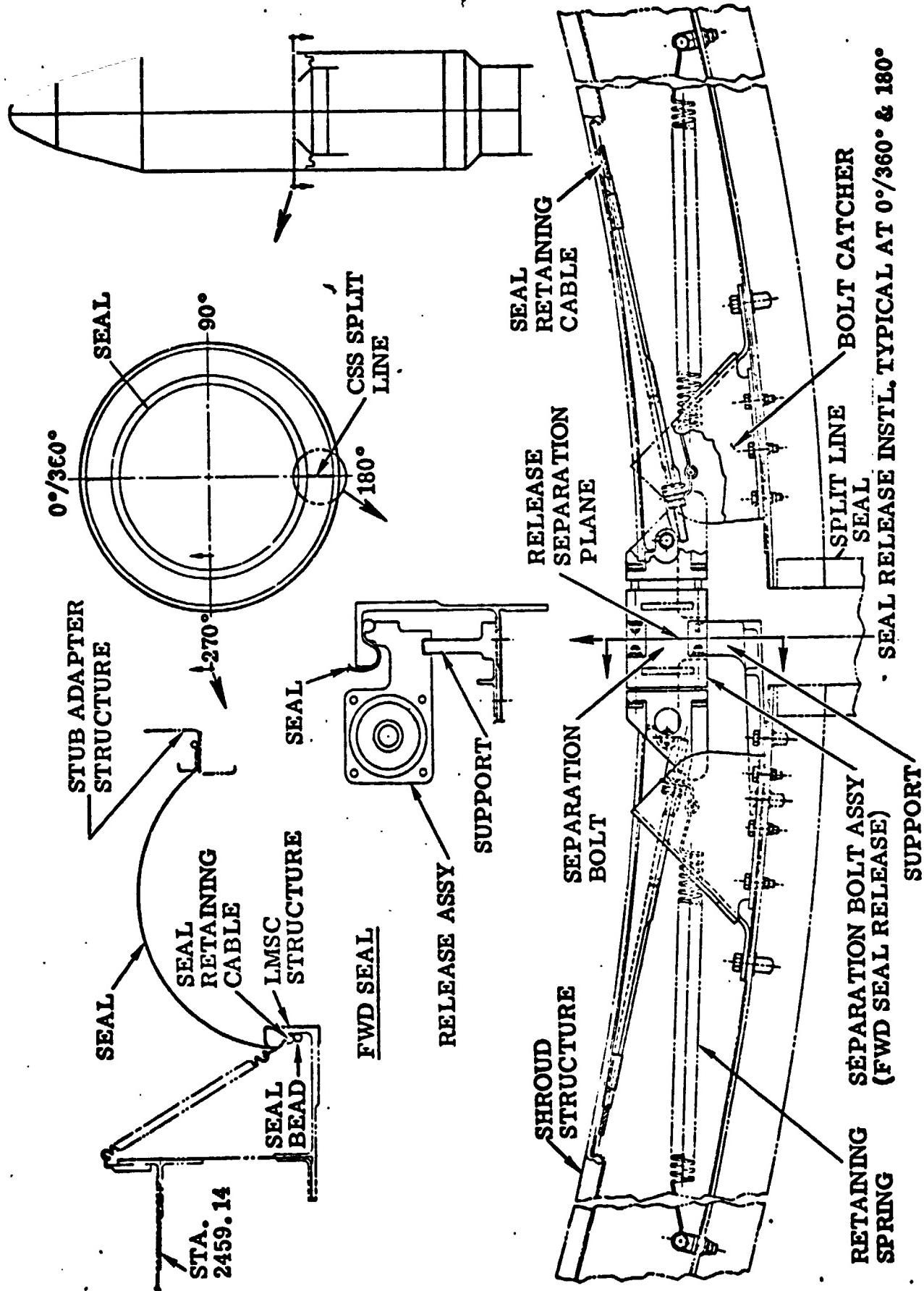


FIGURE 61 FORWARD SEAL

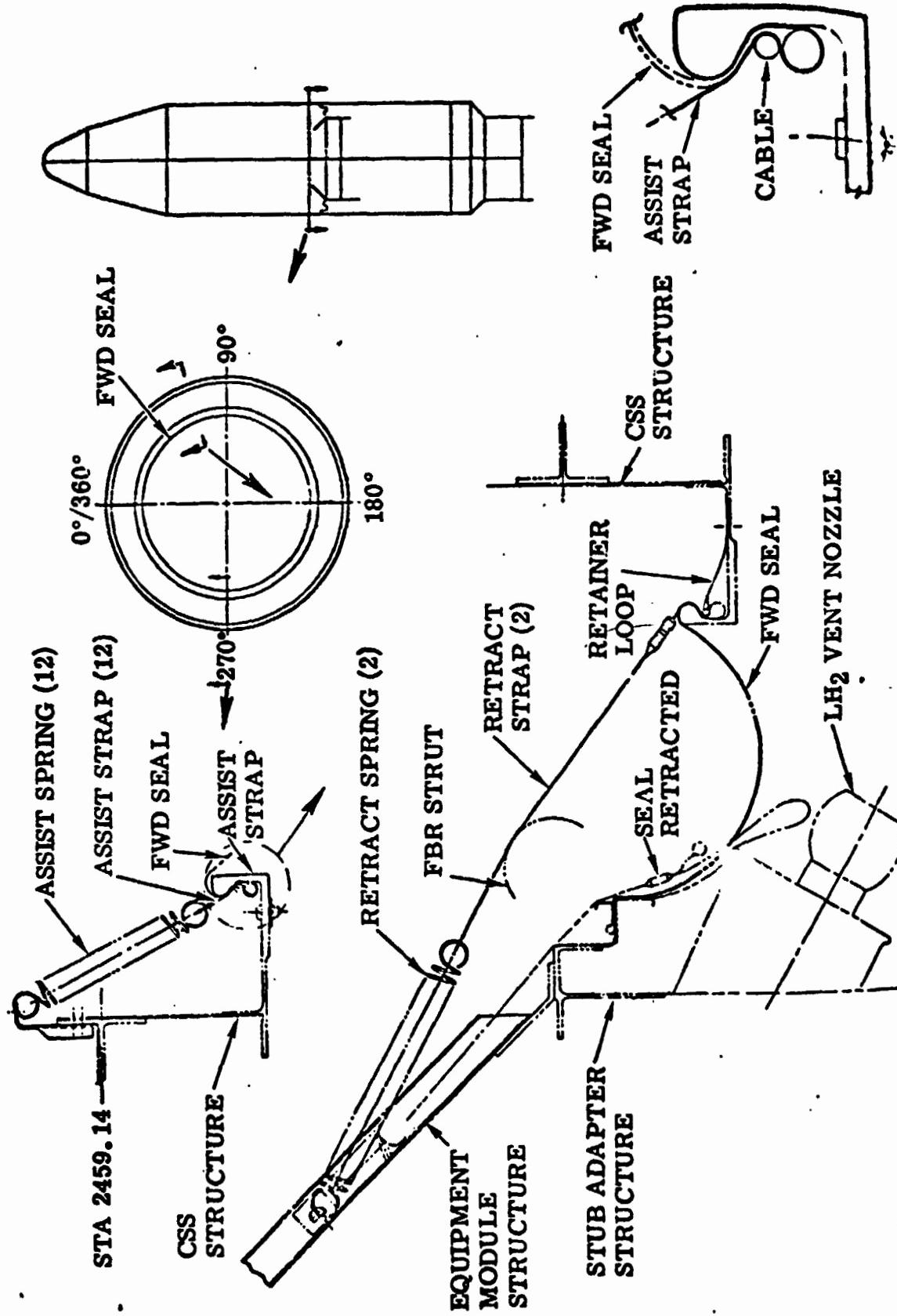


FIGURE 62 FORWARD SEAL RELEASE ASSIST SYSTEM

Super*Zip Separation and Jettison

Super*Zip separation systems, both primary and secondary, are shown in Figures 63 and 64. The systems incorporate a longitudinal and circumferential joint consisting of two explosive cords in a stainless steel tube as shown in Figures 65 and 66. When either cord is ignited, the resultant pressure expands the tube and fractures the frangible doublers.

The secondary system is fired .5 seconds after primary command only in the event the primary system fails to separate the shroud. Each joint is redundantly actuated by electric detonators as shown in Figures 67 and 68. At the payload section, there are detonation transfer lines which bridge the field joint and fire the cord by means of nonelectric detonators (reference Figure 64).

De-activation of the secondary system is accomplished by electrical disconnects located at the base of the shroud as shown in Figure 69. For the TC-2 flight, two of the disconnects (P4J4 and P7J7) were modified by incorporation of an additional 1.125 inch stroke as shown in Figures 69 and 70. CSS jettison tests conducted after the TC-1 flight and the TC-1 flight data indicated the .33 inch stroke disconnect will disengage upon separation of the circumferential joint prior to shroud half rotation. This condition will result in premature de-activation of the secondary system. The increased disconnects eliminate the above condition.

Jettison of the CSS following joint separation is accomplished by eight jettison springs located at the base of the CSS and four helper springs on the split lines as shown in Figure 71.

At T + 318.60 seconds the Super*Zip primary system actuated and separated the CSS from the vehicle. The jettison springs rotated the CSS halves on the hinges until the shroud jettisoned free of the Titan/Centaur vehicle 2.8 seconds later. Breakwires listed in Table 29 provided time of 3°, 8° and 32° CSS half rotation. The time for 3° and 8° angles of rotation are approximately the same for each half indicating a nominal separation and jettison function. At 32° rotation the capped or heavy half time is .3 seconds longer than the uncapped half which is normal performance. Differences in TC-1 and TC-2 CSS rotation times are due to the higher G field in which the TC-2 shroud was jettisoned. TC-2 CSS jettison occurred 45 seconds later than TC-1.

Primary system separation of the CSS was verified by comparison of command times, accelerometer data, hinge strain data and breakwire/disconnect data. Table 30 lists the command times for the primary and secondary systems. At T + 318.60 seconds accelerometers and hinge strain gages verify the Super*Zip primary system fired coincident with primary system command. The secondary system command occurred at 319.10 seconds (as programmed). Also, as per configuration, the secondary system did not fire since the CSS had already rotated over 8°, and disconnected the electrical lines which transmit power to the secondary detonators. Table 30 also lists electrical disconnect times for the .38 and 1.50 inch stroke disconnects verifying that the 1.50 inch stroke disconnect provides proper de-activation of the secondary system.

- NONCONTAMINATING REDUNDANT SYSTEM
- CENTAUR INITIATES COMMANDS
- TITAN PROVIDES POWER

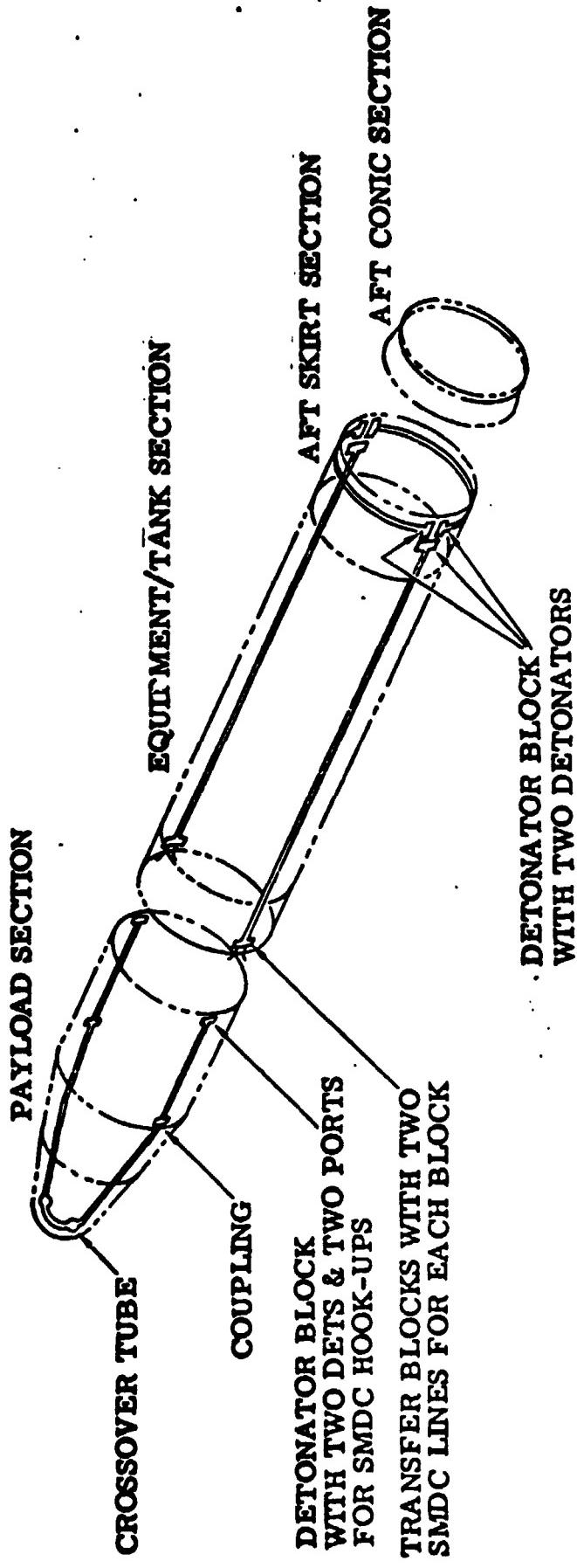
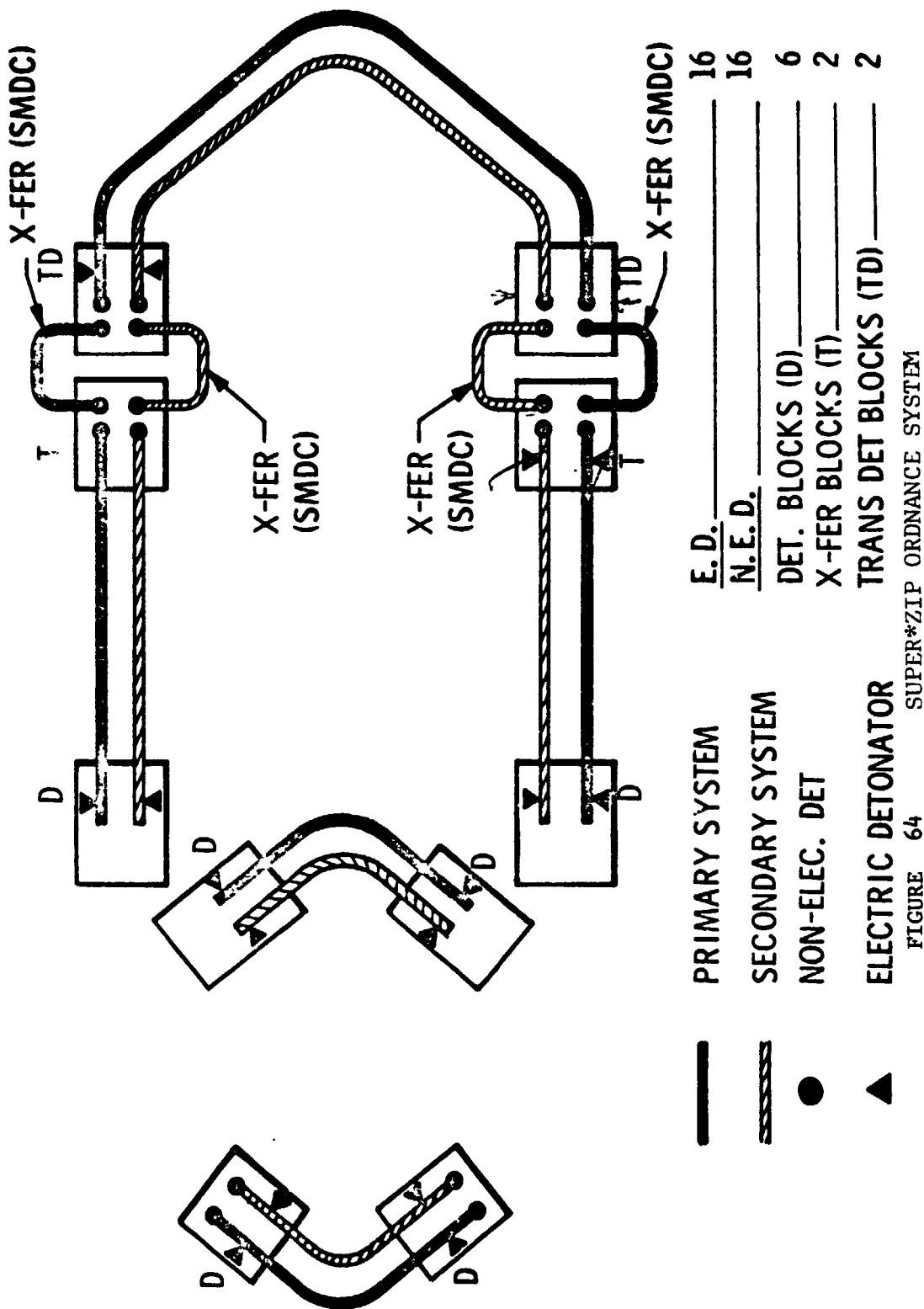


FIGURE 63 SUPER*ZIP SEPARATION SYSTEM



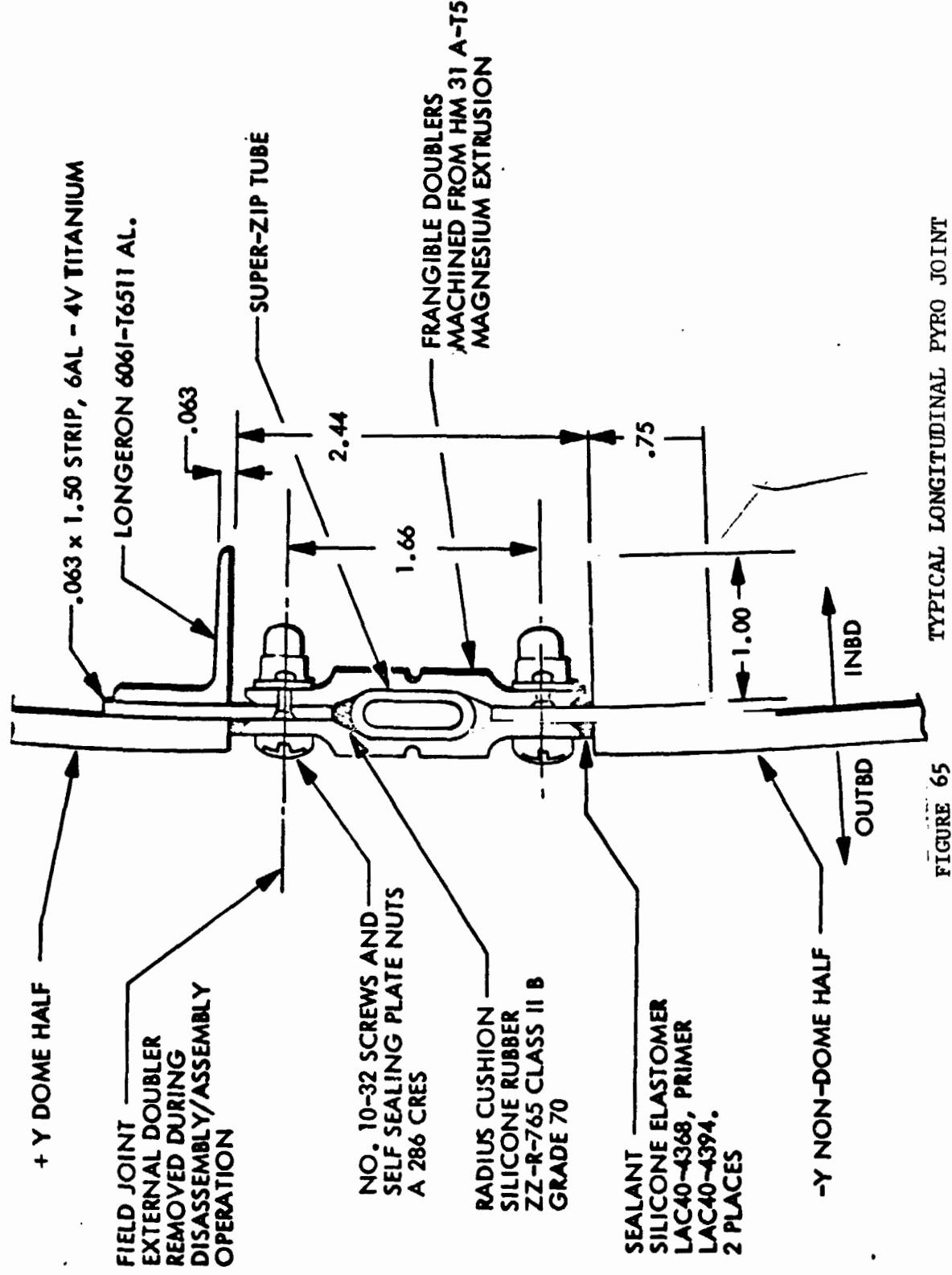


FIGURE 65

TYPICAL LONGITUDINAL PYRO JOINT

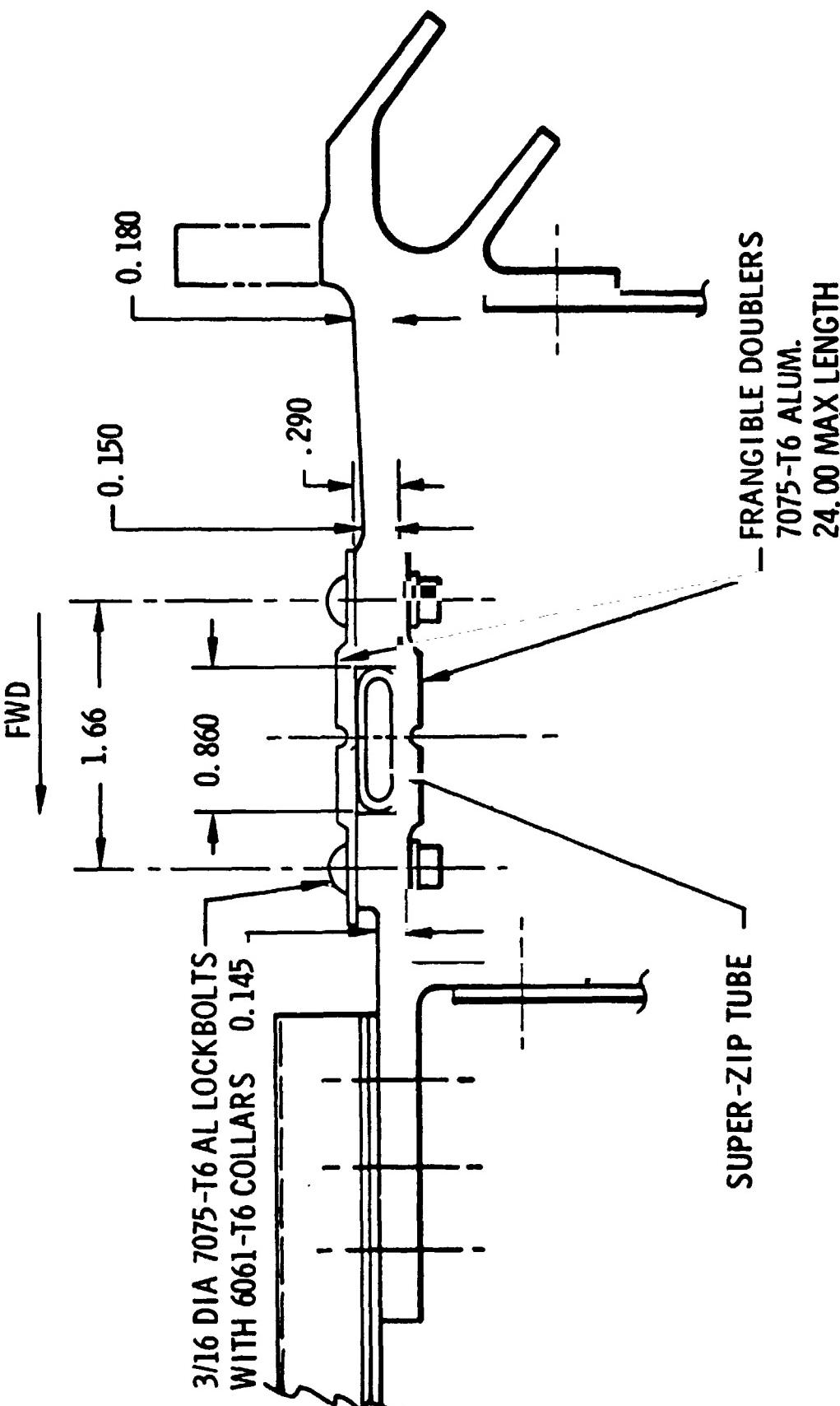


FIGURE 66 TYPICAL CIRCUMFERENTIAL PYRO JOINT

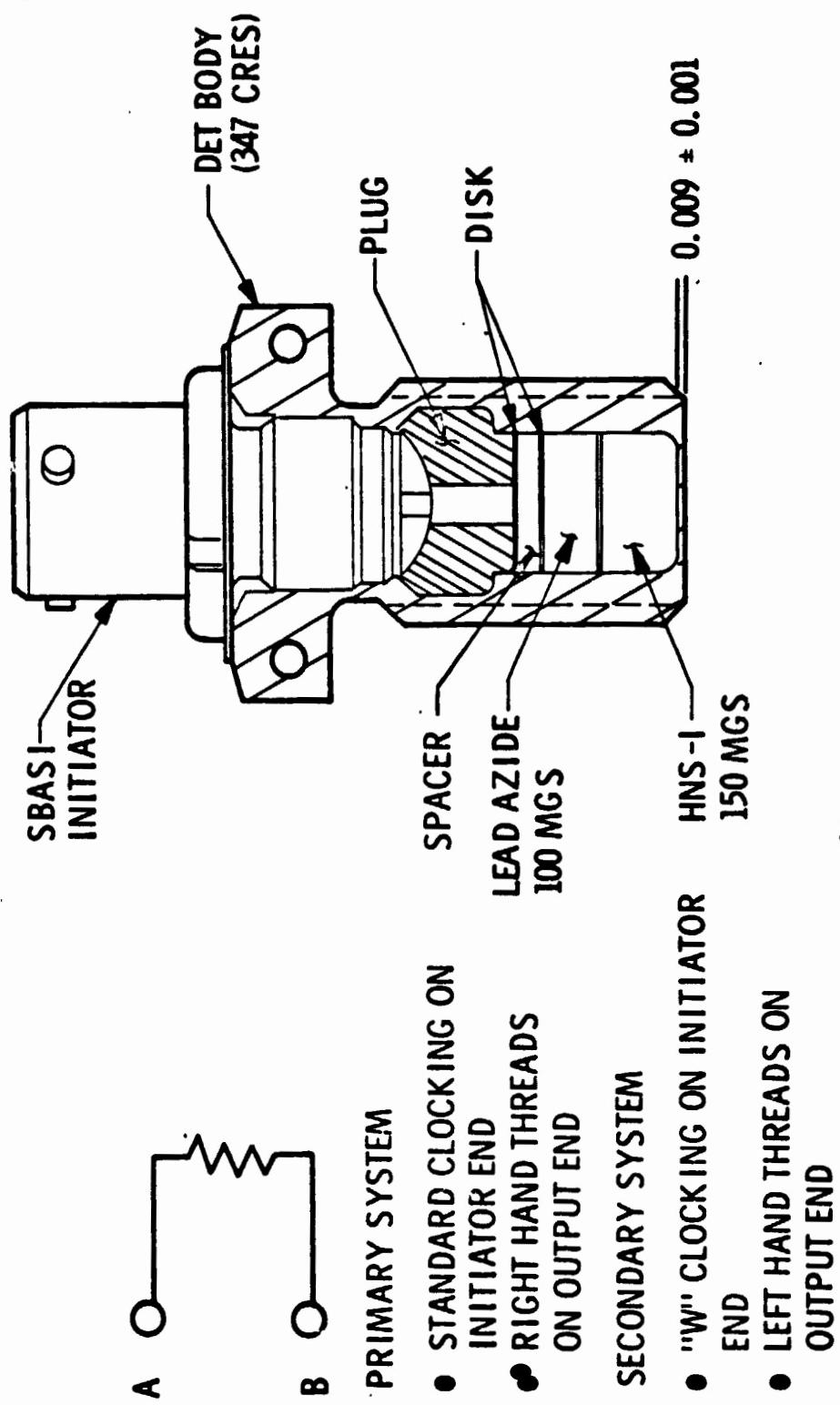


FIGURE 67 ELECTRIC DETONATOR

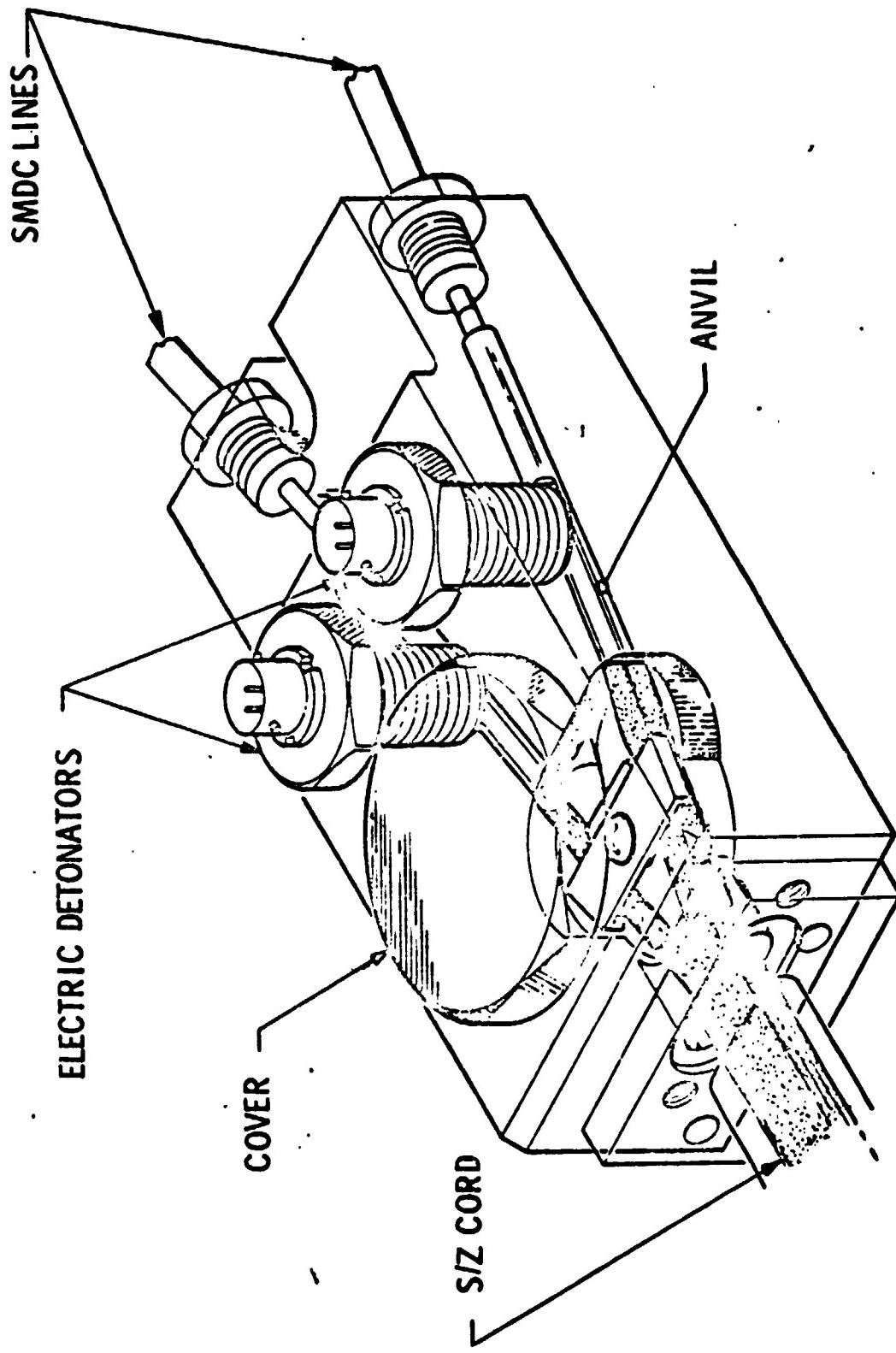


FIGURE 68 DETONATOR BLOCK ASSEMBLY

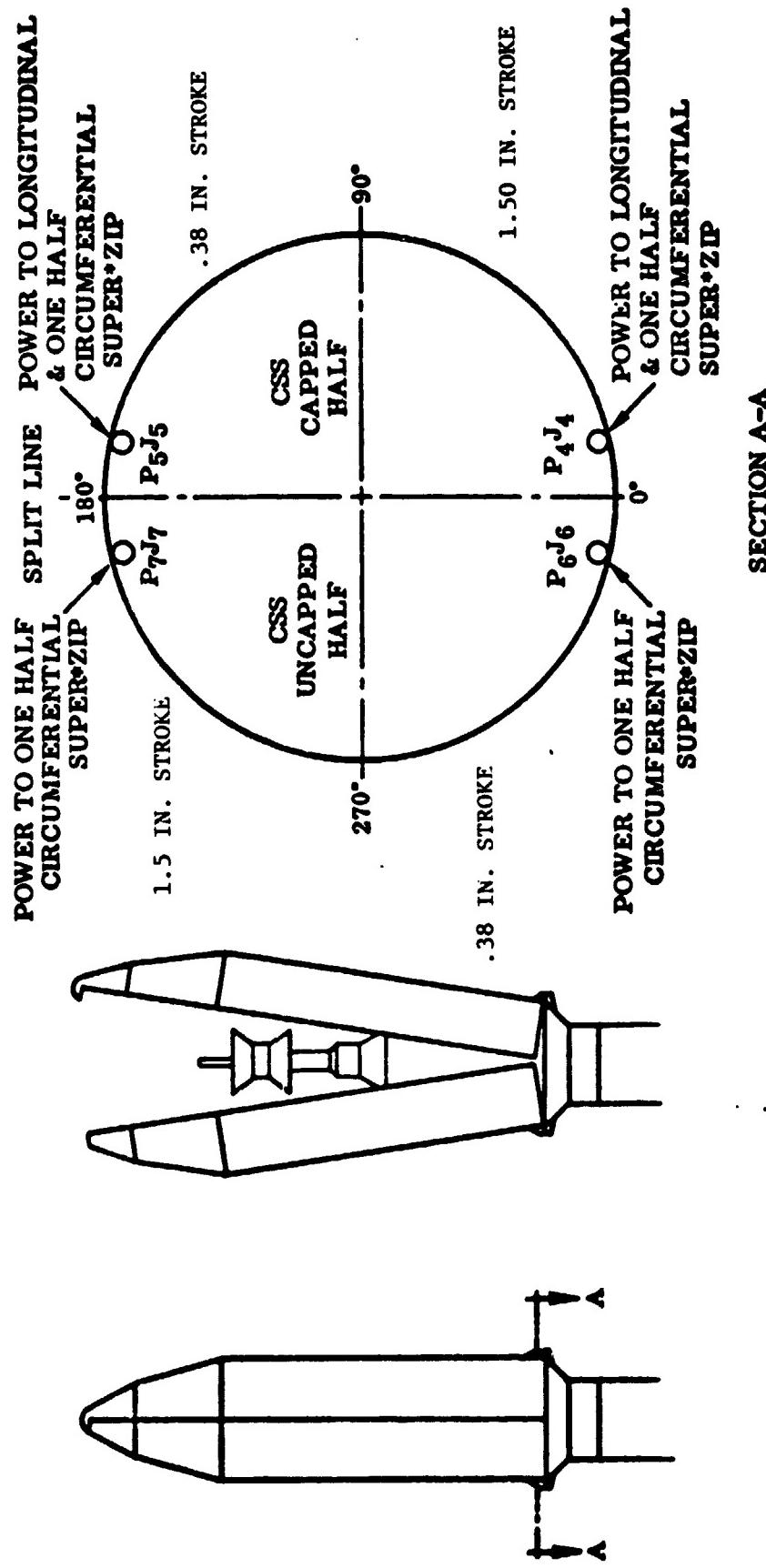
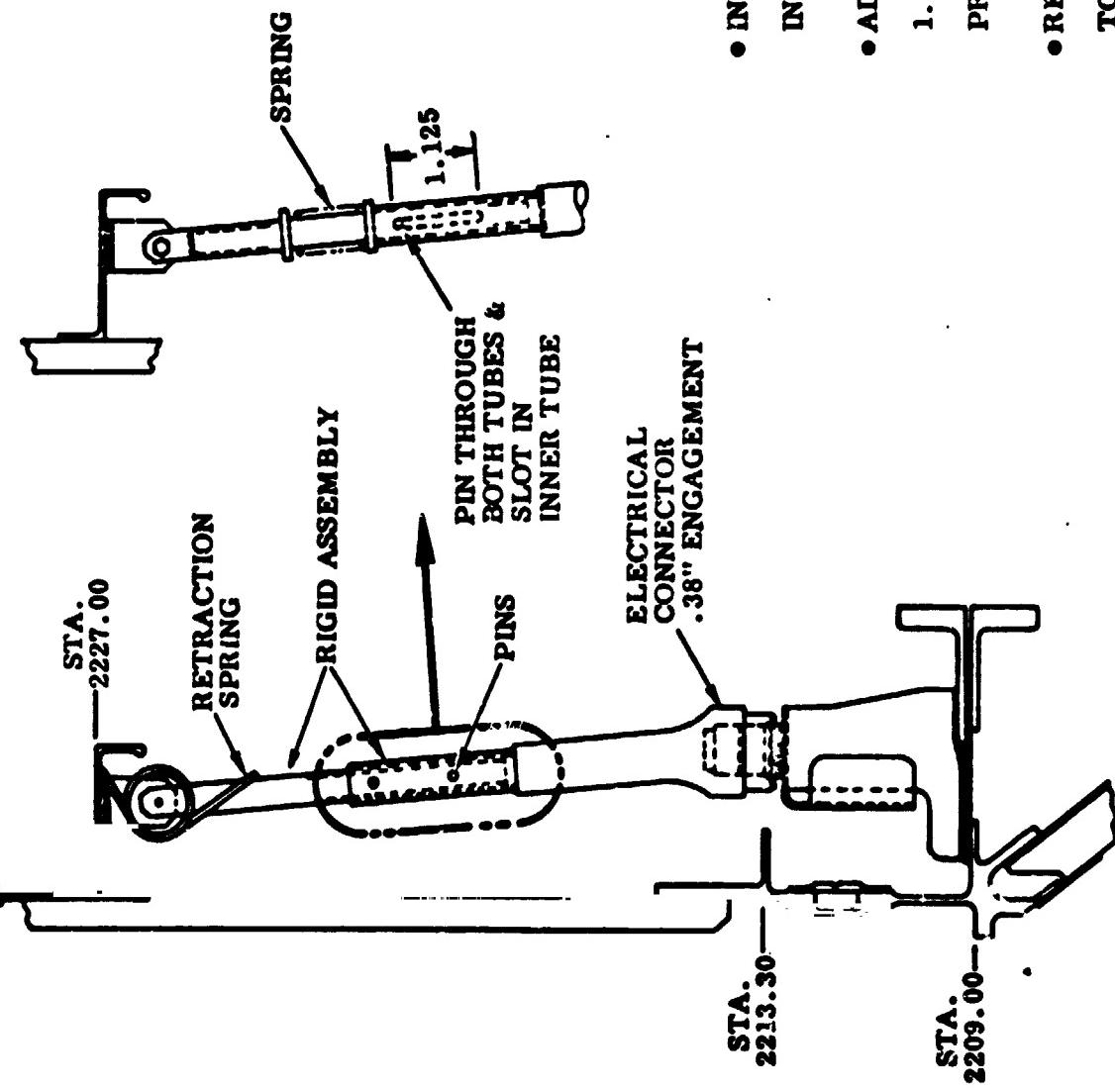


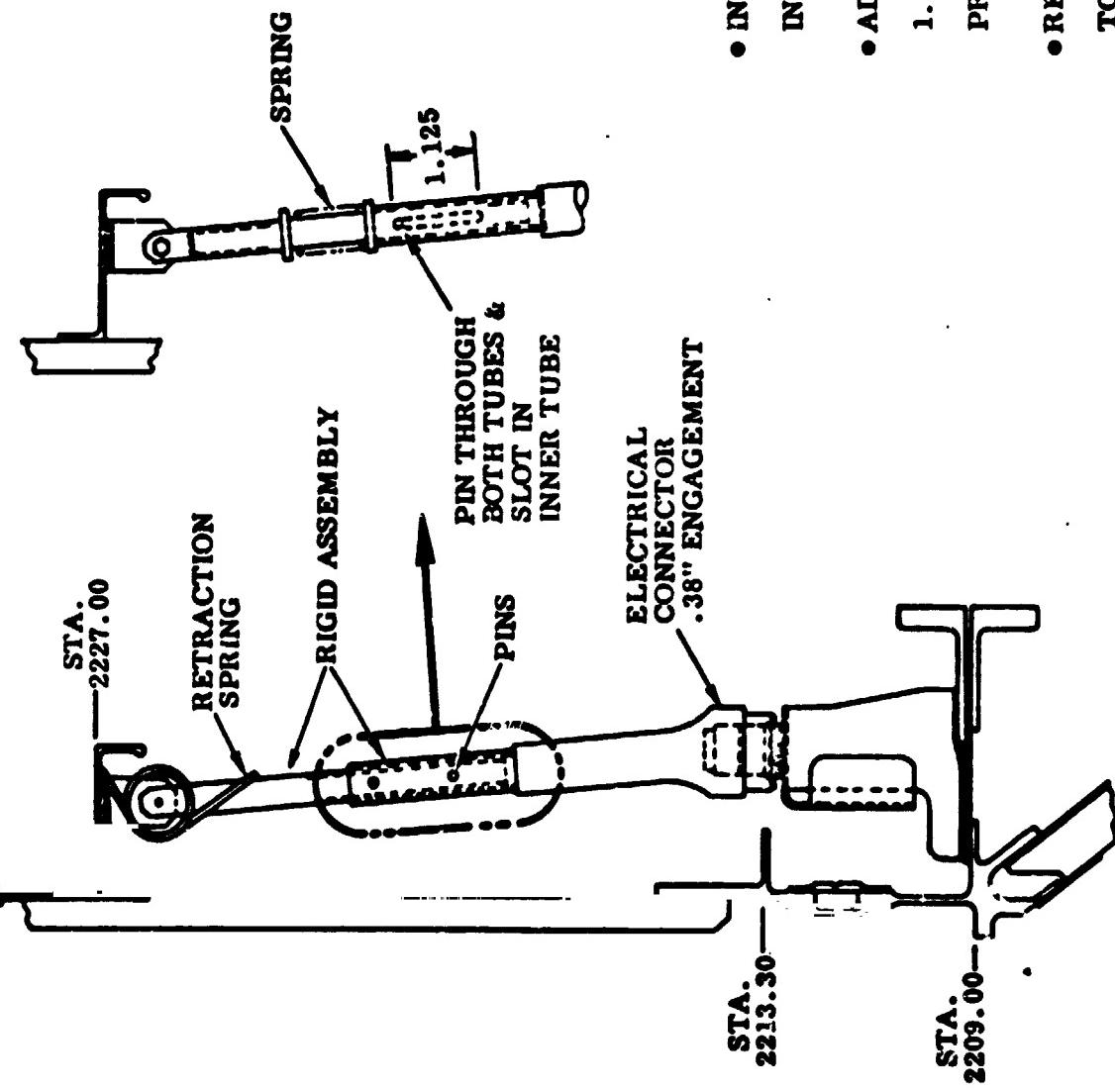
FIGURE 69

SUPER*ZIP SYSTEM ELECTRICAL DISCONNECTS

TC-1 CONFIGURATION



TC-2 AND ON CONFIGURATION



MODIFICATIONS

- INCORPORATE 1.125 IN. STROKE IN BRACKET ASSY.
- ADDED SPRING TO ENSURE 1.125 IN. MOTION OF BRACKET PRIOR TO .38 IN. DISCONNECT TRAVEL.
- RETRACTION SPRING REMOVED TO ELIMINATE SIDELOAD.

FIGURE 70

SUPERZIP SYSTEM ELECTRICAL DISCONNECT MODIFICATIONS

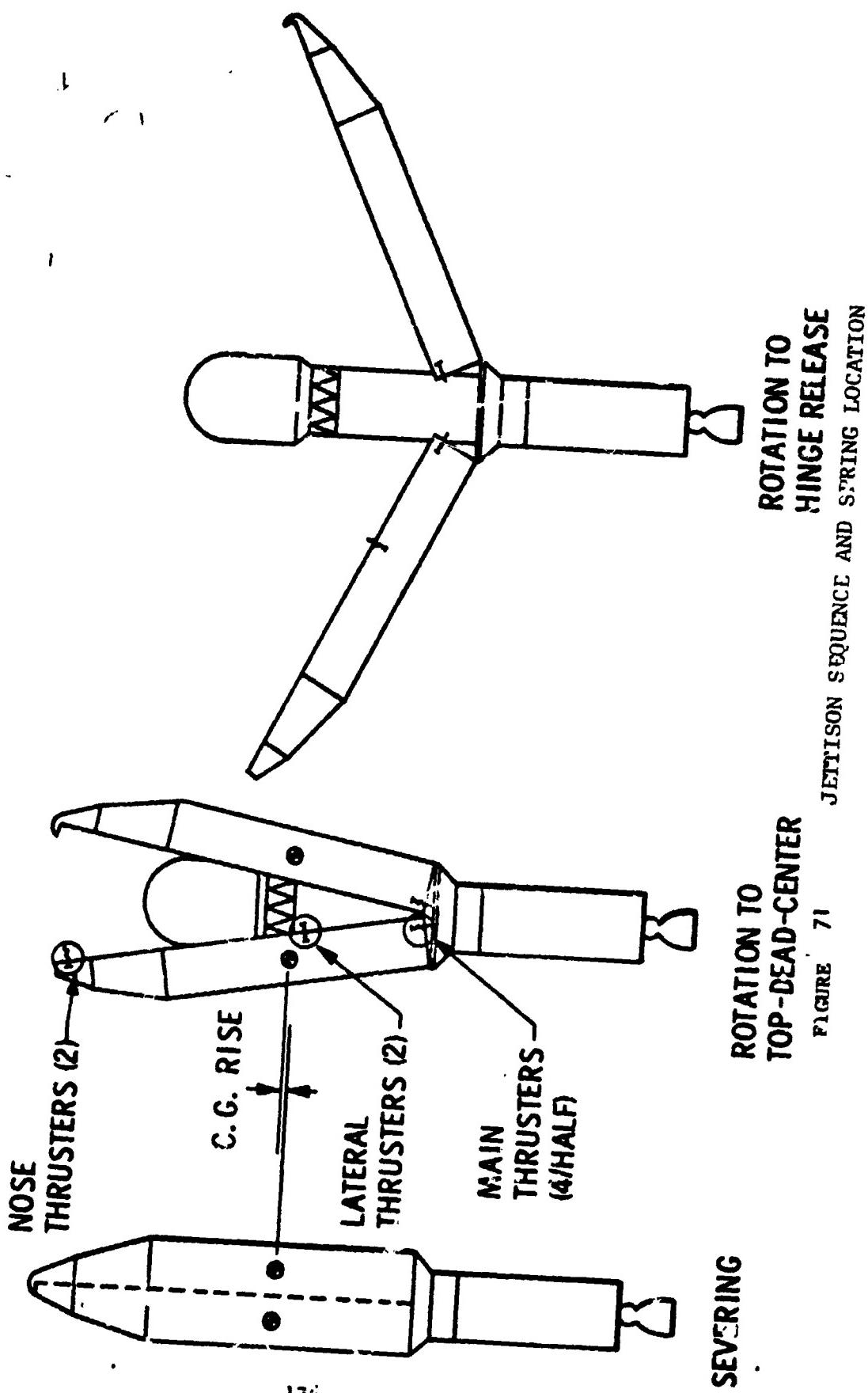


TABLE 29
CSS BREAKWIRE SUMMARY

BREAKWIRE (ROTATION AND LOCATION)	ACTIVATION TIME (SEC)	TIME FROM PRIMARY COMMAND		SAMPLING RATE (HZ)	
		TC-2 (SEC)	TC-1 (SEC)		
3° QUAD I	CAPPED	318.99	.39	.40	697
3° QUAD II		319.01	.41	.42	697
3° QUAD III	UNCAPPED	319.01	.41	.39	697
3° QUAD IV		318.99	.40	.40	697
8° QUAD I-II	CAPPED	319.36	.76	.65	697
8° QUAD III-IV	UNCAPPED	310.36	.75	.72	697
32° QUAD I-II	CAPPED	320.46	1.86	2.02	139
32° QUAD III-IV	UNCAPPED	320.16	1.56	1.84	139

TABLE 30
SUPER*ZIP COMMAND
AND
ELECTRICAL DISCONNECT ACTIVATION TIMES

FUNCTION	LOCATION	ACTIVATION TIME (SEC)	TIME FROM PRIMARY COMMAND		SAMPLING RATE (HZ)
			TC-2 (SEC)	TC-1 (SEC)	
PRIMARY COMMAND	--	318.60	--	--	--
ELECTRICAL DISCONNECT 1.50 in. STROKE	QUAD I (CAPPED)	318.83	.23	N/A	100
ELECTRICAL DISCONNECT .38 in. STROKE	QUAD II (CAPPED)	318.64	.04	.04	100
ELECTRICAL DISCONNECT 1.50 in. STROKE	QUAD III (CAPPED)	318.83	.23	N/A	100
ELECTRICAL DISCONNECT .38 in. STROKE	QUAD IV (UNCAPPED)	318.64	.04	.04	100
SECONDARY COMMAND	--	319.10	.500	.500	--

Shroud Jettison Hinge Loads

The shroud jettison strains were sensed by strain measurements and the strains converted to stress values. Because of the complexity of the jettison loads on the shroud hinges combined with the limitation of the available instrumentation, the loads on the hinges were assessed by comparing flight strains in the aft hinge support longerons to those experienced in the shroud jettison tests and the hinge static load tests.

Strain gage arrays were located on the aft hinge longeron webs. Each array consisted of four uniaxial gages centered on Station 2187 and electrically connected to compensate for temperature variations and to give augmented signal voltage output as shown in Figure 72.

Prior to shroud jettison, stresses in the aft hinge longerons were small in value as expected. The hinge longerons are designed primarily for loading at shroud jettison and only peripheral loads are transmitted to them in the course of the flight.

At shroud jettison the stresses in the four aft hinge longerons went from zero to maximum tension values in 0.04 second as follows:

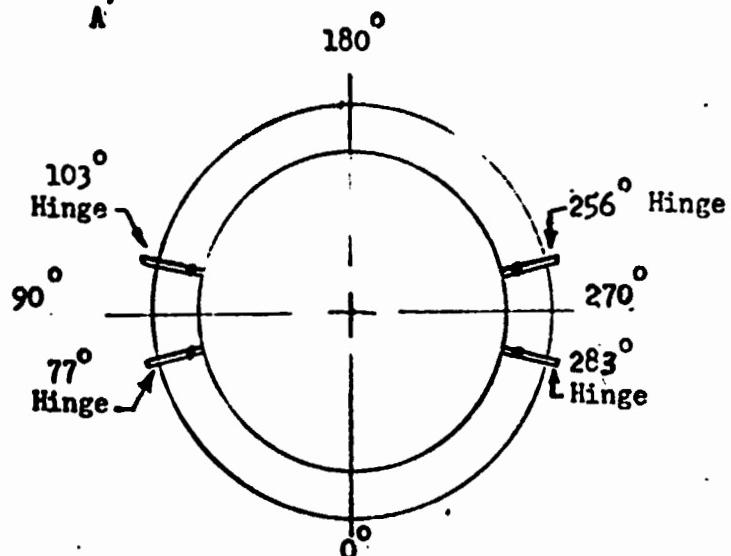
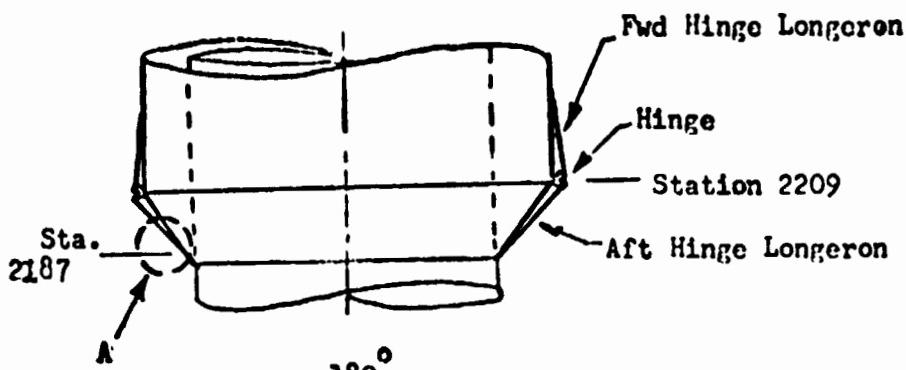
Hinge Longeron at 77° azimuth, 2300 psi tension
Hinge Longeron at 103° azimuth, 2000 psi tension
Hinge Longeron at 257° azimuth, 1950 psi tension
Hinge Longeron at 283° azimuth, 2400 psi tension

These values compare to 2200, 2500, 1800 and 1900 psi, respectively, for TC-1 and to 2900 psi and 1950 psi maximum tension in the Heated/Altitude Jettison Tests Nos. 1 and 2, respectively, and to 6080 psi maximum in the Hinge Static Load Test.

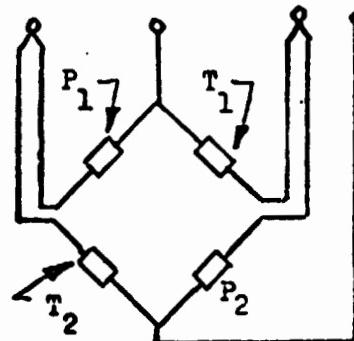
The hinge longeron stresses were oscillatory tension stresses during the initial phase of the jettison event as expected. The oscillations were at approximately 11.5 Hz with the amplitudes damping essentially to zero by 0.6 seconds. From 0.6 seconds until the shroud separated from the vehicle, the hinge longeron stresses were compression stresses of varying magnitudes. The maximum compression stresses were:

Hinge at 77° azimuth, 360 psi compression
Hinge at 103° azimuth, 420 psi compression
Hinge at 257° azimuth, 540 psi compression
Hinge at 283° azimuth, 690 psi compression

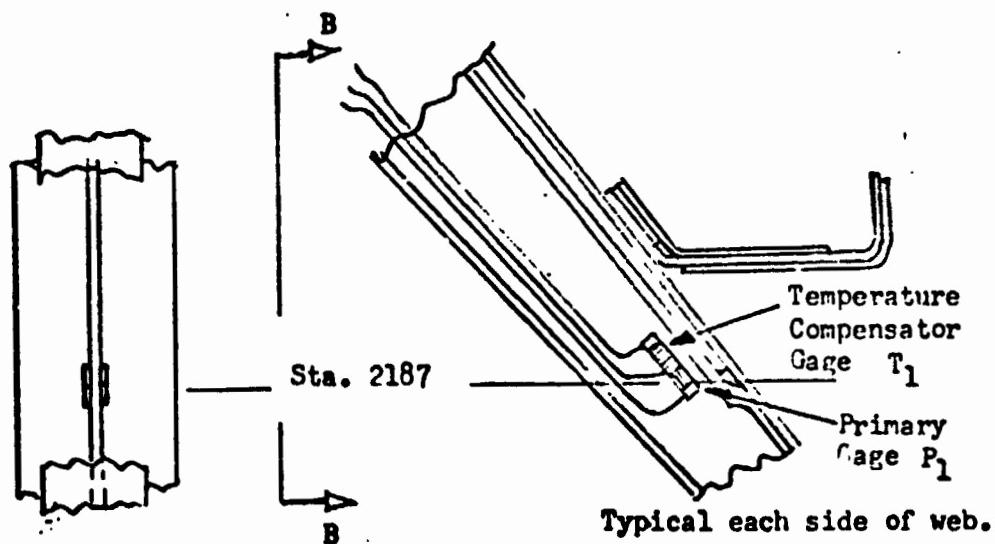
By comparison the maximum compressive stresses in the aft hinge longerons for TC-1 were 1000, 1300, 800 and 700 psi, respectively. Whereas the values in the No. 1 and No. 2 Heated/Altitude Jettison Tests were 400 psi and 500 psi, respectively. The longeron maximum stress value in the Hinge Static Load Test was 7750 psi.



LOOKING FWD



Electrical Circuit



View B B

Enlargement A

Figure 72 Centaur Standard Shroud Hinge Longeron Strain Gages.

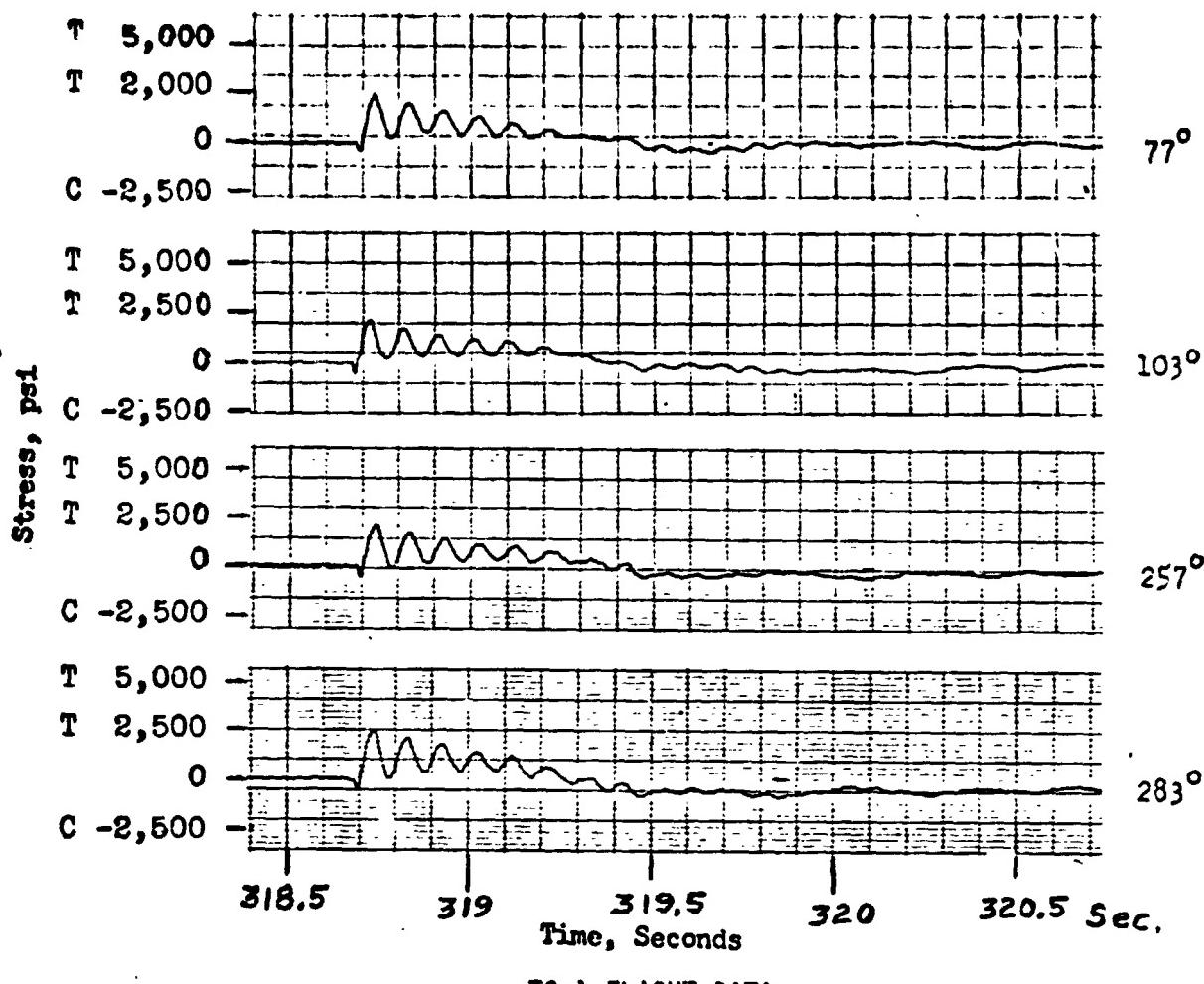
Shroud jettison loads as evidenced by aft hinge longeron strains started at $T + 318.7$ seconds and the last indication of longeron strains which was associated with completed jettison of the shroud from the vehicle was at $T + 321.5$ seconds. The duration of shroud jettison was 2.8 seconds and compares to 2.8 seconds for TC-1 shroud jettison and 2.7 seconds for the Heated/Altitude Jettison Tests.

The stresses in the aft hinge longerons during shroud jettison were of low value and compared well to the Heated/Altitude Jettison Tests data and were considerably less than half of the value of the stresses in the Hinge Static Load Test as shown in Table 31. Data traces of the flight shroud jettison in each aft hinge longeron versus time are compared in Figure 73 to curves from TC-1 shroud jettison. As shown, the traces are similar both in magnitude and in stress fluctuation.

T • Tension
C • Compression

TC-2 FLIGHT DATA

Hinge Location



TC-1 FLIGHT DATA

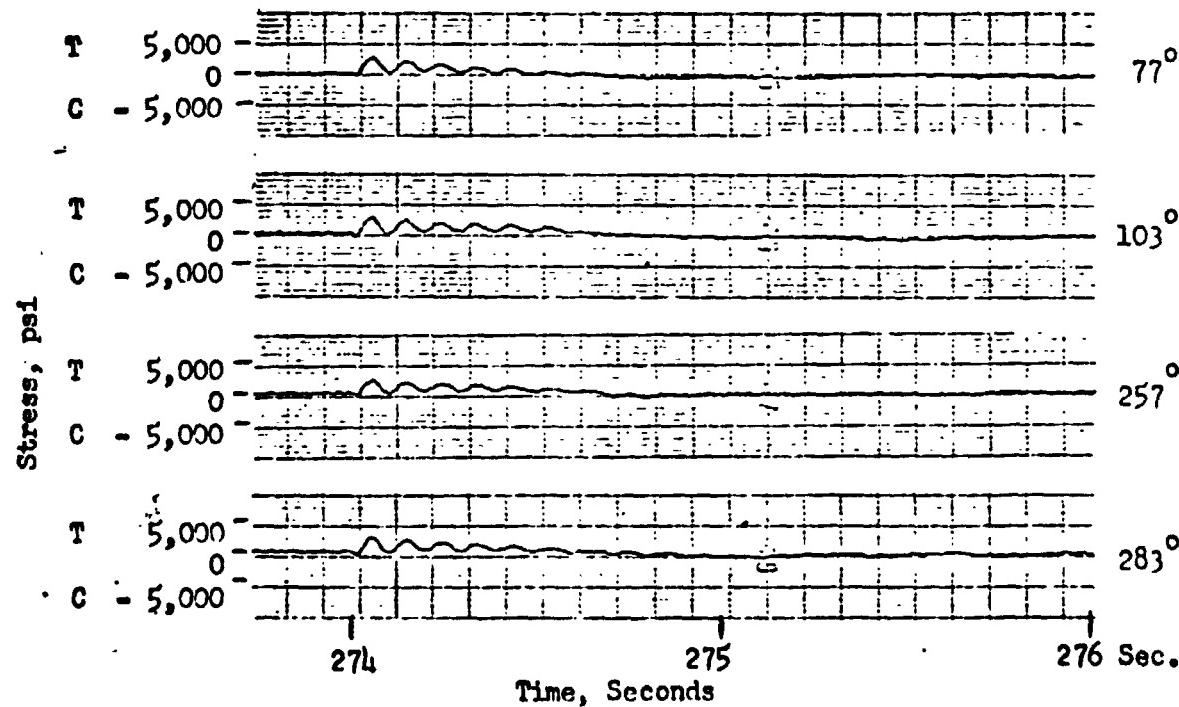
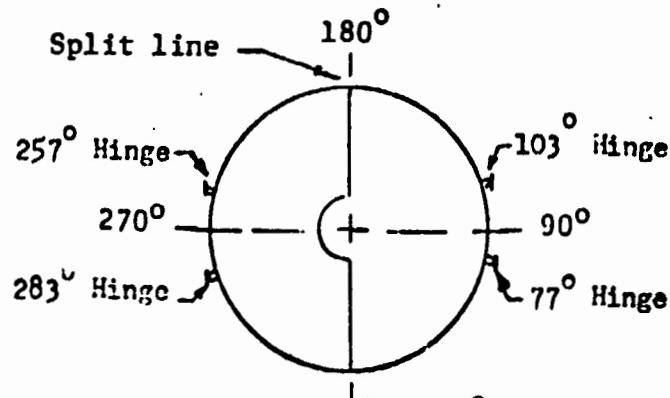


FIGURE 73 AFT HINGE LONGERON STRESSES AT STATION 2187 DURING SHROUD JETTISON

TABLE 31

Hinge Jettison Stresses
in Aft Hinge Longerons at Station 2187.

		Flight Maximums				Test Maximums			
		Capped Half (90°)		Uncapped Half (270°)		Heated Altitude Jettison		Static Struct.	
		Time, Sec.	77° Hinge psi	103° Hinge psi	257° Hinge psi	283° Hinge psi	#1 psi	#2 psi	psi
Max. Tension	TC-2	T+318.72	2300	2000	1950	2400	2400	2200	6080
	TC-1	T+374.03	2200	2500	1800	1900			
Max. Compr.	TC-2	-----	360	400	540	690	750	800	7750
	TC-1	-----	1000	1300	800	700			



Looking Aft

IX CENTAUR D-ITR SYSTEMS ANALYSIS

IX CENTAUR D-ITR SYSTEMS ANALYSIS

Mechanical Systems

Structures

by R. T. Barrett, C. W. Eastwood, R. C. Edwards,
T. L. Seeholzer and J. O. VanVleet

The ISA satisfactorily transferred all Centaur and CSS loadings onto the Titan Skirt structure. The ISA forward ring was completely severed at Titan/Centaur staging and the vehicles separated at a constant acceleration.

The ullage pressures in the Centaur propellant compartments were within prescribed limits. Sufficient pressure was maintained to prevent buckling and maximum pressures did not exceed burst limits of the tank structure.

The structural components located on the forward portion of the Centaur tank satisfactorily supported the payload and electronic packages. The stub adapter structure safely withstood the tangential loading of the six FBR struts.

The Forward Bearing Reactor struts successfully transferred flight loads from the CSS to the Centaur stub adapter. The magnitude of these loads was well within the demonstrated capability.

Interstage Adapter

The interstage adapter (ISA) provides a physical connection between the Titan forward skirt (at Station 2127.43) and the Centaur (at Station 2240.79). In addition, it provides a support ring for the Centaur Standard Shroud at Station 2180.48 as shown in Figure 74.

A separation monitoring device (yo-yo) was mounted between the ISA and the Centaur aft bulkhead (Figure 75). This yo-yo was instrumented and plotted during flight for a total of 15 feet after separation to verify that separation was satisfactory.

The flight loads, both axial and bending moments, on the forward section of the interstage adapter (ISA) were calculated from structural strains that were sensed by strain measurements composed of strain gage arrays. On the section of the ISA forward of the shroud/ISA interface, four strain gage arrays were located at Station 2208 and spaced 90 degrees apart at azimuths 24°, 114°, 204° and 294° as shown in Figure 76. Each array consisted of four uniaxial gages mounted on the stringers and electrically connected as shown in Figure 77.

Prior to propellant tanking of the vehicle, the strain measurements were zeroed. This method of reference required the addition of the weight (in a 1-g field) of the dry Centaur, the forward adapters and equipment, and the Helios-A spacecraft, totalling 8,400 pounds, to all axial loads on the forward ISA. Also, a calibration factor of 0.79 was applied to the indicated bending moments on the ISA. The calibration factor was determined from the imit Load Static Structural Tests (reference 1).

INTERSTAGE ADAPTER

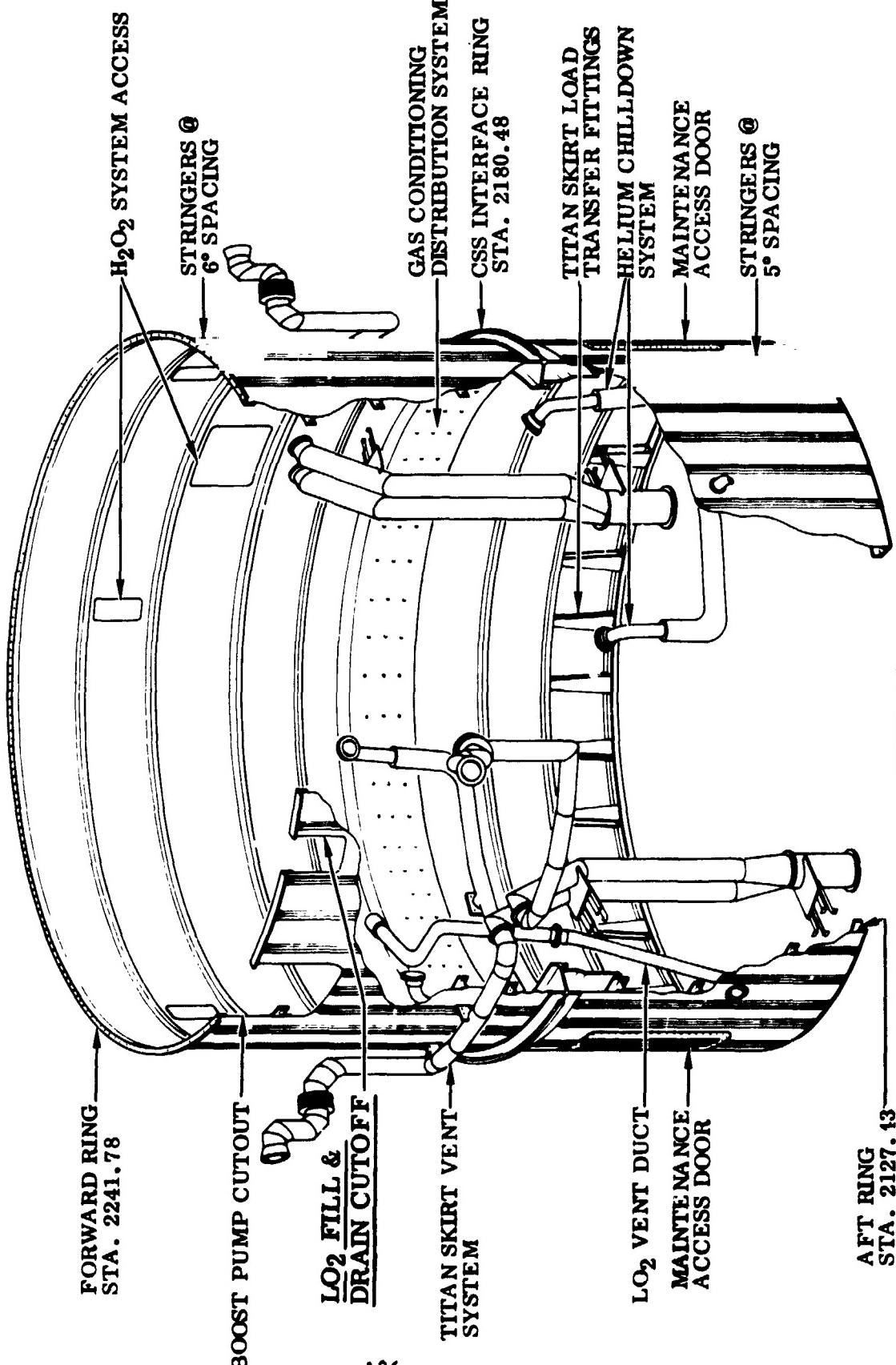


FIGURE 74

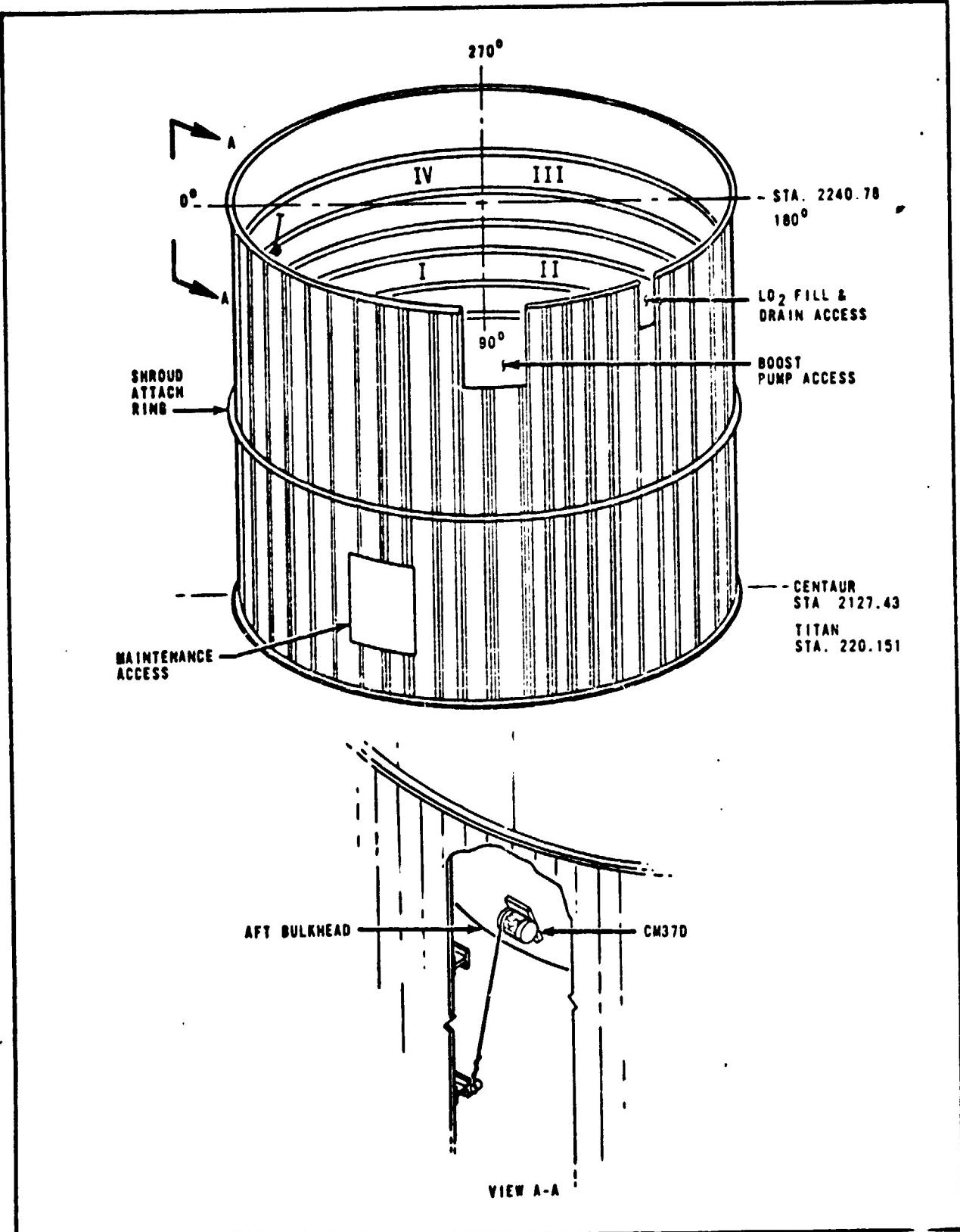


FIGURE 75 TITAN/CENTAUR INTERSTAGE ADAPTER SEPARATION INSTRUMENTATION (Y0-0)

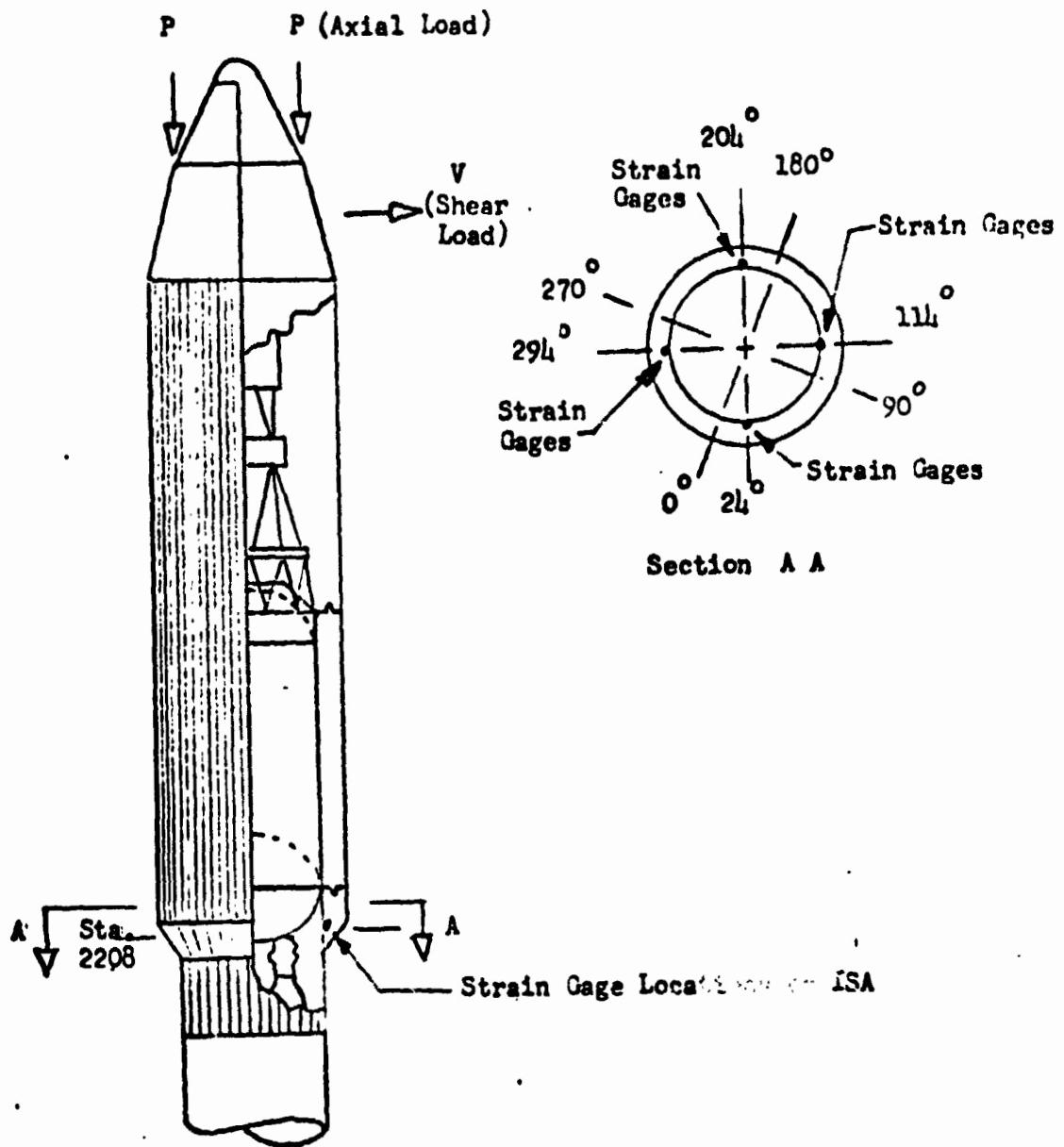
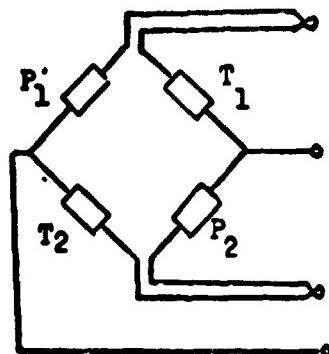
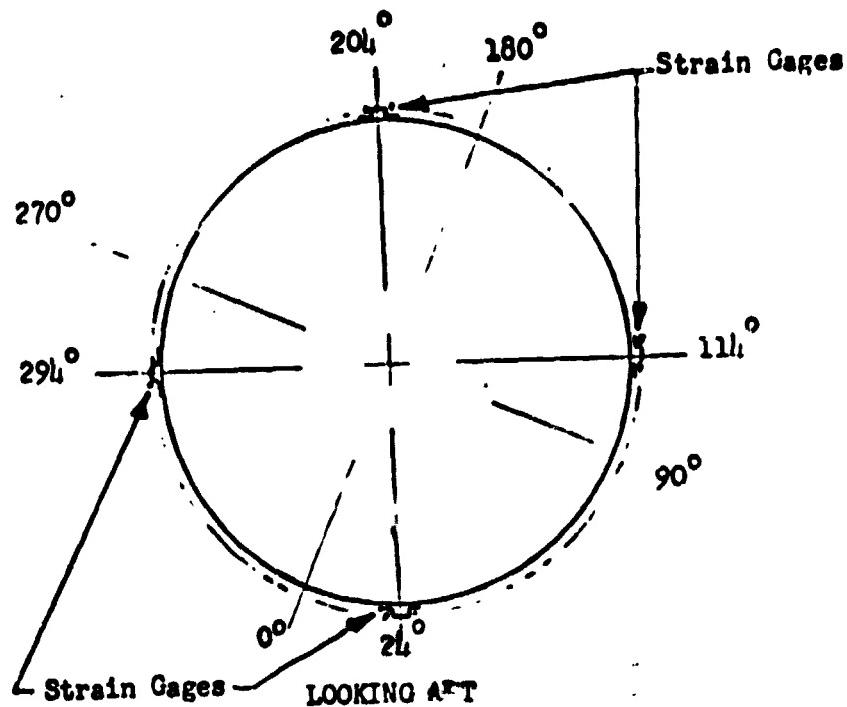
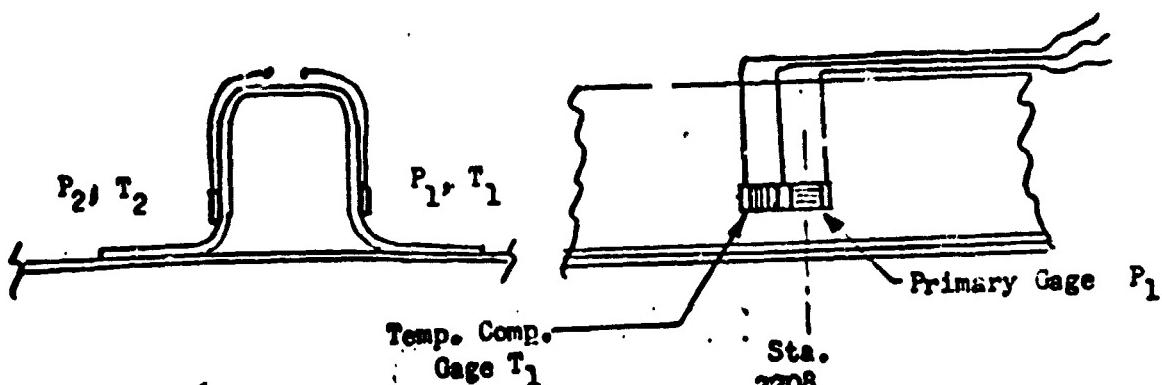


Figure 76 Structural Strain Measurement Locations on ISA.



Electrical Circuit



Typical Each Side of Stringer.

Figure 77 Centaur Interstage Adapter Strain Gages.

The yo-yo separation trace was very smooth (Figure 78), indicating a normal separation. Since the IA is 9.5 feet long and the total yo-yo travel is 15 feet, the ISA cleared the Centaur.

The maximum combined loads on the ISA at Station 2203 were at T + 257 seconds at maximum acceleration during Stage I burn. The equivalent axial load at that time was 128,500 pounds on the compression side and 126,300 pounds compression on the opposite side. Of this equivalent axial load, 127,400 pounds were direct axial load and 1,100 pounds were from a bending moment of 0.03×10^6 inch-pounds.

The maximum bending moment on the ISA at Station 2208 was 1.14×10^6 inch-pounds at T + 38.3 seconds. At the same time the axial load was 62,200 pounds compression at Station 2208 on the ISA. The equivalent axial load was 100,200 pounds on the compressive side and 24,200 pounds compression on the opposite side.

Equivalent axial loads, direct axial loads and bending moment at the various event times during the TC-2 flight are listed in Table 32. Loads applied to the test ISA with the FBR system installed and the equivalent axial loads for TC-1 flight are included in the table for comparison. As shown, the flight maximum equivalent axial load for TC-2 was 80 percent of the TC-1 load and 58 percent of the test load. The flight maximum bending moment was less than 26 percent of the test value maximum. The axial load at Stage I maximum acceleration was 60 percent greater than the test axial load, however, as previously stated, the combined load was only approximately 58 percent of the test value.

Using the bending moments from the ISA at Station 2208 and from the shroud at Station 2294 and correlating the values with the qualification test values, a bending moment value for flight on the ISA/Titan Skirt interface at Station 2127 can be approximated within 20 percent. At T + 38.3 seconds of flight, the value was 12.2×10^6 inch-pounds compared to a test value of 22.9×10^6 inch-pounds. The equivalent axial load at Station 2127 at T + 38.3 seconds calculated by combining the correlated bending moment and the axial load was 503,400 pounds compression compared to a test value of 869,600 pounds and 310,000 pounds tension compared to a test value of 658,400 pounds. In percent of test values, the equivalent axial loads at Station 2127 for TC-2 and TC-1 flights were as follows:

<u>Station 2127 Flight Equivalent Axial Load Type</u>	<u>Percent of Test Equivalent Axial Load</u>	
	<u>TC-2</u>	<u>TC-1</u>
Compression	57.8%	44.1%
Tension	47.1%	29.8%

TO VARIOUS CRIMINAL ACTS

FIGURE 78 TC-2 FLIGHT SEPARATION ($y_0 - y_0$)
READING CM370

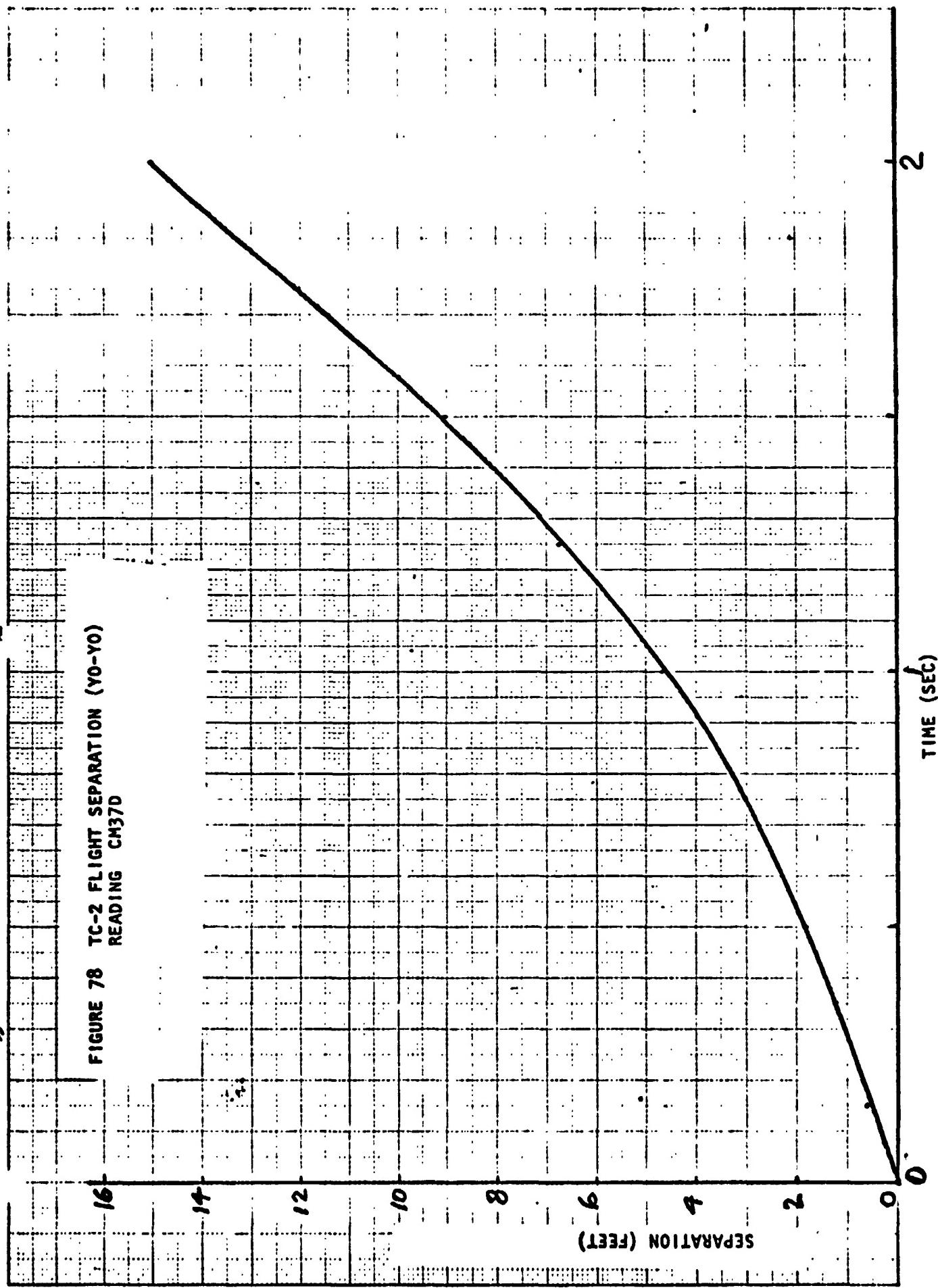


TABLE 32

ISA Structural Flight Loads and Limit Test Loads, Station 2208.
 (Includes weight of Centaur, Propellants, Adapters, Equipment,
 and Helios A Spacecraft forward of Sta. 2208 in all axial values)

Flight Event	Nominal Time, Sec.	Total Axial Load, Lbs.	Bend. Mom., in.lb. x10 ⁶	Vehicle Accel., g	Total Equivalent Axial Load at Extreme Fiber, Lbs.	Compression
		Compress,	TC - 2	TC-2	TC-1	
Zero Reference	T -1	39,800	0.15	1.00	45,500	43,450
-----	T -5	50,400	0.20	1.60	57,000	65,500
Transonic	T -38.3	62,200	1.14	1.80	100,200	94,000
-----	T -41	57,200	0.37	1.80	69,500	100,700
SRM Max Accel	T-105	97,200	0.06	2.70	99,200	115,000
SRM Jettison	T-125	50,900	0.04	1.30	52,400	57,600
Stage I Max Accel	T-257	127,400	0.03	3.60	128,500	149,500
Prior to CSS Jett.	T-318	35,000	0.04	0.95	36,400	-----
Stage II Max Accel	T-467	70,000	0.10	2.08	73.700	84,300
Test Limit Loads						
With FBR until T-100		79,000	4.33	1.00	223,400	

Although TC-2 flight loads were greater than TC-1 values, both TC-2 and TC-1 loads were less than 58 percent of the test verified design loads.

Centaur Tank

The propellant tank forms the primary Centaur vehicle structure (Figure 79). The tank locations and criteria which determine the maximum allowable and minimum required tank pressures during various phases of flight are described in Figure 80. These maximum allowable and minimum require tank pressure limits are compared to actual TC-2 propellant tank pressures in Figure 81. During the flight, the combined ullage and hydrostatic pressure of the liquid hydrogen tank was always less than 29.2 psia and the liquid hydrogen tank ullage pressure was always greater than the minimum required pressure. The oxygen tank pressure was always greater than the combined hydrogen ullage and hydrostatic pressures. The differential pressure between the propellant compartments did not exceed 23.0 psi at any time during flight. The liquid oxygen tank pressure was always less than the maximum allowable pressure.

Stub Adapter

The stub adapter is a ten-foot diameter skin-and-stringer cylinder, 25 inches high, which attaches to the Centaur tank and provides a mounting platform for forward equipment and payloads.

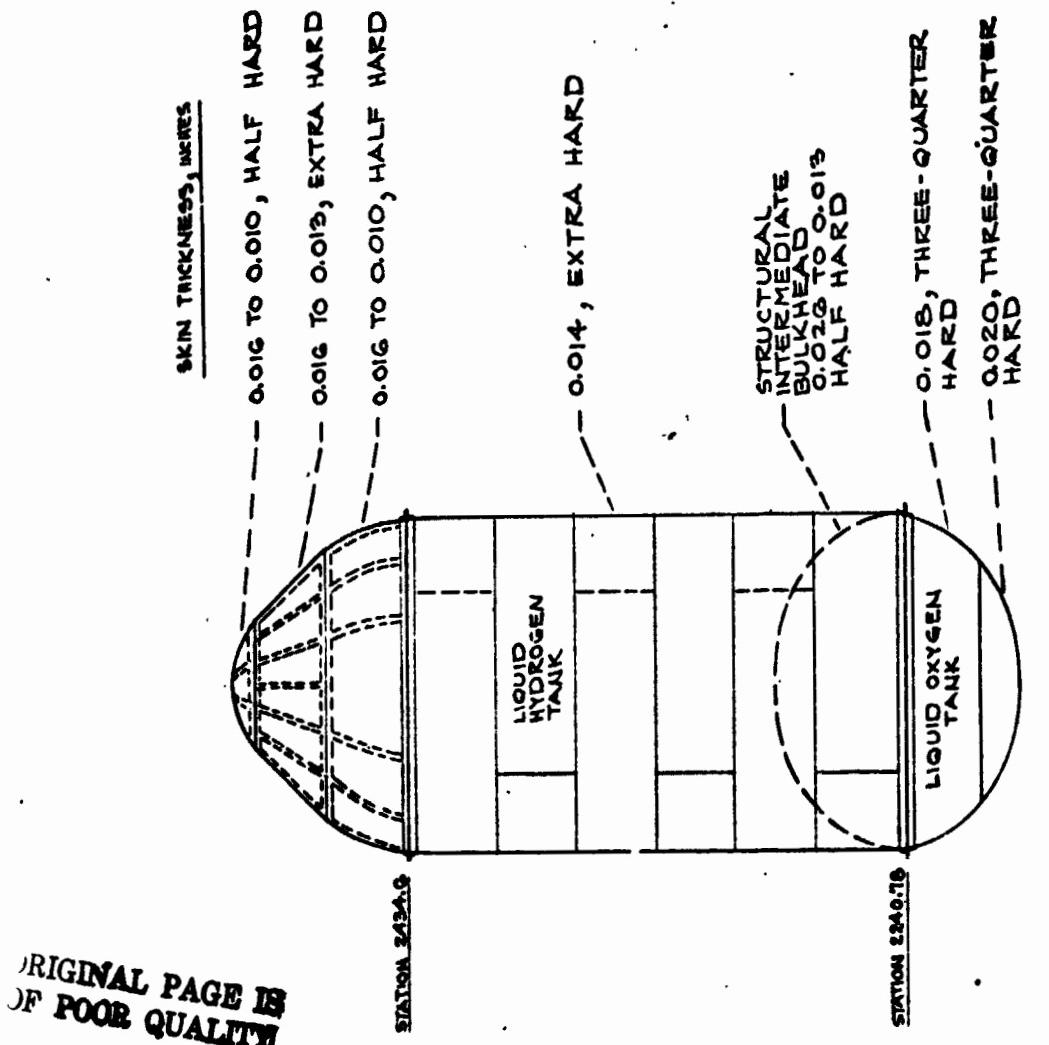
The adapter was not instrumented for strain monitoring - no direct load data for the adapter is available. The design allowable crush pressure for the module is 2.9 psid; measured flight pressures ranged from zero psid to 1.2 psid crush.

Equipment Module

The Centaur equipment module is a conical skin-stringer structure of 10-foot diameter base and five-foot diameter top, 30 inches high, which attaches to the top of the stub adapter. Its function, for TC-2 was to provide a mounting surface for the avionics packages, to act as a thermal insulating cap for the Centaur tank, and to serve as a payload mounting platform. A spring-loaded door in the module opened at liftoff, as scheduled, so that there was no burst or crush pressure on the module during flight. Module pressure just prior to flight was 0.18 psid burst. There was no strain gage data for the equipment module.

Mission Peculiar Adapter

The Helios Mission Peculiar Adapter is a conical aluminum skin-stringer-frame structure joining the aft end of the Delta spin-table assembly to the forward end of the Centaur Equipment Module.



194

FIGURE 79 CENTAUR PROPELLANT TANKS (ALL MATERIAL 301 CRES)

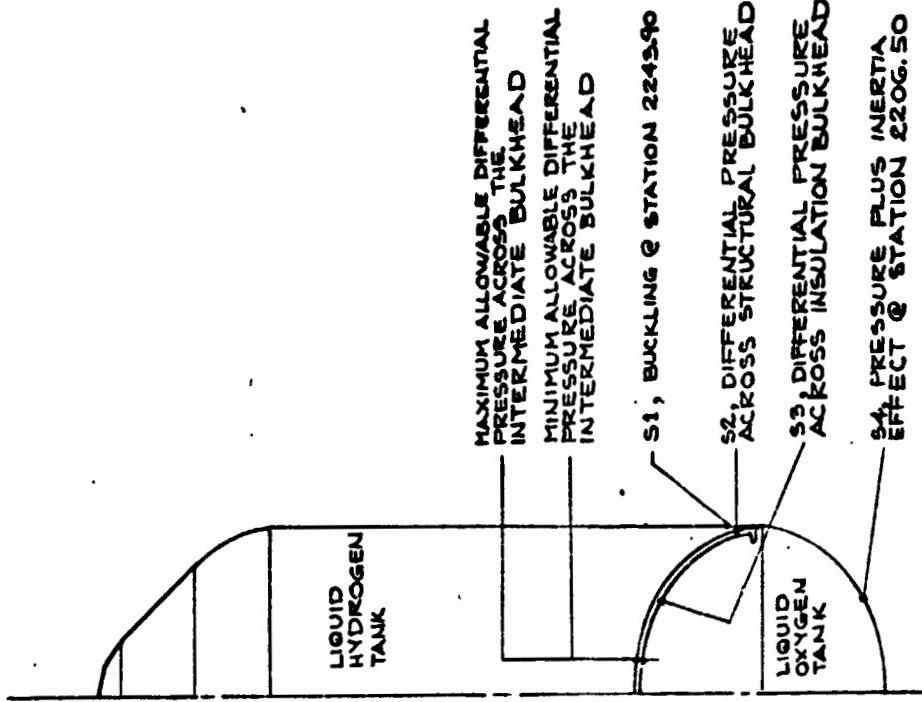


FIGURE 80 TANK LOCATIONS AND CRITERIA WHICH DETERMINE ALLOWABLE PRESSURES

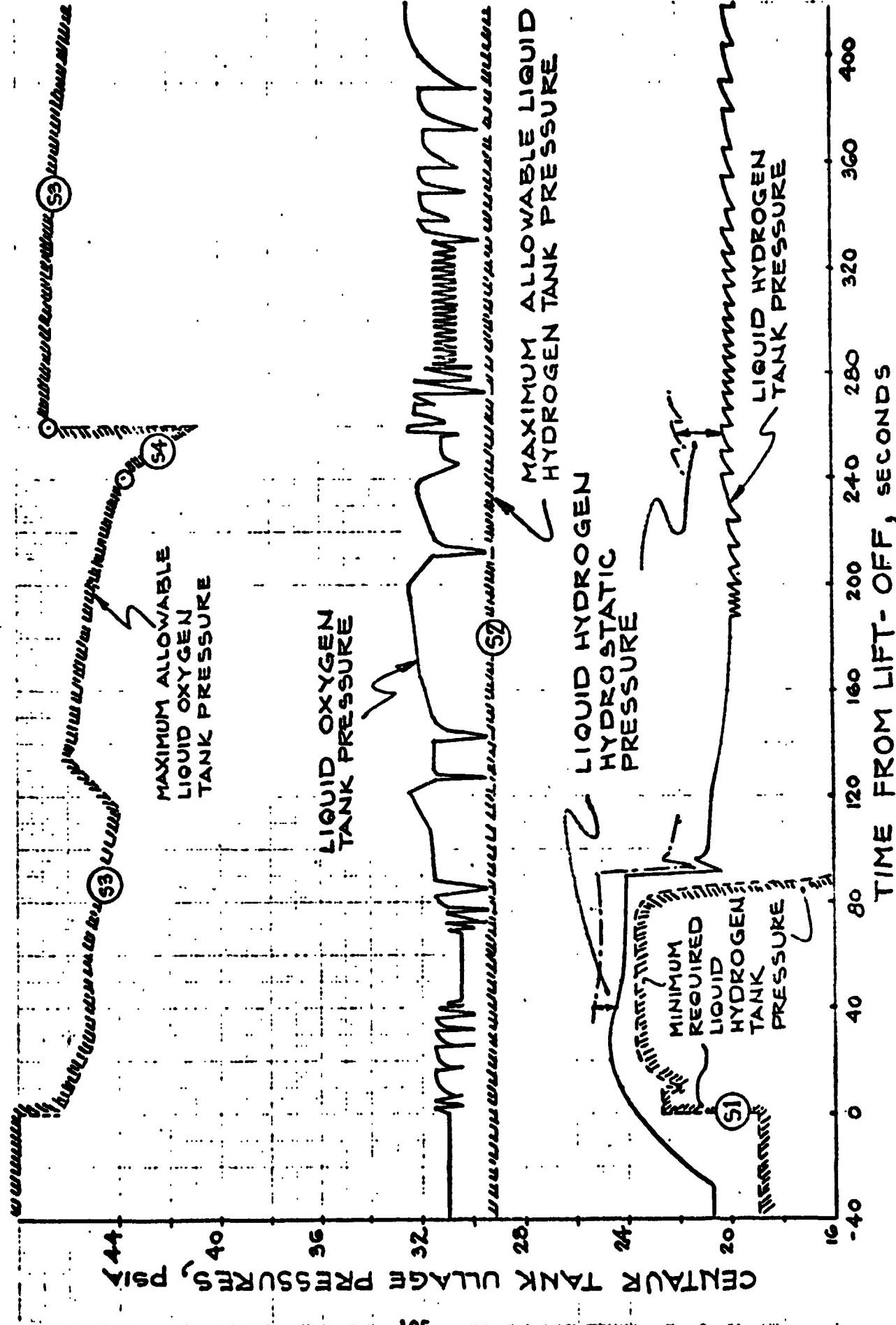
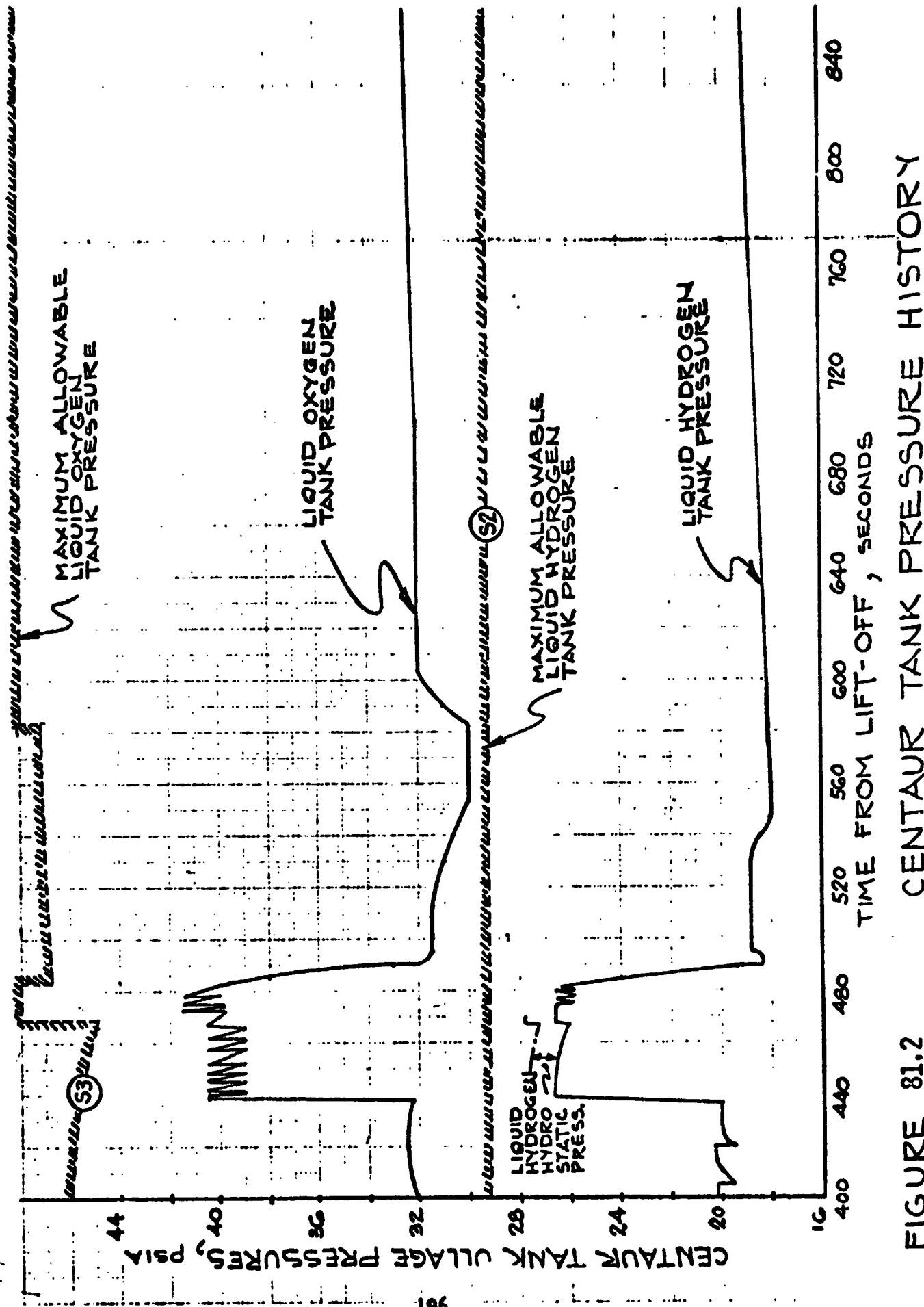


FIGURE 81.1 CENTAUR TANK PRESSURE HISTORY



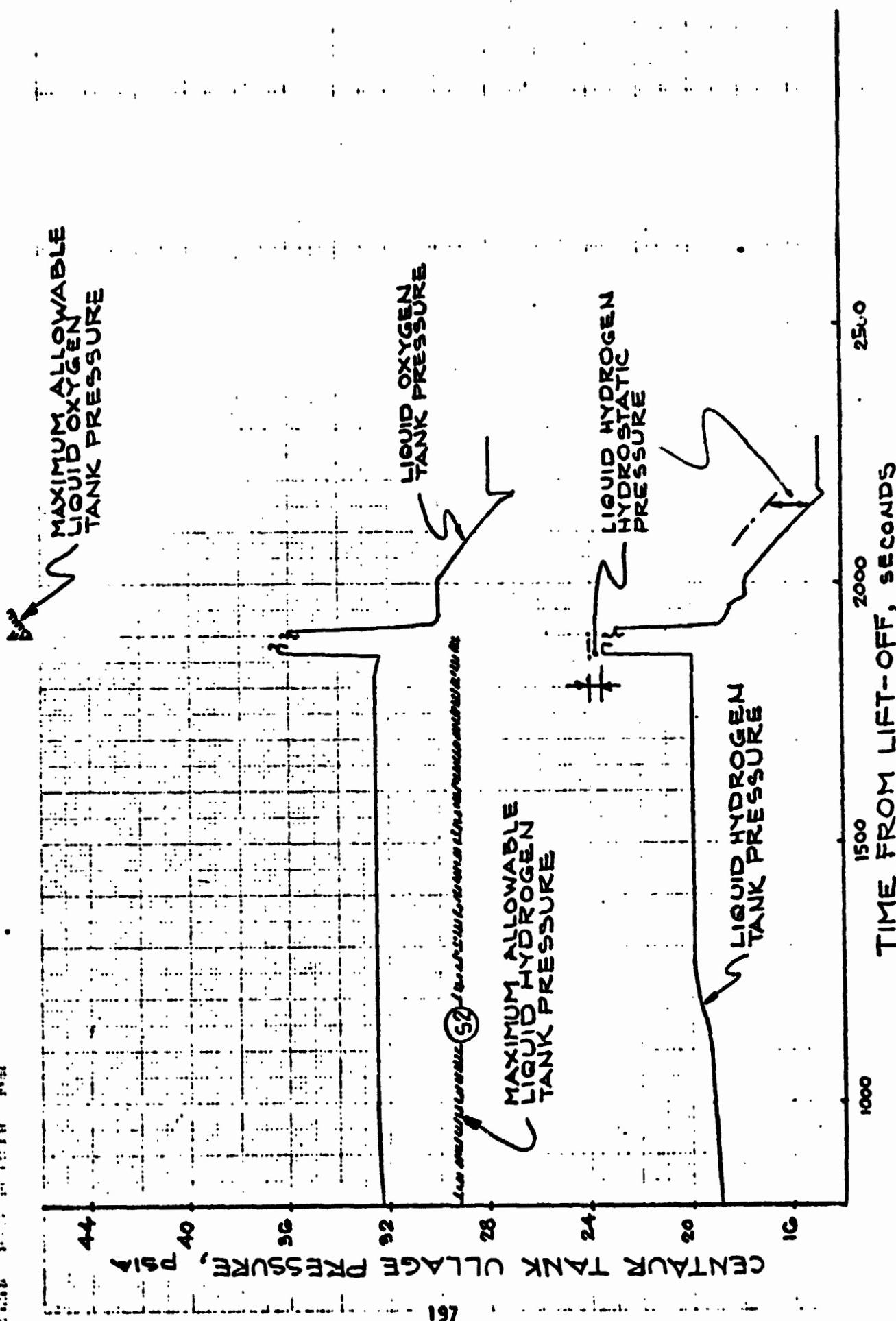


FIGURE 81.3 CENTAUR TANK PRESSURE HISTORY

An environmental shield is attached to the adapter forward ring. The outer edges of the shield are supported from the equipment module aft ring by 12 tubular struts. The shield also serves as a work platform for access to the payload. The shield consists of eight segments, each made from a sandwich panel of balsa wood core with aluminum sheets.

There was no strain gage or pressure data for the Mission Peculiar Adapter.

References

1. C. Eastwood: Centaur Standard Shroud (CSS) Static Limit Load Structural Tests. NASA TMX-71727, April 1975.

Propulsion/Propellant Feed System

by K. W. Baud and W. K. Tabata

RL10 Engine System

Ground Prechill - Liquid helium prechill of the engine fuel pumps on the ground was satisfactory. Listed in Table 33 are the C-1 and C-2 engine fuel pump housing temperatures at liftoff. Each fuel pump housing has a dual element temperature probe, so the primary measurements, CP122T and CP123T, as well as the backup measurements, CP118T and CP119T, are listed. All four measurements indicate both fuel pumps were well below the 100°R maximum at liftoff. Also listed in Table 33 are the C-1 and C-2 engine oxidizer pump housing temperatures (single-element probes) and the C-1 and C-2 engine thrust chamber temperature measurements. All these temperatures were as expected and within the experience of the TC-1 Proof Flight and previous Atlas/Centaur launches.

Prestart - The C-1 and C-2 engine fuel and oxidizer pump housing temperatures and the thrust chamber temperatures at the beginning of the first-burn and the second-burn prestarts are listed in Table 33. For both prestarts, all temperatures were as expected and within the range of previous Centaur flights.

The first burn and second burn had programmed prestart duration of 8 seconds and 17 seconds, respectively. The pump housing temperatures indicate proper cooldown transients during the prestart periods.

Start - The first-burn transients for the C-1 and C-2 engines are shown in Figure 82 for the time period of main engine start (MES) plus 1.0 seconds to plus 1.7 seconds.

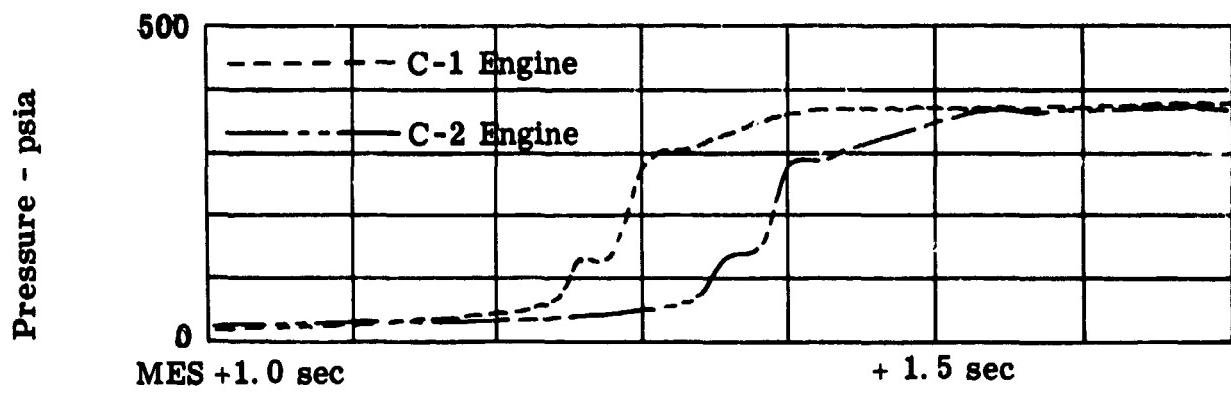
Figure 82a shows the C-1 and C-2 engine chamber pressures. The time to accelerate to 90 percent of steady-state thrust for both engines and the differential acceleration time between the two engines are within previous flight experience. Ignition on both engines (not shown in Figure 82a) occurred at approximately 0.2 seconds after start signal as expected.

The start transients of the oxidizer pump speed, the fuel venturi upstream pressure, the oxidizer pump discharge pressure, and the fuel pump discharge pressure shown in Figures 82b through 82e are all normal.

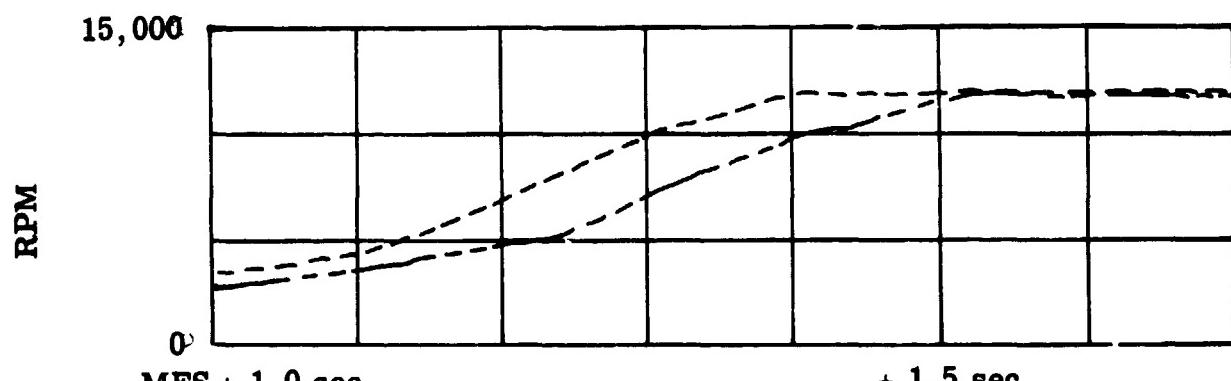
The second-burn start transients are shown in Figure 83. All transients are normal and as expected. The differential acceleration time to 90 percent thrust (Figure 83a) between the C-1 and C-2 engines is approximately 0.3 seconds. This is larger than normal, but not outside of previous flight experience. Atlas/Centaur flight AC-32 had a differential acceleration time on the second burn of approximately 0.27 seconds. The larger differential times would be expected, since acceptance test of the

Table 33 RL10A-3-3 Engine Temperatures

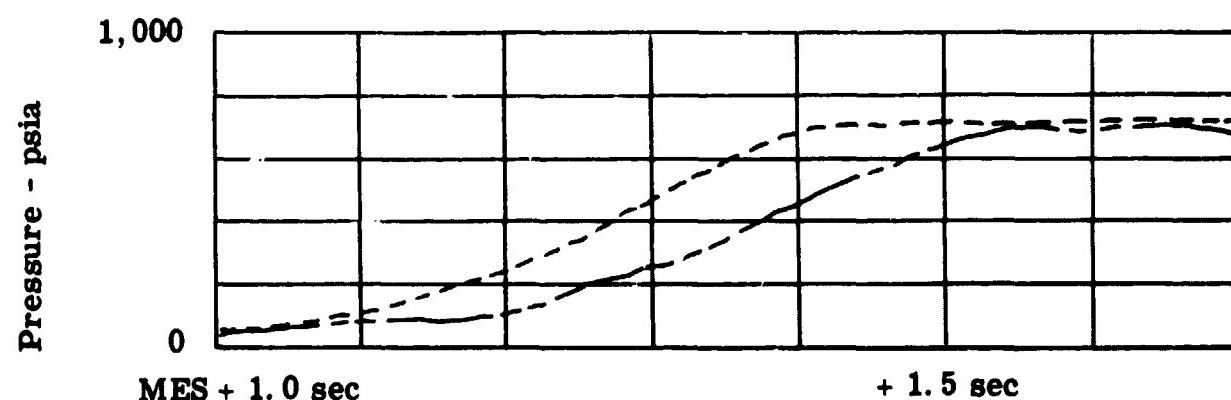
		At Liftoff	At Prestart #1	At Prestart #2
CP124T	C-1 Oxidizer Pump Housing, °R	390	369	316
CP125T	C-2 Oxidizer Pump Housing, °R	409	374	365
CP122T	C-1 Fuel Pump Housing, °R	65	182	216
CP118T	C-1 Fuel Pump Housing (Backup), °R	60	179	209
CP123T	C-2 Fuel Pump Housing, °R	65	182	210
CP119T	C-2 Fuel Pump Housing (Backup), °R	64	179	205
CP63T				
CP741T	C-1 Thrust Chamber, °R	508 - 531	501 - 531	404 - 505
CP743T				
CP745T				
CP98T				
CP742T	C-2 Thrust Chamber, °R	502 - 531	497 - 531	387 - 430
CP744T				
CP746T				



(a) Thrust Chamber Pressure

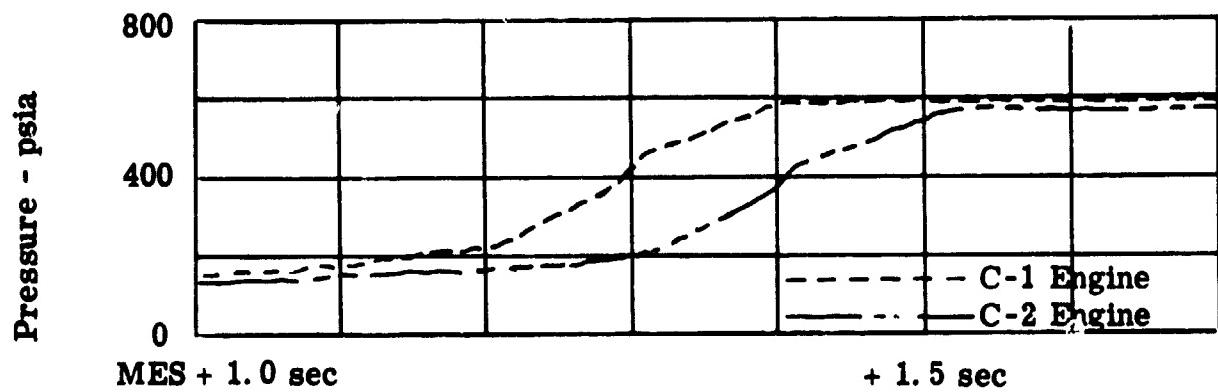


(b) Oxidizer Pump Speed

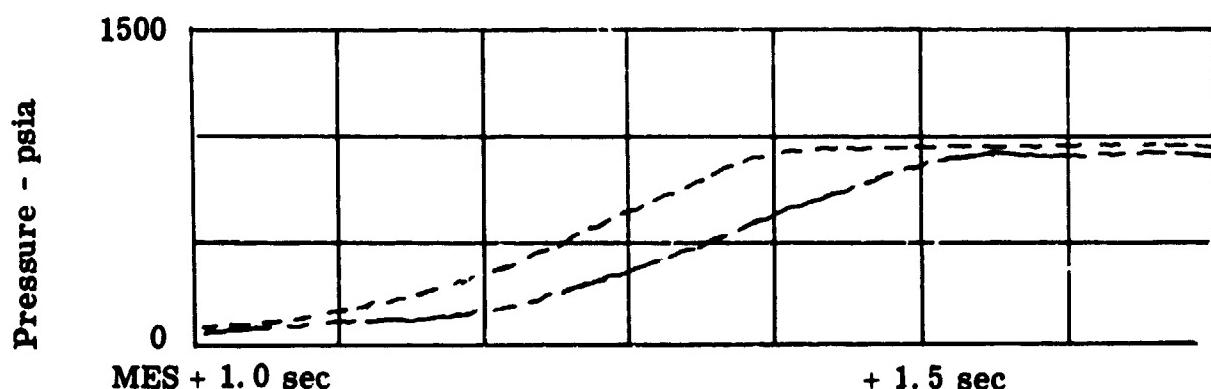


(c) Fuel Venturi Upstream Pressure

Figure 82.1 First-Engine Start Transient

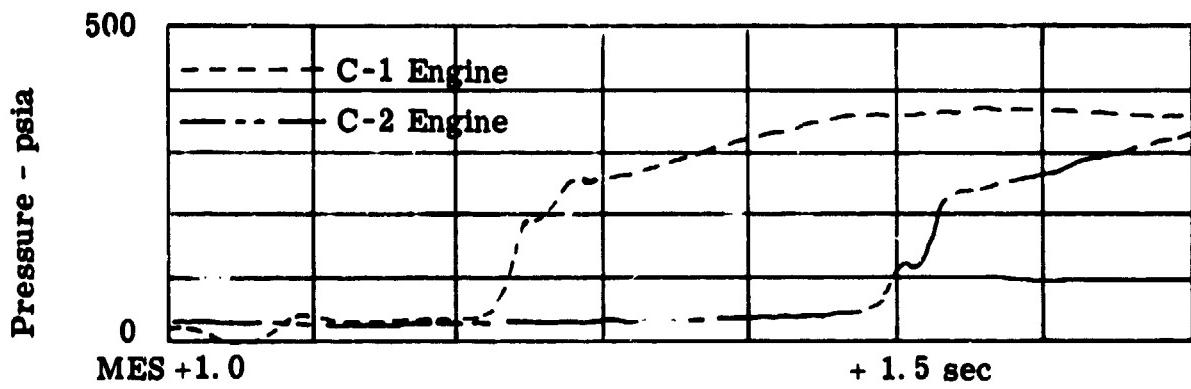


(d) Oxidizer Pump Discharge Pressure

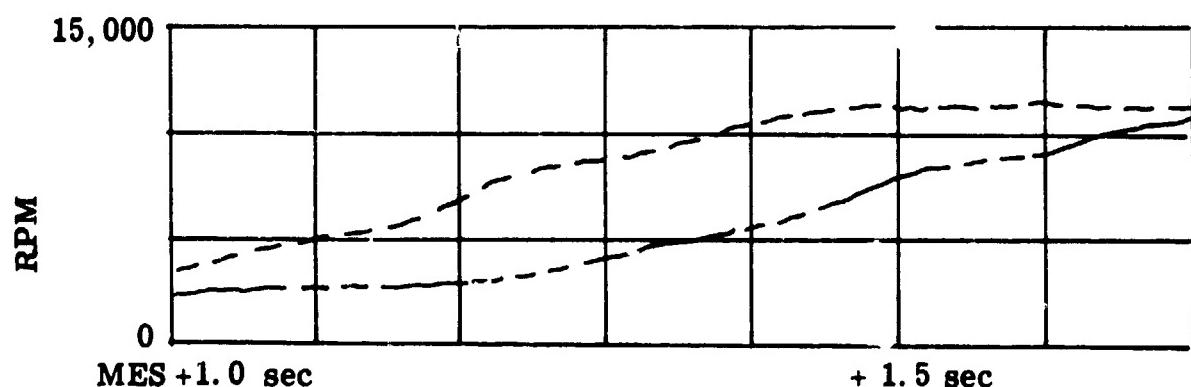


(e) Fuel Pump Discharge Pressure

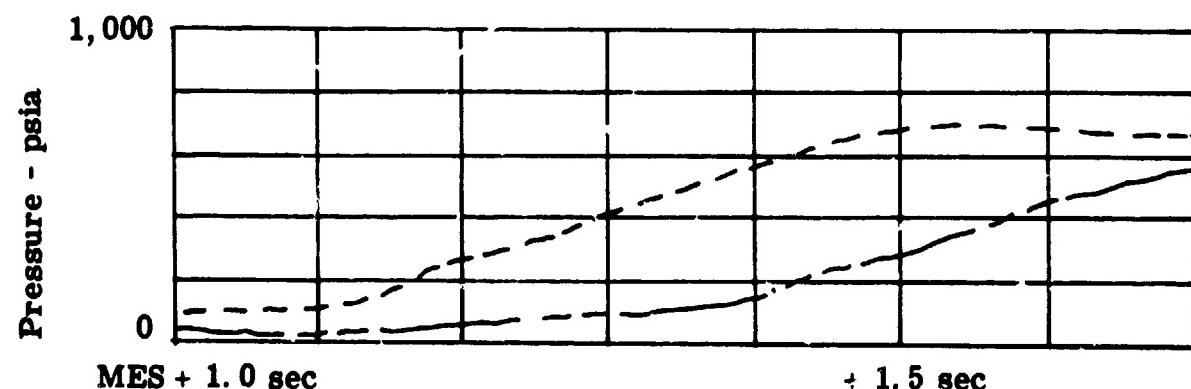
Figure 82.2 First-Engine Start Transient



(a) Thrust Chamber Pressure

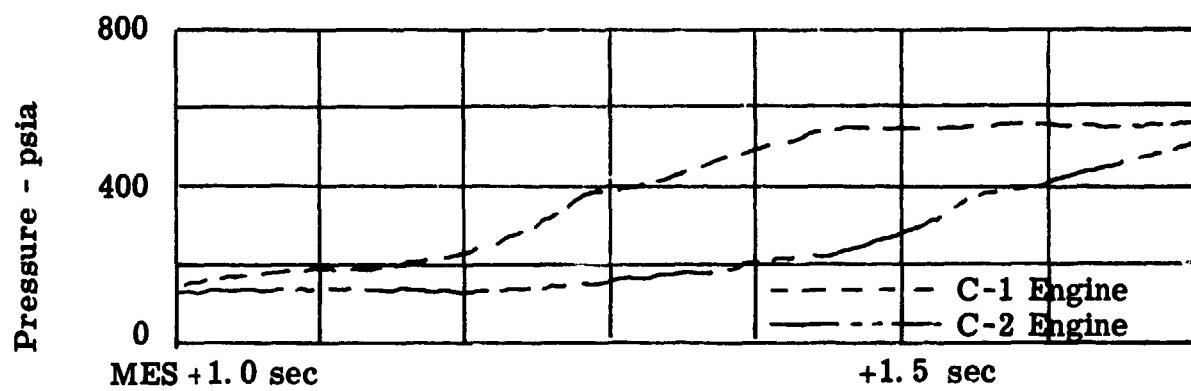


(b) Oxidizer Pump Speed

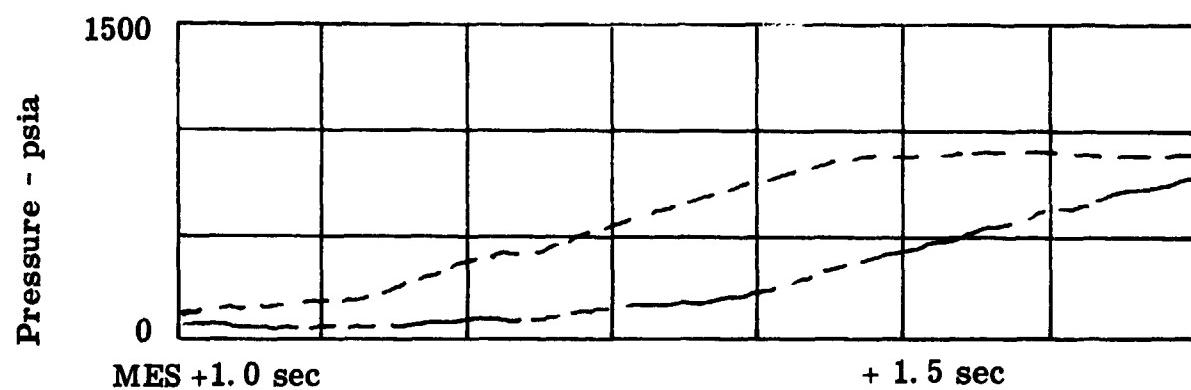


(c) Fuel Venturi Upstream Pressure

Figure 83.1 Second-Engine Start Transient



(d) Oxidizer Pump Discharge Pressure



(e) Fuel Pump Discharge Pressure

Figure 83.2 Second-Engine Start Transient

TC-2 C-2 engine, P641959, and the AC-32 C-1 engine, P641956, indicated both engines were slightly slower to accelerate.

In Figure 83a, the C-1 engine chamber pressure indicates a "dip" to zero pressure at MES + 1.05 seconds. These "dips" in chamber pressure before the engine begins to accelerate have been noted in recent flights since converting to strain-gage type pressure transducers. Engine tests at Pratt & Whitney Aircraft have indicated these "dips" are associated with the flight pressure transducers and not with a physical occurrence in the thrust chamber.

Steady State - The C-1 and C-2 engine steady-state performance was as expected. In Table 34, the measured engine parameters at first main engine cutoff (MECO No. 1) and the second main engine cutoff (MECO No. 2) are compared to engine acceptance test values. All parameters are within the flight instrumentation accuracy of the acceptance test values.

The C-1 and C-2 engine average mixture ratio and total thrust for the first and second burn, as calculated by Pratt & Whitney, are presented in Figure 84.

Shutdown - The shutdown transients of both engines on the first and second burns were normal.

Extended Mission Experiments - After the separation of the Helios A spacecraft, a Centaur extended coast experiment was performed. During the experiment, the RL10A-3-3 engines were satisfactorily ignited two more times and operated satisfactorily for 11 seconds and 48 seconds as programmed.

In summary, the RL10A-3-3 engines operated satisfactorily on the TC-2 mission:

1. The ground prechill was satisfactory.
2. The programmed prestart durations satisfactorily cooled down the pumps on all burns.
3. Engine ignition occurred normally on both engines for all starts.
4. Engine accelerations were normal on both engines for all starts.
5. Steady-state engine operation was normal on both engines on all burns.
6. Engine shutdowns were normal on both engines on all burns.

Propellant Feed System

Propellant feed system performance was satisfactory. A total of three boost pump rotation tests were successfully conducted prior to liftoff.

Special boost pump temperature measurements revealed no abnormal turbine temperatures during the Titan boost phase, except for the LO₂ boost pump

Table 34 RL10A-3-3 Engine Parameters at Shutdown

		MECO #1	MECO#2	Final Acceptance Test Values	Flight Accuracy
CP46P	C-1 Thrust Chamber Pressure	390 psia	390 psia	393 psia	+10 psi
CP47P	C-2 Thrust Chamber Pressure	390 psia	395 psia	393 psia	+10 psi
CP1B	C-1 Oxidizer Pump Speed	12, 450 rpm	12, 300 rpm	12, 353 rpm	+600 rpm
CP2B	C-2 Oxidizer Pump Speed	12, 300 rpm	12, 225 rpm	12, 278 rpm	+600 rpm
CP7P	C-1 Venturi Upstream Pressure	740 psia	750 psia	756 psia	+30 psi
CP8P	C-2 Venturi Upstream Pressure	730 psia	725 psia	735 psia	+30 psi
CP5T	C-1 Turbine Inlet Temperature	394 °R	394 °R	387 °R	+16°R
CP6T	C-2 Turbine Inlet Temperature	372 °R	373 °R	367 °R	+16°R
CP107P	C-1 Oxidizer Pump Disch. Press	608 psia	608 psia	610 psia	+16 psi
CP108P	C-2 Oxidizer Pump Disch. Press	592 psia	588 psia	600 psia	+16 psi
CP194P	C-1 Fuel Pump Disch. Pressure	975 psia	975 psia	985 psia	+30 psi
CP195P	C-2 Fuel Pump Disch. Pressure	960 psia	975 psia	985 psia	+30 psi

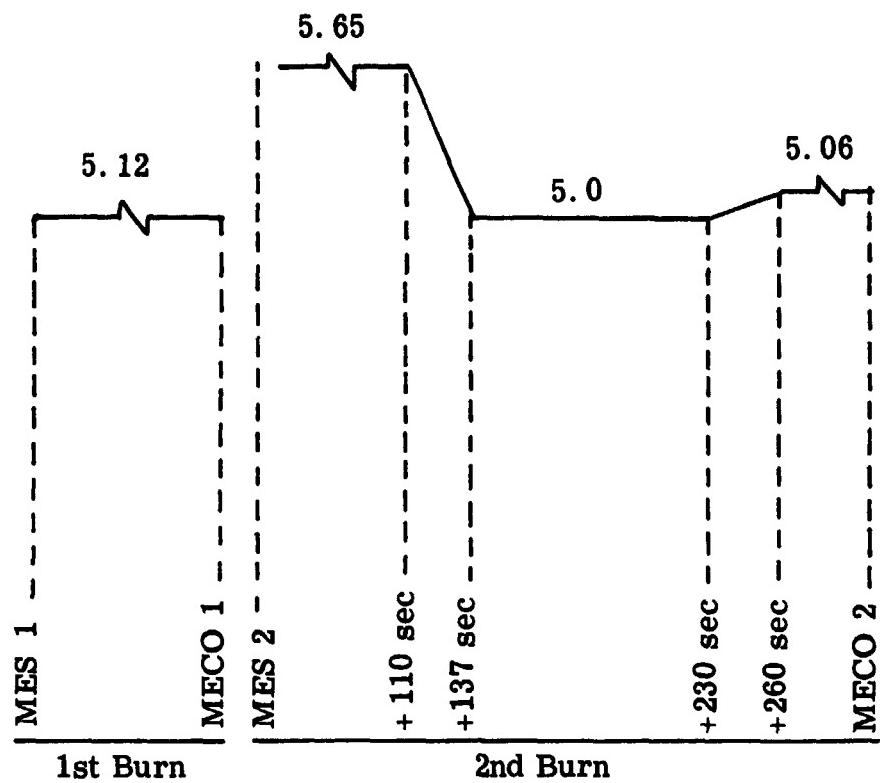


Figure 84.1 TC-2 Steady-State Mixture Ratio C-1 and C-2 Engine Average
(Pratt & Whitney Aircraft data analysis)

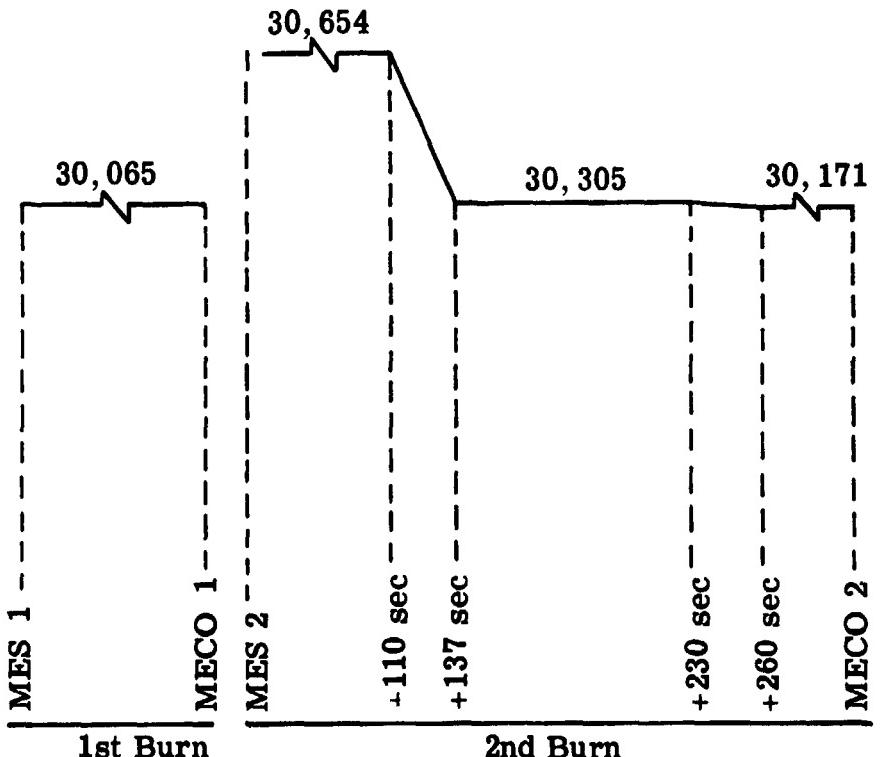


Figure 84.2 TC-2 Steady-State Total C-1 and C-2 Engine Thrust
(Pratt & Whitney Aircraft data analysis)

shaft housing temperature. This measurement indicated the L₂O boost pump shaft housing was approximately 45°F colder than the corresponding measurement on AC-32.

Boost pump operation during each burn was normal. A potential overspeed condition was noted and has been fully investigated. The results indicated no problem for future missions.

The configuration of the propellant feed system was identical to the TC-1 configuration with the following exceptions:

1. Minor changes were made to the boost pump seal cavity purge tubing to enable dewpoint checks to be made.
2. Airborne components were added to provide the capability to rotate the boost pumps using gaseous nitrogen from a ground supply during the countdown.
3. Special instrumentation was added to monitor the temperature and vibration environment of the boost pumps during the Titan boost phase.

The changes made to incorporate the boost pump rotation system consisted of adding a self-sealing disconnect on the aft T-4 second panel, and routing tubing from the disconnect to the L₂O and LH₂ boost pump turbine inlet pressure sense lines as shown in Figure 85. Two check valves were installed in series in the branch legs to each turbine to prevent overboard leakage and cross flow between the two turbines during normal boost pump operation. The turbine inlet pressure sensing lines were rerouted to an existing larger diameter port on the turbine nozzle box to reduce the line pressure drop during the boost pump rotation tests.

Locations of the special temperature and vibration measurements added for TC-2 are as shown in Figures 86 and 87 for the LH₂ boost pump, and in Figures 88 and 89 for the L₂O boost pump.

A total of three boost pump rotation tests were conducted prior to launch. The first two tests were conducted during the countdown of the aborted launch and the third during the countdown of the actual launch. Boost pump performance data obtained during the three rotation tests are summarized in Table 35. Included for comparison are the data from two rotation tests conducted during the TC-2 Terminal Countdown Demonstration (TCD) test conducted October 22, 1974, and the data from the Atlas/Centaur vehicles AC-32 and AC-33. The performance was considered normal for all three rotation tests.

Boost pump performance during both Centaur burns was satisfactory. A summary of the performance data is presented in Table 36.

A potential boost pump overspeed condition was noted during the first 15-second time period after each MECO. During these time periods, residual

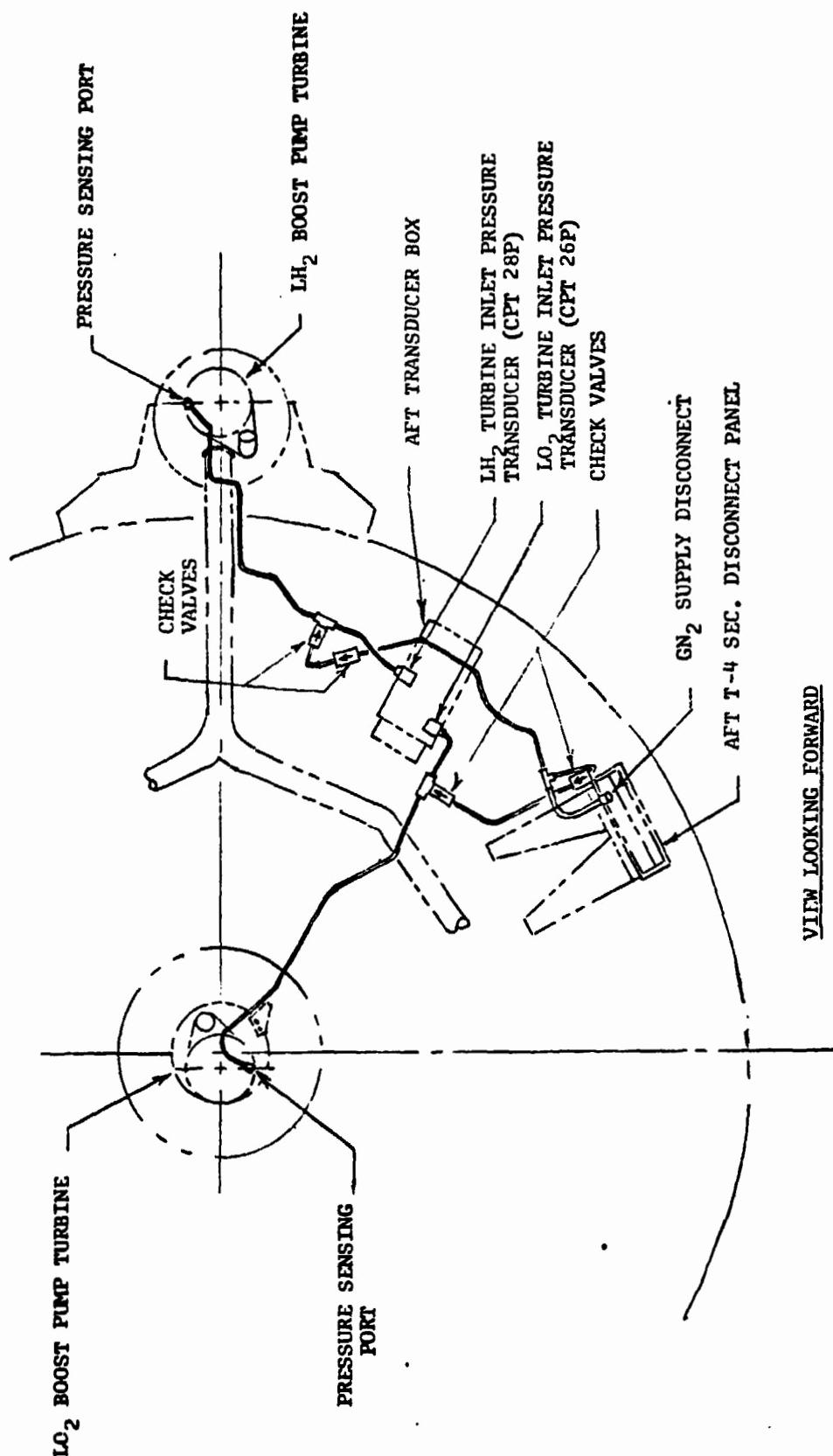


FIGURE 85 BOOST PUMP ROTATION AIRBORNE SYSTEM INSTALLATION SCHEMATIC

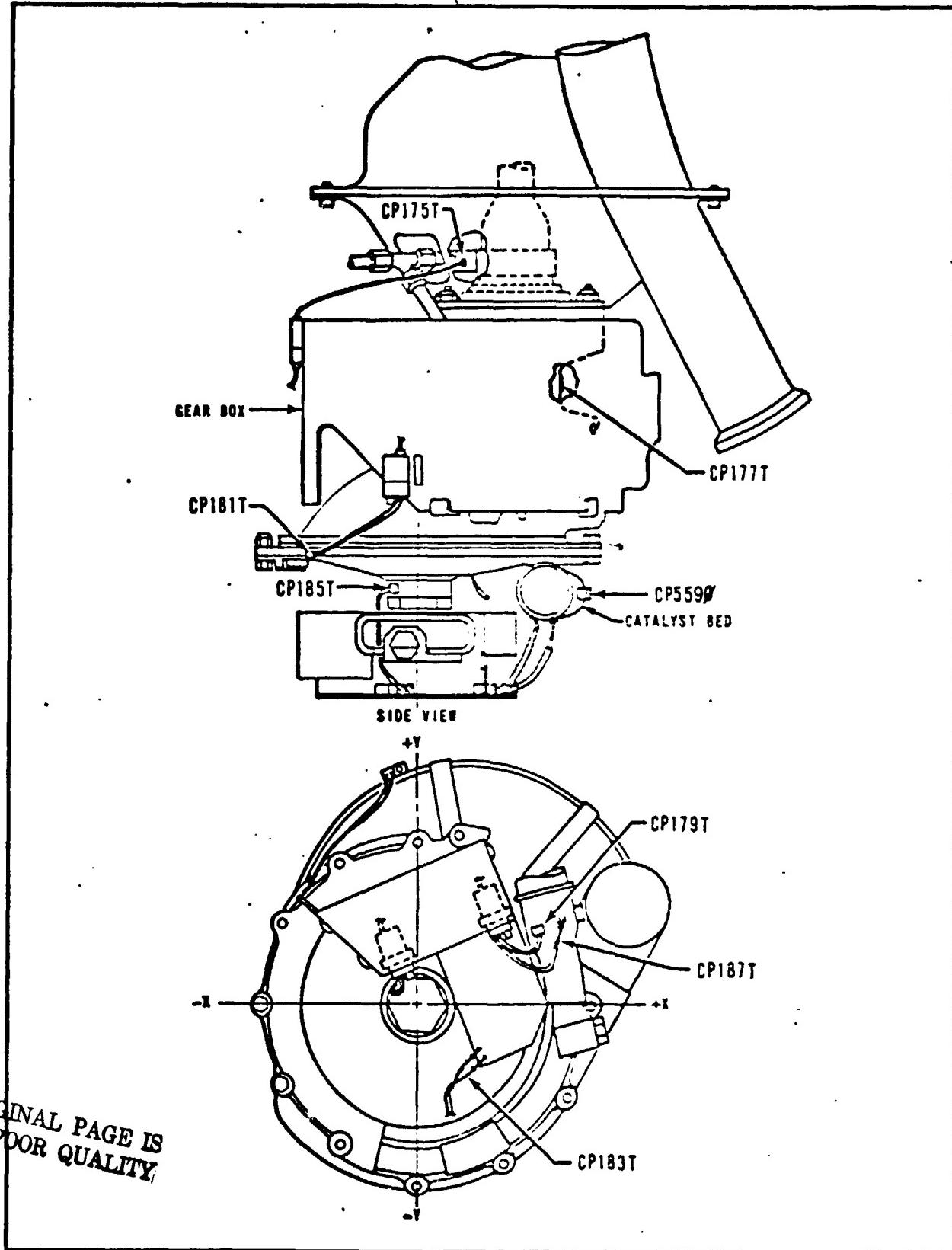


FIGURE 86

CENTAUR LH₂ BOOST TURBINE VIBRATION AND TEMPERATURE
MEASUREMENT LOCATIONS

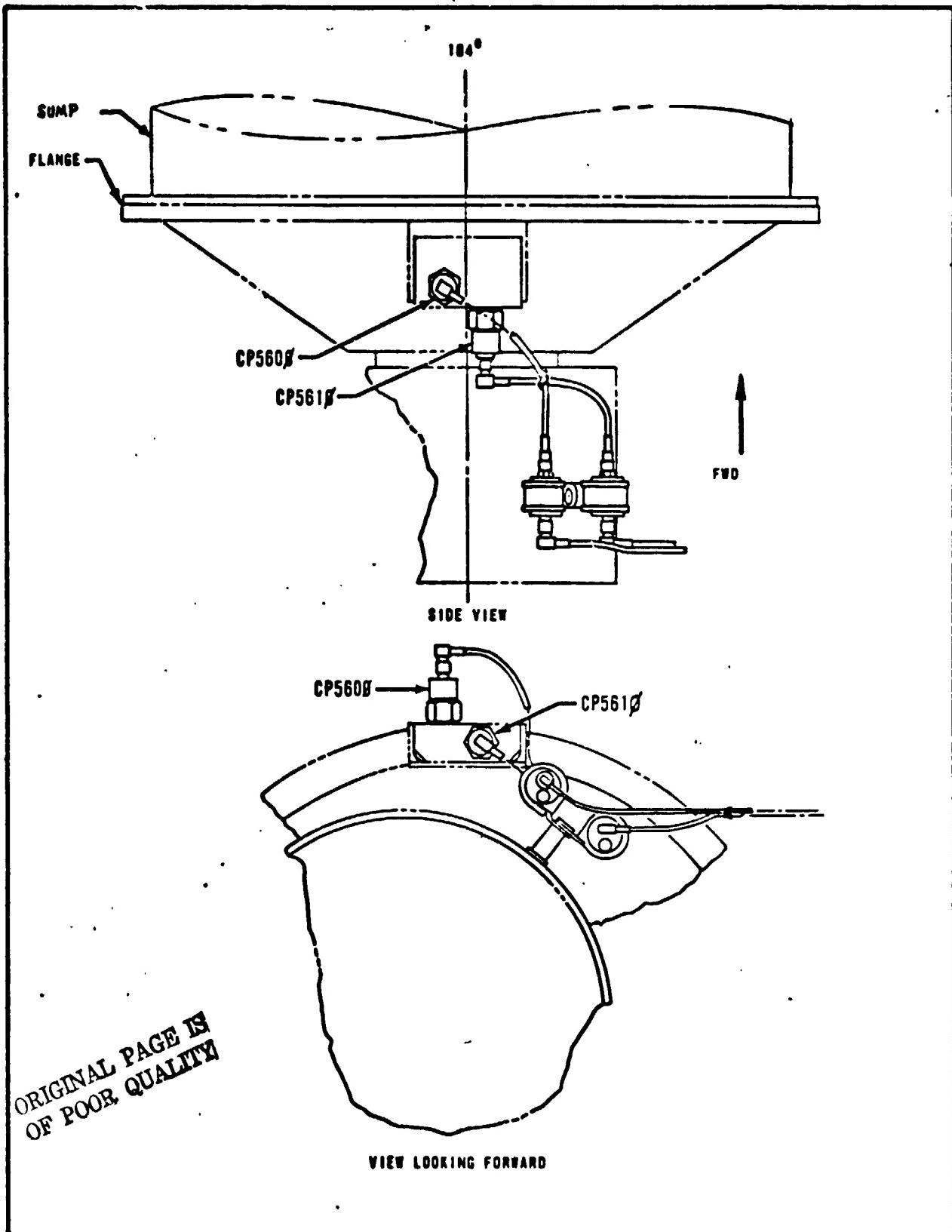


FIGURE 87

CENTAUR LH₂ BOOST PUMP VIBRATION AND TEMPERATURE MEASUREMENT LOCATIONS

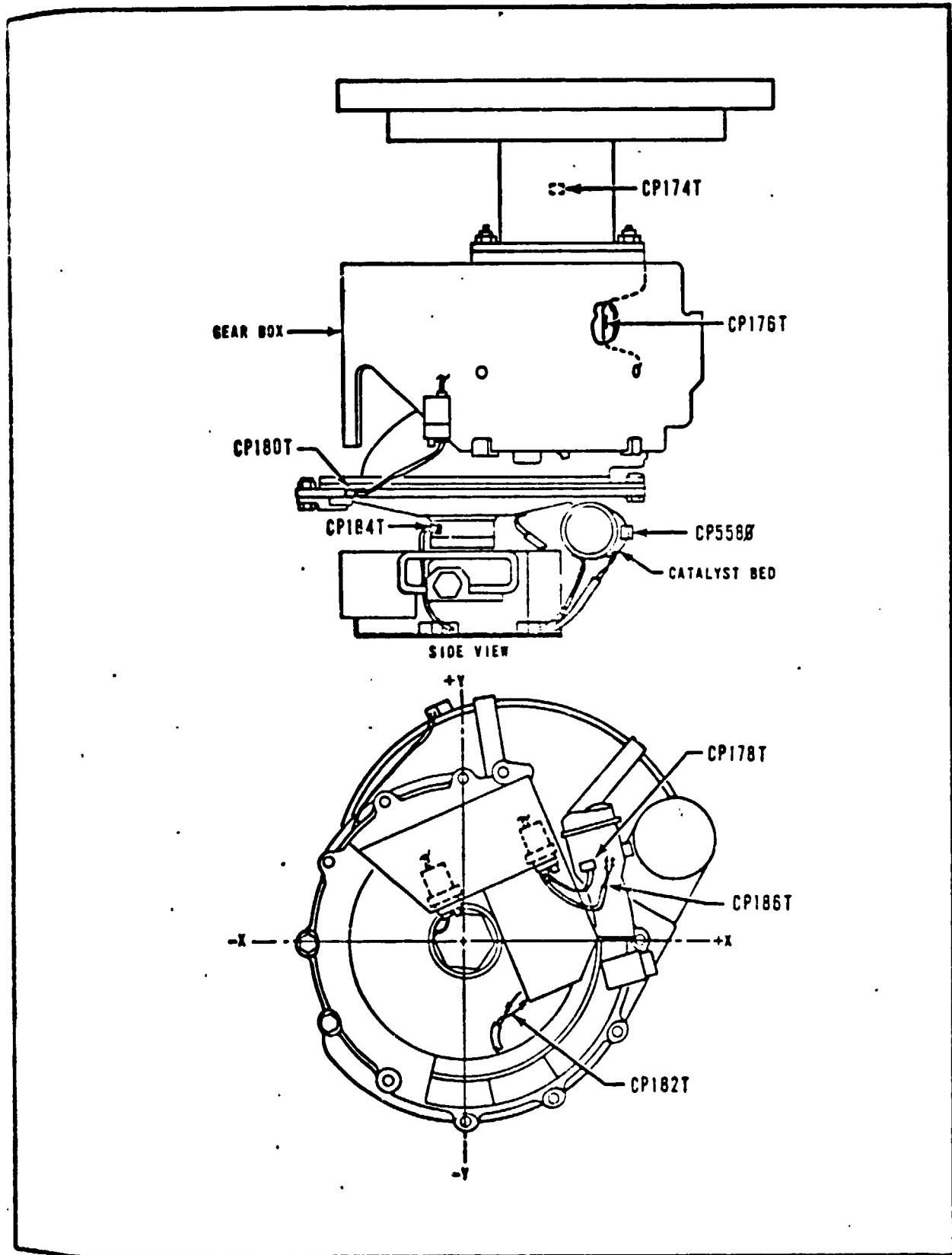


FIGURE 88 CENTAUR LO₂ BOOST PUMP TURBINE VIBRATION AND TEMPERATURE MEASUREMENT LOCATIONS

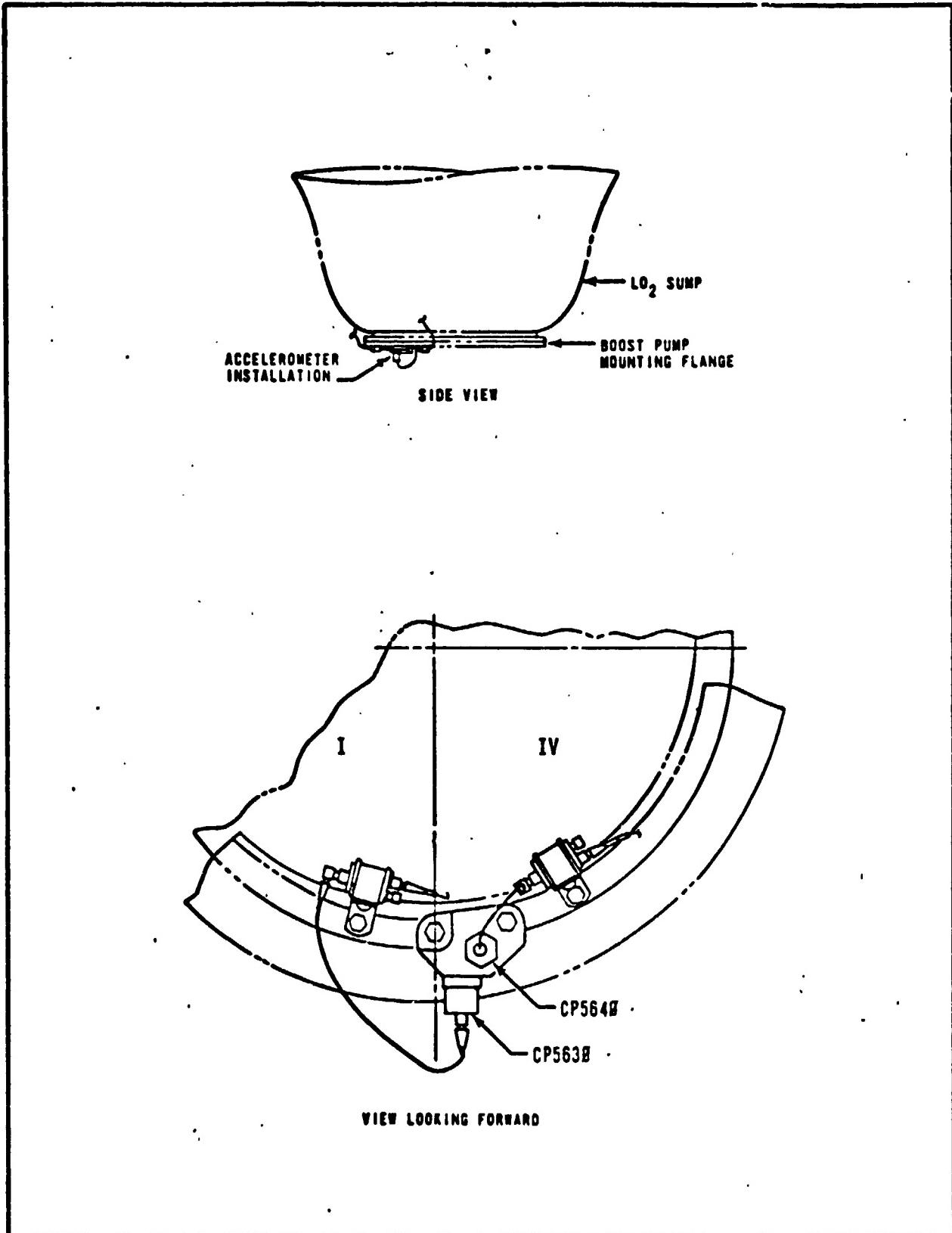


FIGURE 89 CENTAUR LO₂ BOOST PUMP FLANGE VIBRATION AND TEMPERATURE MEASUREMENT LOCATIONS

TABLE 35 SUMMARY OF CENTAUR BOOST PUMP PERFORMANCE DURING PRELAUNCH ROTATION TEST

Parameter	Vehicle and Test										
	TC-2			AC-32			AC-33				
	TCD #1	TCD #2	Abt. Lnc. #1	Abt. Lnc. #2	Launch #1	TCD #1	TCD #2	Launch #1	TCD #1	TCD #2	Launch
Duration of Run (Sec.)	140	204	223	208	223	236	245	194	166	160	190
<u>L02 Boost Pump</u>											
Delay Time to First Rotation (Sec.)	14	17	14	16	13	11	14	14	17	14	15
Nozzle Box Press. at First Rotation (PSIA)	60	60	54	60	54	57	60	60	-	-	-
Steady State Nozzle Box Press. (PSIA)	155	160	152	158	155	157	156	155	163	162	156
Steady State Turbine Speed (RPM)	15,650	16,250	16,575	16,825	16,440	15,900	15,990	16,250	14,300	14,300	15,600
Steady State Pump Delta-P (PSID)	12.6	13.5	14.5	15.7	14.4	15.0	15.0	15.0	15.1	15.1	15.0
Coastdown Time (Sec.)	32	35	38	36	38	35	30	36	32	32	29
<u>LH2 Boost Pump</u>											
Delay Time to First Rotation (Sec.)	23	20	20	20	24	23	19	22	20	25	20
Nozzle Box Press. at First Rotation (PSIA)	87	69	71	70	81	90	69	78	-	-	-
Steady State Nozzle Box Press. (PSIA)	158	161	148	154	152	156	155	155	159	158	156
Steady State Turbine Speed (RPM)	19,800	20,345	20,325	20,450	20,460	20,500	20,500	20,600	21,450	21,130	20,500
Steady State Pump Delta-P (PSID)	3.5	3.4	4.0	4.3	3.9	4.0	4.0	4.0	4.3	4.3	4.3
Coastdown Time (Sec.)	31	33	34	31	34	33	35	29	31	32	41

TABLE 36 SUMMARY OF CENTAUR BOOST PUMP PERFORMANCE FOR FIRST AND SECOND BURN

Parameter Description	Meas. No.	Units	First Burn			Second Burn		
			Prestart	MES	MECO	Prestart	MES	MECO
<u>L02 Boost Pump</u>								
Pump Headrise (Delta-P)	CPT120P	psid	79.5	76.5	30.0	78.7	78.0	30.5
Turbine Speed	CPT15B	rpm	38,300	38,300	33,100	37,700	39,000	33,800
Turbine Inlet Pressure	CPT26P	psia	99	99	102	102	102	102
<u>LH2 Boost Pump</u>								
Pump Headrise (Delta-P)	CPT121P	psid	24.0	21.0	10.8	20.3	Poor Data	11.0
Turbine Speed	CPT16B	rpm	44,200	41,600	40,900	40,900	41,600	40,900
Turbine Inlet Pressure	CPT28P	psia	98	98	102	102	102	102

hydrogen peroxide (H_2O_2) was purged from the boost pump supply lines. The residuals flowed through the catalyst bed of each turbine where it decomposed, thereby supplying energy to the turbine wheel. Concurrent with the purging action, the boost pumps were only partially pumping (which is normal) due either to MECO disturbances displacing liquid from the pump inlet, or due to partial cavitation. The application of partial power to the turbines which were only partially loaded resulted in acceleration of the boost pumps.

A complete investigation of the potential overspeed condition was conducted. The investigation determined that the limited quantity of residual peroxide was not sufficient to produce damaging turbine speeds even under worst case conditions of no pumping action for the entire 15 seconds of purging. Thus, no corrective action was required.

A summary of the propellant feed system temperature data is presented in Table 37 for times of significant events. There were no abnormal or unexpected temperatures noted with one exception. The temperature measurement located on the L_2 boost pump shaft housing (CP174T) indicated temperatures after liftoff that were approximately $45^{\circ}F$ colder than the corresponding measurement on AC-32. A plot of the temperature data from this measurement is presented in Figure 90. Plots of the temperature data from all other special boost pump measurements are presented in Figures 91 and 92 for the L_2 and LH_2 boost pumps, respectively.

It should be noted that the temperature of the L_2 boost pump shaft housing (CP174T), as shown in Figure 90, was very sensitive to the surrounding environment. The temperature decreased rapidly during the boost phase due to convective cooling produced by propulsion compartment venting. The temperature then showed a significant increase during the 80-second time period of thruster firings prior to the first boost pump start, and again during the time period from first boost pump start until Titan/Centaur separation. The relatively large differences between the AC-32 and TC-2 data might, therefore, be within the normal vehicle-to-vehicle dispersions. The limited amount of flight data prohibited an accurate assessment of whether the data was abnormal. All other turbine temperatures were near ambient, so the low L_2 pump shaft housing temperature was not considered a problem.

The L_2 and LH_2 supply duct metal surface temperatures at second boost pump start (see Table 37) were within the preflight predicted ranges. The L_2 duct average metal temperature was predicted to be within the range from $-285^{\circ}F$ to $-252^{\circ}F$; the TC-2 flight value was $-265^{\circ}F$. The LH_2 duct average metal temperature was predicted to be within the range from $-354^{\circ}F$ to $-275^{\circ}F$; the TC-2 flight value was $-307^{\circ}F$.

In summary, performance of the propellant feed system in support of the Helios mission was satisfactory. Boost pump performance during the prelaunch rotation tests and during first and second burn was satisfactory. Special temperature instrumentation on the boost pumps revealed no abnormal temperatures, except the L_2 boost pump shaft housing temperature was approximately $45^{\circ}F$.

TABLE 37 SUMMARY OF CENTAUR PROPELLAN FEED SYSTEM TEMPERATURE DATA

Parameter Description	Meas. No.	T-0 F	BPS #1 F	MES #1 O _F	MEO #1 O _F	SFS #2 F	MES #2 O _F	MEO #2 O _F	Payload Separation
Cryogenic Data									
LH ₂ Boost Pump Inlet	CP32T	-421.2	-421.4	-421.6	-422.1	-421.0	-421.6	-423.8	-423.8
LH ₂ Boost Pump Inlet	CPT33T	-282.1	-292.3	-281.6	-283.0	-280.3	-282.3	-284.9	-285.3
C-1 LO ₂ Pump Inlet	CPT59T	-280.9	-279.5	-280.4	-282.5	>-275.0	>-80.7	-284.7	-284.7
C-1 LH ₂ Pump Inlet	CPT60T	-420.0	-421.0	-419.5	-421.0	>-414.0	>-420.6	-422.7	-422.7
C-2 LO ₂ Pump Inlet	CPT61T	-280.9	-279.3	-280.1	-282.5	-279.5	-280.7	-284.5	-284.5
C-2 LH ₂ Pump Inlet	CPT62T	-419.6	-420.6	-419.2	-421.0	>-414.0	>-420.7	-422.7	-422.7
C-1 LO ₂ Duct Surface	CP750T	-278	-278	-278	-278	-265	-278	-282	-282
C-1 LH ₂ Duct Surface	CP751T	<-400	<-400	<-400	<-400	<-400	<-400	<-400	<-400
L0₂ Boost Pump Turbine									
Rotor Lower Bearing	CPT36T	72	71	98	127	204	216	303	320
Coupling Shaft Housing	CP174T	-9	-72	-70	-76	-51	-49	-36	-33
Gearcase Surface (Output)	CP176T	68	65	74	94	174	175	215	238
Decomp. Chamber (Patch)	CPI78T	113	136	>217	>217	>217	>217	>217	>217
Rotor Housing (Outboard)	CPI80T	63	63	85	>147	>147	>147	>147	>147
Rotor Housing (aft)	CPI82T	68	68	275	688	434	479	909	966
Rotor Access Boss	CPI84T	65	66	81	117	>147	>147	>147	>147
Decomp. Chamber (T/C)	CPI86T	112	136	>597	>597	569	>597	>97	>597
H ₂ Orifice Holder	CP711T	65	60	83	90	106	99	100	104
LH₂ Boost Pump Turbine									
Rotor Lower Bearing	CPT127T	72	70	97	127	190	202	200	299
Coupling Shaft Housing	CPI75T	39	27	26	35	77	76	113	>120
Gearcase Surface (Output)	CP177T	61	58	61	91	156	157	212	218
Decomp. Chamber (Patch)	CPI79T	97	120	>206	>206	>206	>206	>206	>206
Rotor Housing (Outboard)	CPI81T	68	63	92	>147	>147	>147	>147	>147
Rotor Housing (Aft)	CPI83T	56	56	236	654	353	425	841	795
Rotor Access Boss	CPI85T	67	57	68	116	>147	>147	>147	>147
Decomp. Chamber (T/C)	CPI87T	-	-	-	Transducer Failed	-	Data Inval	-	-
H ₂ Orifice Holder	CP710T	76	69	87	91	95	99	107	111
Electrical Connector	CP712T	72	58	61	65	107	137	143	150

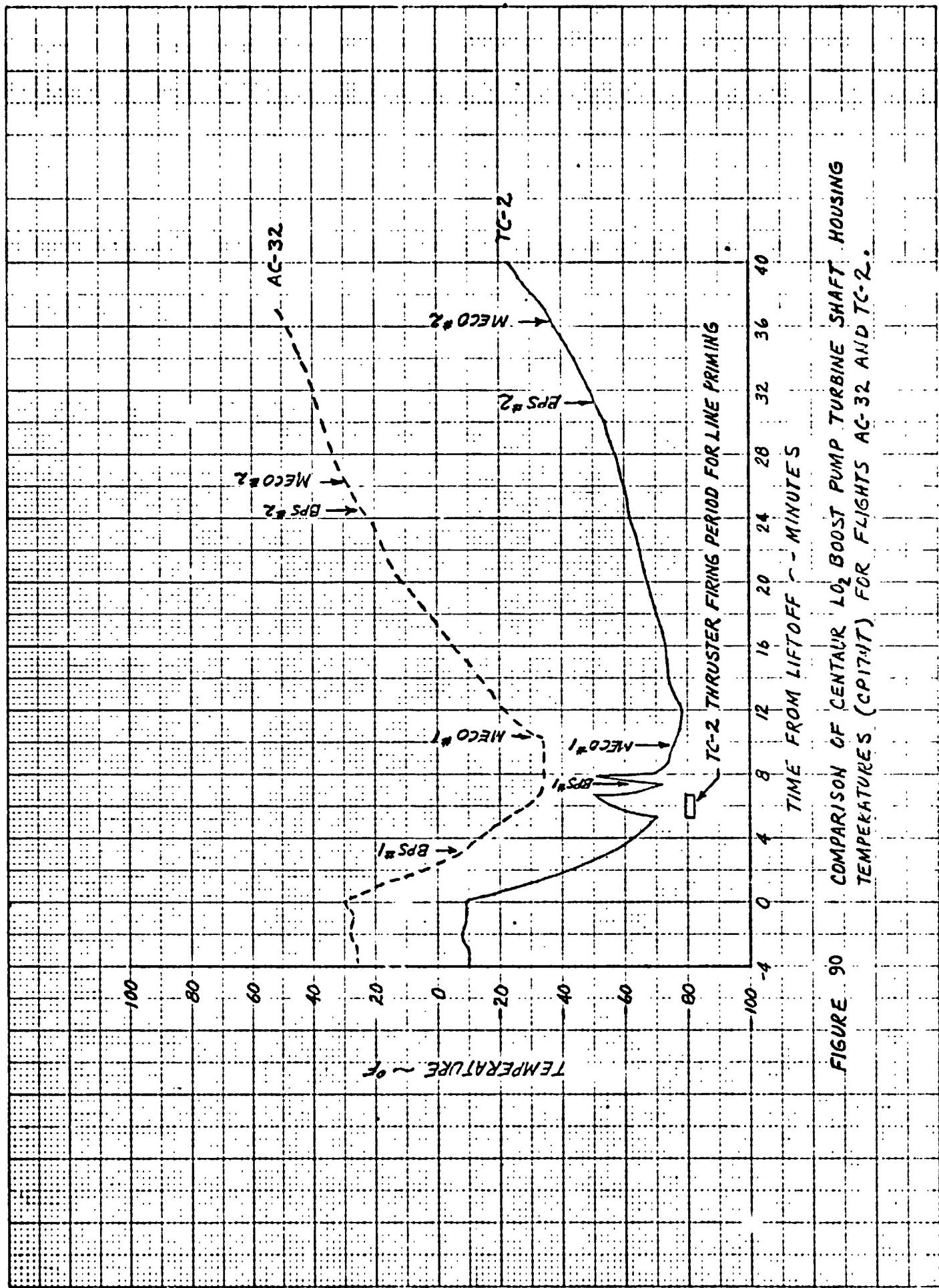


FIGURE 90 COMPARISON OF CENTAUR LO₂ BOOST PUMP TURBINE SHAFT HOUSING TEMPERATURES (CP174T) FOR FLIGHTS AC-32 AND TC-2.

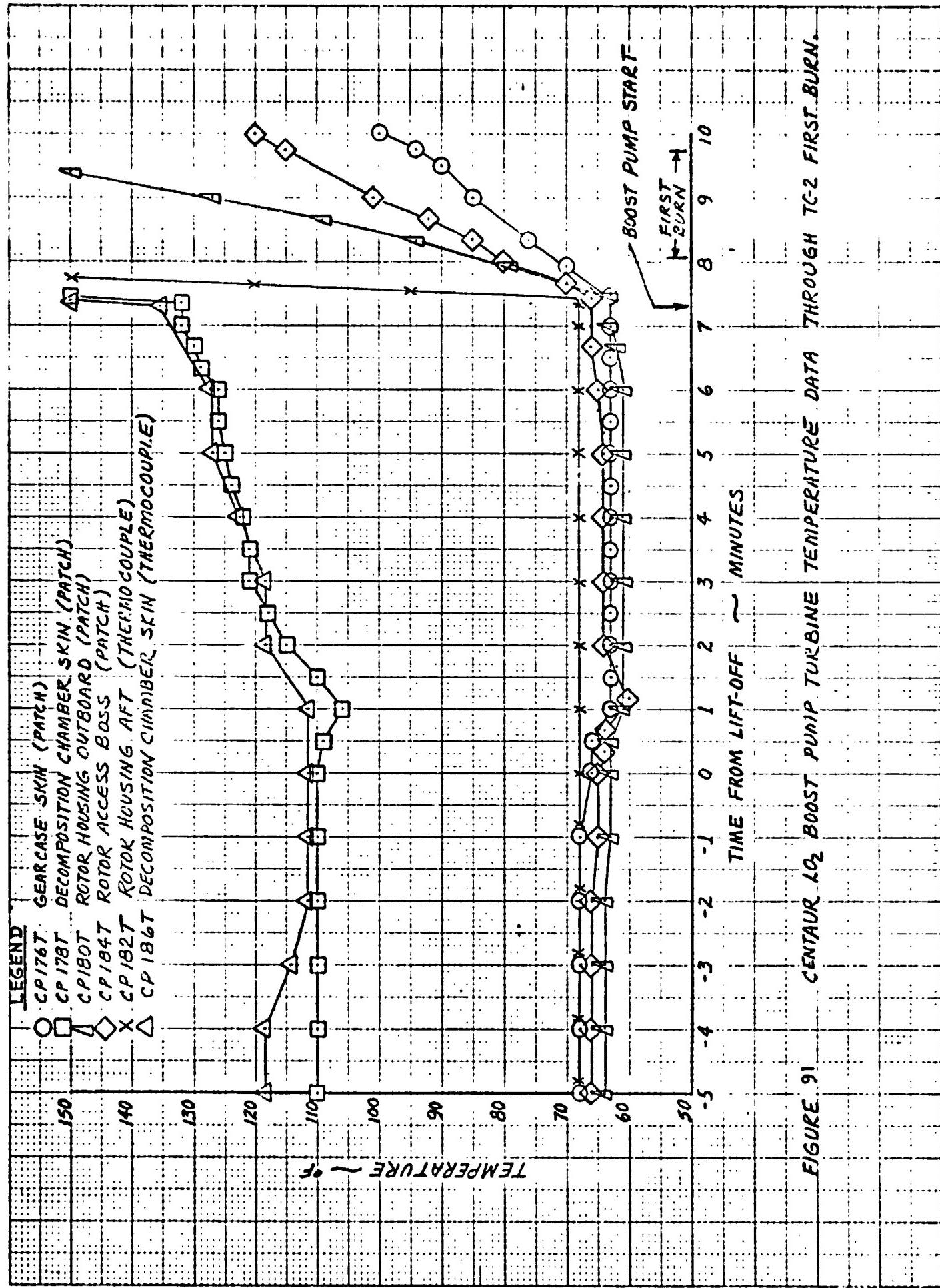


FIGURE 91 CENTAUR LO₂ BOOST PUMP TURBINE TEMPERATURE DATA THROUGH TC-2 FIRST BURN.

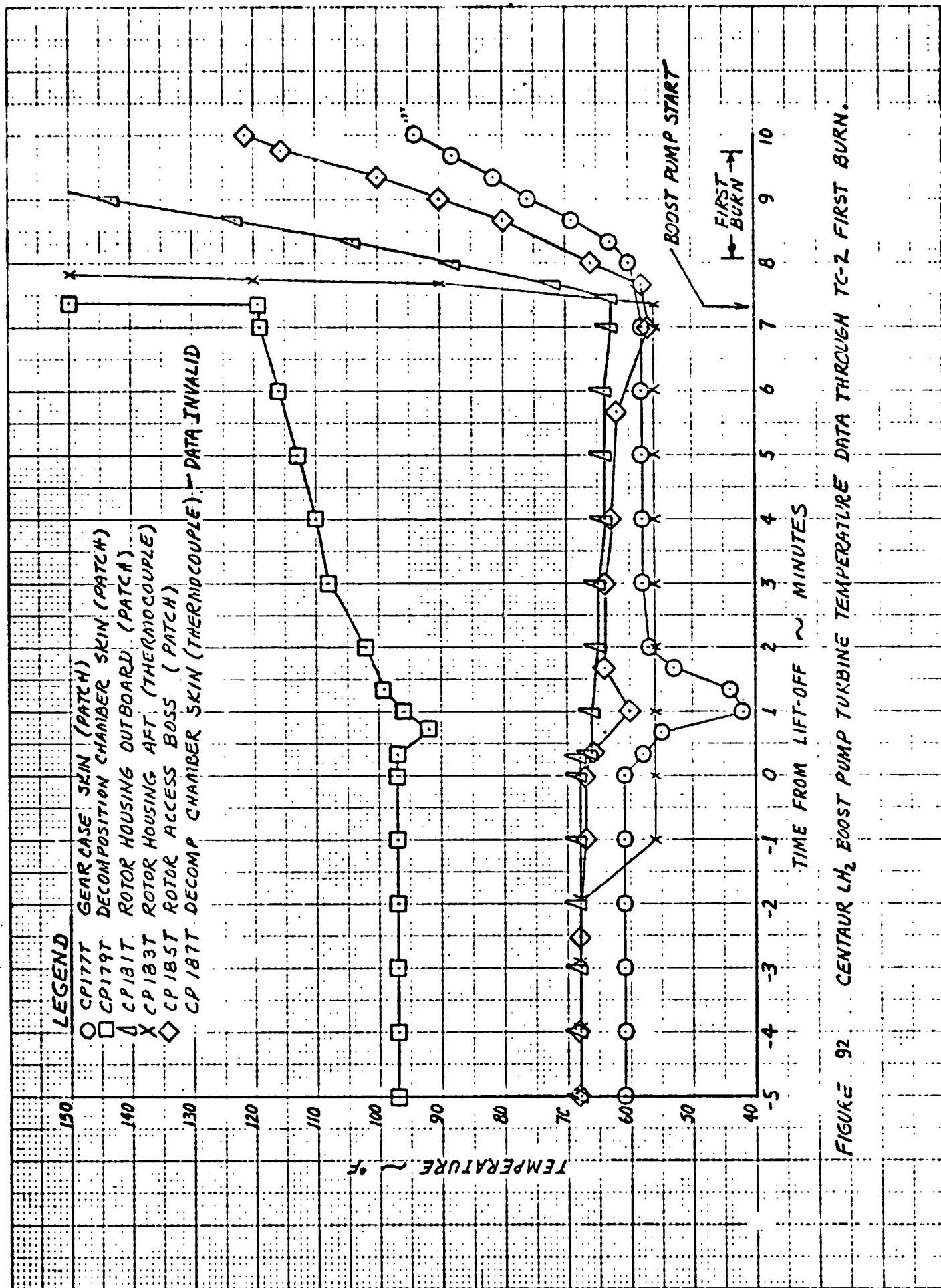


FIGURE 92. CENTAUR LH₂ BOOST PUMP TURBINE TEMPERATURE DATA THROUGH TC-2 FIRST BURN.

colder than on AC-32. The limited quantity of flight data prohibited an accurate assessment of the abnormality of this data. The low temperature had no effect on boost pump operation and was not considered a problem.

A potential boost pump overspeed condition was noted during the first 15 seconds after each MECO. A complete investigation indicated that the potential overspeed condition was not a problem for future Centaur flights.

The LO₂ and LH₂ supply duct metal temperatures at the end of the 24 minute settled coast were within the range of preflight predicted values.

Hydrogen Peroxide Supply and Reaction Control System

by K. W. Baud

The hydrogen peroxide supply and reaction control system performed satisfactorily in support of the Helios mission. All system component and hydrogen peroxide bulk temperatures were maintained within acceptable limits. Programmed thruster firings during the boost phase and settling sequences occurred in the proper sequence and for the proper duration. Lateral directed thrusters responded to the flight control system commands and maintained proper vehicle altitude control.

The configurations of the hydrogen peroxide supply and reaction control systems were identical to the configuration previously flown on TC-1.

The hydrogen peroxide (H_2O_2) supply and reaction control system (RCS) performed satisfactorily from liftoff through spacecraft separation. The RCS was inactive during the time period from liftoff to first main engine cutoff (MECO No. 1) except for programmed firing of four RCS engines before boost pump start and warming firings of the eight lateral engines just prior to MECO No. 1. The performance of the RCS is only briefly discussed in this section. A detailed discussion of the RCS performance in regard to on-off duty cycles and control of the vehicle is presented in the flight control system analysis.

The S2A, Y1, Y2, and S4B thrusters were fired (in that order) for 20 seconds each during the Titan boost phase to remove any large accumulations of gas in the H_2O_2 bottles. The firings were accomplished in rapid succession with no waiting interval. Temperature measurements located on the thrust chamber bodies confirmed proper firing of the S2A, Y1, and S2B thrusters. A temperature measurement was not installed on the Y2 thruster, however, proper firing was evidenced by the response of other temperature measurements inside the Titan/Centaur interstage adapter.

All eight lateral thrusters were simultaneously fired for 10 seconds commencing approximately 20 seconds prior to each MECO. Purpose of the firings was to warm these thrusters prior to entering a long coast. Temperature measurements located on the thrust chamber bodies of four of the thrusters (P3, P4, Y1, and Y3) verified the warming firing was properly performed.

At MECO No. 1, all four axial settling thrusters (S2A, S2B, S4A, and S4B) were fired in a continuous on mode for 250 seconds which provided 24 pounds-thrust for initial propellant settling. During the time period between MECO No. 1 plus 250 seconds and MES No. 2 minus 120 seconds, the propellant settling thrust was reduced to 12 pounds-thrust. S2A and S4A were used for the first half of the 12 pound-thrust mode; S2B and S4B were used for the last half. At MES No. 2 minus 120 seconds, all four axial thrusters were again turned on and remained on until MES No. 2 plus 5 seconds. Proper sequencing and operation of the four axial thrusters were verified by the temperature measurement on each.

Pitch, yaw, and roll control were provided by the eight lateral thrusters during the first coast and between MECO No. 2 and spacecraft separation. Proper vehicle attitude control was provided. See the flight control system analysis for a detailed discussion.

A summary of the H₂O₂ supply and RCS systems temperature data recorded at times of significant events is presented in Table 38. All temperature data were within acceptable limits. The lowest temperature recorded (25°F) was at the CPT714T location during the Titan boost phase. This measurement was located on an unheated section of the L₂O₂ boost pump H₂O₂ supply line. The line contained no H₂O₂ at this time and, being unheated, was quite sensitive to the convective cooling produced by venting of the propulsion compartment. The corresponding temperature on the TC-1 flight was 20°F.

Three of the temperature measurements located on the H₂O₂ lines to the boost pumps (CP159T, CPT361T, and CP833T) revealed temperatures in excess of the normal 140°F upper limit for the H₂O₂ system. Two of these measurements (CPT361T and CP833T) were on unheated lines very near the hot face of the LH₂ turbine rotor housing. High temperatures at these locations, particularly during the coast phase when the lines are empty, were expected and present no problem.

The high temperature indicated at the CP159T location was not expected, but does not present a problem. The high temperature was primarily caused by impingement of the S4A and S4B axial thruster exhaust on this section of empty line during the 4S engine on mode before second boost pump start. The line rapidly cooled with the resumption of H₂O₂ flow after second boost pump start.

In summary, the H₂O₂ supply and RCS systems performed satisfactorily in support of the Helios mission. All programmed thruster firings were accomplished in the proper sequence and for the proper duration. Vehicle attitude control was properly maintained. The minimum temperature (25°F) occurred during the boost phase on the unheated portion of the L₂O₂ boost pump supply line and was expected.

All other temperatures were within the design range of 40°F to 120°F with the exception of three measurements. Two of these measurements were on an unheated line near the hot LH₂ turbine and were expected to be above 120°F. The third measurement was on an empty supply line to the LH₂ turbine which received impingement heating from the axial thrusters in quadrant 4. The temperatures experienced posed no problem since the lines were empty.

TABLE 38 SUMMARY OF H₂O₂ AND RCS TEMPERATURE DATA

Parameter Description	Meas. No.	T-0 °F	BPS #1 °F	MES #1 °F	MECO #1 °F	BPS #2 °F	MES #2 °F	MECO #2 °F	P/L Sep. °F
H2O2 Bulk RCS Bottle Boost Pump Bottle	CP93T CP659T	83 79	83 81	83 81	84 83	86 86	86 86	88 88	88 88
<u>Thruster Chamber Surface</u>									
Y1	CP148T	79	705	671	1077	1043	1077	1161	1212
Y4	CP149T	68	45	45	959	1026	1144	1128	1178
P3	CP375T	68	68	68	875	1161	1110	1060	1110
P4	CP376T	79	79	79	959	841	976	1128	1114
S2A	CP691T	56	637	567	479	1246	1246	637	593
S4A	CP693T	68	68	68	68	1262	1271	671	628
S2B	CP836T	68	908	723	567	1229	1229	637	602
S4B	CP837T	68	68	68	68	1296	1296	671	671
<u>H2O2 Lines to Thrusters</u>									
Quad 1	CPT150T	75	92	94	91	96	94	87	89
Quad 2	CPT151T	76	89	90	92	102	102	114	116
Quad 2/3	CPT152T	74	93	92	92	92	92	96	96
Quad 3	CPT153T	82	100	100	100	96	96	96	96
Quad 4	CPT154T	88	100	101	100	98	98	99	99
Quad 1/4	CPT155T	70	96	95	96	96	96	96	98
<u>H2O2 Lines to Boost Pumps</u>									
Quad 1 LH ₂ (fitting)	CP156T	72	68	80	86	83	91	99	96
Quad 2 LH ₂	CP157T	68	87	87	89	107	91	95	103
Quad 3 LH ₂	CP158T	68	65	65	87	85	83	89	89
Quad 4 LH ₂	CP159T	72	81	89	91	>178	109	95	101
LH ₂ Orifice Inlet	CPT361T	74	61	107	128	107	113	173	183
LO ₂ Orifice Inlet	CPT714T	65	76	99	102	113	100	110	115
Between Feed Valves	CP831T	83	101	91	91	127	111	95	97
LH ₂ Inlet (Near Tee)	CP833T	83	69	78	95	95	99	>147	>147

TABLE 38 SUMMARY OF H₂O₂ AND RCS TEMPERATURE DATA (CONTINUED)

Parameter Description	Meas. No.	T-0 °F	BPS °F	MJS °F	MECO #1 °F	BPS °F	MES °F	MECO #2 °F	P/L Sep. °F
<u>Other</u>									
BPFV #2 Body	CP834T	75	75	83	87				
Bottle Manifold Line	CP756T	87	91	93	93				
H ₂ O ₂ Vent Line	CP832T	83	105	105	105				
						91	91	95	97
						88	88	87	93
									87

Hydraulic System

by T. W. Godwin

Centaur hydraulic system performance was satisfactory. The hydraulic recirculation pumps responded properly when commanded on prior to main engine start (MES 1, MES 2, MES 3, MES 4) and throughout the boost pump spinup test and the blowdown maneuver. In addition, the C-2 recirculation pump was switched on four times automatically by the low temperature thermostat in the C-2 hydraulic manifold. Main system operation was normal throughout the four main engine firings. Startup and shutdown transients, as well as operating pressures, were normal.

The hydraulic system on the TC-2 vehicle incorporated additional temperature instrumentation (power pack, recirculation motor housing and actuator body temperatures) for the purpose of monitoring the effects of long coast period, zero-G operation and orbital maneuvers on system components. This data will be presented in detail in a later report. However, all temperature data obtained for the first two main engine firings are presented, together with pressure data, in Table 39.

No system anomalies were noted.

TABLE 39 CENTAUR HYDRAULIC SYSTEM TC-2 FLIGHT PERFORMANCE

Parameter	Meas. No.	Units	1st Burn			2nd Burn			Blowdown		
			Recirc. ON	MES #1	MECO #1	Recirc. ON	MES #2	MECO #2	Recirc. ON	Recirc. OFF	
Hydraulic System Press.											
C1 Engine	CHT1P	psia	125	1140	1130	126	1132	1120	123	120	
C2 Engine	CHT3P	psia	130	1134	1122	132	1125	1115	128	128	
Temperatures											
C1 power pack	CHT2T	°F	58	59	70	80	80	80	139	87	87
C1 hyd. manifold	CHT5T	°F	65	65	113	75	76	76	170	93	93
C1 recirc. motor hsg.	CH9T	°F	57	51	51	73	73	76	85	85	83
C1 yaw actuator body	CH33T	°F	R0	80	93	87	87	87	140	81	80
C2 power pack	CHT4T	°F	57	56	64	77	76	76	130	66	61
C2 hyd. manifold	CHT6T	°F	45	45	65	70	71	71	159	39	45
C2 recirc. motor hsg.	CH10T	°F	55	47	43	97	101	87	78	78	64
C2 pitch actuator body	CH36T	°F	67	67	84	84	82	82	135	68	65

Pneumatics and Tank Vent Systems

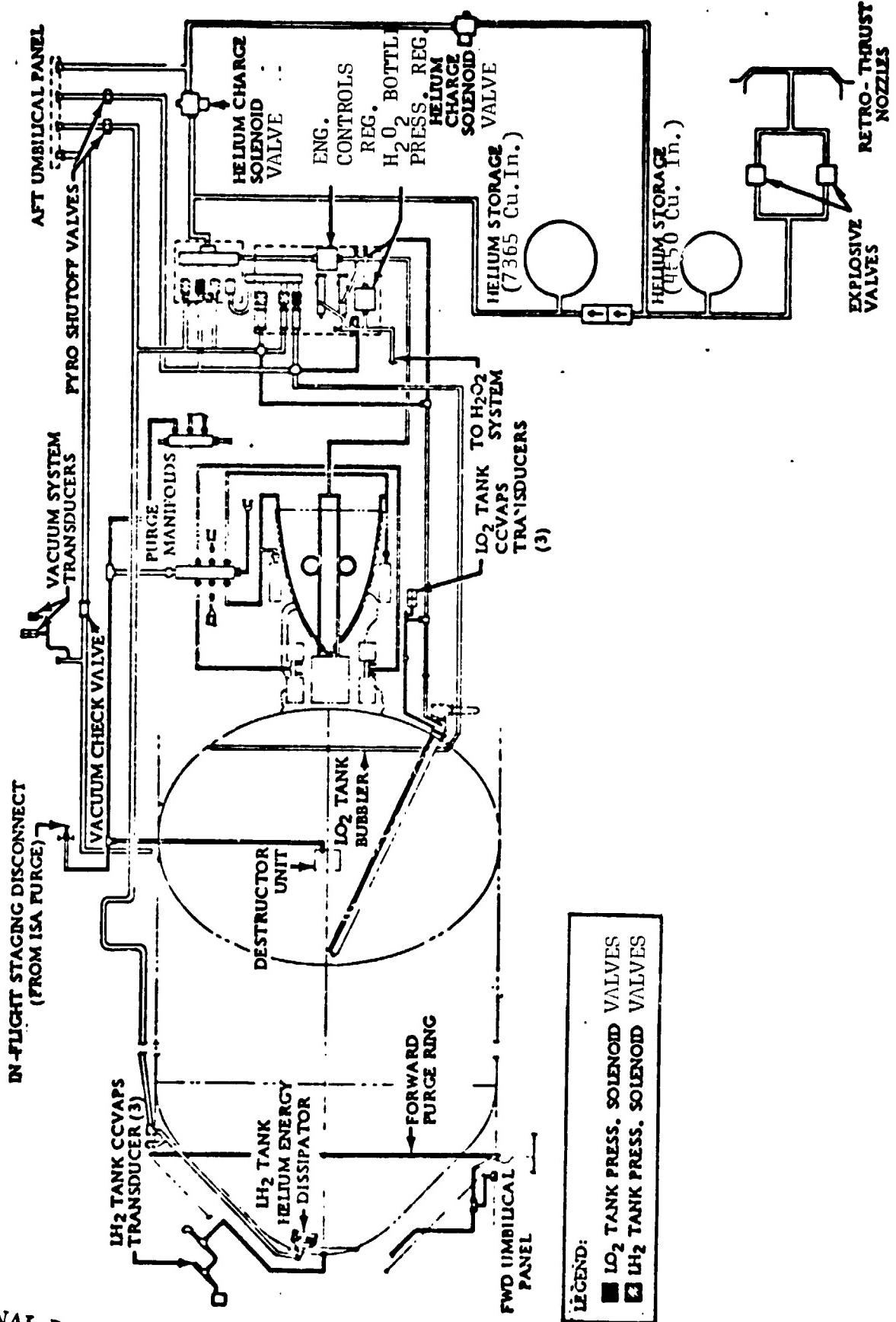
by M. L. Jones

The Centaur pneumatic system, which is shown schematically in Figure 93, was the same as that on TC-1 except in the following areas:

1. Hydrogen tank pressurization - The diameter of the flow metering orifice associated with the number two pressurization valve was changed from 0.157 inches to 0.0995 inches.
2. Helium retro-thrust - This system was added to TC-2 in order to provide the required separation distance between the Centaur and the spacecraft immediately after spacecraft separation and before firing the spacecraft rocket motor. The system consists of two normally closed pyrotechnic valves, mounted in parallel, and two forward canted nozzles. The system is activated by opening the pyrotechnic valves allowing the remainder of the helium in the smaller (4650 cu. in.) bottle to blow down through the two nozzles applying a reverse thrust to the Centaur.
3. Helium storage - This portion of the system was changed by adding two check valves in series between the two helium bottles and an additional helium charge solenoid valve. The check valves were added to isolate the larger (7365 cu. in.) helium bottle from the retro-thrust system. The charge valve was added to permit charging the larger bottle independently of the smaller bottle in order to leak test the check valves.
4. Oxygen tank vent system - The vent nozzle alignment angle was changed from 40°-48° with the vertical to 15°.

Propellant Tank Pressurization and Venting - A time history of the propellant tank ullage pressures is shown in Figure 94. Prior to T-27.8 seconds, the primary hydrogen vent valve, which has a specification operating range from 19.0 to 21.5 psia, regulated the tank pressure. At T-27.8 seconds, the primary hydrogen vent valve was commanded to the locked mode and the tank pressure was allowed to rise in order to satisfy the tank structural strength requirements during liftoff and during the subsonic portion of the flight. A minimum requirement of 23.1 psia at liftoff had been established before the flight. A maximum limit of 24.9 psia had also been established in order to preclude the possibility of venting hydrogen gas overboard before 8 seconds into the flight.

From the time of vent valve lockup until T-8 seconds, the tank pressure was monitored by the computer controlled vent and pressurization system (CCVAPS), which calculated the pressure rise rate and predicted the tank pressure at liftoff. If the CCVAPS prediction had not fallen within the established limits, an automatic launch abort would have been initiated. At T-8 seconds

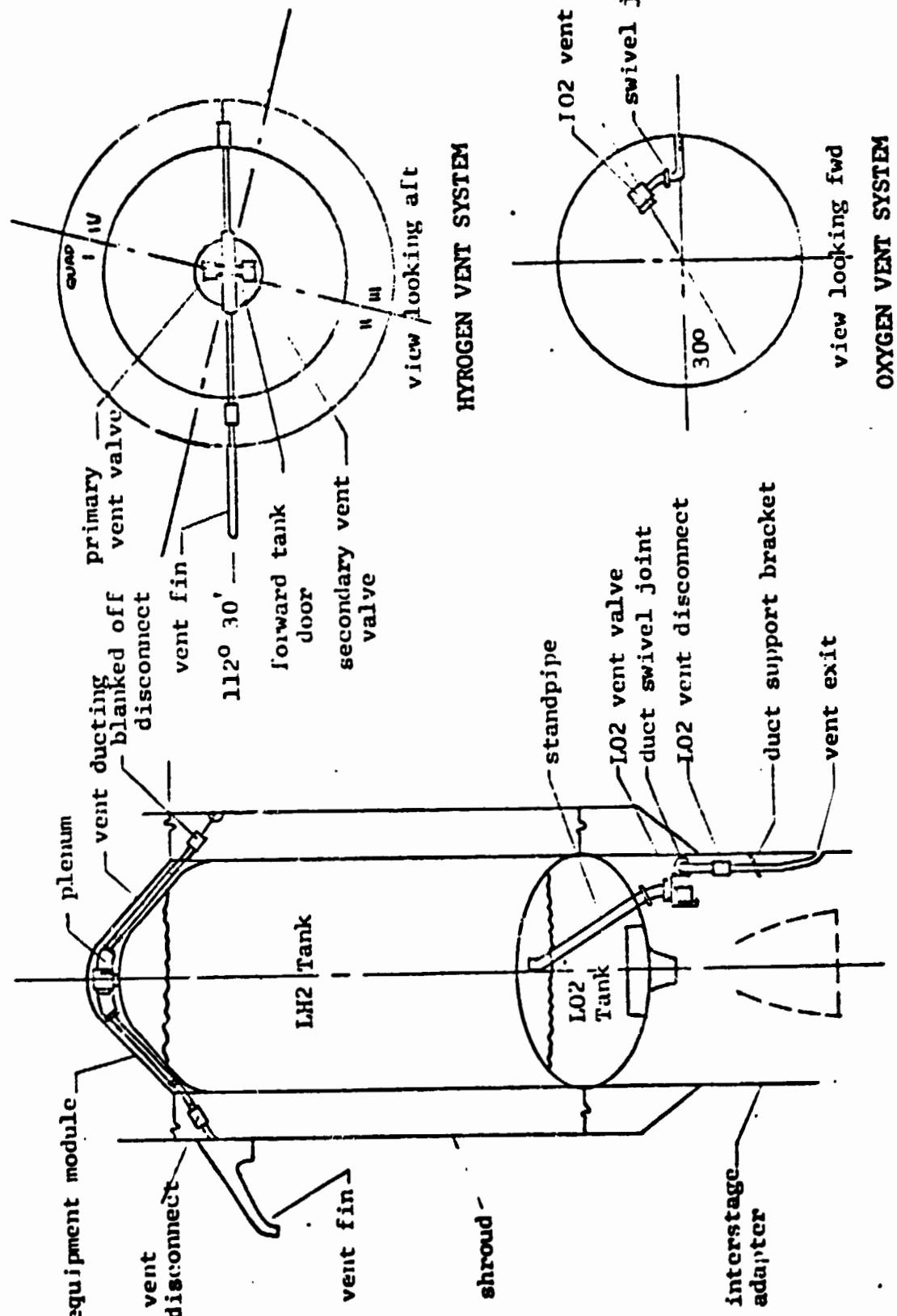


ORIGINAL PAGE IS
OF POOR QUALITY

(a) Pneumatics System

Centaur Pneumatics & Vent Systems

Figure 93.1

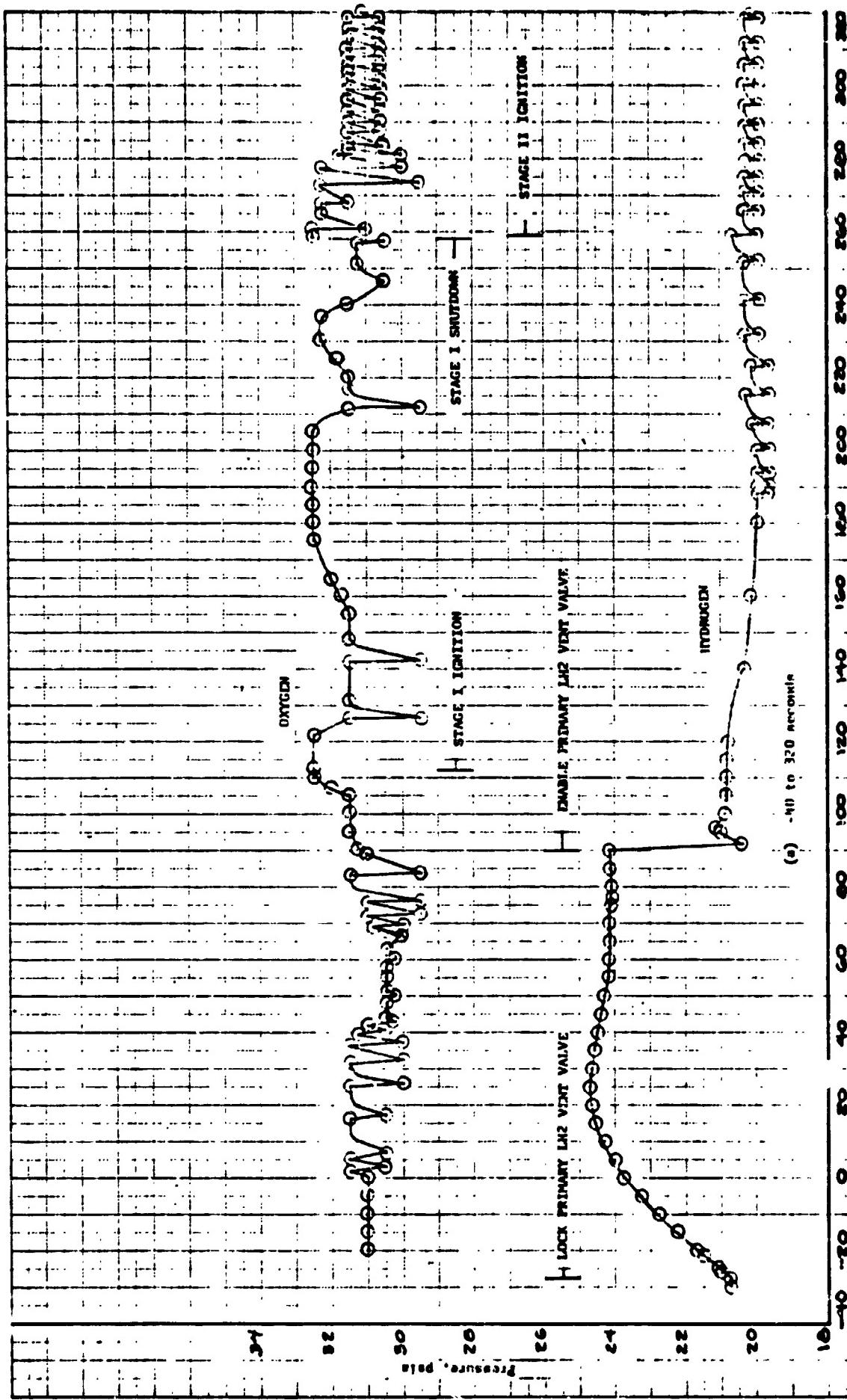


ORIGINAL PAGE IS
OF POOR QUALITY

(b) Vent System

Figure 93.2

Figure 941. Constant-tension ultrasonic pressure-time history, 2002 sec.



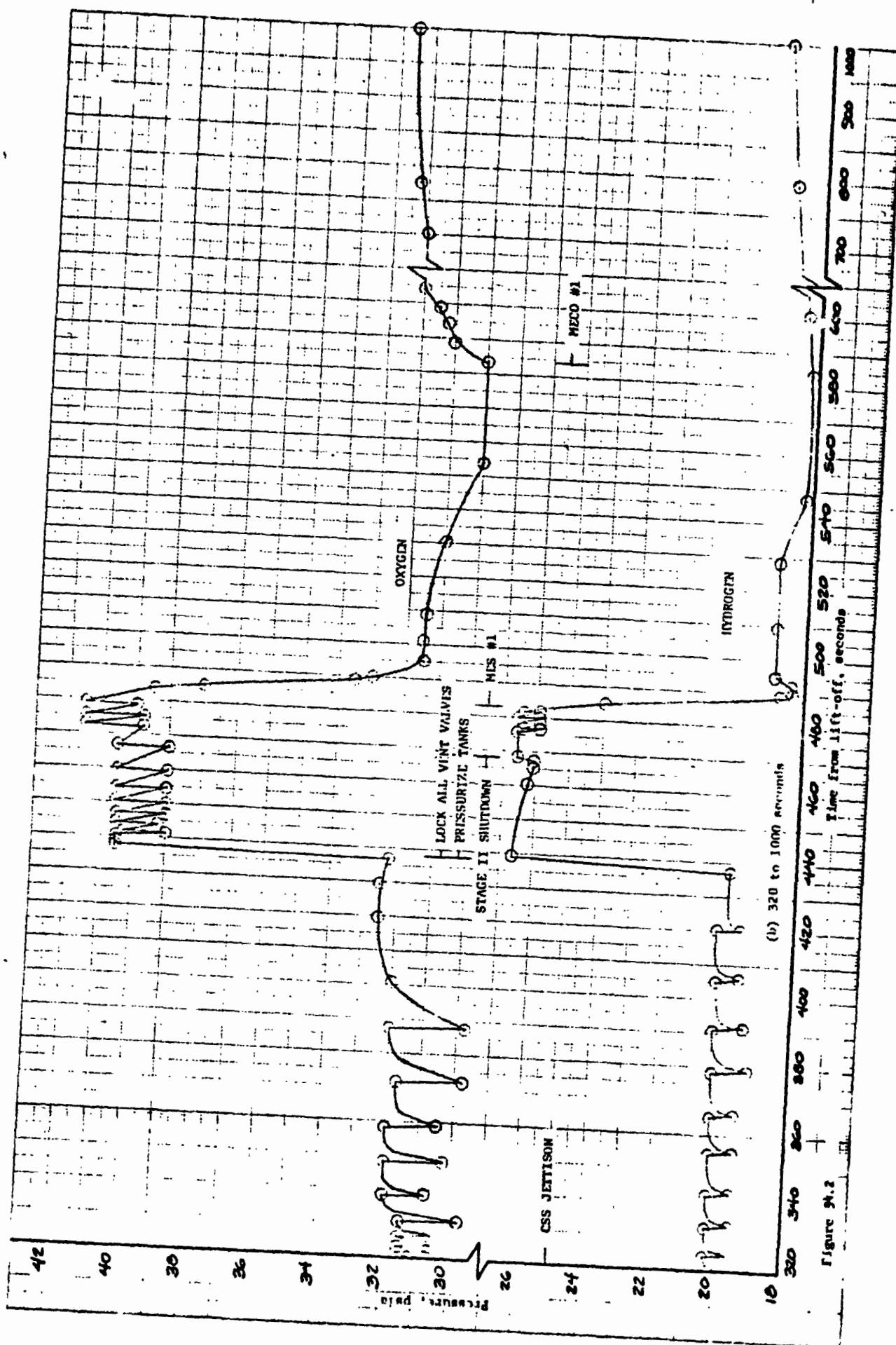


Figure 94.2

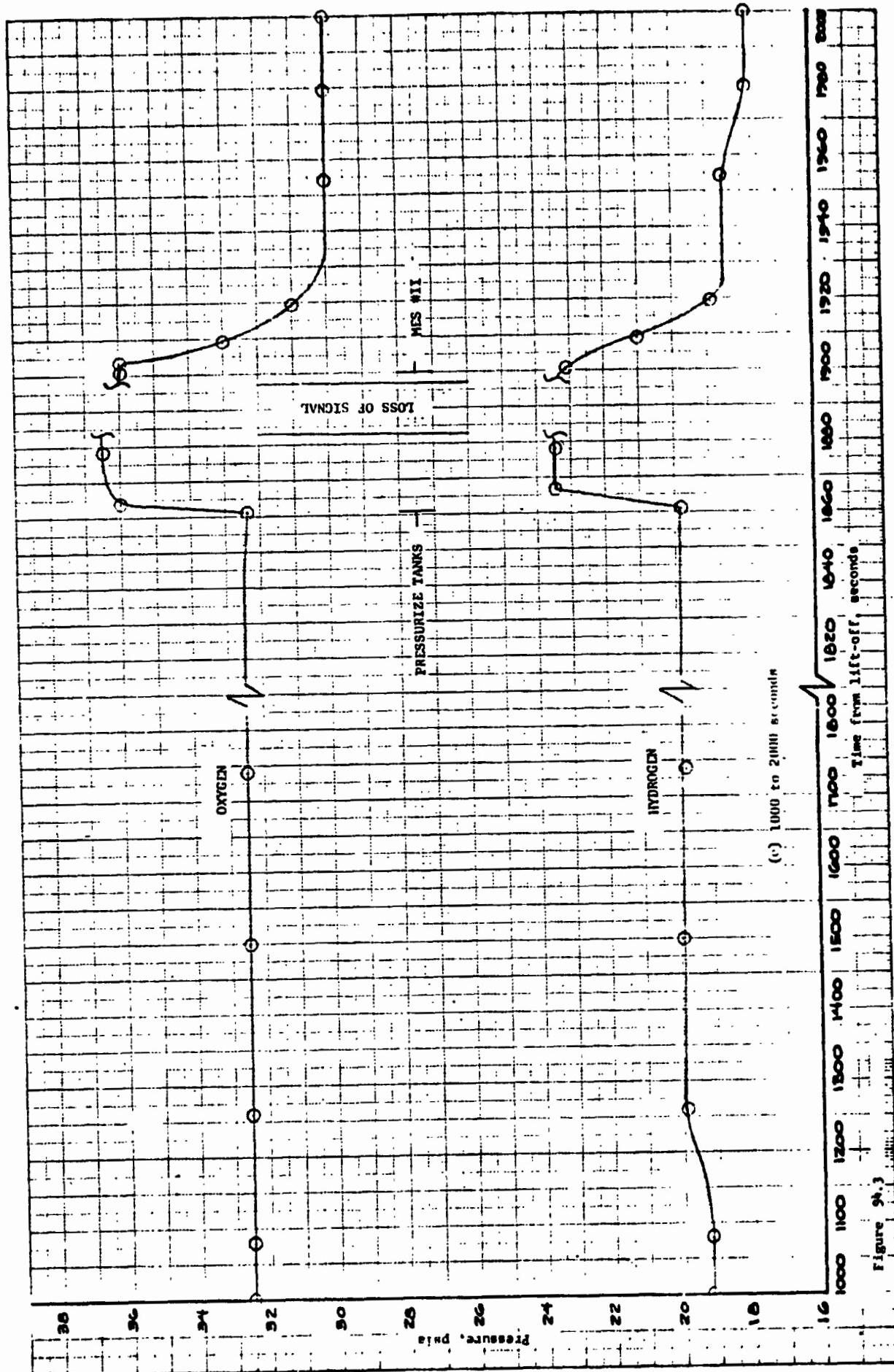
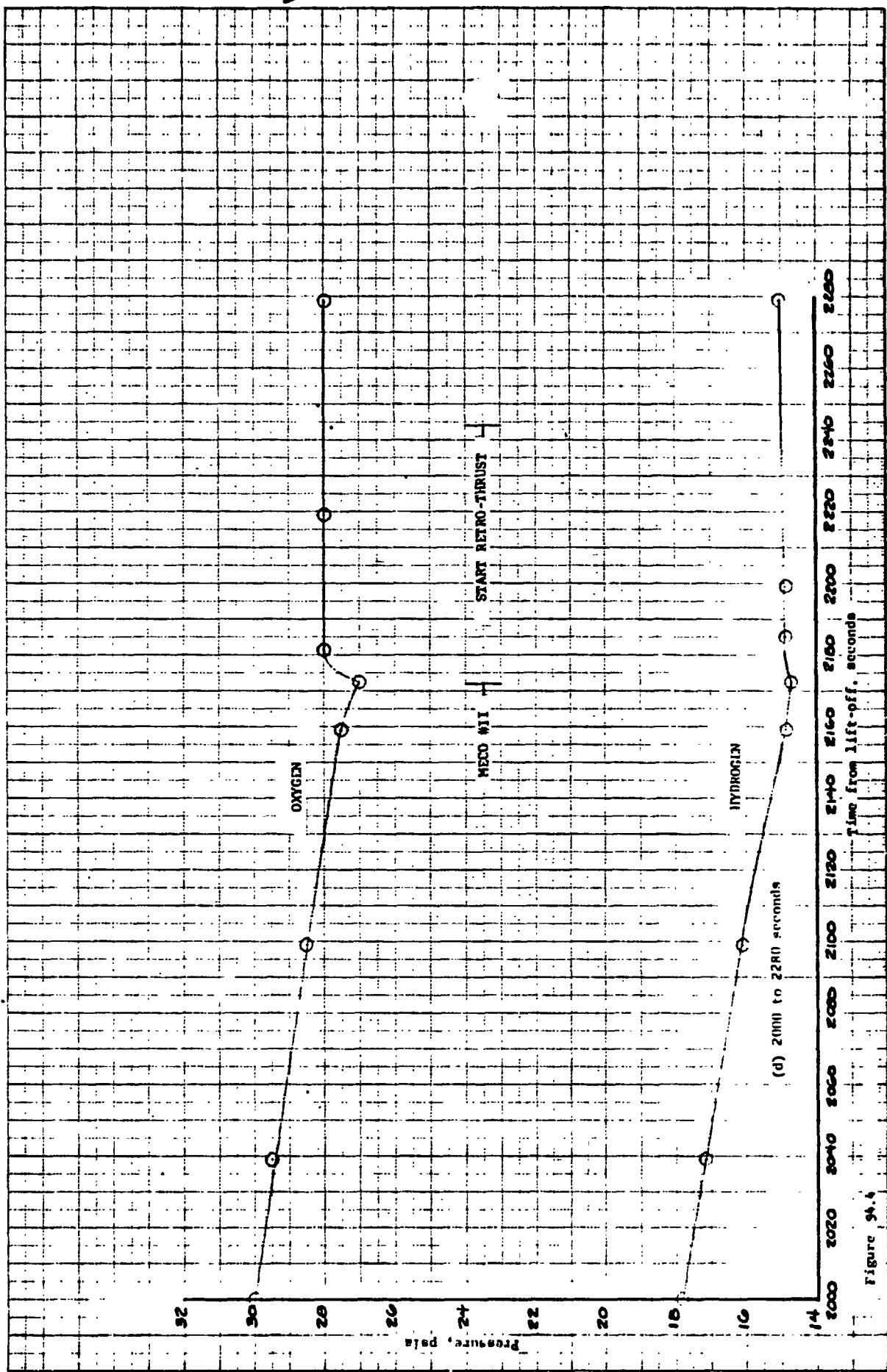


Figure 26.3

Figure 9.



the CCVAPS predicted pressure at liftoff was 23.75 psia. The actual liftoff pressure was 23.78 psia. At T-8 seconds the CCVAPS was deactivated until the start of tank pressurization for the first main engine start sequence.

After liftoff the tank pressure continued to rise, but at a decreasing rate, until it reached 24.7 psia at approximately T+25 seconds. After reaching the peak value, the pressure gradually decreased to 24.15 psia and remained relatively constant until T+90 seconds, when the primary vent valve was commanded to the relief mode. The decreasing rate of pressure rise and the eventual decrease in pressure can be attributed to a combination of factors: decreased convective heat input to the tank from the helium purge gas as it vented overboard during atmosphere ascent, suppressed boiling of the liquid hydrogen as the vehicle acceleration increased; and the increasing of the ullage volume by virtue of the tank changing shape as pressure increased. During the period when the primary vent valve was in the locked mode, the secondary vent valve, which has a specification operating range from 24.8 to 26.8 psia, was in the relief mode in order to protect against overpressurization of the tank.

At T+90 seconds the primary hydrogen vent valve was commanded to the relief mode, and the hydrogen tank vented down to the control range of the vent valve. The valve then began to cycle between its operating limits and continued to cycle until commanded to the locked mode for the start of tank pressurization for first main engine start.

The drop of approximately one psia in the operating limits of the vent valve from T+90 to T+188 seconds and the onset of relatively high frequency cycling can be attributed to the diminishing back pressure on the valve outlet. These are characteristic phenomena of the vent valves and have been observed on other Centaur flights and during acceptance testing of the valves. After T+320 seconds, when the Centaur Standard Shroud was jettisoned, the upper limit of the valve operating range remained essentially the same, but the lower limit dropped approximately 0.3 psia. When the shroud was jettisoned, the cap on the second leg of the vent system was also jettisoned, opening that leg for venting. The dynamic effect of the response time of the valve by the greater flow capacity of the system caused the pressure to decrease to a lower level before the vent valve could close.

The ullage pressure in the oxygen tank was 31 psia at liftoff. The vent valve, which has a specification operating range from 29.0 to 32.0 psia, was in the relief mode. Immediately after liftoff, the vent valve began to cycle between its operating limits and continued to cycle until the beginning of tank pressurization for first main engine start. At T+25 seconds the lower limit decreased about 0.5 psi. Later in the flight during atmospheric ascent, the reseat pressure decreased an additional 0.5 psi. These same operating characteristics were observed on TC-1 and can be attributed, in part, to the diminishing back pressure on the vent system as the vehicle ascended through the atmosphere.

Several times during the boost phase of flight, the ullage pressure rose above 32 psia, the upper specification limit of the vent valve. This also

occurred during TC-1 flight. At approximately T+105 seconds, the pressure rise could have been caused by a decrease in vehicle acceleration near the end of Stage 0 operation. A rapid decrease in the gravity field on the liquid will cause boiling which, in turn, will cause a rapid pressure rise. The same phenomenon occurred at approximately T+258 seconds, the end of Stage 1 operation. The other pressure excursions above 32 psia might have been the result of liquid oxygen ingestion by the vent system.

At T+437 seconds, the oxygen vent valve and both hydrogen vent valves were commanded to the locked mode, and tank pressurization for the first main engine start sequence was initiated. CCVAPS controlled tank pressures to predetermined increases over the pressures at the start of pressurization. These increases were based both upon tank structural limits and boost pump net positive suction pressure requirements. A discussion of the CCVAPS software and performance is presented in the CCVAPS section of this report.

At T+483.2 seconds Centaur first main engine start (MES 1) was initiated. The pressures in both tanks dropped rapidly at first and then decayed gradually until first main engine cutoff (MECO 1) at T+584 seconds. The pressure in the hydrogen tank at MECO 1 was 18.2 psia while that in the oxygen tank was 30 psia. After MECO 1, the pressures in the oxygen tank and hydrogen tank increased to 32.5 and 20 psia, respectively, and remained relatively constant until the beginning of tank pressurization for second main engine start.

At T+1861 seconds tank pressurization for the second main engine start was initiated and controlled by CCVAPS. At T+1899.5 seconds MES 2 was initiated. Again, the tank pressures dropped rapidly at first and then gradually until MECO 2 at T+2172.9 seconds. After MECO 2 both tank pressures increased slightly and remained constant until Centaur retromaneuver.

Helium Storage and Consumption - The helium, which was stored in one 7365 cu. in. bottle and one 4650 cu. in. bottle, was used to pressurize the propellant tanks during engine start sequences, to operate the engine control valves, to pressurize the H₂O₂ bottle, and to provide purges to various parts of the Centaur. The amount of helium consumed during the flight through retromaneuver is summarized in Table 40. It should be noted that the amount of helium used during engine start sequences includes usage for tank pressurization and pressurization of the H₂O₂ bottle while H₂O₂ was being consumed for operating the boost pumps.

Propulsion Pneumatics - The engine controls regulator and the H₂O₂ bottle pressure regulator maintained proper system pressure levels from pressurization of the helium bottles through retromaneuver. The engine controls regulator output pressure at liftoff was 462 psia (allowable limits are 440 to 479 psig), while that of the H₂O₂ bottle pressure regulator was 326 psia (allowable limits are 297-316 psig). Both regulators are referenced to ambient pressure, so after liftoff both output pressures decreased, corresponding to the decrease in ambient pressure, and remained relatively constant after the ambient pressure had decreased to zero.

TABLE 40 SUMMARY OF HELIUM USAGE

Event	Helium Bottle Press. (psia)		Helium Bottle Temp. (°F)		Helium Quantity (Pounds)		Helium Used (Pounds)
	7365 Cu. In.	4650 Cu. In.	7365 Cu. In.	4650 Cu. In.	7365 Cu. In.	4650 Cu. In.	
Liftoff	3195	3495	76	72	9.25	5.88	-
MES I Press'n. (Start)	3460	3495	77	74	9.14	5.16	0.13
MES I Press'n. (End)	3160	3240	61	63	8.67	5.59	0.74
MES II Press'n. (Start)	3080	3160	64	92	8.42	5.21	0.63
MES II Press'n. (End)	2680	2720	39	63	7.76	4.76	1.11
Retromaneuver (Start)	2720	2780	48	81	7.74	4.71	0.07
Retromaneuver (End)	2720	0	48	-	7.74	0	4.71
TOTAL						7.39	

Helium Retro-Thrust - At T+2244.9 seconds, the two normally closed pyrotechnic valves in the helium retro-thrust system were fired, allowing the remainder of the helium in the smaller bottle to discharge through two forward canted nozzles. The discharge of the helium through the nozzles created a reverse thrust on the Centaur, providing a separation distance between the Centaur and the spacecraft. The pressure in the smaller bottle went from 2780 to 0 psia. The pressure in the large bottle remained constant, indicating that the check valves did not leak.

Helium Purge - Throughout the launch countdown, the ground system supplied a helium gas purge to the forward and aft ends of the vehicle. The gas was used to purge the hydrogen tank/shroud annulus, the destruct package, and several propulsion system components. The purge was required to maintain enough pressure differential across the shroud after cryogenic tanking to prevent ground winds inflow. For the launch day wind conditions of approximately 10 MPH, a minimum differential pressure of 0.045 psid was required. At the beginning of hydrogen tanking the pressure dropped momentarily to 0.065 psid but then recovered to 0.171 psid and remained essentially constant until hydrogen vent valve lockup. The pressure then began to rise until it reached a value of 0.225 psid at liftoff.

Computer Controlled Vent and Pressurization System

by E. J. Cieslewicz

The computer controlled vent and pressurization system (CCVAPS), when activated, maintains the L₂O tank and L₂H tank pressures at required levels during various phases of flight. CCVAPS Figure 95 consists of the pressurization system, the vent system, the ullage pressure transducers, the digital computer unit (DCU), and the sequence control unit (SCU).

The DCU monitors the tank pressures during selected periods of the flight and issues appropriate commands to the SCU relays which activate the appropriate pressurization solenoid valves and solenoid-operated vent valves. The DCU is programmed with maximum and minimum allowable tank pressures and pressure increases prior to main engine start. In addition, the DCU is able to detect ullage pressure transducer failures and pressurization solenoid valve failures.

The DCU monitors each tank pressure through three transducers, a primary, a reference, and a backup. In the event of a discrepancy between the outputs of the primary and reference transducers, the DCU uses the output of the backup transducer to determine tank pressure.

During a pressurization sequence, if the DCU monitors an insufficient or excessive increase in pressure (due to a pressurization solenoid valve failure), the DCU commands the flow control valve closed and uses the redundant pressurization solenoid valves (both tanks) for the remaining portion of the flight.

Prior to main engine start, CCVAPS is activated, the pressurization solenoid valves and the solenoid-operated vent valves are activated, and both tank pressures are increased by predetermined amounts and maintained at those levels until main engine start. CCVAPS is deactivated at main engine start.

During the coast phase, CCVAPS is activated to prevent the L₂O tank and L₂H tank pressures from exceeding maximum allowables. The appropriate H₂O₂ engines are fired to settle the propellants, then the solenoid-operated vent valves are deenergized to allow venting.

CCVAPS is also activated after the final main engine cutoff. The L₂O tank is pressurized to prevent an adverse intermediate bulkhead delta P condition.

Propellant Tank Pressurization - The pressurization mode of the CCVAPS computer program was used prior to each Centaur engine start and after the final engine firing. For each of these pressurizations the vent valves were locked by the sequencer module and the CCVAPS module took over the task of pressurization. The pressurization valves were opened and closed cyclicly to increase and maintain propellant tank pressures at predetermined levels sufficient for proper propellant conditions at each engine start and for structural integrity.

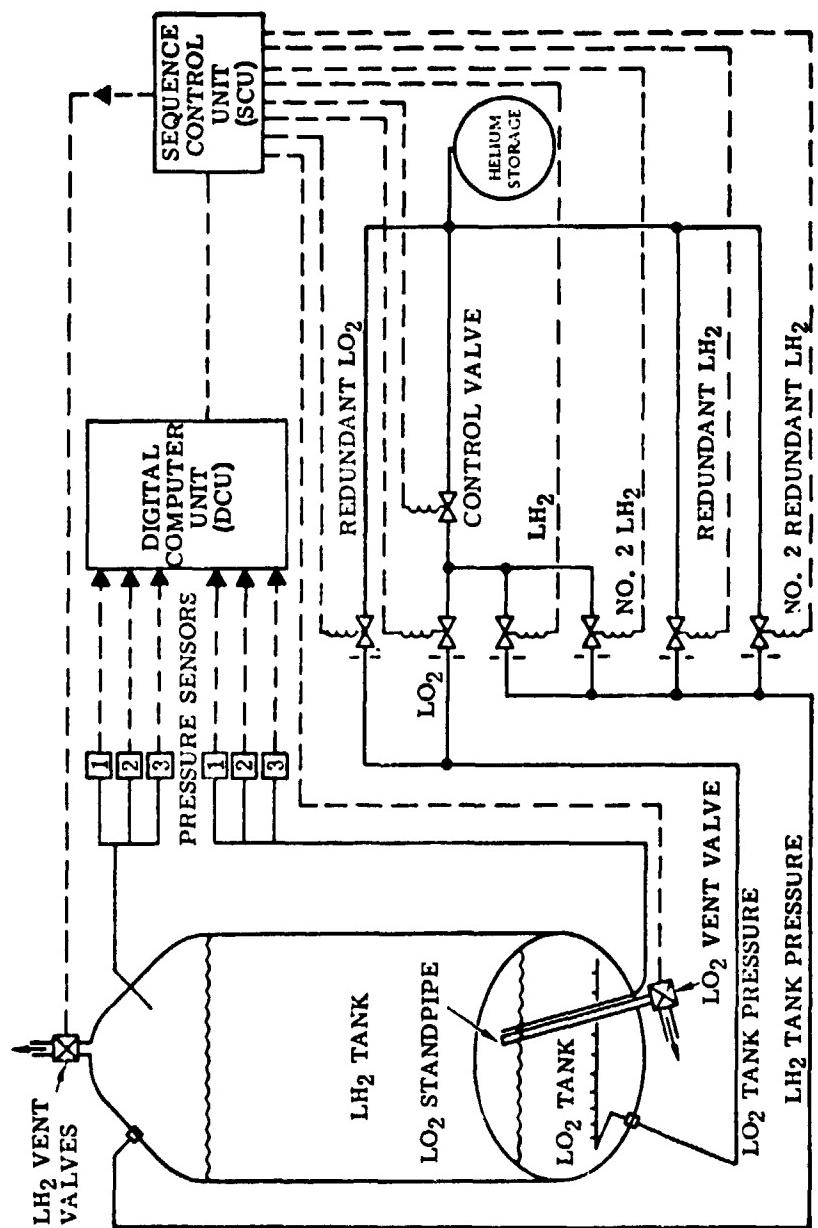


FIGURE 95 COMPUTER CONTROLLED VENT AND PRESSURIZATION SYSTEM

following the final engine firing. The CCVAPS module performed failure checks of the propellant tank transducers and monitored pressurization system valve performance to determine if a switch to redundant systems was necessary. The redundant transducers and the backup pressurization system were not called on by CCVAPS since all systems performed well.

Pressurization for MES 1 - For the first pressurization, the CCVAPS system calculated pressurization valve closing pressures. The computer was programmed to use the lowest of three computed values for the LO₂ tank and the lowest of two computed values for the LH₂ tank. The criteria used for the computations were initial tank pressures at start of pressurization, desired pressure increases above initial pressures for engine start, the structural limits of maximum pressures, and the allowable maximum differential pressure across the propellant tank bulkhead. Table 41 shows the desired delta pressure increases for each tank above the DCU computed initial pressures. The Table also shows the maximum allowable pressures for these tanks.

Prior to Stage II cutoff the LO₂ tank had a third requirement that it be pressurized no higher than 19.2 psi above the calculated initial LH₂ tank pressure to avoid a propellant tank bulkhead delta pressure problem. The computed and selected LO₂ tank pressurization valve closing pressure was based on limiting delta pressure across the bulkhead to only 19.2 psi above the hydrogen tank initial pressure. The required LO₂ tank pressurization valve closing pressure was 39.12 psia. See Table 41 which lists the higher and unused values of closing pressure based on desired increase in tank pressure and the maximum LO₂ tank allowed pressure.

The computed and selected LH₂ tank pressurization valve closing pressure was based on desired delta pressure increase above the initial tank pressure. The required LH₂ tank pressurization valve closing pressure was 25.92 psia, 6.0 psi above the initial LH₂ tank pressure.

Figure 96 shows the pressure profiles of both the LO₂ tank and the LH₂ tank during the pressurization phase prior to the first engine start. The cross hatched bands shown in the figure above and below the clear 0.2 psi control band, illustrate the limits to which CCVAPS will allow tank pressure to vary before the pneumatic system would have been called on to use its redundant components. Had either propellant tank pressure gone above the upper band or below the lower band during this pressurization, a switch in the pressurization would have been made using the backup pressurization valves for both tanks. See Figure 95 for backup components.

Figure 96 cross hatch levels are set at 3.77 psi above the calculated pressurization valve closing pressure and 0.6 psi below the calculated pressurization valve closing pressure minus the 0.2 psi allowed for control deadband on the LO₂ tank pressurization system. The LH₂ tank pressurization system has bands similar to the LO₂ pressurization system and its limits above and below the 0.2 psi deadband are 1.53 psi and 1.7 psi respectively.

TABLE 41

Pressurization Phase, Time of Activation, Seconds	Desired Press. Increase Before Engine Start, PSIA	L02	LH2	Maximum Bulkhead Delta Press. Above LH2 Initial PSIA		L02	LH2	Flight Value Closing Press. Used, PSIA	1st. Cycle Press. Rise Rate PSI/Sec.
				L02 Only	LH2				
Stage II Cutoff -28.5 to	7.76	6.0 *		19.2*	40.5	26.0		39.12	25.92
Stage II Cutoff								8.81	2.24
Stage III Cutoff to MES 1 -0.2	7.76*	6.0*		--	40.5	27.1		39.91	25.92
MES 2 -38.0 to MES 2 -0.2	3.5*	3.4*		--	44.5	28.1		36.11	23.53
								1.21	0.68

- Parameter chosen by CCVAPS for pressurizing valve closing pressure.

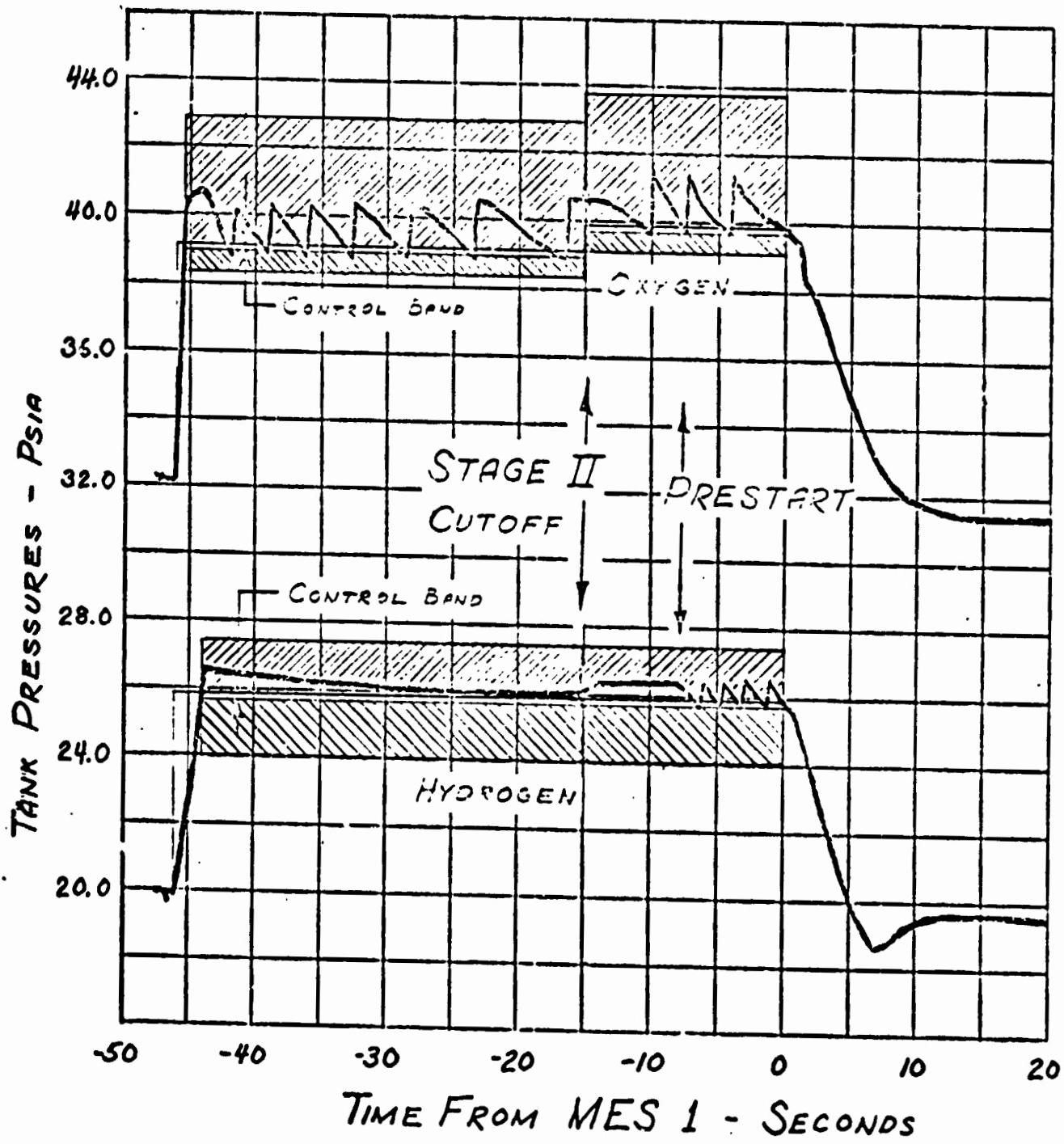


FIGURE 96 CCVAPS CONTROLS & LIMITS LANDS

ORIGINAL PAGE IS
OF POOR QUALITY

The CCVAPS module monitored the pressure rise rate during the first pressurization cycle to determine if tank pressures had increased to a required minimum above initial pressures in an allotted time. The LO₂ tank was to increase 2.0 psi in the first 1.5 seconds, which it did, or the CCVAPS module would have determined that the primary pressurization system had failed and would have switched the system over to the backup system. The initial cycle average pressure rise rate was sufficient at 8.81 psi/second. The LH₂ for the same reason was to increase 1.0 psi in the first 1.5 seconds, which it also did. The initial cycle average pressure rise rate was adequate at 2.24 psi/second.

Before the pressurization valves were opened, the CCVAPS system determined that both initial tank pressures were below maximum tank pressure allowables; otherwise, the pressurization system valves would have remained closed.

In Figure 97 the cross hatched limit bands of the LO₂ tank pressure profile changed at the time of Stage II cutoff. The overshoot and undershoot allowances are the same as those before Stage II cutoff but the upward shift was due to the change in pressurization requirements at this time. At Stage II cutoff the bulkhead delta pressure was no longer critical, therefore, the desired pressure increase above the initial value became the controlling parameter. The pressure calculation for valve closing pressure was 39.91 psia, 7.76 psi above the initial LO₂ tank pressure. The requirement for the LH₂ tank did not change, therefore, the limit bands remained the same as those before Stage II cutoff.

The obvious difference in activity associated with pressurization in Figures 96 and 97 was primarily related to the means of insulation used on the tanks and the methods by which pressurants are added to the tanks. See report section on Pneumatics.

Pressurization for MES 2 - The sequencer module activated CCVAPS for the MES 2 pressurization. CCVAPS computed values for valve closing pressures for both the LO₂ tank and the LH₂ tank. The main criteria used for tank pressurization following the first engine firing was the desired pressure increase above initial pressure, limited, if necessary, by the allowable maximum for each propellant tank. Table 41 shows the desired pressure increases and the allowable maximums for each tank. Also shown are the actual values computed.

The computed and selected LO₂ tank pressurization valve closing pressure was 36.11 psia, 3.5 psi above the initial tank pressure of 32.61 psia. The computed and selected LH₂ tank pressurization valve closing pressure was 23.53 psia, 3.4 psi above the initial value. Figure 97 shows the pressure profiles of both the LO₂ tank and the LH₂ tank during the pressurization phase prior to second engine start. Shown also on this figure are the limits bands in cross hatch and the 0.2 psi control band. The limit bands for system operation are 1.0 psi above closing pressure and 0.6 psi below closing pressure minus the 0.2 psi allowed for control deadband of the LO₂ tank pressurization system. The LH₂ tank pressurization system has bands

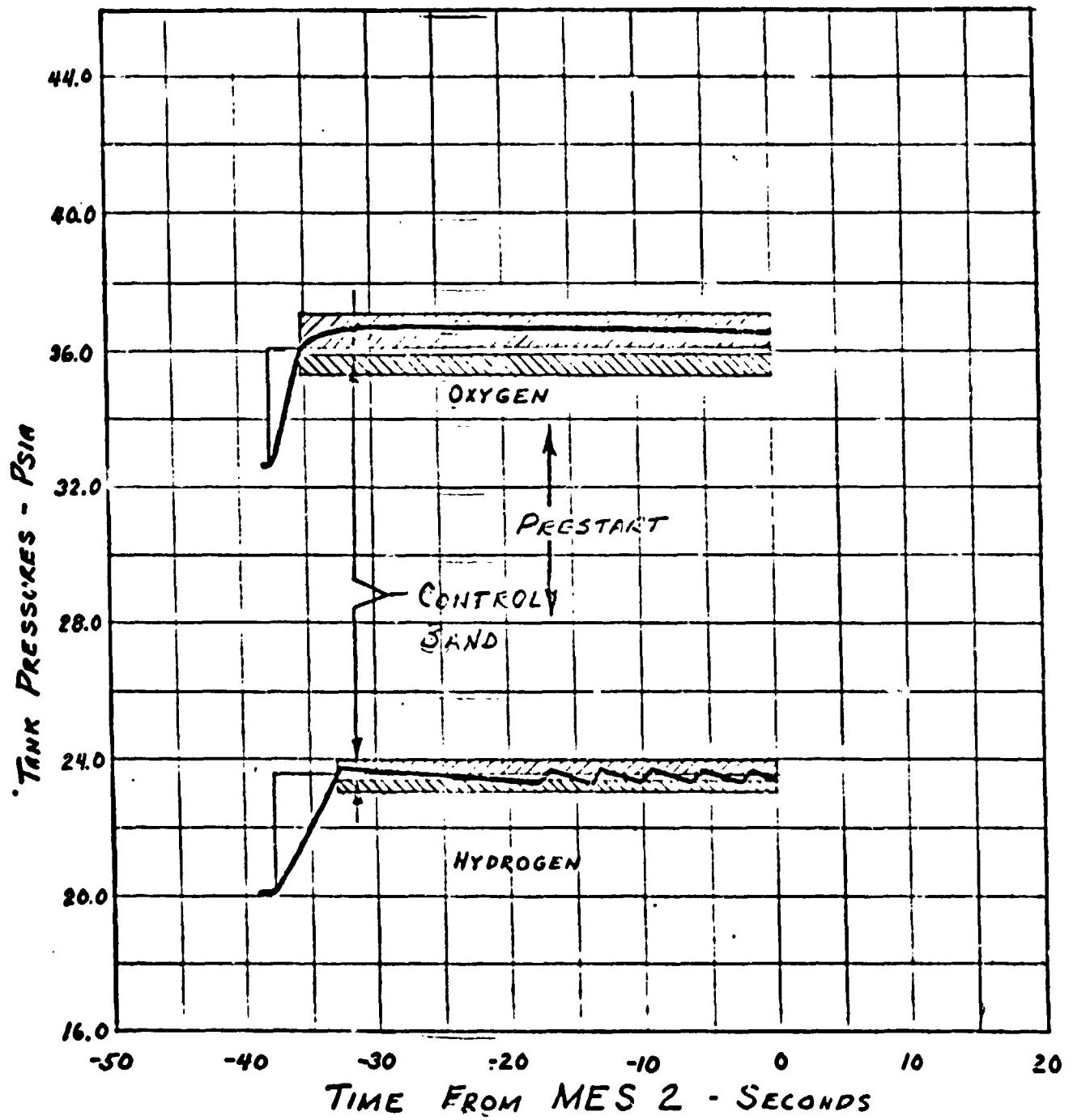


FIGURE 97 CCVAPS CONTROLS & LIMITS BANDS

similar to the LO₂ pressurization system and its limits above and below the 0.2 psi deadband are 0.36 psi and 0.3 psi, respectively.

Pressure rise rates of the propellant tanks were monitored by CCVAPS to assure that the LO₂ tank rose 2.0 psi in the allotted 2.0 seconds. The actual rise rate on the first pressurization cycle was sufficient at 1.21 psi/second. The LH₂ tank was to rise 0.35 psi in the same allotted 2.0 second period. Actual rise rate for the LH₂ tank was adequate at 0.68 psi/second.

Propellant Tank Venting - The venting mode of the CCVAPS computer program was enabled at the times listed in Table 42. Also shown in the Table are the pressure levels used by CCVAPS to trigger the start of a venting sequence. Tank pressures throughout flight were not high enough to trigger a venting routine. Pressures were always below the values listed in Table 42.

TABLE 42

Coast Phase, Times of Activation-Seconds	LO2 Pressure	Vent Enable Pressure, PSIA	LH2 Pressure	Δ Pressure
MECO 1 + 260 to MES 2 -96	≥ 47.0	≥ 28.8		N/A
MECO 2 +300 to MES 3 -96	≥ 42.0	≥ 27.5		$\geq 18.0/\leq 2.6$

Centaur D-1TR and CSS Thermal
Environments and Propellant Behavior

by R. F. Lacovic

Centaur and CSS Component and Environmental Temperatures

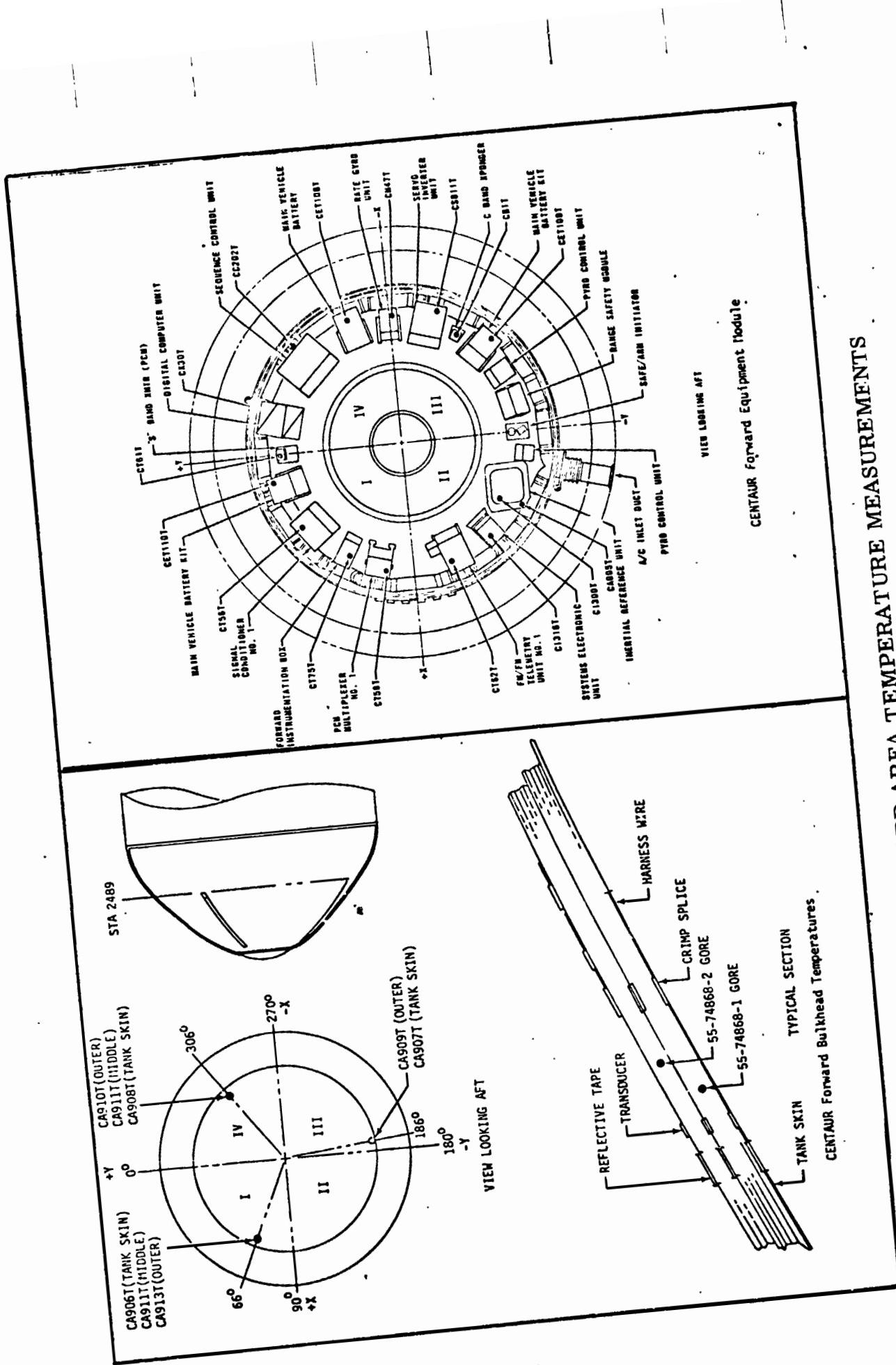
The Centaur vehicle was extensively instrumented in order to assess the component thermal control and environment of the D-1T Centaur configuration. This configuration contained the following new or revised thermal control hardware.

1. LH₂ tank sidewall radiation shielding.
2. Titanium stub adapter.
3. Propellant feed system radiation shielding.
4. H₂O₂ system radiation shielding, heaters, and impingement shields.
5. Prelaunch purging and gas conditioning.
6. Pneumatic and vent system coatings and shielding.
7. Electronic packages coatings and shieldings.

Most of these configuration changes were incorporated in order to make the Centaur thermal performance suitable for long space coast missions. Consequently, as expected the Centaur thermal performance during the Helios portion of the TC-2 mission was satisfactory and well within previous D-1A Centaur flight experience.

The Centaur component and environmental temperatures from liftoff through spacecraft separation are listed herein. These temperatures are compared with TC-1 flight temperature listings to indicate the repeatability of the D-1T thermal control performance during the boost phase. The locations of the sensors used in the following listings are shown in Figures 98 and 99.

Package Temperatures - The electronic and mechanical package temperatures are listed in Table 43. The temperatures at liftoff were all satisfactorily maintained by prelaunch conditioning to well within the 50°F - 90°F prelaunch limits. During the 22 minute parking orbit coast the forward packages (which received sunlight) warmed slightly, and the aft packages (which received no sunlight) cooled slightly. All of the package temperatures were well within their operating limits through spacecraft separation. Three of the package temperatures (CT611T, CT622, and CK30T) did show a more rapid warming trend, but these temperatures were still well below the 160°F operating limit.



CENTAUR FORWARD

FIGURE 9b: 1

ORIGINAL PAGE IS
OF POOR QUALITY

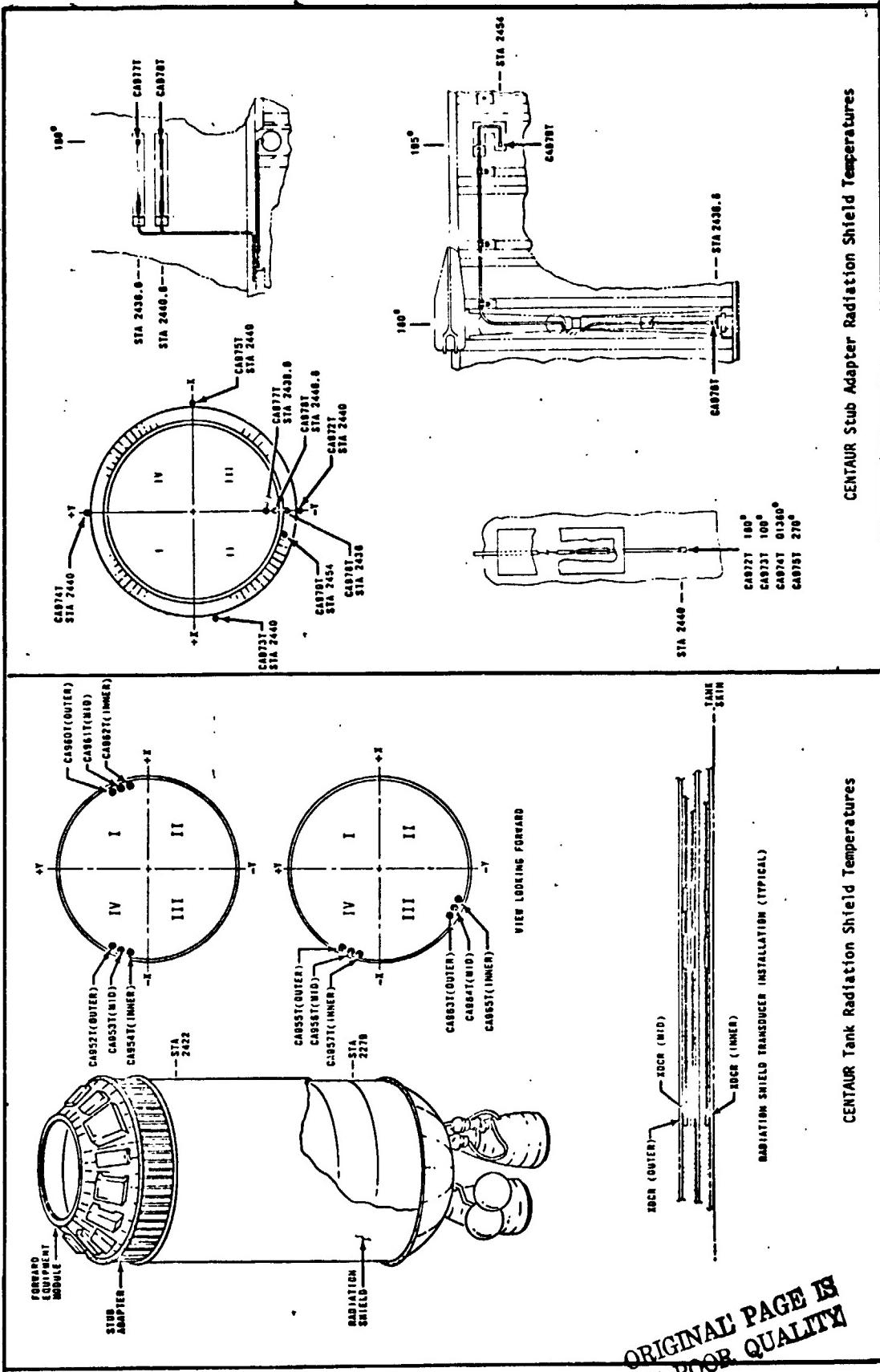


FIGURE 98.2 CENTAUR LH₂ TANK AND STUB ADAPTER RADIATION SHIELDING TEMPERATURE LOCATIONS

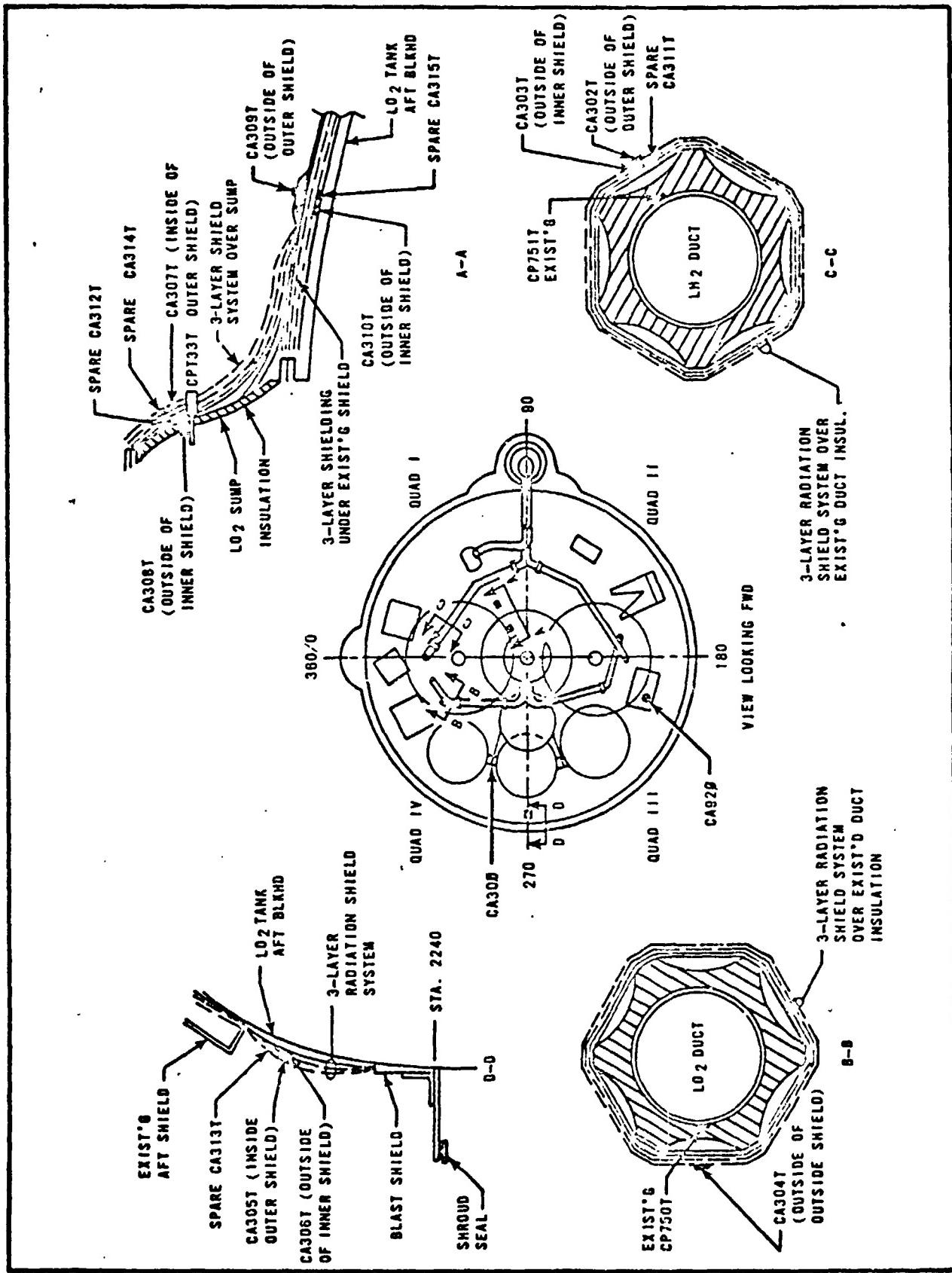


FIGURE 99.1 CENTAUR THRUST SECTION RADIATION SHIELD TEMPERATURES

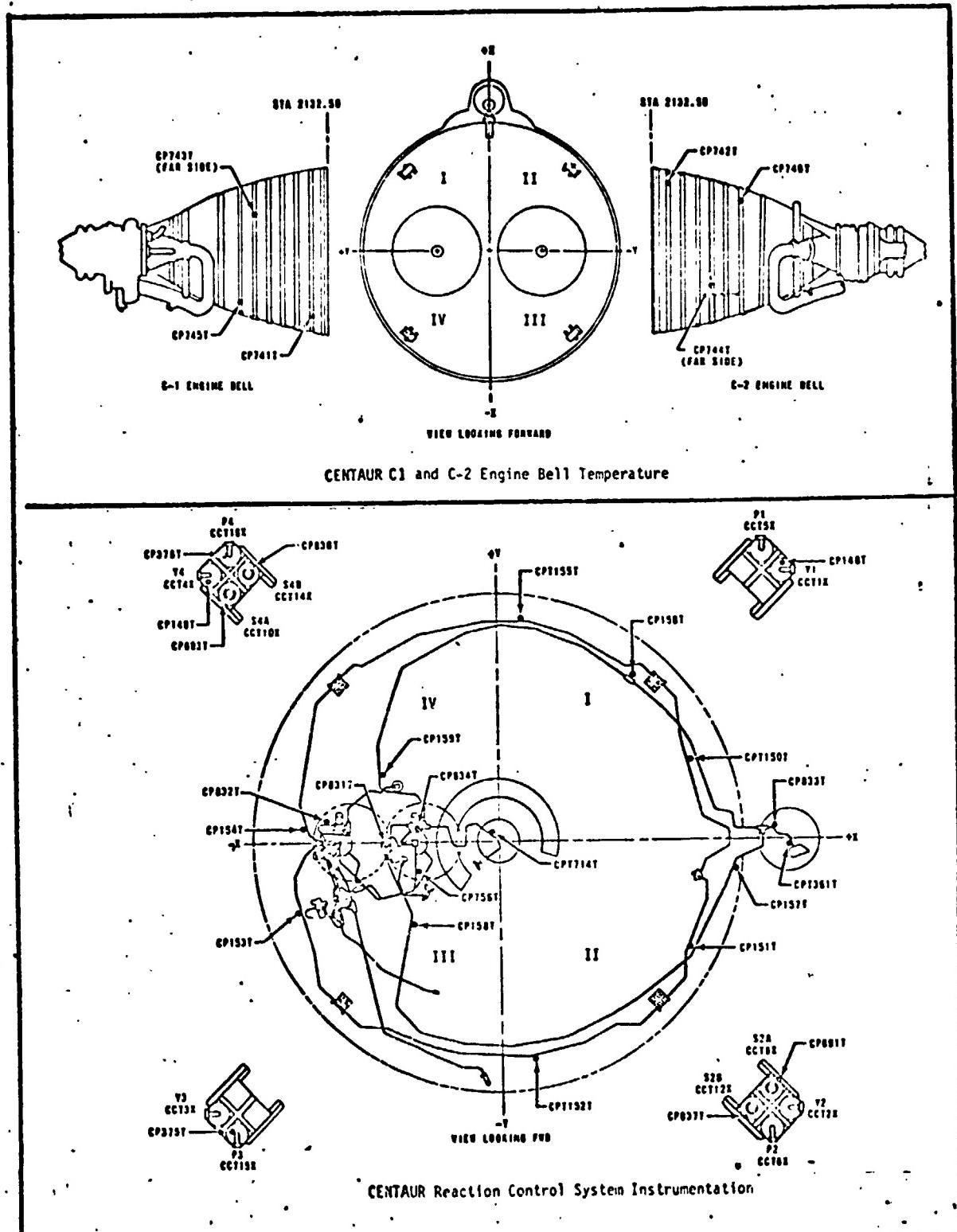


FIGURE 99.2 CENTAUR ENGINE BELL AND REACTION CONTROL SYSTEM INSTRUMENTATION

TABLE 43 PACKAGE TEMPERATURES, TC-2 FLIGHT

Measurement No.	Location	Temperature - °F											
		Liftoff TC-1	TC-2	CSS Jett. TC-2	MES 1 TC-1	740 Sec. TC-2	1000 Sec. TC-2	1500 Sec. TC-2	MES 2 TC-2	S/C Sep.			
CB1T	C-Band Transponder	66	70	73	72	73	72	75	76	77	78	80	
CC202T	SCU Housing Web	64	73	72	63	72	63	72	70	70	70	72	
CE56T	RSC Batt 1 Internal	83	108	99	77	96	77	94	91	85	82	80	
CE57T	RSC Batt 2 Internal	97	79	79	86	78	86	76	74	70	67	66	
CE108T	Main Batt 1 Internal	95	87	98	97	97	97	90	97	93	95	96	
CE109T	Main Batt 2 Internal	81	91	91	82	91	82	92	92	92	92	92	
CE110T	Main Batt 2 Internal	92	77	82	94	82	95	86	86	88	91	93	
CS811T	SIU Skin	65	74	75	67	77	69	77	78	80	82	84	
CI300T	IRU Skin Internal	80	77	84	86	85	85	86	86	85	85	85	
CI316T	SEU Internal	65	72	73	66	73	65	73	73	73	74	76	
CK30T	DCU Skin	77	87	92	87	90	87	94	96	97	102	106	
CM47T	IRGU Gyro Block	77	88	88	80	91	80	89	93	96	97	99	
CT56T	Sig. Conditioner No. 1	62	71	70	61	69	60	69	69	68	68	68	
CT57T	Sig. Conditioner No. 2	82	80	79	81	79	81	79	79	78	78	77	
CT58T	Equipment Mod. MUX 1	63	71	70	63	69	61	69	69	69	65	68	
CT59T	Thrust Section MUX 2	76	70	69	75	69	75	68	68	67	66	66	
CT61T	S-Band XMIR PCM	71	87	98	85	102	92	107	109	116	121	124	
CT62T	S-Band XMIR FM	72	82	88	82	90	83	92	94	95	98	106	
CT75T	Equip Mod Instr.Box	67	73	73	64	72	64	72	72	72	71	71	
CT76T	Aft Bulk.Instr.Box	71	74	72	72	73	69	71	71	71	71	71	
CT77T	C-2 Instr. Box	73	69	66	72	67	69	63	63	62	58	53	
CJ240T	C-1 Servo PSN Hsg.	66	64	63	66	66	68	60	58	52	48	39	
CJ241T	C-2 Servo PSN Hsg.	60	54	57	63	57	63	61	69	67	75	61	
CF133T	Aft Pneu. Panel No. 1	65	60	52	56	53	54	47	46	40	37	34	
CF134T	Aft Pneu. Panel No. 2	66	61	48	56	47	54	43	43	36	33	31	
LO2	Vent Valve Sol.	-142	-120	-149	-127	-178	-161	-154	-142	-135	-126	-142	
CF30T	LH ₂ Prim Vnt Vlv Sol.	-155	-211	-300	-264	-230	-208	-165	-165	-126	-111	-94	

Structural Temperatures - The various Centaur structural temperatures are listed in Table 44. The equipment module temperatures remained nearly constant once the temperatures had stabilized at the end of the ascent venting. The temperatures of the new titanium stub adapter at various times throughout the flight are shown in Figure 100. These temperature profiles compared well with the prelaunch predictions, indicating that the predicted heat transfer rate to the LH₂ tank forward ring had been obtained. The temperature of the inside surfaces of the payload area of the Centaur Standard Shroud are shown in Figure 101. As shown in this figure, the temperatures were far below the 135°F limit, even with the 50 second increase in time to shroud jettison.

Propulsion System and H₂O₂ System Temperatures - The Centaur RL10, propellant feed, and H₂O₂ system temperatures are listed in Tables 45 and 46. All of the temperatures were satisfactory. The propellant feed system temperatures were close to the nominal expected for the radiation shielded configuration. The engine bell and pump temperatures were close to the maximum predicted levels as a result of H₂O₂ engine exhaust impingement and solar heating. The H₂O₂ system temperatures were all between 87°F and 100°F except for a few localized hot spots that received H₂O₂ engine exhaust impingement (such as CP159T) or heat soakback from the boost pump turbine (such as CP361T). The heaters and radiation shield boots maintained good thermal control of the lines. The impingement heating effects during the continuous 80 second H₂O₂ engine firing primary sequence during boost was acceptable and about the same as for TC-1. The C-1 LH₂ pump housing showed the most marked effects of the impingement heating and is shown in Figure 102.

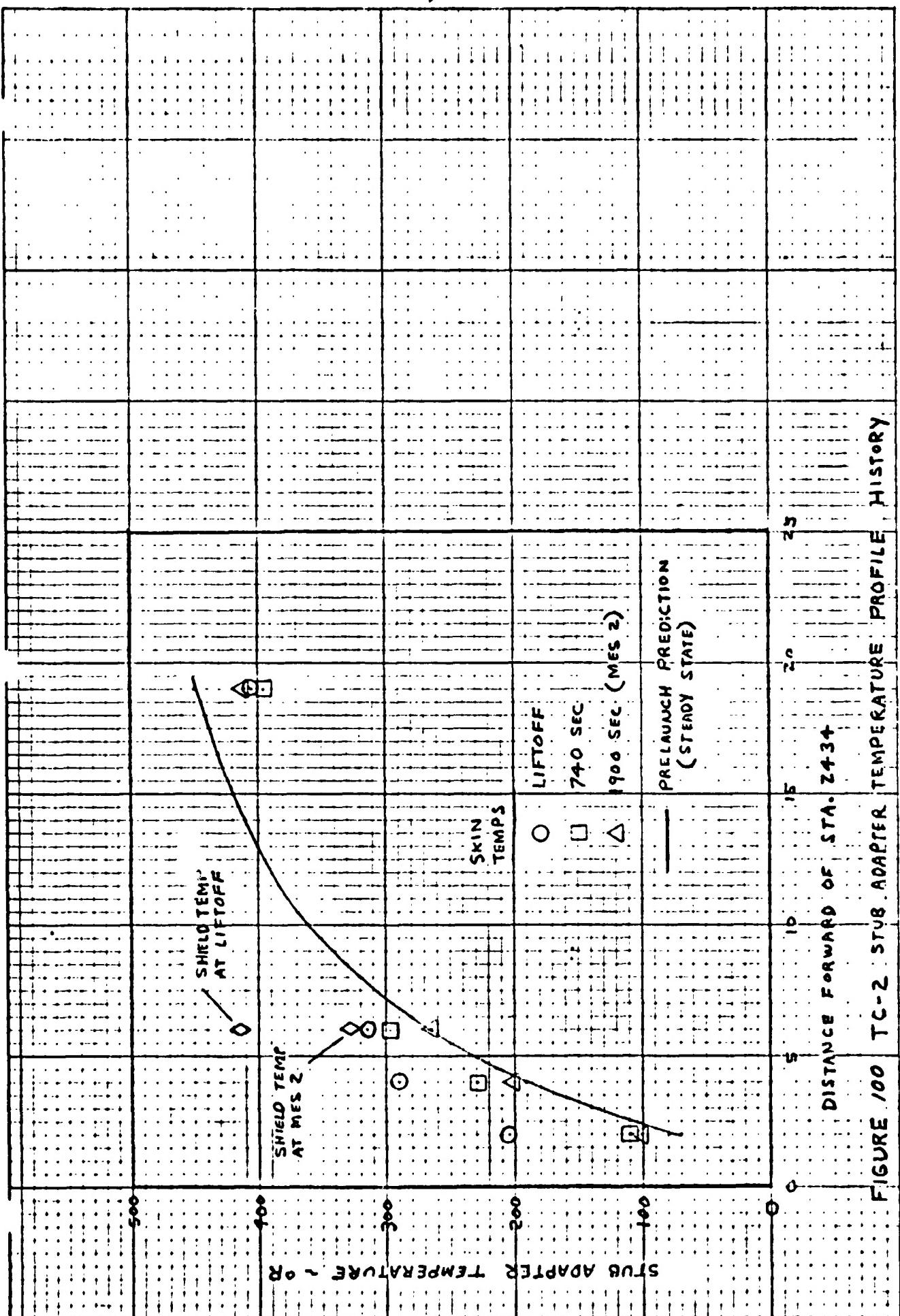
Radiation Shield Temperatures - The Centaur LH₂ tank sidewall, forward bulkhead, sump, feedlines, and LO₂ tank aft bulkhead radiation shield system temperatures are listed in Tables 47 and 48. The thermal performance of these systems was as expected. The temperatures at liftoff were close to previous TC-1 flight and TCD test experiences. During the boost, the rapid venting results in a decrease in shield temperatures. After CSS jettison, the shield temperatures begin to increase to achieve equilibrium with their space environment resulting in large temperature gradients through the shielding. These temperature increases, which continued through spacecraft separation, are in good agreement with calorimeter testing of the shielding which showed that over one hour is required for the shielding to reach a steady state temperature gradient.

The LO₂ tank aft bulkhead did not contain the three layer radiation shielding as it did for TC-1 (the scheduling for the TC-2 reconfiguration did not permit it). This accounts for the large differences between TC-1 and TC-2 temperatures in this area.

TABLE 44 STRUCTURAL TEMPERATURES

Measurement No.	Location	Temperatures - °F												S/C Sep.	
		Liftoff		CSS		Jett.		MES 1		740 Sec.		1000 Sec.			
		TC-1	TC-2	TC-1	TC-2	TC-1	TC-2	TC-1	TC-2	TC-1	TC-2	TC-1	TC-2		
CA90LT		-	69	57	-	-	55	-	-	53	49	47	49	54	
CY19T	S/C Comp. Amb.	-	67	56	-	-	-	-	-	-	-	-	-	-	
CA903T	Eq. Mod. Skin Q4	41	43	30	32	30	34	30	30	30	30	32	32	36	
CA904T	Eq. Mod. Skin Q1	42	41	29	34	29	30	29	29	29	29	27	29	33	
CA905T	IRU Out Mount	67	82	77	63	77	84	76	73	71	80	71	80	106	
CA914T	Eq. Mod. +Z	48	52	41	33	36	44	35	35	32	27	27	26	30	
CA971T	Fill and Drain Port	-404	-413	-413	-405	-417	-406	-417	-417	-417	-417	-417	-417	-417	
CA972T	Stub Adapt. Shld.	180	-43	-61	-115	-121	-123	-64	-123	-137	-142	-132	-132	-56	
CA973T	Stub Adapt. Shld.	100	-84	-71	-71	-156	-144	-105	-147	-168	-177	-71	-71	7	
CA974T	Stub Adapt. Shld. 0	-41	-37	-115	-69	-93	-35	-68	-56	-83	-83	-83	-83	-9	
CA975T	Stub Adapt. Shld.	270	-41	-51	-123	-59	-86	-18	-49	-44	-29	0	0	12	
CA976T	Stub Adapt. Skin	2437	-253	-255	-306	-360	-326	-349	-350	-352	-358	-358	-358	-361	
CA977T	Stub Adapt. Skin	2439	-162	-170	-207	-226	-213	-229	-229	-233	-253	-253	-253	-266	
CA978T	Stub Adapt. Skin	2441	-133	-147	-156	-158	-159	-156	-163	-168	-189	-189	-189	-202	
CA979T	Stub Adapt. Skin	2454	-47	-54	-79	-56	-73	-47	-64	-61	-56	-51	-51	-46	
CA980T	Wire Tnl. LH2 Sump	-177	-211	-275	-121	-213	-150	-184	-184	-189	-200	-211	-211	-209	
CA981T	Wire Tnl. LO2 Tank	23	41	-64	-86	-59	-105	-81	-88	-96	-101	-103	-103	-103	
CA982T	Wire Tnl. Rail 2337	-338	-355	-361	-362	-358	-327	-350	-347	-311	-288	-288	-288	-268	
CA983T	Wire Tnl. Fairlead 2346	-345	-367	-389	-385	-386	-361	-382	-382	-352	-370	-370	-370	-364	
CA984T	Fairlead Cap 2346	-335	-347	-364	-360	-370	-338	-364	-364	-358	-352	-352	-352	-347	
CA985T	Fairlead Support 2346	-350	-367	-392	-395	-396	-373	-392	-392	-392	-384	-384	-384	-386	
CA986T	Fairlead Support 2345	-	-379	-406	-	-403	-	-403	-406	-406	-406	-406	-406	-406	
CA987T	Recirc. Line 2296	-396	-410	-410	-415	-410	-406	-459	-459	-410	-403	-403	-403	-410	
CA988T	Destruct Mount Flt.	10	12	81	-136	-111	-150	-130	-135	-144	-149	-149	-149	-151	
CA989T	Destructor Pod	14	12	-168	-208	-200	-184	-193	-177	-113	-96	-96	-96	-81	

ORIGINAL PAGE IS
OF POOR QUALITY



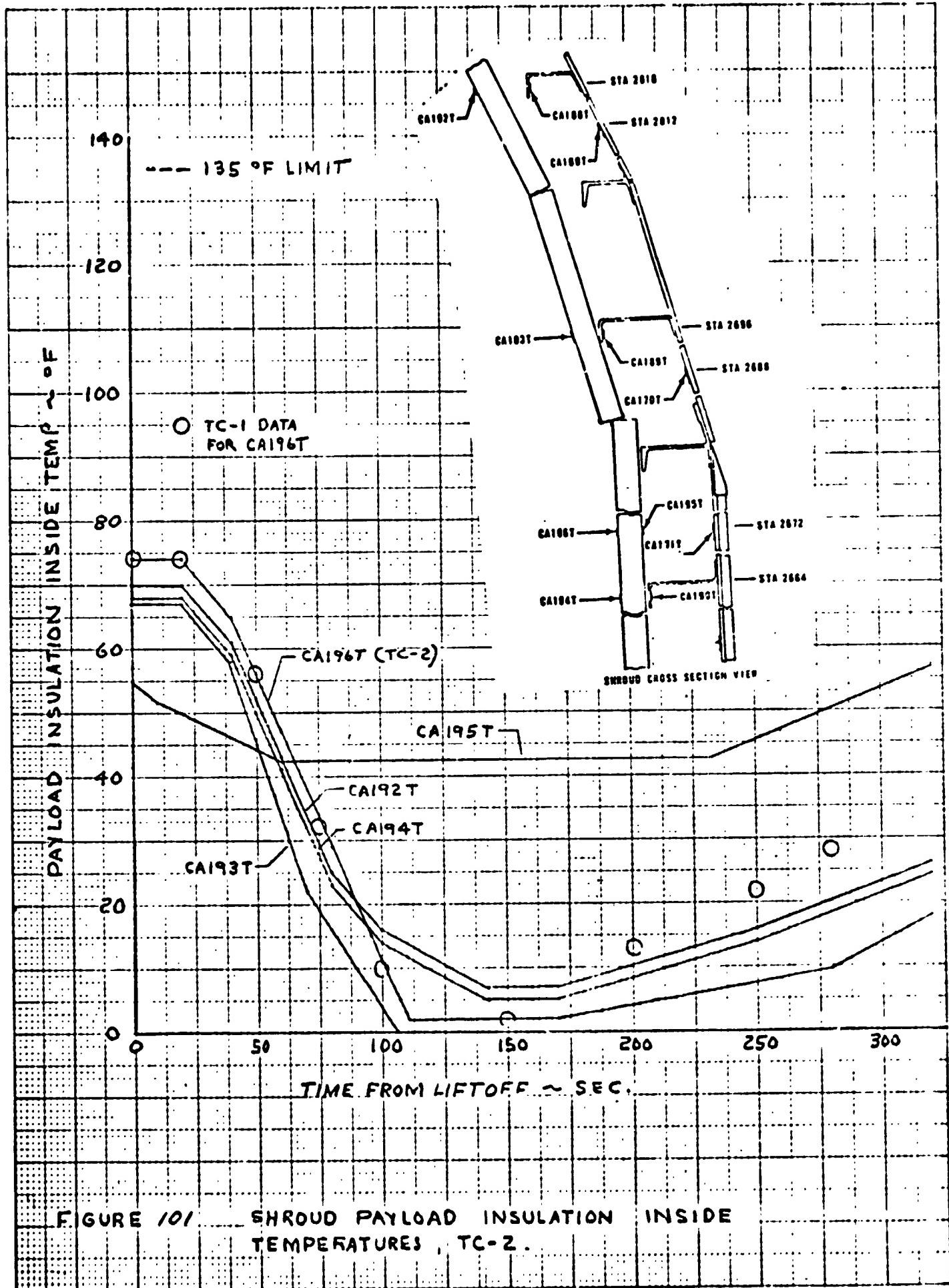


FIGURE 101 SHROUD PAYLOAD INSULATION INSIDE TEMPERATURES , TC-2 .

TABLE 45 PROPULSION SYSTEM TEMPERATURES

Measurement No.	Location	Temperature - °F												S/C Sep.	
		Liftoff				MES 1				740 Sec.				1000 Sec.	
		TC-1	TC-2	CSS	Jett.	TC-1	TC-2	TC-1	TC-2	TC-1	TC-2	TC-1	TC-2	TC-2	TC-2
CP148T	Y-1 Chamber Surf	80	89	69	70	600	-	991	942	963	1070	1105			
CP149T	Y-4 Chamber Surf	75	79	50	75	60	-	992	1112	863	1140	1182			
CP375T	P-3 Chamber Surf	70	79	60	70	69	-	1133	1119	663	1006	635			
CP376T	P-4 Chamber Surf	70	79	60	75	69	-	820	800	742	1384	1077			
CP691T	S2A Chamber Surf	75	75	68	68	68	-	1250	1260	580	1260	570			
CP693T	S4A Chamber Surf	70	79	69	72	69	-	1252	1273	600	1259	620			
CP836T	S4B Chamber Surf	65	75	65	70	75	-	1295	580	1290	1290	650			
CP837T	S2B Chamber Surf	70	70	60	75	70	-	1230	550	1220	1220	630			
CP741T	C1 Eng. Bell	79	67	53	70	67	-	-76	-87	-76	-76	-182			
CP742T	C2 Eng. Bell	70	67	49	61	67	-	-62	-73	-59	-71	-283			
CP743T	C1 Eng. Bell	70	63	49	112	63	-	-66	-62	-94	-52	-171			
CP744T	C2 Eng. Bell	61	63	49	79	63	-	-118	-97	-104	-101	-175			
CP745T	C1 Eng. Bell	61	63	53	53	56	-	-69	-59	-45	-46	-227			
CP746T	C2 Eng. Bell	61	63	53	53	56	-	-62	-62	-69	-38	-161			
CP750T	C-1 LO Duct Surf	-265	-270	-276	-265	-276	-	-276	-296	-274	-263	-279			
CP751T	C-1 LH ₂ Duct Surf	-100	-403	-400	-400	-400	-	-402	-383	-353	-416	-403			
CP752T	C-1 LH ₂ Pmp. Disch.	-342	-344	-235	-325	-252	-	-213	-143	-78	-317	-269			
CP753T	C-1 LH ₂ Pmp. Hsg.	-338	-342	-244	-215	-296	-	-294	-241	-191	-185	-309			
CP754T	C-1 LH ₂ Jckt. Line	-76	-101	-108	-243	-90	-	-276	-273	-210	-168	-283			
CP828T	C-2 Eng. Tbpmp.	-393	-371	-299	-288	-310	-	-318	-304	-263	-231	-347			
CP829T	C-2 Pump Shield	-27	9	-215	-27	9	-	-125	-150	-113	-78	-113			

TABLE 46 H₂O₂ SYSTEM TEMPERATURES

Measurement No.	Location	Temperature - °F											
		Liftoff TC-1	TC-2	CSS Jett. TC-2	MES 1 TC-1	740 Sec. TC-2	1000 Sec. TC-2	1500 Sec. TC-2	MES 2 TC-2	S/C Sep. TC-2			
CP93T	Alt. Cntrl. H ₂ O Btl.	84	85	84	83	85	83	87	87	87	88		
CP659T	3/P H ₂ O Btl.	82	80	80	82	82	83	84	86	87	88		
CP756T	H ₂ O Crossover Line	83	88	90	92	88	92	93	93	93	94		
CP361T	LH ₂ O B/P Sup. Ln.	79	77	63	105	100	136	134	134	116	116		
CP150T	QD ₁ A/C Line	72	76	73	92	90	89	93	95	90	85		
CP151T	QD ₂ A/C Line	74	72	70	84	88	97	63	95	96	102		
CP152T	QD _{2/3} A/C Line	81	72	70	92	92	94	91	90	89	90		
CP153T	QD ₃ A/C Line	80	81	87	96	98	94	96	95	95	96		
CP154T	QD ₄ A/C Line	74	87	87	94	99	93	96	96	96	97		
CP155T	QD ₁ A/C Line	77	70	71	92	95	96	94	95	95	95		
CP156T	QD ₁ LH ₂ B/P Ftg.	74	73	73	82	73	88	84	87	87	95		
CP157T	QD ₂ LH ₂ B/P Ln.	66	69	65	88	90	111	89	87	87	96		
CP158T	QD ₃ LH ₂ B/P Ln.	65	67	59	83	86	85	89	88	88	91		
CP159T	QD ₄ LH ₂ B/P Ln.	68	70	75	89	90	116	114	119	163	109		
CP710T	LH ₂ B/P ² Orf. Holder	77	77	71	81	86	100	100	103	97	96		
CP711T	LO ₂ B/P Orf. Holder	68	66	63	86	65	98	96	99	111	106		
CP712T	LH ₂ B/P Elect.	65	74	53	94	62	102	74	77	89	103		
CP831T	In.Btrwn.B/P Fd.Vlvs.	82	83	96	84	91	95	98	107	119	127		
CP832T	H ₂ O Vent Ln. No. 1	85	82	87	84	87	84	87	88	90	91		
CP833T	LH ₂ O B/P Inlet Ln.	91	84	68	82	73	131	127	101	98	151		
CP834T	B/P Fd. Vlv. 2 Bdy.	73	77	77	84	81	87	90	93	93	92		

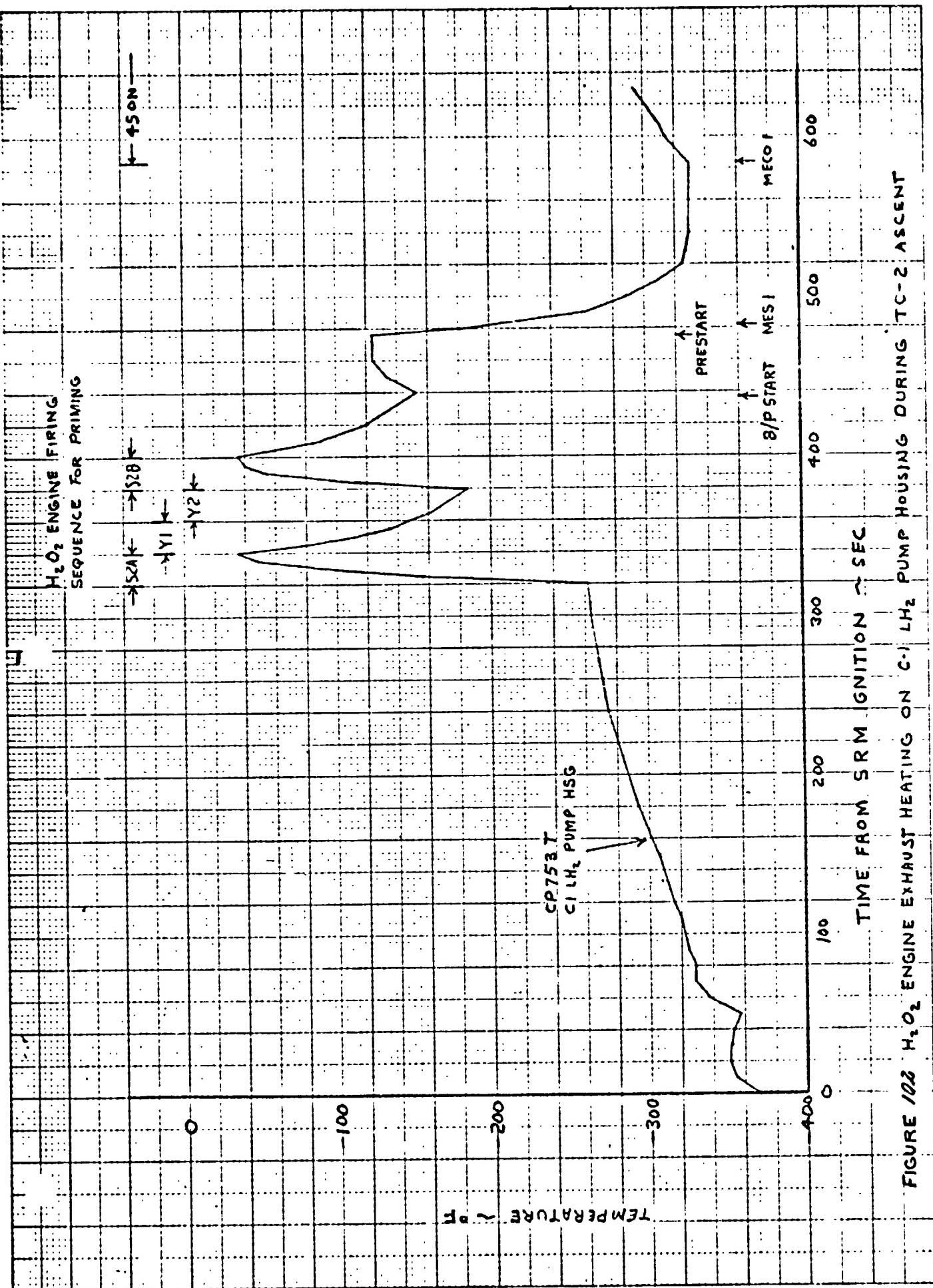


TABLE 47 RADIATION SHIELD TEMPERATURES, TC-2 FLIGHT

Measurement No.	Location	Temperature - °F									
		Liftoff		CSS		MES 1		740 Sec.		1000 Sec.	
		TC-1	TC-2	Jett.	TC-2	TC-1	TC-2	TC-1	TC-2	TC-2	S/C Sep.
CA954T	LH ₂ Tank Sidewall	-294	-304	-396	-330	-326	-295	-277	-270	-262	-246
CA953T	Rad. Shld. Inn 2422 Q4	-251	-270	-370	-275	-297	-207	-235	-211	-182	-135
CA952T	Rad. Shld. Mid 2422 Q4	-133	-118	-321	-71	-142	11	-26	-14	2	41
CA962T	Rad. Shld. Out 2422 Q4	-302	-295	-396	-343	-358	-285	-314	-306	-302	-297
CA961T	Rad. Shld. Inn 2422 Q1	-240	-195	-394	-310	-311	-264	-286	-284	-268	-268
CA960T	Rad. Shld. Mid 2422 Q1	-148	-130	-293	-226	-242	-161	-200	-198	-177	-186
CA957T	Rad. Shld. Out 2422 Q1	-390	-396	-410	-387	-367	-357	-341	-341	-326	-304
CA956T	Rad. Shld. Inn 2279 Q4	-370	-382	-403	-298	-311	-220	-262	-251	-163	-120
CA955T	Rad. Shld. Mid 2279 Q4	-343	-344	-389	-72	-144	15	-26	-26	5	45
CA965T	Rad. Shld. Out 2279 Q3	-395	-396	-410	-382	-389	-359	-355	-347	-344	-341
CA964T	Rad. Shld. Inn 2279 Q3	-379	-382	-406	-345	-352	-264	-306	-293	-275	-256
CA963T	Rad. Shld. Mid 2279 Q3	-361	-352	-403	-91	-279	38	-175	-149	-120	-78
CA966T	LH Sump										
CA967T	Rad. Shld. Out 2247	-350	-358	-336	-270	-277	-131	-238	-235	-115	12
CA968T	Rad. Shld. Mid 2247	-	-367	-367	-	-336	-	-314	-316	-311	-284
CA969T	Rad. Shld. Inn 2247	-379	-389	-392	-382	-361	-361	-358	-379	-396	-376
	Rad. Shld. Out 2235	27	14	-19	-54	-66	-74	-127	-127	-	-211

TABLE 48 BULKHEAD TEMPERATURES, TC-2 FLIGHT

Measurement No.	Location	Temperature - °F									
		Liftoff	CSS Jett.	MES 1	740 Sec.	1000 Sec.	1500 Sec.	MES 2	S/C Sep.		
	TC-1	TC-2	TC-1	TC-2	TC-1	TC-2	TC-1	TC-2	TC-1	TC-2	
CA906T	Forward Bulkhead	-416	-417	-416	-418	-387	-420	-417	-416	-416	-422
CA912T	Bulk Skin Q1	-191	-215	-254	-265	-260	-265	-265	-267	-265	-265
CA913T	Bulk Ins. Mid Q1	-64	-78	-112	-91	-88	-73	-52	-43	-15	3
CA908T	Bulk Ins. Exp. Q1	-418	-416	-417	-422	-412	-415	-420	-418	-417	-422
CA911T	Bulk Skin Q4	-219	-217	-265	-254	-267	-264	-265	-267	-265	-265
CA910T	Bulk Ins. Mid. Q4	-61	-54	-54	-79	-54	-62	-63	-44	-15	-9
CA907T	Bulk Ins. Ext. Q4	-416	-418	-418	-422	-413	-415	-420	-417	-416	-422
CA909T	Bulk Skin +2	-71	-63	-137	-71	-79	-52	-79	-40	-20	-7
	Aft Bulkhead										
CA302T	LO Duct Rad. Shld. Out	63	55	-28	23	-59	-29	-76	-85	-121	-108
CA303T	LH Duct Rad. Shld. Inn	57	44	-28	-4	-51	-29	-75	-119	-164	-174
CA304T	LO Duct Rad. Shld. Out	50	42	16	14	37	182	182	182	182	72
CA305T	Periph. Rad. Shld. Out	1	-51	-98	-85	-63	-79	-72	-28	20	29
CA306T	Periph. Rad. Shld. Inn	-99	-202	-198	-167	-189	-176	-193	-187	-168	-157
CA307T	LO Sump Rad. Shld. Out	39	50	3	1	-6	-58	-63	-70	-96	-106
CA308T	LO Sump Rad. Shld. Inn	-37	-8	-53	-67	-62	-101	-91	-96	-127	-172
CA309T	Aft Bulk Rad. Shld. Out	45	37	-13	10	-17	-24	-42	-47	-70	-85

Centaur Propellant Management

by R. F. Lacovic

Boost Phase Propellant Behavior - The L₂ venting that occurred during the TC-1 boost was again observed during the TC-2 boost. There were indications of liquid venting from T+45 to T+75 seconds, when the L₂ tank vent valve operation reflects the decreasing ambient pressure, and from T+285 to T+300 seconds, when the hydrostatic head is lost at Stage I shutdown. It appears that similar L₂ venting will continue to occur as long as the present TC tanking levels, sequencing, and accelerations are maintained.

It is probable that liquid hydrogen venting also occurred. The L₂ tank liquid/vapor sensor CM241X located at the top of the tank went wet at SRM jettison, as a result of the decrease in vehicle acceleration. Since the L₂ primary vent valve is flowing full at this time, it is likely that some L₂ was vented. CM241X indicated wet for only 2 seconds, as compared with 30 seconds at SRM jettison during the TC-1 flight.

Settled Coast Propellant Behavior - The TC-2 flight provided the first demonstration and verification of the settled coast propellant management techniques for the D-1T Centaur configuration. The new hardware and sequencing associated with these techniques are summarized in Table 49. The resulting propellant management differences, as compared with the D-1A Centaur configuration, are also presented in this table. All of these differences were required as a result of the increased propellant loading and the reduced acceleration levels associated with D-1T Centaur.

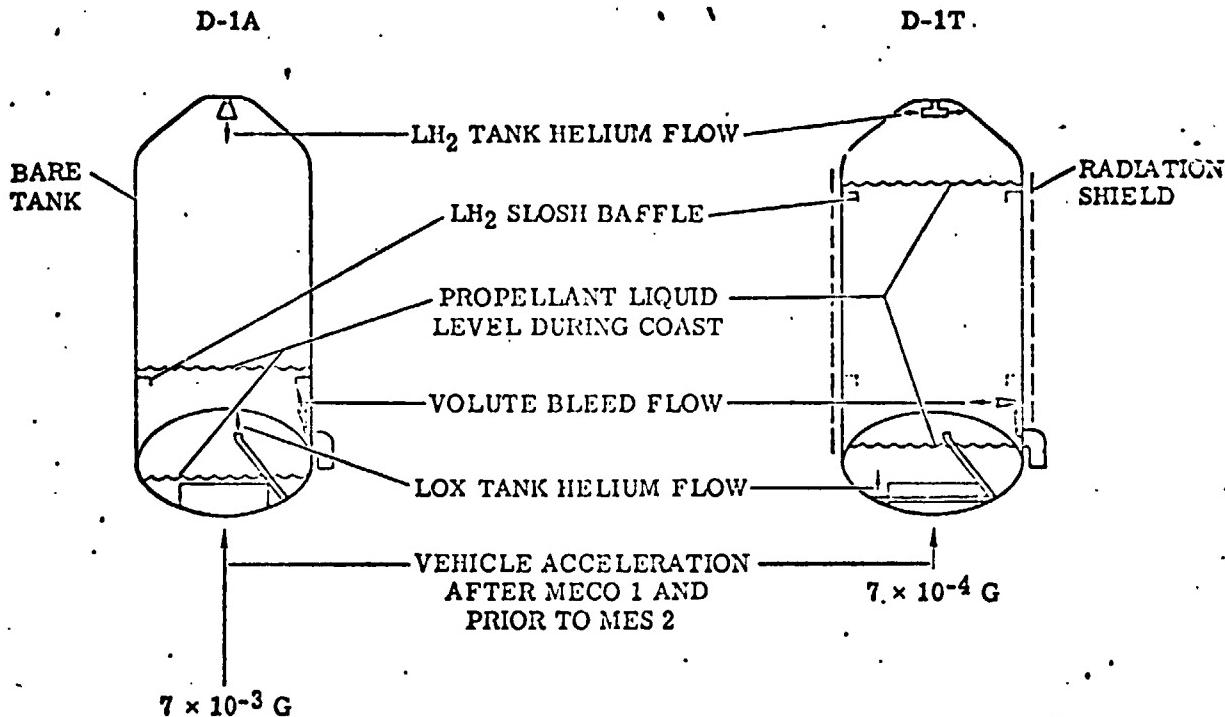
The new, or revised, flight hardware consisted of:

1. An L₂ tank helium energy dissipator to reduce the impact of the pressurant on the liquid surface.
2. A perforated tube in the L₂ tank to inject helium pressure beneath the liquid surface to reduce helium consumption.
3. A revision of the L₂ boost pump volute bleed to redirect the flow away from the liquid surface.
4. A relocation of the L₂ tank slosh baffle to its most forward location to provide propellant damping.
5. The incorporation of L₂ tank sidewall radiation shielding in order to eliminate the need for L₂ tank venting throughout the coast.

The behavior of the propellants throughout the coast was as follows. At MECO 1 the liquid level in the L₂ tank was about 10 inches above the forward slosh baffle. At this location, the baffle provided only 40 percent

TABLE 49

SETTLED COAST PROPELLANT MANAGEMENT DIFFERENCES
BETWEEN D-1A AND D-1T CENTAUR



<u>Item</u>	<u>D-1A Centaur</u>	<u>D-1T Centaur</u>
1. Propellant loading during coast.	25%	90%
2. Propellant settling after MECO 1.	7×10^{-3} g for 76 sec.	7×10^{-4} g for 250 sec..
3. Propellant retention during coast.	4.1×10^{-4} g (Bond Number = 350)	3.4×10^{-4} g (Bond Number = 290)
4. Propellant settling prior to MES 2.	7×10^{-3} g for 40 sec.	7×10^{-4} g for 120 sec.
5. LH ₂ tank venting.	Continuous with balanced thrust.	Computer controlled blowdown. Aft canted nozzles.
6. LH ₂ tank heating.	38,000 BTU/lb. (Bare tank)	3,000 BTU/lb. (Radiation shielded tank).
7. LH ₂ tank pressurization.	a) 7×10^{-3} g b) Axial flow helium energy dissipator. c) Boost pump volute bleed flows upward.	a) 7×10^{-4} g b) Radial flow helium energy dissipator. c) Boost pump volute bleed flows across tank.
8. LO ₂ tank pressurization.	a) 7×10^{-3} g b) Helium is added directly to tank ullage.	a) 7×10^{-4} g b) Helium is injected beneath the liquid surface.
9. LH ₂ tank slosh baffle.	Located at aft end of tank. (Station 2322)	Located at forward end of tank. (Station 2399)

ORIGINAL PAGE IS
OF POOR QUALITY

of its optimum effectiveness in damping LH₂ slosh (for a liquid level 3 inches above the baffle, the effectiveness is 100 percent). The LH₂ behavior at MECO 1 is indicated in Figure 103. At 12 seconds after MECO 1 a large splash of LH₂ had traveled to the top of the tank as indicated by the activations of the four uppermost liquid/vapor sensors. The splash was also indicated by the three forward bulkhead skin temperatures (CA906T, CA907T, and CA908T at Station 2472) which decreased to LH₂ temperature at six seconds after MECO 1. At MECO 1 + 30 seconds the LH₂ began to fall away from the top of the tank as indicated by the drying of CM241X. At MECO 1 + 34 seconds the LH₂ began to fall away from the top of the tank as indicated by the drying of CM241X. At MECO 1 + 34 seconds CM242X (located 12 inches below CM241X) went wet until MECO 1 + 46 seconds, thus indicating the passage of the descending LH₂. An extrapolation of this LH₂ descent rate indicates that it would take about 20 additional seconds for the descending LH₂ to reach the liquid surface at Station 2418.

After this initial splash of LH₂, there was no further indication of LH₂ motion through MES 2. However, since the nearest liquid/vapor sensors to the liquid surface were 8 inches away, it is possible for small LH₂ surface motions to occur without being detected.

The propellant management techniques selected for D-1T Centaur settled coast periods have been verified. The 250 seconds of 4S engine firing after MECO was more than sufficient to control the propellant motion at MECO, even with the non-optimum slosh baffle location. The transition to the 2S engine firing propellant retention mode at MECO 1 + 250 seconds occurred with no indications of propellant motion. There were also no indications of propellant disturbances during the 120 second 4S engine firing period prior to MES 2, which included the LH₂ tank vent and pressurization period and the boost pump dead-head period.

Settled Coast Propellant Tank Pressures - The L₂O tank and LH₂ tank pressure histories throughout the settled coast period are shown in Figure 104. Both the L₂O and LH₂ tank pressures increased sharply for 20 seconds following MECO 1 (1.3 psid L₂O tank, 0.5 psid LH₂ tank). This sharp pressure increase is attributed partly to the release of energy at MECO 1 as a result of the head loss, and partly to the addition of energy resulting from the recirculation and volute bleed flows during the post-MECO boost pump spin down. These energies probably contributed to the post-MECO propellant splashing. Once the tank pressures stabilized, the pressures then increased slowly as a result of the incident space heating. The L₂O tank pressure increased 0.5 psid during the coast from MECO 1 + 20 to MECO 1 + 450 seconds, and zero psid from MECO 1 + 450 seconds to MES 2. This pressure rise was as expected, since the propellant loading was large enough to absorb all of the space heating into the liquid. The LH₂ tank pressure increased only 1.2 psid from MECO 1 + 20 seconds to MES 2. The new LH₂ tank sidewall radiation shielding reduced the pressure rise rate by more than an order of magnitude in comparison with the D-1A Centaur LH₂ tank pressure rise rate. As a result of the small pressure increase, no LH₂ tank venting was required at any time from MECO 1 to the start of tank pressurization.

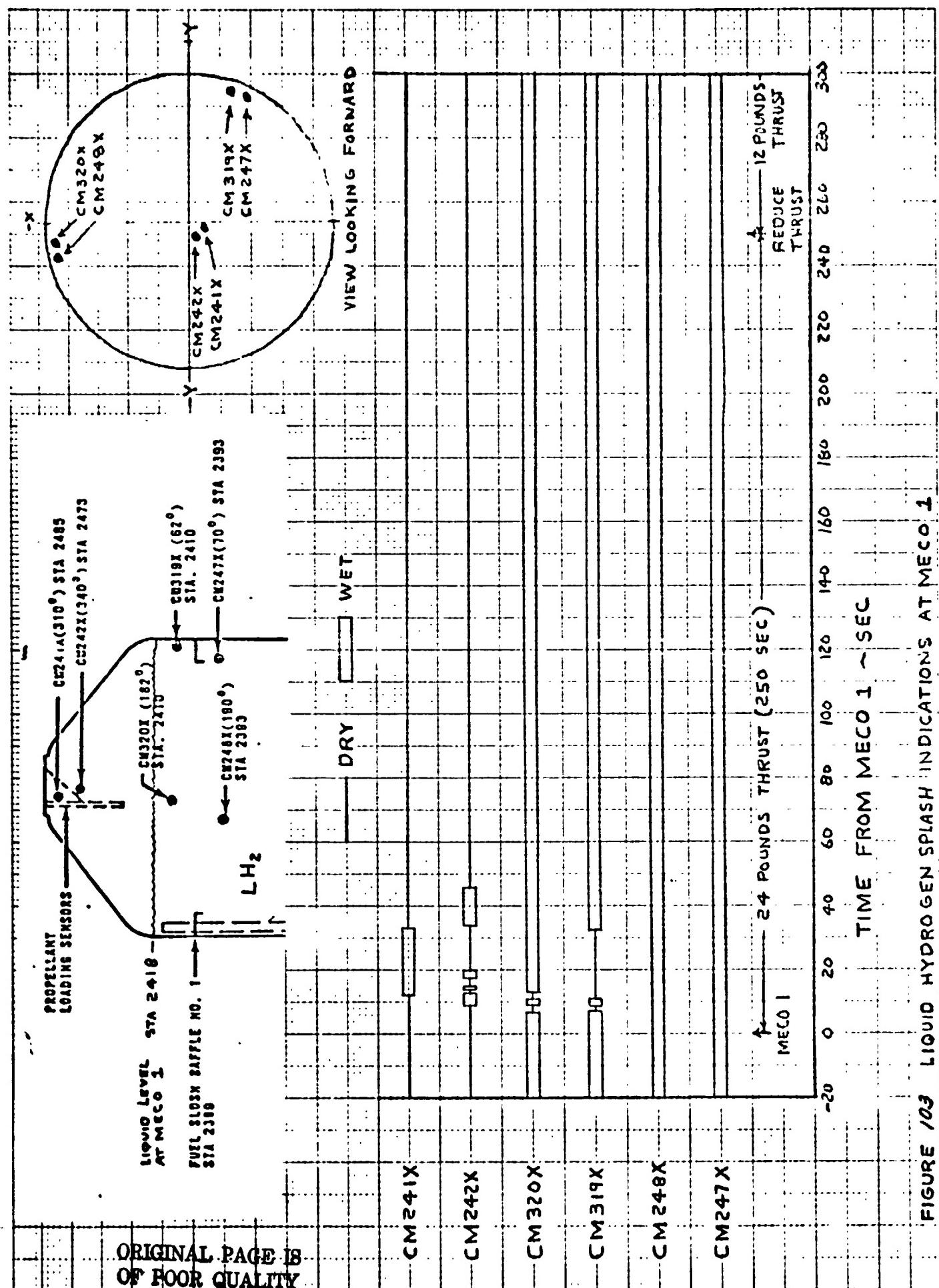
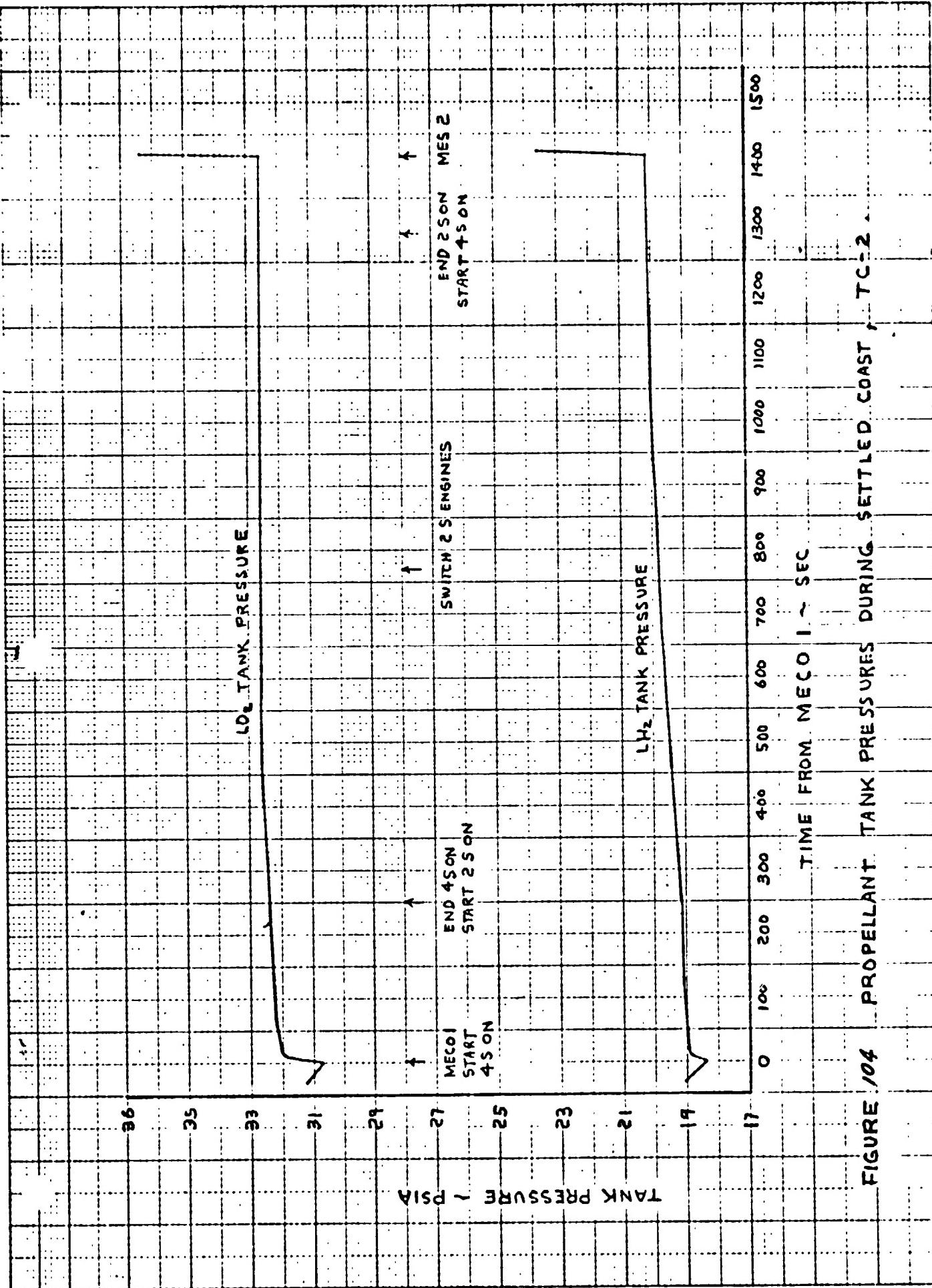


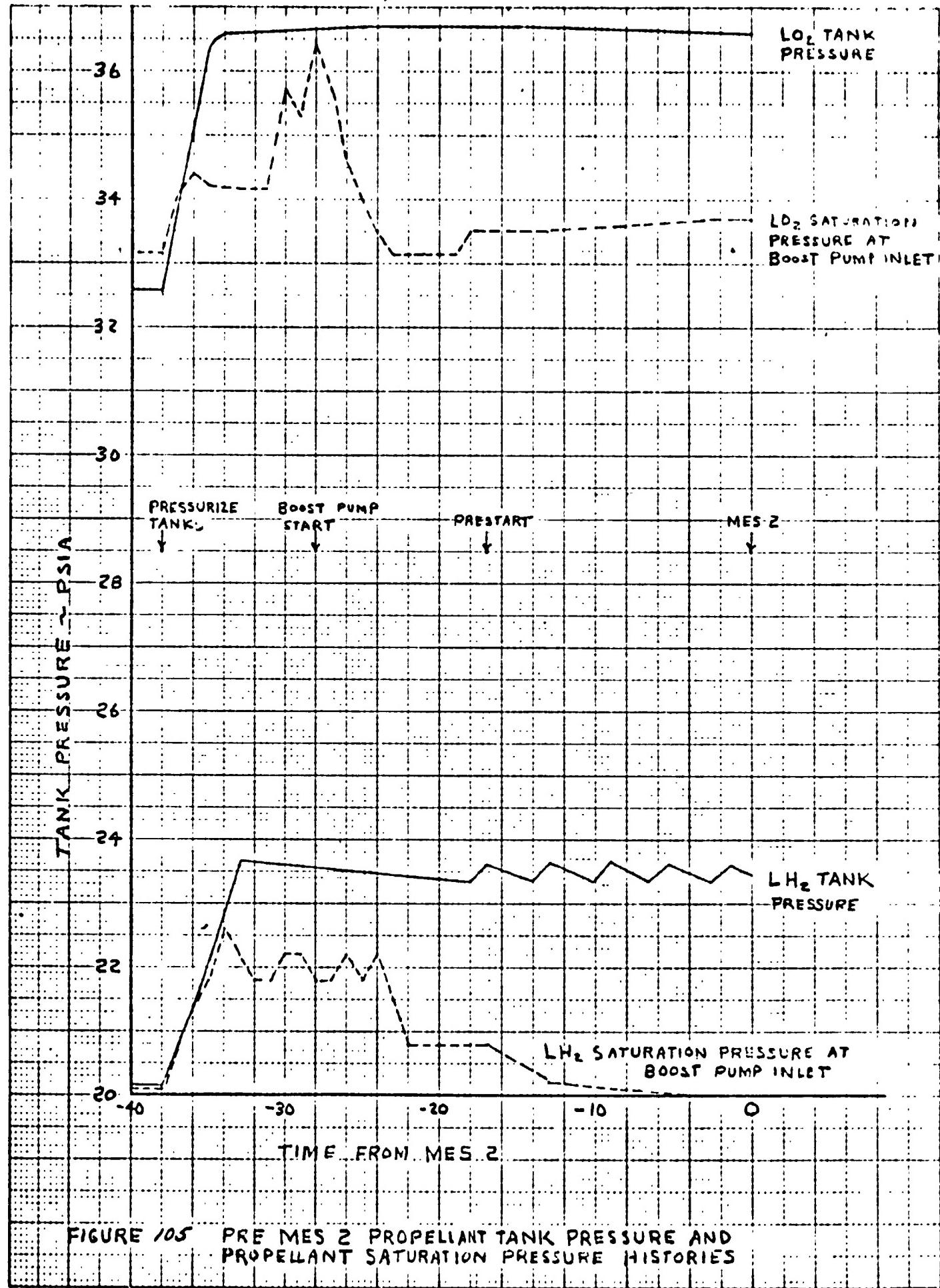
FIGURE 103 LIQUID HYDROGEN SPLASH INDICATIONS AT MECO 1



Tank Pressurization at MES 2 - Many of the propellant management hardware changes for D-1T Centaur were incorporated in order to reduce the helium consumption during pre-MES 2 pressurization. The proximity of the liquid surface and the low vehicle acceleration at this time can result in liquid splashing during pressurization that greatly increases the helium consumed. The new LH₂ tank helium energy dissipator was designed to reduce splashing by adding the helium to the tank at low velocities in a radial direction. The new perforated tube (bubbler) used for pressurizing the L₂O tank, by injecting helium beneath the liquid surface, greatly reduces helium consumption by vaporizing oxygen.

The L₂O tank and LH₂ tank pressure histories during pre-MES 2 pressurization are shown in Figure 105. (The propellant saturation pressures are also shown in Figure 105 to give an indication of the boost pump NPSH.) The quantity of helium required to achieve the 4 psid increase in the L₂O tank was 0.14 pounds. This quantity compares to a predicted quantity of 0.68 pounds if the existing D-1A Centaur mode of pressurization through the L₂O tank standpipe had been used. The L₂O tank bubbler performed as expected, resulting in a rapid and stable L₂O tank pressurization requiring only small quantities of pressurant. The quantity of helium required to achieve the 3.5 psid increase in the LH₂ tank was 0.76 pounds. This compares to a nominal preflight predicted quantity of 0.81 pounds assuming that no LH₂ splashing occurred during the pressurization. The new helium energy dissipator apparently worked as expected.

Post-MECO 2 Liquid Hydrogen Behavior - At MECO 2 the liquid level in the LH₂ tank was about one inch below the aft slosh baffle. The LH₂ motion after MECO 2 is indicated in Figure 106 which shows the liquid/vapor sensor activation times. For 72 seconds after MECO 2 the Centaur was in a zero g coast mode. During this time part of the LH₂ moved to the top of the tank. As a result of MECO disturbances, the release of stored energy from the head loss, and the volute bleed and recirculation flows during the post-MECO boost pump spin down, sensor CM241X at the top of the tank went wet at MECO 2 + 63 seconds. At MECO 2 + 72 seconds the helium retrothrust was activated which provided a thrust in the aft direction ranging from 300 pounds to 10 pounds over a 10 second period. This thrust moved the bulk of the LH₂ forward thus wetting the forward sensors and leaving the aft sensors dry, except for a fillet of liquid around the aft slosh baffle. This liquid/vapor configuration remained throughout the following zero g coast.



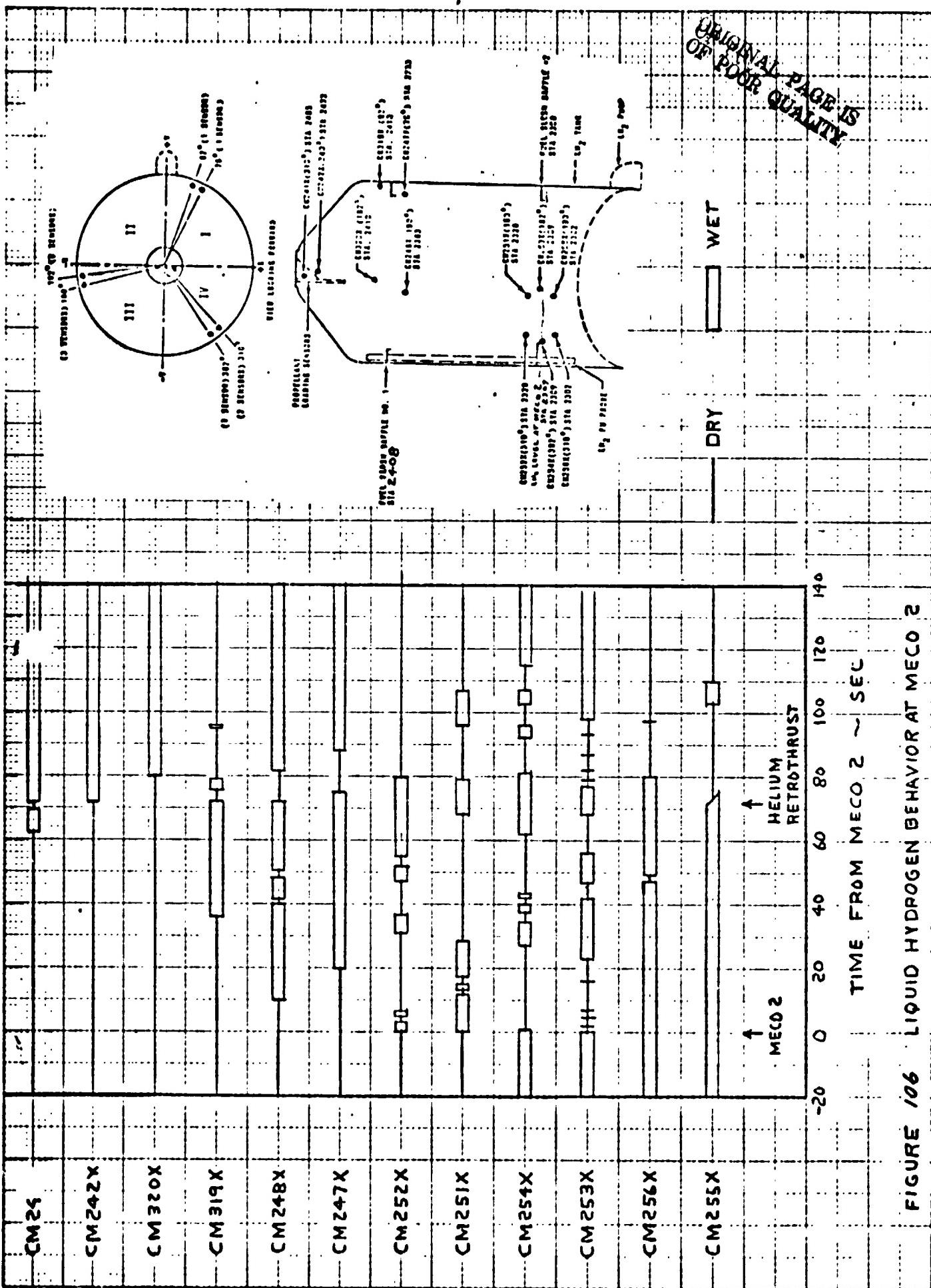


FIGURE 106 LIQUID HYDROGEN BEHAVIOR AT MECO 2

Electrical/Electronic Systems

Electrical Power Systems

by J. B. Nechvatal

The electrical system consists of a power changeover switch (integral part of the Sequence Control Unit), three main batteries (interconnected by a diode assembly), two independent range safety command (vehicle destruct) batteries, and a single 400 Hz inverter (the inverter is an integral part of the Servo Inverter Unit).

The performance of the Centaur electrical system was satisfactory and no unexpected system current demands were noted during the programmed flight period. Transfer of the electrical load from external power to the internal batteries was accomplished at minus 111.2 seconds by the changeover switch and normal transfer characteristics were observed.

The three Centaur busses were supplied by separate 150 ampere-hour batteries, interconnected by a diode assembly. The diode assembly permitted Bus No. 2 battery to supply Bus No. 1 and Bus No. 3 power during surge loads and at possible deletion of capacity of Bus No. 1 and/or Bus No. 3 battery during a long/extended flight sequence. (Bus No. 2 battery has the lowest programmed power drain.)

At liftoff, the three (3) main battery bus voltages were 28.5, 29.0, and 28.7 volts for Bus No. 1, No. 2 and No. 3 batteries respectively. Battery data are shown in Table 50.

Bus No. 1 battery voltage was relatively constant throughout the flight, reflecting only the Bus No. 2 battery variations. Bus No. 2 battery voltage reflected the effects of the Bus No. 3 flight current demands, but remained fairly constant during the programmed flight. Bus No. 3 battery voltage responded normally to level changes resulting from the application and removal of electro-mechanical loads per the programmed flight sequence. A low of 27.5 volts was observed during Main Engine Start Sequence No. 1 (a period of maximum load).

The total Centaur current (as measured by CETIC) was 45.0 amperes at liftoff. Peak currents were recorded during the Main Engine Start Sequences, with a maximum peak at Main Engine Start No. 1. The periods of maximum and minimum current levels relative to Mark Events are shown in Table 51. The flight current profile was consistent with values recorded during preflight tests and no anomalies were observed.

Battery current values with respect to flight programmed events are shown in Table 51.

TABLE 50
CENTAUR BATTERY DATA

	OPEN CIRCUITS VOLTS	T-0 LIFT-OFF VOLTS	LOAD TEST AMPS VS VOLTS
Main Battery - BUS No. 1	35.12	28.5	65A at 27.01V
Main Battery - BUS No. 2	35.11	29.0	65A at 26.8V
Main Battery - BUS No. 3	34.81	28.7	65A at 27.36V
RSC Battery - No. 1	33.71	32.8	10A at 28.96V
RSC Battery - No. 2	33.91	32.9	10A at 29.1V

TABLE 51 TC-2 CENTAUR ELECTRICAL SYSTEM PARAMETERS

MEAS. NO.	DESCRIPTION	UNITS	T- C	T/C SEP.	MES NO. 1	MECO NO. 1	MES NO. 2	MECO NO. 2	MES NO. 3	MECO NO. 3	MES NO. 4	MECO NO. 4	LOS 18250 SEC.
CE1C	Main Battery Current	AMPS	45.0	56.2	64.8	66.5	64.0	45.2	52.0	63.8	45.0	64.0	44.5
CE28V	BUS No. 1 Voltage	VDC	28.5	28.4	28.1	28.3	28.2	28.5	28.5	28.7	28.9	28.9	29.1
CF142C	BUS No. 1 Current	AMPS	10.0	10.0	10.0	10.0	10.0	10.0	10.0	9.9	9.9	9.6	9.6
CE143C	BUS No. 2 Current	AMPS	8.2	8.0	8.1	7.9	7.9	7.9	8.0	8.0	8.0	8.0	7.8
CE144C	BUS No. 3 Current	AMPS	14.2	19.5	24.7	16.5	23.7	16.0	16.3	23.3	15.6	24.0	15.7
CE97C	BUS No. 3 Partial Current	AMPS	2.7	3.6	2.7	1.7	2.7	1.7	2.0	3.2	2.2	3.2	2.2
CE600V	Battery No. 1 Voltage	VDC	28.5	28.4	28.1	28.3	28.2	28.5	28.5	28.7	28.9	28.9	29.1
CE609V	Battery No. 2 Voltage	VDC	29.0	28.7	28.4	28.9	28.5	28.9	28.7	28.8	29.0	29.1	29.1
CE610V	Battery No. 3 Voltage	VDC	28.7	28.7	27.5	28.4	27.6	28.5	27.9	28.8	28.9	28.5	29.0
CE21V	RC. Battery No. 1 Voltage	VT~	32.8	32.8	32.8	32.8	33.4	33.4	33.4	33.5	33.5	33.5	33.5
CE72V	LS.C. Battery No. 2 Voltage	VDC	32.9	32.9	32.9	32.8	33.3	33.3	33.3	33.2	33.2	33.2	33.2
CE844V	Inverter Voltage	VAC	25.9	25.9	25.9	25.9	25.9	25.9	25.9	25.9	25.9	25.9	25.9

ORIGINAL PAGE IS
NOT IN OUR QUALITY

The individual bus currents exhibited normal profiles. Bus No. 1 remained steady between 9.6 to 10.0 amperes, reflecting only the expected variations due to the DCU duty cycle and real time interrupts.

Bus No. 2 current was relatively constant, with the exception of the period of PJ control. Variations of 6.9 to 8.2 were noted during this time interval, which was nominal and as expected. Bus No. 3 current exhibited changes throughout the flight in response to vehicle demands. The maximum current observed was 36.5 amperes at Main Engine first start sequence.

Two individual electronic package currents (IMG and SCU) were monitored via telemetry. The IMG (Inertial Measurement Group) current exhibited normal low level oscillations following platform stabilization (prelaunch function). The load current varied between 6.1 and 6.5 amperes. The SCU (Sequence Control Unit) current also exhibited normal output with a steady state load of 0.18 amperes, and a strobe current of 0.88 amperes. The IMG and SCU are supplied by the Bus No. 1 battery and are part of the total Bus No. 1 load.

Performance of the two range safety command batteries was satisfactory. The voltages at liftoff were 32.8 volts for range safety command no. 1 and 32.9 volts for range safety command no. 2. Voltages remained steady throughout the flight until Main Engine Cutoff No. 1, when the range safety command receivers are turned off and the destruct system is deactivated.

Vehicle AC power was supplied by the Service Inverter Unit. The voltage output of the inverter remained steady at 25.9 volts AC throughout the programmed flight.

Digital Computer Unit

by R. S. Palmer

All DCU inputs and outputs were analyzed. The DCU performed satisfactorily as evidence by proper functioning of flight events and operation of associated systems. The data indicating DCU performance are presented with the flight performance analyses of the associated systems.

Inertial Measurement Group

by D. E. Pope

This flight was the first to use an Inertial Reference Unit containing Kearnott gyros. System performance was satisfactory. Preflight calibration was accomplished, and the measured parameters were subsequently loaded into the vehicle computer. The inertial platform was then final aligned and the flight mode of operation was entered at approximately T-6 seconds.

The maintenance of the inertial reference block to within its specified maximum dynamic gimbal error of ± 60 arc seconds was accomplished. Maximum displacement of gimbals one, two, and three was ± 5 arc seconds as evidenced by the demodulator error signal.

IMG current was nominal with variations from 5.9 to 7.5 amperes. The IRU internal skin temperature was 82°F at liftoff and varied from a minimum of 81°F during first coast to a maximum of 100°F prior to MES 4. The SEU internal skin temperature was 72°F at liftoff and varied to a maximum of 114°F prior to MES 4.

Guidance coast phase accelerometer bias is shifted from the one "g" level measured during calibration by torque generator reaction torque (TGRT). TGRT is a second order torquing non-linearity introduced by pulse rebalancing of the pendulum and is influenced by the matching of the permanent magnets. Long coast periods may, therefore, introduce errors by the accumulation of false acceleration information. Coast bias actuals to predicted are shown:

Table 52

	Actual 1st Coast	Actual 3rd Coast	Predicted
U Accelerometer Bias Error (μg)	+53	+42	+14
V Accelerometer Bias Error (μg)	+67	+72	+32
W Accelerometer Bias Error (μg)	-20	-30	-32

The guidance error model includes a 3 sigma value of $150 \mu\text{gs}$ for accelerometer bias error. Actuals were approximately one-half the 3 sigma error model value; however, the predicted coast phase bias is obtained from measurements

at the component level. These predicted values are shown in Table 52 and with the exception of the W accelerometer, are one-half to one-third of the actual values. The prediction technique will be refined as more flight data becomes available and before predicted values are used in the error model.

Flight Control System

by R. A. Edkin and T. W. Porada

Flight Control Commands

The Digital Computer Unit (DCU) and the Sequence Control Unit (SCU) performed satisfactorily in issuing the flight control system commands to other vehicle systems. The SCU receives its input from the DCU and converts this input into switch commands usable by other vehicle systems.

Table 53 lists the SCU switching sequence and flight events. The column headed "Sequence" shows the time of the event from the start of each phase of flight. The column headed "Planned Time" shows the time after liftoff for each event based upon preflight actual launch time trajectory with launch day winds. The "Actual Time" column shows the time after liftoff that each command was issued by the SCU during flight. Other functions programmed by the DCU software are shown in the table to help in clarifying the flight sequence.

Control Dynamics

The dynamic behavior of the vehicle indicated that a normal environment was experienced. Vehicle dynamic response was evaluated in terms of amplitude, frequency, and duration of rate gyro, attitude error, digitally derived rate (DDR) of attitude error, engine gimbal angles and coast phase control engine firing data. These data indicated that the control system did not impose any severe loading or vibration environment on the vehicle. The vehicle responded normally to all commands and transient disturbances and showed a bounded limit cycle condition throughout flight. Centaur instrumentation rate gyro data are shown tabulated in Table 54 at major flight events.

At the Titan/Centaur separation ($T+472.7$ seconds) event, residual rates before and after separation are shown below:

	Before Separation	After Separation	Requirement
Residual rate, deg./sec.	0.27	0.21	2.0

No evidence of bumping or interference was evident from rate gyro or accelerometer data. The Centaur engines were observed to be at their null positions at the time of separation. A summary of the maximum rates and engine gimbal angles is shown below for the ignition and shutdown transients. Included also are those engine gimbal angles required for the maximum steering commands observed.

TABLE 53.1
TC-2 FLIGHT SEQUENCE OF EVENTS

SCU	SWITCH	EVENT	SEQUENCE	PLANNED TIME-SEC	ACTUAL TIME-SEC
84	Reset	<u>GO INERTIAL</u> (1)	T-6	T-6	T-6
85	Reset				
86	Reset				
-----	-----	<u>SRM IGNITION</u> (07:11:01.057Z)	T=0	T+0	0.0
-----	-----	<u>LIFTOFF</u> (2)	T+0.2	0.2	0.4
57,58	Set	BEGIN ROLL PROGRAM	T+6.5	6.5	6.6
57,58	Reset	END ROLL PROGRAM	T+7.0	7.0	6.7
-----	-----	BEGIN DCU PITCH, YAW PROGRAM	T+10	10.0	10.6
28	Reset	UNLOCK LH ₂ VENT VALVE 1	T+90	90.0	90.0
34	Set	SEP FWD BRG REACTOR	T+100	100.0	100.0
34	Reset	RESET FWD BRG REACTOR	T+102	102.0	102.0
-----	-----	<u>STG 0 SHUTDOWN</u> (3)	STG 0	111.0	111.7
39	Set	RELEASE FWD SEAL	STG 0 + 100	211.0	211.7
39	Reset	RESET FWD SEAL	STG 0 + 103	214.0	214.7
-----	-----	<u>STG 1 SHUTDOWN</u> (4)	STG 1	262.0	258.6
61	Set	UNLATCH SHROUD CMD 1	STG 1 + 60	323.0	319.1
62	Set	UNLATCH SHROUD CMD 2	STG 1 + 60.5	323.5	319.6
8	Set	S2A ON	STG 1 + 61	324.0	320.1

- (1) Go Inertial occurs 25 seconds after the control monitor group sends a command to start the DCU count
- (2) Liftoff - noted by DCU when computed acceleration is greater than 1.4g
- (3) Stage 0 shutdown - noted by DCU when computed acceleration is less than 1.5g
- (4) Stage 1 shutdown - "

TABLE 53.2
TC-2 FLIGHT SEQUENCE OF EVENTS

SCU	SWITCH	EVENT	SEQUENCE	PLANNED TIME-SEC	ACTUAL TIME-SEC
61	Reset	RESET SHROUD CMD 1	STG 1 + 61.5	323.5	320.6
62	Reset	RESET SHROUD CMD 2			
8	Reset	S2A OFF	STG 1 + 81	343.0	340.1
1	Set	Y1 ON			
1	Reset	Y1 OFF	STG 1 + 101	363.0	360.1
2	Set	Y2 ON			
2	Reset	Y2 OFF	STG 1 + 121	383.0	380.1
12	Set	S2B ON			
12	Reset	S2B OFF	STG 1 + 141	403.0	400.1
24	Set	LOCK LO ₂ VENT VALVE	STG 2 - 30.5	439.6	435.1
28	Set	LOCK LH ₂ VENT VALVE 1	"	"	"
31	Set	LOCK LH ₂ VENT VALVE 2	"	"	"
27	Set	OPEN CONTROL VALVE	STG 2 - 28.56	441.54	437.0
29	Set	PRESS LO ₂ TANK	"	"	"
32	Set	PRESS LH ₂ TANK	"	"	"
23	Set	PRIMARY-BOOST PUMPS ON	STG 2 - 28.4	441.7	437.2
18	Set	B/U-BOOST PUMPS ON			
<hr/>		<u>STG 2 SHUTDOWN (5)</u>			
65	Set	STG 2 S/D B/U	STG 2	470.1	468.8
17	Set	C1 CIRC PUMP ON	STG 2 + 0.1	470.2	468.9
21	Set	C2 CIRC PUMP ON			
63	Set	<u>T/C SEPARATION (6)</u>	SEP	475.6	472.7
64	Set				
19	Set	OPEN PRESTART VALVES	SEP + 2.5	478.1	475.2
27	Reset	CLOSE CONTROL VALVE	SEP + 10.22	485.82	482.9

(5) Stage II shutdown - noted by DCU when observed acceleration is less than 1g

(6) T/C separation - commanded by DCU when computed acceleration is less than 0.01g

TABLE 53.3
TC-2 FLIGHT SEQUENCE OF EVENTS

SCU SWITCH		EVENT	SEQUENCE	PLANNED TIME-SEC	ACTUAL TIME-SEC
<u>MES 1 (7)</u>					
22	Set	IGNITERS ON	MES 1	486.1	483.2
20	Set	OPEN START VALVES			
22	Reset	IGNITERS OFF	MES 1 + 4	490.1	487.2
17	Reset	C1 CIRC PUMP OFF	MES 1 + 12	498.1	495.2
21	Reset	C2 CIRC PUMP OFF			
1-4	Set	YAW ENGINES ON	MECO 1-20	564.8	564.0
5,6	Set	PITCH ENGINES ON	MECO 1-20	564.8	564.0
15,16	Set				
1-4	Reset	YAW ENGINES OFF	MECO 1-10	574.8	574.0
5,6	Reset	PITCH ENGINES OFF	MECO 1-10	574.8	574.0
15,16	Reset				
<u>MECO 1 (8)</u>					
23	Reset	PRIMARY-BOOST PUMPS OFF	MECO 1	584.8	584.0
18	Reset	B/U-BOOST PUMPS OFF	"	"	"
20	Reset	CLOSE START VLAVES	"	"	"
19	Reset	CLOSE PRESTART VALVES	"	"	"
8	Set	SETTLING ENGINES ON	MECO 1 + 0.1	584.9	584.1
10	Set	"	"	"	"
12	Set	"	"	"	"
14	Set	"	"	"	"
68,72	Reset	RESET PU SWITCHES	MECO 1 + 1	585.8	585.0
76,80					
12,14	Reset	REDUCE TO 2S ENGINES ON S2B, S4B OFF	MECO 1 + 250	834.8	834.0
<u>CHANGE S ENGINE PAIRS</u>					
8,10	Reset	S2A, S4A OFF	HALFWAY THROUGH 2S		
12,14	Set	S2B, S4B ON	ON MODE		1307.1

(7) MES 1 - commanded by the DCU 10.5 seconds after T/C separation

(8) MECO 1 - commanded by the DCU based on guidance computed time

TABLE 53.4
TC-2 FLIGHT SEQUENCE OF EVENTS

SCU SWITCH		EVENT	SEQUENCE	PLANNED TIME-SEC	ACTUAL TIME-SEC
-----		INCREASE TO 4S ENGINES ON			
8,10	Set	S2A, S4A ON	MES 2-120	1779.7	1779.7
17	Set	C1 CIRC PUMP ON	MES 2-60	1839.7	1839.5
21	Set	C2 CIRC PUMP ON			
27	Set	OPEN CONTROL VALVE	MES 2-38.06	1861.64	1861.4
29	Set	PRESS LO TANK	"	"	"
32	Set	PRESS LH ₂ TANK	"	"	"
23	Set	PRIMARY-BOOST PUMPS ON	MES 2-28	1871.7	1871.5
18	Set	B/U - BOOST PUMPS ON			
19	Set	OPEN PRESTART VALVES	MES 2-17	1882.7	1882.5
27	Reset	CLOSE CONTROL VALVE	MES 2-0.28	1899.42	1899.2
-----		<u>MES 2 (9)</u>			
20	Set	OPEN START VALVES	MES 2	1899.7	1899.5
22	Set	IGNITERS ON			
1-4	Reset	YAW ENGINES OFF	MES 2 + 0.2	1899.9	1899.7
5,6	Reset	PITCH ENGINES OFF	MES 2 + 0.2	1899.9	1899.7
15,16	Reset				
22	Reset	IGNITERS OFF	MES 2 + 4	1903.7	1903.5
8	Reset	END 4S SETTLED THRUST	MES 2 + 5	1904.7	1904.5
10	Reset	"	"	"	"
12	Reset	"	"	"	"
14	Reset	"	"	"	"
17	Reset	C1 CIRC PUMP OFF	MES 2 + 12	1911.7	1911.5
21	Reset	C2 CIRC PUMP OFF			
1-4	Set	YAW ENGINES ON	MECO 2-20	2156.5	2152.9
5,6	Set	PITCH ENGINES ON			
15,16	Set				
1-4	Reset	YAW ENGINES OFF	MECO 2-10	2166.5	2162.9
5,6	Reset	PITCH ENGINES OFF			
15,16	Reset				

(9) MES 2 - commanded by the DCU based upon guidance computed time

TABLE 53.5
TC-2 FLIGHT SEQUENCE OF EVENTS

SCU SWITCH	EVENT	SEQUENCE	PLANNED TIME-SEC	ACTUAL TIME-SEC
-----	<u>MECO 2 (10)</u>			
23 Reset	PRIMARY-BOOST PUMPS OFF	MECO 2	2176.5	2172.9
19 Reset	CLOSE PRESTART VALVES	"	"	"
20 Reset	CLOSE START VALVES	"	"	"
18 Reset	B/U-BOOST PUMPS OFF	"	"	"
68,72 Reset 76,80 Reset	RESET PU SWITCHES	MECO 2 + 1	2177.5	2173.9
95 Reset	ENABLE TE364 IGNITION	MECO 2 + 60	2236.5	2232.9
73,74 Set	FIRE SPIN ROCKETS	MECO 2 + 70	2246.5	2242.9
73,74 Reset	FIRE SPIN ROCKETS (RESET)	MECO 2 + 70.8	2247.3	2243.7
35 Set	FIRE WIRE CUTTERS	MECO 2 + 71	2247.5	2243.9
69,70 Set	SEP TE364/FIRE RETROS	MECO 2 + 72	2248.5	2244.9
69,70 Reset	SEP TE364/FIRE RETROS (RESET)	MECO 2 + 77	2253.5	2249.9
35 Reset	FIRE WIRE CUTTERS (RESET)	MECO 2 + 77.1	2253.6	2250.0
-----	TE364 IGNITION		2290.5	2285.8
-----	BURNOUT		2234.3	2330.7
-----	HELIOS SPACECRAFT SEPARATION		2406.5	2401.5

(10) MECO 2 - commanded by the DCU based upon guidance computed time

Table 54 Centaur Rotational Rates and Engine Gimbal Angles During Powered Flight

<u>Event</u>	<u>Time</u>	<u>Axis</u>	<u>Rate Deg/Sec.</u>	<u>Axis</u>	<u>Gimbal Angle/ Control Capability</u>
MES 1	483.2	Pitch	-1.5	Pitch	+1.3/+3.0
		Yaw	-0.1	Yaw/Roll	-.5/+3.0
		Roll	-1.4		
1st Burn Steering	492.2	Pitch		Pitch	+1.4/+3.0
		Yaw		Yaw/Roll	-2.0/+3.0
		Roll			
MECO 1	584.0	Pitch	-.2		
		Yaw	-.1		
		Roll	-.5		
MES 2	1899.5	Pitch	-4.3	Pitch	+2.4/+3.0
		Yaw	-.4	Yaw/Roll	-.4/+3.0
		Roll	-3.6		
2nd Burn Steering	No Data	Pitch	No	Pitch	No Data
		Yaw	Data	Yaw/Roll	
		Roll			
MECO 2	2172.9	Pitch	0		
		Yaw	0		
		Roll	-.8		
Fire Spin Rockets	2242.9	Pitch	-.06		
		Yaw	0		
		Roll	+.08		

A limit cycle of approximately 0.7 degrees peak-to-peak at 3.5 Hz was observed during the first burn. This is normal operation. During the second burn, data were noisy and sporadic; a similar limit cycle, however, was discernible.

The Centaur first coast showed the following duty cycles. This is defined as the ratio of disturbance torque to control torque quoted in percentage.

Table 55 Attitude Control System Average Duty Cycle

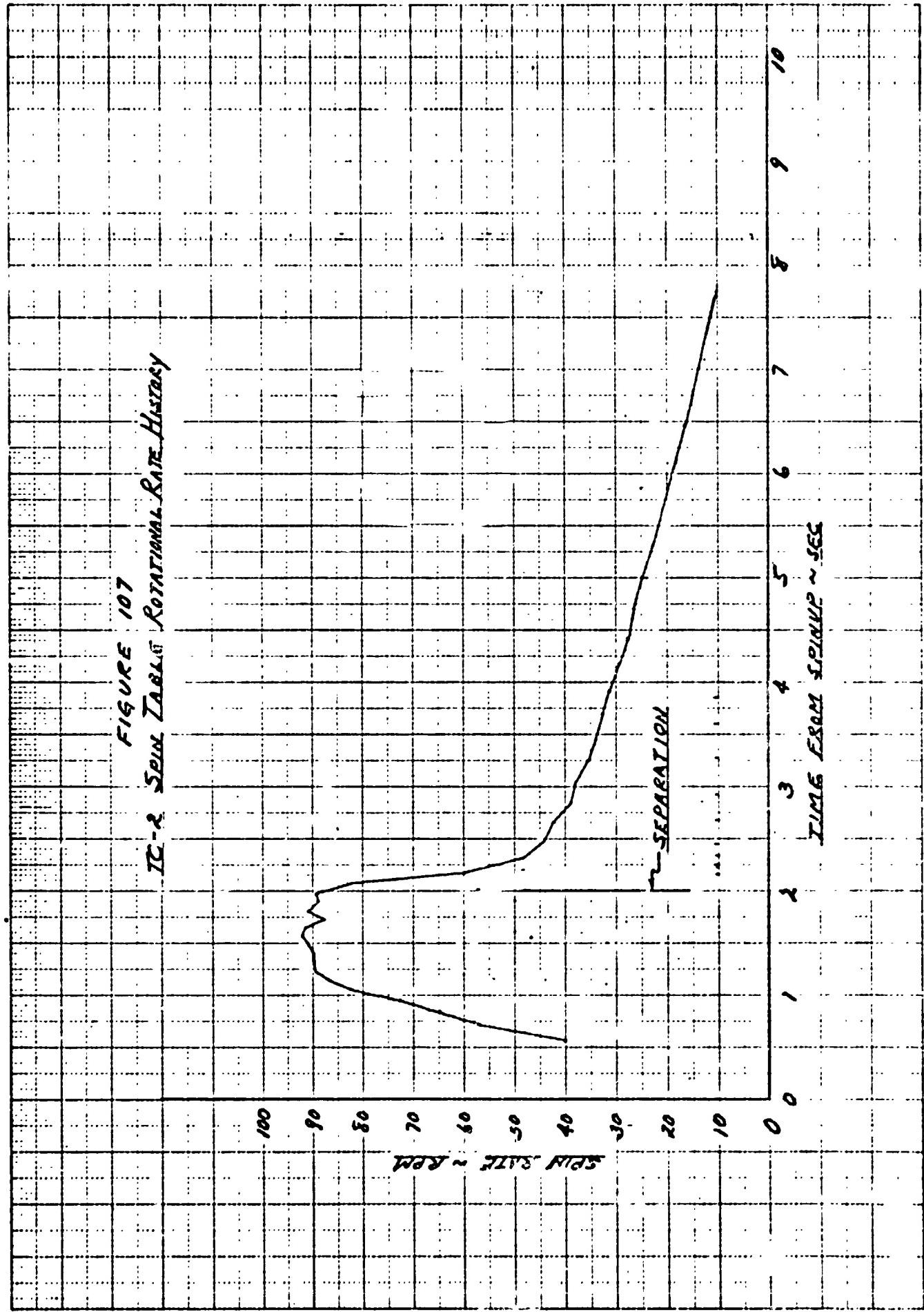
Mode	Axis	Duty Cycle /
Settling 4S ON	Pitch	14.4
	Yaw	1.2
	Roll	0.1
Retention 2SA ON	Pitch	6.9
	Yaw	1.1
	Roll	0.3
Retention 2SB ON	Pitch	5.8
	Yaw	0.1
	Roll	0.8

Following MECO 2, the Centaur aligned the spacecraft to the desired pointing vector and at T+2242.9 seconds spin rockets were commanded to fire. This event achieved a spin rate for the spacecraft of approximately 90 rpm. The spin rate history of the table is shown in Figure 107. It was observed that the spin decay was approximately twice as fast as those observed on Pioneer flights. An impulsive clockwise roll disturbance resulting in a roll rate of 0.4 degrees/second at the spin up event was observed on Centaur. This has been observed on Pioneer flights and is associated with breaking the restraining line which keeps the spin table from rotating during the ascent. It was, however, lower in magnitude as shown below.

Table 56

Vehicle	Roll Rate Due to Breaking Rope	Degrees/Second
Pioneer	AC-27	1.2
Pioneer	AC-30	1.8
Helios	TC-2	0.4

A large propellant residual on TC-2 is the major difference from the Pioneer flights. This difference is under further study to determine if the observed reduction in roll rate can be accounted for by the large propellant use.



Propellant Loading/Propellant Utilization

by K. Semenchuk

Propellant Level Indicating System (PLIS)

The propellant level indicating system (PLIS) consists of a LH₂ probe, LO₂ probe, and LO₂ overfill sensor. LH₂ and LO₂ probes contain three hot wire sensors. The LO₂ overfill sensor contains one hot wire sensor. Each sensor has two redundant sensing elements.

The PLIS is used to indicate the tanking of the propellants to the desired levels. Each sensor gives an indication that a certain level has been reached by the liquid propellant by changing its operating characteristics. This change is detected by the GSE which gives a "wet" or "dry" light indication on the Blockhouse Auxiliary Fuel Tanking Panel.

The LO₂ and LH₂ probe sensors operate at 95 percent, 99.9 percent, and 100.2 percent levels in their respective tanks. The LO₂ overfill sensor is located at approximately 1.75 inches above the 100.2 percent sensor.

The Centaur level indicating system operated satisfactorily during the countdown. At liftoff, both tanks (LO₂ and LH₂) were at 100.2 percent levels.

Propellant Utilization System (PU)

A propellant utilization (PU) system consists of LH₂ and LO₂ sensors, electrical harnesses, a servo positioner mounted on each engine mixture ratio control valve, and electronics circuitry housed within the Servo Inverter Unit (SIU). The SIU provides error detection and valve servo positioner feedback excitation.

The signal generated by this circuitry is processed by the Digital Computer Unit (DCU) for creation of valve position commands. The DCU operates switches in the Sequence Control Unit (SCU) to drive the engine valves to the required position.

The PU system (1) reduces residual mass of one propellant at depletion of the other propellant and (2) reduces errors caused by dispersion due to tanking, liftoff, propellant uncertainties, and engine performance uncertainties.

The PU system controls mixture ratio as a continuous function of the mass ratio of propellants in the tanks.

No PU controls occurred during first and third burns as expected. During first burn, the propellants stayed above the top of the probes; and the third burn was too short (11 secs) for PU control. The propellant utilization system was operated closed loop during second and fourth burns.

The TC-2 Centaur PU flight constants programmed into DCU are shown below.

Table 57 PU Flight Constants

Coast Bias #1	+326 lb. LO ₂
Coast Bias #2	+798 lb. LO ₂
Error Bias	+145 lb. LO ₂
Calibration Offset Bias	-503 lb. LO ₂
C1 S/P Fixed Angle	+0.1 Deg.
C2 S/P Fixed Angle	+1.7 Deg.
C1 Positive Stop	+65.0 Deg.
C1 Negative Stop	-50.5 Deg.
C2 Positive Stop	+65.5 Deg.
C2 Negative Stop	-45.0 Deg.

During the first burn, the PU servo positioners were locked at fixed angles shown above. At MES 2 + 5 seconds, the S/P valves moved to the LO₂ rich limits to compensate for the biases and errors accumulated to this point. At MECO 2 -27 seconds, the valves were set at their last computed values of approximately 7 degrees each. At MES 3 -28 seconds, the PU valves were nulled and remained nulled throughout the third burn as planned. At MES 4 + 5 seconds, the PU system was placed in closed loop control, and the servo positioners immediately moved to the positive stops (LH₂ rich) and remained there throughout the fourth burn.

The LH₂ rich condition during this burn is due to the large coast biases and/or a low boiloff rate of LH₂ during the second and third coast periods. The actual fuel (LH₂) and LOX (LO₂) residuals at MECO 2 and MECO 4 are shown in Table 58 below and are compared to the predicted values.

Table 58 LH₂ and LO₂ Residuals

	LH ₂ (Lbs.)		LO ₂ (Lbs.)	
	Actual	Predicted	Actual	Predicted
At MECO 2				
Total Usable	1048	960	4076	4430
At MECO 4				
Total Usable	290	195	798	724
	220		726	

At the end of the mission, the residual fuel was enough to sustain 13.5 seconds of burn time.

During the third coast period, the heaters on the servo positioners were cycled on-off three times as commanded by the DCU. The temperatures of the servo positioners were 62°F and 59°F for C1 and C2, respectively at liftoff. The lowest temperature recorded was +26°F and the highest never exceeded +62°F for the entire flight.

Instrumentation and Telemetry Systems

by J. M. Bulloch and T. J. Hill

Instrumentation - A total of 569 measurements were instrumented, 523 PCM measurements, 23 twenty-four bit DCU words via the PCM system, and 23 analog measurements.

The following measurements failed to provide valid data during the flight:

CP5640 (LO_2 Boost Pump Flange Longitudinal Vibration) failed to provide any vibration data during the flight. The data level was constant at the 50 percent (Information Bandwidth amplifier bias level). Satisfactory operation of the measurement was observed during prelaunch systems tests. The exact cause of the anomaly is unknown.

CA289T (Tank Skin 2426/90) indicated off scale high until 47 seconds into the flight. The measurement had failed previously during TCD and was not repaired due to inaccessibility of the transducer under the shroud. The most probable cause of the anomaly is a bad connection at the splice joint of the transducer leads to the harness wires. An improved technique for installing these splices has been developed effective TC-5, AC-40 and on.

CP187T (LH_2 Boost Pump Decomposer Chamber) was attenuated throughout the flight. Additionally, negative steps of 4 percent IBW were noted at circ pump start and ignitor firing. Similar characteristics were noted during the FED and TCD. Investigation after the TCD indicated a short circuit in the thermocouple between the reference junction and RMU. Because of the large number of measurements utilizing this RMU connector, it was decided not to troubleshoot or attempt to fix the measurement because of possible damage to the other measurements.

The following measurements exhibited data anomalies during the flight:

CP5630 (LO_2 Boost Pump Flange, Lateral), CP5600 (LH_2 Boost Pump Flange, Lateral), CA886Y (Forward Equipment Module Acoustic). In all cases, recovery was within one to two seconds. The vibration and acoustic data is recoverable during the transient period. This type of bias shift and recovery is typical of a momentary open in the coaxial cable/connector circuits between the accelerometer, 'T' calibration connectors and charge amplifiers.

CA6850 (Payload Adapter Longitudinal) exhibited a +3 percent IBW shift at Forward Bearing Reactor separation. CA6860 (Payload Adapter Radial) exhibited a (-) 5 percent IBW shift at the same time. Both measurements remained shifted for the remainder of the acquisition period. The most probable cause is transducer sensitivity to ambient pressure changes. Testing in the lab has indicated these transducers (27-01922) can drift or exhibit shifts due to abrupt shocks

when the pressure changes from ambient to a vacuum. This discrepancy will be eliminated by modifying the transducer electronics on TC-5 and up and AC-37 and up. CF6T (LO_2 tank ullage temperature) remained off scale high throughout the Cape Canaveral acquisition period except between 145 and 154 seconds. Data during this period showed three separate levels and is considered invalid. Downrange data from Hawaii indicates the measurement was providing valid data prior to the third burn up to MES 3. The measurement had failed during TCD and was not replaced due to transducer inaccessibility. Investigation after the TCD indicated an electrical open circuit within the LO_2 tank. Data indicates the anomaly was at the sensor. No further investigation is planned. It is believed this discrepancy may have been brought about by the unusually extensive handling of the LO_2 standpipe when measurement CF23T was added for the extended mission. CPT33T (LO_2 Boost Pump Inlet Temperature) exhibited positive and negative noise spikes (up to band edge in amplitude) throughout the flight. No data was lost due to these transients. The spiking was caused by interaction in the common leg temperature bridge due to the intermittent nature of the CF6T transducer (see 3 above). This is a known operating characteristic of these common leg circuits.

The following measurements all exhibited data characteristics which are attributed to a faulty splice between the transducer and harness:

CA186T (Superzip Outer 2688/-Z) exhibited an anomalous 15°F positive excursion between 23 and 26 seconds. CA176T (Shroud Skin Station 2551/128) exhibited an anomalous 50°F positive drift between 75 and 86 seconds, returning abruptly to the expected level at 86 seconds. CA969T (LH_2 Sump Radiation Shield Outer Station 2235) stepped off scale high at 472 seconds (T/C separation). Data prior to this time appeared valid. An improved technique for installing these splices has been developed effective TC-5 and on and AC-40 and on.

The following measurements all exhibited data characteristics which may be attributed to the transducer becoming unbonded from the attach structure, resulting in poor thermal contact:

CA288T (Tank Skin Station 2426/0), CA290T (Tank Skin Station 2370/0), and CA293T (Tank Skin Station 2334/0) all exhibited erratic outputs (between 10 and 30 percent 1BW) from prior to liftoff to approximately T + 180 seconds. Data after 180 seconds appears valid.

CA291T (Tank Skin Station 2370/90), CA292T (Tank Skin Station 2370/180), and CA294T (Tank Skin Station 2334/90) all indicated an unexpected warming trend beginning at 472 seconds (Titan/Centaur separation).

CP744T (C2 Engine Bell Station 507 Inboard) indicated a drop in temperature to -112°F at MES 1 when a drop to -305°F was expected. The measurement indicated the expected ambient output prior to MES 1. A thorough analysis of the data from these tank skin temperature measurements has not been completed and so it is not yet known how much of the data is actually questionable. Until the

anomalies are defined, the cause of the (possible) anomalies cannot be determined.

CA894P (ISA Ambient Pressure) exhibited several negative transients during the first 15 seconds of flight. A similar anomaly was noted on TC-1 and on two ambient pressure measurements on AC-31. These transients are attributed to intermittent liftoff of the wiper arm in the transducer. No significant data was lost.

The Conrac transducer used in conjunction with this measurement is no longer being procured and is being phased out by a Servonics transducer.

CPI95P (C2 Pump LH₂ Discharge) did not read less than approximately 15 psia at times when the transducer was actually sensing lower pressure. Since the measurement performed normally at all pressures above approximately 15 psia, the transducer was apparently at fault. It appears that some obstruction prevented the transducer wiper arm from traveling below the 15 psia point (the point at which it rested in a one-atmosphere pressure environment). The transducer had been calibrated over its full range prior to installation and functioned properly at low pressures at that time. The cause of an obstruction that could have developed since that time is a matter for pure speculation. No further investigation is planned because this is the first time this problem has been reported with that type transducer and no data loss occurred in the area of interest for that measurement.

Unexplained 37 Hz oscillation buildups and occasional spiking were observed on measurement CM42R (IRGU Pitch Rate Low Output) after T + 51 minutes during the flight. Similar oscillations and some spiking were also observed on this measurement during prelaunch operations. Maximum amplitudes of the oscillations and spikes did not exceed 15 percent IBW p-p (0.21 deg/sec p-p) and were generally less than 10 percent IBW p-p. The oscillations were not apparent on the rate gyro output monitor (CM41R). A post-flight analysis of the anomaly could not define any rate gyro package problem that could cause the observed phenomena (ref. PR#AG05262CP). The 37 Hz oscillation mode is believed to be the result of aliasing a higher frequency oscillation mode (probably 800 Hz) with the PCM measurement sampling rate (279 samples/sec).

The first launch attempt of this vehicle on December 8, 1974, was aborted due to redline measurement CPT62T (C-2 LH₂ Pump Inlet Temperature) drifting off-scale-high at approximately T-30 minutes. Subsequent investigation revealed a faulty transducer. Failure analysis indicated the cause was due to the improper use of glue to cement the interfacial seal in the connector when the seal is supposed to be press-fit into the connector. Some of the glue inadvertently got onto the connector pins resulting in intermittent operation at cryogenic temperatures. To prevent a future occurrence, survey 2-75 has been initiated to verify that the interfacial seal has not been glued into any connectors for all existing 55-01259 stock.

Telemetry Systems

The performance of the Centaur FM/FM, PCM Link 1, PCM Link 2, and the TE-M-364-4 stage telemetry was satisfactory. A total of 582 measurements were instrumented, 546 on PCM, 23 on the Centaur FM/FM, and 13 on the TE-M-364-4 stage FM/FM.

Signal strengths indicate satisfactory performance of the airborne RF system. This was the first Centaur vehicle to utilize a redundant PCM transmitter. The same PCM bit stream from the DCU was used to modulate different FM transmitters on 2202.5 and 2215.5 MHZ. The dual RF link was to assure data recovery in the post-Helios phase of Centaur flight. Two Hi-gain antennas were also installed on the Centaur for the same purpose. At T + 4173 (MECO 2 + 2000 sec.) all three Centaur RF sources were switched from the omni antennas to the Hi-gain antennas. RF signal strengths rose approximately 30 db at this time, indicating satisfactory performance of the Hi-gain system and RF switches.

Ground Station coverage and participating stations are shown in Figure 108. Two stations reported problems during the flight. ARIA 2 was unable to deploy its antenna and was unable to provide any coverage. As a result, there is a gap in the data available from T + 1130 to AOS at ACN at T + 1246.

The USNS Vanguard reported that it switched to a backup 30-foot antenna to support the flight and that due to a late turning maneuver the ship's superstructure interferred with the signal received by this antenna. Vanguard did have intermittent data coverage from T + 1869 seconds to Johannesburg AOS at T + 1916.

The expected occultation of the signal received at CIF at liftoff did occur in the first second of flight. Coverage was provided at Complex 36 and Hangar J for this period.

FIGURE 108.1

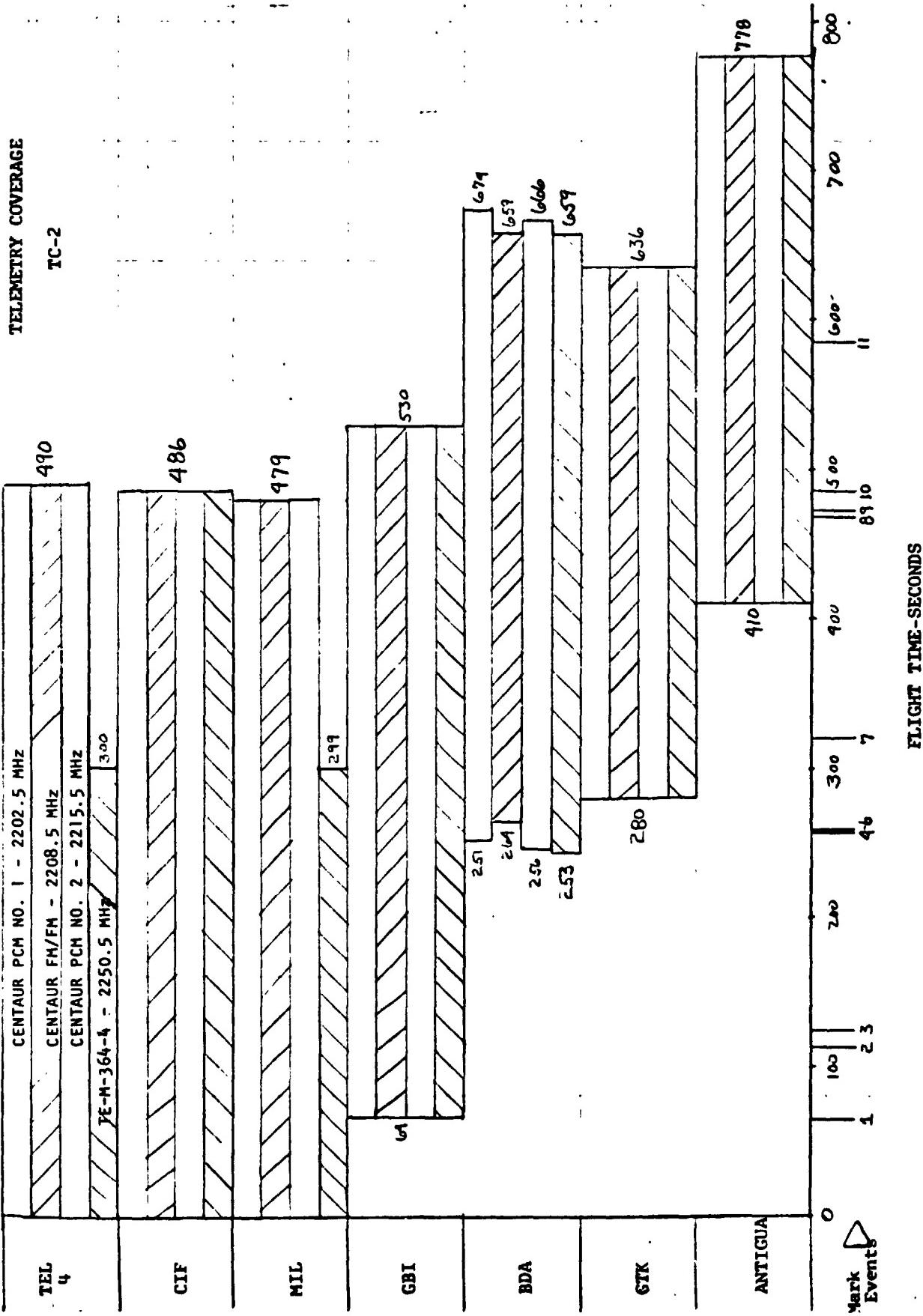


FIGURE 108.2
TC-2 TELEMETRY

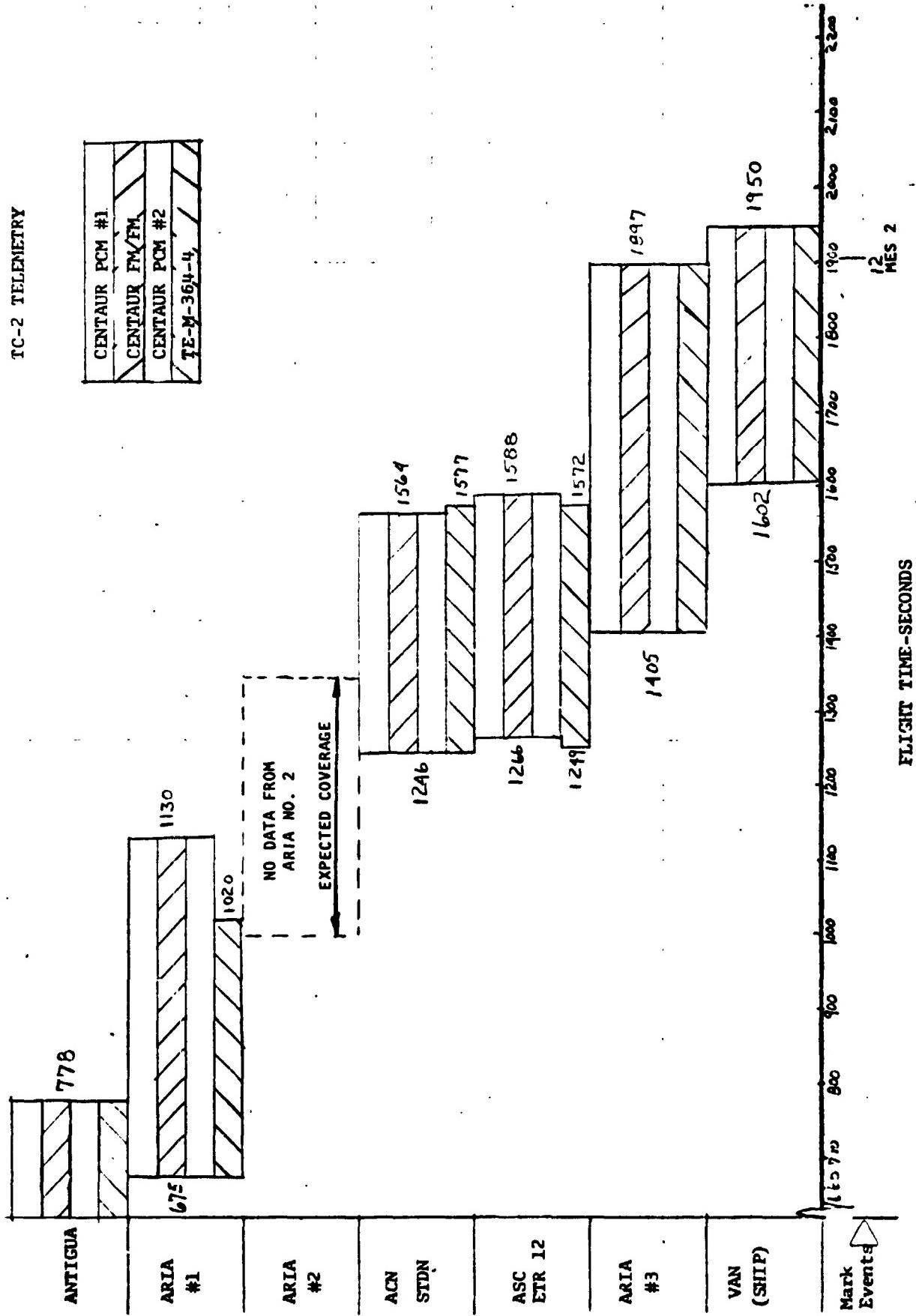


FIGURE 108.3
TC-2 TELEMETRY

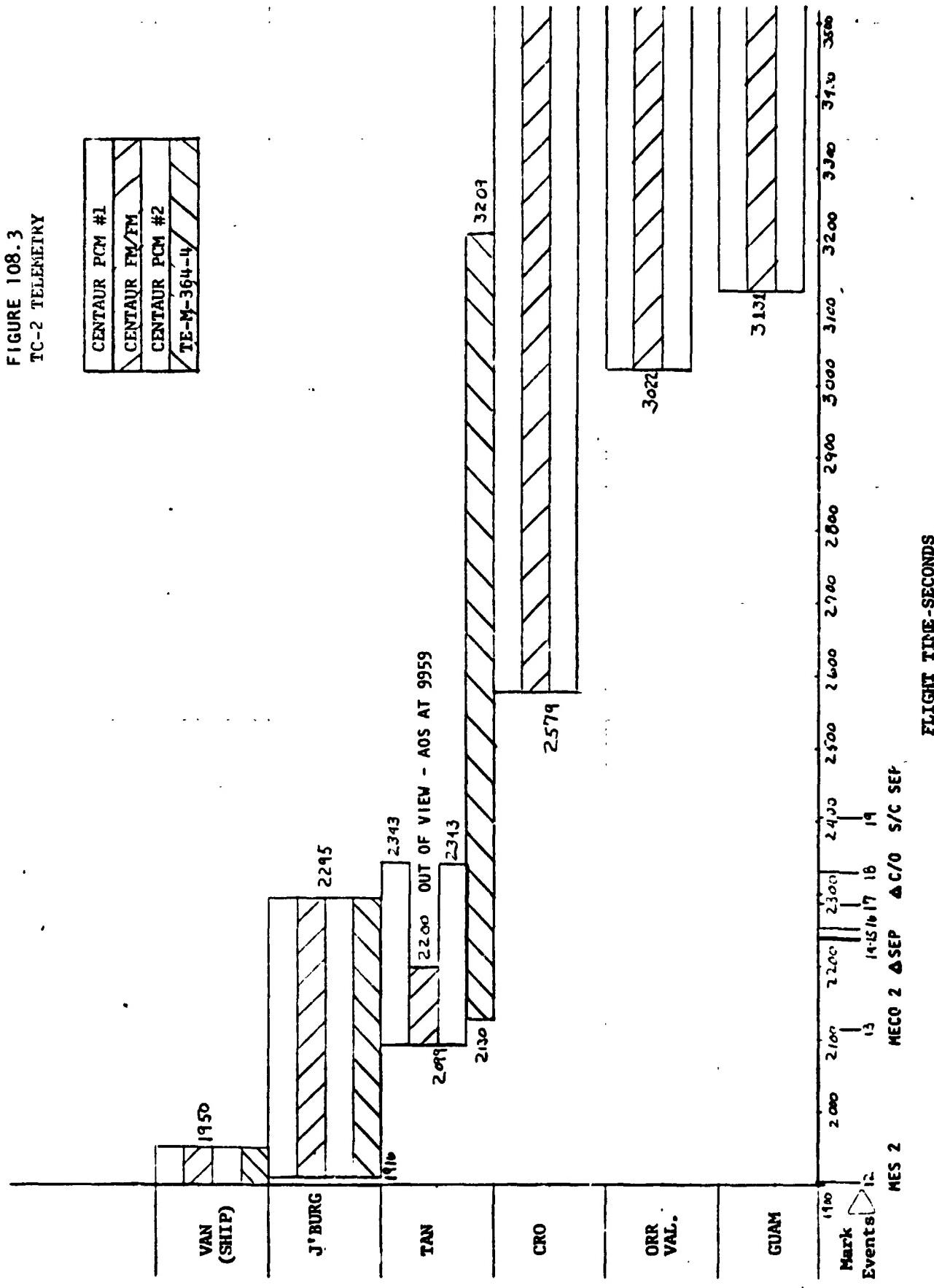
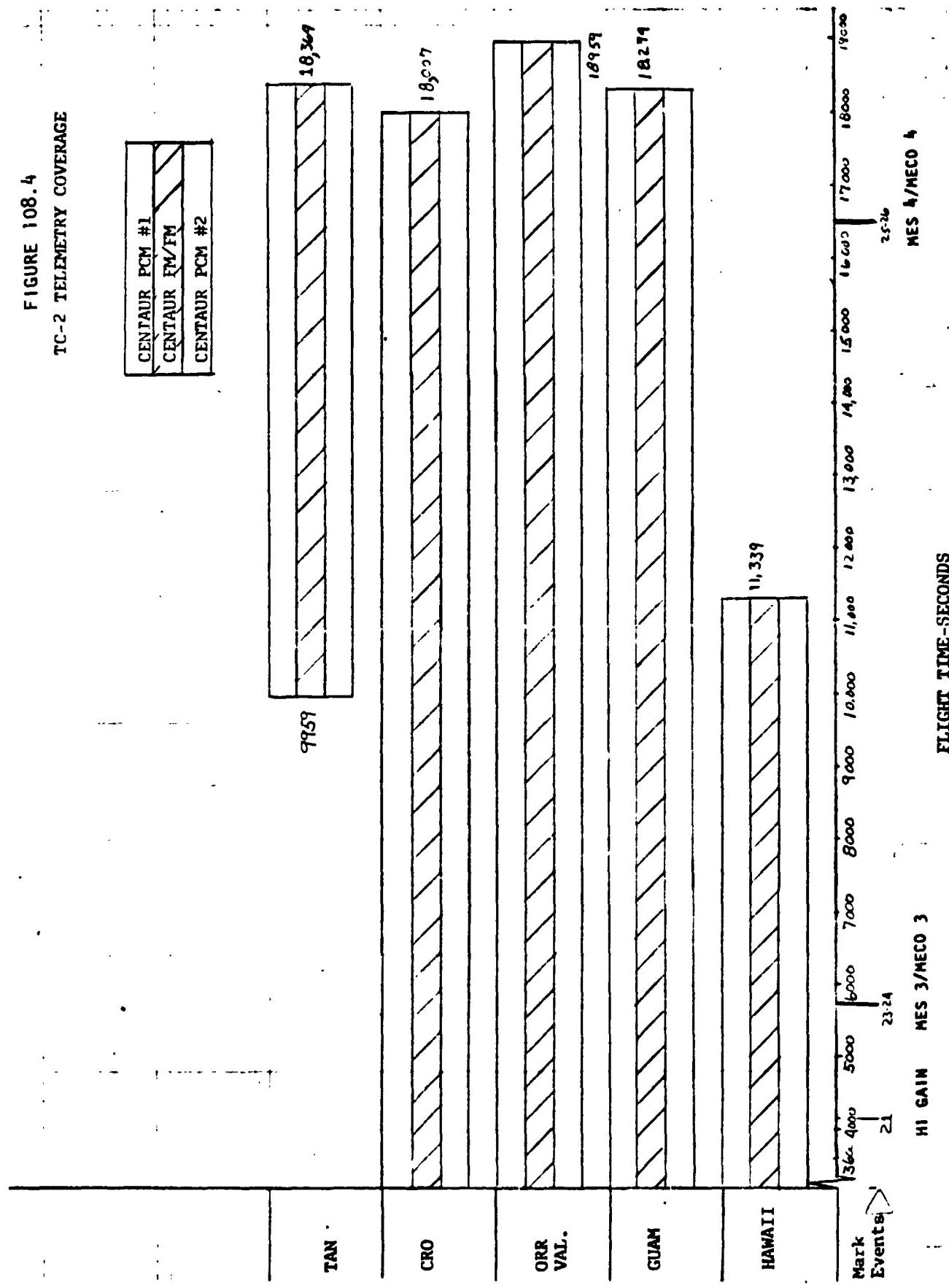


FIGURE 108.4
TC-2 TELEMETRY COVERAGE



Tracking and Range Safety Systems

by T. J. Hill

C-Band Tracking

Operation of the Centaur C-Band Tracking System was satisfactory from lift-off through the Antigua tracking interval with no discrepancies noted. No C-Band coverage was planned from LOS at Antigua until acquisition by Hawaii radar. Data reports from Hawaii and Canton Island note considerable loss of data and intermittent tracking. Canton Island reported no valid data because the wrong range interval was being used.

Tananarive attempted to acquire the Centaur beacon at the end of TE-364 support at T + 2825 but Centaur had already set.

Range Safety Command System

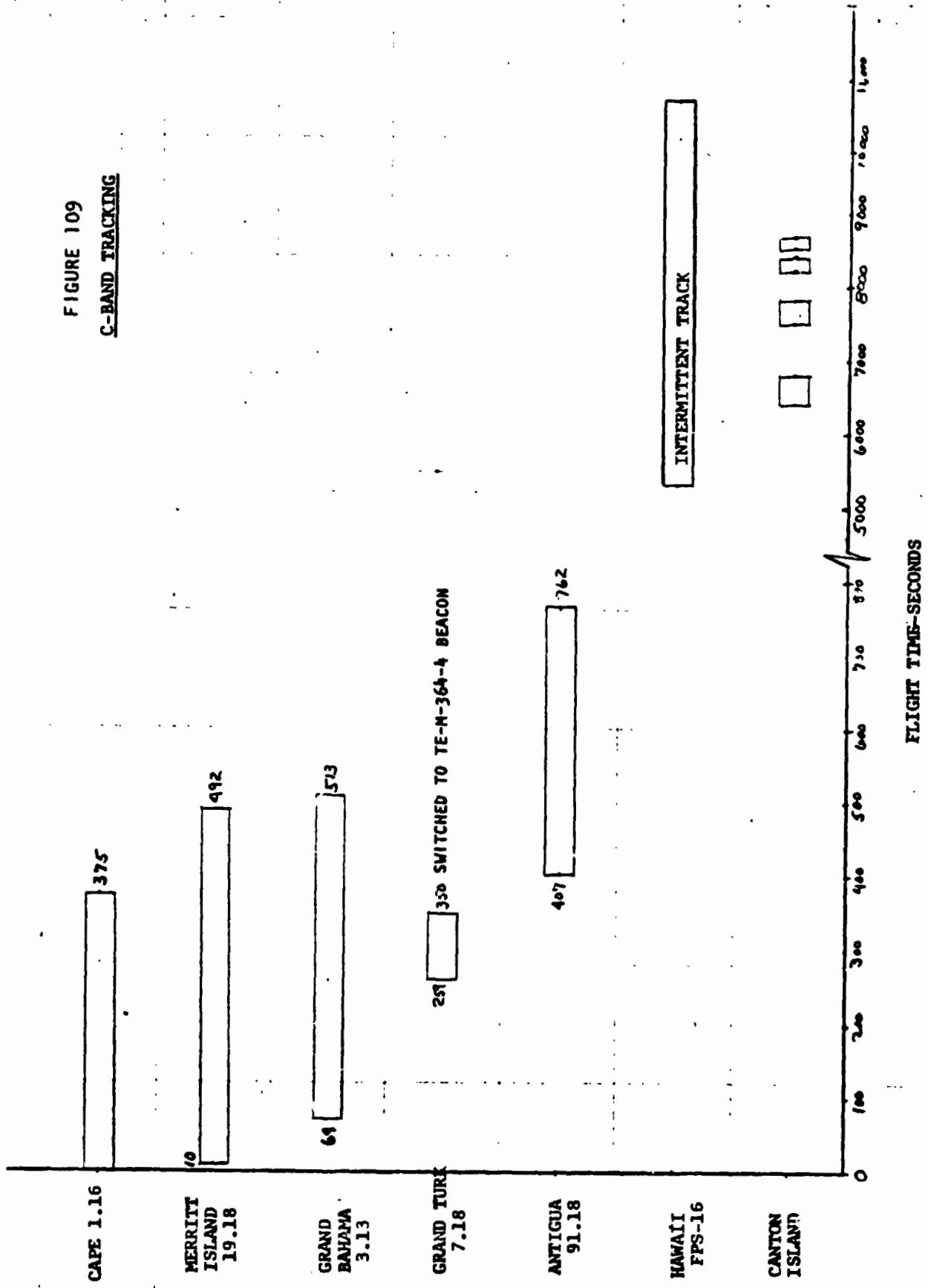
Operation of the Range Safety Command (RSC) system was satisfactory. Signal strength (AGC) data indicated a satisfactory received signal level throughout the flight. Two short duration drops in AGC were noted, as expected, at Titan SRM jettison and shroud jettison. However, system capability was maintained during these periods. System control was maintained as the vehicle flew downrange by switching of RSC transmitter control. Station switching times are presented in the following table.

Table 59

<u>Station</u>	<u>Carrier On (Sec)</u>	<u>Carrier Off (Sec)</u>
Cape Canaveral	-1982	170
Grand Bahama Island	170	460
Antigua	460	733

The Antigua transmitter sent RSC RF disable at 601 seconds resulting in shutdown of the airborne RSC receivers.

FIGURE 109
C-BAND TRACKING



X DELTA TE-M-364-4 SYSTEMS ANALYSIS

X DELTA TE-M-364-4 SYSTEMS ANALYSIS

Mechanical System

by R. C. Edwards

During the TC-2 flight, the Delta structure performed satisfactorily. The payload attach fitting, TE-364-4 motor, and spin table safely withstood the structural loadings imposed during the booster and TE-364 thrust period of flight.

The mechanical events occurred on time and no anomalies were noted. The tension chord that secures the spin table in place functioned satisfactorily. The spin rockets were fired on time, breaking the tension chord. A spin rate of 92.5 RPM was imparted to the TE-364-4 motor and spacecraft. The motor attaching clamp was severed on time and was jettisoned due to its own stored energy. Following clamp band separation, the four spin table petals rotated about hinges at their base to free the TE-364-4 motor from the spin table. The wire cutter device severed the wiring harness between the spin table and the timer mounted on the payload attach fitting. The payload clamp band and the "yo" weight were released on schedule and without any discrepancies noted.

A maximum axial acceleration of 13.6 g's occurred at TE-364-4 burnout. The maximum pressure decrease in the payload compartment was 0.66 psi per second.

A more detailed and extensive report on the performance of the Delta Stage will be published by the McDonnell Douglas Astronautics Company in July 1975.

Propulsion System

by W. K. Tabata

The performance of the TE-M-364-4 solid propellant motor was normal. The ignition delay was 44.0 seconds. The action time of the motor was 43.6 seconds. The action time is defined as the time interval from when the chamber pressure reaches 300 psia on the ascending portion of the chamber pressure time history curve to when it reaches 100 psia on the descending portion of the curve. Combustion was smooth and stable. The maximum chamber pressure was 610 psia.

Electrical System

by C. H. Arth

The telemetry battery was satisfactorily above the redline value (26.0 VDC) at liftoff reading 29.3 VDC. The flight history of the telemetry battery voltage and current indicated normal performance. The ordnance battery satisfied the redline value of 11.0 VDC reading 11.06 VDC at liftoff and performed normally.

Telemetry and Tracking Systems

by T. J. Hill

Three radar stations (BDA, VAN and TAN) of the Space Tracking and Data Acquisition Network reported that the TE-M-364-4 stage beacon was responding with a "weak and lobing" signal. Lobing is defined as received signal strength variations in the transponders pulse returns. The STDN No. 502.3 Network Operations Plan (NOP) for C-Band Systems specifies left-hand circular polarization for Delta antennas. STDN stations would normally configure their stations for linear vertical polarization. Bermuda (BDA), Vanguard (VAN), and Tananarive (TAN) used linear vertical polarization, apparently causing the TE-M-364-4 signal to appear weak and lobing. Stations configurating to circular polarization (Grand Turk, Ascension-STDN and Ascension-ETR) reported nominal signal strengths. The problem appears to be a result of cross-polarization between the TE-M-364-4 and the three STDN stations reporting difficulty.

Station coverage data is included in Section IX in the discussion of the Centaur C-Band tracking.

XI FACILITIES AND AGE

XI FACILITIES AND AGE

Complex 41 Facilities

by M. Crnobrnja

Modifications Since TC-1

The launch of TC-1 Proof Flight resulted in considerable damage to Transporter No. 2 due to a post-launch fire. The damage was assessed by a Launch Damage Committee and the following actions were implemented in response to the recommendations made by the Launch Damage Committee:

1. Close all openings in the transporter base and masts to prevent entry of direct flame and debris.
2. Install heat resistant boots over the SRM umbilical cables.
3. Incorporate bulkheads in the transporter booms.
4. Provide quick-opening latches for access doors at the base of the transporter masts.
5. Eliminate the Firex system for the water deluge system.
6. Initiate a prelaunch closeout inspection of areas at the base of the masts.
7. Revise the post-launch inspection team procedures.
8. Operate the DTS and DRS systems until the launch complex is secure after launch.
9. Add a CO₂ inertion system for the base of the transporter masts and booms.
10. Add a new water deluge system to the base of the transporter masts.
11. Modify the LOX vent line to return LOX to grade rather than dump overboard from Level 9 of the Umbilical Tower.

Facility and Site Operation

All facility systems required for the TC-2 vehicle performed satisfactorily. Launch damage was minimal and typical, if not cleaner, than other Titan launches.

Fluid Systems Operations

by M. Crnobrnja

Titan Propellant Loading

Titan vehicle propellant loading was initiated on F-3 day and completed on F-2 day. Table 60 provides quantities and temperatures of propellants loaded on the Titan stages.

The propellant loading system was identical to TC-1 except for the automatic temperature compensators which have been deleted. System operation was satisfactory.

Centaur Propellant Loading

Centaur propellants were tanked during launch countdown. Significant system operation event times are provided in Table 61. The system operation was satisfactory for launch countdown tanking, detanking during scrub and retanking for launch.

The Centaur loading system was identical to TC-1 except for the rerouting of the LOX vent line from Level 9 to grade.

Liquid Helium System

Liquid helium flow for chilldown of Centaur vehicle turbopumps was initiated during countdown. Table 61 provides system operation event times. System operation was satisfactory.

TABLE 60
TITAN PROPELLANT LOAD SUMMARY

	Indicated Load Lbs.	Bulk Temperature °F
Stage I Fuel	90,338	67.6
Stage II Fuel	24,298	68.0
Stage I Oxidizer	165,850	69.0
Stage II Oxidizer	43,237	70.0
TVC-1 Oxidizer	8,415	70.5
TVC-2 Oxidizer	8,415	70.1

TABLE 61
CENTAUR SYSTEM EVENTS

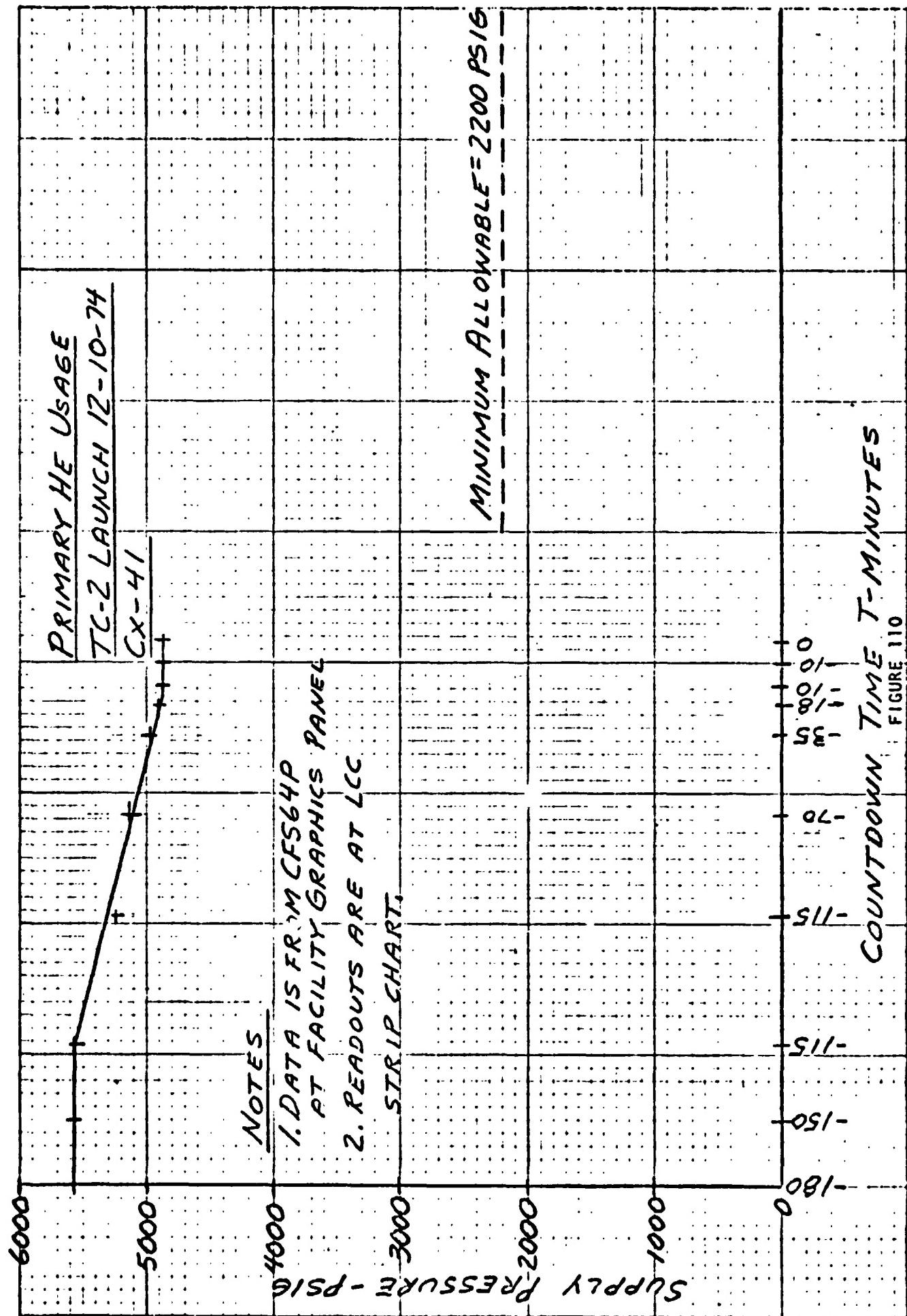
	<u>Planned Time</u> Min:Sec	<u>Actual Time</u> Min:Sec
Start LO ₂ Chilldown	T-180	T-107
Start LO ₂ Tanking	T-98	T-99
Start LH ₂ Chilldown	T-90	T-91
Start LH ₂ Tanking	T-70	T-69
LO ₂ at Flight Level	T-8	T-47
LH ₂ at Flight Level	T-8	T-30
Start LHe Chilldown	T-30	T-20
Secure LH ₂ Tanking	T-0:90	T-0:82
Secure LO ₂ Tanking	T-0:75	T-0:67
Secure LHe Chilldown	T-0:07	T-0:07

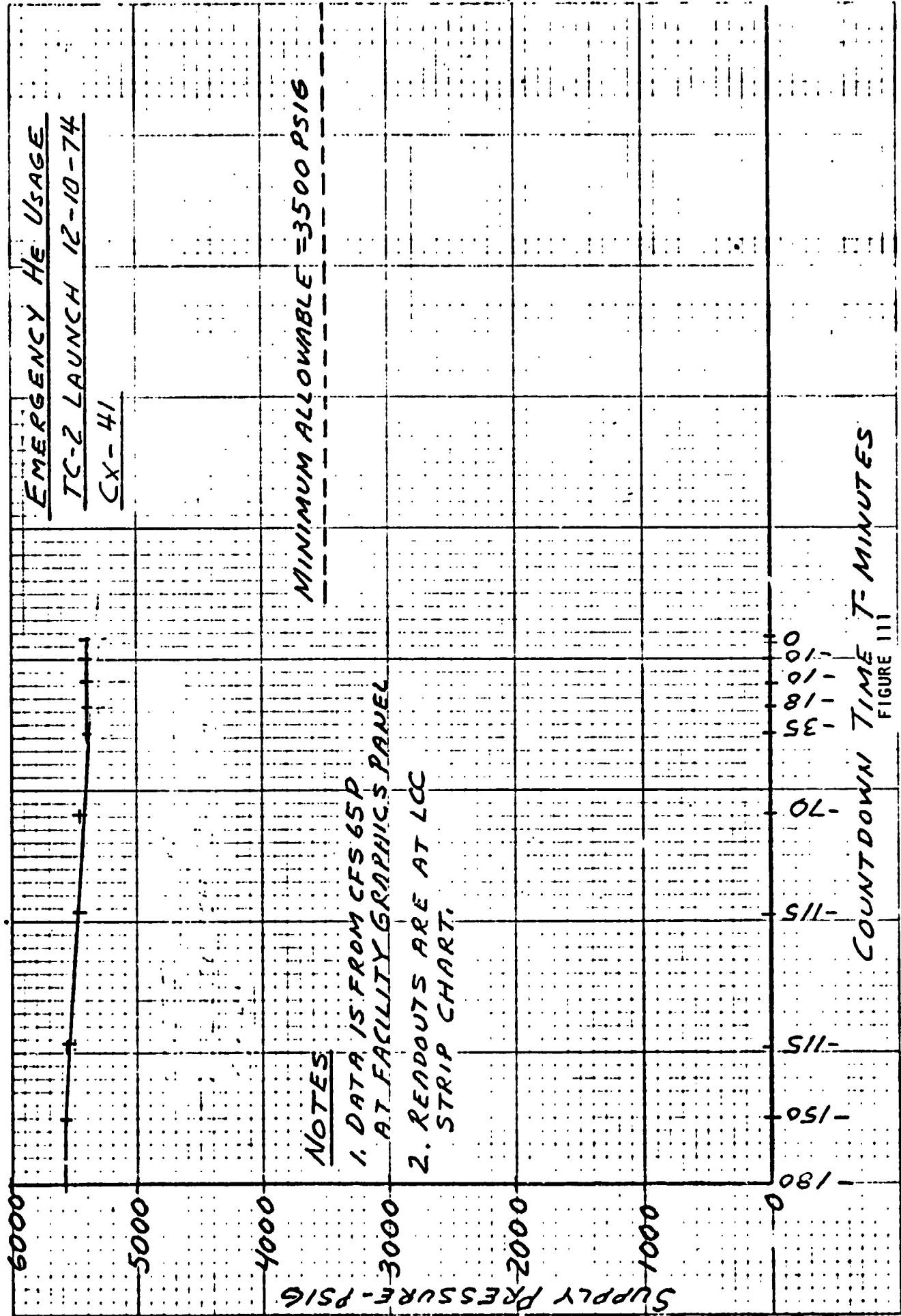
Pneumatic Ground Systems

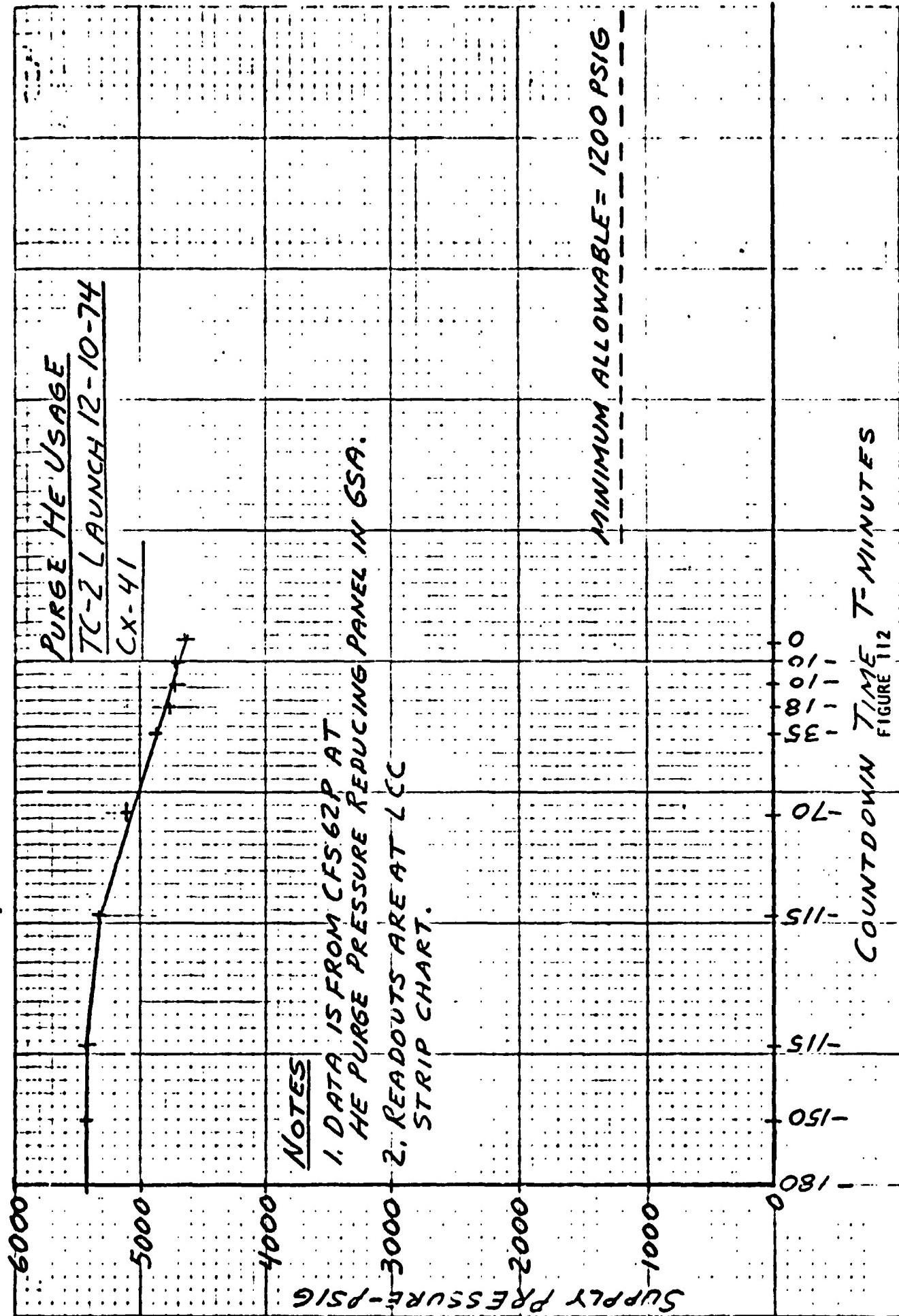
by A. C. Hahn

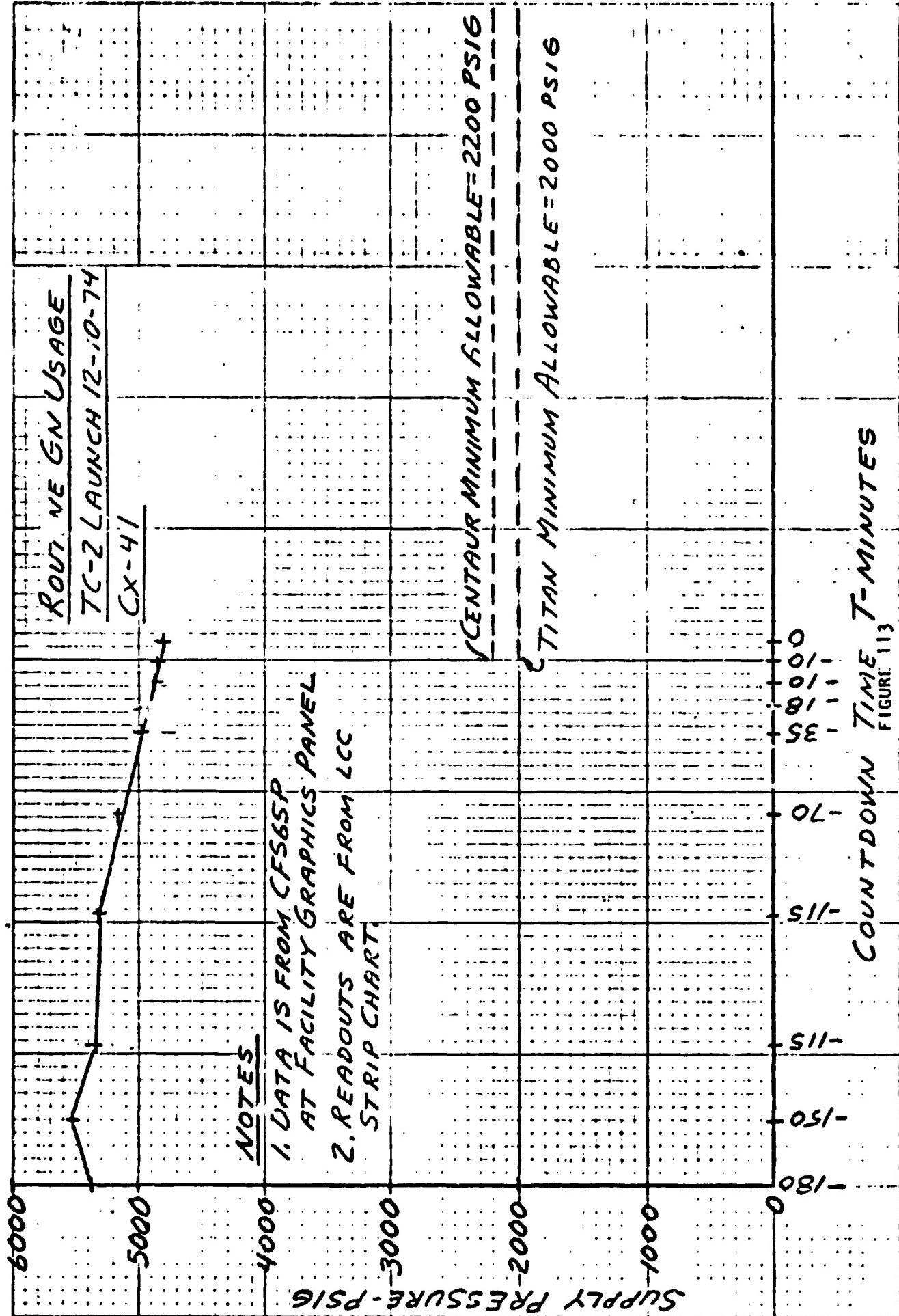
The pneumatic systems include the primary helium, emergency helium, purge helium, and routine nitrogen systems. The three helium systems are peculiar to Centaur. The routine nitrogen storage supplies both the Titan and the Centaur nitrogen systems. Figures 110 through 114 provide information on system operations.

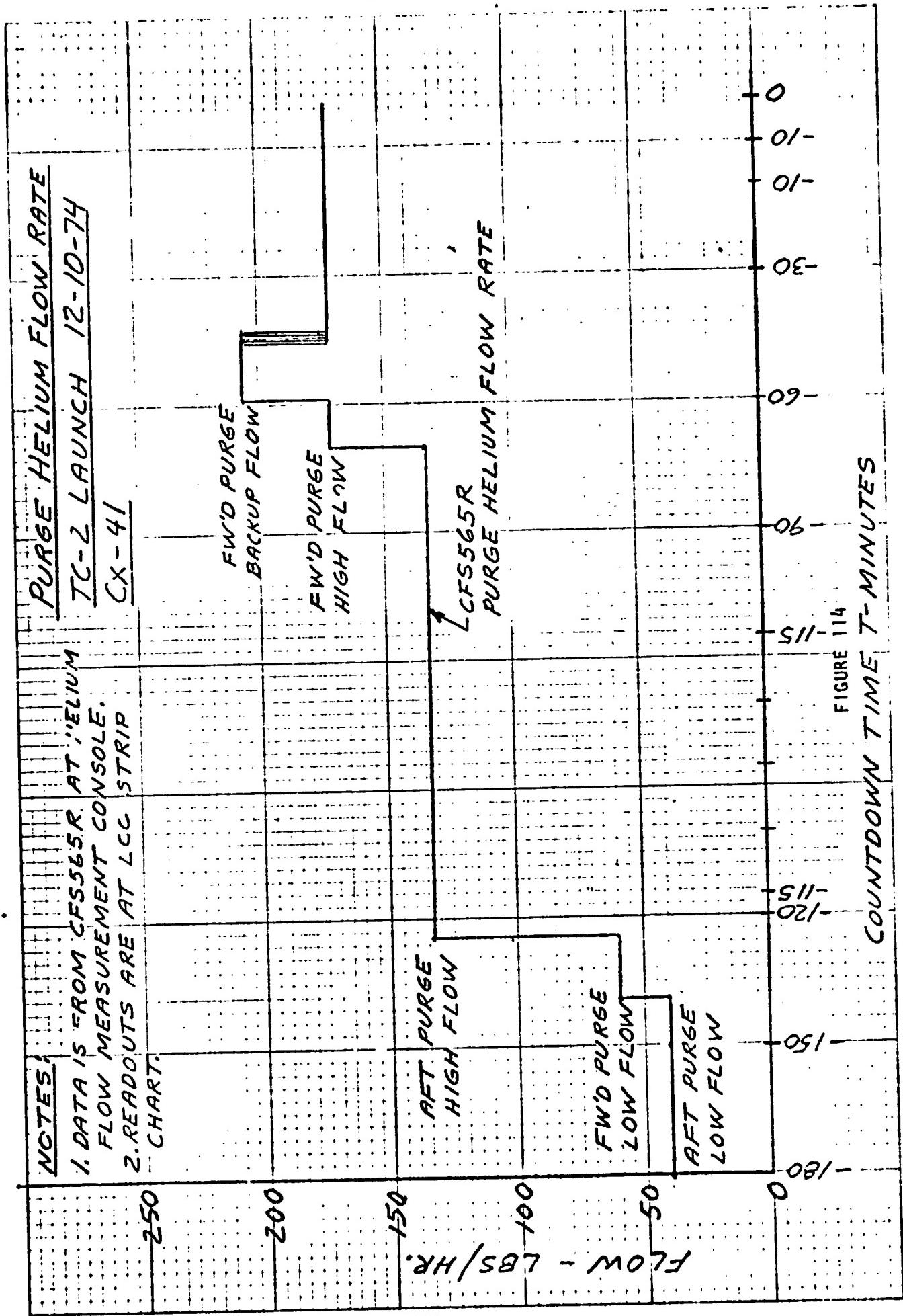
System operation was satisfactory and without anomalies during launch count-down.











Environmental Control Systems

by A. C. Hahn

Titan Air Conditioning System Operation

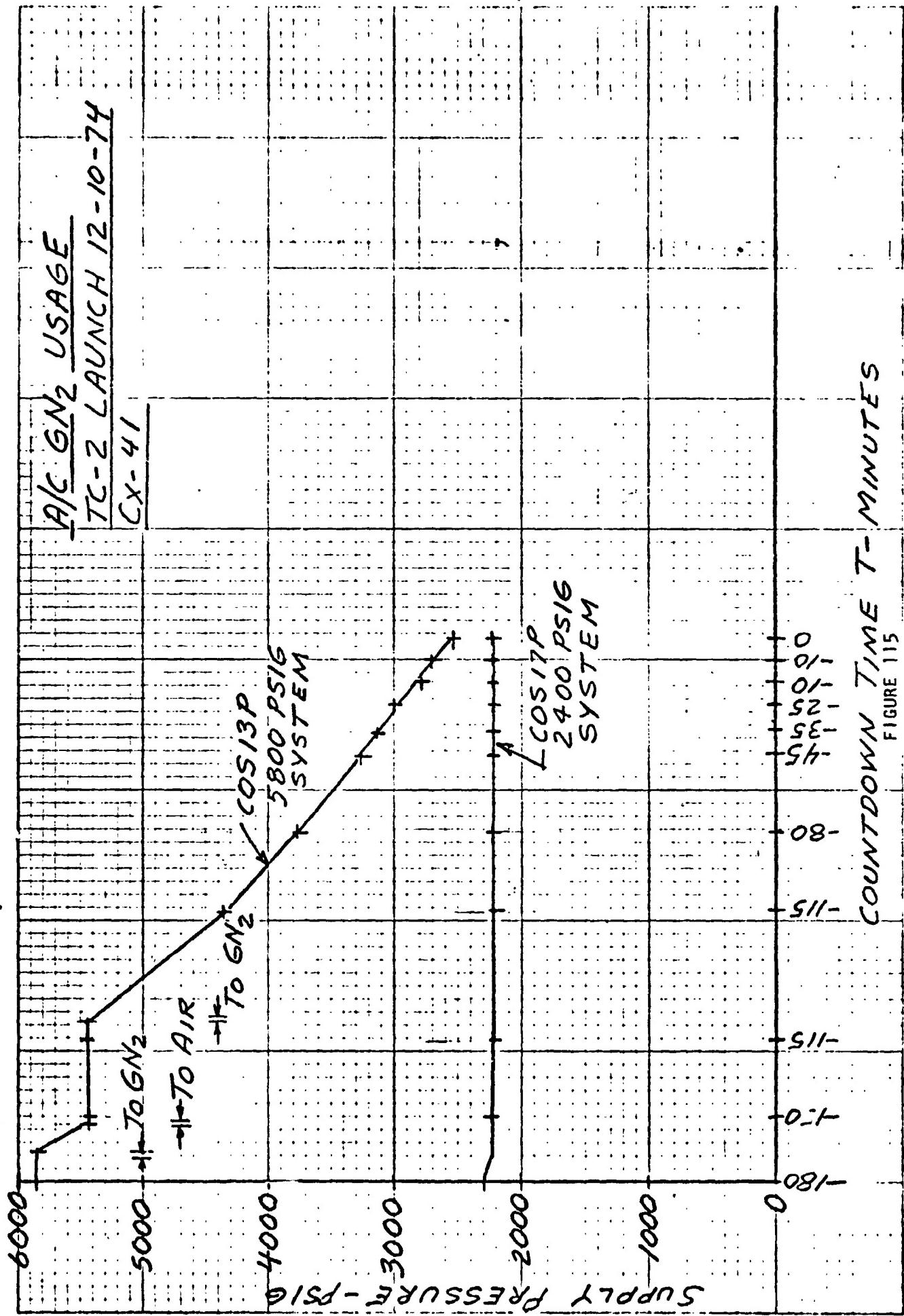
The core air conditioning system supplies conditioned air to compartment 2A and to the start cartridges. System operation was satisfactory and without anomalies during launch countdown.

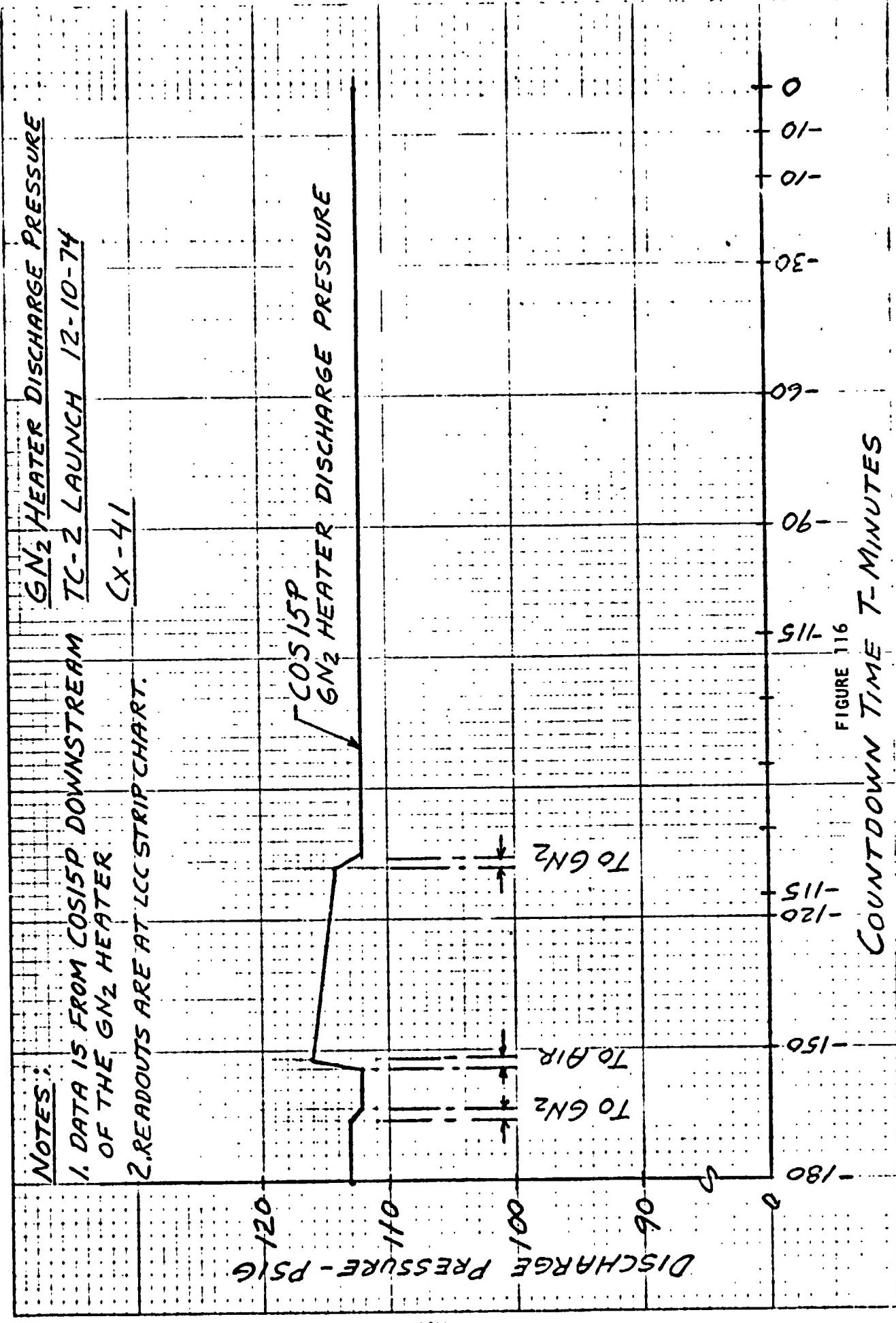
Centaur Environmental Control System

The Centaur Environmental Control System provides conditioned air or gaseous nitrogen to the payload, Centaur equipment module, and interstage adapter compartment. System operation was switched from air to GN₂ early in the one hour hold prior to the start of Centaur propellant loading. Figures 115 through 125 and Table 62 provide information on the GN₂ portion of the system.

System operation was satisfactory and without anomalies during launch countdown.

Right after liftoff the ground half of the payload disconnect separated from the umbilical duct. Movies and measurements of the start of payload duct pressure decay show that the ground half separated from the airborne half of the disconnect properly. The most likely cause of the separation of the ground half from the umbilical duct is severe buffeting. The umbilical duct is supported from the North Mast. Vehicle drift toward the North Mast caused the severe buffeting.





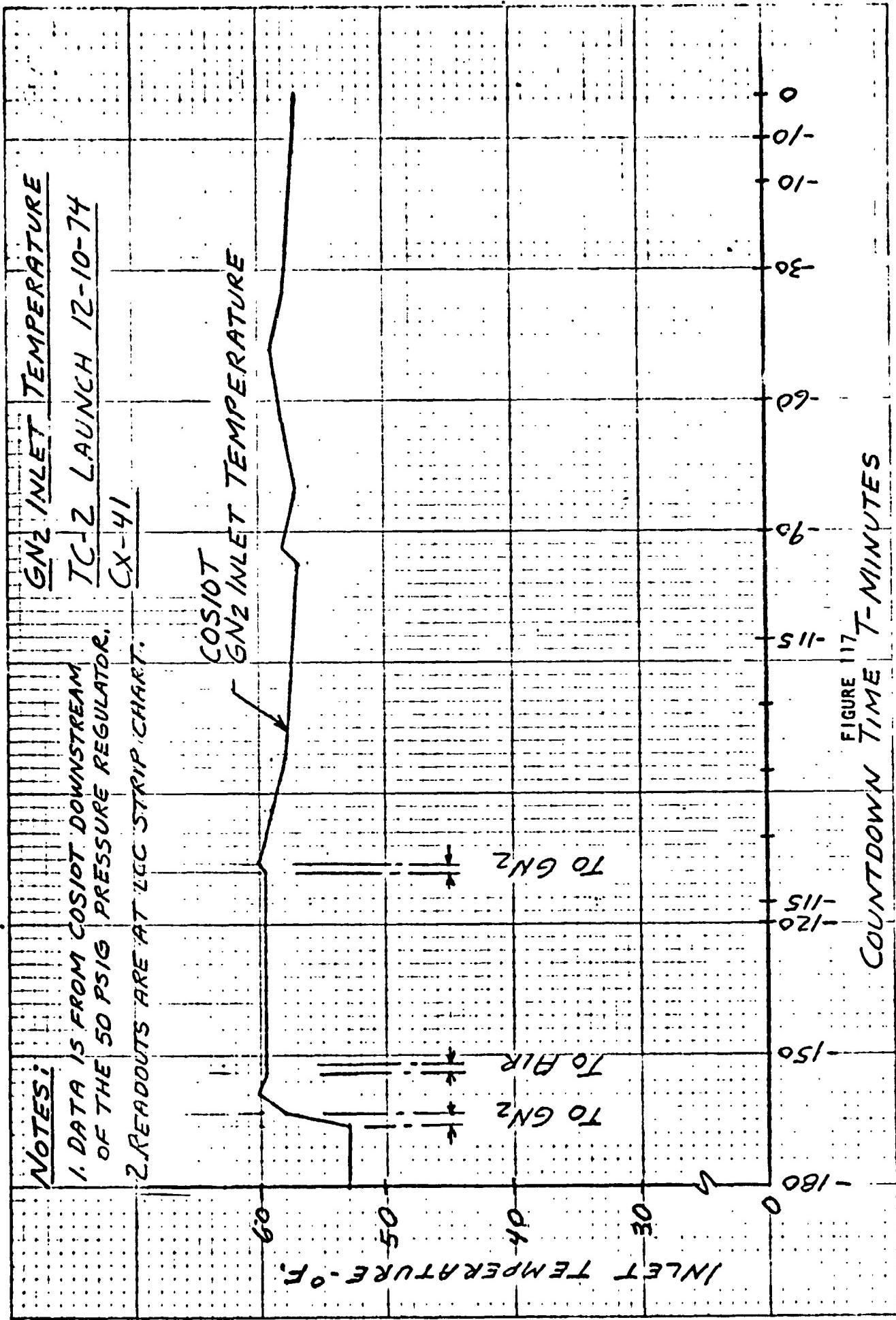


FIGURE 117-T-MINUTES

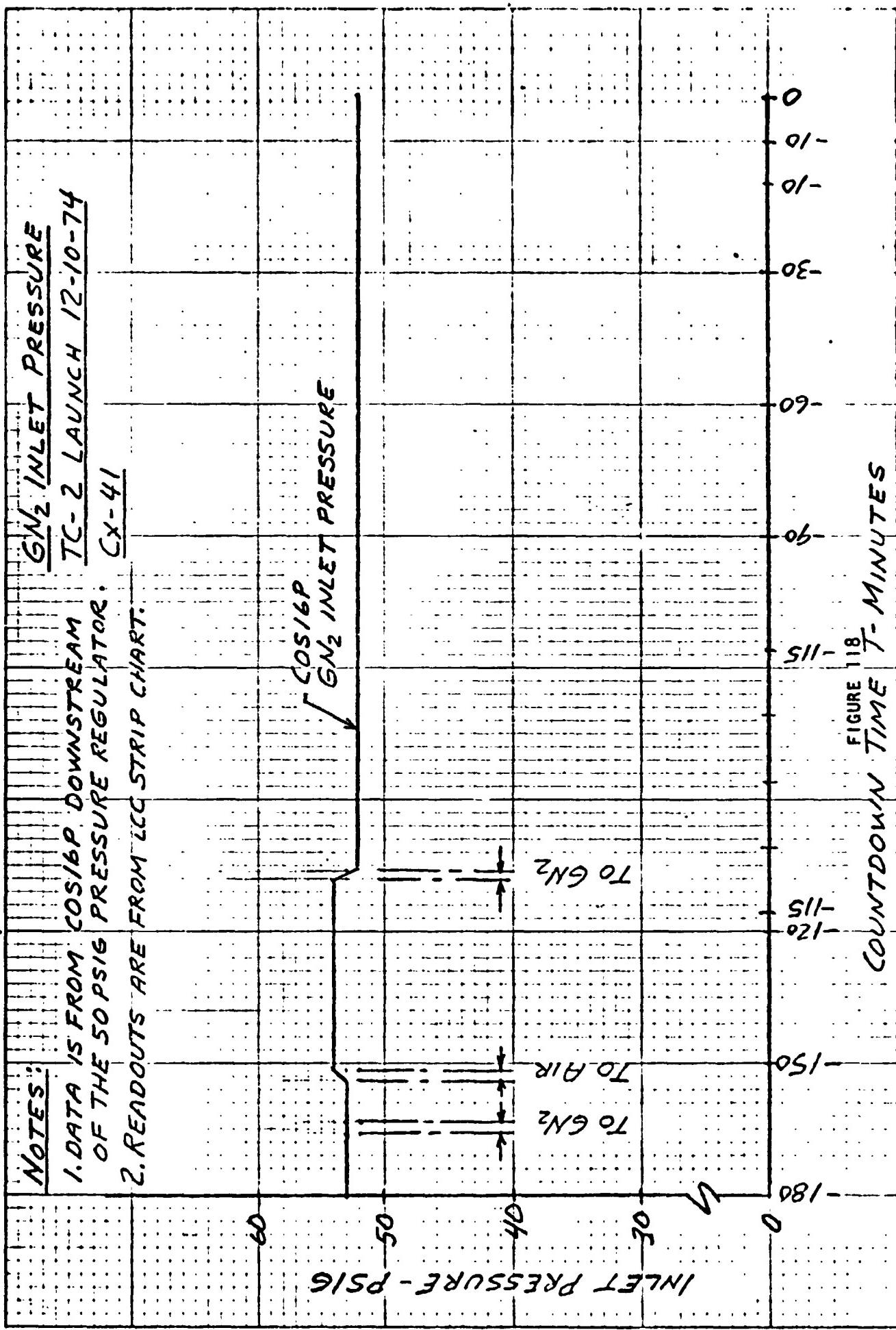
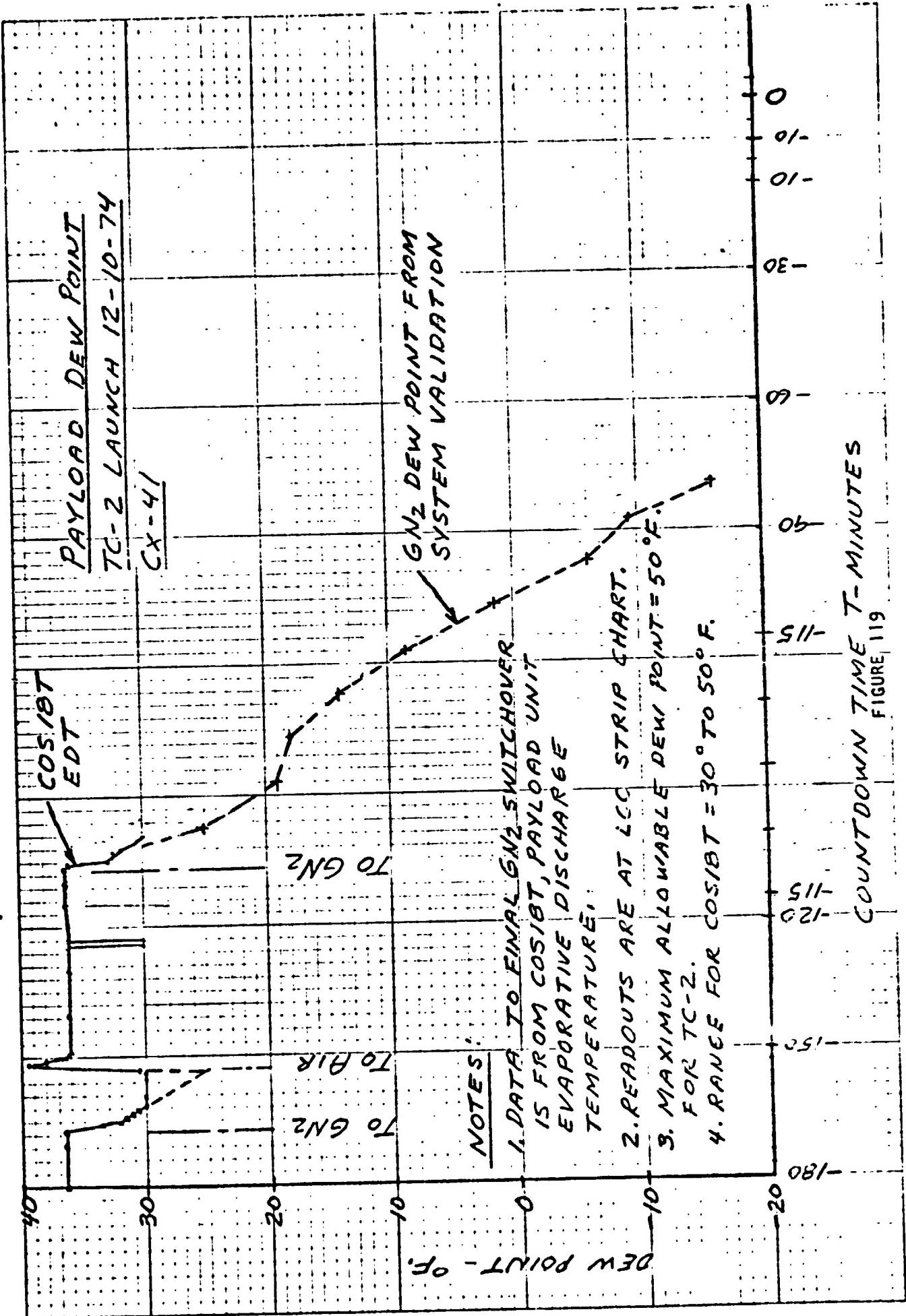


FIGURE 18
COUNTDOWN TIME - MINUTES



COUNTDOWN TIME - MINUTES

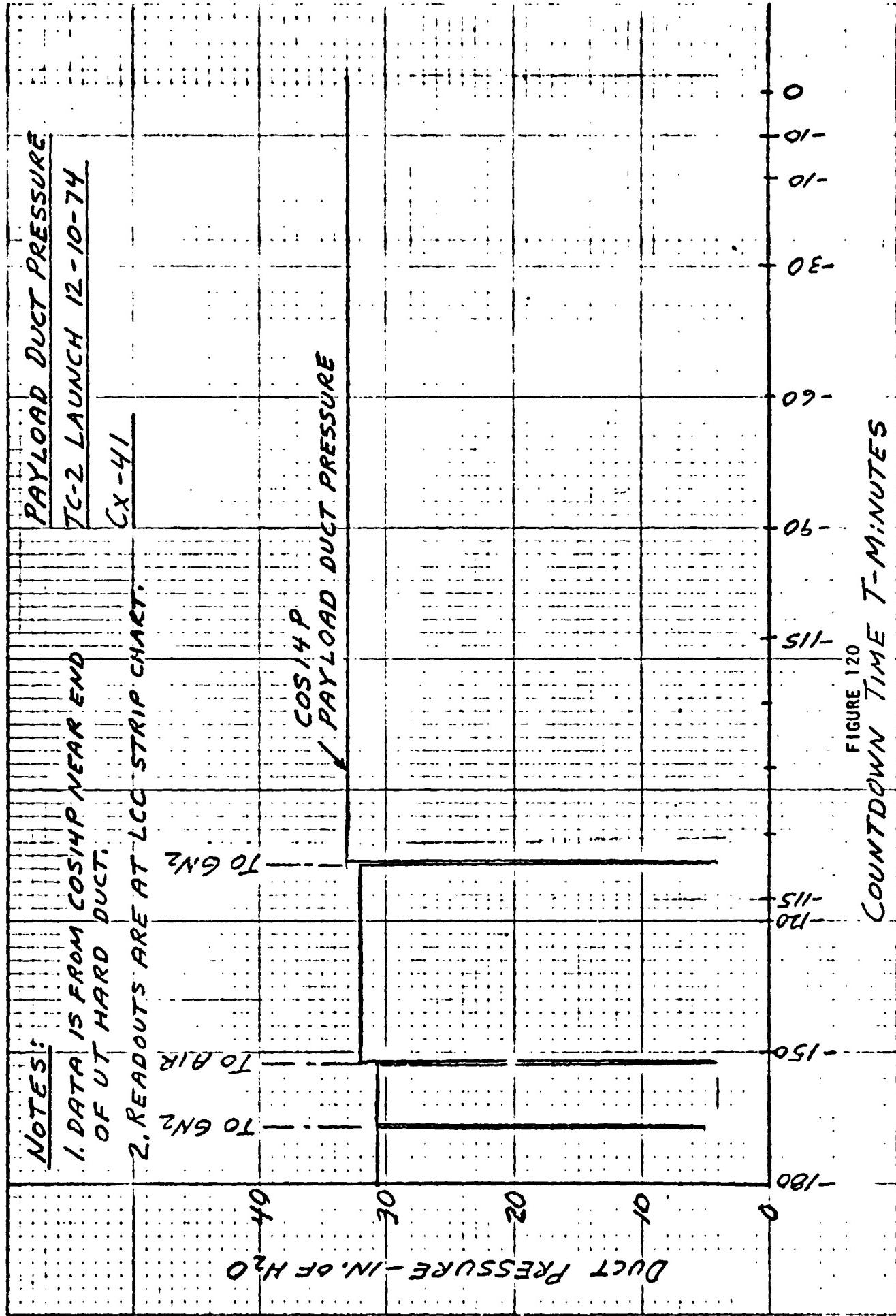


FIGURE 120
COUNTDOWN TIME T-MINUTES

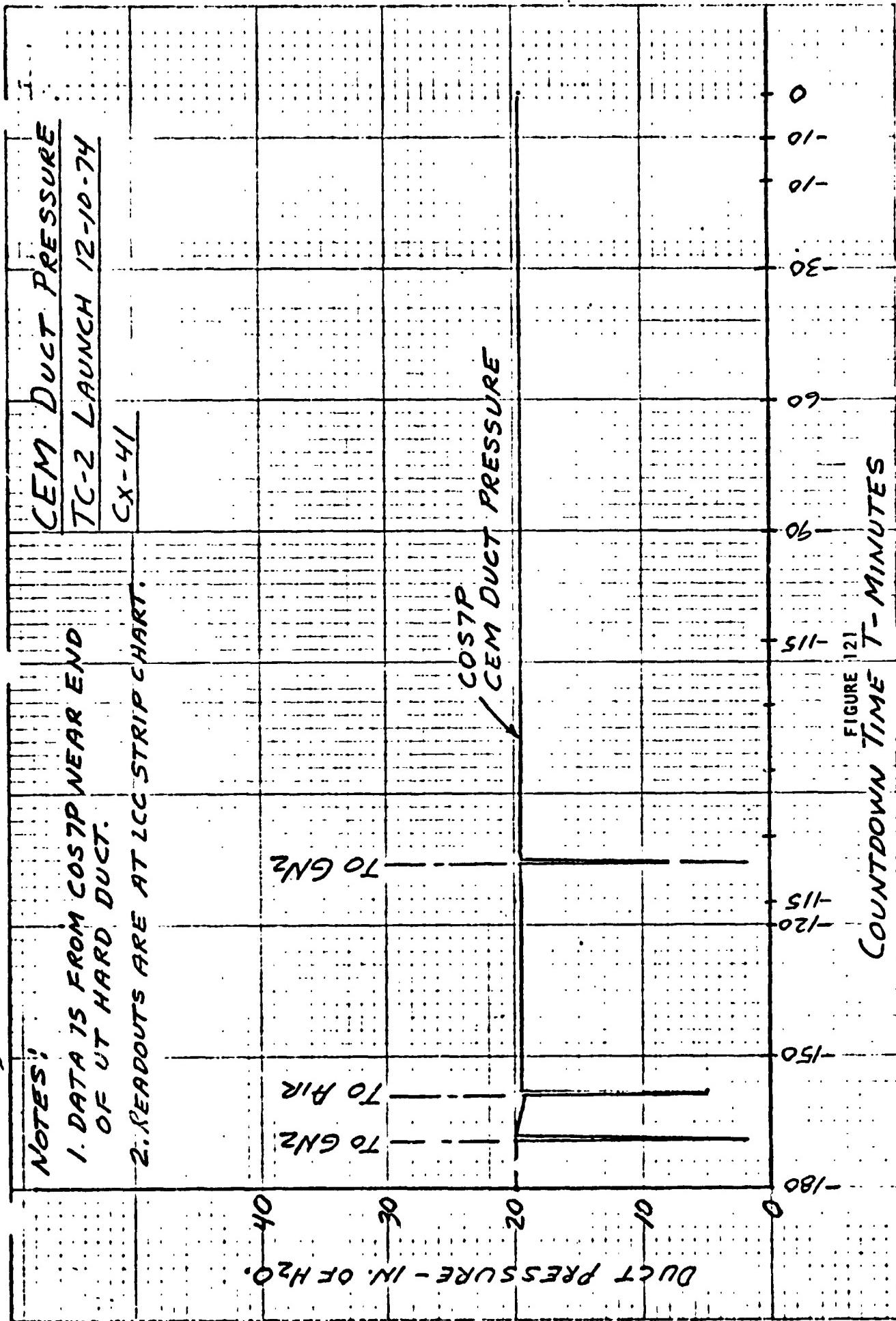
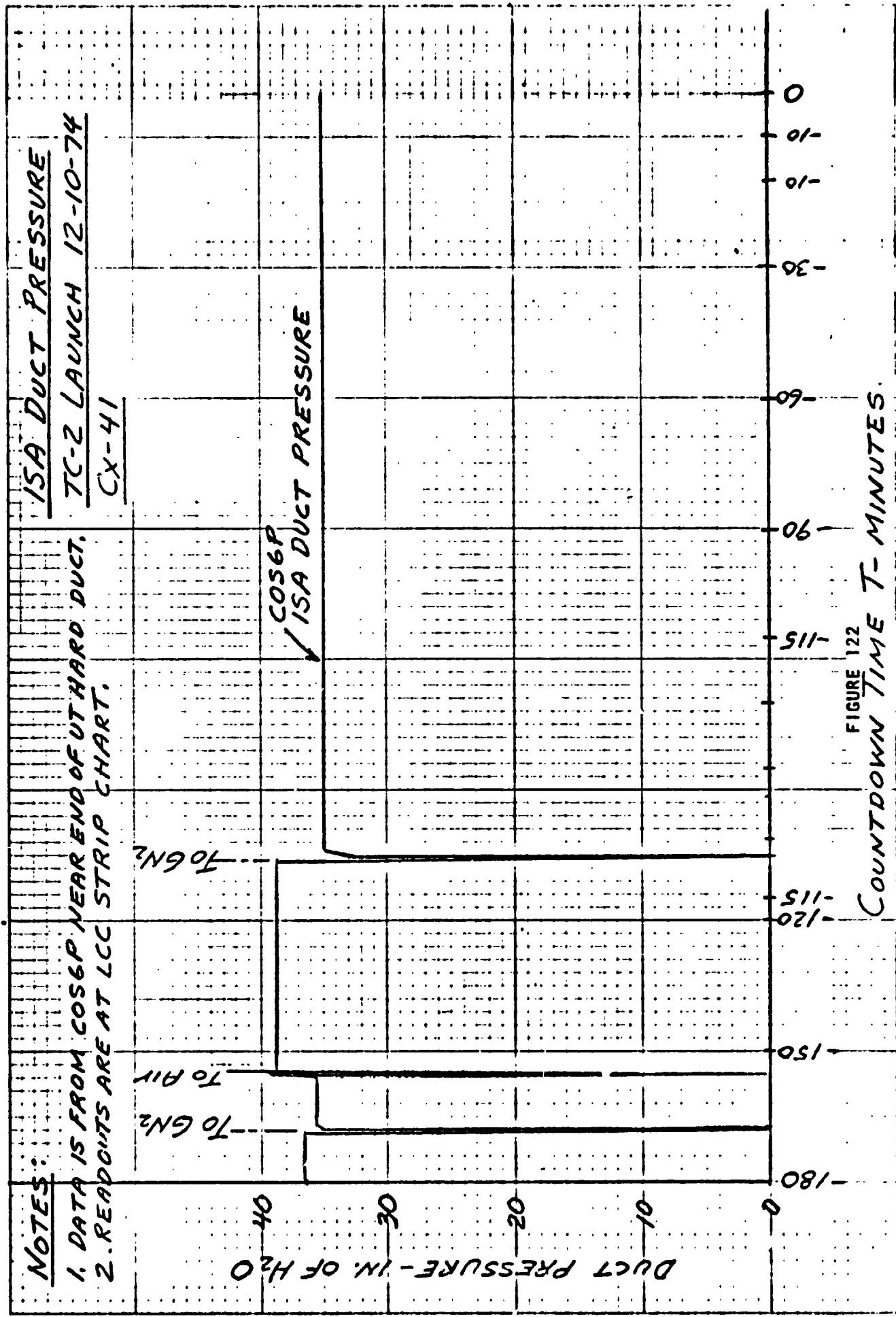


FIGURE 121
COUNTDOWN TIME T-MINUTES



卷之三

NOTES

1. DATA IS FROM COSST AT PAYLOAD DISCONNECT.
 2. READOUTS ARE AT LCC STRIP CHART.

Payload Inlet Temperature

TC-2 LAUNCH 12-10-74

CX-41

MAX. ALLOWABLE

COS ST PAYLOAD INLET TEMP

MIN. ALLOWABLE

206N₂

SII-
021-

051

To G.N.²

081-

INLET FERM.-OF

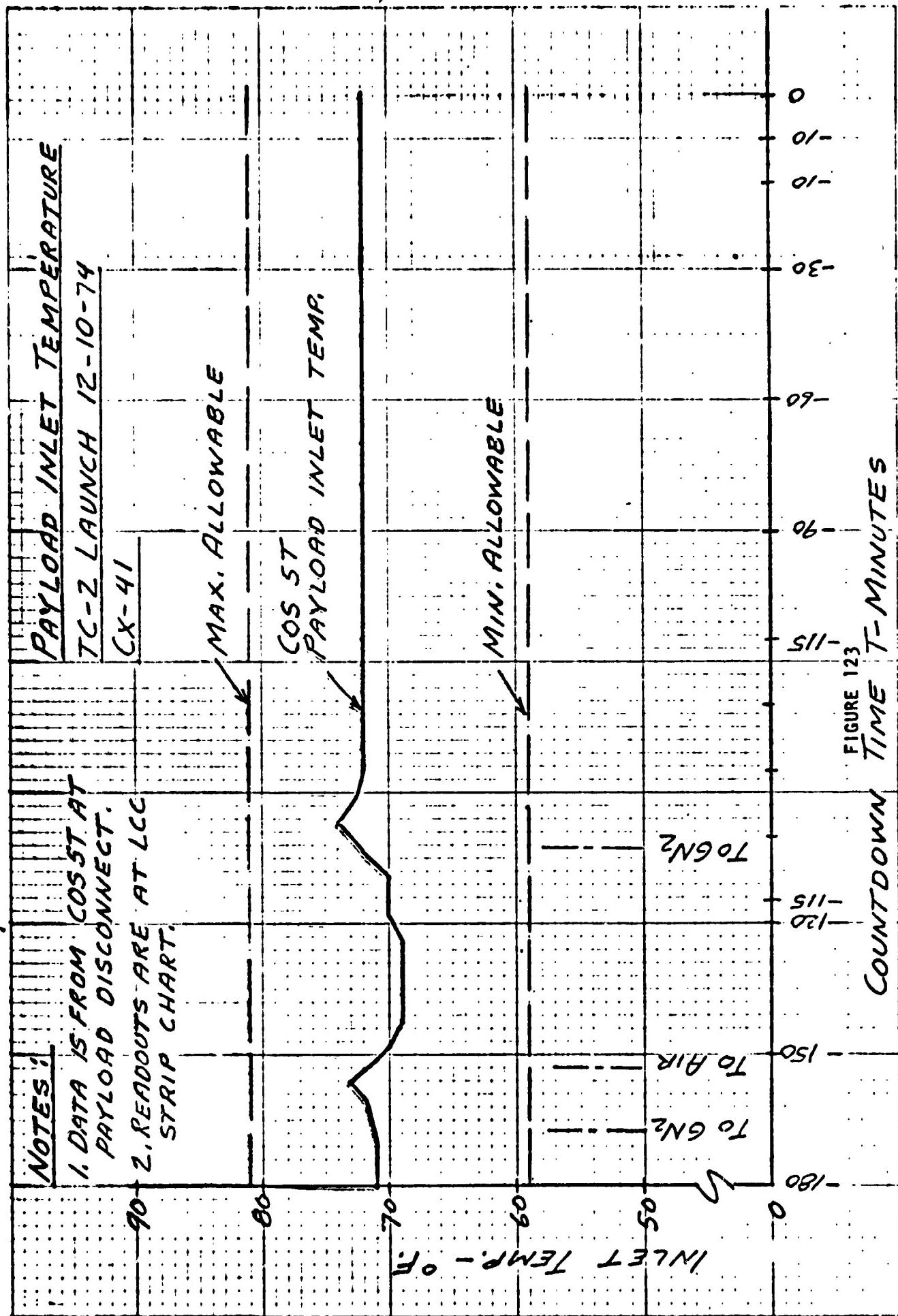
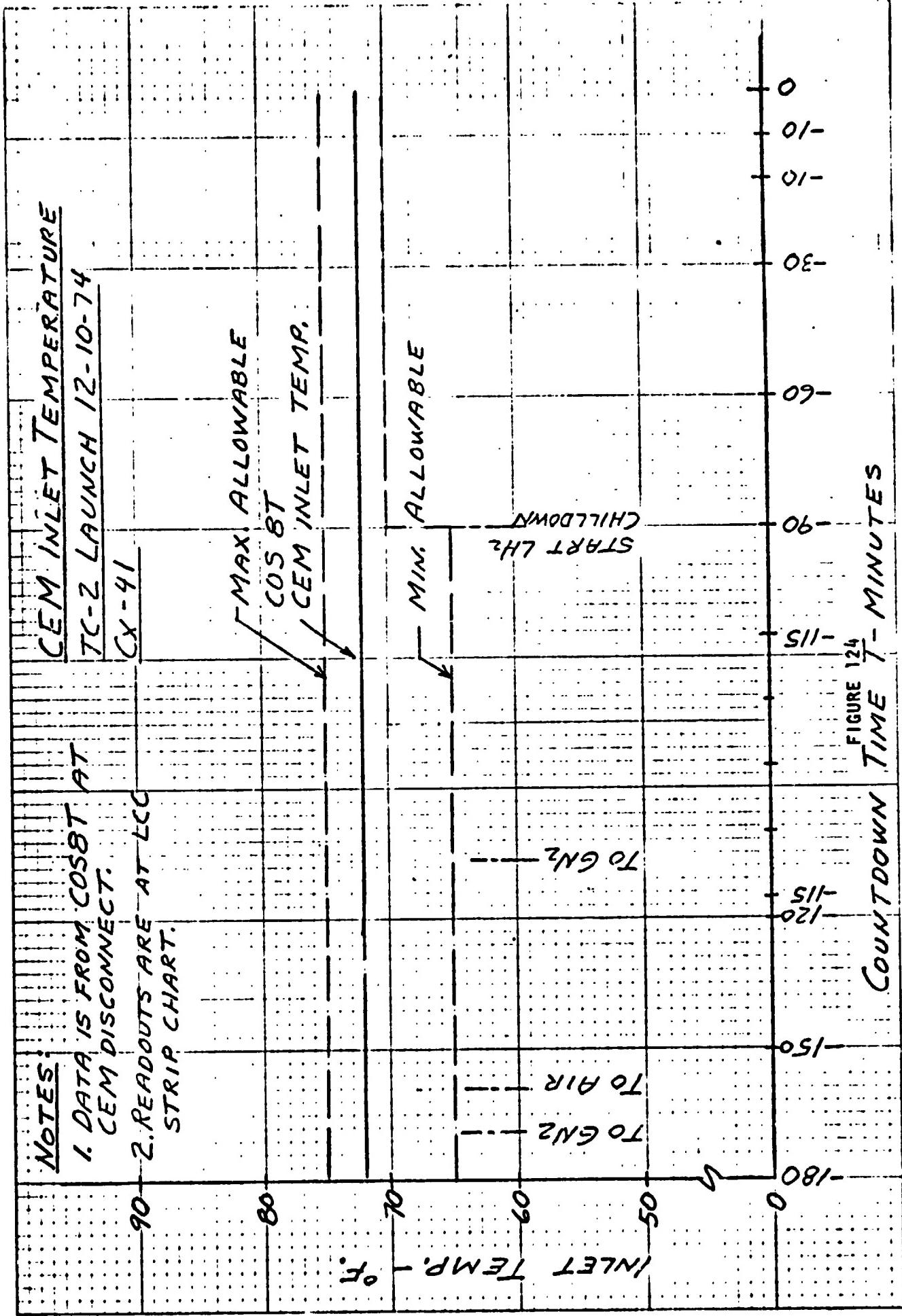


FIGURE 123
COUNTDOWN TIME T-MINUTES



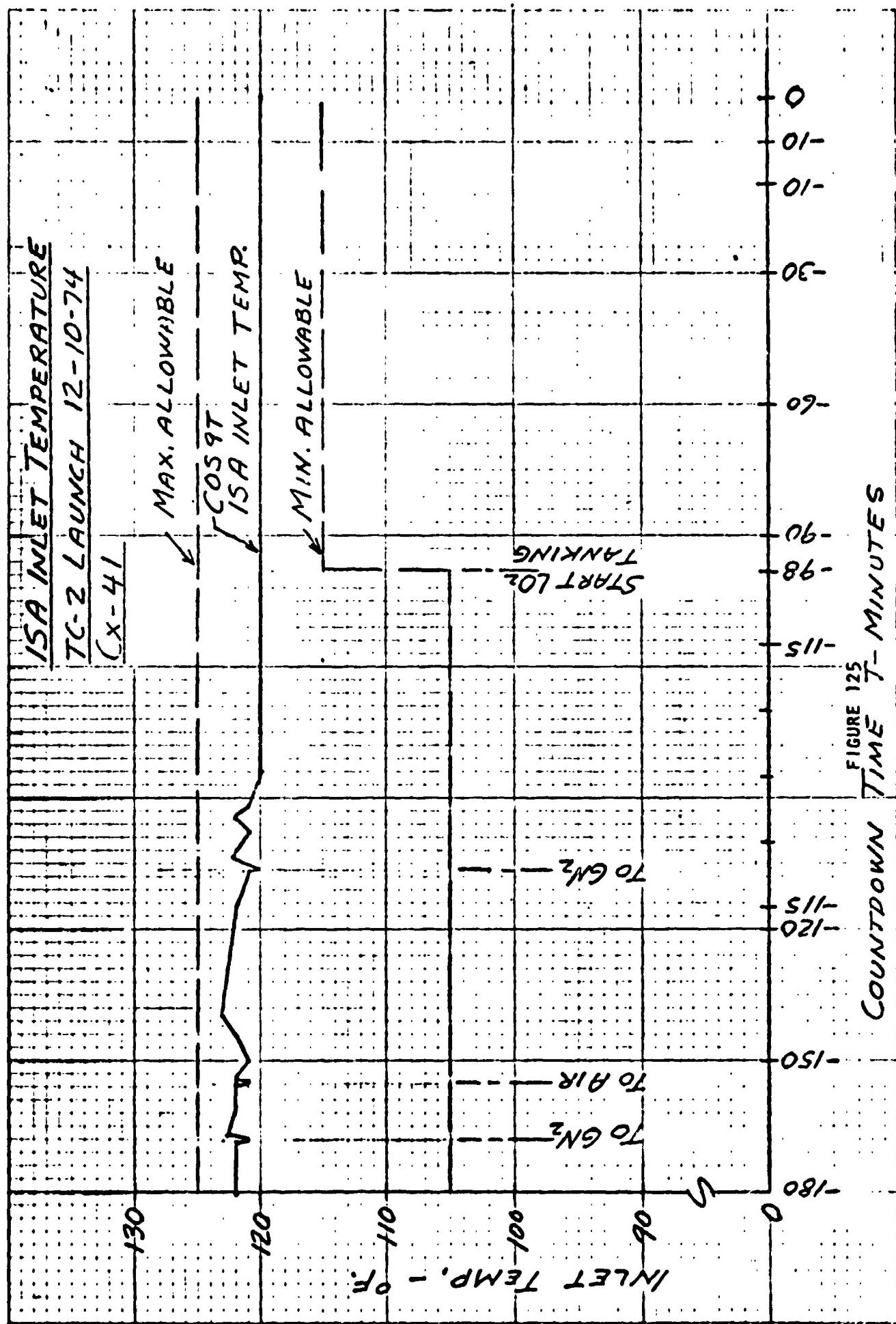


TABLE 62

A/C GN₂ FLOWS

TC-2 LAUNCH - DECEMBER 10, 1974

COMPLEX 41

<u>COMPARTMENT</u>	<u>GN₂ FLOW, LB/MIN</u>		<u>MEASUREMENT</u>
	<u>REQUIRED</u>	<u>ACTUAL</u>	
Payload	120 ₊₅	121	COS24R read at LCC panel meter
CEM	90 ₊₅	90	COS22R read at LCC panel meter
ISA	130 ₊₅	130	COS23R read at LCC panel meter

Data is from flow control assemblies downstream of the A/C units

Electrical Ground Systems

by J. Nestor and H. E. Timmons

Titan Electrical

The Titan electrical ground systems configuration was essentially the same for the launch of TC-2 as it was for TC-1. The launch countdown is initiated and monitored from the Launch Control Console (LCC) in the Launch Control Center. The actual processing of critical readiness and hold functions is performed by the Control Monitor Group (CMG), a time-based automatic countdown controller. The CMG works in conjunction with peripheral equipment such as the Vehicle Checkout Set (VECOS), Tracking and Flight Safety Monitor Group (TFSMG), and Flight Safety Checkout Control Monitor Group (FSCCMG).

The data received during the countdown is transmitted to various recording devices over hardline transmission systems, both from the vehicle and from the ground PCM system. Capability also exists to strip data out of the open loop RF telemetry signal.

The flight of TC-2 was the first usage of a newly built van/transporter set built specifically for NASA programs. The van/transporter set used on TC-1 was one which was obtained from the Air Force, except for the Centaur Mobile Transfer Room (MTR), which was new-build by NASA. The transporter structure and the MTR for TC-2 were essentially copies of the TC-1 equipment. However, the Titan van incorporated both Titan launch control and ground instrumentation equipment into a single van (Figure 126). Previously, this equipment was segregated into two separate vans. The ground instrumentation equipment was new state-of-the-art design incorporating a higher signal level for better noise rejection. The launch control equipment was all built to the original Titan designs, with some of the components being obtained from a program of refurbishment of prototype equipment which had been previously stored at the contractor's plant in Denver. The transporter cabling was also a new design which simplified the overall system wiring and reduced the amount of cabling required.

A few modifications were made to the ground systems after TC-1. The more major changes included the addition of CO₂ and water deluge systems on the transporter for fire prevention, addition of current shunts in the ground power supplies to provide added data for troubleshooting, and the addition of a backup generator at the VIB to provide power in the event of a main AC power outage.

One major change in the data system involved the first usage of the Data Recording and Quick-Look Set (DRQLS) in the VIB. DRQLS replaced the remote Data Recording Set (DRS) previously used in the VIB to evaluate launch control event data. DRQLS provides a magnetic tape recording of the data as well as real time printout of each event change time-tagged to a resolution of 3 milliseconds.

LAUNCH CONTROL AND INSTRUMENTATION VAN

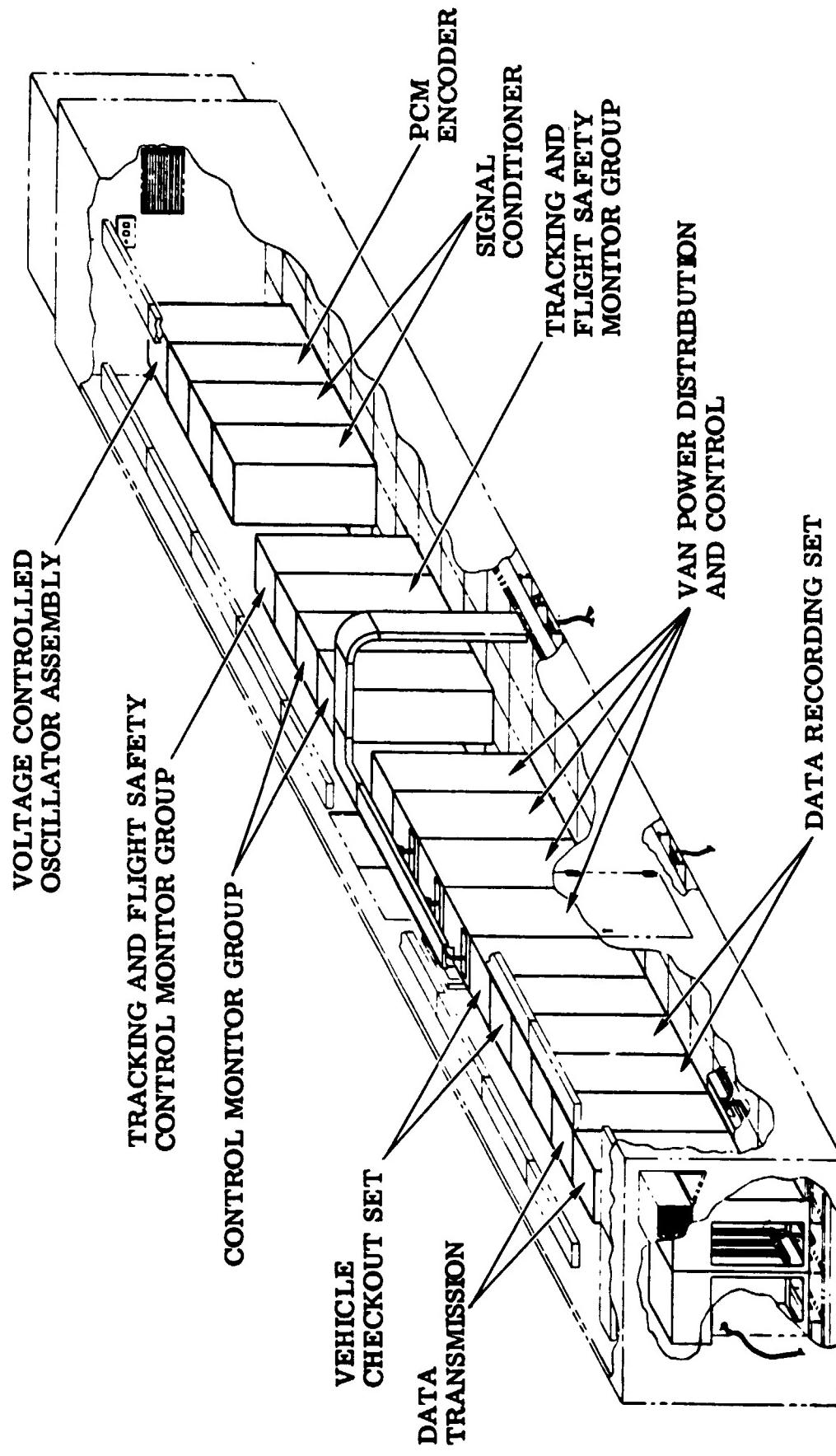


FIGURE 126

The launch of TC-2 was originally scheduled to take place two days earlier than it actually did. This attempt was scrubbed due to the failure of the Centaur LH₂ boost pump inlet temperature transducer.

During the aborted attempt several minor problems occurred in the ground systems. These problems had no impact on the launch attempt nor the actual launch two days later. The problems included five indicating lamps on various items of checkout equipment which were burned out during the launch preps and noise on one channel of data taken during the Automatic Vehicle Verification. An amplifier failed in the strip chart recorder recording LOX Fill and Drain Valve temperature at T-120 minutes. The amplifier was replaced and retested during the one hour built-in hold and performed properly thereafter. When CMG "B" power was applied from the Launch Control Console (LCC) at T-90 minutes, the indicator on the LCC panel failed to light. A check of the data showed that power was on and that this, too, was a burned out lightbulb. The CMG count was then started and all events proceeded normally until the hold and abort for the boost pump transducer failure at T-10 minutes.

The countdown and launch of Titan/Centaur -2 was accomplished with no major launch control or ground instrumentation systems problems. Table 63 provides a list of minor anomalies discussed in the following paragraphs. The count picked up at T-625 minutes at 2:36 p.m., EST (19:36 GMT), on December 9, 1974.

Prior to the start of the countdown the Programmable PCM Decommutator in the VIB used to decommute Titan telemetry data dropped out of synchronization. This decommutator is used to strip various measurements out of the telemetry data stream for display and evaluation. Loss of synchronization results in display readings which are not representative of the actual data.

This problem of "decom dropout" had been present on a random basis since the Terminal Countdown Demonstration (TCD) on October 22, 1974. Troubleshooting had been unable to isolate the cause of the problem. In order to clear the problem once it had occurred, the mylar tape containing the addressing instructions must be read into the memory of the decommutator by use of a tape reader. The time to clear the problem is approximately 3 minutes. As of the launch date, the problem never had occurred more than two or three times in any one day, therefore, there was no launch constraint assigned.

During the launch countdown the problem recurred one time, at approximately T-500 minutes. The memory was reloaded and synchronization reacquired. The problem did not recur any more through the remainder of the launch countdown activities. Had the problem increased in scope such that reloading the memory could not solve it, a backup plan using a secondary data system had been agreed to by the concerned organizations.

TABLE 63 - TITAN LAUNCH CONTROL AND GROUND INSTRUMENTATION ANOMALIES

<u>TIME</u>	<u>PROBLEM</u>	<u>CAUSE</u>
Prior to Countdown	Titan airborne PCM decommutator lost synchronization	Cause unknown
T-300 min.	Titan landline measurement 7703 - "N ₂ O ₄ injectant pressure", dropped approximately 5% in value	Transducer or ground signal conditioner
T + 0.345 sec.	"Stage II Hydraulic Accumulator Precharge Pressure No-Go" indication came on - remained until 2CIE umbilical disconnect	Airborne pressure switch anomaly
T + 0.427 sec.	"VECOS CST Power Enable" signal pulsed off and back on 3 milliseconds later	Cause unknown
T + 0.450 sec.	Titan umbilical disconnect sequence not as predicted	Lanyard overload

At approximately T-300 minutes, Titan measurement 7703 dropped in value approximately 4-5 percent. This is a measurement of the N₂O₄ injectant pressure in the Thrust Vector Control (TVC) tanks on the Solid Rocket Motors (SRM) which is transmitted over the landline instrumentation system. This is a significant measurement in that it is displayed on the Pad Safety Officer's (PSO) console in the Launch Control Center. It is one of the measurements he uses to make a "go/no-go" determination on the status of the launch vehicle. There are two other measurements on the airborne telemetry system which essentially duplicate the suspect measurement. Both of these measurements were steady and agreed in value with each other within 0.5 percent. It was, therefore, determined that the problem was confined to the instrumentation system only, either in the transducer or the ground signal conditioning system. Verbal assurance was given to the PSO by the UTC engineering team that the pressure was proper based on their monitoring of the telemetry data. Based on this assurance and a periodic update over the communications system, the PSO allowed the launch to continue.

The only other ground systems problems occurred after SRM ignition. At 7:11:01.363, 0.306 seconds after SRM ignition but 0.066 seconds before indication of vehicle movement, the Stage II Hydraulic Accumulator Precharge Pressure No-Go indication came on as indicated by Data Recording Set (DRS) channel 028 going high. Normally this would indicate a drop in the precharge pressure below the lower allowable limit. However, the go indication from the same pressure switch did not go off, indicating a problem in the switch itself rather than an actual pressure decay. Both indications went off as expected when the Titan 2C1E umbilical disconnected at 7:11:01.588. The Stage II Hydraulic Accumulator Precharge Pressure Go signal is a core readiness monitor; i.e., is a prerequisite to entering the terminal countdown. Once the terminal countdown begins at T-32 seconds, the pressure is no longer included in the launch ladder. The NO-GO part of the switch provides an indication only and is not involved in the launch sequence.

At 7:11:01.444, again after ignition but prior to liftoff, a signal which goes from the Control Monitor Group (CMG) to the Vehicle Checkout Set (VECOS) pulsed off and back on 3 milliseconds later. The signal, "VECOS CST Power Enabled," is used to turn VECOS power on when a test is to include a plus count demonstration. It is not used at all during a launch. The pulse probably occurred as the result of the vibration caused by the SRM ignition sound wave. The signal is a patched signal using patch cords in a program board. Since it was not significant to the launch and since the patchboard must be removed and repatched prior to the next usage, no attempt will be made to isolate the exact problem.

The disconnect sequence of the Titan umbilicals was not per plan. The Stage I electrical umbilical (1C1E), which was to be the first core umbilical out, actually came out after one of the upper Stage II electrical umbilicals, 2A1E. No detrimental effects of this sequence were noted, the only concern being that the sequence had not previously been tested. The umbilical release sequence on TC-1 had also been different than the desired sequence.

As a result of the evaluation of the TC-1 sequence, it was decided to modify the lanyard rigging associated with all the Titan umbilicals in an attempt to achieve the desired sequence for TC-2. The lanyards for the two Solid Rocket Motor umbilicals, LB1E and RB1E, were shortened by one inch each while the core umbilical lanyards were each lengthened by various amounts (LC1E - 1/4 inch; 2A1E - 3/8 inch; 2A2E - 1/2 inch; 2C1E - 3/4 inch). In addition, an adjustment was made in the J-bar position for LB1E and RB1E which lowered it 1/2 inch. Normally, these adjustments would have resulted in the proper sequence. However, on the TC-2 launch, the J-bar to which the LC1E umbilical was attached became overloaded causing it to deform. This deformation caused the umbilical to release slightly later than predicted. The load in the LC1E lanyard was estimated to be about 250 pounds based on the 3/8 inch permanent deformation which remained at the J-bar after launch. The allowable load limits for the static pull force on this umbilical are 70 to 230 pounds. The dynamics of the launch may have added to the static forces normally encountered during testing which would account for the deformation and resultant late umbilical disconnect. Post-launch review has shown that this sequence is acceptable and no change will be made to the umbilical lanyards for on-going vehicles. Table 64 shows the Titan umbilical sequence.

Centaur Electrical

All systems performed satisfactorily throughout countdown and launch operations. No problems nor any significant discrepancies were observed. The second MTR, in conjunction with Van Set No. 4, was used for the first time in support of a launch, and is scheduled to be used next to support activities for the Viking A (TC-4) launch.

Some important modifications to Complex 41 were implemented after the launch of TC-1 to provide for improved operations and to accommodate TC-2 configuration changes. One of the more significant design improvements, resulting in lower operating costs, was the incorporation of "Local Control" capability in the AGE Building and MTR. The vehicle power and pneumatic systems were modified to permit, at the cognizant engineer's option, the performance of checkout and validation procedures at the complex without the support from the VIB that had previously been necessary. This change permits more expeditious performance of tests involving these two systems, at the same time frees the VIB for other tasks that could be performed concurrently.

The complex was also modified from TC-1 configuration to provide for performance of the boost pump rotation tests as described in Section IX of this report. The propulsion and attitude control system was modified to provide for GSE control to operate and monitor the spin tests from either the AGE Building or the VIB. The change in TC-2 mission requirements from two burn to four burn mandated the use of two airborne helium bottles as in TC-1. This change, as described in Section IX of this report, had the added requirement that the two bottles be capable of being individually charged or discharged. The pneumatic control system was modified to provide this capability from either the complex or the VIB, as well as providing the added instrumentation to permit continuous monitoring of bottle temperatures and pressures via landlines.

TABLE 64 - TITAN UMBILICAL DISCONNECT TIMES
 (CMG T-0 = 7:11:01.018)

<u>UMBILICAL DESIGNATION</u>	<u>TIME OF DISCONNECTION</u>	<u>TIME FROM CMG T-0</u>
	<u>GMT</u>	
LBIE	7:11:01.429	T + 0.411
RBIE	7:11:01.432	T + 0.414
2A1E	7:11:01.468	T + 0.450
1C1E	7:11:01.483	T + 0.465
2A2E	7:11:01.501	T + 0.483
2C1E	7:11:01.585	T + 0.567

Centaur Umbilicals

The Centaur umbilicals performed satisfactorily with one exception. The shroud cavity pressure probe umbilical did not separate as planned. This umbilical consists of a vinyl tube which slips over a 1/4-inch tube which protrudes through the shroud about two inches. The tube is located near the LH₂ fill and drain valve. Between the surface of the shroud and the end of the tube is a coil of wire (tube stripper) to which a retract lanyard is attached. The retract lanyard is actuated with the LH₂ fill and drain valve lanyard. Post-launch examination of the pressure probe umbilical revealed that the tube stripper was not attached to the lanyard and the vinyl tube had fractured with very jagged edges, which seems unusual for vinyl tubing. GDC has performed some special tests to determine the cause of the umbilical failure. The results of the testing are presented in GDC report 671-6-75-10 titled "Shroud Cavity Pressure Probe Umbilical." GDC will maintain the existing configuration of the Shroud Cavity Pressure Probe Umbilical Retract System except that they will replace the present tube stripper with one made from larger diameter wire. The GDC static tests showed the stripper made from the larger diameter wire to have an ultimate strength of 143 lbs. at -100°F as compared to 61 lbs. at -100°F for the stripper used on TC-2.

The Centaur umbilical disconnect sequence is shown in Table 65.

TABLE 65 - CENTAUR UMBILICAL DISCONNECT TIMES
 (CMG T-0 = 7:11:01.018)

<u>EVENT</u>	<u>TIME OF OCCURRENCE</u> <u>GMT</u>	<u>TIME FROM CMG T-0</u>
CMG T-4 Second Command to MTR	7:10:57.037	T-3.981
MTR Relay Actuation - Eject Aftplate & Eject Upper Umbilicals	7:10:57.058	T-3.960
Umbilical 600P2 Ejected	7:10:58.015	T-3.003
Umbilical 600P1 Ejected	7:10:58.231	T-2.787
Aft Door Closed Signal	7:10:58.705	T-2.313
Aft Plate Ejected to CMG	7:10:58.759	T-2.259
CMG T-0.5 Second Command to MTR	7:11:00.538	T-0.480
MTR Relay Actuation - Eject Fill & Drain Valves LH ₂ LO ₂	7:11:00.556 7:11:00.559	T-0.462 T-0.459
LH ₂ Fill & Drain Valve Ejected LO ₂ Fill & Drain Valve Ejected	7:11:00.895 7:11:01.072	T-0.123 T+0.054
CMG T-0 Command to MTR	7:11:01.039	T+0.018
MTR Relay Actuation - Air Conditioning Disconnect	7:11:01.057	T+0.036
Umbilical 600P4 Disconnected (Rise-off) Umbilical 600P5 Disconnected (Rise-off)	7:11:01.690 7:11:01.810	T+0.672 T+0.792

Delta Stage Support Systems

by A. Lieberman

All AGE and facility installations in support of the third stage Delta vehicle and its associated GSE operated satisfactorily during prelaunch and launch operations.

The first-time use of the Delta third stage on the ITL required modifications to the ITL to provide checkout and launch capability. Delta GSE for monitor and control of Delta functions were located in the Launch Control Center No. 1 in the VIB, in Equipment Room No. 2 of the AGE Building and on Level 11 of the MST. Interconnecting cabling was provided between the VIB Delta GSE, PSOC, DTS and Landline PCM systems, the AGE Building Delta GSE, spacecraft umbilical, MST and MTR.

The Delta safe and arm and recorder control panel in the LCC provided remote S&A arming and monitoring as well as remote control of the Delta recorder on Level 11 of the MST. The PSOC provided an arm permission signal to the S&A panel. The Delta TLM and instrumentation control panel in the LCC controlled and monitored Delta stage power.

The GSFC power supply rack in the AGE Building provided ground power for the S&A circuits, local monitor and control of various Delta stage functions and local control of the Delta recorder on the MST. Space and facility power were provided to miscellaneous Delta GSE on Level 11 of the MST for Delta checkout. The recorder monitored the Delta pyrotechnic system during prelaunch operations. In addition, the installation provided simultaneous transmittal of these signals via the MTR to Complex 36 and the CIF.

The Delta portable ground station located in the LCC was cabled to an existing VIB receiving antenna to permit ground checkout of the RF systems with the vehicle at the pad.

Helios A Spacecraft Support Systems

by A. Lieberman

All AGE and facility installations in support of the Helios spacecraft and its peculiar GSE operated satisfactorily during prelaunch and launch operations.

The support of the Helios payload on the ITL required modifications to the ITL to provide checkout and launch capability. Helios GSE for monitor and control of the spacecraft during prelaunch and launch operations were located in the AGE Building and on Level 12 of the MST. Interconnecting cabling was provided between the AGE Building Helios GSE and Level 12 of the MST, the spacecraft umbilical cable and the Range interface to Hangar A0. Ground power and adapter cables to mate with German type connectors were also provided.

Ground checkout of the Helios RF systems was accomplished using a system of reradiating antennas on Level 12 of the MST coupled to a CSS antenna.